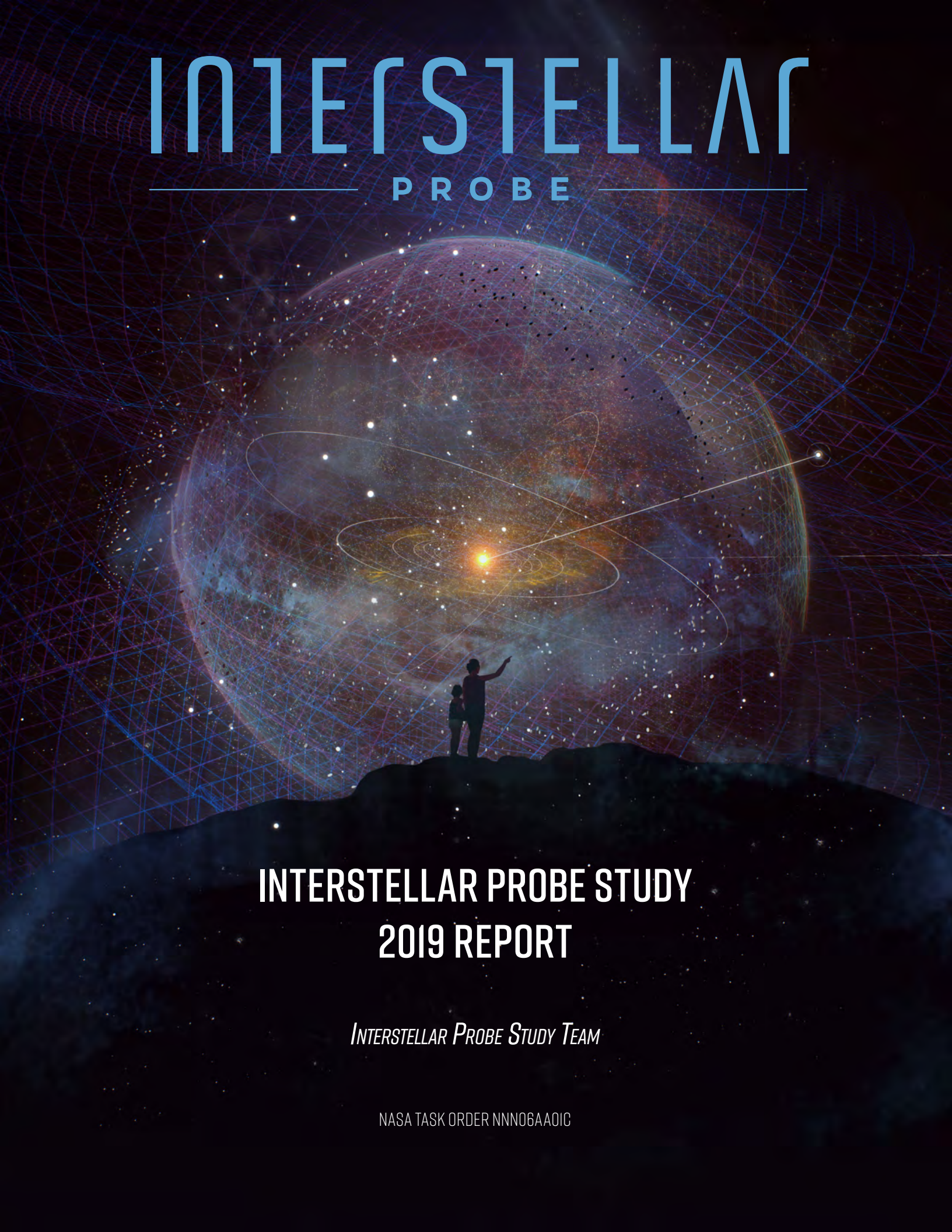

INTERSTELLAR PROBE STUDY 2019 REPORT

Interstellar Probe Study Team

NASA TASK ORDER NNN06AA01C

List of Authors

Primary Team

Name	Position	Affiliation
Ralph L. McNutt, Jr.	Principal Investigator	Johns Hopkins University Applied Physics Laboratory
Michael V. Paul	Project Manager	Johns Hopkins University Applied Physics Laboratory
Glen Fountain	Deputy PM/Senior Advisor & Mission Lifetime Analysis	Johns Hopkins University Applied Physics Laboratory
James P. Mastandrea	Assistant Project Manager	Johns Hopkins University Applied Physics Laboratory
Pontus C. Brandt	Project Scientist	Johns Hopkins University Applied Physics Laboratory
Kathleen E. Mandt	Deputy Project Scientist	Johns Hopkins University Applied Physics Laboratory
Jim Kinnison	Mission Architecture & ACTING Radioisotope Power Systems	Johns Hopkins University Applied Physics Laboratory
Reza Ashtari	Deep Space Communications	Johns Hopkins University Applied Physics Laboratory
Stuart Bale	Heliophysics — Fields	University of California, Berkeley
Alice A. Cocoros	Payload System Engineer	Johns Hopkins University Applied Physics Laboratory
David J. Copeland	Deep Space Communications	Johns Hopkins University Applied Physics Laboratory
Bob DeMajistre	Heliophysics — ENA	Johns Hopkins University Applied Physics Laboratory
André Galli	Heliophysics — Neutrals	University of Bern
Andrea Harman	Program Communications	—
Matthew E. Hill	Heliophysics — Particles	Johns Hopkins University Applied Physics Laboratory
Stephen Jaskulek	Mission Lifetime Analysis	Johns Hopkins University Applied Physics Laboratory
Kathy Kha	Costing & Financial Planning	Johns Hopkins University Applied Physics Laboratory
Carey M. Lisse	Astrophysics Lead	Johns Hopkins University Applied Physics Laboratory
Douglas Mehoke	Solar Shield Analysis and Testing	Johns Hopkins University Applied Physics Laboratory
Parisa Mostafavi	Space Physicist	Johns Hopkins University Applied Physics Laboratory
David Napolillo	Spacecraft Configuration Studies	Johns Hopkins University Applied Physics Laboratory
Romina Nikoukar	Space Physicist	Johns Hopkins University Applied Physics Laboratory
Kimberly J. Ord	Concept of Operations	Johns Hopkins University Applied Physics Laboratory
Elena A. Provornikova	Heliophysics Lead	Johns Hopkins University Applied Physics Laboratory
Gabe Rogers	Spacecraft Control Analysis	Johns Hopkins University Applied Physics Laboratory
Christopher M. Rose	Avionics	Johns Hopkins University Applied Physics Laboratory
Kirby D. Runyon	Planetary Lead	Johns Hopkins University Applied Physics Laboratory
Abigail M. Rymer	Exoplanet Lead	Johns Hopkins University Applied Physics Laboratory
Wayne R. Schlei	Trajectory Analyses	Johns Hopkins University Applied Physics Laboratory
Fazle Siddique	Trajectory Analyses	Johns Hopkins University Applied Physics Laboratory
Clayton Smith	Mission Lifetime Analysis	Johns Hopkins University Applied Physics Laboratory
Robert Stough	SLS Coordination	NASA Marshall Space Flight Center
Drew L. Turner	Heliophysics — Particles	Johns Hopkins University Applied Physics Laboratory

Name	Position	Affiliation
Vikas Vepachedu	Payload System Engineer	Johns Hopkins University Applied Physics Laboratory
Steven R. Vernon	Launch Vehicles Options and Alternatives	Johns Hopkins University Applied Physics Laboratory
Janet Vertesi	Social Science	Princeton University
Sally Whitley	Mission Lifetime Analysis	Johns Hopkins University Applied Physics Laboratory
Lawrence S. Wolfarth	Costing & Financial Planning	Johns Hopkins University Applied Physics Laboratory

Collaborators

Name	Affiliation
Frederic Allegrini	Southwest Research Institute
Nicolas Altobelli	European Space Agency
Brian Anderson	Johns Hopkins University Applied Physics Laboratory
Dan Baker	Laboratory for Atmospheric and Space Physics, University of Colorado, Boulder
Stas Barabash	Institutet för Rymdfysik, Swedish Insitute of Space Physics
Chas Beichman	NASA Jet Propulsion Laboratory
Jean-Loup Bertaux	Institut de Recherche en Sciences de l'Environment
Michel Blanc	Institut de Recherche en Astrophysique et Planétologie
Eric Christian	NASA Goddard Space Flight Center
John Cooper	NASA Goddard Space Flight Center
Mihir Desai	Southwest Research Institute
Kostas Dialynas	Department of Physics, National and Kapodistrian University of Athens
Bruce Draine	Princeton University
Stefan Eriksson	Laboratory for Atmospheric and Space Physics, University of Colorado, Boulder
Hans Fahr	Argelander-Institut für Astronomie
Len Fisk	University of Michigan
Herb Funsten	Los Alamos National Laboratory
Steve Fuselier	Southwest Research Institute
Randy Gladstone	Southwest Research Institute
George Gloeckler	University of Michigan
Mike Gruntman	University of Southern California
Don Gurnett	University of Iowa
Sonny Harman	NASA Ames Research Center
George Ho	Johns Hopkins University Applied Physics Laboratory
Mihaly Horanyi	Laboratory for Atmospheric and Space Physics, University of Colorado, Boulder
Vlad Izmodenov	Институт Космических Исследований
Peter Kollmann	Johns Hopkins University Applied Physics Laboratory
Haje Korth	Johns Hopkins University Applied Physics Laboratory

Name	Affiliation
Bill Kurth	University of Iowa
Rosine Lallement	l'Observatoire de Paris
Lou Lanzerotti	New Jersey Institute of Technology
Benoit Lavraud	Institut de Recherche en Astrophysique et Planétologie
Stefano Livi	Southwest Research Institute
Dick Mewaldt	Space Radiation Lab at California Institute of Technology
Don Mitchell	Johns Hopkins University Applied Physics Laboratory
Eberhard Moebius	University of New Hampshire
Merav Opher	Boston University
Jeewoo Park	NASA Goddard Space Flight Center
Nick Paschalidis	NASA Goddard Space Flight Center
Larry Paxton	Johns Hopkins University Applied Physics Laboratory
Andrew Poppe	University of California, Berkeley
Eric Quemerais	Institut de Recherche en Sciences de l'Environment
Jamie Rankin	Princeton University
Seth Redfield	Wesleyan University
Ed Roelof	Johns Hopkins University Applied Physics Laboratory
Jim Slavin	Harvard & Smithsonian Center for Astrophysics
Veerle Sterken	ETH Zürich
Adam Szabo	NASA Goddard Space Flight Center
Jamey Szalay	Princeton University
Jan-Erik Wahlund	Swedish Institute of Space Physics
Joe Westlake	Johns Hopkins University Applied Physics Laboratory
Bob Wimmer	Christian-Albrechts-Universität zu Kiel
Brian Wood	U.S. Naval Research Laboratory
Peter Wurz	Space Research & Planetary Sciences, Universität Bern
Gary Zank	University of Alabama
Philippe Zarka	l'Observatoire de Paris
Michael Zemcov	Center for Detectors, Rochester Institute of Technology

Distribution Statement

This work was supported by NASA Contract Number NNN06AA01C.

Table of Contents

List of Figures

List of Tables

1. Executive Summary

Astronomical observations of the 20th century led to multiple shifts in our thinking about the scope and scale of the universe. The vast distances (>10 billion light years) and corresponding times scales (set by the finite speed of light) limit our knowledge of the universe—from the nearest stars to the largest galactic structures—to what can be ascertained from remote observations. These observations in turn are enabled by the fundamental particles and phenomena that travel at light speed, namely photons, neutrinos, and gravitational radiation. From these phenomena, the physical laws governing the interplay of matter and energy and the evolution of both, and clues provided by the highest energy cosmic rays, we have gradually constructed notional maps of our location in the grand scheme of the known universe (Figure 1-1).

For just over the last 60 years, we have been exploring our way outward from the Earth with instrumented spacecraft. From the Earth orbit of Sputnik, we have learned about conditions on the other bodies of the solar system as well as those in interplanetary space itself. Limited by propulsion technology and spacecraft reliability and lifetime, our "design reach" has only recently been extended to the Pluto system and the Kuiper Belt Objects beyond. In the meantime, the Voyager 1 and 2 spacecraft, designed for a 4.5-year mission lifetime (Draper et al., 1975; Kohlhase & Penzo, 1977), have completed their 42nd year post launch, resulting in the twin Voyagers becoming the first probes to explore nearby interstellar space, but only by accident.

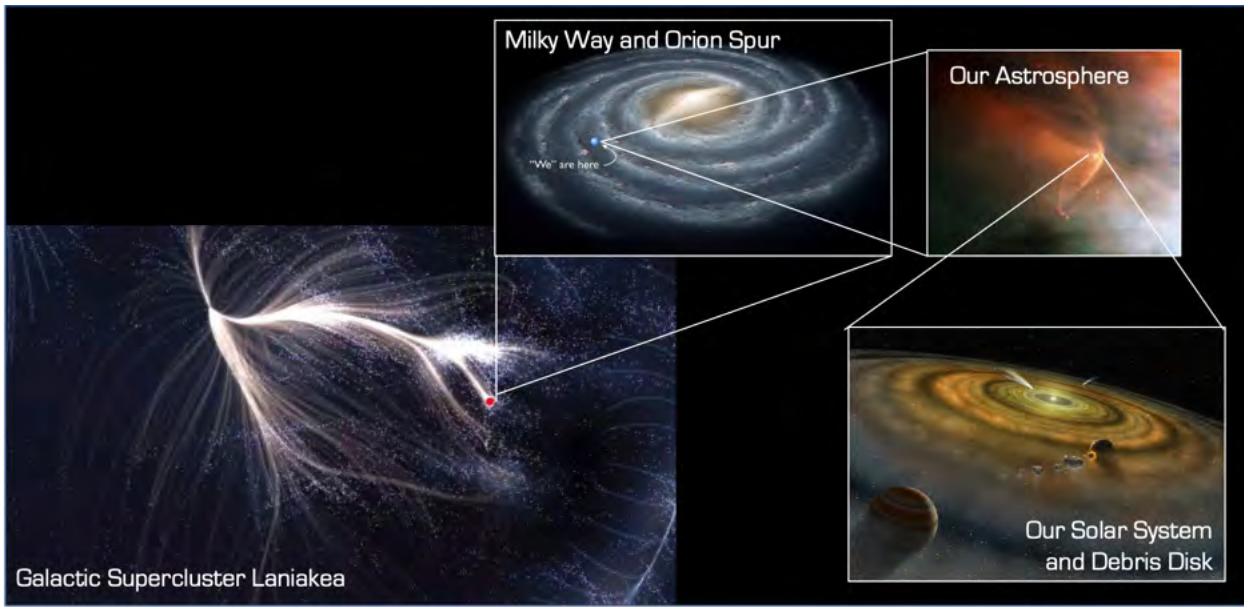

Figure 1-1. The grand scale of our place in the known universe as deduced from remote measurements that began with those of Hubble (1926) less than a century ago and were greatly expanded by the use of the Hubble Space Telescope named in his honor.

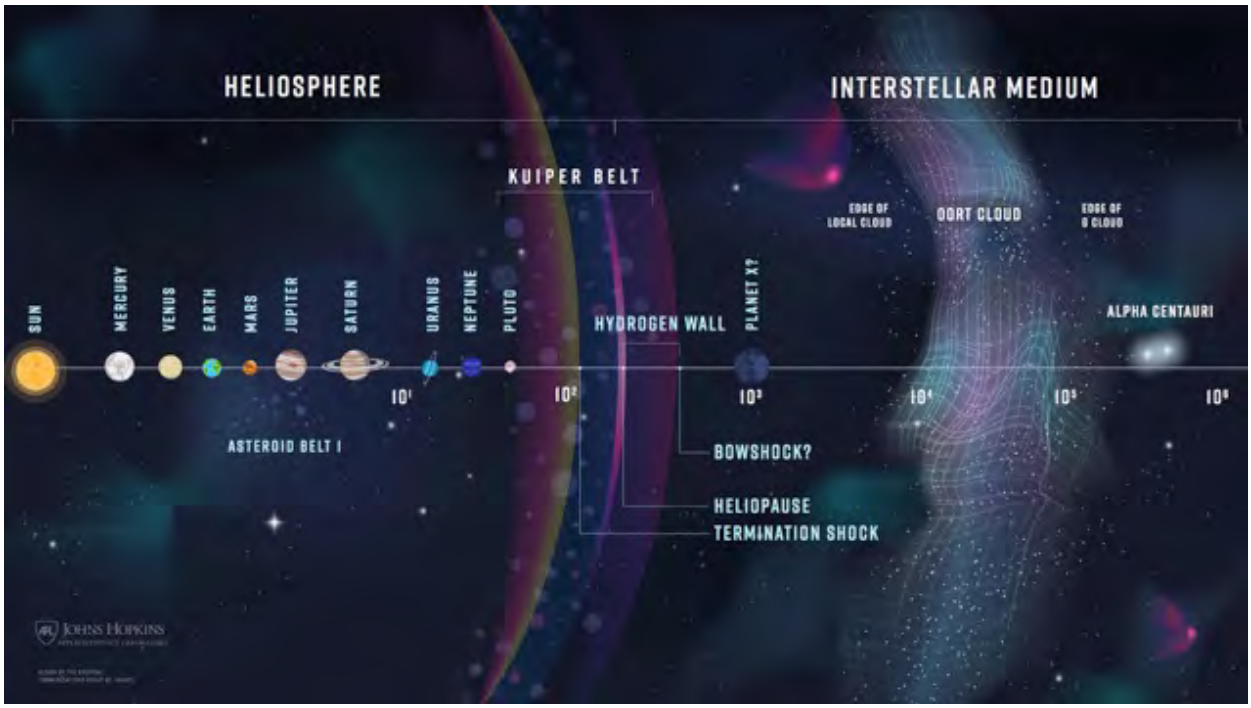

Figure 1-2. An interstellar probe mission to the interstellar medium would be daring, challenging, and inspirational to the public, and it will be a rational first step before attempting to reach another star. The units of the x-axis are astronomical units.

In contrast, the Interstellar Probe mission represents ***humanity's first deliberate step into the space between the stars*** (Figure 1-2). Such a robotic space mission has been under discussion since the beginning of the Space Age and the establishment of NASA. As at the beginning of most such undertakings, the implementation has proven more challenging than first thought, and the concepts brought forward have collectively become known as Interstellar Probe, a robotic, one-way mission into the local interstellar medium. Traveling beyond the Sun's sphere of influence would open remarkable possibilities across NASA's science divisions to explore the environment of the Milky Way and how its past state shaped the emergence of our own habitable solar system. Our own existence as a sentient species provides the only guidance on how to search for—and recognize—life elsewhere among the stars. Interstellar Probe would be NASA's first dedicated mission to venture into the space between our star and other potentially habitable planetary systems and represents perhaps NASA's boldest move to date in space exploration.

The Johns Hopkins University Applied Physics Laboratory has been tasked by NASA to perform a study to determine the feasibility of a "pragmatic" interstellar mission—one that could be launched by the year 2030 and can utilize mature technologies at the time of development. The study began in calendar year (CY) 2018 (13 June 2018) and will continue through early CY 2022 (30 April 2020). The context for this current study is the next "Decadal Survey" effort for NASA's Heliophysics Science Division. Guidance from the science community for NASA's overall science program is provided every 10 years via Decadal Surveys for each of NASA's four science mission divisions: Planetary Science,

Astrophysics, Heliophysics, and Earth Science. The Interstellar Probe has been discussed in the past two Heliophysics Decadal Surveys (NRC, 2003, 2013) and by the general community for long before (Simpson et al., 1960). This current study is being supported by NASA to provide technical input, which can be used for the deliberations of the next Heliophysics Decadal Survey, which will apply for the years 2023–2032. At the same time, NASA's Science Mission Directorate has asked this study to assess what science across all of the divisions could be enabled with such a mission (see Figure 1-3). Recommendations for specific science goals and approaches are the responsibility of the Decadal Survey efforts themselves. In contradistinction, this effort is to investigate what Interstellar Probe missions could technically be implementable within the time period through 2032. To do so, we have outlined and discussed—but not selected—notional, specific science goals, target(s), and/or payload(s) and will continue to do so.

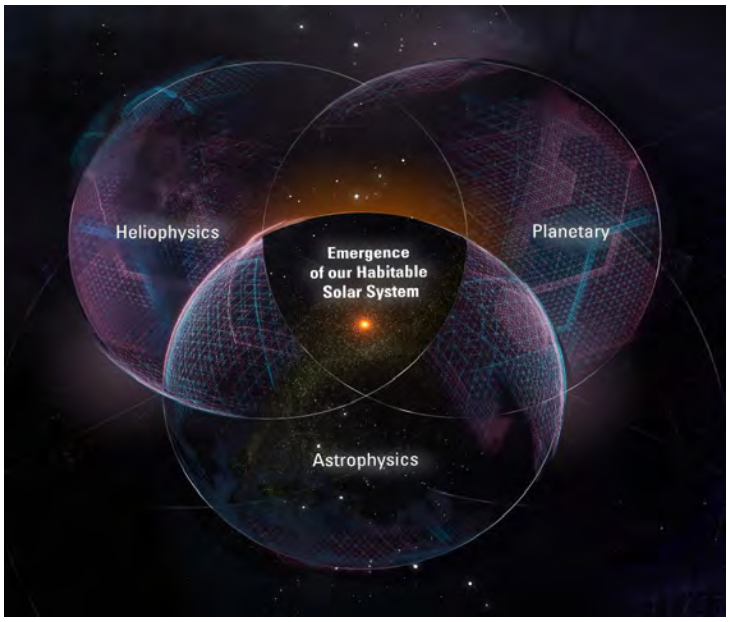

Figure 1-3. Science investigations in multiple disciplines will be enabled by an Interstellar Probe mission.

This report provides a summary of activities beginning in June 2018 and covering our 1st Interstellar Probe Exploration Workshop in October 2018 through the end of fiscal year (FY) 2019 (leading up to, but not including, the 2nd Interstellar Probe Exploration Workshop). Section 2 of this report provides the motivation and historical background for an interstellar probe. The first of our Interstellar Probe Exploration Workshops, which assessed the state of knowledge and gathered information on "next steps" in the domains of interest, was held 10–12 October 2018 at The Explorer's Club in New York City. The 2nd Interstellar Probe Exploration Workshop was held 16–18 October 2019 at the same inspiring venue. A third and fourth workshop are planned for 16–20 November 2020 (all virtual due to the COVID-19 pandemic) and November 2021 (exact dates to be determined). The 2018 workshop provided the information for the sections on science, instruments, and science operations concepts (Sections 2–4). In this report Sections 5 and 6 provide examples of science traceability matrices, and a baseline model payload is shown. Both of these sections will be expanded in greater detail after discussions with the science community at the 2020 workshop and documented in the 2021 and final reports. The major engineering trade study is taking place in 2020; however, initial engineering ground rules and an initial survey of launch options are provided in Section 7. One of the major challenges of an interstellar probe mission is to assure success for a mission requiring 50+ years. This challenge is composed of three elements: spacecraft reliability, sustaining the necessary ground segment infrastructure (including data management), and sustaining a team for such a long period. An initial analysis of some of these factors is given in

Section 8, but much of the spacecraft reliability and analysis of the ground segment will await the results of the engineering trade studies in 2020. Section 9, "Management," describes the tasks as they relate to the Statement of Work, how the study is organized, and the study schedule.

The work carried out in FY 2018 culminated in a broad outline of potential science goals that set the stage for developing the trade space that drove the engineering study in FY 2019 and will continue to do so in FY 2020. The science community will use the resulting documentation of the 2018 and 2019 workshops, as well as the engineering trades being performed in FY 2020, to develop a consensus on an appropriate set of options for a "pragmatic" interstellar probe mission.

1.1. Section 1 References

Draper, R., Purdy, W., Cunningham, G. (1975) *The Outer Planet Mariner Spacecraft.* In Conference on the Exploration of the Outer Planets, American Institute of Aeronautics and Astronautics, St. Louis, MO.

Kohlhase, C.E., Penzo, P.A. (1977) Voyager Mission Description. *Space Science Reviews* 21, 77. doi: 10.1007/bf00200846

NRC (2003) *The Sun to the Earth - and Beyond: A Decadal Research Strategy in Solar and Space Physics*. Washington, DC: The National Academies Press. https://doi.org/10.17226/10477

NRC (2013) *Solar and Space Physics: A Science for a Technological Society*. Washington, DC: The National Academies Press. https://doi.org/10.17226/13060

Simpson, J.A., Chamberlain, J.W., Kraushaar, W., et al. (1960) *Interim Report No. 3*. Washington, DC: Space Science Board.

2. Introduction

This effort, requested by the Heliophysics Division within NASA's Science Mission Directorate (SMD), focuses on a pragmatic interstellar probe with the ability to operate at 1000 au and a design lifetime of 50 years and assesses its technical readiness for a launch in 2030 to help support the next round of Decadal Surveys covering the time frame of 2023–2032. A large, international team of scientists is analyzing the compelling science goals and requirements, iterated with mission architectures led by a team at APL to find realistic solutions that close technically and scientifically.

2.1. What Is "Interstellar Probe"?

2.1.1. History

An interstellar probe mission to the local interstellar medium (LISM) has been discussed and studied since 1960 by multiple teams, including the U.S. Simpson Commission in 1960 (Simpson et al., 1960). The most recent studies have begun to recognize its critical importance for all three of NASA's main science directorates, fueled by the crossing of the heliopause by Voyager 1 and 2, the New Horizons flybys of Pluto and Arrokoth (Stern et al., 2019), and the surveys of cosmic microwave background radiation (CMBR) by the Cosmic Background Explorer (COBE) and the Wilkinson Microwave Anisotropy Probe (WMAP). Perhaps most importantly, with the burgeoning number of exoplanetary systems found by Kepler/K2/Transiting Exoplanet Survey Satellite (TESS), a growing need is emerging for putting the solar system, the relic debris disk, and the surrounding heliosphere into the context of other exoplanetary systems and astrospheres. For example, a heliosphere like our own has likely never been observed because of its relatively low UV intensity at those distances, which has prevented detailed understanding of the habitable properties of the astrosphere and its stellar wind. Also, despite the decisive importance of understanding the circumsolar debris disk, its large-scale distribution remains unconstrained, preventing local ground truth for understanding planetary system formation and evolution in other circumstellar debris disks.

The concept—and the reports generated by it over the years—is hardly new, and in the intervening past six decades human space exploration has progressed from orbiting an automated metal ball about our home world to humans on the Moon, to robotic flybys, orbiters, landers, and sample returns from throughout the solar system, and to five American space probes escaping the gravitational pull of the Sun, following the completion of their primary missions of planetary exploration.

While the latter have made (Pioneer 10 and 11), are making (Voyager 1 and 2), and will continue to make (New Horizons) new discoveries regarding the outer reaches of our heliosphere and the interstellar space outside, none was designed with such tasks as their *raison d'être*, but instead explored nearby galactic space following their completion of their primary missions of planetary exploration. All were designed, built, and flown as American missions by NASA.

As such, this effort takes a hard look at a subset of the science and tasks of many past studies, the most recent comprehensive one being that of the W. M. Keck Institute for Space Studies (KISS) in 2014–2015 (Stone et al., 2015).

It is important to note that new, enabling technologies for flight projects rarely, if ever, emerge in a timescale of less than a decade within NASA at the current budget levels to which NASA is subject for the foreseeable future. Estimating the cost of implementing such technologies is made even more uncertain, making upscope and descope options even more important, especially for a large, strategic mission (National Academies of Sciences et al., 2017), a categorization which will likely include this mission as well.

The five previously mentioned, solar-system-escaping missions all are enabled by a triad of technologies and their implementation. Improvements have been sought in each with substantial investments of both time and money, but the planned-for/hoped-for paradigm shifts in performance have remained, and continue to remain, elusive. These technologies are propulsion, power, and communication. Given the constraints of this study vis-à-vis a near-term implementation time frame, we, therefore, have ruled out the consideration of using nuclear electric propulsion (NEP), radioisotope electric propulsion (REP), photon-pushed sails (solar or laser-powered), nuclear thermal propulsion (NTP), and other exotic means of propulsion, which have been discussed previously in the context of interstellar and interstellar precursor missions (cf., e.g., Chew et al., 2001; Millis, 2010). Similarly, for power, we consider only radioisotope power systems (RPSs) and, of these, only General Purpose Heat Source (GPHS) Radioisotope Thermoelectric Generators (RTGs) and Multi-Mission Radioisotope Thermoelectric Generators (MMRTGs), both of which have application disadvantages but have been used on flight missions and are, in principle, available. Finally, for communication we consider Ka- and X-band radio systems; while these have their inherent limitations in bandwidth, the use of laser communications systems in deep space (beyond ~10 au) has yet to be demonstrated with the required pointing and timing accuracy required for multiple light-hour transmissions and data reception.

Returning to propulsion, solar electric propulsion (SEP), while proven, has limitations on its efficient use for an interstellar probe as it is best used inside of Jupiter's orbit. What we do investigate is the use of a large booster, which can accommodate multiple upper stages, usable either as part of the Earth-departure segment of the launch sequence or as high-thrust kick stages in deep space. While the latter is not typical and will require some engineering development, we judge it to be within the normal and "ordinary" engineering development required for any unique, scientific, deep-space mission. Although there are nominal commercial large rockets under development, e.g., the New Glenn (Blue), Big Falcon Rocket (BFR – SpaceX), we have baselined the Space Launch System (SLS) Block 1B Cargo for our point engineering studies due to the more readily available technical information and its currently planned (and apparently earlier) initial operation capability (IOC). Similarly, we have looked to operational upper stages, e.g., the Star series of Northrop Grumman, while also researching newer planned developments by other commercial vendors.

It is important to note that the study does not purport to center on "the one and only" interstellar probe but rather on this mission as a first step to more advanced missions and capabilities, such

as described most recently in the KISS study (Stone et al., 2015). In addition to promising historically groundbreaking discoveries, the Interstellar Probe necessitates a transformation in the programmatics needed to accommodate lifetime, reliability, and funding requirements for this new type of multigenerational, multidecade operational mission. Paving the way for longer journeys utilizing future propulsion technologies, such as those not invoked here, the Interstellar Probe is the first explicit step we take today on the much longer path to the stars.

This study is not—nor should it be—a replacement for a NASA Science Definition Team (SDT) or Science and Technology Definition Team (STDT). In the same vein as the KISS study (Stone et al., 2015), we reached out to a team of scientists from multiple disciplines, including heliophysics, astrophysics, planetary sciences, and exoplanet science, to assay the current state of the art and level of interest in such a mission. We also attempted to gauge the interest not only within the "traditional" Heliophysics Division of SMD but also within the Planetary and Astrophysics Divisions as well. This community input has been sought and assembled to date via special sessions of the 42nd Committee on Space Research (COSPAR) Scientific Assembly in Pasadena, California, in July 2018 and of the American Geophysical Union (AGU) meeting in Washington, D.C., in December 2017 and 2018, as well as by the 1st Interstellar Probe Exploration Workshop held in October 2018. In addition to adding to some of the thoughts already expressed at the KISS meetings, information was sought—and obtained—on the measurements, measurement techniques, and instrumentation which would be required to address the various science questions raised. Throughout this current study and others before, the primary science goal revolves around how the heliosphere interacts with the LISM. Secondary, or supporting, goals include opportunities for observing Kuiper Belt objects (KBOs), the circumsolar dust disk, the extragalactic background light (EBL), and the solar system from afar as an analogy to an exoplanetary system reflecting the rapidly expanding and evolving sphere of exoplanet research.

The approach has been, and continues to be, to provide a "menu" of scientific goals, questions, measurements, techniques, and instruments from which a credible and compelling mission could be assembled or a starting point for the same could be defined. The emphasis is on providing input which could be useful to a NASA-assembled SDT/STDT rather than on prejudging the choices they might make when "ordering" from such a "menu" (or deciding to look for another "restaurant" altogether).

To make definitive progress on the technical issues within the amounts of funding available, we adopted the very capable, and successful, New Horizons spacecraft as an initial "cut" at a dedicated interstellar probe. This versatile spacecraft has known lifetime, power, and instrument payload capabilities for operation in deep space and so makes for a good starting point in assessing mission capabilities for a variety of rocket boosters and staging considerations. With a launch mass of 478.3 kg (wet, i.e., fully fueled at launch), the mass is about twice that of Pioneer 10 and 11, about half that of Voyager 1 and 2, and also about halfway between that of Ulysses and Parker Solar Probe, all deep-space-flyby or solar-orbit missions.

To scope out mission possibilities under the ground rules noted, we considered three trajectory options. Planetary gravity assists have become the part of the *lingua franca* of solar system trajectory design. Complicated maneuvers involving multiple planets trade mission time against spacecraft mass and onboard propulsive capability. Escape velocity from the solar system using a large launch vehicle from the Earth is just possible today at C_3 ~153 km^2/s^2, for which the asymptotic speed would be approximately zero. It has been well known since the early 1960s (Minovitch et al., 1965) that an optimized gravity assist at Jupiter can provide a trajectory to the Sun, a fast trajectory from the Sun, or a significant plane change for a Sun-orbiting heliocentric trajectory. While multiple gravity assists at Jupiter as well as Saturn and/or Uranus and Neptune can, in principle, provide even faster escapes, there is a significant trade against the timing of the launch window, the Grand Tour opportunities of once every ~176 years being the case in point (Flandro, 1966).

An interstellar probe by definition needs to escape the solar system rapidly, and we have a goal of reaching an asymptotic flyout speed of 20 au/year (~95 km/s). All of the trajectories under consideration employ a Jupiter gravity assist. The window for optimal transfers to Jupiter are set by the Jupiter's synodic period of 398.88 days (~13 months), while the optimal orbit for targeting a given location on the celestial sphere by using a gravity assist occurs roughly every Jupiter revolution about the Sun, with a synodic period of 11.862 sidereal years (4,332.589 days). Hence, there are 10.862~11 optimal Jupiter transfers per revolution of Jupiter about the Sun. The optimally available "aim points" are tied to Jupiter's location and drift through heliolongitudes, but the pattern itself repeats, enabling an easy assessment of how the aim points vary with time.

We have considered three different trajectory options to balance a long flyout time with minimal time spent in the inner solar system prior to escape. That is, we consider only direct-to-Jupiter flight transfers. The first two trajectory options considered both use prograde gravity assists at Jupiter. In the first, all stages are expended in the launch sequence at the Earth, placing the probe into a very high (C_3 > 200 km^2/s^2), hyperbolic escape orbit to Jupiter. In the second option, at least one of the upper stages in the launch stack is "held back" for use in a prograde burn at Jupiter. The flyout energy is now less but must still be above ~100 km^2/s^2 in order to reach Jupiter directly. In addition, engineering modifications must be made as needed for the kick stage to survive the ~1 yearlong Jupiter cruise and work reliably.

The so-called "Oberth maneuver" (or "solar-Oberth maneuver"), first documented by Oberth in 1929 (Oberth, 1970), makes use of the fact that the energy gain in a propulsive maneuver can be extremely large when the burn is made deep in the gravity well of the Sun when the probe speed around the Sun is already very high (the Option 2 trajectory can be considered as a "Jupiter-Oberth" maneuver for the same reason. In order to perform such a burn at very close distances to the Sun to maximize their efficacy, the orbital speed of the Earth imparted to the probe at launch (~29.8 km/s) along with the associated angular momentum must be removed. This is such a large speed that the only way of doing this currently is to "rebound" from Jupiter by using a retrograde Jupiter gravity assist prior to the Oberth burn at the Sun. The required launch C_3s are ~110–120 km^2/s^2, depending upon the perihelion aim point. The complicating factor is the spacecraft and the kick stage must both be protected by a thermal shield up to, during, and after the burn

while the stack is close to the Sun. The closer the perihelion, the larger the potential boost for a given rocket stage and the larger (and hence more massive) the thermal shield—which drives the imparted speed change down. These trades drive families of configurations to an optimal closest approach to the Sun, and hence and optimal flyout speed, in a way that inherently ties together stage performance, mission design, and thermal shield design. While Option 3 provides the most apparent promise, it is also the most complex to analyze. An additional complication is that there is no way to actually run a full-up flight test without actually flying the mission.

To make a first cut at addressing these trades and what performance could be achieved by a near-term mission, we have examined 39 different flight configurations across these three mission options. This approach provides a first-order cut at disconnecting the mission performance from the payload and spacecraft configuration flown.

These ingredients, along with some initial thoughts about long-term (up to ~50-year) mission planning and functioning, have been presented to members of the study community via the meetings already mentioned as well as others, both domestic and international, both to socialize the concepts studied and to provide feedback useful for the next study phase.

2.1.2. Interstellar Probe Science Goals

As with its implementation, the science goals of an interstellar probe have undergone various formulation changes over the years. Initially focused on a variety of fields with measurements enabled by locations far from Earth (Despain et al., 1971; Ehricke, 1971; Parker, 1967), more realistic science goals were seen as building upon the then-upcoming Pioneer 10 and 11 missions (Dessler & Park, 1971). The first "integrated" set of goals came from the JPL Interstellar Precursor studies of the late 1970s (Jaffe et al., 1977) with extension to astrophysical goals as part of the thousand astronomical units (TAU) studies of the 1980s (Nock, 1987). By the time of the Holzer report (Holzer et al., 1990), the science goals stabilized and have endured since, while exact details and formulations have continued to vary (Stone et al., 2015). As with all missions, at some level the exact goals that set the basis for the Level 1 requirements of a confirmed mission tie to the particularities of the instrumentation, mission architecture, and mission trajectory. Against this backdrop, one can nonetheless capture the essential, and generally agreed upon, science goals for an interstellar probe mission.[1]

2.1.2.1. Primary Goal: Understand the Heliosphere as a Habitable Astrosphere

The solar system is encased in a magnetic bubble spanned by the expanding solar wind. As it plows through galactic space, the properties of the solar wind and the interstellar environment shape

[1] It is worth noting that the earliest serious studies of interstellar travel led to the early conclusion that, given actual travel between the stars required greatly advanced technology (if it was even possible at all), physical travel would be so difficult that only radio communication with other intelligent lifeforms in the galaxy would be possible (Sagan, 1963; von Hoerner, 1962). This led to the early investigations loosely captured as communication with extraterrestrial intelligence (CETI), since rebranded as the search for extraterrestrial intelligence (SETI). While the notion of actually travelling to other star systems continues to surface (e.g., Tollefson, 2016; Weinstein-Weiss et al., 2018), even the proponents agree that this is an activity which will not be possible for decades, and so it is well outside the scope of the effort under consideration here.

this "heliosphere," which is the astrosphere of our Sun. The complex processes at its interface shield the solar system from the very high energy cosmic rays that otherwise would have bombarded and affected the chemical evolution of the planetary atmospheres. Despite its crucial importance for understanding the physics and habitability of our "astrosphere" and others out there, its global structure and astrophysical processes continue to be mysteries that can be solved only by flying a probe with comprehensive plasma and fields measurements through the interface region and imaging the heliosphere from the outside in UV and energetic neutral atoms (ENAs).

2.1.2.2. Supporting Goal: Understand the Origin and Evolution of Planetary Systems

The solar system was formed from a collapsing nebula of dust and gas, where gravitational accretion and collisions formed rocky asteroids, icy comets, and KBOs in the protoplanetary disk (PPD), then planets and moons as most these objects merged and accreted further. The relic planetesimals of this era of formation in the first 100 Myr, i.e., the small bodies that did not become planets and moons, were relegated to the asteroid and Kuiper belts and the Oort cloud. Further sculpting and diminution of these relic populations occurred as the planets migrated and scattered most of the remnants to produce the belt substructures we see today. During all these processes—planetary formation, planetesimal scattering, relic body evolution—secondary dust from the bodies is created due to impacts, grinding, and sputtering. Much of this dust is emitted into circumsolar orbits, creating and supplying the solar system's debris disk. This disk extends from inside the orbit of Mercury (the so-called "F-ring") to the heart of the Kuiper Belt (as recently detected by New Horizons (Poppe et al., 2019)). Similar debris disks have been observed around thousands of other stars and similarly hold immense information on how exoplanetary systems form and evolve. However, almost nothing is known about the large-scale structure of our own circumsolar debris disk since we live inside it and foreground emissions obscure its overall structure. Therefore, there is no local ground truth for the critical interpretation of other circumstellar disks. By implementing a relatively simple low-mass and low-power dust detector and infrared camera instrument suite onboard Interstellar Probe, the 3D structure of the debris disk can be captured and the bottleneck in our understanding planetary system formation and evolution can be removed.

The recent New Horizons flyby of the Pluto and MU69 KBO systems has returned an incredible wealth of knowledge about these objects and revolutionized our understanding of the Kuiper Belt. Just as we have built up our understanding of the diversity of objects in the main asteroid belt by repeated close flybys of individual objects by spacecraft on their way to outer solar system destinations (e.g., Galileo/Gaspra, ROSETTA/Steins), an interstellar probe can allow us to have the third (and potentially fourth and fifth) flybys of a KBO ever accomplished. Plotting an interstellar probe trajectory to allow flyby observations of several key KBOs, especially types of KBOs not yet encountered (ones in the 100-km-radius size range and giant non-resonant KBOs), would greatly expand our knowledge of their properties and provide direct insight in to the detailed formation processes of the Kuiper Belt itself.

2.1.2.3. Supporting Goal: Explore the Universe Beyond the Circumsolar Dust Cloud

Just as the CMBR contains huge amounts of diagnostic information that has allowed us to revolutionize our understanding of the Big Bang and the era of our universe's formation, the cosmic

infrared background radiation (CIBR) contains huge amounts of diagnostic information about the era of galaxy formation. However, the light from the nearby relic debris disk dust, (a.k.a. the "zodiacal" cloud or "Zody") not only obscures its larger structure, but also completely overwhelms the remnant light in the diffuse cosmic backgrounds produced in the time when galaxies first formed. This may be the biggest stumbling block in experimental astrophysics today since it leaves theories of galaxy and stellar formation without any constraints. An interstellar probe carrying a simple infrared mapping spectrometer (the same relatively simple infrared detector used for determining solar system's debris disk structure) to outside the zodiacal cloud (i.e., well outside its relic planetesimal source regions in the Main Asteroid Belt and the Kuiper Belt) would thus eliminate the local foreground Zody emissions and help unveil the early universe of the first stars and galaxies by making the first truly unobscured CIBR measurements.

2.2. Scope of this Study

This study is built upon certain guiding principles: launch in the decade 2023–2033, return valuable science to Heliophysics Division and also to the Planetary Science and Astrophysics Divisions of the NASA SMD, and maintain a programmatic and mission architecture that controls cost and cost risk. These principles led to decisions made by the study leadership to ensure that NASA's investment would be in the mission itself and not into speculative technologies with uncertain maturation dates. A small spacecraft, built upon conventional architecture and with conventional technology, can be readied for launch in the next decade and return the promised science value without incurring the cost overruns that have plagued recent missions (Chaplain, 2016, 2017, 2018, 2019; National Academies of Sciences et al., 2017). These decisions made by the study team defined the scope of the study in the following ways:

- Launch vehicle: NASA's SLS is the baseline launch vehicle for Interstellar Probe. The study team worked closely with the SLS payload accommodation team to determine SLS's capabilities for high-escape-velocity (characteristic energy, or "C_3") configurations. SLS has enormous capacity for lift in its first and second stages. This study delves into SLS's high C_3 capability by adding existing systems as upper stages in the analysis (Ralph L. McNutt et al., 2019).
- Power system: This study considers the GPHS-RTG and MMRTG as power sources for the mission. The RPSs used over the past few decades, from the Galileo mission to Jupiter to the Mars Curiosity rover, have enabled significant advances in space science and exploration. The current supply of 238-Pu and the maturity of existing RPS heat-to-electricity conversion technologies make them suitable candidates for the Interstellar Probe spacecraft power supply (R. L. McNutt, Jr. et al., 2015). Although NASA is making investments in new technologies for power conversion for RPSs (Zakrajsek, 2019), none of these are expected to be mature enough in the Interstellar Probe launch window to be acceptable for a large strategic mission with a multidecade mission time line.
- Payload mass: The payload mass was fixed at 60 kg. The history of the Parker Solar Probe notional payload mass through decades of mission studies (Anderson et al., 1976; APL, 2008; Averell et al., 1965; Axford et al., 1995; De Moraes & Gage, 1965; Feldman et al., 1989; Fox et al., 2015; Gloecker et al., 1999; Gloeckler et al., 1999a; Gloeckler et al., 1999b; Hall et al., 1962; Haviland, 1958; Lundholm et al., 1964; Martin, 1965; McComas et al.,

2005; McComas et al., 2008; R. L. McNutt et al., 1995; Möbius et al., 2000; Neugebauer & Davies, 1978; J. E. Randolph, 1996; J. R. Randolph, 1978; Staehle et al., 1999), resulted in a wide-ranging set of estimated mission costs. This tight tracking and control of mass was crucial to programmatic success. This study hopes to employ the same discipline as the contents of the payload evolve.

- Spacecraft model: New Horizons was used as a model for the spacecraft for this study (Fountain et al., 2008). The power level, launch mass, and payload accommodation allow the parameters above to be met while promising a realizable mission. The success of New Horizons through both the Pluto encounter (Stern et al., 2015)and the recent KBO flyby (Stern et al., 2019) show that significant science can be done from a platform at that size.

Each of these defining points must be revisited as the concept of a pragmatic interstellar probe mission matures. Refinement of the science return, the instruments comprising the model payload, the spacecraft system and engineering, the trajectory analysis, and the mission concept of operations will reduce uncertainties and the resultant programmatic risk.

The scope of this study includes the following:

- Analysis of the SLS capability to achieve the high C_3 required for Interstellar Probe, including the addition of upper stages
- Definition of a multidisciplinary science return, including identification of current-design payload components that address the science goals
- Trajectory analyses to determine a path to achieving 1000 au over a 50-year mission with conventional propulsion technology, including the option of a solar-Oberth maneuver
- Analyses to determine a materials-based limit for the perihelion distance for a solar-Oberth maneuver
- Design studies to bound the size and mass of a shield to protect the system during a possible close approach to the Sun, including multiple existing kick-motors, across a range of perihelion distances
- Design study to determine the launch mass of the various configurations considered above

2.3. Section 2 References

Anderson, J.D., Colombo, G., Friedman, L.D., Lau, E.L. (1976, 17-20 September) *An Arrow to the Sun.* In Atti dei Convegni Lincei, Dott. G. Bardi, Tipografo dell'Accademia Nazionale dei Lincei, Pavia.

APL (2008) *Solar Probe+ Mission Engineering Study Report*. Laurel, MD: Johns Hopkins University Applied Physics Laboratory.

Averell, J., Hoyer, S., Lundholm, J.G., Prohaska, E.S. (1965) A Close-Approach Solar Probe Design Feasibility and Mission Study. *Journal of Spacecraft and Rockets* 2(4), 550-557. doi: 10.2514/3.28227

Axford, W.I., Feldman, W., Forman, M.A., Habbal, S.R., Ling, J.C., Moses, S., Title, A., Woo, R., Young, D.T. (1995) *Close Encounter with the Sun - Report of the Minimum Solar Mission Science Definition Team, Scientific rationale and mission concept*. Pasadena, CA: Jet Propulsion Laboratory.

Chaplain, C. (2016) *NASA: Assessment of Major Projects*. Washington, DC: United States Government Accountability Office.

Chaplain, C. (2017) *NASA: Assessments of Major Projects*. Washington, D.C.: United States Government Accountability Office.

Chaplain, C. (2018) *NASA: Assessments of Major Projects*. Washngton, DC: United States Government Accountability Office.

Chaplain, C. (2019) *NASA: Assessment of Major Projects*. Washington, DC: United States Government Accountability Office.

Chew, G., Doyle, M., Stancati, M. (2001) *Interstellar Spaceflight Primer*. Schaumburg, IL: Science Applications International Corporation.

De Moraes, C., Gage, D. (1965) *Mission Objectives and Design Considerations for a Scientific Solar Probe* In Unmanned Spacecraft Meeting 1965, American Institute of Aeronautics and Astronautics, Los Angeles, CA.

Despain, L.G., Hennes, J.P., Archer, J.L. (1971, 28-30 June) *Scientific Goals of Missions Beyond the Solar System.* In 17th Annual Meeting American Astronautical Society, Seattle, WA.

Dessler, A.J., Park, R.A. (1971, 28-30 June) *The First Step Beyond the Solar System.* In 17th Annual Meeting American Astronautical Society, Seattle, WA.

Ehricke, K.A. (1971, 28-30 June) *The Ultraplanetary Probe.* In 17th Annual Meeting American Astronautical Society, Seattle, WA.

Feldman, W., Mellott, M., Tsurutani, B., et al. (1989) *Solar Probe Scientific Rationale and Mission Concept: A Report of the 1989 Solar Probe Science Study Team* (JPL D-6797). Pasadena, CA: Jet Propulsion Laboratory.

Flandro, G.A. (1966) Fast Reconaissance Missions to the Outer Solar System Utilizing Energy Derived from the Gravitational Field of Jupiter. *Astron. Acta* 12(4), 329-337.

Fountain, G.H., Kusnierkiewicz, D.Y., Hersman, C.B., et al. (2008) The New Horizons Spacecraft. *Space Science Reviews* 140, 23-47. Retrieved from http://adsabs.harvard.edu/abs/2008SSRv..140...23F

Fox, N.J., Velli, M.C., Bale, S.D., et al. (2015) The Solar Probe Plus Mission: Humanity's First Visit to Our Star. *Space Science Reviews*, 1-42. doi: 10.1007/s11214-015-0211-6

Gloecker, G., Feldman, W., Habbal, S.R., et al. (1999) *Solar Probe: First Mission to the Nearest Star*. Laurel, MD: The Johns Hopkins University Applied Physics Laboratory.

Gloeckler, G., Suess, S., Habbal, S.R., McNutt, R.L., Jr., Randolph, J.E., Title, A.M., Tsurutani, B.T. (1999a) Solar Probe: A Mission to the Sun and Inner Core of the Heliosphere. *Geophyical Monograpgh* 109, 237-246.

Gloeckler, G., Suess, S.T., Habbal, S.R., McNutt, R.L., Randolph, J.E., Title, A.M., Tsurutani, B.T. (1999b). Solar Probe: A Mission to the Sun and the Inner Core of the Heliosphere. In Burch, J.L., Carovillano, R.L., Antiochos, S.K. (Eds.), *Sun-Earth Plasma Connections* (Vol. 109, pp. 237-246).

Hall, C.F., Nothwang, G.J., Hornby, H. (1962) Solar Probes - A Feasibility Study. *Aeorspace Engineering*, 22-30.

Haviland, R.P. (1958, 25-30 August) *Considerations of the Solar Probe.* In IXth International Astronautical Federation Congress, Springer-Verlag, Amsterdam.

Holzer, T.E., Mewaldt, R.A., Neugebauer, M. (1990) *The Interstellar Probe: Scientific Objectives for a Frontier Mission to the Heliospheric Boundary and Interstellar Space*. Ballston, VA: NASA.

Jaffe, L.D., Ivie, C.V., Lewis, J.C., Lipes, R., Norton, H.N., Stearns, J.W., Stimpson, L.D., Weissman, P. (1977) *An Interstellar Precursor Mission*. Pasadena, CA: Jet Propulsion Laboratory.

Lundholm, J., J. G., Prohaska, E.S., Hoyer, S., Averell, J. (1964) *A Close Approach Solar Probe Design Feasibility and Mission Study*. Paper presented at the 1st Annual Meeting, Washington, DC. http://dx.doi.org/10.2514/6.1964-496.

Martin, J.P. (1965) *Scientific Objectives and Instrumentation for a Solar Probe*. Paper presented at the Unmanned Exploration of the Solar System, Denver, CO.

McComas, D.J., Velli, M., Lewis, W.S., et al. (2005) *Solar Probe: Humanity's First Visit to a Star.* In Proceedings of the Conference Solar Wind 11 - SOHO 16, ESA,, Whistler, Canada.

McComas, D.J., Acton, L.W., Balat-Pichelin, M., et al. (2008) *Solar Probe Plus: Report of the Science and Technology Definition Team*. Greenbelt, MD: NASA.

McNutt, R.L., Reynolds, E.L., McAdams, J.V., Bokulic, R.S., Bhatnagar, V., Williams, B.D., Willey, C.E., Myers, R., Gefert, L.P. (1995) Mission to the Sun - The Solar Pioneer. *Anticipating a Solar Probe* 17(3), 21-30.

McNutt, R.L., Wimmer-Schweingruber, R.F., Gruntman, M., et al. (2019) Near-Term Interstellar Probe: First Step. *Acta Astronautica* 162, 284-299. doi: https://doi.org/10.1016/j.actaastro.2019.06.013

McNutt, R.L., Jr., Aleman, S.M., Amato, M.J., et al. (2015) *Nuclear Power Assessment Study - Final Report*. Laurel, MD: NASA Glenn Research Center.

Millis, M.G. (2010) *Progress in Revolutionary Propulsion Physics.* In 61st International Astronautical Congress, International Astronautical Federation, Prague, Czech Republic.

Minovitch, M.A., Aeronautics, U.S.N., Administration, S. (1965) *Utilizing Large Planetary Perturbations for the Design of Deep-space, Solar-probe, and Out-of-ecliptic Trajectories*: Jet Propulsion Laboratory, California Institute of Technology. Retrieved from https://books.google.com/books?id=YnowuQAACAAJ

Möbius, E., Gloeckler, G., Goldstein, B., Habbal, S.R., McNutt, R.L., Jr., Randolph, J.E., Title, A., Tsurutani, B. (2000) Here Comes Solar Probe! *Advances in Space Research* 25(9), 1961-1964.

National Academies of Sciences, Engineering, and Medicine (2017) *Powering Science: NASA's Large Strategic Science Missions*. Washington, DC: The National Academies Press. doi:10.17226/24857

Neugebauer, M., Davies, R.W. (1978) *A Close-Up of the Sun* (JPL Publication 78-70). Pasadena, CA: Jet Propulsion Laboratory.

Nock, K. (1987). TAU - A Mission to a Thousand Astronomical Units. In *19th International Electric Propulsion Conference*: American Institute of Aeronautics and Astronautics.

Oberth, H. (1970) *Ways to Spaceflight* (Agence Tunisienne de Public-Relations, T., Tunisia, 1970, Trans.): National Aeronautics and Space Administration. Retrieved from https://ia600503.us.archive.org/21/items/nasa_techdoc_19720008133/19720008133.pdf

Parker, E.N. (1967) The Dynamical State of the Interstellar Gas and Field. III. Turbulence and enhanced diffusion. *The Astrophysical Journal* 149, 535.

Poppe, A.R., Lisse, C.M., Piquette, M., Zemcov, M., Horányi, M., James, D., Szalay, J.R., Bernardoni, E., Stern, S.A. (2019) Constraining the Solar System's Debris Disk with In Situ New Horizons Measurements from the Edgeworth-Kuiper Belt. *The Astrophysical Journal* 881. doi: 10.3847/2041-8213/ab322a

Randolph, J.E. (1996) NASA Solar Probe Mission and System Concepts. *Advances in Space Research* 17(3), 3-12. doi: 10.1016/0273-1177(95)00491-V

Randolph, J.R. (1978) *Solar Probe Study*. Paper presented at the A close-up of the Sun, Jet Propulsion Laboratory.

Sagan, C. (1963) Direct Contact Among Galactic Civilizations by Relativistic Interstellar Spaceflight. *Planetary and Space Science* 11, 485-498.

Simpson, J.A., Chamberlain, J.W., Kraushaar, W., et al. (1960) *Interim Report No. 3*. Washington, DC: Space Science Board.

Staehle, R.L., Brewster, S.C., Carraway, J.B., et al. (1999) Ice & Fire: Missions to the Most Difficult Solar System Destinations… on a Budget. *Acta Astronautica* 45(4), 423-439. doi: 10.1016/S0094-5765(99)00162-9

Stern, S.A., Bagenal, F., Ennico, K., et al. (2015) The Pluto System: Initial Results from Its Exploration by New Horizons. *Science* 350(6258), 292. doi: 10.1126/science.aad1815

Stern, S.A., Weaver, H.A., Spencer, J.R., et al. (2019) Initial Results from the New Horizons Exploration of 2014 MU_{69}, a Small Kuiper Belt Object. *Science* 364(6441), eaaw9771. doi: 10.1126/science.aaw9771

Stone, E., Alkalai, L., Friedman, L., et al. (2015) *Science and Enabling Technologies for the Exploration of the Interstellar Medium*. Pasadena, CA: Keck Institute for Space Studies.

Tollefson, J. (2016) Billionaire backs plan to send pint-sized starships beyond the Solar System. *Nature* 2019(May). doi: 10.1038/nature.2016.19750

von Hoerner, S. (1962) The General Limits of Space Travel: We May Never Visit Our Neighbors in Space, But We Should Start Listening and Talking to Them. *Science* 137(3523), 18-23. doi: 10.1126/science.137.3523.18

Weinstein-Weiss, S., Rayman, M., Turyshev, S., et al. (2018) A Science-Driven Mission Concept to an Exoplanet. *Journal of the British Interplanetary Society* 71, 140-150.

Zakrajsek, J.F. (2019) Implementation of Cross-Agency Nuclear Applications. *Nuclear and Emerging Technologies for Space (NETS) 2019*. Retrieved from https://ntrs.nasa.gov/citations/20190002791

3. The Compelling Science Cases

Our star is one of a hundred billion stars in the galaxy that plows through the interstellar gas—plasma and dust made up of the material from supernova remnants. With its dynamic solar wind, the Sun carves out the enormous habitable magnetic bubble harboring the solar system we live in. The unique interaction responsible for upholding the boundary of the heliosphere, also applicable to the vast range of other astrospheres in our galaxy, represents one of the most outstanding problems in space physics today. Beyond the heliosphere, the unexplored local interstellar medium (LISM) presents a completely new territory that is decisive for the heliospheric interaction and holds the key to understanding our galactic home.

An interstellar probe traveling far beyond the heliopause (HP) would represent humanity's first deliberate step into the galaxy and would perhaps be the boldest move in space exploration since humans landed on the moon. The realization that Earth-like planets may exist elsewhere fuels our drive to understand, now more than ever, the origin of our habitable solar system, harbored by the heliosphere plowing through interstellar space.

Voyager 1 and 2 have uncovered mysteries at the heliospheric boundary that are forcing a complete reassessment of the fundamental plasma physics in this astrophysical regime. From deep inside the heliosphere, imaging from the IBEX and Cassini missions has revealed completely unexpected features that remain unexplained. New Horizons has explored the farthest object ever visited by a robotic spacecraft, and this object is only the tip of the iceberg of Kuiper Belt Objects (KBOs) and dwarf planets that hold the key to understanding planetary system formation. Although the large-scale structure of our circumsolar debris disk remains hidden from vantage points inside the zodiacal cloud, the Atacama Large Millimeter/submillimeter Array (ALMA) has recently revealed surprisingly young and structured circumstellar disks, implying that theories of planetary system formation will have to be revised. Also, the diffuse extragalactic background light accumulated from all the red-shifted light of early galaxies holds the key to understanding the formation of these galaxies shortly after the Big Bang, but is again obscured by the zodiacal cloud.

Below is a discussion of the science goals for and the example questions pertaining to an interstellar probe across heliophysics, planetary physics, and astrophysics that builds on current results from missions, previous studies, and a series of community workshops and meetings, including the Committee on Space Research (COSPAR), the American Geophysical Union Fall Meeting, and the Interstellar Probe Workshop in New York City in October 2018. Measurement approaches and the current state of instrumentation that could meet the science requirements are summarized at the end of the section to demonstrate that closure could be achieved with today's instrument technology.

3.1. Primary Science Goals: Understand Our Heliosphere as a Habitable Astrosphere and Its Place in the Galaxy

3.1.1. Outstanding Science Questions

3.1.1.1. What Is the Global Nature of the Heliosphere?

Despite decades of studies, we still do not understand the global heliosphere, the space in our galaxy carved by the Sun and its expanding solar wind. The heliosphere presents a unique opportunity to study in detail the only accessible (for now) example of a fundamental and common astrophysical phenomenon—formation of an astrosphere around a star (Figure 3-1). Current in situ and remote-sensing observations continue to generate more puzzles challenging our view on the heliosphere. The structure of the heliosphere results from the complex interaction of space plasmas of different origins—solar and galactic. This interaction involves the solar wind plasma and solar magnetic field, interstellar medium (ISM) plasma and magnetic field, ISM neutral particles, solar energetic particles, and galactic cosmic rays (V. V. Izmodenov, 2009; M. Opher, 2016; Pogorelov, Fichtner, et al., 2017; Zank, 1999). Incoming interstellar hydrogen atoms charge exchange with solar plasma protons in the heliosphere. This key process determines the size of the

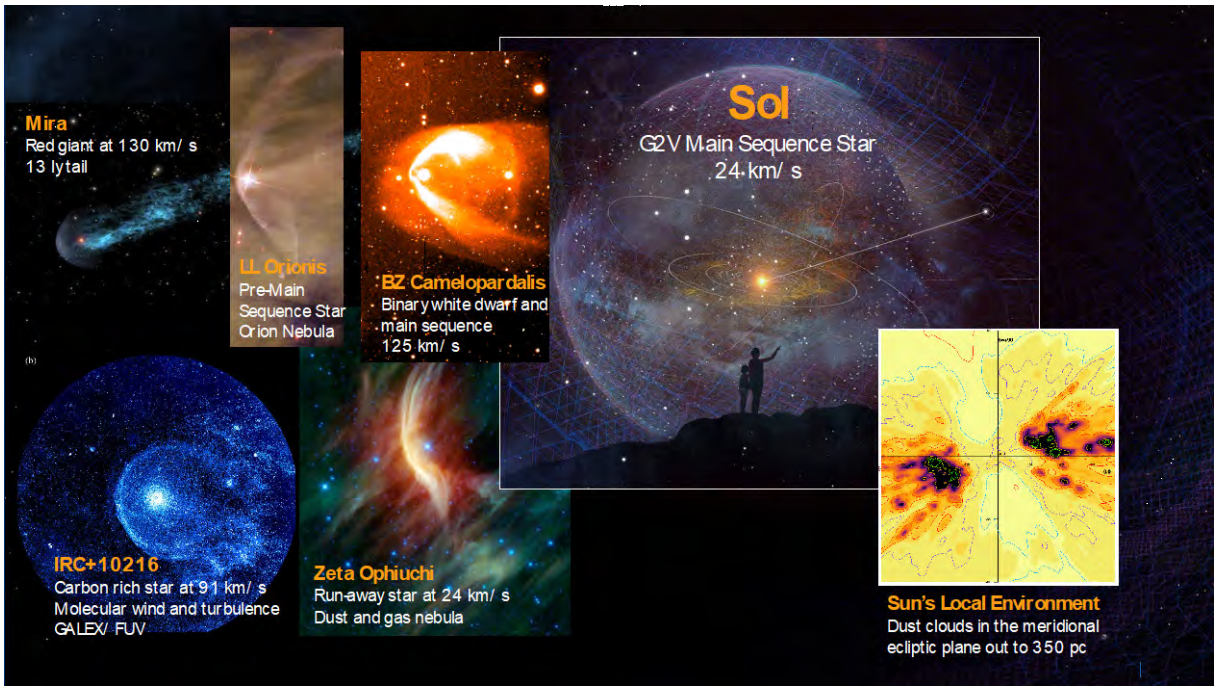

Figure 3-1. As our type-G2V star plows through the galactic interstellar medium, it forms the habitable astrosphere harboring the entire solar system we live in. Of all other astrospheres, one of our habitable type has never been observed, and yet we are only at the very beginning of uncovering our own. An interstellar probe through the heliospheric boundary into the LISM would enable us to capture its global nature and would represent humanity's first step into the galaxy, where unpredictable discoveries await. Images courtesy of NASA, except "Sun's Local Environment" (Rosine Lallement, 2020).

heliosphere and solar wind properties at large distances from the Sun. Ions born in a charge-exchange process are picked up by the solar wind and become energized. Energetic particles in the outer heliosphere dominate the pressure balance. This in particular creates a unique plasma regime in the heliosheath, the outermost layer of the heliosphere, which is filled with energetic particles. The solar magnetic field pervading the heliosphere was found to play an important role in the 3D shape of the heliosphere. A predominantly azimuthal magnetic field leads to collimation of the solar wind flow in the heliosheath toward the solar rotation axis (V. V. Izmodenov & Alexashov, 2015) and can produce a "croissant"-like shape of the heliosphere (M. Opher et al., 2015). Other studies suggest that magnetic reconnection of the sector solar magnetic field can result in a complex heliosheath structure and allow mixing of interstellar and solar matter (Swisdak et al., 2013). Solar activity changing with the solar cycle creates temporal variations in the heliosphere. Varying solar wind dynamic pressure causes motions of the heliosphere boundaries, creating a "breathing" heliosphere (V. Izmodenov et al., 2005; V. V. Izmodenov et al., 2008; Pogorelov et al., 2009; Provornikova et al., 2014; H. Washimi et al., 2011).

From outside, the heliosphere shape is affected by the interstellar magnetic field (ISMF) (B-field). Its direction and magnitude far away from the heliosphere (presumably >500 astronomical units [au]) are poorly constrained. The only existing estimates are from extrapolation of in situ Voyager measurements of B-field just outside the heliosphere (within few tens of astronomical units) or from remote-sensing energetic neutral atom (ENA) and Lyman-alpha observations. Voyager 1 entered the ISM in August 2012 and has provided the first direct measurements of the LISM B-field within ~25 au from the heliosphere boundary. Voyager 1 observed draped ISM B-field with the average magnitude <B> ~ (0.48 ± 0.04) nT (Burlaga & Ness, 2016), which is significantly stronger than the magnetic field in the heliosheath of ~0.1 nT. Voyager 2 joined Voyager 1 on its interstellar journey in November 2018 and observed B-magnitude <B> of ~0.7 nT. The fact that both Voyager spacecraft show no change in B-direction in the ISM compared to B-field inside the heliosphere was completely unexpected. The direction remained dominantly azimuthal after HP crossing (Burlaga, Ness & Stone, 2013), while the ISM field is thought to be inclined to azimuthal direction. The magnitude of the ISM B-field inferred from IBEX ENA data is ~0.25–0.3 nT (Heerikhuisen et al., 2014). Different magnetic field magnitudes from in situ and remote observations suggest that there may be variations of B-field in the ISM due to the presence of the heliosphere. Among the top scientific objectives of the Interstellar Probe is to characterize the complex interactions of the plasma, magnetic field, and neutral interstellar gas taking place from ~30 au (the distant supersonic solar wind) through the interaction region out to the pristine ISM. Voyager's in situ measurements of the magnetic field and plasma waves, as well as its observations of charged particles (suprathermal tails, anomalous cosmic rays [ACRs], and galactic cosmic rays [GCRs]), provided a glimpse of these phenomena (Burlaga, Ness & Stone, 2013; Krimigis et al., 2013; E. C. Stone et al., 2013).

Although it is well understood now that pickup ions (PUIs) are one of the most important components in the outer heliosphere, their role in the solar wind heating and energy partition at the termination shock (TS) and transient shocks is hotly debated. An additional open question is the sources of "inner-source" PUIs throughout the solar wind and the mechanisms of their origin. The Solar Wind

Around Pluto (SWAP) instrument on New Horizons made observations of the suprathermal PUIs in the outer heliosphere beyond Jupiter's orbit for the first time. PUIs dominate the thermal solar wind, with PUI pressure typically being larger than the thermal solar wind and magnetic pressure (D. J. McComas et al., 2017). PUIs strongly mediate the structure of shocks in the outer heliosphere (Mostafavi et al., 2017, 2018). Even though PUIs are only a few percent of the total proton density at a shock, they contain most of the internal particle pressure (Zirnstein, McComas, et al., 2018). Although New Horizons measures PUIs, the spacecraft likely will lose its power before reaching the heliosheath, where PUIs play a dominant role and were not measured by Voyager 1 and 2. Global modeling of the heliosphere interaction with the ISM with kinetic treatment of PUIs (Malama et al., 2006) showed that in the presence of PUIs, the heliosheath becomes thinner, in agreement with Voyager observations. A recent study by Merav Opher et al. (2018) suggests that PUIs play a critical role in the energy flow in the outer heliosphere, deflating the heliosphere and producing a smaller and rounder shape. Determining relative pressures of particles and fields (thermal solar wind, thermal interstellar plasma, local and transmitted PUIs and the magnetic field) with comprehensive measurements throughout the heliosphere boundary regions will aid in understanding the key processes determining this region.

Since early hydrodynamic models, the heliosphere was viewed having a comet-like shape (Baranov et al., 1970; Baranov & Malama, 1993). Modern kinetic-magnetohydrodynamic (MHD) models show a similar type of heliosphere shape, with the tail extending to thousands of astronomical units (V. V. Izmodenov & Alexashov, 2015; Pogorelov, Fichtner, et al., 2017) (Figure 3-2, left and right panel). However, another scenario was suggested by M. Opher et al. (2015); Merav Opher et al. (2018), where the heliosphere has a croissant-like shape with two jets of the solar wind confined by the solar magnetic field (Figure 3-2, center panel). ENA imaging on the Cassini/INCA and IBEX missions points to two different shapes of the heliosphere (Figure 3-3). INCA observations of high-energy ENAs in 10–45 keV indicates that the heliosphere has a quasi-spherical shape with no

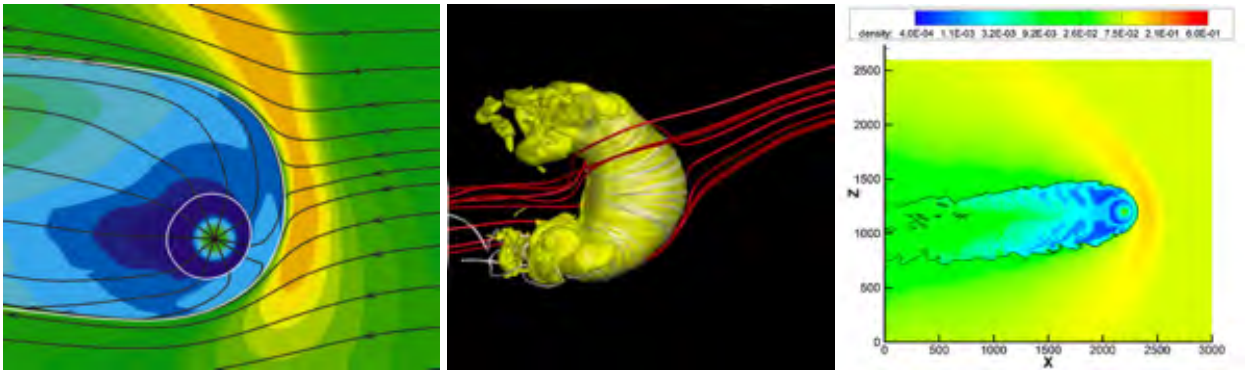

Figure 3-2. The global physical nature of the heliosphere eludes our understanding and requires new physics to be incorporated in models. (Left) A 3D kinetic-MHD model by the Moscow group showing the heliosphere with the tail (reproduced from V. V. Izmodenov and Alexashov (2015) with permission; © AAS). (Center) "Croissant"-like heliosphere with two jets (reproduced from M. Opher et al. (2015) with the permission of AIP Publishing). (Right) A 3D global model with solar cycle variations showing the heliosphere with the tail (reprinted from Pogorelov, Fichtner, et al. (2017) with permission; © 2017 Springer).

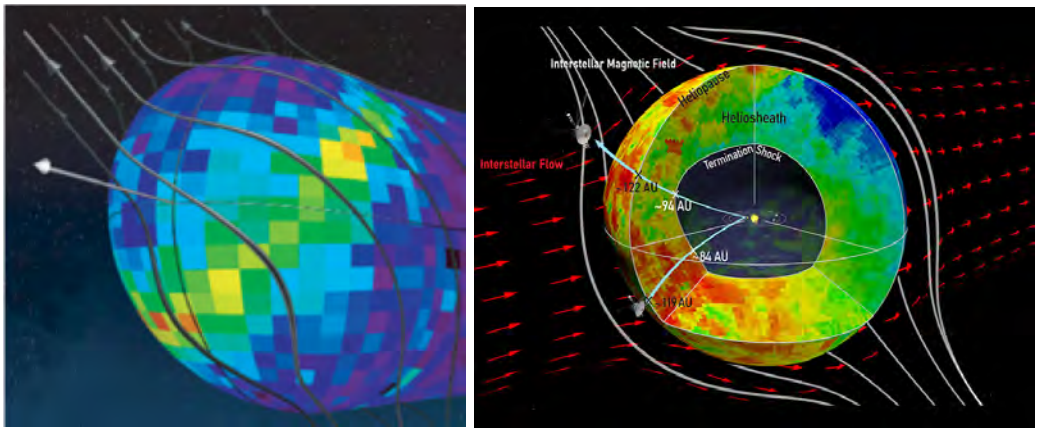

Figure 3-3. Remote ENA observations from inside the heliosphere by IBEX (left) (from D. J. McComas, Allegrini, Bochsler, Bzowski, Christian, et al. (2009); reprinted with permission from AAAS) and Cassini (right) (reprinted from Dialynas et al. (2017) with permission; © 2017 Springer Nature Limited) yield different global pictures. IMAP will close the gap on this inconsistent understanding with improved instrumentation (D. J. McComas et al., 2018). The decisive observations will be made by the Interstellar Probe traversing the interaction boundary into the LISM, where ENA images will provide the first external view of our own habitable astrosphere.

tail (Dialynas et al., 2017). IBEX ENA observations show a signal from the downwind direction (opposite to the heliosphere "nose") persistent over a solar cycle. This signal was interpreted as coming from an extended heliospheric tail (Schwadron & Bzowski, 2018). Different models and observations point to different hypotheses about the shape of the heliosphere. The community is in need of new dedicated measurements to understand the physical nature of the interaction between the Sun and the LISM and to resolve these important problems.

It has been established that the interface at the heliosphere edge consists of the TS, where the solar wind slows down, and the HP, the boundary separating hot solar wind and cold interstellar plasma. The TS location was predicted to be ~90 au (Baranov & Malama, 1993) a decade before Voyager 1 and 2 crossed the TS at 94 au (Voyager 1; December 2004) and 84 au (Voyager 2; August 2007). Voyager discovered that across the TS, 80% of the solar wind kinetic energy upstream was transferred into the suprathermal component in the heliosheath, the PUIs (John D. Richardson et al., 2008). Heliosheath thermal plasma turned out to be much cooler (by an order of magnitude) than expected. The heliosheath is dominated energetically by PUIs. Voyager 1 and 2 were not capable of measuring PUIs, leaving a gap in particle measurements with suprathermal energies between ~1 keV (thermal plasma) and 40 keV. The TS is the largest shock in the heliosphere and was expected to play a major role in acceleration of ACRs. However, Voyager presented evidence that ACR intensities continued to increase as the spacecraft traveled farther into the heliosheath (Figure 3-4) (Cummings et al., 2009; Decker et al., 2008). The role of the TS and heliosheath in ACR acceleration and how thermal plasma, PUIs, ACRs, and waves affect the TS structure are still open questions.

While current models reproduce the location of the TS, their HP location is much farther than Voyager 1 and 2 observed. Voyager 1 crossed the HP in August 2012 at the distance ~122 au, which

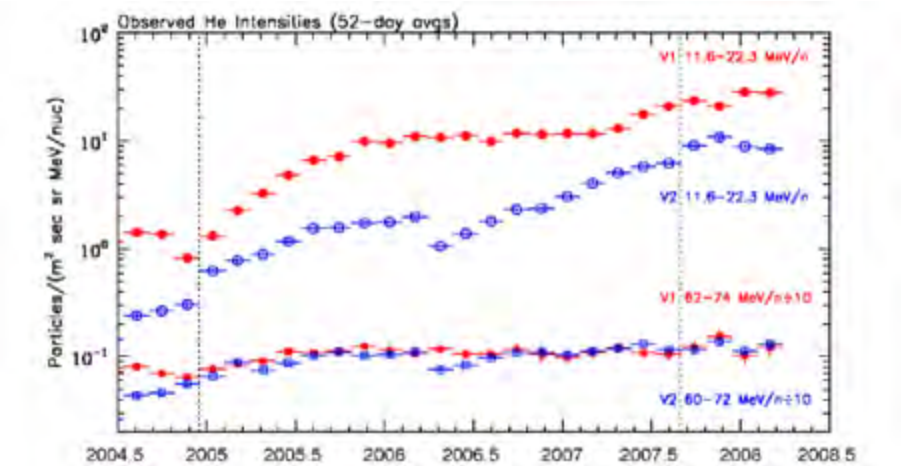

Figure 3-4. Acceleration at the TS and unexpected unfolding ACR intensities in the heliosheath. The two vertical dotted lines mark the times of the TS crossing by Voyager 1 and Voyager 2 (reprinted from Edward C. Stone et al. (2008) with permission; © 2021 Springer Nature Limited).

is 28 au past the TS crossing. Very recently, comparison of data on different instruments on Voyager 2 showed that the spacecraft crossed the HP at the distance 119 au in November 2018, which is 35 au past the TS crossing. Voyager 1 and 2 are traveling roughly 30° above and below the ecliptic plane. Although the two Voyager spacecraft are separated by 60° in heliolatitude and ~170 au in distance, the HP crossing distances are remarkably similar. This suggests that the HP could be *quasi-spherical* in the upwind (toward the ISM inflow direction) with the radius ~120 au (Roelof, Fall AGU 2019 poster). Both Voyager spacecraft revealed that the thickness of the heliosheath is ~30 au. This is smaller, by at least a factor of two, than predicted by existing state-of-the-art global models of the heliosphere, which give a thickness of 50–60 au (V. V. Izmodenov & Alexashov, 2015; M. Opher et al., 2015; Pogorelov, Fichtner, et al., 2017). Although different ideas to explain a thin heliosheath were pursued (Gloeckler & Fisk, 2015; V. V. Izmodenov et al., 2014; Malama et al., 2006; Merav Opher et al., 2018), a complete physical picture of the heliosheath eludes description. The shape of the heliosphere, the structure of its boundary, and the physical nature of the heliosheath remain the most outstanding questions in heliophysics.

Unexpected Heliosphere Boundary—Not a Surface

A traditional view of the HP was that it is a tangential discontinuity separating solar wind plasma and interstellar plasma flowing along the HP surface. However, Voyager in situ observations showed that the HP is not an ideal boundary but instead has so-called “porous” structure. Beginning on day 210 of 2012, Voyager 1 measured a series of dropouts in the intensities of energetic particles that originated in the heliosphere: ACRs (Krimigis et al., 2013). At the same time as the dropouts, abrupt increases in the GCR particles that originated outside the heliosphere and an increase in the magnetic field intensity were observed (Burlaga & Ness, 2013). Finally, on around day 238, the ACRs dropped to noise levels and the GCRs underwent a final increase (Figure 3-5). Both have since exhibited no significant variations, which indicated that Voyager 1 crossed the HP. Similar but not identical changes in particles were observed during Voyager 2’s HP crossing in November 2018 (Figure 3-5). This similarity in energetic particle behavior at HP crossings that are

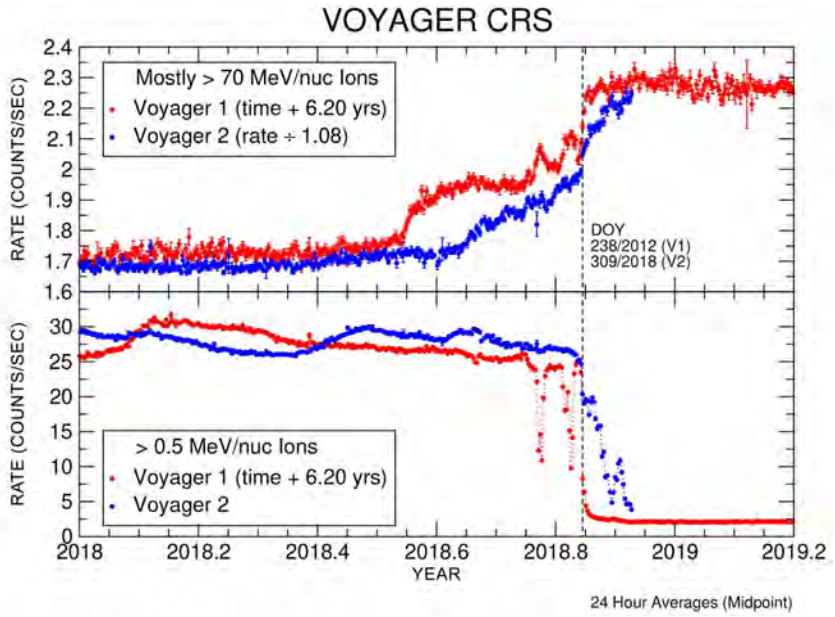

Figure 3-5. The Cosmic Ray Subsystem instrument on Voyager 1 and 2 observed similar increases in cosmic rays and decreases in lower energy particles as both spacecraft exited the heliosphere. Cosmic rays originate outside the heliosphere, and lower energy particles originate inside. (Image credit: NASA/JPL-Caltech.)

170 au apart is remarkable. Several theories were explored to understand a complex interplay between magnetic fields and energetic particles at the heliosphere boundary. Swisdak et al. (2013) presented a model of the HP crossing at Voyager 1's location that produced particle and magnetic signatures consistent with the observations and concluded that Voyager 1 had entered interstellar space. There were other explanations, including time-dependent instabilities (Florinski, 2015), flux transfer events (Schwadron & McComas, 2013b), and turbulence reconnection (Grygorczuk et al., 2014).

However, absence of dedicated direct measurements of thermal plasma, and especially of PUIs (Figure 3-6), left many questions unanswered. Additionally, the expected change in magnetic field direction was not observed, nor was the expected turbulence of the field. In fact, the magnetic field was exceptionally smooth after and beyond the crossings. Was the boundary that both Voyager spacecraft crossed at ~120 au the HP? Or could it be that the HP is well beyond the current locations of Voyager 1 and 2? (Fisk & Gloeckler, 2013; Gloeckler & Fisk, 2015, 2016). While even now it is generally believed that both Voyager spacecraft have crossed the HP, IBEX and Cassini observations of ENAs (Dialynas et al., 2017; Galli et al., 2016) provide evidence that Voyager 1 and 2 have not yet crossed the HP but rather entered and thus discovered *an entirely new plasma interaction region* (Fisk & Gloeckler, 2013).

Unexplored Hydrogen Wall around the Heliosphere and Other Astrospheres

The hydrogen wall (H-wall) is a dense layer of hydrogen formed in the very local interstellar medium (VLISM) in front of the heliosphere (Figure 3-7, left). The ISM plasma is slowed down and

diverted around the heliosphere. An H-wall is created by H atoms that originate in a charge exchange between ISM H and decelerated ISM plasma. The H-wall was first predicted by models of the outer heliosphere (Baranov & Malama, 1993). Analogously to the H-wall, there is an oxygen wall of secondary interstellar oxygen atoms that originated in a charge exchange between oxygen ions and hydrogen (V. Izmodenov et al., 1997). Heliosphere H-wall absorption was discovered for the first time by Jeffrey L. Linsky and Wood (1996) in the Lyman-alpha spectra toward Alpha Centauri measured by the Goddard High Resolution Spectrograph/Hubble Space Telescope (HST) (Figure 3-7, right). The presence of an H-wall was inferred from Voyager UVS Lyman-alpha data (Eric Quémerais et al., 2000). Recent analysis of Voyager 1/UVS data suggests that there could be a dense layer of hydrogen atoms near the HP (Katushkina et al., 2017). The layer produces a contribution to the Lyman-alpha emission in agreement with observations. Lyman-alpha data from New Horizons/Alice also suggest the presence of an additional source of emission—near the heliosphere or more distant—with brightness of ~40 R (Gladstone et al., 2018). The HST found evidence of the presence of an H-wall around other stars, indicating that the H-wall is a common phenomenon for astrospheres. The most relevant example is the H-wall detected by (B. E. Wood et al., 2004) and around Alpha Centauri A and B by line-of-site absorption measurements. Although these observations are sufficient for a positive detection of an H-wall, the statistics are too low to construct an image of the astrosphere around the Alpha Centauri binary system. With the orbital period of A and B of 79.91 years and their separation range between 11 and 35 au, it would indeed make for a very intriguingly dynamic astrosphere.

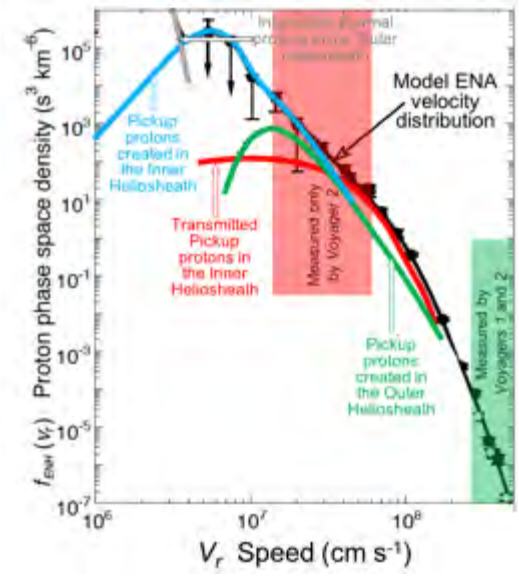

Figure 3-6. The relatively narrow energy ranges measured by the Voyager mission have left significant gaps in our understanding of the plasma physics of the outer heliosphere. (Image courtesy of G. Gloeckler.)

The H-wall was never observed in situ, and its properties (e.g., spatial extension, shape, enhancement of hydrogen [and oxygen] in H-wall [O-wall] compared to pristine ISM) are not known. One of the important questions is how far the influence of the heliosphere extends into the ISM in different directions, toward the nose, sides, and tail. Another open question is how the H-wall outside the HP is related to similar structures detected around other astrospheres. Observations of backscattered Lyman-alpha emission from hydrogen outside of the heliosphere on Interstellar Probe will provide unique information about global distribution of H atoms near the heliosphere in the H-wall and farther away in the local interstellar cloud (LIC).

Depending on the ISM parameters (speed, magnetic field strength, temperature), the bow shock may form or not in the VLISM ahead of the heliosphere (D. J. McComas, Alexashov, et al., 2012; D. J. McComas, Dayeh, et al., 2012; Zank et al., 2013). Bow shock structure can also be influenced by the charge-exchange process between plasma and neutral particles.

Figure Permission Pending

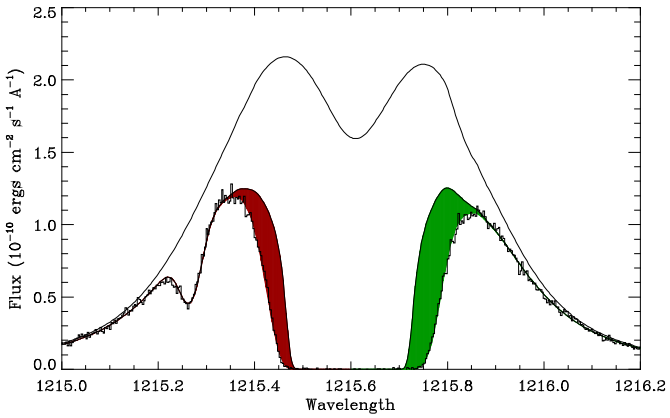

Figure 3-7. (Left) Hydrogen density enhancement in the hydrogen wall around the heliosphere (Balogh & Izmodenov, 2005; Baranov & Malama, 1993; Baranov & Malama, 1995; Gruntman et al., 2001). (Right) Hydrogen Lyman-alpha line shape observed toward a late-type star by the Hubble Space Telescope. Excess absorption on the blue and red sides indicates the presence of astrospheric and heliospheric H-wall absorption, respectively (Brian E. Wood, 2004).

Puzzling Interactions at Heliosphere Boundary Imprinted in ENA Sky Images

ENAs emanate from any hot plasma embedded in a cold neutral gas, and these atoms can be used to image the plasma from remote vantage points. In addition to the spatial information about the plasma, ENA images contain information about its composition, energy distribution, and bulk velocity. ENAs that originate in the outer heliosphere beyond the TS carry important information about interaction between the solar wind and ISM. ENAs are produced in a charge exchange between energetic plasma ions and ISM neutrals. The IBEX mission and the INCA instrument on Cassini produced all-sky ENA flux maps over a wide energy range. IBEX images ENAs with energies of 0.2–4.3 keV from 1 au (D. J. McComas, Allegrini, Bochsler, Bzowski, Collier, et al., 2009). Cassini/INCA measured ENAs in a higher energy range (5.4–55 keV) (Krimigis et al., 2009) in orbit about Saturn. IBEX discovered a completely unpredicted narrow ribbon of ENA emission in 1 keV coming from the outer heliosphere (D. J. McComas, Allegrini, Bochsler, Bzowski, Christian, et al., 2009). Cassini/INCA data revealed an ENA belt in energies around 4–13 keV (Figure 3-8). The IBEX ribbon appears to be ordered by the ISM B-field outside the heliosphere, e.g., ribbon ENAs are coming from regions where the radial component (with respect to the Sun) of the LISM B-field is zero (Schwadron et al., 2009). Over a dozen different mechanisms for ENA ribbon formation have been proposed (D. J. McComas et al., 2014). Among them is a model in which ribbon ENAs are produced outside of the heliosphere (in the "outer heliosheath") via the formation of PUIs from neutral solar wind and a second charge exchange that creates the returning ENAs (Heerikhuisen et al., 2009). One key challenge for this model is how the PUIs are retained long enough either close to 90° in pitch angle or spatially to produce the observed ribbon intensity, which has been addressed with several proposed competing mechanisms (Gamayunov et al., 2010; Giacalone & Jokipii, 2015; Isenberg, 2014; Schwadron & McComas, 2013a). The Cassini/INCA ENA belt in the sky is organized similarly to (but not perfectly with) the IBEX ribbon. Where and how the IBEX ribbon and INCA belt are produced and the relationship between these sources is a hot debate in the community. Also, all-sky maps

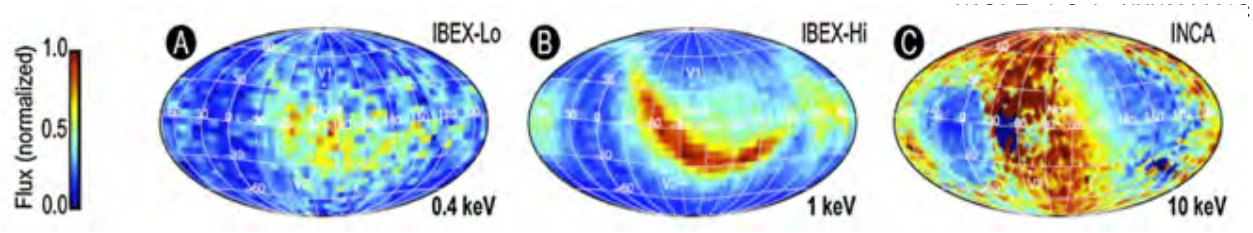

Figure 3-8. Global distributions of ENAs reveal complex interactions between the solar wind and ISM. The origin of the bright ENA ribbon (B) and its relationship to the ENA belt seen by INCA are open questions. Observations from IBEX-Lo (A), IBEX-Hi (B), and Cassini/INCA (C) are shown (from D. J. McComas et al. (2018)).

from IBEX show a diffuse signal of global ENA emissions, known as the globally distributed flux, which appeared around the IBEX ribbon (Schwadron et al., 2009). Several studies have suggested a number of possible sources for the globally distributed ENAs: transmitted and reflected solar wind ions in the inner heliosheath, and transmitted, reflected, and injected PUIs in the heliosheath and beyond the HP (Desai et al., 2014; Zirnstein et al., 2014). Although the energy spectra of globally distributed ENAs were established in the energy range from 0.1 to 6 keV by IBEX observations (Fuselier et al., 2012; Fuselier et al., 2014), the source of low-energy (~0.05–0.5 keV) ENAs is still not understood (Gloeckler & Fisk, 2015; Zirnstein et al., 2014; Zirnstein, Kumar, et al., 2018).

The upcoming IMAP mission to be launched in 2024 will explore particle acceleration processes at 1 au in detail and connect these to ENA production at the heliosphere boundary to address fundamental questions about the heliosphere (D. J. McComas et al., 2018). Although IMAP will provide a great deal of new information on the plasma structures of the outer heliosphere, it will be limited by the ambiguities of the internal vantage point. The Interstellar Probe mission will image the heliosphere from the outside, allowing it to see the overall shape of the heliosphere and how the plasma is distributed within it directly without the ambiguities of the internal vantage point. Interstellar Probe will allow us to study the ribbon and belt structure; it will be immediately obvious whether these structures originate within the heliosheath or result from processes beyond. Further, depending on the selected trajectory, the source of the ribbon/belt structures could be sampled in situ. Together with concurrent ENA imaging from 1 au, ENA observations on Interstellar Probe will allow true tomography of the outer heliosphere, which will reveal the structures and processes in 3D.

Past and current heliosphere observations brought many remarkable discoveries. These point to the uniqueness of the plasma environment around the Sun and its orbiting planets shaped by the complex interactions between solar and galactic material. While substantial progress has been made in understanding various components of the interaction, the fundamental processes determining the global nature of the heliosphere are missing. A dedicated set of in situ and remote-sensing measurements is required to address the most outstanding questions about the heliosphere. In situ measurements include plasma ions, electrons and neutrals in the solar wind and ISM, the solar and ISM magnetic field, waves and turbulence, PUIs (not measured by Voyager 1 and 2), energetic particles, and cosmic rays. Mapping ENA fluxes and extreme ultraviolet (EUV)

emission from outside the heliosphere for the first time will reveal the heliosphere shape and properties of the VLISM.

3.1.1.2. How Do the Sun and Galaxy Affect the Dynamics of the Heliosphere?

The Sun influences the dynamics of the entire heliosphere and its boundaries through the 11-year activity cycle. Even at 145 au, Voyager 1 still detects a significant influence of the dynamic Sun. From solar minimum to solar maximum, the solar wind dynamic pressure changes by a factor of two. Models predict that the heliosphere boundaries, the TS and HP, globally and locally respond to the solar wind dynamic pressure changes and move inward and outward (V. Izmodenov et al., 2005; V. V. Izmodenov et al., 2008; Pogorelov et al., 2009; Provornikova et al., 2014; Haruichi Washimi et al., 2007; H. Washimi et al., 2011). The TS is more responsive to the solar wind changes and can move in and out by 10 au. Average variations in HP position toward the heliosphere nose during the solar cycle are predicted to be smaller, ~3–5 au. The solar wind varies on different time and spatial scales during the solar cycle. Coronal mass ejections (CMEs) emerging from the Sun predominantly during solar maximum travel in the interplanetary space (J. D. Richardson et al., 2006), interact with each other, and merge, producing large-scale global merged interaction regions (GMIRs) (Burlaga, 1993). GMIRs are characterized by high pressure and magnetic fields in the outer heliosphere. These structures generate significant changes in solar wind parameters. GMIRs modulate cosmic-ray intensities in the heliosphere (Burlaga & Ness, 1998). GMIRs typically drive shocks that propagate through the heliospheric interface, interacting with the TS and HP and affecting particle acceleration processes and ENA production. Large pressure fluctuations of solar origin drive disturbances beyond the HP in the VLISM (Burlaga, Ness, Gurnett, et al., 2013; Gurnett et al., 2015; Schwadron & McComas, 2017).

During the declining phase of the solar cycle, the solar wind in the heliosphere is dominated by long-lived corotating interaction regions (CIRs) (Burlaga et al., 2003). CIRs are characterized by an enhanced magnetic field, plasma density, and pressure, and are bounded by a pair of shocks typically forming at ~2–5 au. CIR shocks are efficient accelerators of particles—both ions and electrons. Observations of CIRs by Voyager 2 and Pioneer 10 in the inner heliosphere within 10 au showed that the dynamic pressure in CIRs may increase by a factor of 15−30. At larger heliospheric distances, CIRs expand and merge into more complex structures but continue to affect plasma, fields, and particles. Near 45 au, Voyager 2 data show the sequence of recurring sharp, shock-like increases in the solar wind speed during the solar minimum in 1994−1995 that very much resemble forward shocks. These recurrent structures are associated with quasiperiodic enhancements in ~1-MeV energetic particles. One would expect that these structures propagate further to the heliosheath and beyond into the LISM. In fact, Voyager 1 magnetic field data from the LISM reveal an interval (2014.6–2015.4) with ~28-day oscillations in B (Burlaga & Ness, 2016). This suggests that the Sun influences this region. However, the origin of these oscillations is not yet explained. The nature of the interaction between structures evolved from CMEs and CIRs and heliospheric boundaries, as well as their effects on the VLISM, still challenges our understanding.

By now Voyager 1 has traveled 25 au in the interstellar space, which was expected to be a quiet medium with not much dynamics expected. However, Voyager 1 made a remarkable discovery by

observing shock waves in this region. The shocks are presumably driven by solar transients that reached the heliosphere boundary and propagated to the LISM. The first shock in the LISM was observed by Voyager 1 at the end of 2012 (Burlaga, Ness, Gurnett, et al., 2013). The important property of the LISM shock is its very smooth nature and very large width, being ~10^4 times broader than a shock with similar properties often observed in the solar wind near Earth. The shock properties in the LISM are dramatically different from ones inside the heliosphere. Why shocks are so broad and what processes determine their structure in the LISM are open questions. A recent study (Mostafavi & Zank, 2018) suggests that the LISM is collisional because the electron and proton collisional mean-free paths are small compared to the almost featureless LISM. The weak LISM shock is very broad, and its structure is controlled by particle collisions and not by the wave-particle interactions observed inside the heliosphere. The nature of the LISM plasma is different compared to the heliosphere plasma and needs to be explored more carefully. In situ measurements in the LISM are critical to understanding the physics of shock waves, pressure waves, and associated particle energization in this region.

Heliosphere Influenced by the Local Interstellar Medium and Shielded against It

Beyond the HP, Voyager 1 observed a draped ISM magnetic field, indicating that the heliosphere distorts the ISM magnetic field around it. Surprisingly, the ISM magnetic field in front of the heliosphere has a direction resembling the azimuthal (east-west on average) solar magnetic field (Burlaga & Ness, 2016). This was completely unexpected, given that based on several indirect observations, the ISM field was believed to be inclined to the east-west direction (V. V. Izmodenov, 2009; M. Opher et al., 2009). The ISM field is distinctly different from the heliosheath magnetic field (Burlaga & Ness, 2016). In the heliosheath, the field is relatively weak (B ~ 0.1 nT) and highly variable showing sector boundaries. Beyond the HP, the average B is relatively strong (0.48 nT measured by Voyager 1 and 0.7 nT measured by Voyager 2) and does not change significantly. The ENA IBEX ribbon orientation currently provides one of the important constraints on the ISM direction (Funsten et al., 2013; D. J. McComas, Allegrini, Bochsler, Bzowski, Christian, et al., 2009; Schwadron et al., 2009; Zirnstein et al., 2016). While Voyager 1 and 2 are observing the draped ISM field and ISM plasma, this region is still significantly perturbed by the Sun. The open questions for the Interstellar Probe mission are (1) what is the magnetic field magnitude and direction in the ISM, and (2) does it influence the shape of the heliosphere?

Our galactic neighborhood, the partially ionized LIC, affects the heliosphere, determining its global structure. LIC hydrogen coming to the heliosphere interacts with the solar wind plasma in the charge-exchange process. The charge exchange removes momentum from the solar wind, controlling the locations of the heliosphere boundaries (Baranov & Malama, 1993) and the properties of the solar wind at large distances from the Sun. Charge exchange creates PUIs, which play a dominant role in the heliosheath pressure (Gloeckler & Geiss, 2004). ISMF draping around the heliosphere affects its shape (M. Opher & Drake, 2013; M. Opher et al., 2017). The ISM hydrogen and plasma parameters (number density, velocity, and temperature) and magnitude and direction of the ISM field are key parameters to measure on the Interstellar Probe.

With the Voyager observations, it is now established that the heliosphere, the only known habitable astrosphere, shields 75% of GCRs, an important constituent for the development of life on Earth (Figure 3-9). Even with this shielding, however, variations in the solar cycle and in Earth's magnetic field allow variations in the flux of GCRs, potentially driving significant changes in atmospheric chemistry that may, in turn, affect the biosphere (Krivolutsky, 1999; Pavlov et al., 2005). Without a relatively quiet host star like the Sun, an Earth-like planet could face a much greater flux of GCRs, with more severe implications for life (Atri et al., 2013; Grenfell et al., 2007; Tabataba-Vakili et al., 2016). Tentative connections have been made between GCRs and cloud cover, climate, and aerosol distributions (Marsh & Svensmark, 2000). To better understand the extent and impact of GCRs on the Earth, then, it is imperative that we have a clearer understanding of the connection between the heliosphere, the LIC, and GCR fluxes via in situ measurements.

3.1.1.3. What Is the Nature of the Local Interstellar Medium?

Sun Leaving Local Interstellar Cloud to the Next Interstellar Destination

The Sun is moving at 26 km/s in the direction of the edge of the LIC, and it is believed that it will leave the LIC in <1900 years (Figure 3-10). The edge is <0.07 pc = 7000 au upstream. The LIC is one of many interstellar clouds clustered in the Local Bubble, a region of low-density hot gas extending to ~100 pc from the Sun (R. Lallement et al., 2003). What will be the next hosting interstellar cloud for the Sun and its heliosphere is an open hot question. J. D. Slavin and Frisch (2008) summarized properties of the LIC obtained from spectroscopic ISM measurements: n(H) = 0.19 – 0.2 cm^{-3}, n(e) = 0.07 ± 0.01 cm^{-3}, T = 6300 ± 340 K, fractional H ionization ~0.2, inflow velocity 26.3 km/s. The other three interstellar clouds closest to the Sun are G-cloud (Rosine Lallement, 2007) in front of Alpha Centauri (1.3 pc), Blue cloud (Redfield & Linsky, 2001) in front of Sirius (2.6 pc), and Mic cloud, which is formed at the interaction region between the collided LIC and G-cloud (Redfield & Linsky, 2008) (Figure 3-11, left). G-cloud (it is so called because of its location on the galactic center side) is cooler and slightly faster moving than the LIC. The Blue cloud may be a detached piece of

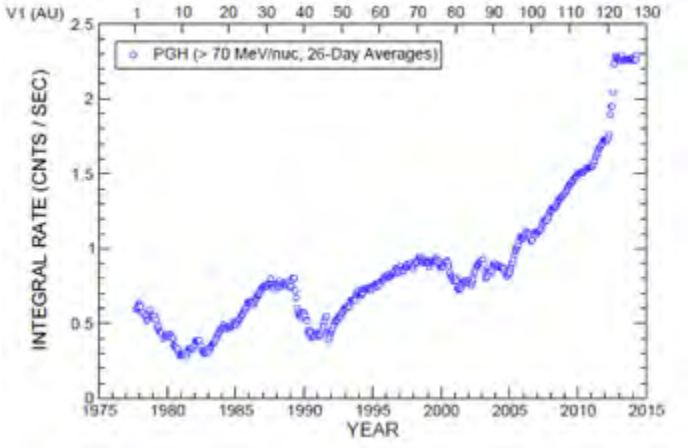

Figure 3-9. Voyager 1: Heliosheath shields 75% of galactic cosmic rays coming to the heliosphere from the interstellar medium. Plot generated from Voyager CRS Rates Time History.

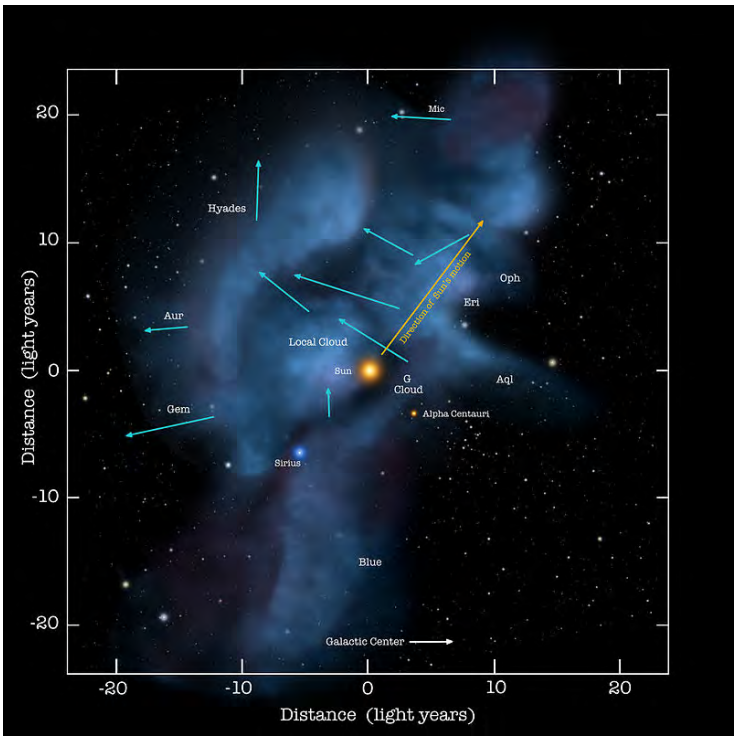

Figure 3-10. The Sun is on the way to exiting the Local Interstellar Cloud and entering another unexplored interstellar region. (Image credit: NASA/Goddard/Adler/U. Chicago/Wesleyan.)

the LIC with properties changed by EUV radiation. Mic cloud has a filamentary and turbulent nature, with the shape resembling the boundary of the G-Cloud and LIC. Fifteen interstellar clouds were identified within 15 pc of the heliosphere (Figure 3-11, right).

Interstellar Probe would provide the first sampling of LISM material that is unprocessed by the HP. It is not yet known how far the influence of the heliosphere really extends into the LISM, but it is thought to be located beyond a possible bow wave/shock at a distance of >500 au. The two Voyager spacecraft provided the first unique in situ measurements of the LISM just beyond the HP but approach their end of operation at ~160–170 au from the Sun, well before reaching the unperturbed LISM. EUV measurements obtained by Interstellar Probe of the ISM in different lines of sight (LOSs) could bring new understanding of inhomogeneity, velocity, and temperature distribution in the pristine LISM.

Investigating the Origin and Evolution of Matter in the Galaxy

The unprocessed LISM holds the key to understanding not only the global heliospheric interaction but also how matter in the galaxy originated and evolved. The elemental and isotopic composition

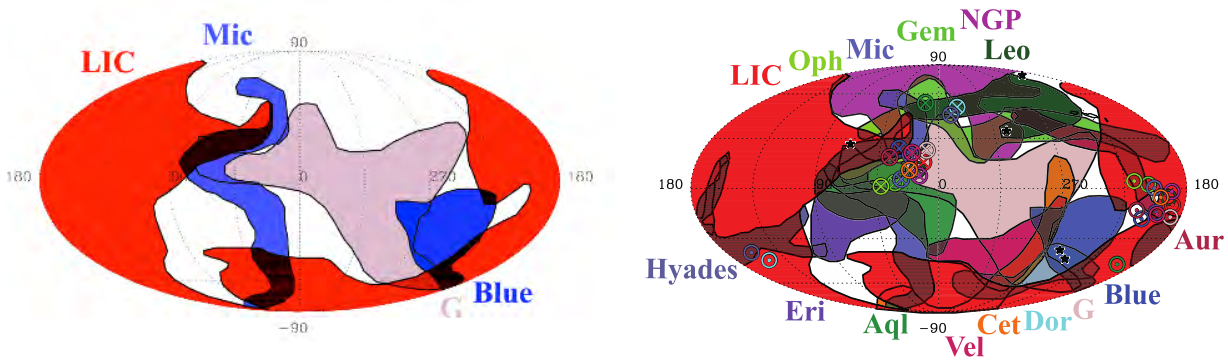

Figure 3-11. Galactic environment near the heliosphere. (Left) The four interstellar clouds closest to the Sun (J. L. Linsky & Redfield, 2013). (Image courtesy of S. Redfield.) (Right) Fifteen interstellar clouds located within ~15 pc of the heliosphere (reproduced and adapted from Redfield and Linsky (2008) with permission; © AAS).

of gas is the only direct measurement that can be used to constrain models of stellar nucleosynthesis and therefore formation of matter in the galaxy. Interstellar dust (ISD) grains are the building blocks of both stellar and planetary systems and are therefore critical to understand the evolution in the galaxy.

After the Big Bang, only a small number of the light elements (such as H, D, Li and Be) existed. Stellar nucleosynthesis then subsequently formed essentially all elements heavier than Li, with the isotopes ^{13}C, ^{18}O, ^{22}Ne, and ^{38}Ar produced during different stages of stellar evolution than the main isotopes. Given that the relative abundances of isotopes are fractioned much less than the elemental abundances, isotope ratios therefore remain the more critical constraints on nucleosynthesis models. Of particular importance are ratios such as D/H ^{3}He/^{4}He, ^{13}C/^{12}C, ^{18}O/^{16}O, ^{22}Ne/^{20}Ne, and ^{38}Ar/^{36}Ar.

The LISM consists of material in multiple hot, warm, and cold phases, each of which is characterized by different temperatures, densities, and stages of ionization—both atomic and molecular—as well as ISD grains. These are the condensed phases of the ISM, transporting the heavy elements produced by stellar nucleosynthesis through the different ISM phases. Although representing only ~1% of the mass of the ISM, ISD grains contribute significantly to the different evolutionary processes of the galaxy and are the building blocks of new stellar/planetary systems forming upon collapses of cold molecular clouds. Dust condensation from gaseous heavy elements occurs both in certain circumstellar environments as well as in protostellar nebulae. ISD grains ensure the transport and mixing of heavy elements across the different phases of the ISM, where they undergo multiple cycles of formation and destruction (Zhukovska et al., 2008). Any modern model describing galactic chemical evolution must therefore take their life cycles through the ISM into consideration.

A direct in situ characterization of the ISD grains in the warm gas and dust phase surrounding the solar system, the LISM, and their interaction with the gas phase therefore enables an understanding of the true nature of the current building blocks of planetary systems in our galaxy.

So far, information on the LISM has been gathered using three approaches. The first approach uses LOS observations of the light absorption of nearby stars to reveal the depletion of heavy elements in the gas phase. Under the assumption that the solar photosphere element abundance is a good reference for the LISM, one can deduce that the heavy missing elements are condensed as ISD grains. This approach yields various possible constitutive models of local ISD (Kimura et al., 2003). However, given that these are observations along LOSs of element depletion, they can be attached with strong biases.

The second approach relies on detecting gas and dust that penetrate the heliosphere. Because of the motion of the Sun with respect to the LISM, gas and dust are entering the solar system, where some can be detected. ISD grains enter the heliosphere with 26 km/s with respect to the Sun from a direction at 79° ecliptic longitude and −8° ecliptic latitude, well aligned with the flow of neutral helium (Frisch et al., 1999; Gruen et al., 1994; Witte et al., 2004). The relatively low velocity dispersion of the ISD flux entering the solar system is indicative of particles in Brownian motion within the LISM, with no group velocity component. Another ISD stream, decoupled dynamically from the ISM, may have been recorded during Earth-based radar measurements and tentatively linked to the debris disk of Beta Pictoris (Baggaley, 2000), but this remains under speculation.

The third approach uses the detection of interstellar PUIs formed from ionized neutral LISM atoms penetrating the heliosphere (Gloeckler & Geiss, 1998). Neutral helium, as well as ISD grains, could also be directly detected by instruments carried by the Ulysses spacecraft, coming from the apex direction of motion of the Sun (Grun et al., 1993; Witte et al., 1993). However, because of the sensitivity of those instruments, combined with various filtering processes of the LISM material at the HP and after entering the heliosphere (Grün & Landgraf, 2001; Linde & Gombosi, 2000; Mann et al., 2010; Jonathan D. Slavin et al., 2012; V. J. Sterken et al., 2013), the data cannot unambiguously constrain the constitutive models of the ISD from the LISM and present a historical stumbling block for studying the important LISM properties directly. Figure 3-12 and Figure 3-13 show the ISD flux filtering resulting from the solar radiation pressure and interaction of the charged grains with the interplanetary magnetic field (IMF).

Furthermore, neither the main ISD stream entering the solar system from the neutral gas direction and detected in situ nor the (large, >20 μm) grains detected via radar measurements provide access to the lower size regime of the dust grains responsible for the starlight extinction measured from the ultraviolet (UV) to the infrared (IR), which led to a seminal ISD grain average size distribution—"the MRN distribution"—in the ISM (Mathis et al., 1977). Indeed, the lower-size-range (<0.2 μm) grains responsible for the interstellar extinction curves are prevented from entering the heliosphere because of their interaction with the magnetic field at the solar bow shock (Linde & Gombosi, 2000; Jonathan D. Slavin et al., 2012).

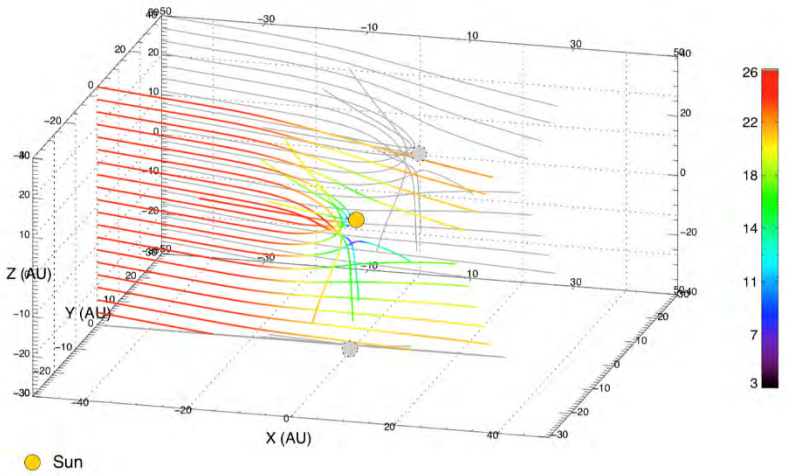

Figure 3-12. Simulated trajectories of ISD grains entering the heliosphere along the solar apex direction and subject to deflections because of the solar radiation pressure effect combined with the Lorentz forces. The particles shown on this plot have a radiation pressure-to-gravity ratio of 1.5 and a charge-to-mass ratio of 1.5 C/kg (V. J. Sterken et al., 2012).

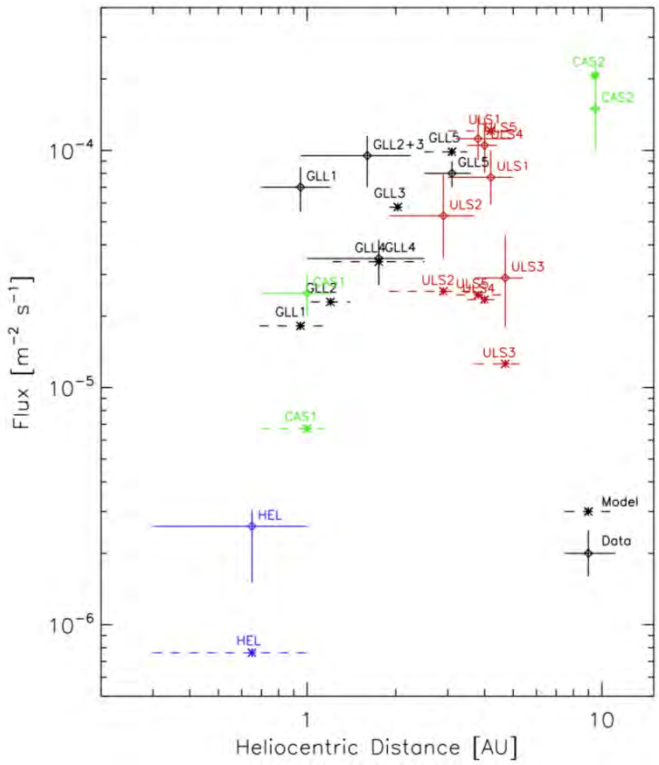

Figure 3-13. ISD dust flux as measured (and compared with models) by four different spacecraft carrying dust instruments, as a function of the heliocentric distance (Krüger et al., 2019). The overall trend is a reduction in the ISD flux the closer one gets to the Sun, with fluctuations of the measured flux values for a given heliocentric distance being the result of the interaction of the charged grains with the IMF, whose configuration is itself driven by the solar activity.

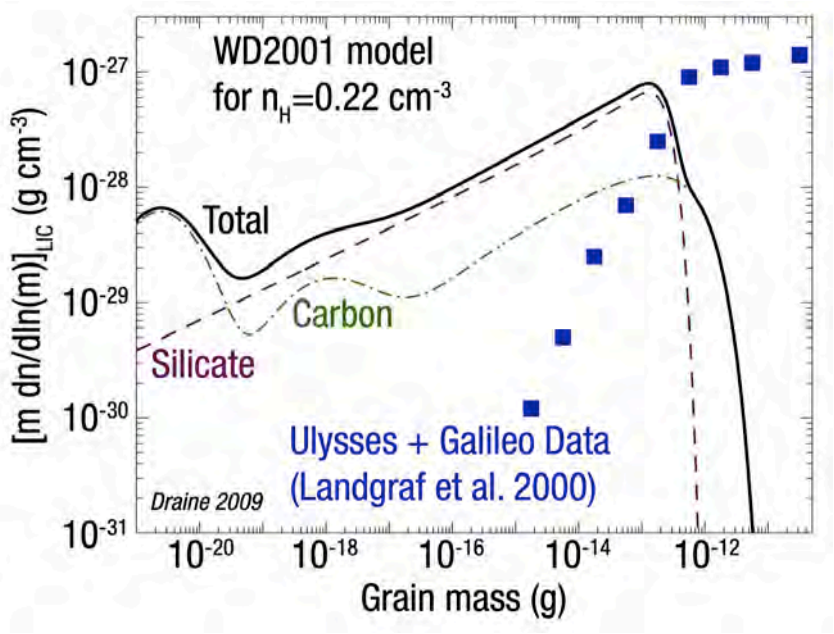

Figure 3-14. Interstellar particles with masses of $5 \times 10^{-13} < m < 2 \times 10^{-11}$ g have fluxes in the solar system observed by Ulysses and Galileo (red squares) far above that expected based on a fit to the optical and infrared extinction of the light from nearby stars (blue curve), scaled to the hydrogen density nH ≃ 0.22 cm^{-3} of the local interstellar cloud outside the heliosphere. The lack of particles with $m << 5 \times 10^{-13}$ g is expected because of their filtration in the outer heliosphere. The peak near 3×10^{-21} g is expected because of their filtration in the outer heliosphere. The peak near 3×10^{-21} g consists of polycyclic aromatic hydrocarbons (reprinted from Draine (2009) with permission; © 2008 Springer Nature).

As a consequence, the ISD component measured so far by dust instruments onboard interplanetary probes within the solar system shows grains with a size in excess of the MRN. While those larger grains will contain most of the LISM condensed mass, their low volume number density in the ISM results in optical depth that is too low to make a significant contribution to the interstellar extinction curve (Krüger et al., 2019) and therefore escape analysis via astronomical means.

Only an interstellar probe leaving the heliosphere would enable, for the first time, measurement of the composition, flux, and flow direction of small-sized (tens of nanometers) to large-sized (equal to or greater than micrometer size) particles. The small particles are most numerous (power-law size distribution), and the high relative velocity of the Interstellar Probe facilitates detection of these smallest particles. This will provide unprecedented information about the composition and volume number densities of the surrounding interstellar cloud dust. Sampling the ISD grain population in the LISM would also provide a measurement of the level of chemical homogenization of the particles. This seems to be the case for the ISD grains large enough to enter the heliosphere and studied by the dust instrument onboard the Cassini spacecraft (Altobelli et al., 2016). All grains detected contained silicate-forming elements, and the abundance of Mg, Si, Ca, and Fe was compatible with those elements being fully condensed from the LISM gas phase. The absence in the Cassini data of particles whose composition would correspond to a condensation

process in circumstellar envelopes (“stardust”), like the carbon-bearing grains SiC, can be explained by the fact that such particles are unable to condense directly from the ISM phase, and would be destroyed during their re-cycling across the various ISM phases. However, it must be noted that the Stardust mission reported on the presence of sulfide-bearing particles (Veerle J. Sterken et al., 2014) not seen in the Cassini data. Only an interstellar probe could verify the existence of pristine “stardust” that would stand out—as a result of the characteristic composition imposed by the environment of their formation—from the “average” LISM silicate-bearing dust population detected by Cassini.

Multiple other astrospheres have been observed in IR that show interactions with their surrounding ISD (Cox et al., 2012). Zeta Ophiuchi (Figure 3-1) is an example of a young and massive star interacting with a relatively dense dust cloud. The star is plowing through its ISM at a speed of ~24 km/s, possibly once torn away from a binary system. The prominent bow-shock-shaped bright region consists of dust deflected in the interaction with the stellar wind. Understanding how ISD interacts with our own heliosphere would therefore enable a dramatically improved understanding of the environment around other astrospheres. However, the ISD grain size, which determines dust charging properties, is largely unknown in the ISM. This means that models on how the heliosphere filters interstellar material by size and chemical composition and how this depends on the solar cycle are very ill constrained.

Unknown Galactic Lyman-Alpha Background

Observations of backscattered Lyman-alpha emission on Interstellar Probe from outside the heliosphere open the possibility of a unique diagnostic of the spatial and temporal distribution of hydrogen properties in the LIC and possibly the other closest clouds: density, velocity, and temperature. In the LISM (at ~400 au), simulations predict the intensity of the backscattered Lyman-alpha to be on the order of 5 R or less for the antisolar direction (Gruntman, 2004). Measurements of Lyman-alpha radiation at 300–400 au with high sensitivity present a unique opportunity to obtain galactic background in Lyman-alpha. Observation of the galactic background from the inner heliosphere is very difficult because of the bright glow of interstellar H inside the heliosphere. Rosine Lallement et al. (2011) analyzed Lyman-alpha data from the UVS instrument on Voyager as it was leaving the heliosphere. They discovered that in addition to the smooth heliospheric emission, the UVS detects a galactic Lyman-alpha emission on the order of few rayleighs. The emission is mainly concentrated in the plane of the galaxy. Milky Way Lyman-alpha data can be used to test the complex radiative transfer models that are developed for distant galaxies.

3.2. Origin and Evolution of Planetary Systems

The formation and evolution of our solar system, and others, is one of the most compelling science questions in planetary science and astrophysics today. It derives directly from the quest to understand how matter in the solar system and ISM originated and evolved, which is one of the top priorities recommended in the Planetary Science Decadal Survey, *Vision and Voyages* (NRC, 2011). The distribution of worlds in the solar system and the structure of the circumsolar debris disk hold the key to understanding not only the formation and evolution of this solar system but also the

increasing diversity of exoplanetary systems and unexpectedly structured circumstellar debris disks. The rich data sets acquired via flybys by an interstellar probe of one or two KBOs or dwarf planets would significantly elevate the understanding of the state of the early system and subsequent evolution. Observations from an outbound solar system escape trajectory would illuminate the structure of the circumsolar debris disk, greatly adding to initial dust measurements by New Horizons (A. R. Poppe et al., 2019).

3.2.1. Planetary Science and the Compelling Worlds of KBOs

3.2.1.1. Formation and Evolution of Planets and Smaller Worlds as Evidenced in the Outer Solar System

Three key regions can be considered in the solar system: (1) the terrestrial planets where metals, silicates, and some liquids can exist, often under protective atmospheres; (2) the gaseous and icy giant planets with numerous icy moons; and (3) the zone beyond Neptune where Pluto and many small icy worlds reside, including KBOs, dwarf planets, and comets. Comets and KBOs have historically been considered "time capsules" from the formation of the solar system, and the composition of their comae is used to make conclusions about the formation of other solar system worlds (K. E. Mandt et al., 2015). A primary goal of the European Space Agency's Rosetta mission was to explore the composition of a coma in great detail, using it as a "Rosetta Stone" for solar system formation (Glassmeier et al., 2007). Observations of the noble gas abundances have been particularly important, revolutionizing our understanding of how ices were processed in the protosolar nebula, as illustrated in Figure 3-15 (Mousis et al., 2018). In situ exploration of such a time capsule had never taken place until the time of writing this report (2019), which coincided with New Horizons' flyby of the contact binary KBO 2014 MU69 and the study of its ices—further revolutionizing our understanding of the solar system while building on the comet and Pluto system stories. What has been particularly important about the exploration of MU69 is the discovery that contact binaries appear to be common in the outer solar system and the discovery of an extremely high abundance of refractory methanol ice and orangish tholin. However, with only two KBO systems explored in situ, we are only just beginning to understand what KBO formation means to the bigger picture of planetary formation.

As the largest members of the KBOs, dwarf planets are particularly important not only because they are the most common class of planet (numbering near 130 for worlds > 500 km in diameter) but also because they illustrate the diversity of evolutionary tracks possible for planets. It is important to note that Pluto is differentiated—likely with a subsurface ocean (Kamata et al., 2019)—and its materials have gone through significant internal and surface densification, differentiation, and processing (F. Nimmo et al., 2016; Telfer et al., 2018). Unlike smaller KBOs, Pluto also has an atmosphere that transports volatiles across its surface, where chemistry and atmospheric loss evolve Pluto's composition over time (K. Mandt et al., 2017; K. E. Mandt et al., 2016; Young et al., 2018). Therefore, one must be careful comparing Pluto and other dwarf planets with comets not only because they are large enough to gravitationally bind the most volatile of species (Schaller & Brown, 2007b) but also because of the dwarf planets' complex evolutionary history relative to the

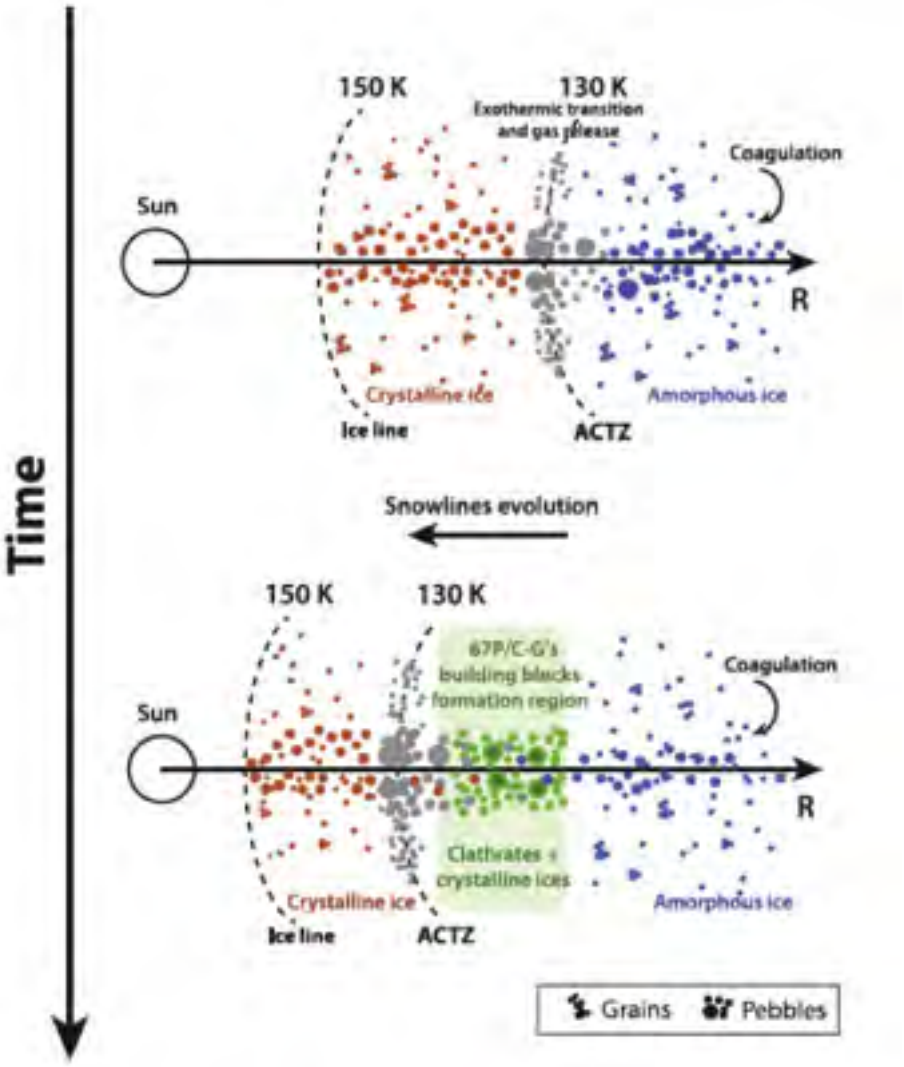

Figure 3-15. Illustration of the formation conditions of ice grain precursors of planetesimals that formed the objects in the Kuiper Belt and that added mass to each of the giant planets (K. E. Mandt et al., 2020).

smaller worlds (Keane et al., 2016; Francis Nimmo et al., 2017). Furthermore, the fascinating complexity of Pluto's evolution emphasizes the need for exploration of other planets in the Kuiper Belt to conduct comparative planetology of the outer solar system.

Models of our solar system must accurately reproduce the size, composition, and dynamical distributions observed between the smallest KBOs and the largest planets. Some models are coming close; however, it is easier to do this on a small scale or a large scale than to completely model all aspects of our solar system simultaneously. For example, it is very difficult to explain the geological and compositional differences between Pluto and Triton, similar-sized objects formed in the 20- to 30-au region of the protoplanetary disk (PPD).

As it is, all observed objects are "present day," and we infer from their conditions, both dynamically and physically, what our solar system and the solar nebula might have looked like in earlier

epochs. Interestingly, within each region of the solar system, we find binaries and discrete objects whose characteristics can be used to provide significant constraints to models. We also recognize that formation of such systems is highly dependent on the thermal properties within the regions where they reside. For example, thermally driven formation models work for near-Earth asteroid binaries but not for Kuiper Belt binaries; the latter seem to require copious amounts of disk gas and streaming instabilities to produce gravitational collapse into proto-KBO bodies. Likewise, object size is important, allowing for retention of ices and gases at various distances from the Sun. Therefore, a full inventory of observations of objects throughout our solar system, remotely and in situ, is required for proper modeling and understanding of the proto-solar nebula and the history of our solar system as a whole.

While no one mission can independently accomplish all the needed observations, missions that build on each other will eventually fill in the observational phase space while numerical models are developed to consider the physical interactions of such objects over long and short timescales. A huge amount has been learned from just the first and second in situ flybys produced by the New Horizons mission. An interstellar probe mission that can produce the third, fourth, and maybe even fifth KBO close flyby has the ability to provide even more information, especially when combined with Earth-based long-duration studies of individual objects and systems.

3.2.1.2. Dwarf and Giant Planets, Moons, and Small KBOs

The dwarf planets of the Kuiper Belt are a unique class of solar system world. Dwarfs are the most common type of solar system planet, outnumbering giant and terrestrial planets by two orders of magnitude. Understanding dwarf planets' present state, evolution, and origin is thus an essential component to constraining the evolution of a habitable astrosphere. Surface compositions (volatiles, organics, ices) and geological landforms (faults, cryovolcanoes, craters, dunes, flows, etc.) can reveal the current state and evolution of small planets' surfaces and interiors. Dwarf planets are comparable in size to the mid-sized and large satellites of the giant planets but are formed in drastically different accretional, radiogenic, and tidal heating environments. Thus, their interiors record different physical processes and different information about solar system formation. They let us both examine the earliest epochs of solar system formation and also study processes divorced from the complexities of giant planet formation and evolution.

While the Kuiper Belt is a dynamically gentle environment, it hosts surprisingly active worlds. The exploration of Pluto by New Horizons provides a useful analog for other dwarf planets. Observations of extreme geologic diversity on Pluto caused a paradigm shift in planetary science. Pluto demonstrates that even small amounts of solar and radiogenic heating (and zero present-day tidal heating) are sufficient to produce geologic activity that rivals Earth and Mars. While there is some hint of comparable geologic activity on other planets in the Kuiper Belt, only future in situ reconnaissance will tell us for sure.

Exploration of the Kuiper Belt is also highly likely to lead to new, unexpected discoveries. Voyager 2 surprised us when it revealed Triton to be a craterless (i.e., young) world, with active geysers (B.

A. Smith et al., 1989). New Horizons shocked the world when it uncovered Pluto's "heart"—Sputnik Planitia—a vast, actively convecting nitrogen and methane ice glacier (McKinnon et al., 2016; Stern et al., 2015; Trowbridge et al., 2016). Pluto's informally named Cthulhu Macula is a low-albedo equatorial band composed of complex organic molecules produced by airfall from photolyzed atmospheric methane. Transport of methane from Pluto has mantled Charon's north polar region (Grundy et al., 2016). Pluto was shown to have methane, CO, and N_2 distributions across a water-ice bedrock. The Kuiper Belt's other planets show a remarkable degree of heterogeneity—from Eris' high albedo (Sicardy et al., 2011), to Haumea's extremely oblate shape and ring (Ortiz et al., 2017), to Quaoar's young, hydrate, and crystalline water-ice composition (Barucci et al., 2015). Interstellar Probe will allow us to explore more of these dynamic and surprising planets.

In addition to revealing surface geology and activity, Voyager and New Horizons demonstrated that fast flyby missions can provide critical insights into worlds' interior structure and geophysical evolution. One of the most surprising results from New Horizons' flyby of Pluto was the inference of a subsurface ocean, confirming thermal models suggesting the commonality of subsurface liquid-water oceans throughout dwarf planets' histories (Bierson et al., 2018; Hammond et al., 2016; Kamata et al., 2019; Robuchon & Nimmo, 2011). For Pluto, such an ocean could have persisted until 2.5 Ga, and possibly up to the present (Conrad et al., 2019; Kamata et al., 2019; Robuchon & Nimmo, 2011). Detecting and exploring subsurface oceans are of critical important to planetary science; not only are they potentially habitable, but they also are unique geophysical laboratories providing insight into the thermal evolution of planetary systems. Most methods for identifying and confirming ocean worlds either require the presence of an external time-varying gravity or magnetic field or require specialized instruments capable of probing the deep interior structure (F. Nimmo & Pappalardo, 2016). Despite lacking these instruments, New Horizons was able to infer the presence of a subsurface ocean from a combination of remote-sensing geologic observations. The single long-range imaging camera on New Horizons (LOng Range Reconnaissance Imager [LORRI]) enabled measurements of Pluto's global shape, hemispheric topography, and regional tectonic structures, as well as detection of its impact basins—all of which hint at the presence of a subsurface ocean (Keane et al., 2016; F. Nimmo et al., 2016). For instance, New Horizons revealed no tidal bulge (i.e., Pluto has high sphericity) and no crustal flexure around tectonic faults; these observations imply an interior that was once liquid and an inelastic crust down to at least 10 km depth (Conrad et al., 2019). Similar observations of Triton by Voyager 2 have led to the hypothesis of a subsurface ocean on that moon as well. Interstellar Probe will be able to make comparable observations of another dwarf planet, which may enable similar geologic inferences of the deeper interior structure and geophysical evolution. If Pluto and similar planets had or have interior liquid-water oceans, they could thus be potential abodes for life, past or present. The timeline of subsurface ocean freezing, using evidence from surface tectonic and cratering features, thus constrains the timeline of ocean-world subsurface habitability. Global geometry can indicate global expansion (e.g., freezing of a large ocean; Beyer et al. (2017)), planetary despinning, orbital migration, and/or true polar wander (Keane et al., 2016), further constraining subsurface mass distributions.

Beyond probing the shape and spin of planets, magnetic field measurements from an interstellar probe would undoubtedly provide new, independent insights into interior structure. For example, the detection and characterization of a dynamo-driven magnetic field at a Kuiper Belt planet would immediately revolutionize our understanding of the formation and evolution of these small planets.

Images with high-resolution pixel scales (tens to hundreds of meters per pixel) of surface features enable many geophysical investigations on the surfaces of planets. While tectonic and crater landforms are useful probes of the interior of planets, surface geomorphology and dynamics provide further glimpses into the diversity of dwarf planets' surficial evolution. Using Pluto, Charon, and Triton as dwarf planet analogs, other planets' landscapes could include the following:

- Sublimation landforms, including penitentes (Earth), bladed terrain (Pluto) (Moores et al., 2017; White et al., 2019), and accrescent and decrescent terrain (J. M. Moore et al., 2015)
- Cryovolcanoes, such as the putative cryovolcanoes Wright and Piccard Mons (Pluto), which feature gently sloping flanks and proportionally large summit calderas (Kelsi N. Singer et al., 2018) or widespread flood cryovolcanism, such as hypothesized for Charon (Beyer et al., 2018; Schenk et al., 2018)
- Glaciation, such as the Sputnik Planitia nitrogen ice convecting glacier (Howard et al., 2017; White et al., 2019)
- Impact craters:
  - Large (more than tens of kilometers in diameter) craters can constrain the crustal viscosity and heat flow based on their depth-to-diameter ratios (White et al., 2017).
  - The size-frequency distribution of craters reflects the size-frequency distribution of the impactor population and thus the size population of small KBOs (K. N. Singer et al., 2019).
  - Craters expose vertical and lateral heterogeneities in geologic units, revealing stratigraphic relationships and relative ages.
  - Global orientation of faults and large basins could indicate the planet has "tipped over" and experienced true polar wander, as is likely the case from the evidence of the glacier-filled Sputnik basin (Keane et al., 2016).
  - Glacial or possibly fluvial channels, such as those discovered on Pluto (Howard et al., 2017), indicate viscous flow across the surface.

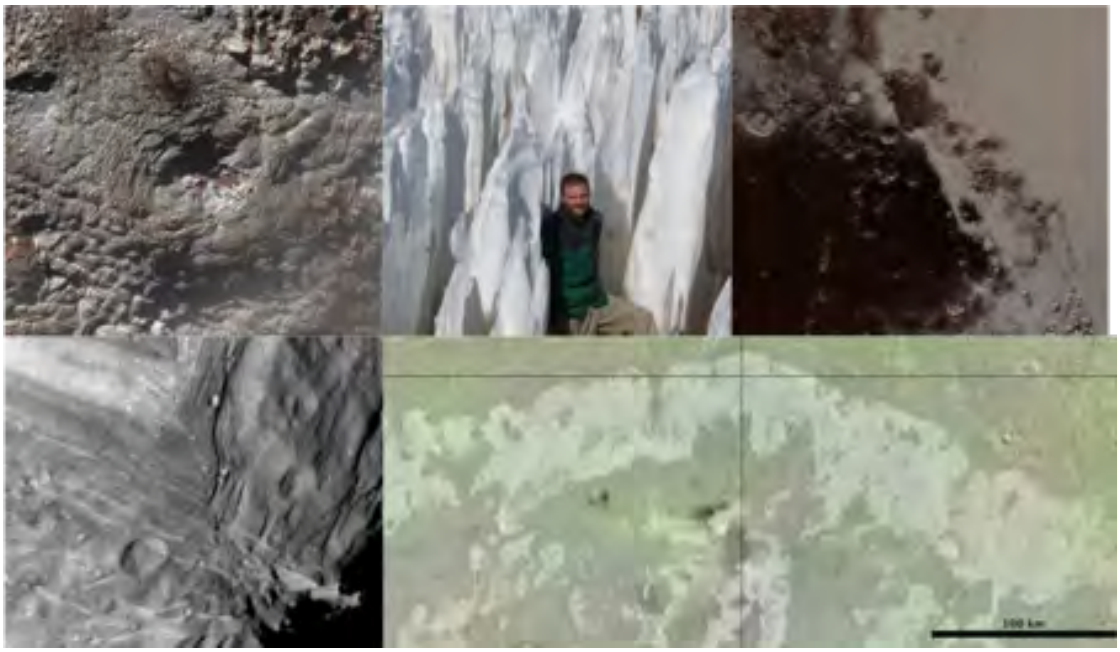

Figure 3-16. (Top Left) Cryovolcanic edifice of Wright Mons, Pluto (NASA PIA11707). (Top Center) Sublimation-driven penitentes on Earth (image credit: S. de Silva). (Top Right) N_2 glaciation and organics-rich cratered highlands on Pluto (NASA PIA11707). (Bottom Left) Extensional grabens and a possible mantle convection corona on Miranda (NASA PIA01354). (Bottom Right) Sublimation-eroded cliffs on Triton (JMARS/P. Schenk). (Image credit: NASA/JPL-Caltech/Arizona State University; Runyon et al. (2019).)

Quaoar's size (D ~ 1092 km; roughly the same size as Charon) and spectral characteristics suggest that it is a fascinating planet worthy of closer scrutiny, especially because it appears to have an intermediate amount of surface volatiles (CO, N_2, CH_4; e.g., M. E. Brown (2008)) between volatile-poor small KBOs and the volatile-rich planets Pluto and Eris. The types, distributions, and albedos of landforms on the encounter hemisphere will constrain their formation processes. The presence of crystalline volatile ices (e.g., CH_4, C_2H_6, NH_3–H_2O) on Quaoar's surface (Barucci et al., 2015; Schaller & Brown, 2007a) could suggest recent cryovolcanism and sublimation-driven surface geology with possibilities for aeolian processes and bedforms (dunes) and erosional yardangs. Higher-order hydrocarbons (e.g., tholins) from hydrocarbon photolysis would be more stable than methane (Schaller and Brown, 2007) and could form albedo patchworks, similar to Pluto. Observed crater size-frequency distributions would constrain the impactor flux population for heavily cratered terrains and show relative ages between geologic units. Crater ejecta emplacement mechanisms will be hinted at by the range of ejecta morphologies. Faults, pits, and bands will provide constraints on tectonic processes and may enable modeling of the interior, revealing whether Quaoar ever had water in contact with hot rock, with astrobiological implications. Regarding an atmosphere, spectroscopic UV observations and high phase-angle imaging and radio sounding could reveal an atmosphere and hazes around Quaoar, as was done for Pluto (Gladstone et al., 2016).

With a known population of nearly 130, dwarf planets are the most common type of planet in the solar system, offering many more target options than just Quaoar. Any one of these planets would

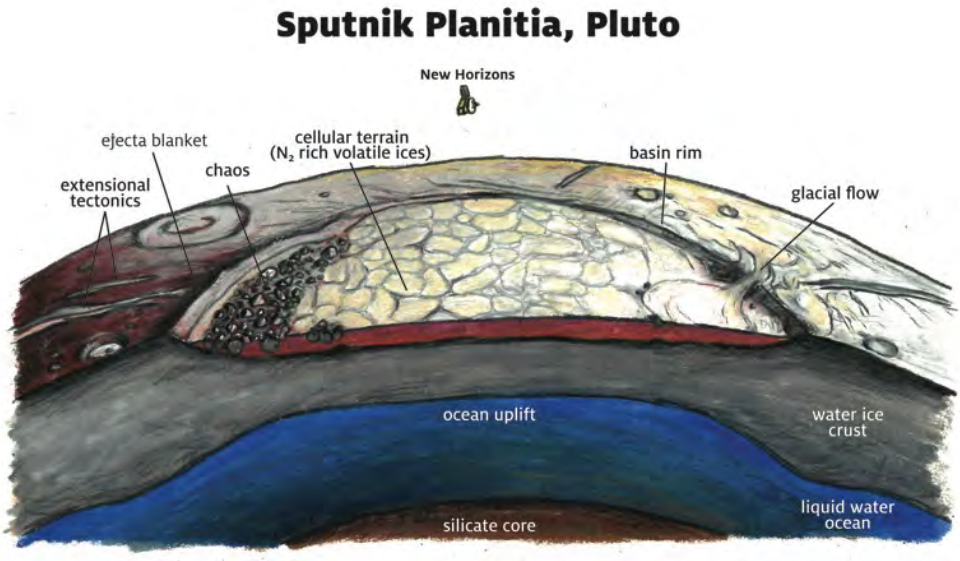

Figure 3-17. Notional geophysical cross-section cartoon through Pluto. Topography and fault networks can reveal the past or present existence of a subsurface ocean. (Image credit: James Tuttle Keane, JPL/Caltech.)

be a compelling flyby target for Interstellar Probe for the purposes of filling out the Kuiper Belt census of small planets. Many of the above considerations for Quaoar are the same for other potential target planets. As discussed by Brown (M. E. Brown, 2008; Michael E. Brown, 2012), Makemake, like Quaoar, is also transitional between volatile rich and poor. Haumea, although volatile depleted, is rotating quickly enough (4 hours) to be oblong in dimension while still resting in hydrostatic equilibrium. In contrast to these and the majority of dwarf planets, Pluto, Triton, Eris, and Sedna are volatile rich, offering insights into planetary diversity and formation scenarios

While ground-based observations can survey large populations of KBOs to study the dynamics of this region of our solar system, they are limited by what diffraction-limited optics and Earth-based geometry allow. For objects in the Kuiper Belt, this means that we can only sample the phase angle of an object up to ~2–3° (the angular distance of the Earth's orbit as seen from the Kuiper Belt). Over time, the orientation of these objects changes based on their long-term (>200 year) orbits around the Sun; however, the observational angular limits remain the same. As a spacecraft traverses different regions of our solar system, it has the ability to observe KBOs and other objects from much larger phase angles, allowing us to better sample the surface properties; e.g., the reflection of sunlight off a smooth or rough surface can change drastically with solar incident angle (A. Verbiscer et al., 1990; A. J. Verbiscer & Veverka, 1990, 1992). The New Horizons mission has made great use of this technique by observing nearly 25 KBOs at extended phase angles (Porter et al., 2016). In fact, New Horizons has used phase angle observations to sample all of the different dynamical classes of KBOs (classical circular orbit objects, objects in mean motion resonances with Neptune, and scattered objects) as well as objects of differing sizes (dwarf planets as well as ~30-km KBOs). Clearly, the Kuiper Belt-based observations of 25 objects are a small sample of the projected 10^4 100+-km objects in the Kuiper Belt (Petit et al., 2008), but they are a solid start.

Likewise, observations from spacecraft are not limited by the day-night cycle of the Earth. This is true for orbiting satellites as well as planetary missions, but fundamentally, observations over time, unhindered by the day/night cycle, allow us to obtain an unbiased measurement of object light curves far from the Sun to better understand their true angular momentum properties. They also allow us to determine general shape and, under the right conditions, to identify contact or resolved binaries. The latter provides significant constraints on formation models because they are observed in the current Kuiper Belt and must have either been created recently (unlikely based on the physics of the objects observed) or survived during dynamical mixing caused by migration of the giant planets.

3.2.1.3. Opportunities for Giant Planet Flybys

Although Jupiter and Saturn have both had dedicated orbiting missions (Galileo and Juno at Jupiter and Cassini at Saturn) a number of non-incremental science goals can be achieved from a fast flyby such as that provided by Interstellar Probe, and unique science can also be achieved by looking back at these objects from the distant solar system. The Jovian magnetosphere is by far the largest object in the solar system, with a magnetotail that stretches out to the orbit of Saturn. This enormous magnetosphere is continuously being mass loaded by plasma originating from the volcanic moon Io, which leads to closed magnetized regions of plasma being centrifugally torn off and escaping down the magnetotail. While such "plasmoids" are known to exist, their large-scale morphology and motion have eluded previous spacecraft because of their slower speed and trajectory. The fast Jupiter flyby by the New Horizons spacecraft in 2007 provided novel interpretations of this mass loss down Jupiter's enormous magnetotail region that could never be studied from the relatively slow (and relatively near planet) orbiting platforms (D. J. McComas et al., 2007). A Jupiter gravity assist (JGA) by an interstellar probe would provide an even faster snapshot through the Jovian magnetotail, depending on the exact maneuver required to best achieve a high asymptotic speed out of the solar system. By nature, an interstellar probe would carry dedicated fields and

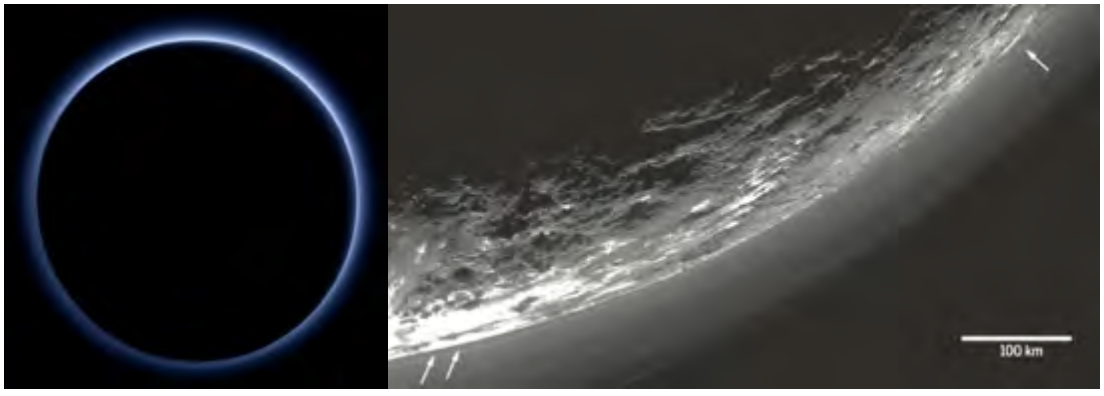

Figure 3-18. (Left) Forward scattering of sunlight by haze (likely tholin) particles in Pluto's atmosphere produces a blue plutonian solar eclipse (image credit: NASA PIA19964). (Right) Haze layers detected in Pluto's atmosphere by the LORRI camera, where the arrows show a haze layer 5 km above the ground (left) intersecting the ground at right (reprinted from Gladstone et al. (2016) with permission from AAAS).

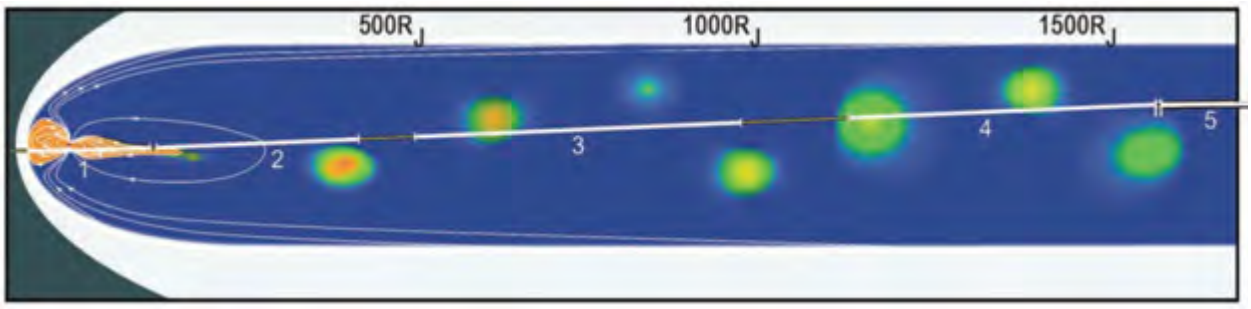

Figure 3-19. Schematic diagram of a meridional cut through Jupiter's magnetotail (top) shows the plasma disk near Jupiter and notional large plasmoids (colored) moving down the tail, past New Horizons. This is from just after New Horizons' inbound crossing of Jupiter's magnetopause late on day of year 56, 2007, through closest approach at ~32 R_J, and back down the magnetotail to >2500 R_J (reprinted from D. J. McComas et al. (2007) with permission from AAAS).

particle instrumentation, which would reveal several important details about the magnetotail structure and dynamics that the payload of New Horizons could not.

Other Jovian targets include the enigmatic moon Io where New Horizons also observed active eruptions of volcanoes (Spencer et al., 2007). Io is a challenging target to fly close to because of the high-radiation environment near its orbit around Jupiter and therefore is one of the lesser-studied solar system moons despite being a very high value science target. The fast speed of Interstellar Probe results in a relatively modest total ionizing dose of radiation but still imposes requirements on sufficient background rejection techniques of cameras and instrumentation. This is, as always, a trade-off between science return, mass, and complexity of the instrumentation.

If Interstellar Probe was able to fly past Saturn, it would be the first fast flyby of that planet since the Voyager era, providing a snapshot in time that would complement the Cassini mission data set by, in particular, extending our observations at Saturn to include post-Saturn solstice observations of system activity.

The following table has examples of questions that Interstellar Probe could address at the solar system gas and ice giant planets, along with suggested tests.

Table 3-1. Solar System Planetary Science Questions

Question or Science Goal	Testing Scheme
Giant planets as laboratories to understand the solar system and extrasolar planets	Very distant multispectral time-series imaging of giant planets as single pixels can aid interpretation of similar imaging of exoplanets
Are the 0cean worlds (especially Europa, Io, Ganymede, Enceladus, Triton) active in the coming decades?	Imaging of plumes and/or new surficial deposits
Why are the ice giant magnetic fields so complex, and how do they interact with the solar wind, planetary atmospheres, and satellites?	Magnetometer, ENA cameras, and plasma instrument in situ measurements
Constrain atmospheric heat balance, composition, and dynamics of giant planets	Atmospheric thermal IR or microwave imaging
Are Triton and other moons also ocean worlds?	Magnetometer measurements of any induced magnetic fields

Ice giant planets (Uranus and Neptune) are the only major category of solar system worlds never to have had a dedicated mission and represent one of the largest groups of detected exoplanets (Fulton et al., 2017). We know very little about our own ice giants, and the potential science return from a modern-era spacecraft flyby is immense. White papers submitted to the Planetary Science Decadal Survey 2013–2023 and the Heliophysics Science Decadal Survey 2013–2023 provide a persuasive case for missions to our ice giants (Uranus or Neptune). Three key points highlight the importance of sending a mission to these ice giants. First, they represent a class of planet that is not well understood and that is fundamentally different from the gas giants (Jupiter and Saturn), terrestrial planets, and dwarf planets. Ice giants are, by mass, ~65% water and other so-called "ices," such as methane and ammonia. Despite the "ice" name, these species are thought to exist primarily in a massive, super-critical liquid-water ocean. No current model for their interior structure is consistent with all observations. A second key factor is the importance of Neptune-class planets to exoplanet studies. Third, they might be host to unique types of ocean worlds. Depending on fly-out direction, an interstellar probe could provide very valuable observations during a flyby of an ice giant.

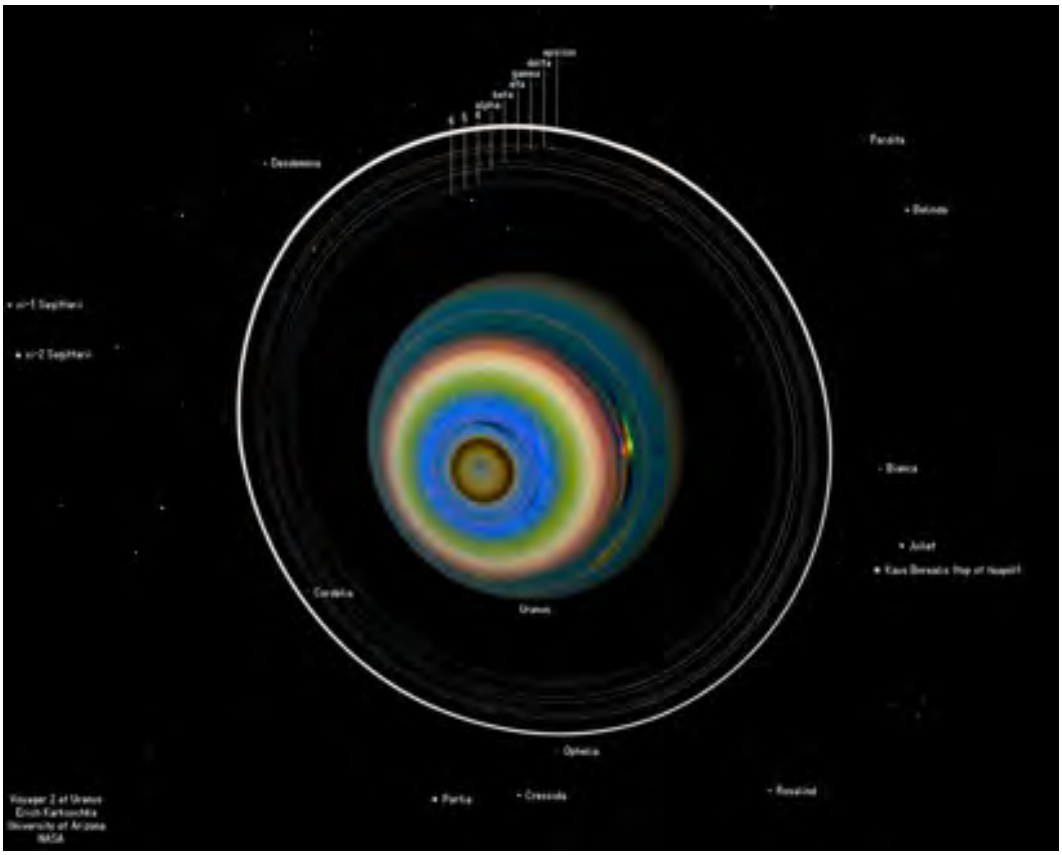

Figure 3-20. The southern hemisphere of Uranus indicates a flurry of previously unknown atmospheric phenomena, hinting at an unusual feature in the interior of the planet (reprinted from Witze (2014) with permission; © 2014 Springer Nature Ltd.).

Naturally the transit time of any planetary flyby would be relatively short. While several days would be spent traversing the inner Jovian system and moons, <10 hours will be spent on the outbound portion after the assist. Similarly, during a potential ice giants flyby, only several hours would be spent traversing the system because these flybys would likely occur after any JGA (or solar Oberth maneuver). Although seemingly short, observations and measurements during gas or ice giant flybys are certain to return science data of high value because of the instrumentation that is much improved over past missions such as Voyager and Pioneer.

3.2.1.4. The Solar System as a Habitable Exoplanetary System

A vantage point far away from the Sun offers a historically unique opportunity to observe the solar system as an analog of exoplanetary systems and would provide critical information to telescope observations of other exoplanetary systems. On 14 February 1990, Voyager 1 captured a series of images of six of the planets from a distance of 40.5 au from the Sun. The assembled series (Figure 3-21) has become known as the "family portrait" of the solar system and represents the only image "looking back" at the solar system from the outside. The famous "Pale Blue Dot" is a part of this image sequence. In November 2010, the MESSENGER spacecraft obtained a similar image of eight planets but from roughly the orbit of Mercury.

These portraits continue to inspire humanity, in particular the Pale Blue Dot that gave rise to the book by the same name by Carl Sagan. With the increasing abundance of exoplanetary systems observed, using the solar system as an exoplanetary analog has become more important, not only for philosophical reasons but also primarily for scientific reasons. Absorption spectra during exoplanetary transits are the primary means of probing atmospheric composition and have led to several discoveries. The reflectance spectrum at different phases as an exoplanet orbits its star potentially could provide information on cloud patterns, continents, and ocean coverage. However, all of today's exoplanetary observations are limited to one-pixel observations and therefore require comparative observations of well-known planets such as Earth, Venus, and Mars (Jiang et al., 2018). Therefore, observations of reflectance and transit absorption spectra of the solar system planets are extremely valuable measurements that will provide critical ground truth for exoplanetary observations. However, observations of transiting solar system planets are rare from

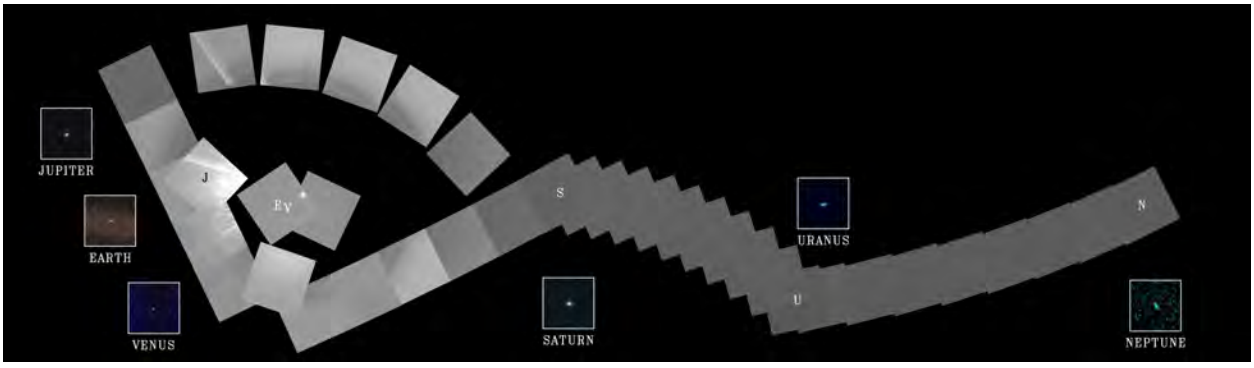

Figure 3-21. The "family portrait" of our solar system was obtained by the Voyager 1 mission on 14 February 1990 from a distance of 40.5 au. The famous image of Earth—"Pale Blue Dot"—is a part of this series. (Image credit: NASA JPL.)

Earth. For example, Venus transits are generally only visible from Earth every 243 years (with the last in 2012) and have provided a wealth of data on that type of planet as an exoplanet. Direct (reflectance) observations of Earth have only recently been made by the DSCOVR satellite (see, for example, Figure 3-22, left), where the resolution was degraded to resemble an exoplanet in order to better understand how Earth-like planets are manifest as exoplanets.

This type of analysis is vital in helping us to understand the increasing wealth of information from telescopes such as Kepler, TESS, and the James Webb Space Telescope—not forgetting of course the increasingly powerful ground-based arrays and radio interferometers. An interstellar probe leaving the solar system would be an appropriate platform from which to provide both direct and transit observations of solar system planets. Because of their relatively short orbital periods, the inner planets of our habitable zone (Venus, Earth, Mars) lend themselves to direct reflectance spectra to help guide identification of cloud patterns, ocean and continents, and more, as outlined by, for example, Jiang et al. (2018). Absorption spectra during transits would contribute to better interpretations of exoplanetary atmospheric composition measurements.

3.2.2. The Circumsolar Debris Disk: A Window to Planetary System Formation

Planetesimal belts and dusty debris disks are known as the "signposts of planet formation" in planetary systems. The overall brightness of a disk provides information on the amount of sourcing planetesimal material, while asymmetries in the shape of the disk can be used to search for perturbing planets within the system or external forces from outside the system such as interstellar gas. Our solar system is known to house two such belts, the asteroid belt and the Edgeworth-Kuiper Belt (EKB), and two debris disks sourced mainly by planetesimal collisions and comet evaporative sublimation.

However, the overall structure of the solar system's debris disk is poorly understood in toto because we live inside of it; e.g., how much dust is produced from the EKB is not well understood because the near-Sun comet contributions dominate near-Earth space and only one spacecraft,

Figure 3-22. (Left) An image of Earth captured by the DSCOVR satellite (image credit: NASA). (Right) Artist's impression of a rocky planet transiting across a red dwarf star (image credit: European Southern Observatory/L. Calçada).

New Horizons, has ever flown a dust counter through the EKB (Horányi et al., 2008; Piquette et al., 2019). Understanding how much dust is produced in the EKB would give us a much better idea of the total number of bodies in the belt (especially the smallest ones) and their dynamical collisional state (K. N. Singer et al., 2019). Even for the inner zodiacal cloud, questions remain concerning its overall shape and orientation with respect to the ecliptic and invariable planes of the solar system; they are not explainable from perturbations caused by the known planets alone (Stenborg & Howard, 2017).

Understanding the large-scale structure of our circumsolar debris disk has become even more important with the increasing number of groundbreaking images of circumstellar disks and PPDs by the ALMA observatory (Isella et al., 2016). Together with the detailed information of the dynamics, composition, and mass distribution of the solar system bodies, knowledge of the large-scale structure of the circumsolar debris disk would provide the needed critical model constraints to make a dramatic leap in our understanding of planetary formation in general.

3.2.2.1. Composition and Structure of the Circumsolar Dust Cloud

Dust grains of the inner solar system have undergone extensive study and are sourced primarily from the Jupiter-family comets (JFCs) with small contributions from asteroids and both Halley-type comets (HTCs) and Oort-cloud comets (OCCs) (see Figure 3-23) (Nesvorný et al., 2010b; Nesvorný, Janches, et al., 2011; Nesvorný, Vokrouhlický, et al., 2011; Pokorný et al., 2014; A. R. Poppe et al., 2019). In comparison, the dust distribution in the outer solar system beyond ~5 au is not as well constrained. Here, dust grains are most likely dominated by the sources in the EKB with additional contributions from comets (Kuchner & Stark, 2010; Landgraf et al., 2002; Andrew R. Poppe, 2016; A. R. Poppe et al., 2019). Several processes act on the transport of dust through the outer solar system, including gravitation, solar wind and Poynting-Robertson drag, and stellar radiation pressure (Burns et al., 1979; Gustafson, 1994). Trapping of grains born from the EKB may occur through mean motion resonances with Neptune as the dust grains migrate inward (Liou & Zook, 1999). When grains eventually break free from these resonances, they continue to diffuse inward, where they can either be gravitationally ejected from the solar system by one of the giant planets or reach the inner solar system.

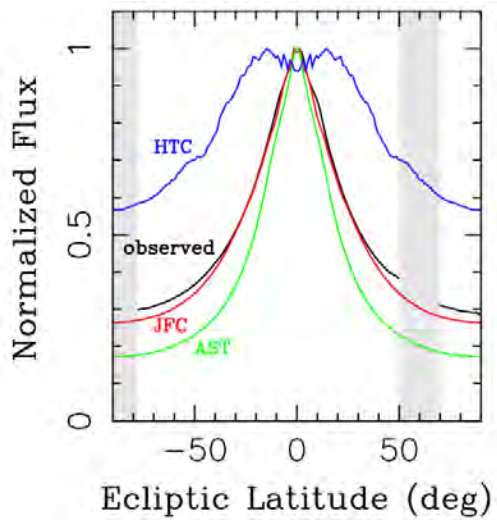

Figure 3-23. Comparison of the JFC (red), HTC (blue), and asteroidal (AST) model with IRAS 24-µm observational normalized flux curves versus ecliptic latitude (reprinted from Nesvorný et al. (2010b) with permission; © AAS).

Infrared Astronomy Satellite (IRAS) and Cosmic Background Explorer (COBE) scans, Infrared Space Observatory (ISO) and Spitzer spectroscopy, and visible data on scattered zodiacal light (Hahn et al., 2002; Kelsall et al., 1998; Nesvorný et al., 2010a; Rowan-Robinson & May, 2013) have generated many theoretical models for the spatial distribution

of zodiacal dust as well as suggestions as to its origins and composition (e.g., Figure 3-24). These models must explain the "Zody band" structures associated with asteroid collisional families, the strong ecliptic-plane-to-ecliptic-pole surface brightness decrease, and the asteroid-like spectrum for the Zody band found in the near-IR that shifts to a comet-like dust thermal emission spectrum in the mid-IR (Tsumura et al., 2010). Typically, these models incorporate a fan-like structure with the dust density following both a radial power law and an exponential vertical distribution with scale height increasing with radial distance from the Sun. Grain properties include a variety of sizes (5–100 µm) and compositions (Reach et al., 2003); however, numerous questions remain. These "fan" models show that the cloud consists of a combination of cometary dust, dust originating in the asteroid belt, and dust entering the solar system from the ISM. Rowan-Robinson and May (2013) found a ratio of 70%:22%:7.5%, respectively, for these three components (Figure 3-24). By contrast, Nesvorný et al. (2010b) found that 85–95% of the cloud comes from JFCs, with the remainder from main-belt asteroids and OCCs. More importantly, little is known about how these contributions vary with distance from the Sun, particularly on the far side of the asteroid belt. Indeed, at 4 au, the Rowan-Robinson and May (2013) results are inconsistent with direct measurements of dust concentration from the Ulysses spacecraft by a factor of 10. Today, it is still not known whether the basic composition of EKB grains is similar to that of KBOs, and thus conforms to our understanding of solar system formation. Several important questions remain unanswered, such as the processes acting on grains after their creation, and the presence of organics.

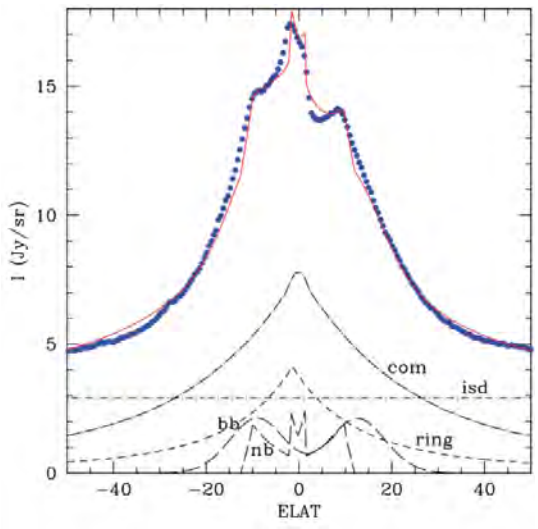

Figure 3-24. Comparison of IRAS 25-µm scans to various model components of interplanetary and interstellar dust (Rowan-Robinson & May, 2013).

Thus, Interstellar Probe represents a unique opportunity to examine the structure of the zodiacal cloud as a function of distance from the Sun. The dust cloud will diminish in brightness by almost a factor of 100 between 1 and 10 au at visible and IR wavelengths because of the combined decline in IPD density (Figure 3-25a), solar irradiation, and grain temperature (from ~270 K at 1 au down to ~85 K at 10 au; Figure 3-25b). In particular, an interstellar probe instrument could measure the falloff in zodiacal brightness between 0.5 and 50 µm as Interstellar Probe voyages outward and would help us to quantify the contributions of these different dust components. Of particular importance will be monitoring the brightness while Interstellar Probe traverses and exits the asteroid belt and Kuiper Belt. A modest spectrophotometric capability using selected medium- or narrow-band filters could also probe dust grain composition as a function of distance. Determining the ratios between different dust sources (e.g., asteroid, JFCs, KBOs, OCCs, and ISM dust) and their variation with distance would provide important constraints on the ongoing production of IPD.

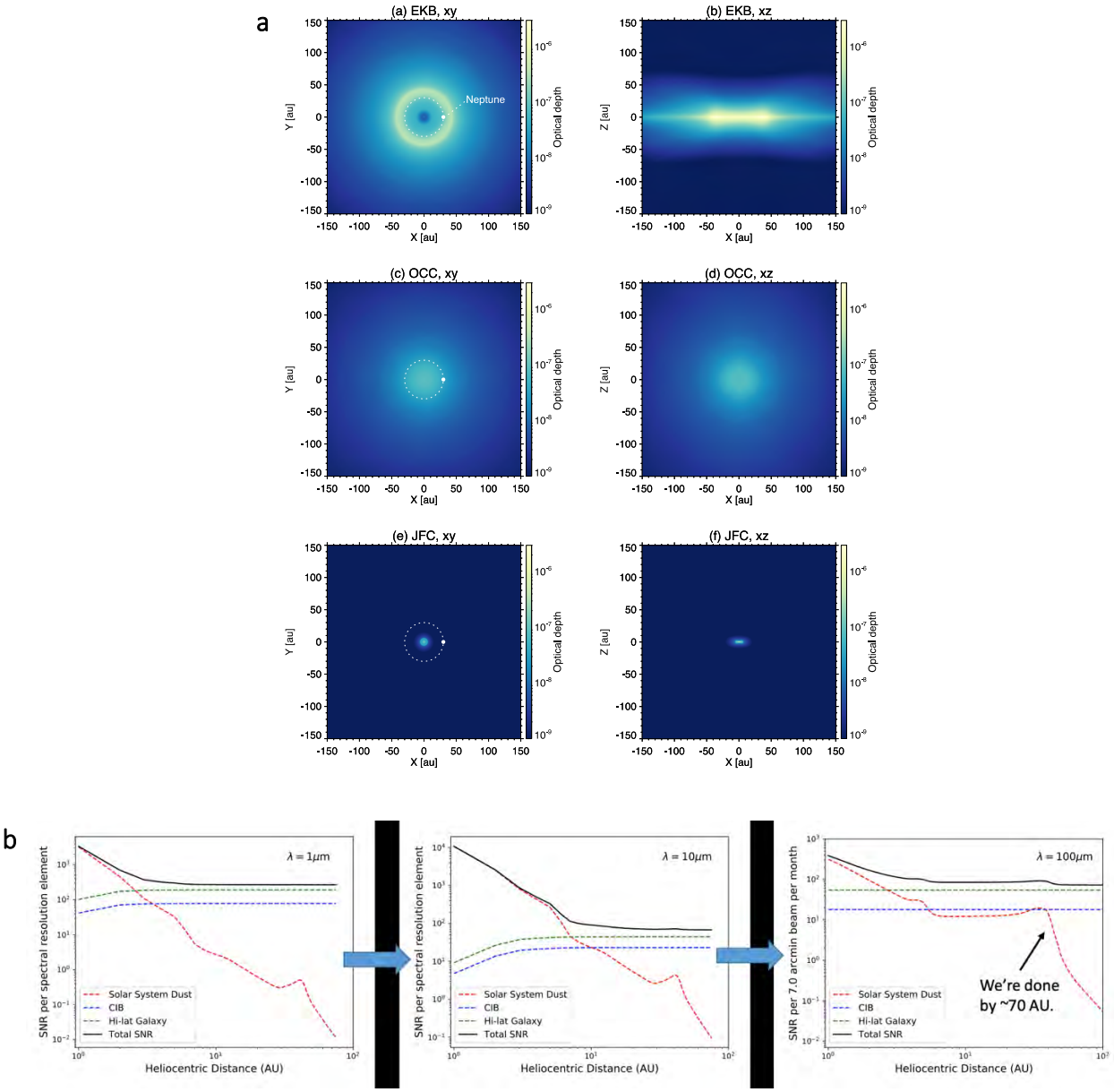

Figure 3-25. (a) Predicted dust cloud morphologies arising from solar system JFCs and OCCs as well as Kuiper Belt (EKB) sources (Figure courtesy of A. Poppe; A. R. Poppe et al. (2019)). (b) Estimated sky fluxes from the solar system dust cloud, the galaxy, and the CIB as a function of Interstellar Probe's distance from the Sun at 1, 10, and 100 μm.

Information about the large-scale structure of the circumsolar dust disk could be obtained in two ways: by pointed lookback IR measurements once the spacecraft is far outside the zodiacal cloud and via continuous IR measurements during the outbound trajectory. The latter technique would require repeated LOS mapping of the hemisphere forward of 90° solar elongation at different heliocentric distances. This would provide brightness measurements of the cloud from a continually changing vantage point, until the signal ultimately vanishes as Interstellar Probe exits the cloud. With appropriate inversion techniques (such as the Radon transform used in magnetic resonance

imaging), one would be able to extract unprecedented 3D maps of the zodiacal dust distribution and produce revolutionary new constraints for current physical models of the cloud, particularly beyond 5 au.

Finally, knowledge of the Zody cloud's large-scale structure not only would provide insight into current solar system processes that generate and subsequently shape the cloud but also would help inform us about ancient solar system evolutionary events such as giant planet migration and planetesimal scattering (as in the late heavy bombardment [LHB]) and could conceivably put constraints on the presence (or absence) of any undetected (to date) far outer solar system bodies (like Planet X).

3.2.2.2. The Circumsolar Debris Disk Versus Protoplanetary Disks

Since their initial discovery by IRAS in 1983 (Aumann et al., 1984), hundreds of circumstellar disks around nearby stars have been revealed by Wide-field Infrared Survey Explorer (WISE), Spitzer, Herschel, and HST spectrophometry and now ALMA and Large Binocular Telescope Interferometer (LBTI) interferometry (Wyatt, 2008). They are seen around stars of all ages. For example, the HL Tauri system shows a remarkable PPD ring and gap structure, indicative of already solid planetary bodies in formation in a system that is likely less than 0.1 Myr old (Akiyama et al., 2016). Other observations show likely gas-giant formation in action in young (1–5 Myr old) gas-rich disks like HD 100546 (Grady et al., 2001). The images of older, gas-poor disks like HR 4796A (~10 Myr old), HD 32297 (~30 Myr old), and Fomalhaut (~440 Myr) show a well-developed, one-ring structure far from the central star, which begs the question: Is this a common feature of more mature systems such as our own solar system at 4.571 Gyr old, or is it due to the slow rate at which A-stars form planets? The mature Eta Corvi system at 1.4 Gyr is highly anomalous because of its very bright Kuiper Belt debris disk ring coupled with inner system primitive dust, suggesting an ongoing LHB-like event is occurring (Lisse et al., 2012; Marino et al., 2016). Overall, models suggest disks formed from the Kuiper Belt are common but those formed from asteroid belts are rare (Patel et al., 2014; Schneider et al., 2018); whether this is a selection effect resulting from the sensitivity of present-day instrumentation or the simple fact that all systems formed with an outer edge to their PPDs, and hence an outer Kuiper Belt (while inner stable asteroid belts require unusual and rare planetary orbital stability conditions), remains to be determined.

Recent results from the LBTI survey (Ertel et al., 2018; Ertel et al., 2019) suggest that the typical debris disk density around mature stars like the Sun is in the 5–10 "Zody" range, where 1 Zody is equivalent to the current solar system zodiacal cloud brightness at 11 μm. While this is good news for efforts attempting to directly image planets around other stars (in that circumstellar dust is unlikely to create much of a con-

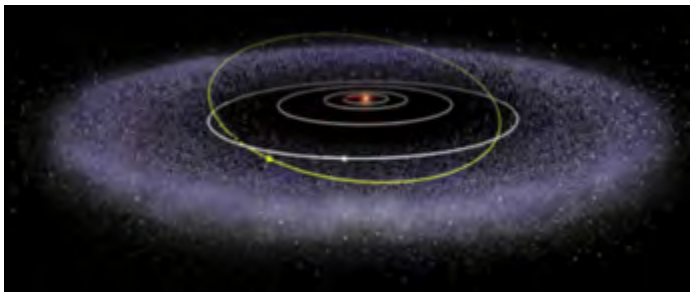

Figure 3-26. IPDs encode chemical diversity of the Edgeworth-Kuiper Belt. (Image credit: ESA/Plank.)

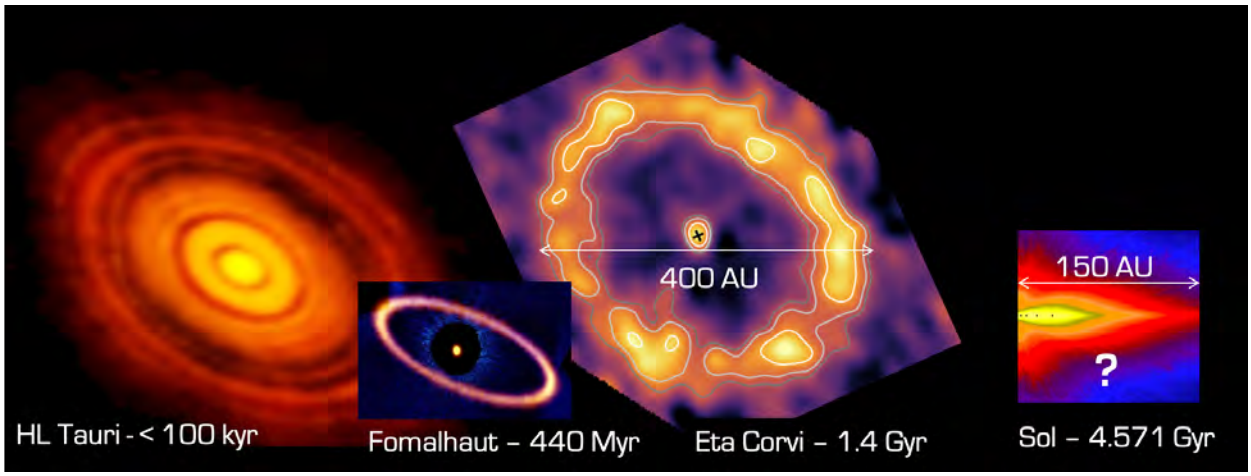

Figure 3-27. The ALMA observatory has begun to deliver a wide range of sensitive, high-spatial-resolution images of circumstellar disks that are completely revising our understanding of when and how planets around stars are formed. The systems range from extremely early planetary formation in PPD systems like HL Tauri (likely less than 100,000 years old), to the older Eta Corvi system (1.4 Gyr old) with its bright circumstellar Kuiper Belt debris disk and inner system belt. The large-scale structure of our own circumsolar debris disk (right) is largely unknown because all remote observations have been made from inside the dust cloud where the foreground IR emissions obscure the larger picture, while only one dust counter, New Horizons/Student Dust Counter, has ever been flown past 10 au from the Sun. (Image credit: NASA.)

founding background signal versus the starlight reflected and reemitted from an exoplanet), it also suggests that our own system is dust-deficient. Is this true, and if so, is it because our system is "planet-rich," and planets efficiently clean out the local dust reservoirs, like the Kuiper and asteroid belts, as Greaves and Rice (2011) have argued, or is it because the solar system never suffered much planetary migration, and therefore never created a huge amount of relic dust sources to create a dense debris disk (Meshkat et al., 2017)? The answer to these questions bear on whether nearby Sun-like systems like Tau Ceti (G8V, ~6 Gyr old), with denser Kuiper Belts than ours, could have harbored life-bearing planets (Greaves et al., 2004).

Enabled by a purpose-defined spectrophotometric imaging and in situ dust sampling instrument suite and its trajectory through all of the known solar system debris disk sources, Interstellar Probe would make a groundbreaking contribution to our understanding of the zodiacal cloud's structure, composition, and sourcing, finally providing us with local ground truth good enough to interpret exodisks. With this in hand, we will have a new ability to understand the past and present of an exosystem, to remove the exosystem foregrounds from exodisks that can interfere with the detection of exoplanets. Lastly, characterizing the dust environment is of decisive importance for the feasibility of launching small, high-speed spacecraft ("chipsats") beyond the solar system, where dust impacts would deliver detrimental amounts of energy.

3.3. The Universe beyond the Circumsolar Dust Cloud

3.3.1. Understanding the Infrared Sky

Earth's atmosphere presents a daunting foreground to measurements of the faint and diffuse emission from our cosmos. Glow from the night sky is typically orders of magnitude brighter than that from the diffuse astrophysical background, and at some wavelengths, observations are precluded entirely (Leinert et al., 1997). Even early in the space age it was known that such measurements would need to be performed from space, whether using suborbital or orbital platforms (Berkner et al., 1961). The advent of cryogenically cooled telescopes in space, first IRAS, which launched in 1983 (Beichmann, 1988), and then COBE, which launched in 1989, gave us our first detailed views of the IR sky. IRAS found that the local IPD cloud as traced by the zodiacal light has a characterizing temperature of ~270 K and a mean optical depth toward to ecliptic pole of ~10^{-7} (M. G. Hauser et al., 1984), and the COBE/Diffuse InfraRed Background Experiment (DIRBE) instrument allowed detailed models of the local IPD cloud to be made both at wavelengths where the emission is scattered sunlight ($\lambda < 3.5$ μm) and in thermal emission ($\lambda > 3.5$ μm; (Kelsall et al., 1998).

It quickly became apparent that, at most IR wavelengths, understanding the component of astrophysical emission from outside our solar system would be a demanding task. The zodiacal light is a bright position- and time-varying source of emission whose spectral and spatial morphology challenges measurement of large-scale structure in the light from our and other galaxies. Its brightness has historically contributed to significant uncertainties and errors not only in our determination of the aggregate light from the extragalactic universe but also in our understanding of the LISM and interstellar radiation fields (Zemcov et al., 2018).

Measurements from within Earth's 1-au orbital separation from the Sun are embedded within the local zodiacal dust cloud and offer only a single, obscured point from which to observe. Escaping the inner solar system and making observations far from the bright light of the Sun can offer significant advantages requiring only modest telescopes (Zemcov et al., 2018). The Interstellar Probe presents humanity's first real opportunity to design and optimize astrophysical instrumentation for which the problems associated with a 1-au vantage point could be eliminated, and so truly open our understanding of the faint and diffuse universe for the first time.

3.3.2. How Did Galaxies Form and Evolve in the Universe?

The formation of stars in galaxies throughout the universe's history is accompanied by the release of photons from both gravitational and nuclear mechanisms (Cooray, 2016; Michael G. Hauser & Dwek, 2001). This diffuse background, called the extragalactic background light (EBL; Figure 3-28), is present at all wavelengths where we have looked, and different wavelength regimes offer important insights into a variety of physical emission mechanisms in the universe. Diffuse cosmic

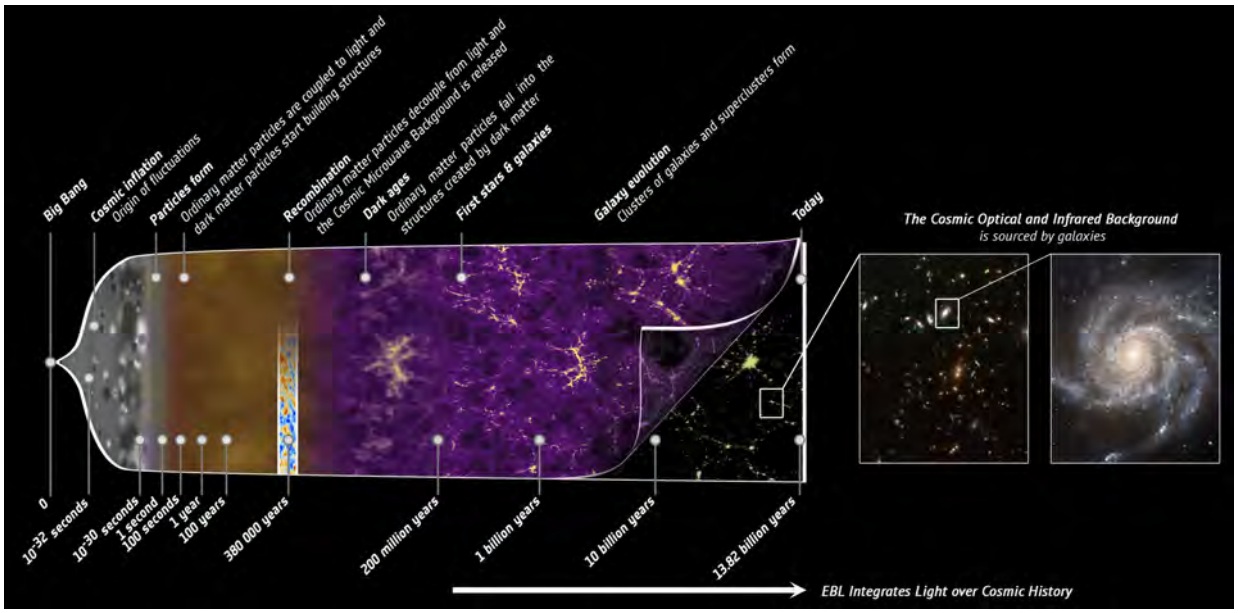

Figure 3-28. The EBL in the context of cosmic history. The EBL integrates all photons emitted throughout the history of the cosmos and thus is a tracer of large-scale structure formation, galaxy assembly, and fundamental physics. The cosmic optical and IR backgrounds are produced by stars and galaxies in the universe and thus trace emission all the way from the epoch of reionization to today. We can constrain the total light from galaxies by counting galaxies in deep images, as shown at left, but also by observing their aggregate emission without the need to resolve them into individual sources of emission. (Figure adapted from ESA/Planck.)

background radiation in the optical and IR parts of the electromagnetic spectrum sourced by the formation of and emission from stars is an expected relic of galaxy assembly (Low & Tucker, 1968). Measurements of the EBL at these wavelengths provide insights into large-scale structure formation, the history of nucleosynthesis, and even beyond-standard model physics in the universe.

At the shorter end of the IR regime into optical wavelengths, the EBL is largely sourced by starlight in galaxies near the peak of their characteristic blackbody emission at 0.5–2 μm. This emission is integrated over the history of galaxies at redshifts (z) < 5 and thus appears as a broad spectral feature in the range 1–10 μm. The EBL at these wavelengths is usually called the cosmic optical background (COB). Light from star-forming regions as reprocessed by dust grains in galaxies also sources an approximately thermal background at mid-IR to FIR wavelengths. This is known as the cosmic infrared background (CIB; Figures 3-29 and 3-30), and it is a probe of the aggregate star formation of the universe integrated over time. Together, the COB and CIB trace the emplacement and lives of stars over cosmic history.

There are a number of ways to constrain the EBL at these wavelengths. One possibility is to count the number of galaxies as a function of brightness in a particular region of the sky (Helgason et al., 2014). This method only ever produces a lower limit to the emission because it relies on the assumptions that (1) the survey in question has found all galaxies, no matter how faint or diffuse, and (2) all photons in the universe are sourced in resolved galaxies. Because we have recently

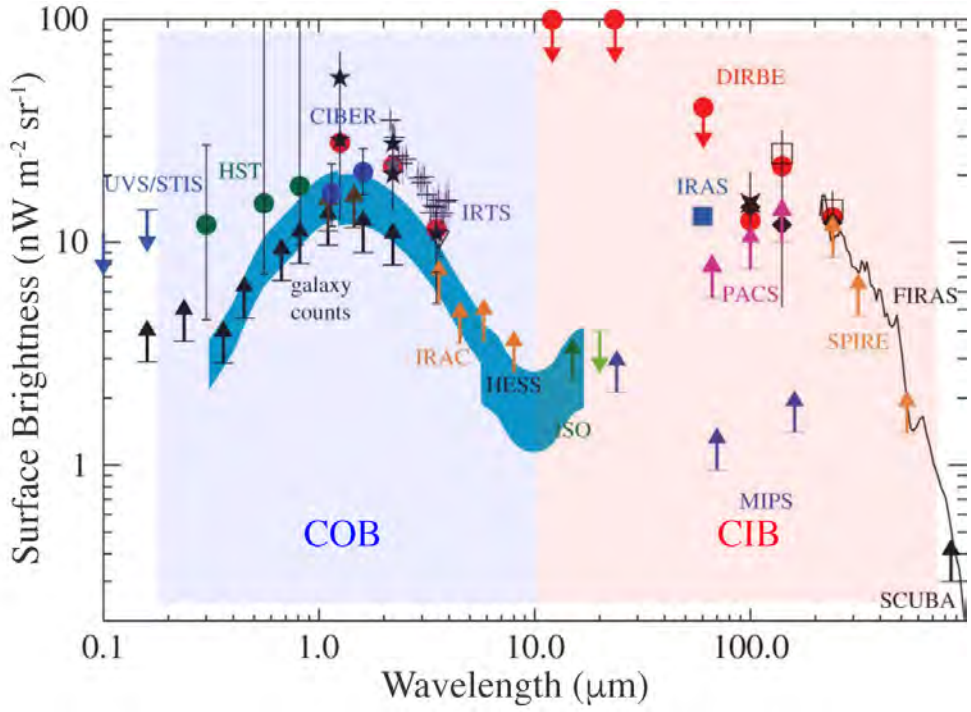

Figure 3-29. Energy density of diffuse backgrounds in the universe, showing the release of energy from star formation in the optical (COB) as reradiated energy in the IR (CIB). Our current direct photometric measurements at λ < 200 μm are strongly contaminated by zodiacal light and require significant understanding of this complex foreground to interpret. A definitive measurement would come from a capable instrument operating in the distant solar system where the light from local dust is much fainter than these extragalactic backgrounds. (Figure adapted from Cooray (2016).)

found large populations of faint and diffuse galaxies (van Dokkum et al., 2015), and there is evidence for significant populations of stars cast out of galaxies as well (Zemcov et al., 2014), both of these assumptions can be questioned. A second method of determining the brightness of the COB/CIB is to use pair production of γ-rays (Stecker et al., 1992). High-energy photons can interact with lower-energy photons and produce electron-positron pairs in the universe, and as a result, high-energy γ-rays see the EBL as an attenuating "fog" in the universe. Over cosmological distances, significant fractions of γ-ray photons are converted to electron-positron pairs and are lost from a source's spectrum. By comparing the observed spectrum of a blazar source to an estimate of its intrinsic spectrum, the strength of the attenuation can be measured. This effect has been successfully used to infer the brightness of the COB/CIB in the past (e.g., HESS Collaboration, 2017; Acciari et al., 2019). However, it is also prone to uncertainties from assumptions that are difficult to quantify (Dwek & Krennrich, 2013). First, we must assume we understand the intrinsic spectrum of the γ-ray source, which because of the presence of complex particle physics is challenging. Second, some shape for the EBL must be assumed, and priors based on galaxy counts or other information must be placed on the COB/CIB to be constrained. Although these assumptions can be managed, it is very difficult to place fully understood uncertainties on the results.

The only assumption-free method to measure the COB/CIB is to perform direct photometry on the background. In this method, a small-aperture telescope is used to measure the absolute brightness of a patch of sky. Stars and other local sources of photons are masked or otherwise removed from the estimate, and multiple fields are imaged to show that the residuals are isotropic on the sky. If local sources of emission have been properly accounted, the resulting signal is a measurement of the COB/CIB. The primary importance of these direct EBL measurements is that they provide a *cosmic consistency test*, wherein the total number of photons observed through photometry can be compared with the number inferred from galaxy counting or γ-ray attenuation. If the assumptions and foregrounds inherent in all of these methods have been properly accounted, they will agree. More interestingly, a verified disparity between such measurements can provide evidence for new sources of photons in the optical and IR parts of the electromagnetic spectrum, which includes relatively prosaic causes like stars outside of galaxies or very early populations of galaxies, or the possibility of more profound physics like dark matter decay and Lorentz violation in high-energy sources.

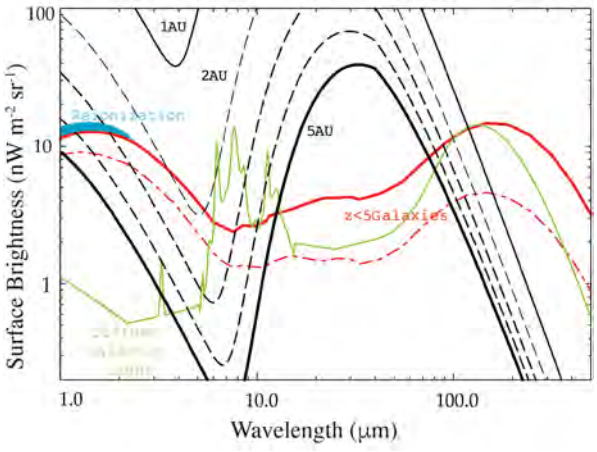

Figure 3-30. Predicted energy density of the combined COB and CIB (solid red line), the foreground from interplanetary dust (black lines) and diffuse galactic light at high galactic latitudes (green line), and the predicted contribution from reionization (teal region). The reduction in the interplanetary dust foreground is shown as a function of heliocentric distance from 1 to 5 au. Beyond Jupiter, the reionization signal is larger than the dust foreground and can be isolated from z < 5 galaxies. (Figure adapted from Cooray (2016).)

As an example of the power of these kinds of measurements, we can look to very-long-IR wavelengths where local foregrounds are faint and we have a relatively unobscured view of the EBL. The Planck and Herschel missions, in combination with a variety of ground-based data, have been used to probe the redshift distribution of the CIB emission, which is determined by the redshift distribution of the emitting galaxies, their dust content, and the history of structure formation in the universe (Korochkin & Rubtsov, 2018). In this method, fluctuations in the CIB are compared with other tracers of large-scale structure in the cosmos, for example gravitational lensing (Omori et al., 2017), to determine the common components and the history of the emission. This approach offers us the ability not only to check the consistency of the aggregate emission through direct photometry of the CIB but also to disentangle its emissive history from cosmological structure formation and other astrophysical factors of interest.

At shorter wavelengths, our own zodiacal cloud obscures our view of the visible and near-IR CIB. Even in space, the zodiacal foreground is at least 10 and at some wavelengths 1000 times brighter than the COB/CIB, and properly accounting for this foreground is challenging. Although some progress has been made in the optical and into the near-IR (Kalevi Mattila & Väisänen, 2019), in the mid-

IR this kind of observation is virtually impossible from the Earth's 1-au orbit. As a result of misestimation of the foreground, the systematic errors of current photometric measurements of the EBL exceed the integrated light from all galaxies outside our own by factors of at least several (K. Mattila, 2003, 2006). Although measurements of the EBL from distant vantage points exist (Zemcov et al., 2017), these have been made with instruments that are not expressly designed for this purpose and have significant systematic errors of their own. A purpose-built instrument designed with systematic error reduction and control in mind could perform a definitive measurement of the COB and CIB and allow us to match the promise of this method in understanding the cosmos. Enabled by its location and trajectory, Interstellar Probe offers the exciting opportunity to open the window to the CIB at wavelengths from 0.5 to 100 μm as it travels outward beyond 5 au.

3.3.2.1. Searching for the Earliest Stars and Galaxies in the Cosmos

The holy grail of COB measurements is the search for emission from the very earliest stars and (proto)galaxies in the universe at $z > 5$. After the release of the cosmic microwave background radiation in the early stages of the universe's history, the cosmos was filled with purely neutral hydrogen and helium that slowly cooled and collapsed under gravity as the universe expanded. Over time, over-densities in this material began to form stellar nurseries in which the first stars in the universe were born. These stars and their offspring are thought to have been very massive and UV-bright, and thus efficiently burned away the neutral gas in a process called reionization. We have strong evidence that the process of reionization was well underway by $z \sim 8$ and essentially complete by $z \sim 6$, but our census of the sources of emission at these high redshifts is woeful. Because large cosmic structures like galaxies take time to evolve, reionization is thought to have been dominated by very faint, small objects perhaps most similar to modern-day globular clusters or dwarf galaxies (Loeb & Barkana, 2001). However, our current techniques to search for these objects are limited to the most massive end of the mass distribution of galaxies (Salvaterra et al., 2011), and these galaxies were not the dominant sources of photons in the early universe.

Interestingly, the process of reionization is thought to produce a diffuse background with a strong spectral feature from Lyman absorption. As a result, emission from the earliest epoch of star and galaxy formation is present in the EBL, redshifted into near-IR wavelengths today. Through careful comparison of a sufficiently precise measurement of the COB to galaxy counts and other constraints, it should be possible to separate the small signal from the epoch of reionization and measure the total emission from all cosmic sources at $z > 5$, regardless of their mass or other characteristics. This kind of measurement will provide a crucial test of models of reionization, including the characteristics of early stars and protogalaxies, the nature and thermodynamics of the gas, as well as its scattering and absorption properties. A properly designed spectral imager on the Interstellar Probe could reach the surface brightness sensitivity and systematic error control necessary to disentangle these various sources of emission and search for the diffuse reionization component of the COB in direct emission for the first time.

3.3.3. Dust in the Milky Way

Through processes similar to those responsible for the zodiacal Light, dust in the interstellar radiation field of the galaxy produces a diffuse glow called the diffuse galactic light (DGL; Leinert et al., 1998). The DGL is present both in scattered light at optical/near-IR wavelengths and in thermal emission at longer wavelengths. At the FIR wavelengths probed by IRAS, DIRBE, and Planck, the galactic emission (typically called cirrus at high galactic latitudes) is well understood. Our understanding of the galactic emission at shorter wavelengths, particularly at high galactic latitudes, is less mature. At near-IR wavelengths, this light is typically very faint, even compared with the EBL, but because it contains a wealth of information about the physical environment where it originates and the dust that emits or scatters it into our LOS, it is worth taking advantage of the opportunity for an unobscured view to better understand it. This is a particularly salient topic in view of measurements at other wavelengths where new forms of emission have been found (Ichiki, 2014) or are required to explain existing results (Zemcov et al., 2014).

At near- and mid-IR wavelengths, the DGL has a rich phenomenology (Draine & Hensley, 2013). It is present in scattering, in emission by diffuse gas, as lit by emission from ions and molecules, and possibly in dust luminescence. By separating the measured emission into different components, we can constrain the size of dust particles in different parts and phases of the ISM, constrain their thermodynamic properties, and understand their chemical makeup and interaction with the interstellar radiation field (Brandt & Draine, 2012). The Interstellar Probe offers a unique vantage point from which to observe dust in our own ISM, and thereby allow us to tie properties in our galaxy to those we find around us in the local and distant universe.

3.3.4. Opportunities for Very Long Baseline Observations: Distribution of Planets and Massive Remnants

Microlensing of distant stars by foreground massive objects is a time-domain technique where abrupt changes in the light curve of a monitor star can betray the presence of (normally invisible) lensing bodies between the source and observer. Microlensing is the most effective method for finding exoplanets beyond the snow line of their stars, which has been a difficult part of parameter space for exoplanet discovery (Figure 3-31). Because this technique does not rely on receiving light from the lensing object itself, it is uniquely sensitive to any massive body, including compact stellar objects (Wyrzykowski et al., 2011) and even free-floating planets (Mróz et al., 2017). The mass and distance of a lensing object are degenerate in point source-point lens events, but this degeneracy

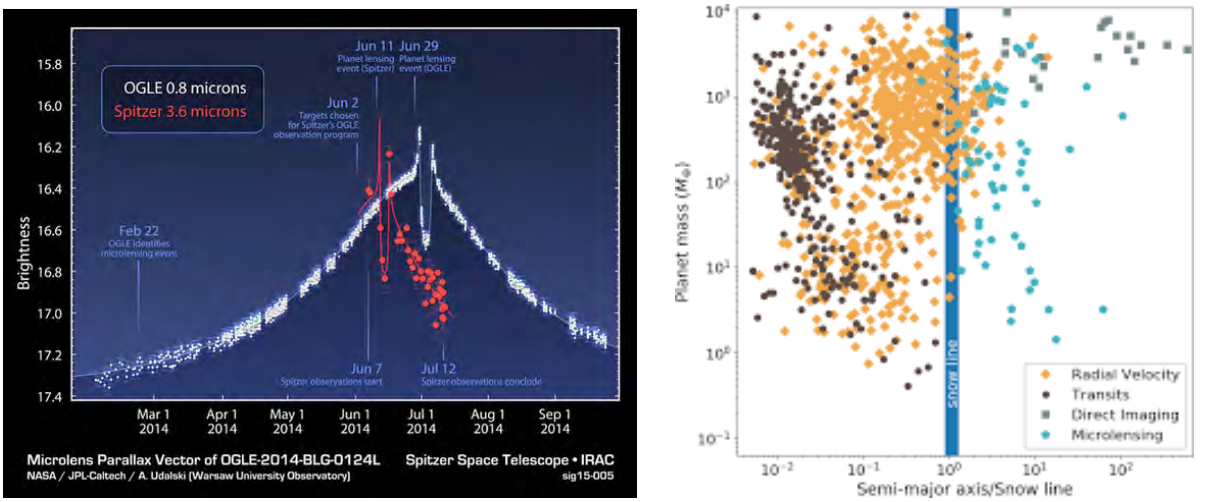

Figure 3-31. Microlensing exoplanet science. (Left) Example of a real microlensing light curve for system OGLE-2014-BLG-0124L. The observed microlensing light curve peak intensity seen by the Spitzer Space Telescope 4 days before the Earth-based OGLE peak was about 0.23 mag brighter, even though Spitzer was about the same distance from the Sun as the Earth. Just the parallax induced by Spitzer being ~50° around the Sun in its trailing orbit was enough to create this much-observed difference between the two measurements; imagine how much different the light curves obtained by the Interstellar Probe at 10, 50, or 100 au from the Sun will be (image credit: NASA/JPL-Caltech/Warsaw University). (Right) Plot of detected exoplanet mass versus exoplanet distance from Earth. Of the current techniques of exoplanet detection, only microlensing can detect exoplanets farther away than 2 kpc, and thus planets around stars in different galactic stellar populations (e.g., bulge stars) than the Sun's (Tsapras, 2018).

can be broken if the event can be measured by observing it from multiple, widely separated locations (Buchalter & Kamionkowski, 1997; Andrew Gould & Loeb, 1992). For events with extremely high magnification, the separation required for this degeneracy breaking is as small as Earth's radius (A. Gould et al., 2009), but these are rare. More commonly, parallax is measured either because the event is long enough for Earth to move in its orbit during the event (Muraki et al., 2011), or by obtaining simultaneous light curves from Earth- and space-based observatories such as Spitzer and K2 (Dong et al., 2007; Street et al., 2016; Yee et al., 2015; Zhu et al., 2017).

To illustrate this, a 1 M_sun object at 4 kpc lensing a source at 8 kpc has a projected outermost radius at the solar system of 4 au. Any observer within this region will see the object lens the source star over the same time frame, although the maximum magnification and time of peak will vary as a result of the different closest approach separations observed from different locations. A unique science case only possible from vantage points far from Earth is to follow up exoplanet lensing events with photometry to break the mass-distance lensing degeneracy (Zemcov et al., 2018). The lens mass to which this method is sensitive changes as a function of heliocentric distance, with planet-mass objects available in the inner solar system and stellar-mass compact objects like neutron stars and black holes available in the outer solar system. For the same parameters as the preceding example, for a 10 M_sun black hole the radius of interest is 25.5 au. A number of theories for the formation of these objects have been proposed, from primordial objects formed soon after

the Big Bang (Carr et al., 2016) to the remnants of stellar evolution (Elbert et al., 2018), but the difficulties of observing non-accreting black holes at large in the galaxy have precluded quantification. Because merging stellar-mass binary black holes are one source of the recent detections of gravitational wave events (Abbott et al., 2016), these studies are salient.

In terms of requirements on an interstellar probe, this science requires either close-to-continuous monitoring of a field in tandem with monitoring from Earth or flagged events from an Earth-based microlensing survey observed in close to real time. Both strategies would be available to an astrophysical instrument on Interstellar Probe but would require either large data telemetry rates or fast command upload and execution to catch events in time. The fields that are usually chosen for microlensing are crowded fields close to the galactic plane, which places significant requirements on the telescope's angular resolution to prevent confusion. Further, this science requires pointed observations that are stable over a several-days-long time frame (at a minimum) and thus would require a very stable platform in terms of both attitude and the detector read chain. In our study, we concluded that a viable strategy for microlensing science would require a >0.3-m optical or near-IR wide-field telescope on a pointed platform. In the inner solar system, we could focus on planetary-mass objects, while in the outer solar system, we could focus on compact stellar remnants, which would require the instrument to be available for science for at least a few years. Although we would not need to point at a given field for months, the trade would need to be that the pointing of the telescope would be commandable within <24 hours. These all place significant engineering requirements on an astrophysical instrument, add significant mass, and are not easily compatible with a spinning spacecraft. Therefore, we conclude that this kind of science may be not be possible with Interstellar Probe as currently envisioned.

3.4. Measurement Approaches

In the following sections, we discuss the possible measurement approaches that could be used to address the science questions presented above. We describe the measurement and mission requirements that derive from these approaches. We summarize the current state of instrumentation and any optimizations that would further improve performance or relax resource requirements. It is important to note that no fundamentally new instrument technology is required to achieve the science discussed above. The groundbreaking science discoveries that await are all enabled by location. An example science payload is presented to frame the range of resource requirements that will directly feed into the science operations, mission architecture, and resulting asymptotic speed. Several trade-offs between science and mission scenarios will be done from this initial starting point.

3.4.1. Magnetic Field Measurements

Measuring the vector magnetic fields in the outer heliosphere and the LISM is critical for understanding the global shape and nature of the heliosphere and its interaction with the ISM. The Voyager 1 and 2 in situ magnetic field measurements in the VLISM revealed smooth but strongly draped field lines. Measurements of the magnetic field strength and direction well beyond the HP are essential to identify the ISMF properties and the detailed mechanisms of how the heliosphere

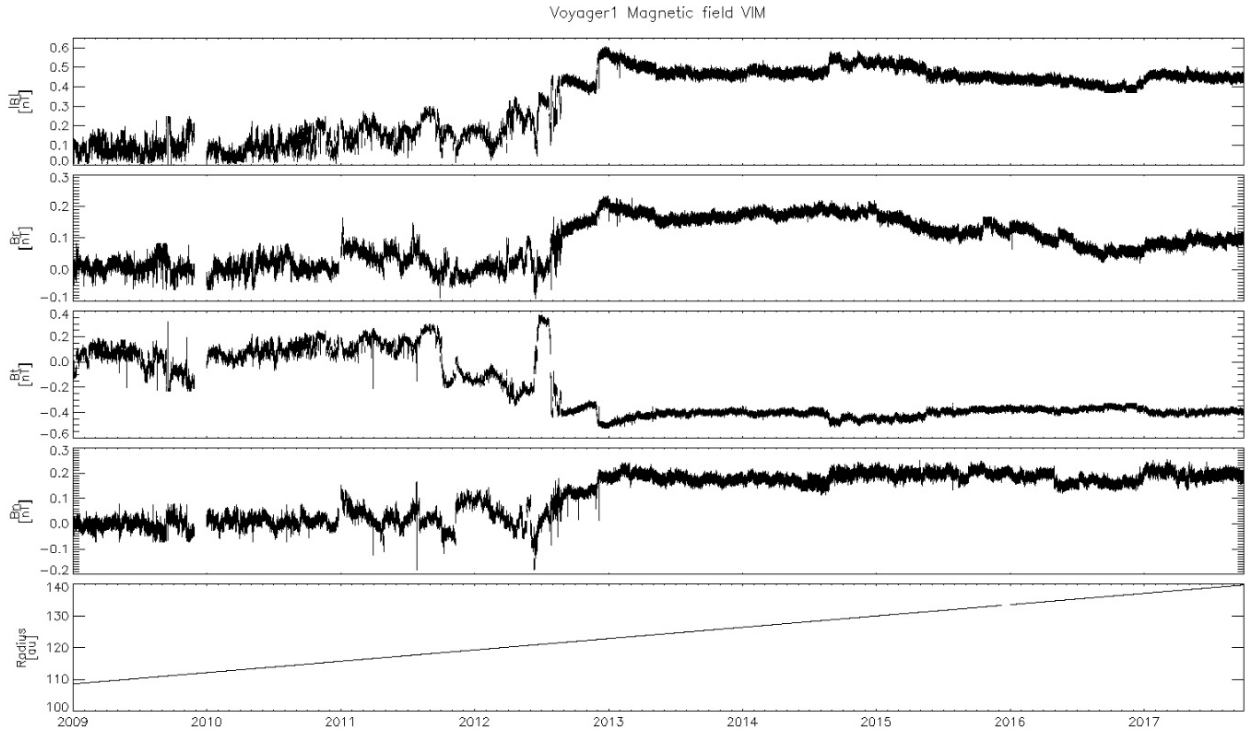

Figure 3-32. Voyager 1 magnetic field measurements from 2009 to 2018 covering both the inner and outer heliosheath. (Image courtesy of A. Szabo.)

interacts with the ISM. Measuring the magnetic field orientation in the LISM is also critical to distinguish between different ribbon generation mechanisms. Magnetic field measurements are also critical to properly understand charged particle properties. The relative angle between the particle propagation and the local magnetic field, known as pitch angle, provides important information on the source and distance of the particle energization.

3.4.1.1. Measurement Requirements

The lowest fields measured by the Voyager spacecraft were encountered in the inner heliosphere and reached as low as 0.05 nT. Therefore, vector components as low as 0.01 nT have to be measured reliably and even lower to address the role of turbulence. To identify the mechanisms responsible for the interaction of the heliosphere with the ISM and determine the pitch angle distribution of charged particles, the full vector magnetic field has to be measured. The outer heliosheath magnetic field has relatively low variability on the 48-second scale of the Voyager measurements (see Figure 3-32). Thus, a uniform 10- to 60-second measurement cadence is sufficient. In addition, traveling through the inner and outer heliosheath requires decades of travel time, necessitating very high temporal stability of the instruments.

3.4.1.2. Mission Requirements

To measure the extremely small magnetic fields of the outer heliosphere, a stringent magnetic cleanliness program has to be implemented for the spacecraft and for all of the instruments. Such a program has been successfully executed recently for the MMS mission (Russell et al., 2016) and

for the outer heliospheric mission Cassini (Narvaez, 2004). To minimize the impact of spacecraft generated fields, the magnetometers are typically placed on a boom away from the spacecraft. The 14-m Voyager magnetometer booms with two fluxgate magnetometers at different distances to observe the differential spacecraft fields were sufficient to reach an accuracy of ~0.1 nT. Occasional spacecraft rolls around the spacecraft-Earth axis provide additional calibration points for two of the three components. The Voyager spacecraft needed to perform such roll maneuvers every 30–60 days to maintain the required accuracy.

3.4.1.3. Current State of Magnetometers

While traditional fluxgate magnetometers are reliable for long-term, low-power operation and can measure the required low field levels at high cadence, they are not providing absolute measurements and require in-flight calibration to deal with their intrinsic drifts. On the other hand, scalar magnetometers provide an absolute measurement with a high sensitivity of 1 pT/√Hz and the absolute accuracy of 0.01-nT magnetometers (Acuña et al., 2002; Gilles et al., 2001), but only at high field strengths (hundreds of nanoteslas), and their long-term operation is still being proven. A dual fluxgate magnetometer configuration such as on Voyager would therefore be a reliable option on an interstellar probe, although low-field scalar magnetometers are being researched.

Table 3-2. Flown Magnetometer Resources and Capabilities

Mission	Instrument	Mass (kg)	Power (W)	Bitrate (bps)	Capabilities	TRL and Heritage	References/Notes
Cassini	Vector Helium + Fluxgate Magnetometer (MAG)	3.2 without boom (1.22 kg scalar, 1.97 kg vector)	6.8 W (2.3 W scalar, 4.5 W vector)	3600	3 axes Dual configuration 0.01–10 nT, 10–60 s Power includes 1-W heater	9	Dougherty et al. (2004) https://solarsystem.nasa.gov/missions/cassini/mission/spacecraft/cassini-orbiter/magnetometer/mag-technical-write-up/ E. J. Smith et al. (2001)
MESSENGER	Magnetometer with 3.6-m boom (MAG)	4.09	5.13	1130	3 axes	9	Anderson et al. (2007) Bale et al. (2016)
MMS	Digital Fluxgate Magnetometer	0.228 (sensor and board)	0.45		Dynamic range: ±650 nT (low range); ±10,500 nT (high range) Non-linearity: <3 × 10^{-5} (low range); <6 × 10^{-4} (high range) Noise density at 1 Hz: <8 pT/√Hz (low range); <100 pT/√Hz (high range)	9	Russell et al. (2016)

3.4.2. Charged Particle Measurements

Among the top scientific objectives of an interstellar probe is the characterization of the complex interactions of the plasma, magnetic field, and neutral interstellar gas taking place from ~30 au (the distant supersonic solar wind), through the heliosheath, out to the pristine ISM. Voyager's in situ measurements of the magnetic field and plasma waves, as well as its observations of charged particles (suprathermal tails, ACRs, and GCRs), provided a glimpse of these phenomena but also uncovered more surprises, as discussed above.

PUIs play a dominant role in the force balance in the heliosheath and are created everywhere by charge exchange of the local plasma with the interstellar neutral gas, both in the LISM and inside the HP. In the inner heliosphere, PUIs are also produced by photoionization and electron impact ionization of the local interstellar gas that is able to penetrate close to the Sun. PUIs are mostly singly charged and have unique velocity distribution functions, with a sharp cutoff at twice the bulk speed of the local plasma. PUIs play a dominant role in the dynamics of the outer heliosphere and LISM because they carry most of the particle pressure (Gloeckler & Fisk, 2015). Their crucial role in the dynamics of the outer heliosphere and the LISM could not be studied with Voyager 1 and 2 because PUIs were and are not measured by those spacecraft. Therefore, it is essential for an interstellar probe to determine the relationship between the thermal plasma and the energetic particles in the LISM as well as identify any other thermal populations over the energy range of tens of electronvolts to hundreds of kiloelectronvolts, where Voyager left a gap at 5–30 keV.

Thermal and suprathermal plasmas (up to tens of kiloelectronvolts) are traditionally measured by electrostatic analyzers (ESAs) to determine the energy to charge (E/q) of the ions. When of time-of-flight (TOF) measurements are added to determine the ion's velocity, the particle's mass, energy, and charge can be uniquely identified.

To determine the energization pathway of ACRs and determine their elusive source, measurements of protons, He, O, and other heavy ions from hundreds of kiloelectronvolts to 1 GeV/nuc as well as their anisotropies are required. GCRs in the 1 MeV/nuc to 1 GeV/nuc range are deflected by the heliosphere, and thus more than 75% of GCRs never reach the inner solar system where they otherwise could affect the chemical evolution of atmospheres. Therefore, it is important for general habitability to understand how an astrosphere shields its planetary system from GCRs. However, GCR anisotropies are sensitive to remote field variations and are therefore used as an effective remote diagnostic of the field configuration of the heliosphere, and once beyond the HP, they provide insight into how the solar disturbances can propagate deep into the ISM (Gurnett et al., 2015; Hill et al., 2019; Krimigis et al., 2013; Rankin et al., 2019). Well into the pristine ISM, where our Sun no longer has direct influence, the vantage point of an interstellar probe would allow spectra of GCRs that are unperturbed by the heliosphere to be obtained and therefore would provide further insight into their source and interaction with the galaxy.

The measurement technique for the high energy ranges of ACRs and GCRs is rather well developed and relies on a stacked solid-state detector telescope. Several such detectors have flown, such as the Solar Isotope Spectrometer on ACE (E. C. Stone et al., 1998). The upper energy range is directly

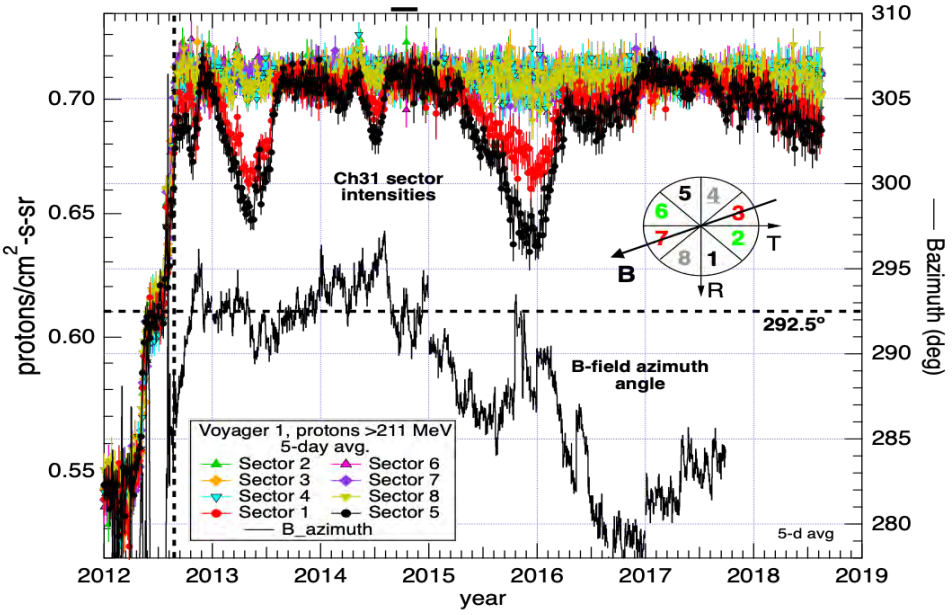

Figure 3-33. Voyager 1 LECP measurements have shown that GCRs can exhibit coherent time-dependent anisotropies in interstellar space. This seems to arise from disturbances that induce mirroring regions that modulate the GCR intensities, resulting in a narrow dropout at 90° pitch angle. (Image courtesy of R. Decker.)

related to mass because material is needed to totally stop the particle in the detector to obtain the measurement. Maximum angular coverage could be achieved by using a spinning platform and multiple telescopes to cover several look directions simultaneously.

While the physics within the heliosphere has been previously addressed with Ulysses/SWICS and ACE/SWICS observations (Allegrini et al., 2005; Geiss et al., 1995; Gloeckler et al., 1992; Gloeckler & Geiss, 1996; Schwadron et al., 2000), lack of full 3D velocity distribution function measurements (i.e., arrival directions of ions) and the small geometric factor of SWICS inhibited the progress and understanding of the particle processes in the heliosphere. For example, neither the origin nor the production mechanism for "inner-source" PUIs has been established (Allegrini et al., 2005; Gloeckler & Geiss, 1996), and while the cosmologically important density of pickup $^3He^+$ was measured for the first time with Ulysses/SWICS (Gloeckler et al., 1992), this value had a large uncertainty.

Table 3-3 below summarizes example specific measurement objectives and their respective measurement requirements.

Table 3-3. Measurement Requirements for Various Charged Particle Populations

Measured Particle Populations	Measurement Requirements
Bulk thermal plasma of the solar wind (SW) or the interstellar wind (IW)	(a) Density, velocity, and parallel and perpendicular temperatures (b) Full 3D velocity distribution functions (vdfs) of H^+ and He^{++} for bulk speeds from ~0 to 1000 km/s
Thermal plasma of SW or IW minor ions	Full 3D vdfs of $^3He^{++}$ and of *high* charge state C, N, O, Ne, Mg, Si, S, A, and Fe for bulk speeds from ~0 to 1000 km/s
Locally created PUIs (interstellar and inner source) from 1 au to the heliopause	Full 3D vdfs of $^3He^+$ and of *singly charged* and *low* charge state He, C, N, O, Ne, Mg, Si, S, Ar, and Fe for bulk speeds from ~0 to 1000 km/s
Suprathermal tails	Full 3D vdfs of H^+, He^{++}, and He^+, as well as dominant charge states (both low and high) of C, N, O, Ne, Mg, Si, S, A, and Fe from 15 to 500 keV per charge
ACR and GCR anisotropies	Full 3D vdfs of H, He, C, N, O, Ne, Mg, Si, S, Ar, and Fe from 0.2 to 1 GeV/nuc
Electrons	Full 3D vdfs of electrons from a few tens of electronvolts to 30 MeV

Table 3-4. Examples of Current Charged Particle Instruments That Have Flown, Are in Operation, or Are in Development

Mission	Instrument	Mass (kg)	Power (W)	Bitrate (bps)	Capabilities	TRL and Heritage	References/Notes
ACE	Solar Wind Electron Proton Alpha Monitor (SWEPAM)	6.8	Nominal: 5.8 Peak: 6.1	1000	Elemental isotopic composition, electron and ion instruments separate H, He, e-; E/Q dist.; ~0.001 MeV/nuc	9	Russell et al. (1998)
ACE	Solar Wind Ion Composition Spectrometer (SWICS)	6	Nominal: 5 Peak: 6.1	504	Chemical/isotopic composition of solar and ISM 2 ≤ Z ≤ 30; Z, E; ~0.001 MeV/nuc; E/Q, TOF-E	9	Russell, C. T., et al. (1999) *The Advanced Composition Explorer Mission*. Springer Science+Business Media Gloeckler et al. (1998)
ACE	Solar Energetic Particle Ionic Charge Analyzer (SEPICA)	38.3	Nominal: 16.5 Peak: 17.5	608	Ionic charge states of energetic particles from 0.2 MeV/nuc to 5 MeV/nuc 2 ≤ Z ≤ 30; Q, Z, E, ~ 1; E/W; dE/dx - E	9	Russell, C.T., et al. (2000) *The Advanced Composition Explorer Mission*. Springer Science+Business Media
IMAP	CoDICE (Plasma + Solar Wind)	6.1	10.8	2500	3D velocity distribution function and ionic charge state/mass composition/arrival direction - 0.5–80 keV/q ions, 0.03–5 MeV/nuc ions, 20–600 keV electrons	6	D. J. McComas et al. (2018)
IMAP	SPICES (Suprathermal + PUI)	~12.55	~30.5	~10500	In development	~5	No reference

Mission	Instrument	Mass (kg)	Power (W)	Bitrate (bps)	Capabilities	TRL and Heritage	References/Notes
JUICE	JENI	7.4 (sensor), 7.0 (shielding)	7.6	500	Combined energetic ion and ENA camera ~1–300 keV/nuc (ENA), 5 MeV ions, FOV: 90° × 120°, 2° res (>10 keV H)	8	Brandt et al. (2019), in press
JUICE	JoEE	1.3 (sensor), 1.9 (shielding)	1.2	<500	Energetic electrons 25 keV – 1 MeV, deltaE/E ≤ 20%, FOV: 12° × 180°, deltaomega = 12° × 22°	8	P. Brandt, personal communication
New Horizons	PEPSSI	1.5	2.5	91	Ion detector, FOV: 160° × 12°, ion energy detection range 20 keV – 1 MeV	9 Heritage: MESSENGER/EPS, Firewheel/ICT, MEPA/AMPTECCE	McNutt et al. (2008)
New Horizons	SWAP	3.3	2.8	280	Electrostatic analyzer - 35 eV – 7.5 keV ΔE/E~0.085	9	D. McComas et al. (2008)
Parker Solar Probe	SWEAP (Solar Wind)	8	10	1500	0.5–30 keV/q ΔE/E ~ 0.3 Interstellar PUI: 3He+, 4He+, N+, O+, 20Ne+, 22Ne+, Ar+ Inner source PUI: C+, O+, Mg+, Si+ Mass and charge state of H-Fe ions: 1.4×10^{-3} cm^2 sr eV/eV 6° × 360°	9 Heritage: Parker Solar Probe/SWEAP, ACE/SWICS	Kasper et al. (2016)
Parker Solar Probe	Suprathermals and Energetic Ions (Epi-Lo)	5.1	5	500	0.03–5 MeV/nuc 1 – >60 amu 12° × 10° × 7° over 360° 0.2 cm^2 sr	>8 Heritage: Parker Solar Probe, ACE, Juno, MMS, Van Allen Probes, Solar Orbiter	Clark et al. (2016) D. J. McComas et al. (2016) Rodríguez-Pacheo, J., et al. (2019) The Energetic Particle Detector (EPD) Energetic particle instrument suite for the Solar Orbiter mission, Astronomy & Astrophysics, accepted

Mission	Instrument	Mass (kg)	Power (W)	Bitrate (bps)	Capabilities	TRL and Heritage	References/Notes
ACE	Solar Isotope Spectrometer (SIS)	22.4	Nominal: 17.5 Peak: 22.4	1992	2 ≤ Z ≤ 30; Z, M, E, ~ 20 MeV/nuc; dE/dx - E	9	Russell, C. T., et al. (2001) *The Advanced Composition Explorer Mission*. Springer Science+Business Media
Solar Orbiter	Suprathermal Ion Spectrograph (SIS)	6.8	3.8	400	50 keV/nuc – 14 MeV/n for CNO two telescopes, pointing 130° apart, FOV 22°, geo factor 0.2 cm^2 sr	Heritage: ACE/ULEIS, STEREO/SIT	Gómez-Herrero et al. (2017) Rodríguez-Pacheo, J., et al. (2019) The Energetic Particle Detector (EPD) Energetic particle instrument suite for the Solar Orbiter mission, *Astronomy & Astrophysics*, accepted

3.4.2.1. Further Optimizations

In general, no new technologies are required to meet the measurement requirements. However, solutions are needed to optimize mass, power, and data volume to meet the large required dynamic range of particle intensities, energies, and charge states within the resource constraints of an interstellar probe mission.

3.4.3. ENA Imaging of Global Heliospheric Interactions

ENA imaging is a powerful tool for remotely diagnosing space plasma interactions to reveal the global morphology and dynamics of ion distributions in planetary magnetospheres, solar wind interaction with weakly magnetized planets, and also the heliospheric interaction with the LISM. ENAs are generally produced through charge exchange between ions and neutrals. Given the central role of charge exchange in the interaction between the heliosphere and the LISM, ENA imaging is one of the more effective tools for remotely probing several aspects of this interaction.

Several missions have used ENA cameras to study the magnetospheres of Earth (Astrid, IMAGE, TWINS, IBEX, Double Star), Saturn (Cassini), Mars and Venus (Mars and Venus Express), and soon also Jupiter (JUICE). Hsieh et al. (1992) was the first to extend the application of ENA imaging to the heliosphere and hypothesized that it could provide information on the morphologies of transient shocks, CIRs, and the TS. Gruntman and Fahr (2000) developed this idea further with detailed analysis showing the ENA intensities for three different types of TSs (a gas-dynamical strong shock, a weak shock with thermalized pickup protons, and a weak shock with non-thermalized protons). Funsten et al. (1994) presented a detection technique that would enable ENA imaging in the 0.2- to 6-keV range. Based on these results and others, IBEX was proposed in 2003 and later launched in 2008 (D. J. McComas, Allegrini, Bochsler, Bzowski, Collier, et al., 2009). The famous IBEX ribbon was reported after about 1 year of operations by D. J. McComas, Allegrini, Bochsler, Bzowski,

Christian, et al. (2009). Krimigis et al. (2009) reported ENA observations from INCA at higher energies than IBEX and concluded that the observations did not conform to the current models of a comet-shaped heliosphere.

In the low energy range from 10 eV to several kiloelectronvolts, ENA imaging targets the direct interstellar neutral flow of H (26 eV), He, O, and Ne but also can detect ENAs resulting from the complex interaction between the interstellar plasma deflected at the HP likely producing the so-called secondary streams (Kubiak et al., 2014; Park et al., 2016). Given the vast scales of the heliospheric boundary, an imaging cadence of a month or less is required. An angular resolution of ~3° would be required to separate the secondary from the primary stream and to constrain the temperature of the interstellar plasma believed to cause the secondary stream. Note that the high asymptotic speed of an interstellar probe would make the detection of these low-energy ENAs beyond the HP very difficult because of the apparent shift in energy due to spacecraft motion away from the Sun.

The detection of low-energy neutrals relies on charge conversion of the primary neutral particles such that conventional analysis techniques can be used to determine their composition and velocity. The conversion techniques include use ultrathin foils (~μg/cm^2), conversion surfaces, and electron impact ionization.

Several important features appear in the medium (from ~1 keV), such as the ribbon. In the high (tens of kiloelectronvolts) energy range, the continuation of the ribbon, the belt, appears. Furthermore, in this high energy range, the ion lifetime against charge exchange is much longer such that ENA images from ~50 keV will reveal more of the large-scale structure of the heliosheath. Ultrathin foils in both of these energy ranges are used exclusively because they have higher efficiency than any conversion surface or ionization technique at those energies. Although ENAs readily penetrate foils well below 1 keV, their angular scattering is significant, resulting in a very degraded angular resolution. To overcome this challenge, collimators that physically restrict the acceptance angle of the incoming particles have been used, such as on IBEX-Hi (Funsten et al., 2009). The drawback of a collimator is a dramatic decrease in the geometric factor. Above ~5–10 keV, the angular scattering decreases rapidly to ~2° or less for the thinnest achievable carbon foils (~0.5 μg/cm^2) (Allegrini et al., 2016), eliminating the need for a collimator; hence, a larger geometric factor and wide field of view (FOV) can be achieved. For these reasons, two different instrument types are still required to cover the medium-to-high energy ranges with a high angular resolution. This is the case on the IMAP mission, where IMAP-Hi and Ultra cover these ranges.

ENA observations most efficiently cover the sky from a spinning platform because the source is rather extended across the sky. This is particularly true for the high-energy ENA cameras that can accommodate a wider FOV. For the low- and medium-energy ENA cameras that often only have a restricted FOV, a mechanically scanning platform enables wider sky coverage, as is the case with the IMAP-Lo camera on board IMAP (D. J. McComas et al., 2018).

ENA imaging from the changing vantage point of an outward trajectory much beyond 10 au would offer critical constraints on the hypotheses of the global structure, the ribbon, and the secondary

stream that are not possible from IBEX, Cassini, and IMAP. Once beyond the HP, a vantage point in the ecliptic in the range of 45°–135° off the longitude of the nose would be preferred to obtain the first ENA images of the heliosphere from the outside that could be used to determine the shape of the heliosphere and differentiate between a bubble-like heliosphere and one with a tail, or something not foreseen (Figure 3-3). On a Sun-pointed spinning spacecraft, this would require an FOV that comes very close to the Sun direction without running the risk of light contamination. In addition, ENA images from inside the heliosphere while traveling outward would be needed in the nose direction. To satisfying these two needs, two cameras would be desired, or one with an FOV that is close to 180° in relation to the spin axis.

Table 3-5. Summary ENA Imaging Objectives and Requirements

Measurement Objectives	Measurement Requirements
Ribbon	0.4–6 keV, H, ~2° angular resolution
Belt, force balance in the heliosheath	5–40 keV, H, ~5° angular resolution
Global heliospheric structure	≥50 keV, H, He, O, ≤10° angular resolution
Primary interstellar neutral flow (velocity, temperature, density)	E 10–2000 eV, DE/E ~ 0.5, counting dynamic range ~10^6, FOV 2pi Ram with 3 × 3°, composition for H, D, He, O, Ne
Secondary interstellar neutral flow viewed from inside the heliosphere (velocity, temperature, density)	E 10–2000 eV, DE/E ~ 0.5, counting dynamic range ~10^6, FOV 2pi Ram with 3 × 3°, composition for H, D, He, O, Ne

Table 3-6. Examples of Current ENA Instruments That Have Flown, Are in Operation, or Are in Development

Mission	Instrument	Mass (kg)	Power (W)	Bitrate (bps)	Capabilities	TRL and Heritage	References/Notes
JUICE	JENI	7.4 (sensor), 7.0 (shielding)	7.6	500	combined energetic ion and ENA camera ~1–300 keV/nuc (ENA), 5-MeV ions, FOV: 90° × 120°, 2° res (>10 keV H)	8	Brandt et al. (2020), in press
Cassini	Ion and Neutral Camera (INCA)	6.9	3	500	≥1.5° (electron optics limit) 90° × 120° <7 keV/nuc – 3 MeV/nuc (ENA) H, He, O, S GF: ≤1.8 cm^2 sr Efficiency: 0.2 (H)	9	Krimigis et al. (2004)

Mission	Instrument	Mass (kg)	Power (W)	Bitrate (bps)	Capabilities	TRL and Heritage	References/Notes
Chandrayaan-1	SARA/CENA	1.98	10	2000	ENA 10 eV – 3.2 keV 1–56 amu H, O, Na/Mg/Si/Al-group, K/Ca-group, Fe group FOV: 15° × 160° Efficiency: 0.01–1% G-factor/sector^{-2} cm^2 sr eV/eV at 3.3 keV	9	Barabash et al. (2009)
IBEX	IBEX-Lo	11.5	3.46	100	10–2000 eV (32 energy channels) H, He, O, Ne 45 × 2° pixels using scanning platform	9	D. J. McComas, Allegrini, Bochsler, Bzowski, Collier, et al. (2009) Fuselier et al. (2009) D. J. McComas, Allegrini, Baldonado, et al. (2009)
IBEX	IBEX-Hi	7.37	0.65	100	0.38–6.0 keV 6.5° 3 × 10^{-3} cm^2 sr eV/eV at 2.2 keV (double coincidence, incl. eff.)	9	D. J. McComas, Allegrini, Bochsler, Bzowski, Collier, et al. (2009) Funsten et al. (2009)
IMAGE	High-Energy Neutral Atom Imager (HENA)	19.05	14.6	~1700	Energy range: ~10–300 keV/nuc Energy resolution: ≤0.25 Mass resolution: H and Heavies FOV: 120° × 90° Angular resolution: ≥3° Sensitivity: 0.3 cm^2 sr (H), 1.6 cm^2 sr (O)	9	Mitchell et al. (2000)
IMAGE	Medium-Energy Neutral Atom Imager (MENA)	13.9	22.5	4300	FOV: 140 × 360 Energy range: 1–70 keV Energy resolution: 80% H, O	9	Pollock et al. (2000)

Mission	Instrument	Mass (kg)	Power (W)	Bitrate (bps)	Capabilities	TRL and Heritage	References/Notes
IMAGE	Low-Energy Neutral Atom Imager (LENA)	20.75	13.1	500	ENA 15–1250 eV E/dE = 1 1–20 amu	9	T. E. Moore et al. (2000)
IMAP	Ultra	~7.4	~7.6	~500	combined energetic ion and ENA camera ~1–300 keV/nuc (ENA), 5-MeV ions, FOV: 90° × 120°, 2° (>10 keV H)	8	Brandt et al. (2020), in press
IMAP	IMAP-Lo	N/A	N/A	N/A	Energy range: 5–1000 eV Pointing knowledge: 0.1° Angular resolution: 9° FWHM		D. J. McComas et al. (2018)
IMAP	IMAP-Hi	N/A	N/A	N/A	Angular resolution: 4° Energy range: 0.41–15.6 keV Energy resolution: ≤ 0.45 (E_FWHM/E) SNR: >100 Mass resolution (M/ΔM): 5		D. J. McComas et al. (2018)

3.4.3.1. Further Optimizations

ENA cameras that exist today can achieve the science goals of an interstellar probe, but current masses for the low, medium, and high energy ranges amount in total to ~30 kg or more, which is a significant fraction of any payload mass allocation. Therefore, efforts to optimize mass by, for example, combining instrumentation of different energy ranges are desirable.

High angular resolution at low energies with a relatively compact instrument remains a challenge. Collimation and charge conversion technology are areas that are seeing development and improvements. With the recent developments in additive manufacturing techniques ("3D printing"), specialized collimators are less of challenge nowadays. Although efficiencies in charge conversion surfaces or foils have improved some over the last decade, it remains an element that limits the overall sensitivity.

While low-energy (<1 keV) imaging requires a different technique, medium-energy (1–10 keV) and high-energy (10–100 keV) imaging has the potential of being combined to enable a more compact ENA imaging payload. The challenge here is to maintain a sufficiently high angular resolution (<5°) down to low energies without sacrificing the geometric factor too much at the higher energies, where ENA intensities are lower (but angular scattering in the foil is small). For example, IMAGE/MENA, IBEX-Hi, and IMAP-Hi all used collimators that restricted the attainable solid angle and therefore the geometric factor. Corresponding high-energy ENA cameras (IMAGE/HENA,

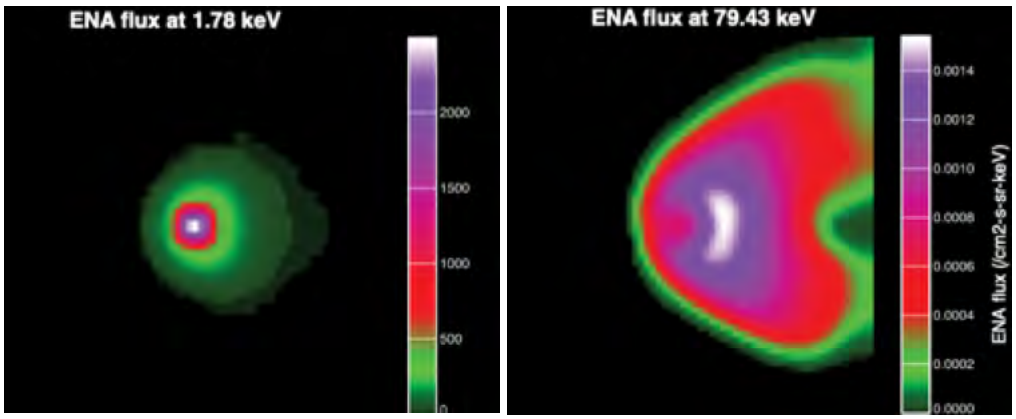

Figure 3-34. Simulations of the heliosphere from a side-view vantage point at 250 au demonstrating the expected general views at different energies. Plasma flows are taken from the MHD model by Opher et al. (2015) and thus do not assume any ribbon or other observed features. (Left) At low energies, the neutralized solar wind dominates the images, and in the heliosheath, ions are lost to charge exchange after a relatively short convection distance. (Right) At higher energies, ions survive for long distances in the heliosheath, providing more complete images of the global heliospheric shape. (Image courtesy of B. DeMajistre; Demajistre et al. (2018).)

Cassini/INCA, IMAP-Ultra) do not require collimation and therefore have larger geometric factors. Acceptable trades here could include the use of ultrathin graphene foils (Allegrini et al., 2016) that can be made thinner than amorphous carbon foils because of their superior strength. This would minimize the angular scattering at the low-energy end. Another trade includes using one sensor with one collimated aperture and one non-collimated aperture, which would add to the complexity of such an instrument.

Although ENA intensities from the heliosheath are generally very low ($\leq 10^{-4}$ particles per cm^2 sr s keV), their dynamics is such that required integration times are on the order of days or more. Therefore, a high signal-to-noise ratio (SNR) is important in addition to maximizing the geometric factor within the available mass allocation. Backgrounds include cosmic rays and UV, and experience from past missions implies that triple coincidences are needed, in particular at the higher energies that may reveal the larger heliospheric structure.

3.4.3.2. Sampling Interstellar Gas Composition and Isotopes

As discussed above, the elemental composition of the interstellar neutral gas inside and outside the heliosphere is a critical property of the ISM as well as how the heliospheric boundary processes modify it. Determining the relative isotopic composition of major neutral components of the LISM is also important for testing nucleosyntheses models. Important ratios to measure include D/H, ^{3}He/^{4}He, ^{13}C/^{12}C, ^{18}O/^{16}O, ^{22}Ne/^{20}Ne, and ^{38}Ar/^{36}Ar as well as the abundance of Li compared to the SS value. Isotopic measurements of the neutral ISM component provide an understanding of these properties well before an interstellar probe reaches the pristine LISM, whereas the isotopic composition of the corresponding ions may not be representative of the pristine LISM, which is believed to start at 500–600 au.

There is a considerable discussion about how tightly the ions and neutrals are coupled in the VLISM (i.e., at the edge of our cloud at a few thousand astronomical units). While the mean-free path of neutrals is very large, the mean-free path for interstellar ions is only a few hundred astronomical units. In addition, ions are affected by the ISMF and the electromagnetic fields associated with the boundary of the cloud. Thus, at 1000 au, ions and neutrals might not be in equilibrium.

Measurements should be performed along the spacecraft trajectory at regular intervals with direct measurements about a day every week, which requires a sensitivity of ~10^{-3} cm^{-3}. Collecting gas samples in a chamber over ~6 months is a complementary method to increase the statistics of the sample and could achieve a sensitivity of 10^{-6} cm^{-3}. In general, a background rejection sufficient to measure 0.1 neutrals/cm^3 in an ambient of 1E6 neutrals/cm^3 is required. Instrument FOV must be pointed within 10° of the ram direction to collect gas samples, with occasional pointing away from the ram direction to allow for background measurements.

Table 3-7. Current State of Neutral Gas Mass Spectroscopy

Measurement Objectives	Measurement Requirements
Elemental composition of LISM	H to Fe, m/Δm > 200 (1σ)
Molecular composition	Mass range 1–150 u/e (regular), 1–300 u/e (high mass range)
Major isotope ratios	D/H, ^{3}He/^{4}He, ^{13}C/^{12}C, ^{18}O/^{16}O, ^{22}Ne/^{20}Ne, ^{38}Ar/^{36}Ar
Attenuation inside termination shock region	Time cadence 1 × week
Possible pileup at heliopause	Time cadence 1 × week
Composition of pristine LISM	Mass 1–56

Table 3-8. Examples of Current Neutral Mass Spectrometers That Have Flown, Are in Operation, or Are in Development

Mission	Instrument	Mass (kg)	Power (W)	Bitrate (bps)	Capabilities	TRL and Heritage	References/Notes
Rosetta	Rosetta Orbiter Spectrometer for Ion and Neutral Analysis (ROSINA)	34.8 16 for DFMS 15 for RTOF	49 19 for DFMS 24 for RTOF	20000	Magnetic mass spectrometer, reflectron-type TOF mass spectrometer – molecules up to 300 amu Mass range: 12–150, resolution: m/dm > 3000 for DFMS Mass range: 1– 500, resolution > 500 for RTOF	7	Balsiger et al. (2007) Wurz, P., et al. The ROSINA Neutral Gas Mass Spectrometer on Rosetta
LADEE	NMS	3.5	5	1	Isotope ratios: D/H, ^{3}He/^{4}He, ^{13}C/^{12}C, ^{18}O/^{16}O, ^{22}Ne/^{20}Ne, ^{38}Ar/^{36}Ar Li abundance m/Δm > 100 at 1σ Sensitivity: 0.1 cm^3	9 Cassini, LADEE, Rosetta	Mahaffy et al. (2014) Balsiger et al. (2007) Waite et al. (2004)
Luna-Resurs	NGMS	3.5	6.8–23	1000000	Mass range: 1–1000	<9	Fausch et al. (2018)

Mission	Instrument	Mass (kg)	Power (W)	Bitrate (bps)	Capabilities	TRL and Heritage	References/Notes
Cassini	Ion Neutral Mass Spec-trometer (INMS)	10.3	23.3	1495	Mass range: 1–99 Daltons	9	Waite et al. (2004)
JUICE	NMS	3.1 (sensor only)	11.8–18.5	10–1000	Mass range: 1–1000 amu Mass resolution: m/Δm > 1100 FOV: 10° × 300°	8	P. Wurz, personal com-munication

3.4.4. UV Imaging of Interstellar Hydrogen

There is a long history of measurements of interplanetary Lyman-alpha emissions (Eric Quémerais et al., 2006). The sensors range from very simple single-element devices (e.g., channeltrons) to larger, sophisticated spectrographs (e.g., Hopkins Ultraviolet Telescope [HUT] and HST) on astronomical missions. One can achieve a reasonable map of interplanetary and/or interstellar H Lyman-alpha with a relatively simple system.

The integrated line brightness near Earth varies across the sky between 400 and 1400 R depending on the phase of the solar cycle. In the outer solar system, brightness levels of a few tens of rayleighs, although dim, are sufficient to produce statistically valid and useful signals. In the ISM at 400 au, the scattering of the solar radiation on interstellar hydrogen would contribute <5 R (Gruntman & Izmodenov, 2004). However, a contribution from the galactic plane of ~10 R has been detected from the study of the Voyager UVS data and correlated with H alpha emissions from H II regions (Rosine Lallement et al., 2011).

Table 3-9. Lyman-Alpha Spectrographic Imaging

Measurement Objectives	Measurement Requirements
Measure interplanetary and LISM H phase space density	Spectrally resolved Lyman-alpha line profile observations (<20 km/s, preferably <3 km/s) with a sensitivity of <1 R/res. element
Characterize the diffuse galactic Lyman-alpha to constrain radiation transfer in galaxies	Spectrally resolved Lyman-alpha profile over a wide range with ≤20 km/s resolution

The interplanetary hydrogen Lyman-alpha line at 121.6 nm is created from resonant scattering of solar photons by interplanetary and interstellar atomic hydrogen. The scattering process is resonant in the rest frame of the H atom, so that the line's integrated intensity and the shape of the line provide important diagnostics about the distribution of hydrogen atoms in the LISM, including their number density, temperature, and bulk velocity. These are critical parameters defining the size and behavior of the heliospheric interface.

A range of UV instruments with varying complexity have been flown on planetary missions, including the Ultraviolet Spectrometer (UVS) on board Voyager 1 and 2 (Broadfoot et al., 1977), the Alice Ultraviolet Imaging Spectrograph on board New Horizons (A. S. Stern et al., 2008), and the Solar Wind Anisotropies (SWAN) spectrograph on board SOHO (Bertaux et al., 1995). In general, there

are two fundamental types of approaches: the first uses a photodetector to collect all of the emission in the Lyman-alpha line to measure the LOS intensity, and the second uses a hydrogen absorption cell to reconstruct the Lyman-alpha line profile. The absorption cell uses its internal H atoms as a narrow-band absorption feature. The motion of a spacecraft provides a Doppler-shift of this narrow absorption feature against the interstellar H emissions. By observing in different directions and at different times of year (for a solar orbiting platform), the absorption cell blocks out different parts of the interstellar line. The active H cell scatters out a portion of the incoming Lyman-alpha line, determined by where the line center of the H in the absorption cell appears to fall on the observed Lyman-alpha. The amount of attenuation depends on the number of H atoms in the cell. That H fraction is zero when the cell is off. When the cell is activated, a tiny fraction of the H_2 gas is dissociated in H. Those are the H atoms that provide the absorption. The second approach is to use a high-resolution spectrograph. The most common approach is to operate the spectrograph an Echelle configuration that fully resolves the Lyman-alpha line shape.

Table 3-10. Examples of Current UV Instruments That Have Flown, Are in Operation, or Are in Development

Mission	Instrument	Mass (kg)	Power (W)	Bitrate (bps)	Capabilities	TRL and Heritage	References/Notes
Voyager	UVS	4.52	3.2	160	3.3 nm		
New Horizons	YVS	4.4	4.4	—	0.9 nm		
SOHO	SWAN	13.25	11	200	0.001 nm (with absorption cell)		
HST	STIS	N/A	N/A	N/A	0.008 nm		
MAVEN	IUVS Echelle	22	28	—	0.007 nm		
DMSP	SSUSI	25.4	28	3800	115–180 nm in 165 bins	9	Paxton et al. (1999) Paxton et al. (1993)
New Horizons	Alice	4.5	4.4		Spectral range: 52–187 nm Spectral resolution: 0.36 nm	9	S. A. Stern et al. (2008)
SOHO	Solar Wind Anisotropies (SWAN)	13.25	11	200	Spectral range: 115–180 nm Spectral resolution: 0.001 nm (absorption cell)	9	Bertaux et al. (1995) In Phase-A study for the SIHLA Mission. PI; Paxton.
MAVEN	IUVS	22	28		Spectral range: Spectral resolution: 0.007 nm	9	
Voyager	UVS	4.5	3.5		Wavelengths: 1.5 nm resolution; 53–170 nm range	9	https://nssdc.gsfc.nasa.gov/nmc/experiment/display.action?id=1977-084A-04 http://vega.lpl.arizona.edu/voyager_uvs/instrument.html

While a photodetector approach with a hydrogen absorption cell can be made with low mass, power, and data rates, it only provides indirect information on the line shape and therefore the

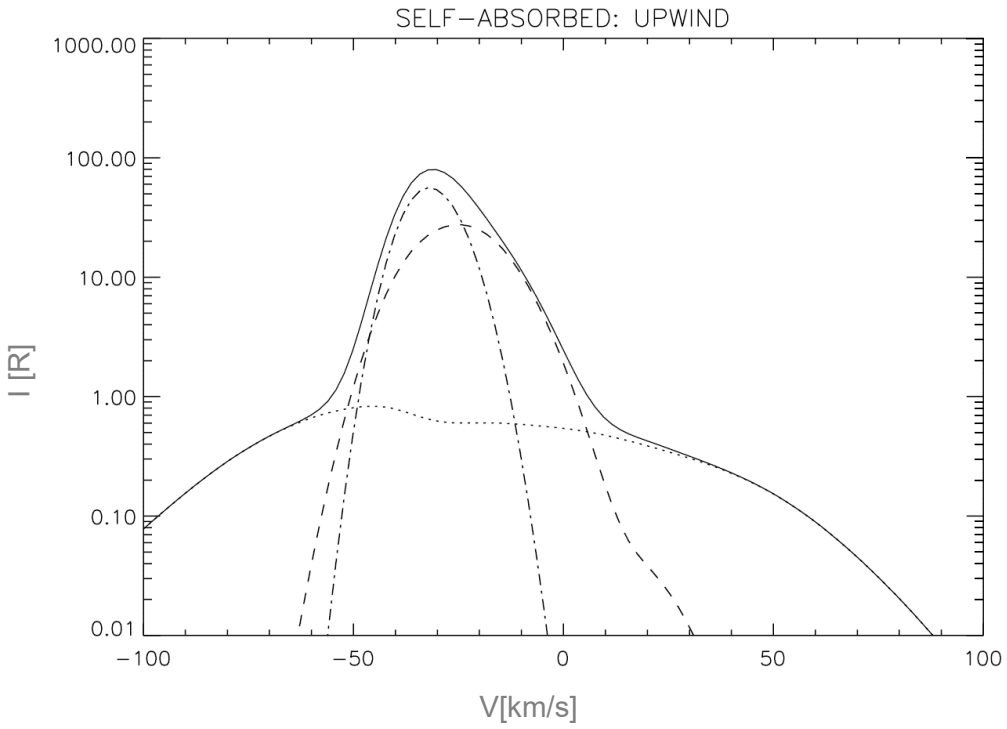

Figure 3-35. Line profile computed for an observer at 1 au, in kilometers per second. The dotted line is the emission of the hot hydrogen (H) population from the inner heliosheath. The dashed-dotted and dashed lines are for the pristine and the secondary H component created in the outer heliosheath, respectively. The ratios between populations vary with distance (reprinted from E. Quémerais and Izmodenov (2002) with permission).

LISM properties. A high-resolution spectrograph directly resolving the line shape offers the best remote measurements of column density, temperature, and velocity of the H flow but requires more resources (see Table 3-10). The use of scanning platforms to provide sky maps independently of spacecraft orientation would add to the complexity, mass, and power.

As shown in Figure 3-35, the hot, secondary, and pristine components of the hydrogen flow set the measurement requirements for spectral resolution. Although an equivalent resolution of 20 km/s would capture all components, 3 km/s resolution would be required to well distinguish the three. One needs to consider the SNR of the measured line profiles as well to determine the detection thresholds of the components. Information about the 3D distribution of the hydrogen wall and other structures could be obtained by observing multiple LOSs on the way out. This is an important trade-off because it adds to the complexity in terms of a scanning platform or multiple optical heads.

3.4.5. Radio and Plasma Wave Measurements

Voyager has demonstrated the importance of low-frequency radio and plasma wave measurements for an interstellar probe mission. Even as close as 15 au to the Sun, the Voyager PWS instruments were able to detect radio emissions in the range of ~1.8–3.6 kHz that we now know are generated in the ISM near and beyond the HP (Gurnett et al., 1993; Kurth et al., 1984). The emis-

sions are generated at the local plasma frequency by mode conversion from electron plasma oscillations, similar to type III radio emissions or narrow-band radio emissions from Earth's bow shock. Furthermore, we know that the radio emissions are triggered by disturbances originating in solar transient events that propagate through the heliosphere and inner heliosheath until they interact with the HP, where shocks or pressure pulses are transmitted through the HP into the ISM.

Figure 3-36. Low-frequency radio emissions generated at and beyond the heliopause via mode conversion from electron plasma oscillations in the foreshock of shocks and pressure pulses moving through the ISM (Kurth & Gurnett, 2003).

Once in the ISM, the Voyager 1 and 2 detected narrow-band, bursty electron plasma oscillations at the local electron plasma frequency, providing accurate measurements of the plasma density, even to the extent of showing density jumps that match the jump in the magnetic field at shocks (Gurnett et al., 2013). Hence, whether by radio emissions detected within the heliosphere or by plasma oscillations in the heliosphere and ISM, the wave signatures provide evidence of the influence of the Sun on the LISM and independent diagnostics of the interstellar plasma density, even in the absence of a working plasma instrument such as in the case of Voyager 1. Also, radio direction finding can localize the source of radio emissions from locations beyond ~15 au and could complement a dust investigation by detecting hypervelocity dust impacts from all directions.

Onboard spectrum analysis of digitized waveforms could be used to optimize the data volume significantly. Such capabilities already exist in missions such as the Van Allen Probes and Juno. For example, onboard spectral line detection would enable the onboard identification of radio emissions or plasma oscillations, allowing an onboard determination of n_e, in the latter case. Onboard quasi-thermal noise (QTN) spectrum analysis would enable fitting the plasma wave spectrum to an electron density and bi-Maxwellian temperature distribution, enabling the ability to downlink n_e, T_c, and T_h as opposed to high-resolution spectra on an ongoing basis. The addition of a sounder capability to stimulate the plasma frequency would provide electron densities in the inner heliosheath where the Debye length is much too large to allow for QTN spectroscopy with a reasonable antenna length. And finally, onboard dust detection would enable a much higher duty cycle for identifying impulses due to hypervelocity dust impacts rather than by downlinking voluminous waveforms. The resulting data set would be a time-tag and amplitude of detected impulses. Such software was implemented in the Cassini RPWS.

In summary, a radio plasma wave investigation would require a frequency range of up to ~10 kHz with 5% spectral resolution, corresponding to an equivalent of 10% density resolution. The full waveform could be telemetered at low duty cycle, and onboard processing could provide plasma

electron frequency and dust detection at low telemetry rates. A spinning and electromagnetically clean spacecraft would be required, with antenna lengths of at least 10 m.

Table 3-11. Radio and Plasma Wave Spectrometer

Measurement Objectives	Measurement Requirements
Observe at least one electric field component of radio emissions generated at and beyond the heliopause	Frequency up to 5 kHz (10 kHz for margin) Sensitivity at 3 kHz 7×10^{-7} V/m or better
Observe electron plasma oscillations for densities of 1 cm^{-3} or lower	Frequency up to 10 kHz
Determine density to within 10%	Spectral resolution ($\Delta f/f$) of 5% or better
Cadence (variable, consistent with telemetry constraints)	One spectrum per second to one spectrum per minute (can be varied to meet telemetry restrictions)
Burst mode (onboard, with ability to downlink at very low duty cycle)	Capture 16k 16-bit waveform samples at ~30 ksps for onboard analysis and possible downlink at very low duty cycle; required for assessment of onboard processing and high-resolution snapshots
Onboard spectrum analysis to minimize telemetry	FFT with ability to average and bin spectra
QTN spectral analysis	Onboard fitting to transmit Ne and Te to ground with minimal telemetry
Dust impact detection	Onboard analysis

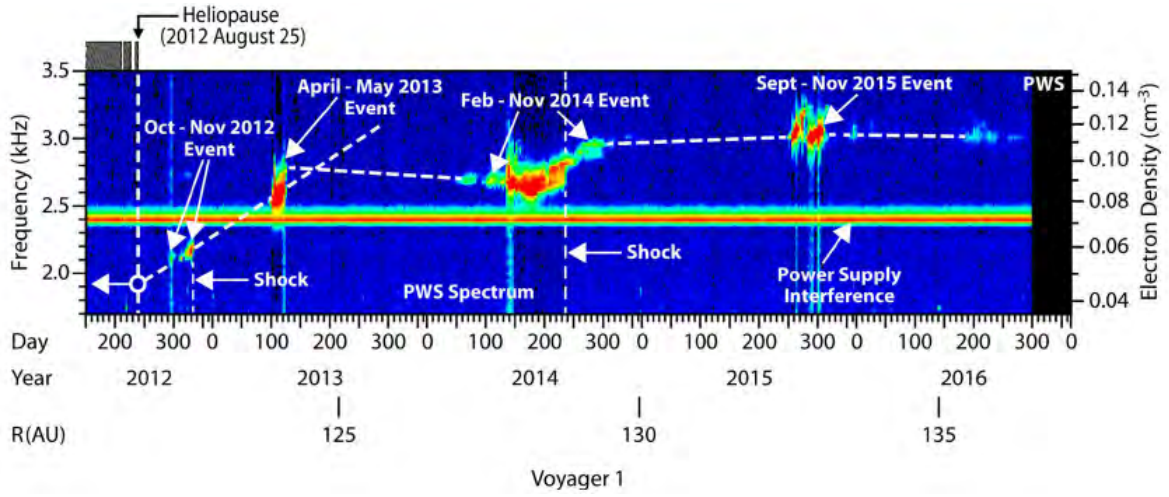

Figure 3-37. Electron plasma oscillations observed beyond the heliopause showing the increase in interstellar plasma density in the LISM (reproduced from Pogorelov, Heerikhuisen, et al. (2017) with permission; © AAS).

Table 3-12. Examples of Current Plasma Wave Instruments That Have Flown, Are in Operation, or Are in Development

Mission	Instrument	Mass (kg)	Power (W)	Bitrate (bps)	Capabilities	TRL and Heritage	References/Notes
Galileo	Plasma Wave Spectrometer (PWS)	7.14	6.8	Low: 240, High: 806400	Electric: 5.62 Hz to 5.65 MHz, magnetic: 5.62 Hz to 160 kHz	9	Gurnett et al. (1992)
Parker Solar Probe	Plasma Wave Instrument	6	1.5	100	Includes sensor, wire antennas, shielding, harness	9	Bale et al. (2016)
Voyager	PWS	1.4 (without boom)	1.1/1.6	16 bps for typical survey, 115 kbps for burst	E-field spectra to 56 kHz, waveform burst mode	9	https://nssdc.gsfc.nasa.gov/nmc/experiment/display.action?id=1977-084A-13 Scarf and Gurnett (1977)
Van Allen Probes	Wave instrument (part of EMFISIS suite)	15.5 (main electronics including MAG electronics and radiation shielding)	14.2 (entire suite)	7.5 kbps survey (full suite), burst modes ranging to 1.3 Mbps	3-channel E, 3-channel B to 12 kHz, 1 channel E to 500 kHz	9	Kletzing et al. (2013)

3.4.6. Multispectral Flyby Imaging

The concept of operations for imaging a planet during a fast flyby benefits from the experience of the New Horizons team during the flybys of the Pluto-Charon system and KBO 2014 MU69. What follows is not a detailed imaging plan but rather is intended to show that a fast flyby is within the performance envelope of a New Horizons-like spacecraft, which could serve as the baseline for an interstellar probe. While New Horizons' flybys were ~14 km/s relative to the targets, we assume an interstellar probe flyby of 50 km/s for the purposes of this exercise. The main constraint is angular acceleration of the apparent motion of the target along the focal plane of the cameras, and that is more a function of spacecraft slew rate and rate change than proper motion. New Horizons can slew at 1.5 deg/s, although it commonly slews slower at around 1 deg/s. Accelerating the spacecraft to that rotation rate takes on the order of a few seconds. Time-delay integration (TDI) for New Horizons' Ralph imager must occur at slew rates no faster than 1000 µrad/s, or ~0.06 deg/s, and must not change during an image acquisition. This imaging slew rate could be increased on future missions by enhancing the imaging detector sensitivity, such as by co-adding more pixels in the direction of the image scan, and software modifications can enable variable-rate TDI imaging.

TDI imaging allows for measuring compositions by acquiring multispectral images. TDI imaging easily accomplishes this by fixing color strips across the imaging chip, allowing images to be built up of the same regions in different visible and IR wavelengths in the same way as New Horizons' Ralph camera (Reuter et al., 2008). With complementary metal-oxide semiconductor (CMOS) detectors, it is possible to have a camera that functions both as a TDI imager and as a framing camera; this is the approach being used for the Europa Imaging System camera for the Europa Clipper

mission (Elizabeth Turtle, personal comm.). Thus, one camera can combine the capabilities of New Horizons' Ralph and LORRI cameras.

Angular rate and rate acceleration are not a problem for a New Horizons-like spacecraft: traveling at 14.44 km/s at a distance of 3500 for the MU69 flyby, the target's instantaneous radial velocity was 0.24 deg/s. This was said by the engineers to be at the limit of capability for the LORRI framing camera (Cheng et al., 2008), which does not use TDI. The three pixels of smear in the along-track direction in the highest-resolution LORRI image of MU69 are due to the spacecraft slewing for the sake of Ralph's TDI imaging. This 0.24 deg/s angular rate is well within the spacecraft's 1–1.5 deg/s slew rate limit, and so image motion compensation would have been possible for even a framing camera.

Table 3-13. Visible Near Infrared (VISNIR) Flyby Camera

Measurement Objectives	Measurement Requirements
Constrain target size (primary and satellites) and mass; density (derived value)	10s km/pixel, low phase angle, global imaging
Map global and selected regional geology and geomorphology	1 km/pixel (global) 100 m/pixel (regional) resolution
Map surface composition, especially methane	>3 band color imaging (suggested channels: 400–500 nm, 500–575 nm, 575–700 nm, 780–975 nm, 860–910 nm)
Constrain topography	Stereo imaging
Map planet's terminator	High SNR (>20); high pointing accuracy
Constrain bolometric Bond albedos	Global imaging at broad range of phase angles
Constrain atmospheric clouds/hazes	High-phase-angle (>110°) panchromatic imaging; <5 km/pixel
Characterize atmospheric and surface time variability	Panchromatic imaging, vertical resolution < 5 km/pixel
Search for other moons and rings	High-phase-angle (>~160°) panchromatic imaging

Consider Interstellar Probe flying by a planet (e.g., Quaoar) at 3500 km from the surface, moving at 50 km/s. The proper motion of the planet would be 0.82 deg/s, which is within a New Horizons-like spacecraft's ability to compensate for by slewing (1.5 deg/s maximum) against the spacecraft motion. To build up a TDI image at a New Horizons-like rate of 0.06 deg/s, the spacecraft must slew at 0.76 deg/s against the velocity vector, although this does not account for angular acceleration produced by changing spacecraft-target distance. The spacecraft can conduct multiple such scans by slewing near the maximum rate parallel to the velocity vector to once again point the cameras ahead of the planet, thus resetting for another imaging scan. To a casual observer, the spacecraft would thus appear to wobble; this was done for New Horizons' encounter with Pluto and MU69. In this way, multiple imaging scans can be acquired leading up to, during, and after closest approach to provide stereo views, global coverage at high resolution, and views at variable phase angles. However, other considerations should inform imaging operations, such as desiring global, high-phase-angle imaging over the planet's terminator, which would occur near closest approach when a LORRI-like camera FOV would span only a few kilometers on the surface.

The scenario above assumes perfect knowledge of the target's location (especially in the down-track/Sun-radial direction), which is far from true, however. A more conservative flyby distance of, e.g., 10,000–20,000 km could mitigate this, which would likewise reduce the necessary spacecraft slew rate and angular acceleration, although at a larger (i.e., worse) pixel scale. Mosaicking around the planet's position error ellipse would likewise help ensure it was imaged. Finally, a closed-loop onboard centroiding (autonomous navigation) capability could be used, which is not a capability of New Horizons (Harch, 2016).

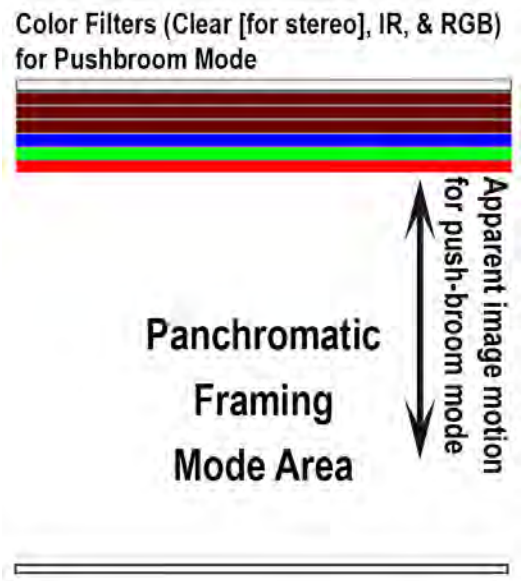

Figure 3-38. Schematic focal plane electronics to allow imaging via both time-delay integration ("push broom") and framing modes. Color filters fixed to the imaging sensor allow multi-wavelength visible and near-IR imaging in TDI mode, which uses spacecraft motion to build up an image line by line. Panchromatic strips at either end of the imaging sensor will permit stereo imaging to resolve a planet's topography. Panchromatic framing images will allow distant reconnaissance observations for both navigation and astronomical observations.

KBO flybys would require panchromatic (~0.3–0.8 µm) and multispectral (~0.9–3.5 µm) wavelengths to allow mapping of methane distribution (e.g., Grundy et al., 2016). Resolution of 100 m/pixel at ~12,000-km distance would be required to resolve important landforms (equivalent to ~5 µrad), which was implemented for New Horizons/LORRI. Framing mode would be used for the panchromatic range and push-broom mode for the multispectral, which has been baselined for Europa Clipper/EIS. Exposures would range from milliseconds to seconds with fast CMOS readouts. Multi-pixel bin modes, including full CMOS binning (one giant pixel) could be implemented for astrophysical and other low-SNR observations. A single-pass push-broom capability using two clear "filters" would allow for parallax-based stereo imaging to obtain topography.

Precise target location knowledge would be required with automatic pointing updating from wide-angle star trackers and LORRI scans. Passive cooling as done on New Horizons would work in the IR part of the spectrum beyond ~20 au. For reference, the LORRI camera on board New Horizons (Cheng et al., 2008) was ~8.6 kg and consumed 15 W in full operations. Data volume is in the gigabit range but could follow the successful scheme on New Horizons, where data were downlinked over years after the flyby.

Table 3-14. Examples of Current VISNIR Imagers That Have Flown, Are in Operation, or Are in Development

Mission	Instrument Type	Instrument	Mass (kg)	Power (W)	Bitrate (bps)	Capabilities	TRL and Heritage	References/Notes
DART	Panchromatic Imager	DRACO	9	4.95		High resolution, high SNR panchromatic imaging 208 aperture, 400-1000 nm, .29 deg full angle FOV		Fletcher, Z. J. et al. "Design of the Didymos Reconnaissance and Asteroid Camera for OpNav (DRACO) on the Double Asteroid Redirection Test (DART)
New Horizons	VISNIR (VIR)	Long Range Reconnaissance Imager (LORRI)	8.6	15	Variable; 1-3 kbps	Panchromatic (~0.3-0.8 µm) and multispectral (~0.3-2 µm) 100 m/px at 10,000 km: <5µrad (baselined ~LORRI optics) Framing (panchromatic) and pushbroom (multispectral) modes (baselined ~EIS electronics) Single-pass pushbroom stereo capability Millisecond to multiple second exposures Tolerance needed to observer planet-Sun transits beyond 30 AU as exoplanet analog. Also could observe moons crossing planets' disks.	9	Conard, S. J., et al. "Design and fabrication of the new horizons long-range reconnaissance imager." Astrobiology and Planetary Missions. Vol. 5906. International Society for Optics and Photonics, 2005. Hawkins, S. Edward, et al. "The Mercury dual imaging system on the MESSENGER spacecraft." Space Science Reviews 131.1-4 (2007): 247-338. Cheng, A. F., et al. "Long-Range Reconnaissance Imager on New Horizons." Space Science Reviews, vol. 140, no. 1-4, pp. 189-215
New Horizons	VISNIR (VIR)	Multi-spectrical Visible Imaging Camera (MVIC)	10.5	7.1	Variable; 1-3 kbps	Visible imaging; 400–975 nm (panchromatic); 4 color filters (Blue, Red, Methane, Near-IR); FOV 5.7◦ × 0.15◦ (stare, pan), or 5.7◦ × arbitrary (scan); IFOV 20 µrad/pixel	9	

3.4.7. Space Physics Observations During Planetary and KBO Flybys

The capabilities of the heliospheric suite of instrumentation outlined above exceed the requirements for magnetospheric measurements during planetary flybys. This is because intensities and field strengths are significantly higher. However, this imposes the additional requirement on instrumentation to handle the large dynamic range of the two vastly different environments.

During other flybys of non- or weakly magnetized bodies, measurement objectives include investigating the deflection of the plasma flow around the body and the exchange of material between the space environment and its surface. This includes the following:

- measuring the deflection of the interplanetary or interstellar magnetic fields and the plasma properties around the object that can provide the first indications of the presence and properties of an atmosphere
- measurements of material originating from the surface or atmosphere that is picked up by the plasma flow (PUI)
- intensity, spectra, and elemental composition of particle bombardment of the surface that alters its properties, such as reddening due to radiolysis (molecular dissociation) by cosmic rays

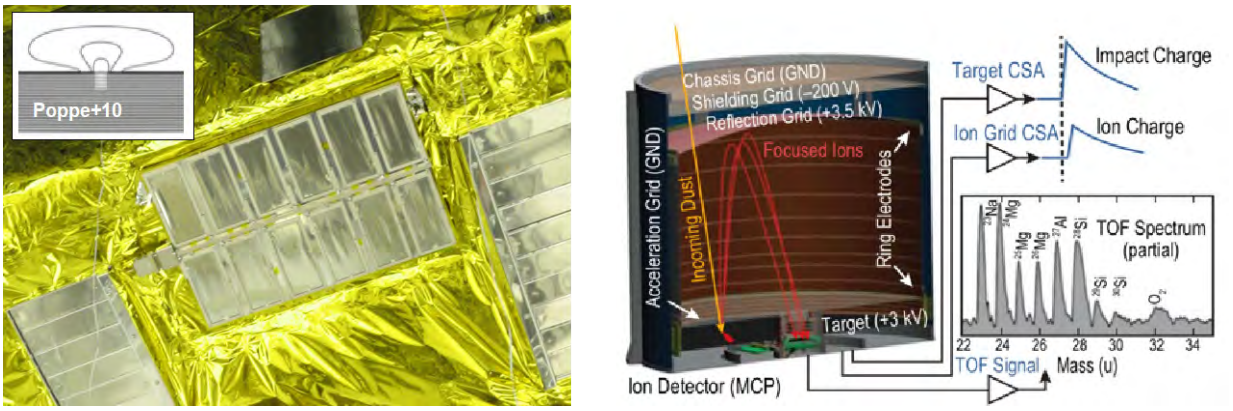

Figure 3-39. While a dust counter provides integrated flux measurements with simple interfaces and low resources, a dust composition analyzer provides insight into the chemical evolution of the galaxy. (Left) The Student Dust Counter on board New Horizons (image credit: NASA/Johns Hopkins University Applied Physics Laboratory/Southwest Research Institute). (Right) A functional drawing of IMAP/IDEX capable of elemental and isotopical separation (D. J. McComas et al., 2018).

- electric and magnetic field fluctuations that can provide insights into the process responsible for acceleration and loss of surface or atmospheric material into space, or that modifies space weathering and redistribution of surface material

3.4.8. In Situ Dust Detection

Combined impact flux measurements of EKB and ISD grains in the outer solar system have been made by the New Horizons Student Dust Counter (SDC). A dust counter provides integrated measurements that are essential for constraining the dust distribution in the solar system, with relatively simple interfaces and low resources (see Table 3-15 below). While useful counting contributions to the study of IPD and ISD have come from radio wave instruments (e.g., Voyager and Cassini), they were even cruder, unable to measure the impacting dust particle mass, speed, or composition.

Table 3-15. Interstellar Probe Dust Detector Measurement Objectives and Requirements

Measurement Objectives	Measurement Requirements
Collect a statistically significant number of EKB and ISD grains	Effective area ≥ 100 cm^2; near-ram and upstream pointing for ISD
Determine the composition of interplanetary and interstellar grains	TOF dust mass spectrometer; 1–500 amu, m/Δm ≥ 200

However, discriminating the relative number fluxes is difficult, and characterizing the compositional diversity of these grain populations is not possible with the New Horizons/SDC instrument and thus does not provide any direct insights into the chemical evolution of the galaxy. A dust composition analyzer capable of measuring the impactor fluxes for interplanetary and interstellar grains would directly sample and measure the composition of IPD and ISD grains. It would be able to identify the abundance of major rock-forming elements (Na, Mg, Al, Si, K, Ca, Fe) and detect the presence of minor elements and organic molecules. IPDs and ISDs will be discriminated both compositionally and by their impact speeds, which are inferred based on the structure of impact

charge signals to the analyzer. Building on the New Horizons measurements of dust fluxes, compositional analyzer measurements will be able to discriminate and catalog the various dust populations throughout the solar system. IPDs encode the chemical diversity of the Kuiper Belt. Having a robust accounting of the EKB dust density and compositional distribution as a function of heliocentric distance would allow us to better understand the origins and evolution of the Kuiper Belt because each grain encodes the composition of its parent body. By accumulating many compositional spectra of EKB grains, Interstellar Probe would be able to characterize the compositional diversity of the Kuiper Belt. Dust composition analyzers that have flown or are scheduled for flight include Cassini/CDA, Europa Clipper/SUDA, and IMAP/IDEX. Near-ram pointing configurations would be required for any in situ dust measurements and for ISD measurements, with an optimal trajectory close to the upstream direction.

Table 3-16. Examples of Current Dust Instruments That Have Flown, Are in Operation, or Are in Development

Mission	Instrument	Mass (kg)	Power (W)	Bitrate (bps)	Capabilities	TRL and Heritage	References/Notes
Cassini	Cosmic Dust Analyzer (CDA)	17.151	12	524	M/ΔM>50	9	Srama, R., et al. "The Cassini Cosmic Dust Analyzer." *Space Science Reviews*, vol. 114, no. 1-4, 2004, pp. 465-518
LADEE	Dust Detector (LDEX)	3.6	5	579	M/ΔM>200 <1˚ 1-70 km/s >0.3 μm	9	Horányi, M., Sternovsky, Z., Lankton, M. et al. Space Sci Rev (2014) 185: 93. https://doi.org/10.1007/s11214-014-0118-7
Europa Clipper	SUDA	N/A	N/A	N/A	200-250 M/ΔM; 1-250 amu	9	S. Kempf, Personal Comm.
In Development	Interstellar Dust Analyzer	9 to 11	12 to 15	10	<1 μm Composition	TRL=6 Casini/CDA, IMAP/IDEX, Europa Clipper/SUDA	Szalay+2019, 2nd Interstellar Probe Exploration Workshop, NYC.
New Horizons	SDC	1.9	5	900	10^{-12} – 10^{-9} g, 0.5-10 μm	9	Szalay, J. et al. Dust Measurements by the Student Dust Counter Onboard the New Horizons Mission to Pluto, https://www.hou.usra.edu/meetings/lpsc2015/pdf/1701.pdf

3.4.9. Optical and IR Spectral Imaging

A wide-spectrum imaging instrument on Interstellar Probe will enable a wide range of remote science. To produce the maximum science return, such an instrument would need to (1) produce spectral resolution $R = \lambda/\Delta\lambda \sim 100$ images of the sky in the optical and near-IR, from 0.5 to 15 μm in wavelength; (2) produce spectral resolution $R \sim 2$ images of the sky in discrete bands from 25 to 100 μm in wavelength; (3) have angular resolution of at least several arcseconds in the optical and several arcminutes in the far-IR; and (4) map the full 2π steradians of the sky in the direction

of the outward trajectory of the probe. Such an instrument would be able to address the full range of science discussed in sections 3.3 and 3.4, namely imaging of IPD and measurements of the diffuse galactic and extragalactic backgrounds.

Observing the surface brightness of the IPD as a function of position on an outward trajectory will enable tomographic measurement of the cloud's structure and spectrum through the Radon transform. These data would be interesting all the way from the Sun out to 100 au and beyond. The inner solar system is brightest at near-IR wavelengths, while measurements of the EKB are particularly compelling in the FIR, where the cold dust grains are emitting thermal radiation and the contrast with the various backgrounds that exist is maximal (A. R. Poppe et al., 2019). Such far-IR imagery would inform us about the dust cloud's thermodynamic state, while the VISIR spectrometer would provide maps of the inner cloud's dust particle size and composition. Such full-spectrum IR remote sensing would map the visible extent of the inner, near-Earth zodiacal cloud and determine whether it connects smoothly into an outer cloud or whether there is a second outer cloud sourced by the Kuiper Belt and isolated by the outer planets, as predicted by (Kuchner & Stark, 2010; Andrew R. Poppe, 2016). Such measurements would allow us to make a map of the inner solar system and EKB dust distributions that could be compared directly against images in other exoplanetary systems.

If possible, observing at high phase angle by looking back toward the Sun could enable deep searches for the presence of rings and dust clouds around discrete sources, such as possible strong individual sources of the debris clouds like Planet X, or the Haumea family collisional fragments, rings of the Centaur Chariklo, or dust emitted from spallation off the six known bodies of the Pluto system. Such "Pale Blue Dot" images would provide interesting data to compare to current and

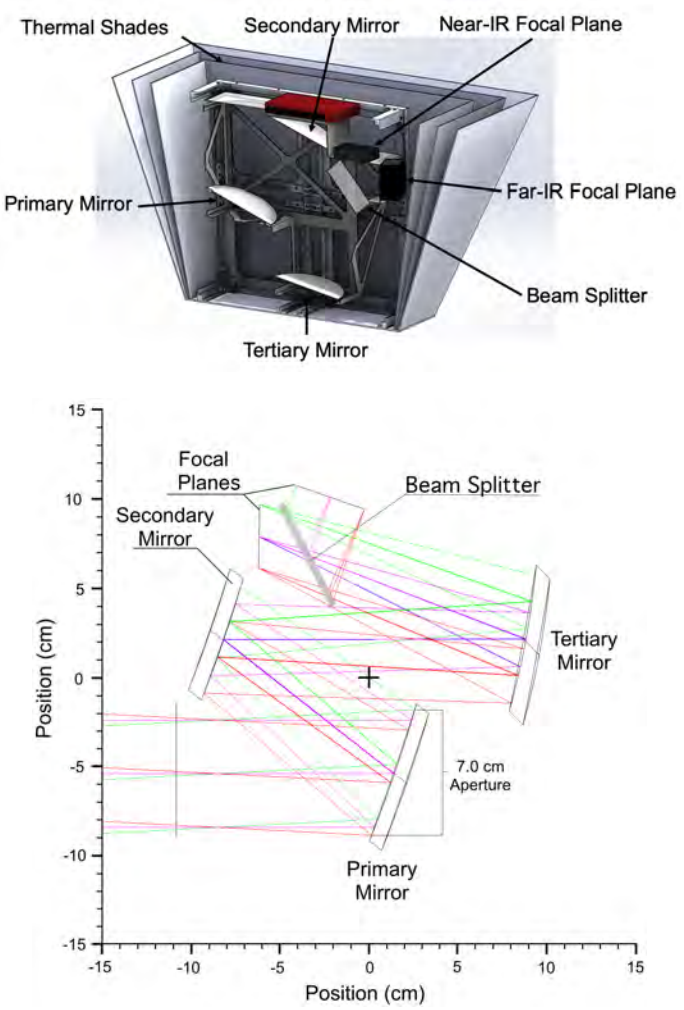

Figure 3-40. Illustrative layout of a wide-band spectral imager utilizing a 7-cm clear aperture free-form off-axis telescope. The near-IR (0.5–10 µm) and FIR (25–100 µm) channels are split by a beam splitter and use 2k × 2k H2RG and single-element photoconductor detectors, respectively. (Image and figure courtesy of M. Zemcov.)

future measurements of exoplanets. The same remote sensors would be designed and available to map the surfaces of any KBOs encountered along Interstellar Probe's trajectory.

The same instrument could also be used to make definitive measurements of the extragalactic background light. The 0.5- to 15-µm VISIR camera could take very sensitive images of the sky in many patches to search for the isotropic component of emission as well as separate the galactic and extragalactic components. At the shorter-wavelength end, such an instrument would easily have the sensitivity to detect and separate the reionization signal from the extragalactic background, thereby producing important constraints on the physics of the earliest stars and galaxies in the universe. Over the whole range, comparison to the γ-ray and galaxy counting measurements would allow searches for a wide range of beyond-standard model physics.

Using new technologies and passively cooled detectors, a suitable low size, weight, and power system VISIR spectrometer/far-IR imager has been specified for the study baseline design. A single two-channel spectroscopic imager on a 7-cm telescope with a ~3° FOV could meet all the science requirements using off-the-shelf, field-tested technologies. The telescope would use modern, free-form optics to maximize the instrument's throughput while minimizing size and mass. VISIR photodetection would be provided by a H2RG HgCdTe detector of the type developed for the NEOCAM mission. Operation in the FIR from 25 to 100 µm would use high-heritage photoconduction detectors (Poglitsch et al., 2010). The VISIR detector array would be cooled to ~30K, and the longer wave detectors would be cooled to ~3K to achieve high sensitivity. Thermal shade technology proven by, e.g., the Planck mission would be used to passively cool the instrument. Such passive cooling would place stringent restrictions on the ability of the instrument to point in the direction of the Sun until later in the mission, when the solar irradiance would be small. At VISIR wavelengths, spectral discrimination could be accomplished by a fixed linear variable filter above the focal plane with N spectral elements, each covering 1/N of the FOV. Different wavelength bands could be sampled sequentially as the camera steps N times across the FOV, an approach that has been used on New Horizons with great success. Although small, the telescope aperture gives a diffraction-limited beam of 0.8–16 inches (0.5–10 µm) and 1.5–6 feet (25–100 µm), which will be adequate to mask or subtract stars from images using known catalogs to reveal the underlying diffuse component (Zemcov et al., 2017). The camera would be equipped with a cold shutter to measure the dark current and instrumental background. Based on a preliminary study shown in Figure 3-40, approximate mass and power estimates for a purely passively cooled system are 4 kg and 3 W.

Table 3-17. Optical and IR Spectral Imager Objectives and Requirements

Measurement Objectives	Measurement Requirements
Structure and composition of the inner zodiacal cloud	R ~ 100 spectral imaging over 0.5–15 μm
Structure and composition of the EKB dust	R ~ 2 imaging over 25–100 μm
Mapping of the dust cloud structure in the mid-solar system	R ~ 2 imaging over 0.5–15 μm
Searches for IPD structures (trails, clumps, rings)	Angular resolution < 10 arcmin at all wavelengths
Maps of diffuse galactic light	Imaging > 100° in one linear dimension in both near-IR and far-IR
Extragalactic background absolute photometry	R ~ 20 spectral imaging over 0.5–10 μm Angular resolution < 10 inches at 1 μm Multiple >5° fields to prove statistical isotropy
Spectrum of epoch of reionization	R ~ 50 spectral imaging over 0.5–3 μm Angular resolution < 5 inches at 1 μm

The operation of the imager may impose requirements on the pointing ability of the spacecraft. For a three-axis-stabilized spacecraft, operation at the shortest wavelength would require pointing at the ~0.5-inch level over a 300-s exposure with the ability to step in increments of 0.1° to make exposures at multiple wavelengths. It is important to note that this imager would also be available to take images of solar system bodies such as KBOs as Interstellar Probe traverses the solar system.

In case of a limited thrust budget of an Interstellar Probe, it is important for instruments to be able to return science in a slow-spinning spin-stabilized mode. In such a mode, a scan mirror would be required to stabilize the image of the sky during an exposure. Ideally, the camera would image the 2π steradian away from the Sun as a function of heliocentric distance to permit reverse-modeling of the IPD cloud.

In the future, instrument trades to be studied include (1) the optimal and acceptable spin rates, (2) scan mirror technologies and heritage, (3) the technical feasibility of an active pointing system for the instrument subassembly, (4) passive cooling schemes and impacts on detector noise properties, and (5) data volume capabilities and restrictions and their impact on survey design.

Table 3-18. Examples of Current IR Instruments That Have Flown, Are in Operation, or Are in Development

Mission	Instrument	Mass (kg)	Power (W)	Bitrate (bps)	Capabilities	TRL and Heritage	References/Notes
New Horizons	RALPH (MVIC and LEISA)	10.5	7.1	Variable; 1-3 kbps	75 mm aperture, 658 mm Effective Focal Length, MVIC panchromatic images (400 to 975 nm), medium resolution, high SNR multispectral imaging, blue, red, IR, methane filters, LEISA is a wedged filter infra-red spectral imager (1.25-2.5 micron)	9	Reuter, D.C. Ralph: A Visible/Infrared Imager for the New Horizons Pluto/Kuiper Belt Mission, 2005.
OSIRIS-Rex	OVIRS	17.8	8.8	Variable; 914 kbps (max,OSIRIS-Rex)	Wavelength range: 0.4 - 4.3 μm Resolving power (λ/Δλ): 125 - 560 (higher for longer wavelengths)		Simon-Miller A. A., "OSIRIS-REx OVIRS: A Scalable Visible to Near-IR Spectrometer for Planetary Study," 44th Lunar and Planetary Science Conference (2013)
In Development	VISIR Spectral Mapper	4	3	10 bps	0.5-15.0 μm, R ~100 1-D imaging spectrometer 10 μrad x 10 urad + 50 to 100 μm single element 10'x10' photometer	TRL = 9 for VISNIR flight instrument: Voyager/IRIS, Galileo/NIMS, Cassini/VIMS, ROSETTA/VIRTIS, NH RALPH/LEISA Using H2RG Detector: Deep Impact HRI/IR, OREX/OVIRS, JWST/NIRSPEC TRL = 5 Using "Speckle" Low Mass/Power Design: CIBER 2	Deep Impact HRI/IR: D.L. Hampton et al. Space Science Reviews 2005, 117:43 New Horizons/RALPH-LEISA: D.C. Reuter et al. 2008, Space Science Reviews 140:129 OSIRIS-REX/OVIRS: D.C. Reuter et al. 2018, Space Sci Rev 2018, 214:54 Zemcov, Personal Communication and 1st Interstellar Probe Exploration Workshop

3.5. Section 3 References

Abbott, B.P., Abbott, R., Abbott, T.D., et al. (2016) The Rate of Binary Black Hole Mergers Inferred from Advanced LIGO Observations Surrounding GW150914. *The Astrophysical Journal* 833. Retrieved from https://ui.adsabs.harvard.edu/abs/2016ApJ...833L...1A

Acciari, V.A., Ansoldi, S., Antonelli, L.A., et al. (2019) Measurement of the extragalactic background light using MAGIC and Fermi-LAT gamma-ray observations of blazars up to z = 1. *Monthly Notices of the Royal Astronomical Society* 486, 4233. doi: 10.1093/mnras/stz943

Acuña, M.H., Anderson, B.J., Russell, C.T., Wasilewski, P., Kletetschka, G., Zanetti, L., Omidi, N. (2002) NEAR Magnetic Field Observations at 433 Eros: First Measurements from the Surface of an Asteroid. *Icarus* 155, 220-228. Retrieved from https://ui.adsabs.harvard.edu/abs/2002Icar..155..220A

Akiyama, E., Hasegawa, Y., Hayashi, M., Iguchi, S. (2016) Planetary System Formation in the Protoplanetary Disk around HL Tauri. *The Astrophysical Journal* 818, 158. doi: 10.3847/0004-637x/818/2/158

Allegrini, F., Schwadron, N.A., McComas, D.J., Gloeckler, G., Geiss, J. (2005) Stability of the inner source pickup ions over the solar cycle. *Journal of Geophysical Research (Space Physics)* 110. Retrieved from https://ui.adsabs.harvard.edu/abs/2005JGRA..110.5105A

Allegrini, F., Ebert, R.W., Funsten, H.O. (2016) Carbon Foils for Space Plasma Instrumentation. *Journal of Geophysical Research: Space Physics* 121(5), 3931-3950. doi: 10.1002/2016ja022570

Altobelli, N., Postberg, F., Fiege, K., et al. (2016) Flux and composition of interstellar dust at Saturn from Cassini's Cosmic Dust Analyzer. *Science* 352, 312-318. Retrieved from https://ui.adsabs.harvard.edu/abs/2016Sci...352..312A

Anderson, B.J., Acuña, M.H., Lohr, D.A., Scheifele, J., Raval, A., Korth, H., Slavin, J.A. (2007) The Magnetometer Instrument on MESSENGER. *Space Sci. Rev.* 131, 417–450. doi: https://doi.org/10.1007/s11214-007-9246-7

Atri, D., Hariharan, B., Grießmeier, J.-M. (2013) Galactic Cosmic Ray-Induced Radiation Dose on Terrestrial Exoplanets. *Astrobiology* 13, 910. doi: 10.1089/ast.2013.1052

Aumann, H.H., Gillett, F.C., Beichman, C.A., de Jong, T., Houck, J.R., Low, F.J., Neugebauer, G., Walker, R.G., Wesselius, P.R. (1984) Discovery of a shell around alpha Lyrae. *The Astrophysical Journal* 278, L23. doi: 10.1086/184214

Baggaley, W.J. (2000) Advanced Meteor Orbit Radar observations of interstellar meteoroids. *Journal of Geophysical Research* 105, 10353. doi: 10.1029/1999ja900383

Bale, S.D., Goetz, K., Harvey, P.R., et al. (2016) The FIELDS Instrument Suite for Solar Probe Plus. *Space Sci. Rev.* 204, 49–82. doi: https://doi.org/10.1007/s11214-016-0244-5

Balogh, A., Izmodenov, V. (2005) The Heliosphere and Its Boundaries. In Institute, I.S.S. (Ed.), *The Solar System And Beyond: Ten Years Of The ISSI* (pp. 151-163): ESA Publications Division.

Balsiger, H., Altwegg, K., Bochsler, P., et al. (2007) Rosina – Rosetta Orbiter Spectrometer for Ion and Neutral Analysis. *Space Science Reviews* 128(1), 745-801. doi: 10.1007/s11214-006-8335-3

Barabash, S., Bhardwaj, A., Wieser, M., et al. (2009) Investigation of the Solar Wind-Moon Interaction Onboard Chandrayaan-1 Mission with the SARA Experiment. *Current Science* 96, 526-532.

Baranov, V.B., Krasnobaev, K.V., Kulikovskii, A.G. (1970) A Model of the Interaction Between Solar Wind and Interstellar Medium. *Akademiia Nauk SSSR Doklady* 194, 41. Retrieved from https://ui.adsabs.harvard.edu/abs/1970DoSSR.194...41B

Baranov, V.B., Malama, Y.G. (1993) Model of the Solar Wind Interaction with the Local Interstellar Medium Numerical Solution of Self-Consistent Problem. *Journal of Geophysical Research* 98, 15157-15164. Retrieved from https://ui.adsabs.harvard.edu/abs/1993JGR....9815157B

Baranov, V.B., Malama, Y.G. (1995) Effect of Local Interstellar Medium Hydrogen Fractional Ionization on the Distant Solar Wind and Interface Region. *Journal of Geophysical Research* 100, 14755-14762. Retrieved from https://ui.adsabs.harvard.edu/abs/1995JGR...10014755B

Barucci, M.A., Dalle Ore, C.M., Perna, D., Cruikshank, D.P., Doressoundiram, A., Alvarez-Candal, A., Dotto, E., Nitschelm, C. (2015) (50000) Quaoar: Surface Composition Variability. *Astronomy and Astrophysics* 584. Retrieved from https://ui.adsabs.harvard.edu/abs/2015A&A...584A.107B

Beichmann, C.A. (1988) The Study of Star Formation with IRAS. In (Vol. 297, pp. 148).

Berkner, L.V., Odishaw, H., Teichmann, T. (1961) Science in Space. *Physics Today* 14, 67. doi: 10.1063/1.3057166

Bertaux, J.L., Kyrölä, E., Quémerais, E., et al. (1995) SWAN: A Study of Solar Wind Anisotropies on SOHO with Lyman Alpha Sky Mapping. In Fleck, B., Domingo, V., Poland, A. (Eds.), *The SOHO Mission*. Dordrecht, The Netherlands: Springer.

Beyer, R.A., Nimmo, F., McKinnon, W.B., et al. (2017) Charon Tectonics. *Icarus* 287, 161. doi: 10.1016/j.icarus.2016.12.018

Beyer, R.A., Spencer, J., McKinnon, W.B., et al. (2018) *The Nature and Origin of Charon's Smooth Plains*. https://ui.adsabs.harvard.edu/abs/2018DPS....5050608B.

Bierson, C.J., Nimmo, F., McKinnon, W.B. (2018) Implications of the Observed Pluto-Charon Density Contrast. *Icarus* 309, 207. doi: 10.1016/j.icarus.2018.03.007

Brandt, T.D., Draine, B.T. (2012) The Spectrum of the Diffuse Galactic Light: The Milky Way in Scattered Light. *The Astrophysical Journal* 744, 129. doi: 10.1088/0004-637x/744/2/129

Broadfoot, A.L., Sandel, B.R., Shemansky, D.E., et al. (1977) Ultraviolet Spectrometer Experiment for the Voyager Mission. *Space Science Reviews* 21, 183-205. Retrieved from https://ui.adsabs.harvard.edu/abs/1977SSRv...21..183B

Brown, M.E. (2008) The Largest Kuiper Belt Objects. In *The Solar System Beyond Neptune* (pp. 335). Tucson, AZ: University of Arizona Press,.

Brown, M.E. (2012) The Compositions of Kuiper Belt Objects. *Annual Review of Earth and Planetary Sciences* 40, 467. doi: 10.1146/annurev-earth-042711-105352

Buchalter, A., Kamionkowski, M. (1997) Rates for Parallax-shifted Microlensing Events from Ground-based Observations of the Galactic Bulge. *The Astrophysical Journal* 482, 782-791. Retrieved from https://ui.adsabs.harvard.edu/abs/1997ApJ...482..782B

Burlaga, L.F. (1993) Solar Wind Behavior Throughout the Heliosphere. *Advances in Space Research* 13, 27. doi: 10.1016/0273-1177(93)90386-p

Burlaga, L.F., Ness, N.F. (1998) Magnetic Field Strength Distributions and Spectra in the Heliosphere and Their Significance for Cosmic Ray Modulation: Voyager 1, 1980-1994. *Journal of Geophysical Research* 103, 29719. doi: 10.1029/98ja02682

Burlaga, L.F., Wang, C., Richardson, J.D., Ness, N.F. (2003) Evolution of Magnetic Fields in Corotating Interaction Regions from 1 to 95 AU: Order to Chaos. *The Astrophysical Journal* 590, 554. doi: 10.1086/374926

Burlaga, L.F., Ness, N.F. (2013) Magnetic Field Strength Fluctuations and the q-Triplet in the Heliosheath: Voyager 2 Observations from 91.0 to 94.2 AU at Latitude 30° s. *The Astrophysical Journal* 765, 35. doi: 10.1088/0004-637x/765/1/35

Burlaga, L.F., Ness, N.F., Gurnett, D.A., Kurth, W.S. (2013) Evidence for a Shock in Interstellar Plasma: Voyager 1. *The Astrophysical Journal* 778, L3. doi: 10.1088/2041-8205/778/1/l3

Burlaga, L.F., Ness, N.F., Stone, E.C. (2013) Magnetic Field Observations as Voyager 1 Entered the Heliosheath Depletion Region. *Science* 341(6142), 147-150. doi: 10.1126/science.1235451

Burlaga, L.F., Ness, N.F. (2016) Observations of the Interstellar Magnetic Field in the Outer Heliosheath: Voyager 1. *The Astrophysical Journal* 829. Retrieved from https://ui.adsabs.harvard.edu/\#abs/2016ApJ...829..134B

Burns, J.A., Lamy, P.L., Soter, S. (1979) Radiation Forces on Small Particles in the Solar System. *Icarus* 40, 1. doi: 10.1016/0019-1035(79)90050-2

Carr, B.J., Kohri, K., Sendouda, Y., Yokoyama, J.i. (2016) Constraints on Primordial Black Holes from the Galactic Gamma-Ray Background. *Physical Review D* 94. Retrieved from https://ui.adsabs.harvard.edu/abs/2016PhRvD..94d4029C

Cheng, A.F., Weaver, H.A., Conard, S.J., et al. (2008) Long-Range Reconnaissance Imager on New Horizons. *Space Science Reviews* 140, 189-215. Retrieved from https://ui.adsabs.harvard.edu/\#abs/2008SSRv..140..189C

Clark, G., Allegrini, F., McComas, D.J., Louarn, P. (2016) Modeling the Response of a Top Hat Electrostatic Analyzer in an External Magnetic Field: Experimental Validation with the Juno JADE-E Sensor. *Journal of Geophysical Research: Space Physics* 121(6), 5121-5136. doi: https://doi.org/10.1002/2016JA022583

Conrad, J.W., Nimmo, F., Schenk, P.M., et al. (2019) An Upper Bound on Pluto's Heat Flux from a Lack Of Flexural Response of Its Normal Faults. *Icarus* 328, 210. doi: 10.1016/j.icarus.2019.03.028

Cooray, A. (2016) Extragalactic Background Light Measurements and Applications. *Royal Society Open Science* 3, 150555. Retrieved from https://ui.adsabs.harvard.edu/abs/2016RSOS....350555C

Cox, N.L.J., Kerschbaum, F., van Marle, A.J., et al. (2012) A far-infrared survey of bow shocks and detached shells around AGB stars and red supergiants. *Astronomy & Astrophysics* 537. doi: 10.1051/0004-6361/201117910

Cummings, A.C., Tranquille, C., Marsden, R.G., Mewaldt, R.A., Stone, E.C. (2009) Radial and latitudinal gradients of anomalous cosmic ray oxygen in the inner heliosphere. *Geophysical Research Letters* 36. Retrieved from https://ui.adsabs.harvard.edu/abs/2009GeoRL..3618103C

Decker, R.B., Krimigis, S.M., Roelof, E.C., Hill, M.E., Armstrong, T.P., Gloeckler, G., Hamilton, D.C., Lanzerotti, L.J. (2008) Mediation of the Solar Wind Termination Shock by Non-Thermal Ions. *Nature* 454(7200), 67. doi: 10.1038/nature07030

Demajistre, R., Brandt, P.C., Roelof, E.C., Westlake, J.H., Gruntman, M., McNutt, R.L., Jr. (2018) *Using Energetic Neutral Atoms to study the structure of the Outer Heliosphere from Vantage Points Several Hundred AU from the Sun*. https://ui.adsabs.harvard.edu/abs/2018AGUFMSH33C3661D.

Desai, M.I., Allegrini, F.A., Bzowski, M., et al. (2014) Energetic Neutral Atoms Measured by the Interstellar Boundary Explorer (IBEX): Evidence for Multiple Heliosheath Populations. *The Astrophysical Journal* 780, 98. doi: 10.1088/0004-637x/780/1/98

Dialynas, K., Krimigis, S.M., Mitchell, D.G., Decker, R.B., Roelof, E.C. (2017) The Bubble-Like Shape of the Heliosphere Observed by Voyager and Cassini. *Nature Astronomy* 1(5). doi: http://dx.doi.org/10.1038/s41550-017-0115

Dong, S., Udalski, A., Gould, A., et al. (2007) First Space-Based Microlens Parallax Measurement: Spitzer Observations of OGLE-2005-SMC-001. *The Astrophysical Journal* 664, 862-878. Retrieved from https://ui.adsabs.harvard.edu/abs/2007ApJ...664..862D

Dougherty, M.K., Kellock, S., Southwood, D.J., et al. (2004) The Cassini Magnetic Field Investigation. *Space Sci. Rev.* 114, 331-383. doi: 10.1007/s11214-004-1432-2

Draine, B.T. (2009) Perspectives on Interstellar Dust Inside and Outside of the Heliosphere. *Space Science Reviews* 143, 333-345. Retrieved from https://ui.adsabs.harvard.edu/abs/2009SSRv..143..333D

Draine, B.T., Hensley, B. (2013) Magnetic Nanoparticles in the Interstellar Medium: Emission Spectrum and Polarization. *The Astrophysical Journal* 765, 159. doi: 10.1088/0004-637x/765/2/159

Dwek, E., Krennrich, F. (2013) The extragalactic background light and the gamma-ray opacity of the universe. *Astroparticle Physics* 43, 112. doi: 10.1016/j.astropartphys.2012.09.003

Elbert, O.D., Bullock, J.S., Kaplinghat, M. (2018) Counting black holes: The cosmic stellar remnant population and implications for LIGO. *Monthly Notices of the Royal Astronomical Society* 473, 1186-1194. Retrieved from https://ui.adsabs.harvard.edu/abs/2018MNRAS.473.1186E

Ertel, S., Absil, O., Defrère, D., Augereau, J.-C., Mennesson, B. (2018) Prospects for the characterisation of exo-zodiacal dust with the VLTI. *Experimental Astronomy* 46, 401. doi: 10.1007/s10686-018-9600-7

Ertel, S., Kamath, D., Hillen, M., et al. (2019) Resolved Imaging of the AR Puppis Circumbinary Disk. *The Astronomical Journal* 157, 110. doi: 10.3847/1538-3881/aafe04

Fausch, R.G., Wurz, P., Tulej, M., Jost, J., Gubler, P., Gruber, M., Lasi, D., Zimmermann, C., Gerber, T. (2018, 3-10 March 2018) *Flight Electronics of GC-Mass Spectrometer for Investigation of Volatiles in the Lunar Regolith.* In 2018 IEEE Aerospace Conference, IEEE, Big Sky, MT.

Fisk, L.A., Gloeckler, G. (2013) The Global Configuration of the Heliosheath Inferred from Recent Voyager 1 Observations. *The Astrophysical Journal* 776. Retrieved from https://ui.adsabs.harvard.edu/abs/2013ApJ...776...79F

Florinski, V. (2015) Magnetic Flux Tube Interchange at the Heliopause. *The Astrophysical Journal* 813, 49. doi: 10.1088/0004-637x/813/1/49

Frisch, P.C., Dorschner, J.M., Geiss, J., et al. (1999) Dust in the Local Interstellar Wind. *The Astrophysical Journal* 525, 492. doi: 10.1086/307869

Fulton, B.J., Petigura, E.A., Howard, A.W., et al. (2017) The California-Kepler Survey. III. A Gap in the Radius Distribution of Small Planets. *The Astronomical Journal* 154, 109. doi: 10.3847/1538-3881/aa80eb

Funsten, H.O., McComas, D.J., Moore, K.R., Scime, E.E., Thomsen, M.F. (1994) Imaging of magnetospheric dynamics using low energy neutral atom detection. *Washington DC American Geophysical Union Geophysical Monograph Series* 84, 275. doi: 10.1029/GM084p0275

Funsten, H.O., Allegrini, F., Bochsler, P., et al. (2009) The Interstellar Boundary Explorer High Energy (IBEX-Hi) Neutral Atom Imager. *Space Science Reviews* 146(1-4), 75-103. doi: 10.1007/s11214-009-9504-y

Funsten, H.O., DeMajistre, R., Frisch, P.C., et al. (2013) Circularity of the Interstellar Boundary Explorer Ribbon of Enhanced Energetic Neutral Atom (ENA) Flux. *The Astrophysical Journal* 776(1), 30. doi: 10.1088/0004-637X/776/1/30

Fuselier, S.A., Bochsler, P., Chornay, D., et al. (2009) The IBEX-Lo Sensor. *Space Science Reviews* 146(1-4), 117-147. doi: 10.1007/s11214-009-9495-8

Fuselier, S.A., Allegrini, F., Bzowski, M., et al. (2012) Heliospheric Neutral Atom Spectra Between 0.01 and 6 keV From IBEX. *The Astrophysical Journal* 754(1), 14. doi: 10.1088/0004-637x/754/1/14

Fuselier, S.A., Allegrini, F., Bzowski, M., et al. (2014) Low Energy Neutral Atoms From the Heliosheath. *The Astrophysical Journal* 784(2), 89. doi: 10.1088/0004-637x/784/2/89

Galli, A., Wurz, P., Schwadron, N.A., et al. (2016) THE Roll-Over of Heliospheric Neutral Hydrogen Below 100 eV: Observations and Implications. *The Astrophysical Journal* 821(2), 107. doi: 10.3847/0004-637x/821/2/107

Gamayunov, K., Zhang, M., Rassoul, H. (2010) Pitch Angle Scattering in the Outer Heliosheath and Formation of the Interstellar Boundary EXplorer ribbon. *The Astrophysical Journal* 725, 2251. doi: 10.1088/0004-637x/725/2/2251

Geiss, J., Gloeckler, G., Fisk, L.A., von Steiger, R. (1995) C^+ Pickup Ions in the Heliosphere and Their Origin. *Journal of Geophysical Research* 100, 23373-23378. Retrieved from https://ui.adsabs.harvard.edu/abs/1995JGR...10023373G

Giacalone, J., Jokipii, J.R. (2015) A New Model for the Heliosphere's "IBEX Ribbon". *The Astrophysical Journal* 812, L9. doi: 10.1088/2041-8205/812/1/l9

Gilles, H., Hamel, J., Chéron, B. (2001) Laser Pumped ^{4}He Magnetometer. *Review of Scientific Instruments* 72, 2253. doi: 10.1063/1.1364667

Gladstone, G.R., Stern, S.A., Ennico, K., et al. (2016) The Atmosphere of Pluto as Observed by New Horizons. *Science* 351, aad8866. doi: 10.1126/science.aad8866

Gladstone, G.R., Pryor, W.R., Stern, S.A., et al. (2018) The Lyman-α Sky Background as Observed by New Horizons. *Geophysical Research Letters* 45, 8022. doi: 10.1029/2018gl078808

Glassmeier, K.-H., Boehnhardt, H., Koschny, D., Kührt, E., Richter, I. (2007) The Rosetta Mission: Flying Towards the Origin of the Solar System. *Space Science Reviews* 128, 1. doi: 10.1007/s11214-006-9140-8

Gloeckler, G., Geiss, J., Balsiger, H., et al. (1992) The Solar Wind Ion Composition Spectrometer. *Astronomy and Astrophysics Supplement Series* 92, 267-289. Retrieved from https://ui.adsabs.harvard.edu/abs/1992A&AS...92..267G

Gloeckler, G., Geiss, J. (1996) Abundance of ^{3}He in the Local Interstellar Cloud. *Nature* 381, 210-212. Retrieved from https://ui.adsabs.harvard.edu/abs/1996Natur.381..210G

Gloeckler, G., Cain, J., Ipavich, F.M., et al. (1998) Investigation of the Composition of Solar and Interstellar Matter Using Solar Wind and Pickup Ion Measurements with SWICS and SWIMS on the ACE Spacecraft. In Russell, C.T., Mewaldt, R.A., Von Rosenvinge, T.T. (Eds.), *The Advanced Composition Explorer Mission* (pp. 497-539). Dordrecht, The Netherlands: Springer.

Gloeckler, G., Geiss, J. (1998) Interstellar and Inner Source Pickup Ions Observed with Swics on Ulysses. *Space Science Reviews* 86(1-4), 127-159. doi: 10.1023/a:1005019628054

Gloeckler, G., Geiss, J. (2004) Composition of the local interstellar medium as diagnosed with pickup ions. *Advances in Space Research* 34, 53. doi: 10.1016/j.asr.2003.02.054

Gloeckler, G., Fisk, L.A. (2015) More Evidence That Voyager 1 Is Still in the Heliosphere. *The Astrophysical Journal* 806(2). doi: 10.1088/2041-8205/806/2/l27

Gloeckler, G., Fisk, L.A. (2016) Energetic Neutral Hydrogen Observations Demonstrate that Voyager 1 is Not Observing the Extraordinarily Strong Interstellar Magnetic Field. *The Astrophysical Journal* 833. Retrieved from https://ui.adsabs.harvard.edu/abs/2016ApJ...833..290G

Gómez-Herrero, R., Rodriguez-Pacheco, J., Wimmer-Schweingruber, R., et al. (2017) *The Solar Orbiter Mission: An Energetic Particle Perspective*. Retrieved from arXiv:1701.04057

Gould, A., Loeb, A. (1992) Discovering Planetary Systems through Gravitational Microlenses. *The Astrophysical Journal* 396, 104. Retrieved from https://ui.adsabs.harvard.edu/abs/1992ApJ...396..104G

Gould, A., Udalski, A., Monard, B., et al. (2009) The Extreme Microlensing Event OGLE-2007-BLG-224: Terrestrial Parallax Observation of a Thick-Disk Brown Dwarf. *The Astrophysical Journal* 698, L147-L151. Retrieved from https://ui.adsabs.harvard.edu/abs/2009ApJ...698L.147G

Grady, C.A., Polomski, E.F., Henning, T., et al. (2001) The Disk and Environment of the Herbig Be Star HD 100546. *The Astronomical Journal* 122, 3396. doi: 10.1086/324447

Greaves, J.S., Wyatt, M.C., Holland, W.S., Dent, W.R.F. (2004) The Debris Disc Around τ Ceti: A Massive Analogue to the Kuiper Belt. *Monthly Notices of the Royal Astronomical Society* 351, L54. doi: 10.1111/j.1365-2966.2004.07957.x

Greaves, J.S., Rice, W.K.M. (2011) Do All Sun-Like Stars Have Planets? Inferences from the Disc Mass Reservoirs of Class 0 Protostars. *Monthly Notices of the Royal Astronomical Society* 412, L88. doi: 10.1111/j.1745-3933.2011.01011.x

Grenfell, J.L., Grießmeier, J.-M., Patzer, B., Rauer, H., Segura, A., Stadelmann, A., Stracke, B., Titz, R., Von Paris, P. (2007) Biomarker Response to Galactic Cosmic Ray-Induced NO_x and the Methane Greenhouse Effect in the Atmosphere of an Earth-Like Planet Orbiting an M Dwarf Star. *Astrobiology* 7, 208. doi: 10.1089/ast.2006.0129

Gruen, E., Gustafson, B., Mann, I., Baguhl, M., Morfill, G.E., Staubach, P., Taylor, A., Zook, H.A. (1994) Interstellar Dust in the Heliosphere. *Astronomy and Astrophysics* 286, 915. Retrieved from https://ui.adsabs.harvard.edu/abs/1994A&A...286..915G

Grun, E., Zook, H.A., Baguhl, M., et al. (1993) Discovery of Jovian dust streams and interstellar grains by the Ulysses spacecraft. *Nature* 362, 428. doi: 10.1038/362428a0

Grün, E., Landgraf, M. (2001) Fast Dust in the Heliosphere. *Space Science Reviews* 99, 151-164. Retrieved from https://ui.adsabs.harvard.edu/abs/2001SSRv...99..151G

Grundy, W.M., Cruikshank, D.P., Gladstone, G.R., et al. (2016) The Formation of Charon's Red Poles from Seasonally Cold-Trapped Volatiles. *Nature* 539, 65-68. Retrieved from https://ui.adsabs.harvard.edu/abs/2016Natur.539...65G

Gruntman, M., Fahr, H.J. (2000) Heliopause Imaging in EUV: Oxygen O^+ Ion 83.4-nm Resonance Line Emission. *Journal of Geophysical Research* 105, 5189. doi: 10.1029/1999ja000345

Gruntman, M., Roelof, E.C., Mitchell, D.G., Fahr, H.J., Funsten, H.O., McComas, D.J. (2001) Energetic Neutral Atom Imaging of the Heliospheric Boundary Region. *Journal of Geophysical Research: Space Physics* 106(A8), 15767-15781. doi: https://doi.org/10.1029/2000JA000328

Gruntman, M. (2004) Instrumentation for Interstellar Exploration. *Advances in Space Research* 34, 204. doi: 10.1016/j.asr.2003.04.064

Gruntman, M., Izmodenov, V. (2004) Mass transport in the heliosphere by energetic neutral atoms. *Journal of Geophysical Research: Space Physics (1978–2012)* 109(A12). doi: 10.1029/2004ja010727

Grygorczuk, J., Czechowski, A., Grzedzielski, S. (2014) Why are the Magnetic Field Directions Measured by Voyager 1 on Both Sides of the Heliopause so Similar? *The Astrophysical Journal* 789, L43. doi: 10.1088/2041-8205/789/2/l43

Gurnett, D.A., Kurth, W.S., Shaw, R.R., Roux, A., Gendrin, R., Kennel, C.F., Scarf, F.L., Shawhan, S.D. (1992) The Galileo Plasma Wave Investigation. *Space Science Reviews* 60(1), 341-355. doi: 10.1007/BF00216861

Gurnett, D.A., Kurth, W.S., Allendorf, S.C., Poynter, R.L. (1993) Radio Emission from the Heliopause Triggered by an Interplanetary Shock. *Science* 262, 199-203. Retrieved from https://ui.adsabs.harvard.edu/abs/1993Sci...262..199G

Gurnett, D.A., Kurth, W.S., Burlaga, L.F., Ness, N.F. (2013) In Situ Observations of Interstellar Plasma with Voyager 1. *Science* 341(6153), 1489-1492. doi: 10.1126/science.1241681

Gurnett, D.A., Kurth, W.S., Stone, E.C., Cummings, A.C., Krimigis, S.M., Decker, R.B., Ness, N.F., Burlaga, L.F. (2015) Precursors To Interstellar Shocks of Solar Origin. *The Astrophysical Journal* 809. Retrieved from https://ui.adsabs.harvard.edu/abs/2015ApJ...809..121G

Gustafson, B.A.S. (1994) Physics of Zodiacal Dust. *Annual Review of Earth and Planetary Sciences* 22, 553. doi: 10.1146/annurev.ea.22.050194.003005

Hahn, J.M., Zook, H.A., Cooper, B., Sunkara, B. (2002) Clementine Observations of the Zodiacal Light and the Dust Content of the Inner Solar System. *Icarus* 158, 360. doi: 10.1006/icar.2002.6881

Hammond, N.P., Barr, A.C., Parmentier, E.M. (2016) Recent Tectonic Activity on Pluto Driven by Phase Changes in the Ice Shell. *Geophysical Research Letters* 43, 6775. doi: 10.1002/2016gl069220

Harch, A.P. (2016) Accommodating Navigation Uncertainties in the Pluto Encounter Sequence Design. In *SpaceOps 2016 Conference*.

Hauser, M.G., Gillett, F.C., Low, F.J., Gautier, T.N., Beichman, C.A., Neugebauer, G., Aumann, H.H., Baud, B., Boggess, N., Emerson, J.P. (1984) IRAS Observations of the Diffuse Infrared Background. *The Astrophysical Journal* 278. Retrieved from http://scholar.google.com/scholar?q=IRAS observations of the diffuse infrared background&btnG=&hl=en&num=20&as_sdt=0%2C22

Hauser, M.G., Dwek, E. (2001) The Cosmic Infrared Background: Measurements and Implications. *Annual Review of Astronomy and Astrophysics* 39, 249-307. Retrieved from https://ui.adsabs.harvard.edu/abs/2001ARA&A..39..249H

Heerikhuisen, J., Pogorelov, N.V., Zank, G.P., Crew, G.B., Frisch, P.C., Funsten, H.O., Janzen, P.H., McComas, D.J., Reisenfeld, D.B., Schwadron, N.A. (2009) Pick-Up Ions in the Outer Heliosheath: A Possible Mechanism for the Interstellar Boundary Explorer Ribbon. *The Astrophysical Journal* 708(2). doi: 10.1088/2041-8205/708/2/l126

Heerikhuisen, J., Zirnstein, E.J., Funsten, H.O., Pogorelov, N.V., Zank, G.P. (2014) The Effect of New Interstellar Medium Parameters on the Heliosphere and Energetic Neutral Atoms from the Interstellar Boundary. *The Astrophysical Journal* 784, 73. doi: 10.1088/0004-637x/784/1/73

Helgason, K., Cappelluti, N., Hasinger, G., Kashlinsky, A., Ricotti, M. (2014) The Contribution of z <~ 6 Sources to the Spatial Coherence in the Unresolved Cosmic Near-infrared and X-Ray Backgrounds. *The Astrophysical Journal* 785, 38. doi: 10.1088/0004-637x/785/1/38

Hill, M.E., Allen, R.C., Kollmann, P., Brown, L.E., Decker, R.B., McNutt, R.L., Krimigis, S.M. (2019) Influence of Solar Disturbances on Galactic Cosmic Rays in the Solar Wind, Heliosheath, and Local Interstellar Medium: ACE, New Horizons, and Voyager Observations. *Astrophysics Journal*.

Horányi, M., Hoxie, V., James, D., et al. (2008) The Student Dust Counter on the New Horizons Mission. *Space Science Reviews* 140, 387-402. Retrieved from https://ui.adsabs.harvard.edu/abs/2008SSRv..140..387H

Howard, A.D., Moore, J.M., Umurhan, O.M., et al. (2017) Present and Past Glaciation on Pluto. *Icarus* 287, 287. doi: 10.1016/j.icarus.2016.07.006

Hsieh, K.C., Shih, K.L., Jokipii, J.R., Grzedzielski, S. (1992) Probing the Heliosphere with Energetic Hydrogen Atoms. *The Astrophysical Journal* 393, 756. doi: 10.1086/171543

Ichiki, K. (2014) CMB Foreground: A Concise Review. *Progress of Theoretical and Experimental Physics* 2014, 06B109. doi: 10.1093/ptep/ptu065

Isella, A., Guidi, G., Testi, L., et al. (2016) Ringed Structures of the HD 163296 Protoplanetary Disk Revealed by ALMA. *Physical Review Letters* 117(25), 251101. doi: 10.1103/PhysRevLett.117.251101

Isenberg, P.A. (2014) Spatial Confinement of the IBEX Ribbon: A Dominant Turbulence Mechanism. *The Astrophysical Journal* 787, 76. doi: 10.1088/0004-637x/787/1/76

Izmodenov, V., Malama, Y.G., Lallement, R. (1997) Interstellar Neutral Oxygen in a Two-Shock Heliosphere. *Astronomy and Astrophysics* 317, 193. Retrieved from https://ui.adsabs.harvard.edu/abs/1997A&A...317..193I

Izmodenov, V., Malama, Y., Ruderman, M.S. (2005) Solar Cycle Influence on the Interaction of the Solar Wind with Local Interstellar Cloud. *Astronomy & Astrophysics* 429(3), 1069-1080. doi: 10.1051/0004-6361:20041348

Izmodenov, V.V., Malama, Y.G., Ruderman, M.S. (2008) Modeling of the Outer Heliosphere with the Realistic Solar Cycle. *Advances in Space Research* 41(2), 318-324. doi: 10.1016/j.asr.2007.06.033

Izmodenov, V.V. (2009) Local Interstellar Parameters as They Are Inferred from Analysis of Observations Inside the Heliosphere. *Space Science Reviews* 143, 139-150. Retrieved from https://ui.adsabs.harvard.edu/abs/2009SSRv..143..139I

Izmodenov, V.V., Alexashov, D.B., Ruderman, M.S. (2014) Electron Thermal Conduction as a Possible Physical Mechanism to Make the Inner Heliosheath Thinner. *The Astrophysical Journal* 795, L7. doi: 10.1088/2041-8205/795/1/l7

Izmodenov, V.V., Alexashov, D.B. (2015) Three-Dimensional Kinetic-MHD Model of the Global Heliosphere with the Heliopause-Surface Fitting. *The Astrophysical Journal Supplement Series* 220(2), 32. doi: https://iopscience.iop.org/article/10.1088/0067-0049/220/2/32

Jiang, J.H., Zhai, A.J., Herman, J., Zhai, C., Hu, R., Su, H., Natraj, V., Li, J., Xu, F., Yung, Y.L. (2018) Using Deep Space Climate Observatory Measurements to Study the Earth as an Exoplanet. *The Astronomical Journal* 156(1), 26. doi: 10.3847/1538-3881/aac6e2

Kamata, S., Nimmo, F., Sekine, Y., Kuramoto, K., Noguchi, N., Kimura, J., Tani, A. (2019) Pluto's Ocean is Capped and Insulated by Gas Hydrates. *Nature Geoscience* 12, 407. doi: 10.1038/s41561-019-0369-8

Kasper, J.C., Abiad, R., Austin, G., et al. (2016) Solar Wind Electrons Alphas and Protons (SWEAP) Investigation: Design of the Solar Wind and Coronal Plasma Instrument Suite for Solar Probe Plus. *Space Science Reviews* 204(1), 131-186. doi: 10.1007/s11214-015-0206-3

Katushkina, O.A., Quémerais, E., Izmodenov, V.V., Lallement, R., Sandel, B.R. (2017) Voyager 1/UVS Lyman α Measurements at the Distant Heliosphere (90–130 AU): Unknown Source of Additional Emission. *Journal of Geophysical Research: Space Physics* 122(11). doi: 10.1002/2017ja024205

Keane, J.T., Matsuyama, I., Kamata, S., Steckloff, J.K. (2016) Reorientation and Faulting of Pluto Due to Volatile Loading Within Sputnik Planitia. *Nature* 540, 90. doi: 10.1038/nature20120

Kelsall, T., Weiland, J.L., Franz, B.A., et al. (1998) The *COBE* Diffuse Infrared Background Experiment Search for the Cosmic Infrared Background. II. Model of the Interplanetary Dust Cloud. *The Astrophysical Journal* 508, 44-73. Retrieved from https://iopscience.iop.org/article/10.1086/306380/fulltext/37785.text.html

Kimura, H., Mann, I., Jessberger, E.K. (2003) Elemental Abundances and Mass Densities of Dust and Gas in the Local Interstellar Cloud. *The Astrophysical Journal* 582, 846. doi: 10.1086/344691

Kletzing, C.A., Kurth, W.S., Acuna, M., et al. (2013) The Electric and Magnetic Field Instrument Suite and Integrated Science (EMFISIS) on RBSP. *Space Science Reviews* 179, 127-181. Retrieved from https://ui.adsabs.harvard.edu/abs/2013SSRv..179..127K

Korochkin, A.A., Rubtsov, G.I. (2018) Constraining the Star Formation Rate with the Extragalactic Background Light. *Monthly Notices of the Royal Astronomical Society* 481, 557-565. Retrieved from https://ui.adsabs.harvard.edu/abs/2018MNRAS.481..557K

Krimigis, S.M., Mitchell, D.G., Hamilton, D.C., et al. (2004) Magnetosphere Imaging Instrument (MIMI) on the Cassini Mission to Saturn/Titan. *Space Science Reviews*, 233-329. doi: 10.1007/s11214-004-1410-8

Krimigis, S.M., Mitchell, D.G., Roelof, E.C., Hsieh, K.C., McComas, D.J. (2009) Imaging the Interaction of the Heliosphere with the Interstellar Medium from Saturn with Cassini. *Science* 326(5955), 971-973. doi: 10.1126/science.1181079

Krimigis, S.M., Decker, R.B., Roelof, E.C., Hill, M.E., Armstrong, T.P., Gloeckler, G., Hamilton, D.C., Lanzerotti, L.J. (2013) Search for the Exit: Voyager 1 at Heliosphere's Border with the Galaxy. *Science* 341(6142), 144-147. doi: 10.1126/science.1235721

Krivolutsky, A.A. (1999) Global Structure of Ozone Response to Solar and Galactic Cosmic Ray Influence (Ground Based and Satellite Data Analysis). *Advances in Space Research* 24, 597. doi: 10.1016/s0273-1177(99)00477-9

Krüger, H., Strub, P., Altobelli, N., Sterken, V.J., Srama, R., Grün, E. (2019) Interstellar Dust in the Solar System: Model Versus in Situ Spacecraft Data. *Astronomy and Astrophysics* 626, A37. doi: 10.1051/0004-6361/201834316

Kubiak, M.A., Bzowski, M., Sokó, J.M., Swaczyna, P., Grzedzielski, S., Alexashov, D.B., Izmodenov, V.V., Möbius, E., Leonard, T., Fuselier, S.A. (2014) Warm Breeze from the Starboard Bow: A New Population of Neutral Helium in the Heliosphere. *The Astrophysical Journal Supplement Series* 213(2), 29. Retrieved from http://scholar.google.com/scholar?q=Warm breeze from the starboard bow: A new population of neutral helium in the heliosphere&btnG=&hl=en&num=20&as_sdt=0%2C22

Kuchner, M.J., Stark, C.C. (2010) Collisional Grooming Models of the Kuiper Belt Dust Cloud. *The Astronomical Journal*, 1007. doi: 10.1088/0004-6256/140/4/1007

Kurth, W.S., Gurnett, D.A., Scarf, F.L., Poynter, R.L. (1984) Detection of a Radio Emission at 3 kHz in the Outer Heliosphere. *Nature* 312, 27-31. Retrieved from https://ui.adsabs.harvard.edu/abs/1984Natur.312...27K

Kurth, W.S., Gurnett, D.A. (2003) On the Source Location of Low-Frequency Heliospheric Radio Emissions. *Journal of Geophysical Research: Space Physics* 108(A10). doi: https://doi.org/10.1029/2003JA009860

Lallement, R., Welsh, B.Y., Vergely, J.L., Crifo, F., Sfeir, D. (2003) 3D Mapping of the Dense Interstellar Gas Around the Local Bubble. *Astronomy and Astrophysics* 411, 447-464. Retrieved from https://ui.adsabs.harvard.edu/abs/2003A&A...411..447L

Lallement, R. (2007) The Local Interstellar Medium: Peculiar or Not? *Space Science Reviews* 130, 341. doi: 10.1007/s11214-007-9178-2

Lallement, R., Quémerais, E., Bertaux, J.-L., Sandel, B.R., Izmodenov, V. (2011) Voyager Measurements of Hydrogen Lyman-α Diffuse Emission from the Milky Way. *Science* 334, 1665. Retrieved from https://ui.adsabs.harvard.edu/abs/2011Sci...334.1665L

Lallement, R. (Producer) (2020) Into the Unknown Local Interstellar Cloud. *Interstellar Probe Webinar*. Retrieved from http://interstellarprobe.jhuapl.edu/Resources/Meetings/agenda.php?id=85.

Landgraf, M., Liou, J.-C., Zook, H.A., Grün, E. (2002) Origins of Solar System Dust beyond Jupiter. *The Astronomical Journal* 123, 2857. doi: 10.1086/339704

Leinert, C., Richichi, A., Haas, M. (1997) Binaries Among Herbig Ae/Be Stars. *Astronomy and Astrophysics* 318, 472. Retrieved from https://ui.adsabs.harvard.edu/abs/1997A&A...318..472L

Linde, T.J., Gombosi, T.I. (2000) Interstellar dust filtration at the heliospheric interface. *Journal of Geophysical Research* 105, 10411. doi: 10.1029/1999ja900149

Linsky, J.L., Wood, B.E. (1996) The α Centauri Line Of Sight: D/H Ratio, Physical Properties of Local Interstellar Gas, and Measurement of Heated Hydrogen (the "Hydrogen Wall") Near the Heliopause. *The Astrophysical Journal* 463, 254. doi: 10.1086/177238

Linsky, J.L., Redfield, S. (2013) *The Local ISM in Three Dimensions: Kinematics, Morphology and Physical Processes*. Presentation. European Southern Observatory. Retrieved from https://www.eso.org/sci/meetings/2013/UVASTRO/LISM_in_3D.pdf.

Liou, J.-C., Zook, H.A. (1999) Signatures of the Giant Planets Imprinted on the Edgeworth-Kuiper Belt Dust Disk. *The Astronomical Journal* 118, 580. doi: 10.1086/300938

Lisse, C.M., Wyatt, M.C., Chen, C.H., Morlok, A., Watson, D.M., Manoj, P., Sheehan, P., Currie, T.M., Thebault, P., Sitko, M.L. (2012) Spitzer Evidence for a Late-Heavy Bombardment and the Formation of Ureilites in η Corvi at ~1 Gyr. *The Astrophysical Journal* 747, 93. doi: 10.1088/0004-637x/747/2/93

Loeb, A., Barkana, R. (2001) The Reionization of the Universe by the First Stars and Quasars. *Annual Review of Astronomy and Astrophysics* 39, 19. doi: 10.1146/annurev.astro.39.1.19

Low, F.J., Tucker, W.H. (1968) Contribution of Infrared Galaxies to the Cosmic Background. *Physical Review Letters* 21(22), 1538-1541. doi: 10.1103/PhysRevLett.21.1538

Mahaffy, P.R., Richard Hodges, R., Benna, M., et al. (2014) The Neutral Mass Spectrometer on the Lunar Atmosphere and Dust Environment Explorer Mission. *Space Science Reviews* 185(1), 27-61. doi: 10.1007/s11214-014-0043-9

Malama, Y.G., Izmodenov, V.V., Chalov, S.V. (2006) Modeling of the Heliospheric Interface: Multi-Component Nature of the Heliospheric Plasma. *Astronomy and Astrophysics* 445, 693. doi: 10.1051/0004-6361:20053646

Mandt, K., Luspay-Kuti, A., Hamel, M., Jessup, K.-L., Hue, V., Kammer, J., Filwett, R. (2017) Photochemistry on Pluto: Part II HCN and Nitrogen Isotope Fractionation. *Monthly Notices of the Royal Astronomical Society* 472, 118. doi: 10.1093/mnras/stx1587

Mandt, K.E., Mousis, O., Marty, B., Cavalié, T., Harris, W., Hartogh, P., Willacy, K. (2015) Constraints from Comets on the Formation and Volatile Acquisition of the Planets and Satellites. *Space Science Reviews* 197, 297. doi: 10.1007/s11214-015-0161-z

Mandt, K.E., Eriksson, A., Edberg, N.J.T., et al. (2016) RPC Observation of the Development and Evolution of Plasma Interaction Boundaries at 67P/Churyumov-Gerasimenko. *Monthly Notices of the Royal Astronomical Society* 462, S9. doi: 10.1093/mnras/stw1736

Mandt, K.E., Mousis, O., Lunine, J., Marty, B., Smith, T., Luspay-Kuti, A., Aguichine, A. (2020) Tracing the Origins of the Ice Giants Through Noble Gas Isotopic Composition. *Space Science Reviews* 216(5), 99. doi: 10.1007/s11214-020-00723-5

Mann, I., Czechowski, A., Meyer-Vernet, N., Zaslavsky, A., Lamy, H. (2010) Dust in the Interplanetary Medium. *Plasma Physics and Controlled Fusion* 52, 124012. doi: 10.1088/0741-3335/52/12/124012

Marino, S., Matrà, L., Stark, C., et al. (2016) Exocometary Gas in the HD 181327 Debris Ring. *Monthly Notices of the Royal Astronomical Society* 460, 2933. doi: 10.1093/mnras/stw1216

Marsh, N.D., Svensmark, H. (2000) Low Cloud Properties Influenced by Cosmic Rays. *Physical Review Letters* 85, 5004. doi: 10.1103/PhysRevLett.85.5004

Mathis, J.S., Rumpl, W., Nordsieck, K.H. (1977) The Size Distribution of Interstellar Grains. *The Astrophysical Journal* 217, 425. doi: 10.1086/155591

Mattila, K. (2003) Has the Optical Extragalactic Background Light Been Detected? *The Astrophysical Journal* 591, 119. doi: 10.1086/375182

Mattila, K. (2006) The 1-μm Discontinuity in the Extragalactic Background Light Spectrum: An Artefact of Foreground Subtraction. *Monthly Notices of the Royal Astronomical Society* 372, 1253. doi: 10.1111/j.1365-2966.2006.10934.x

Mattila, K., Väisänen, P. (2019) Extragalactic Background Light: Inventory of Light Throughout the Cosmic History. *Contemporary Physics* 60, 23. doi: 10.1080/00107514.2019.1586130

McComas, D., Allegrini, F., Bagenal, F., et al. (2008) The Solar Wind Around Pluto (SWAP) Instrument Aboard New Horizons. *Space Science Reviews* 140(1), 261-313. doi: 10.1007/s11214-007-9205-3

McComas, D.J., Allegrini, F., Bagenal, F., Crary, F., Ebert, R.W., Elliott, H., Stern, A., Valek, P. (2007) Diverse Plasma Populations and Structures in Jupiter's Magnetotail. *Science* 318, 217. doi: 10.1126/science.1147393

McComas, D.J., Allegrini, F., Baldonado, J., et al. (2009) The Two Wide-Angle Imaging Neutral-Atom Spectrometers (TWINS) NASA Mission-of-Opportunity. *Space Science Reviews* 142(1-4), 157-231. doi: 10.1007/s11214-008-9467-4

McComas, D.J., Allegrini, F., Bochsler, P., et al. (2009) Global Observations of the Interstellar Interaction from the Interstellar Boundary Explorer (IBEX). *Science* 326(5955), 959-962. doi: http://dx.doi.org/10.1126/science.1180906

McComas, D.J., Allegrini, F., Bochsler, P., et al. (2009) IBEX—Interstellar Boundary Explorer. *Space Science Reviews* 146(1-4), 11-33. doi: 10.1007/s11214-009-9499-4

McComas, D.J., Alexashov, D., Bzowski, M., et al. (2012) The Heliosphere's Interstellar Interaction: No Bow Shock. *Science* 336(6086), 1291-1293. doi: 10.1126/science.1221054

McComas, D.J., Dayeh, M.A., Allegrini, F., et al. (2012) The First Three Years of IBEX Observations and Our Evolving Heliosphere. *The Astrophysical Journal Supplement Series* 203, 1. doi: 10.1088/0067-0049/203/1/1

McComas, D.J., Lewis, W.S., Schwadron, N.A. (2014) IBEX's Enigmatic Ribbon in the Sky and Its Many Possible Sources. *Reviews of Geophysics* 52(1), 118-155. doi: 10.1002/2013rg000438

McComas, D.J., Alexander, N., Angold, N., et al. (2016) Integrated Science Investigation of the Sun (ISIS): Design of the Energetic Particle Investigation. *Space Science Reviews* 204(1), 187-256. doi: 10.1007/s11214-014-0059-1

McComas, D.J., Zirnstein, E.J., Bzowski, M., et al. (2017) Seven Years of Imaging the Global Heliosphere with IBEX. *The Astrophysical Journal Supplement Series* 229(2), 41. doi: 10.3847/1538-4365/aa66d8

McComas, D.J., Christian, E.R., Schwadron, N.A., et al. (2018) Interstellar Mapping and Acceleration Probe (IMAP): A New NASA Mission. *Space Science Reviews* 214(8), 116. doi: 10.1007/s11214-018-0550-1

McKinnon, W.B., Nimmo, F., Wong, T., et al. (2016) Convection in a Volatile Nitrogen-Ice-Rich Layer Drives Pluto's Geological Vigour. *Nature* 534, 82-85. Retrieved from https://ui.adsabs.harvard.edu/abs/2016Natur.534...82M

McNutt, R.L., Livi, S.A., Gurnee, R.S., et al. (2008) The Pluto Energetic Particle Spectrometer Science Investigation (PEPSSI) on the New Horizons Mission. *Space Science Reviews* 140(1-4), 315-385. doi: 10.1007/s11214-008-9436-y

Meshkat, T., Mawet, D., Bryan, M.L., et al. (2017) A Direct Imaging Survey of Spitzer-detected Debris Disks: Occurrence of Giant Planets in Dusty Systems. *The Astronomical Journal* 154, 245. doi: 10.3847/1538-3881/aa8e9a

Mitchell, D.G., Jaskulek, S.E., Schlemm, C.E., et al. (2000) High Energy Neutral Atom (HENA) Imager for the IMAGE Mission. In Burch, J.L. (Ed.), *The IMAGE Mission* (pp. 67-112). Dordrecht, The Netherlands: Springer.

Moore, J.M., Howard, A.D., Schenk, P.M., et al. (2015) Geology Before Pluto: Pre-Encounter Considerations. *Icarus* 246, 65. doi: 10.1016/j.icarus.2014.04.028

Moore, T.E., Chornay, D.J., Collier, M.R., Herrero, F.A., Johnson, J., Johnson, M.A., Keller, J.W., Laudadio, J.F., Lobell, J.F., Ogilvie, K.W. (2000) *The Low-Energy Neutral Atom Imager for IMAGE*. Dordrecht, The Netherlands: Springer. Retrieved from http://scholar.google.com/scholar?q=The low-energy neutral atom imager for IMAGE&btnG=&hl=en&num=20&as_sdt=0%2C22

Moores, J.E., Smith, C.L., Toigo, A.D., Guzewich, S.D. (2017) Penitentes as the Origin of the Bladed Terrain of Tartarus Dorsa on Pluto. *Nature* 541, 188. doi: 10.1038/nature20779

Mostafavi, P., Zank, G.P., Webb, G.M. (2017) Structure of Energetic Particle Mediated Shocks Revisited. *The Astrophysical Journal* 841, 4. doi: 10.3847/1538-4357/aa6f10

Mostafavi, P., Zank, G.P. (2018) The Structure of Shocks in the Very Local Interstellar Medium. *The Astrophysical Journal* 854, L15. doi: 10.3847/2041-8213/aaab54

Mostafavi, P., Zank, G.P., Webb, G.M. (2018) The Mediation of Collisionless Oblique Magnetized Shocks by Energetic Particles. *The Astrophysical Journal* 868, 120. doi: 10.3847/1538-4357/aaeb91

Mousis, O., Ronnet, T., Lunine, J.I., Maggiolo, R., Wurz, P., Danger, G., Bouquet, A. (2018) Synthesis of Molecular Oxygen via Irradiation of Ice Grains in the Protosolar Nebula. *The Astrophysical Journal* 858, 66. doi: 10.3847/1538-4357/aab6b9

Mróz, P., Udalski, A., Skowron, J., et al. (2017) No Large Population of Unbound or Wide-Orbit Jupiter-Mass Planets. *Nature* 548, 183-186. Retrieved from https://ui.adsabs.harvard.edu/abs/2017Natur.548..183M

Muraki, Y., Han, C., Bennett, D.P., et al. (2011) Discovery and Mass Measurements of a Cold, 10 Earth Mass Planet and Its Host Star. *The Astrophysical Journal* 741. Retrieved from https://ui.adsabs.harvard.edu/abs/2011ApJ...741...22M

Narvaez, P. (2004) The Magnetostatic Cleanliness Program for the Cassini Spacecraft. *Space Science Reviews* 114, 385-394. Retrieved from https://ui.adsabs.harvard.edu/abs/2004SSRv..114..385N

Nesvorný, D., Jenniskens, P., Levison, H.F., Bottke, W.F., Vokrouhlický, D., Gounelle, M. (2010a) Cometary Origin of the Zodiacal Cloud and Carbonaceous Micrometeorites. Implications for Hot Debris Disks. *The Astrophysical Journal* 713, 816. doi: 10.1088/0004-637x/713/2/816

Nesvorný, D., Jenniskens, P., Levison, H.F., Bottke, W.F., Vokrouhlický, D., Gounelle, M. (2010b) Cometary Origin of the Zodiacal Cloud and Carbonaceous Micrometeorites. Implications for Hot Debris Disks. *The Astrophysical Journal* 713, 816-836. Retrieved from https://ui.adsabs.harvard.edu/abs/2010ApJ...713..816N

Nesvorný, D., Janches, D., Vokrouhlický, D., Pokorný, P., Bottke, W.F., Jenniskens, P. (2011) Dynamical Model for the Zodiacal Cloud and Sporadic Meteors. *The Astrophysical Journal* 743, 129. doi: 10.1088/0004-637x/743/2/129

Nesvorný, D., Vokrouhlický, D., Pokorný, P., Janches, D. (2011) Dynamics of Dust Particles Released from Oort Cloud Comets and Their Contribution to Radar Meteors. *The Astrophysical Journal* 743, 37. doi: 10.1088/0004-637x/743/1/37

Nimmo, F., Hamilton, D.P., McKinnon, W.B., et al. (2016) Reorientation of Sputnik Planitia Implies a Subsurface Ocean on Pluto. *Nature* 540, 94. doi: 10.1038/nature20148

Nimmo, F., Pappalardo, R.T. (2016) Ocean Worlds in the Outer Solar System. *Journal of Geophysical Research (Planets)* 121, 1378. doi: 10.1002/2016je005081

Nimmo, F., Umurhan, O., Lisse, C.M., et al. (2017) Mean Radius and Shape of Pluto and Charon from New Horizons Images. *Icarus* 287, 12. doi: 10.1016/j.icarus.2016.06.027

NRC (2011) *Vision and Voyages for Planetary Science in the Decade 2013-2022*. Washington, DC: The National Academies Press.

Omori, Y., Chown, R., Simard, G., et al. (2017) A 2500 deg^2 CMB Lensing Map from Combined South Pole Telescope and Planck Data. *The Astrophysical Journal* 849, 124. doi: 10.3847/1538-4357/aa8d1d

Opher, M., Bibi, F.A., Toth, G., Richardson, J.D., Izmodenov, V.V., Gombosi, T.I. (2009) A Strong, Highly-Tilted Interstellar Magnetic Field Near the Solar System. *Nature* 462, 1036. doi: 10.1038/nature08567

Opher, M., Drake, J.F. (2013) On the Rotation of the Magnetic Field Across the Heliopause. *The Astrophysical Journal* 778, L26. doi: 10.1088/2041-8205/778/2/l26

Opher, M., Drake, J.F., Zieger, B., Gombosi, T.I. (2015) Magnetized Jets Driven by the Sun: The Structure of the Heliosphere Revisited. *The Astrophysical Journal* 800. doi: https://doi.org/10.1088/2041-8205/800/2/L28

Opher, M. (2016) The Heliosphere: What Did We Learn in Recent Years and the Current Challenges. *Space Science Reviews* 200, 475-494. Retrieved from https://ui.adsabs.harvard.edu/abs/2016SSRv..200..475O

Opher, M., Drake, J.F., Swisdak, M., Zieger, B., Toth, G. (2017) The Twist of the Draped Interstellar Magnetic Field Ahead of the Heliopause: A Magnetic Reconnection Driven Rotational Discontinuity. *The Astrophysical Journal* 839, L12. doi: 10.3847/2041-8213/aa692f

Opher, M., Loeb, A., Drake, J., Toth, G. (2018) A Predicted Small and Round Heliosphere. *arXiv e-prints*. Retrieved from https://ui.adsabs.harvard.edu/\#abs/2018arXiv180806611O

Ortiz, J.L., Santos-Sanz, P., Sicardy, B., et al. (2017) The Size, Shape, Density and Ring of the Dwarf Planet Haumea from a Stellar Occultation. *Nature* 550, 219-223. Retrieved from https://ui.adsabs.harvard.edu/abs/2017Natur.550..219O

Park, J., Kucharek, H., Möbius, E., Galli, A., Kubiak, M.A., Bzowski, M., McComas, D.J. (2016) IBEX Observations of Secondary Interstellar Helium and Oxygen Distributions. *The Astrophysical Journal* 833(2), 130. doi: 10.3847/1538-4357/833/2/130

Patel, R.I., Metchev, S.A., Heinze, A. (2014) A Sensitive Identification of Warm Debris Disks in the Solar Neighborhood through Precise Calibration of Saturated WISE Photometry. *The Astrophysical Journal Supplement Series* 212, 10. doi: 10.1088/0067-0049/212/1/10

Pavlov, A.A., Pavlov, A.K., Mills, M.J., Ostryakov, V.M., Vasilyev, G.I., Toon, O.B. (2005) Catastrophic Ozone Loss During Passage of the Solar System Through an Interstellar Cloud. *Geophysical Research Letters* 32, L01815. doi: 10.1029/2004gl021601

Paxton, L., Meng, C.-I., Fountain, G., et al. (1993) *SSUSI: Horizon-to-Horizon and Limb-Viewing Spectrographic Imager for Remote Sensing of Environmental Parameters.* In Proceedings of SPIE 1764, Ultraviolet Technology IV, SPIE, San Diego, CA.

Paxton, L., Christensen, A., Humm, D., et al. (1999) *Global Ultraviolet Imager (GUVI): Measuring Composition and Energy Inputs for the NASA Thermosphere Ionosphere Mesosphere Energetics and Dynamics (TIMED) Mission* (Vol. 3756): SPIE. 10.1117/12.366380

Petit, J.-M., Kavelaars, J.J., Gladman, B., Loredo, T. (2008) Size Distribution of Multikilometer Transneptunian Objects. In Barucci, M.A., Boehnhardt, H., Cruikshank, D.P., et al. (Eds.), *The Solar System Beyond Neptune* (pp. 71). Tucson, AZ: University of Arizona Press,.

Piquette, M., Poppe, A.R., Bernardoni, E., et al. (2019) Student Dust Counter: Status Report at 38 AU. *Icarus* 321, 116. doi: 10.1016/j.icarus.2018.11.012

Poglitsch, A., Waelkens, C., Geis, N., et al. (2010) The Photodetector Array Camera and Spectrometer (PACS) on the Herschel Space Observatory. *Astronomy and Astrophysics* 518, L2. doi: 10.1051/0004-6361/201014535

Pogorelov, N.V., Heerikhuisen, J., Zank, G.P., Borovikov, S.N. (2009) Influence of the Interstellar Magnetic Field and Neutrals on the Shape of the Outer Heliosphere. *Space Science Reviews* 143(1-4), 31-42. doi: 10.1007/s11214-008-9429-x

Pogorelov, N.V., Fichtner, H., Czechowski, A., et al. (2017) Heliosheath Processes and the Structure of the Heliopause: Modeling Energetic Particles, Cosmic Rays, and Magnetic Fields. *Space Science Reviews* 212(1-2), 193-248. doi: 10.1007/s11214-017-0354-8

Pogorelov, N.V., Heerikhuisen, J., Roytershteyn, V., Burlaga, L.F., Gurnett, D.A., Kurth, W.S. (2017) Three-Dimensional Features of the Outer Heliosphere Due to Coupling Between the Interstellar and Heliospheric Magnetic Field. V. The Bow Wave, Heliospheric Boundary Layer, Instabilities, and Magnetic Reconnection. *The Astrophysical Journal* 845(1). doi: https://doi.org/10.3847/1538-4357/aa7d4f

Pokorný, P., Vokrouhlický, D., Nesvorný, D., Campbell-Brown, M., Brown, P. (2014) Dynamical Model for the Toroidal Sporadic Meteors. *The Astrophysical Journal* 789, 25. doi: 10.1088/0004-637x/789/1/25

Pollock, C.J., Asamura, K., Baldonado, J., et al. (2000) Medium Energy Neutral Atom (MENA) Imager for the IMAGE Mission. In Burch, J.L. (Ed.), *The IMAGE Mission* (pp. 113-154). Dordrecht, The Netherlands: Springer.

Poppe, A.R. (2016) An Improved Model for Interplanetary Dust Fluxes in the Outer Solar System. *Icarus* 264, 369-386. doi: 10.1016/j.icarus.2015.10.001

Poppe, A.R., Lisse, C.M., Piquette, M., Zemcov, M., Horányi, M., James, D., Szalay, J.R., Bernardoni, E., Stern, S.A. (2019) Constraining the Solar System's Debris Disk with In Situ New Horizons Measurements from the Edgeworth-Kuiper Belt. *The Astrophysical Journal* 881. Retrieved from https://ui.adsabs.harvard.edu/abs/2019ApJ...881L..12P

Porter, S.B., Spencer, J.R., Benecchi, S., et al. (2016) The First High-phase Observations of a KBO: New Horizons Imaging of (15810) 1994 JR_1 from the Kuiper Belt. *The Astrophysical Journal* 828, L15. doi: 10.3847/2041-8205/828/2/l15

Provornikova, E., Opher, M., Izmodenov, V.V., Richardson, J.D., Toth, G. (2014) Plasma Flows in the Heliosheath along the Voyager 1 and 2 Trajectories due to Effects of the 11 yr Solar Cycle. *The Astrophysical Journal* 794, 29. doi: 10.1088/0004-637x/794/1/29

Quémerais, E., Sandel, B.R., Bertaux, J.L., Lallement, R. (2000) Outer Heliosphere Ly-α Measurements: 1993 to 1998. *Astrophysics and Space Science* 274, 123. doi: 10.1023/a:1026591705751

Quémerais, E., Izmodenov, V. (2002) Effects of the Heliospheric Interface on the Interplanetary Lyman Alpha Glow Seen at 1 AU from the Sun. *Astronomy and Astrophysics* 396, 269. doi: 10.1051/0004-6361:20021396

Quémerais, E., Lallement, R., Ferron, S., Koutroumpa, D., Bertaux, J.L., Kyrölä, E., Schmidt, W. (2006) Interplanetary Hydrogen Absolute Ionization Rates: Retrieving the Solar Wind Mass Flux Latitude and Cycle Dependence with SWAN/SOHO Maps. *Journal of Geophysical Research: Space Physics (1978–2012)* 111(A9). doi: 10.1029/2006ja011711

Rankin, J.S., Stone, E.C., Cummings, A.C., McComas, D.J., Lal, N., Heikkila, B.C. (2019) Galactic Cosmic-Ray Anisotropies: Voyager 1 in the Local Interstellar Medium. *The Astrophysical Journal* 873. Retrieved from https://ui.adsabs.harvard.edu/abs/2019ApJ...873...46R

Reach, W.T., Morris, P., Boulanger, F., Okumura, K. (2003) The Mid-Infrared Spectrum of the Zodiacal and Exozodiacal Light. *Icarus* 164, 384. doi: 10.1016/s0019-1035(03)00133-7

Redfield, S., Linsky, J.L. (2001) Microstructure of the Local Interstellar Cloud and the Identification of the Hyades Cloud. *The Astrophysical Journal* 551, 413-428. Retrieved from https://ui.adsabs.harvard.edu/abs/2001ApJ...551..413R

Redfield, S., Linsky, J.L. (2008) The Structure of the Local Interstellar Medium. IV. Dynamics, Morphology, Physical Properties, and Implications of Cloud-Cloud Interactions. *The Astrophysical Journal* 673, 283-314. Retrieved from https://ui.adsabs.harvard.edu/abs/2008ApJ...673..283R

Reuter, D.C., Stern, S.A., Scherrer, J., et al. (2008) Ralph: A Visible/Infrared Imager for the New Horizons Pluto/Kuiper Belt Mission. *Space Science Reviews* 140, 129-154. Retrieved from https://ui.adsabs.harvard.edu/\#abs/2008SSRv..140..129R

Richardson, J.D., Liu, Y., Wang, C., Burlaga, L.F. (2006) ICMES at Very Large Distances. *Advances in Space Research* 38, 528. doi: 10.1016/j.asr.2005.06.049

Richardson, J.D., Kasper, J.C., Wang, C., Belcher, J.W., Lazarus, A.J. (2008) Cool Heliosheath Plasma and Deceleration of the Upstream Solar Wind at the Termination Shock. *Nature* 454(7200), 63. doi: 10.1038/nature07024

Robuchon, G., Nimmo, F. (2011) Thermal Evolution of Pluto and Implications for Surface Tectonics and a Subsurface Ocean. *Icarus* 216, 426. doi: 10.1016/j.icarus.2011.08.015

Rowan-Robinson, M., May, B. (2013) An Improved Model for the Infrared Emission from the Zodiacal Dust Cloud: Cometary, Asteroidal and Interstellar Dust. *Monthly Notices of the Royal Astronomical Society* 429, 2894. doi: 10.1093/mnras/sts471

Runyon, K., Mandt, K., Brandt, P., Paul, M., Lisse, C., McNutt, J., R.. (2019) *Planetary Imaging During Fast Flybys by Interstellar Probe.* In EPSC-DPS Joint Meeting 2019, Geneva, Switzerland.

Russell, C.T., Mewaldt, R.A., von Rosenvinge, T.T. (1998) *The Advanced Composition Explorer Mission*. The Netherlands: Springer. 10.1007/978-94-011-4762-0

Russell, C.T., Anderson, B.J., Baumjohann, W., et al. (2016) The Magnetospheric Multiscale Magnetometers. *Space Science Reviews* 199(1-4), 189-256. doi: 10.1007/s11214-014-0057-3

Salvaterra, R., Ferrara, A., Dayal, P. (2011) Simulating High-Redshift Galaxies. *Monthly Notices of the Royal Astronomical Society* 414, 847. doi: 10.1111/j.1365-2966.2010.18155.x

Scarf, F.L., Gurnett, D.A. (1977) A Plasma Wave Investigation for the Voyager Mission. *Space Science Reviews* 21(3), 289-308. doi: 10.1007/BF00211543

Schaller, E.L., Brown, M.E. (2007a) Detection of Methane on Kuiper Belt Object (50000) Quaoar. *The Astrophysical Journal* 670, L49-L51. Retrieved from https://ui.adsabs.harvard.edu/abs/2007ApJ...670L..49S

Schaller, E.L., Brown, M.E. (2007b) Volatile Loss and Retention on Kuiper Belt Objects. *The Astrophysical Journal* 659, L61. doi: 10.1086/516709

Schenk, P.M., Beyer, R.A., McKinnon, W.B., et al. (2018) Breaking Up Is Hard to Do: Global Cartography and Topography of Pluto's Mid-Sized Icy Moon Charon from New Horizons. *Icarus* 315, 124. doi: 10.1016/j.icarus.2018.06.010

Schneider, A.D., Dullemond, C.P., Bitsch, B. (2018) Surface Waves in Protoplanetary Disks Induced by Outbursts: Concentric Rings in Scattered Light. *Astronomy and Astrophysics* 617, L7. doi: 10.1051/0004-6361/201833965

Schwadron, N.A., Geiss, J., Fisk, L.A., Gloeckler, G., Zurbuchen, T.H., von Steiger, R. (2000) Inner Source Distributions: Theoretical Interpretation, Implications, and Evidence for Inner Source Protons. *Journal of Geophysical Research* 105, 7465-7472. Retrieved from https://ui.adsabs.harvard.edu/abs/2000JGR...105.7465S

Schwadron, N.A., Bzowski, M., Crew, G.B., et al. (2009) Comparison of Interstellar Boundary Explorer Observations with 3D Global Heliospheric Models. 326(5955), 966-968. doi: 10.1126/science.1180986 %J Science

Schwadron, N.A., McComas, D.J. (2013a) Spatial Retention of Ions Producing the IBEX Ribbon. *The Astrophysical Journal* 764, 92. doi: 10.1088/0004-637x/764/1/92

Schwadron, N.A., McComas, D.J. (2013b) Is Voyager 1 Inside an Interstellar Flux Transfer Event? *The Astrophysical Journal* 778, L33. doi: 10.1088/2041-8205/778/2/l33

Schwadron, N.A., McComas, D.J. (2017) Effects of Solar Activity on the Local Interstellar Magnetic Field Observed by Voyager 1 and IBEX. *The Astrophysical Journal* 849, 135. doi: 10.3847/1538-4357/aa8fd5

Schwadron, N.A., Bzowski, M. (2018) The Heliosphere Is Not Round. *The Astrophysical Journal* 862(1), 11. doi: 10.3847/1538-4357/aacbcf

Sicardy, B., Ortiz, J.L., Assafin, M., et al. (2011) A Pluto-Like Radius and a High Albedo for the Dwarf Planet Eris from an Occultation. *Nature* 478, 493-496. Retrieved from https://ui.adsabs.harvard.edu/abs/2011Natur.478..493S

Singer, K.N., Schenk, P.M., Beyer, R.A., et al. (2018) *Cryovolcanism on Pluto and Charon*. https://ui.adsabs.harvard.edu/abs/2018EGUGA..20.5761S.

Singer, K.N., McKinnon, W.B., Gladman, B., et al. (2019) Impact Craters on Pluto and Charon Indicate a Deficit of Small Kuiper Belt Objects. *Science* 363, 955. doi: 10.1126/science.aap8628

Slavin, J.D., Frisch, P.C. (2008) The Boundary Conditions of the Heliosphere: Photoionization Models Constrained by Interstellar and in Situ Data. *Astronomy and Astrophysics* 491, 53-68. Retrieved from https://ui.adsabs.harvard.edu/abs/2008A&A...491...53S

Slavin, J.D., Frisch, P.C., Müller, H.-R., Heerikhuisen, J., Pogorelov, N.V., Reach, W.T., Zank, G. (2012) Trajectories and Distribution of Interstellar Dust Grains in the Heliosphere. *The Astrophysical Journal* 760, 46. doi: 10.1088/0004-637x/760/1/46

Smith, B.A., Soderblom, L.A., Banfield, D., et al. (1989) Voyager 2 at Neptune: Imaging Science Results. *Science* 246, 1422. doi: 10.1126/science.246.4936.1422

Smith, E.J., Dougherty, M.K., Russell, C.T., Southwood, D.J. (2001) Scalar Helium Magnetometer Observations at Cassini Earth Swing-By. *J. Geophys. Res.* 106(A12), 30129-30139. doi: doi:10.1029/2001JA900115

Spencer, J.R., Stern, S.A., Cheng, A.F., et al. (2007) Io Volcanism Seen by New Horizons: A Major Eruption of the Tvashtar Volcano. *Science* 318, 240. doi: 10.1126/science.1147621

Stecker, F.W., de Jager, O.C., Salamon, M.H. (1992) TeV Gamma Rays from 3C 279: A Possible Probe of Origin and Intergalactic Infrared Radiation Fields. *The Astrophysical Journal* 390, L49. doi: 10.1086/186369

Stenborg, G., Howard, R.A. (2017) The Evolution of the Surface of Symmetry of the Interplanetary Dust from 24° to 5° Elongation. *The Astrophysical Journal* 848, 57. doi: 10.3847/1538-4357/aa8ef0

Sterken, V.J., Altobelli, N., Kempf, S., Schwehm, G., Srama, R., Grün, E. (2012) The Flow of Interstellar Dust into the Solar System. *A&A* 538, A102. Retrieved from https://doi.org/10.1051/0004-6361/201117119

Sterken, V.J., Altobelli, N., Kempf, S., Krüger, H., Srama, R., Strub, P., Grün, E. (2013) The Filtering of Interstellar Dust in the Solar System. *Astronomy and Astrophysics* 552, A130. doi: 10.1051/0004-6361/201219609

Sterken, V.J., Westphal, A.J., Altobelli, N., et al. (2014) Stardust Interstellar Preliminary Examination X: Impact speeds and directions of interstellar grains on the Stardust dust collector. *Meteoritics and Planetary Science* 49, 1680. doi: 10.1111/maps.12219

Stern, A.S., Slater, D.C., Scherrer, J., et al. (2008) ALICE: The Ultraviolet Imaging Spectrograph Aboard the New Horizons Pluto–Kuiper Belt Mission. *Space Science Reviews* 140(1-4), 155. doi: 10.1007/s11214-008-9407-3

Stern, S.A., Slater, D.C., Scherrer, J., et al. (2008) ALICE: The Ultraviolet Imaging Spectrograph Aboard the New Horizons Pluto-Kuiper Belt Mission. *Space Science Reviews* 140, 155-187. Retrieved from https://ui.adsabs.harvard.edu/abs/2008SSRv..140..155S

Stern, S.A., Bagenal, F., Ennico, K., et al. (2015) The Pluto System: Initial Results from Its Exploration by New Horizons. *Science* 350, aad1815. doi: 10.1126/science.aad1815

Stone, E.C., Cohen, C.M.S., Cook, W.R., et al. (1998) The Cosmic-Ray Isotope Spectrometer for the Advanced Composition Explorer. *Space Science Reviews* 86, 285-356. Retrieved from https://ui.adsabs.harvard.edu/abs/1998SSRv...86..285S

Stone, E.C., Cummings, A.C., McDonald, F.B., Heikkila, B.C., Lal, N., Webber, W.R. (2008) An Asymmetric Solar Wind Termination Shock. *Nature* 454(7200), 71-74. doi: 10.1038/nature07022

Stone, E.C., Cummings, A.C., McDonald, F.B., Heikkila, B.C., Lal, N., Webber, W.R. (2013) Voyager 1 Observes Low-Energy Galactic Cosmic Rays in a Region Depleted of Heliospheric Ions. *Science* 341(6142), 150-153. doi: 10.1126/science.1236408

Street, R.A., Udalski, A., Calchi Novati, S., et al. (2016) Spitzer Parallax of OGLE-2015-BLG-0966: A Cold Neptune in the Galactic Disk. *The Astrophysical Journal* 819. Retrieved from https://ui.adsabs.harvard.edu/abs/2016ApJ...819...93S

Swisdak, M., Drake, J.F., Opher, M. (2013) A Porous, Layered Heliopause. *The Astrophysical Journal* 774. Retrieved from https://ui.adsabs.harvard.edu/abs/2013ApJ...774L...8S

Tabataba-Vakili, F., Grenfell, J.L., Grießmeier, J.-M., Rauer, H. (2016) Atmospheric Effects of Stellar Cosmic Rays on Earth-Like Exoplanets Orbiting M-Dwarfs. *Astronomy and Astrophysics* 585, A96. doi: 10.1051/0004-6361/201425602

Telfer, M.W., Parteli, E.J.R., Radebaugh, J., et al. (2018) Dunes on Pluto. *Science* 360, 992. doi: 10.1126/science.aao2975

Trowbridge, A.J., Melosh, H.J., Steckloff, J.K., Freed, A.M. (2016) Vigorous Convection as the Explanation for Pluto's Polygonal Terrain. *Nature* 534, 79-81. Retrieved from https://ui.adsabs.harvard.edu/abs/2016Natur.534...79T

Tsapras, Y. (2018) Microlensing Searches for Exoplanets. *Geosciences* 8(10), 365. Retrieved from https://www.mdpi.com/2076-3263/8/10/365

Tsumura, K., Battle, J., Bock, J., et al. (2010) Observations of the Near-infrared Spectrum of the Zodiacal Light with CIBER. *The Astrophysical Journal* 719, 394. doi: 10.1088/0004-637x/719/1/394

van Dokkum, P.G., Abraham, R., Merritt, A., Zhang, J., Geha, M., Conroy, C. (2015) Forty-Seven Milky Way-Sized, Extremely Diffuse Galaxies in the Coma Cluster. *The Astrophysical Journal* 798, L45. doi: 10.1088/2041-8205/798/2/l45

Verbiscer, A., Helfenstein, P., Veverka, J. (1990) Backscattering from Frost on Icy Satellites in the Outer Solar System. *Nature* 347, 162. doi: 10.1038/347162a0

Verbiscer, A.J., Veverka, J. (1990) Scattering Properties of Natural Snow and Frost: Comparison with Icy Satellite Photometry. *Icarus* 88, 418. doi: 10.1016/0019-1035(90)90092-n

Verbiscer, A.J., Veverka, J. (1992) Mimas: Photometric Roughness and Albedo Map. *Icarus* 99, 63. doi: 10.1016/0019-1035(92)90171-3

Waite, J.H., Lewis, W.S., Kasprzak, W.T., et al. (2004) The Cassini Ion and Neutral Mass Spectrometer (INMS) Investigation. In Russell, C.T. (Ed.), *The Cassini-Huygens Mission: Orbiter In Situ Investigations* (Vol. 2, pp. 113-231). Dordrecht, The Netherlands: Springer.

Washimi, H., Zank, G.P., Hu, Q., Tanaka, T., Munakata, K. (2007) A Forecast of the Heliospheric Termination-Shock Position by Three-dimensional MHD Simulations. *The Astrophysical Journal* 670, L139. doi: 10.1086/524358

Washimi, H., Zank, G.P., Hu, Q., Tanaka, T., Munakata, K., Shinagawa, H. (2011) Realistic and Time-Varying Outer Heliospheric Modelling. *Monthly Notices of the Royal Astronomical Society* 416, 1475. doi: 10.1111/j.1365-2966.2011.19144.x

White, O.L., Schenk, P.M., Bellagamba, A.W., Grimm, A.M., Dombard, A.J., Bray, V.J. (2017) Impact Crater Relaxation on Dione and Tethys and Relation to Past Heat Flow. *Icarus* 288, 37. doi: 10.1016/j.icarus.2017.01.025

White, O.L., Moore, J.M., Howard, A.D., et al. (2019) Washboard and Fluted Terrains on Pluto as Evidence for Ancient Glaciation. *Nature Astronomy* 3(1), 62-68. doi: 10.1038/s41550-018-0592-z

Witte, M., Rosenbauer, H., Banaszkiewicz, M., Fahr, H. (1993) The Ulysses Neutral Gas Experiment: Determination of the Velocity and Temperature of the Interstellar Neutral Helium. *Advances in Space Research* 13, 121. doi: 10.1016/0273-1177(93)90401-v

Witte, M., Banaszkiewicz, M., Rosenbauer, H., McMullin, D. (2004) Kinetic Parameters of Interstellar Neutral Helium: Updated Results from the ULYSSES/GAS-Instrument. *Advances in Space Research* 34(1), 61-65. doi: 10.1016/j.asr.2003.01.037

Witze, A. (2014) Gas Giant Spins a Surprise. *Nature*. doi: 10.1038/nature.2014.16333

Wood, B.E. (2004) Astrospheres and Solar-like Stellar Winds. *Living Reviews in Solar Physics* 1. Retrieved from https://ui.adsabs.harvard.edu/abs/2004LRSP....1....2W

Wood, B.E., Müller, H.-R., Zank, G.P., Izmodenov, V.V., Linsky, J.L. (2004) The Heliospheric Hydrogen Wall and Astrospheres. *Advances in Space Research* 34, 66-73. Retrieved from https://ui.adsabs.harvard.edu/abs/2004AdSpR..34...66W

Wyatt, M.C. (2008) Evolution of Debris Disks. *Annual Review of Astronomy and Astrophysics* 46, 339. doi: 10.1146/annurev.astro.45.051806.110525

Wyrzykowski, L., Skowron, J., Kozłowski, S., et al. (2011) The OGLE View of Microlensing Towards the Magellanic Clouds - IV. OGLE-III SMC Data and Final Conclusions on MACHOs. *Monthly Notices of the Royal Astronomical Society* 416, 2949-2961. Retrieved from https://ui.adsabs.harvard.edu/abs/2011MNRAS.416.2949W

Yee, J.C., Udalski, A., Calchi Novati, S., et al. (2015) First Space-based Microlens Parallax Measurement of an Isolated Star: Spitzer Observations of OGLE-2014-BLG-0939. *The Astrophysical Journal* 802. Retrieved from https://ui.adsabs.harvard.edu/abs/2015ApJ...802...76Y

Young, L.A., Kammer, J.A., Steffl, A.J., et al. (2018) Structure and Composition of Pluto's Atmosphere from the New Horizons Solar Ultraviolet Occultation. *Icarus* 300, 174. doi: 10.1016/j.icarus.2017.09.006

Zank, G.P. (1999) Interaction of the Solar Wind with the Local Interstellar Medium: A Theoretical Perspective. *Space Science Reviews* 89(3-4), 413-688. doi: 10.1023/a:1005155601277

Zank, G.P., Heerikhuisen, J., Wood, B.E., Pogorelov, N.V., Zirnstein, E., McComas, D.J. (2013) Heliospheric Structure: The Bow Wave and the Hydrogen Wall. *The Astrophysical Journal* 763, 20. doi: 10.1088/0004-637x/763/1/20

Zemcov, M., Smidt, J., Arai, T., et al. (2014) On the Origin of Near-Infrared Extragalactic Background Light Anisotropy. *Science* 346, 732. doi: 10.1126/science.1258168

Zemcov, M., Immel, P., Nguyen, C., Cooray, A., Lisse, C.M., Poppe, A.R. (2017) Measurement of the Cosmic Optical Background Using the Long Range Reconnaissance Imager on New Horizons. *Nature Communications* 8, 15003. doi: 10.1038/ncomms15003

Zemcov, M., Arcavi, I., Arendt, R., et al. (2018) Astrophysics with New Horizons: Making the Most of a Generational Opportunity. *Publications of the Astronomical Society of the Pacific* 130, 115001. Retrieved from https://ui.adsabs.harvard.edu/abs/2018PASP..130k5001Z

Zhu, W., Udalski, A., Huang, C.X., et al. (2017) An Isolated Microlens Observed from K2, Spitzer, and Earth. *The Astrophysical Journal* 849. Retrieved from https://ui.adsabs.harvard.edu/abs/2017ApJ...849L..31Z

Zhukovska, S., Gail, H.-P., Trieloff, M. (2008) Evolution of Interstellar Dust and Stardust in the Solar Neighbourhood. *Astronomy and Astrophysics* 479, 453-480. Retrieved from https://ui.adsabs.harvard.edu/abs/2008A&A...479..453Z

Zirnstein, E.J., Heerikhuisen, J., Zank, G.P., Pogorelov, N.V., McComas, D.J., Desai, M.I. (2014) Charge-Exchange Coupling Between Pickup Ions Across the Heliopause and its Effect on Energetic Neutral Hydrogen Flux. *The Astrophysical Journal* 783, 129. doi: 10.1088/0004-637x/783/2/129

Zirnstein, E.J., Heerikhuisen, J., Funsten, H.O., Livadiotis, G., McComas, D.J., Pogorelov, N.V. (2016) Local Interstellar Magnetic Field Determined From the Interstellar Boundary Explorer Ribbon. *The Astrophysical Journal* 818(1). doi: 10.3847/2041-8205/818/1/L18

Zirnstein, E.J., Kumar, R., Heerikhuisen, J., McComas, D.J., Galli, A. (2018) Stochastic Acceleration of˜0.1-5 keV Pickup Ions in the Heliotail. *The Astrophysical Journal* 860, 170. doi: 10.3847/1538-4357/aac3de

Zirnstein, E.J., McComas, D.J., Kumar, R., Elliott, H.A., Szalay, J.R., Olkin, C.B., Spencer, J., Stern, S.A., Young, L.A. (2018) In Situ Observations of Preferential Pickup Ion Heating at an Interplanetary Shock. *Physical Review Letters* 121, 075102. doi: 10.1103/PhysRevLett.121.075102

4. Science Operations Concept

The first stage of this study focused on identifying science targets and their preliminary trade-offs. A more detailed analysis of operations concepts given these targets will be performed in the second stage of the study.

4.1. Fly-Out Direction

The orbital position of Jupiter opens solar system escape in a specific direction every 12 years. Ultimately, the fly-out direction is driven by science, but is therefore a trade with launch date if the trajectory is kept in the ecliptic plane. Because of the slingshot motion around Jupiter (gravity assist) planned for two of the mission architecture options, any ecliptic inclination would decrease the asymptotic speed for the same amount of propulsion and mass. For a solar Oberth maneuver, this decrease would be less significant. The following science drivers have been considered and discussed during the 1st Interstellar Probe Exploration Workshop and would need to be traded against each other to select an optimal fly-out direction for a final mission architecture.

4.1.1. Heliospheric and Interstellar Science

The science questions relevant to the heliosphere and local interstellar medium (LISM) are the highest priority that should drive the primary operational scenario. The global shape of the heliosphere is one of the most outstanding questions that could be uniquely answered from an external vantage point. Given that the scientific debate revolves around a bubble shape versus a bifurcated tail structure, a vantage point displaced sufficiently in ecliptic longitude from the nose direction would be a good option.

Reaching the LISM as fast as possible has been expressed to be of high scientific importance. This would allow time for long-term investigations and increase the chances of surviving instruments reaching the unperturbed LISM. The shortest distance to the heliopause (HP) is in the general direction of the nose.

IBEX and Cassini (and IMAP in several years) observations clearly identify directions that would be extremely valuable to measure in situ. Foremost, the intriguing “ribbon” or “belt” appears as a great circle with a cone angle of ~70° around the interstellar medium (ISM) magnetic field direction, and so intersects the ecliptic plane in two places (Figure 4-1). Neither of the Voyager spacecraft are flying through these regions. Also, the region around the heliospheric nose may contain significant plasma pressure in the heliosheath that may move gradually in ecliptic latitude, as has been indicated by IBEX observations (Schwadron et al., 2014). Voyager 2 measured flows that were consistent with directions away from a pressure maximum and not the nose direction (McComas & Schwadron, 2014). Energetic neutral atom (ENA) imaging during the traversal of the heliosphere phase would offer a changing vantage point and viewing angles against the ENA sources, which would be crucial to constrain, for example, the radial location of the ribbon and its generation mechanism. This would also guide the future science operations.

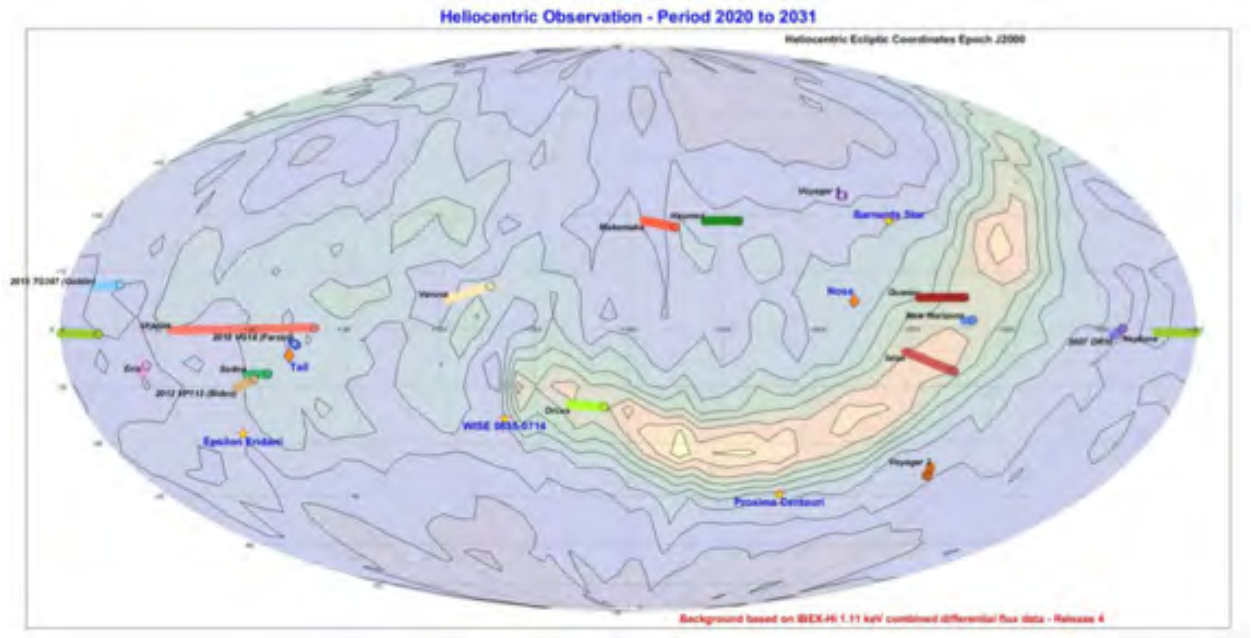

Figure 4-1. The ultimate fly-out direction of an interstellar probe is dictated by the primary heliophysics science goal traded with the speed and launch year. The image shows the sky in ecliptic coordinates with the contours of 1-keV ENA emissions as measured by the IBEX mission and also shows the ribbon. The locations of planets, dwarf planets, and Kuiper Belt Objects (KBOs) are shown for the 2030–2040 period. A trajectory through the ribbon in the ecliptic plane at ~295° ecliptic longitude would also enable an external imaging of the heliospheric shape and offer a potential flyby of Quaoar.

The existence and exact shape of a heliotail is still debated, as discussed above. Flying out down a potential heliotail would definitively determine the HP distance in that direction. However, doing so would come at the expense of a much longer flight time to reach the pristine LISM. Furthermore, an imaging vantage point from directly down the tail would not be optimal for discerning the shape of the heliosphere. Flying along one of the directions of two theorized jets would provide direction measurements of the turbulent scale sizes of that region, which could be a very important constraint on the nature of the global heliospheric interaction with the LISM.

4.1.2. Kuiper Belt Object (KBO) Targets

There are a vast number of KBOs, so any direction governed by heliophysics would offer at least one opportunity for a flyby of a compelling object (Figure 4-1). Targeting larger worlds, such as dwarf planets, would allow the fascinating geology and potential habitability of these small planets to be investigated while providing context for understanding the other Kuiper planets of Pluto, Charon, and Triton. A flyby of Quaoar, at a heliocentric distance of 44 astronomical units (au), lies in a direction that intersects the ribbon and achieves an external vantage point to image the heliospheric shape. Secondary flybys of sub-planetary KBOs (typically <400 km in diameter) could occur as opportunistic alignments allow, but even small trajectory corrections (tenths of degrees) require significant amount of propellant.

Eris, the most massive known Kuiper Belt planet, will be situated near the heliosphere's tail, located ~96 au away. Although exploring Eris would be technically possible for Interstellar Probe, the decision to fly by there would have to be weighed in light of other science priorities.

While it is hard to select exactly what object or system might be most interesting in combination with the logistics of a flyby trajectory, some of the most interesting targets might include one or more objects that are part of the Haumea collisional family. One of the major successes of the Dawn mission was its confirmation, on a variety of levels, of the genetic link between Vesta, the Vestite dynamical family, and the collected Vesta meteorites. Although we do not expect to pick up any Haumea-family meteorites from Earth's surface, genetic linking of spectroscopic and/or surface properties between proposed Haumea family members and Haumea itself would be clear confirmation of many modeling efforts to understand the physics of collisions, dynamics, and interactions of objects in the Kuiper Belt. Similar arguments could be made for other multi-body systems in the Kuiper Belt.

The probability of lining up two or more KBOs is small, in particular if one of the flybys is fixed. With the high speeds of Interstellar Probe, there is little to no room for course adjustments because they would take a significant amount of fuel. For example, MU69 was ~0.2° off the initial direction of New Horizons, and a significant amount of fuel was required to achieve the desired flyby distance. This implies that all targets preferably should be identified early in the development phase to ensure that any operational requirements are incorporated into the mission design. The closest analog is, of course, the identification of MU69, a task that was not straightforward from the Hubble Space Telescope. By the time Interstellar Probe is in full development, the James Webb Space Telescope will have been operational for at least several years, and there should therefore be improved capabilities to search for suitable targets. Given the known density of small and large KBOs in the outer solar system, one would expect at most two to be sufficiently aligned to be realistic for flybys without expending too much fuel.

4.1.3. Planetary Targets

A Jupiter gravity assist (JGA) is part of all of the mission architecture options in this study. Given the high science return of past planetary flybys, science operations at Jupiter are a high priority, except during the mission-critical kick-stage burn. The approximate traversal of the Jovian system, from entrance to exit (bow shock crossing) of the magnetosphere (including the burn at closest approach) would be on the order of several hours.

Both the Uranus and Neptune systems would be compelling flybys because they would enable exploration of the planets, their moons, and their exotic magnetospheres. For launches in the 2030s, Uranus would lie in the direction of the heliotail and Neptune would lie ~110° off the nose direction and not fall within the ribbon.

Batygin and Morbidelli (2017) hypothesized the existence of a fifth giant planet with a semimajor axis >250 au. If a discovery of such a trans-Neptunian giant planet were confirmed well before the

launch of an interstellar probe, it might necessitate a reprioritization of science targets and operations of an interstellar probe and could revolutionize our view of the solar system's structure and evolution.

4.1.4. Circumsolar Debris Disk

An optimal vantage point for the disk would be at high inclination, which would enable direct imaging of azimuthal structure and gaps in the disk caused by planetary interaction. However, not only would this come at a significant cost of asymptotic speed, but it would prevent in situ sampling of the dust in the disk on the way out through the ecliptic. For a trajectory in the ecliptic plane, infrared (IR) imaging could be performed from the changing vantage point, which would provide good information for retrieving the large-scale distribution of the dust in the disk, including potential gaps associated with planetary interactions. Once at a distance beyond the inner zodiacal cloud, the ecliptic vantage point would provide direct constraints on its vertical scale heights. It would certainly be beneficial to study techniques for optimizing the retrieval of the large-scale structure.

4.1.5. Example Optimal Fly-Out Direction

Although there is a need for several other detailed trade-off studies, providing one example illustrates some of the acceptable compromises that must be made. An example direction toward Quaoar satisfies flying through the ribbon close to the ecliptic, and sufficiently away from the nose direction to achieve a side view of the heliosphere that could discern its global shape. Quaoar is only ~8° off the ecliptic plane, which would keep the losses in speed at a minimum. As discussed in section 7, this option would require a launch either just before 2030 or in the late 2030s.

4.2. Spin versus Three-Axis Stabilized

Whereas particle and field measurements prefer a spinning platform to maximize angular coverage, flybys of KBOs would require a three-axis-stabilized platform to maximize image collection during fast flybys in low-light conditions.

It is possible to switch from a spin-stabilized mode to a three-axis-stabilized mode, as was the case with New Horizons, which used hydrazine thrusters to control attitude and spin. The use of hydrazine thrusters also eliminates the risk associated with relying on gyroscopic wheels. However, carrying long plasma wave antennas (>>10 m) and magnetometer booms complicates such operations. Deploying wire antennas and booms is considered a mission-critical maneuver, so deployment and stowage should naturally be avoided as much as possible. Rigid antennas have been flown and successfully deployed on several missions, including the Van Allen Probes, where they reached a length of 7 m each, totaling 14 m tip to tip in the spin-axis direction (Kletzing et al., 2013).

A few approaches were discussed to deal with the need for long-wave antennas that require centrifugal deployment, while also satisfying the need for three-axis stabilization during a potential KBO flyby. The first one was to centrifugally deploy long-wave antennas after a KBO flyby, which would be well before the termination shock. After the last planned flyby, thrusters would be used

to spin up the spacecraft to the desired rate, deploying wire antennas and booms in the process. However, this is considered a mission-critical maneuver. Such a deployment of long antennas (>>10 m) would be very risky given the light travel time and may not be advisable at such large distances. Therefore, a potential KBO flyby may necessitate a mission architecture that relies on rigid (~10 m) plasma wave antennas. A partial deployment of a magnetometer boom could be considered to support the particle measurements. A second approach discussed is to use a de-spun platform that would track the KBO during the flyby. Reliability and cost issues were noted, and this approach was deferred for later analysis.

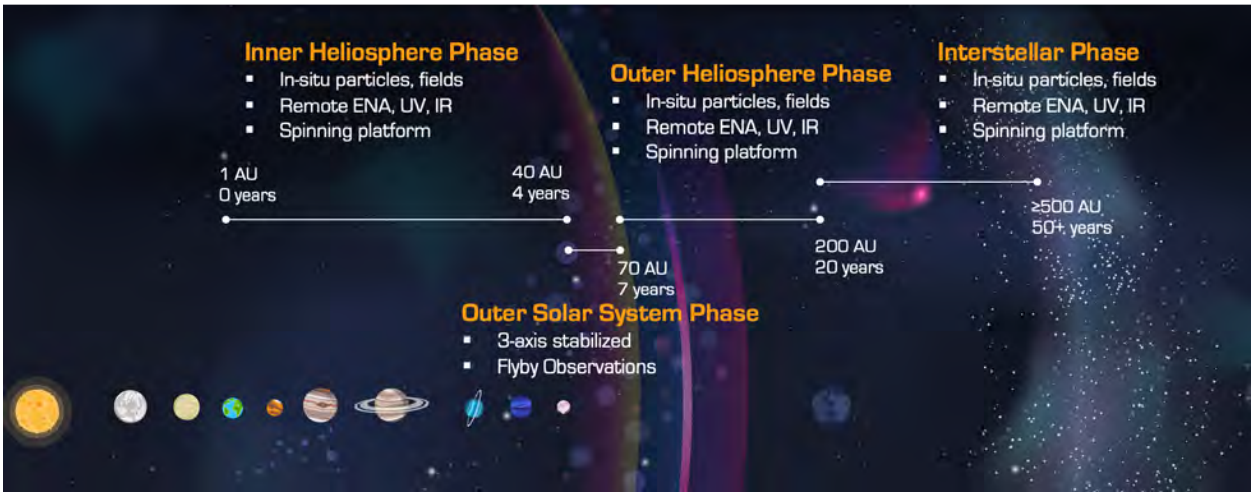

Figure 4-2. An example operation scenario would be divided into three phases and focused on the primary heliophysics goal as indicated. A potential KBO flyby would necessitate three-axis stabilization and may require rigid plasma wave antennas.

4.3. Example Mission Phases and Operations

To illustrate some of the compromises that may be required, we outline below a notional example of science operations over the lifetime of the mission (Figure 4-2). Following other successful missions, such as Cassini, the Interstellar Probe mission could be divided into phases with different primary sciences with unique operational constraints.

4.3.1. Inner Heliosphere Phase

The inner heliosphere phase would begin after commissioning after launch, with no operations during JGA or solar Oberth maneuver, as discussed in section 7. Firing solid rocket engines, especially after a longer in-space storage, is considered a mission-critical maneuver; therefore, any science operations during such a maneuver would not be advisable.

Operations before and after a solar Oberth maneuver would have to be carefully traded off with the increased thermal requirements on instrumentation versus the loss of science observations, but with thermal designs dedicated for the colder conditions in the outer heliosphere. Such trades have been performed before— on the JUICE mission for example—where some of the instruments

have elected to not operate during Venus gravity assist to better accommodate the cold environment of Jupiter.

This phase would last ~4–6 years out to the first KBO flyby (assuming ~10 au/year). Particle and fields observations are of high value in the inner heliosphere, in particular to follow the evolution of pickup ions. Remote imaging from the changing vantage would be an important observation that would provide further information on the large-scale structure of the heliosphere and the temporal evolution of the ENA emission patterns whose source regions eventually would be encountered and investigated in situ. If IR line-of-sight measurements were being conducted, they would start in this phase and provide important information to constrain the vertical scale heights of the zodiacal cloud. Beyond ~10 au, it would be possible to start detecting the cosmic IR background (CIB) as well. In situ dust measurements would provide important information not only on the zodiacal dust but also on the interstellar dusts that penetrate the heliosphere against which measurements in the LISM could be compared. Ultraviolet (UV) measurements of the Lyman-alpha background would be valuable in the heliospheric nose direction to retrieve information about the H-wall and the interstellar H flow.

4.3.2. Outer Solar System Phase

The spacecraft would have to be in a three-axis mode to perform flyby tracking of a KBO. All flyby targets in this example would preferentially have to be identified well before launch to accommodate the needed resources to support operations. Downlink would start as soon as flyby observations are completed, but the expectation is that data would be downlinked over Ka-band over several years. Having a solid commitment of the Deep Space Network or similar large dishes is an important point that could make a significant difference in downlink times. In between two flybys, the spacecraft would remain in three-axis mode or slowly spinning.

Although, one of the main goals of the mission architecture study is to maximize asymptotic speed, extreme flyby speeds well in excess of 45 km/s would potentially have a very severe impact on flyby science that could be obtained for such a fast flyby. Developments for complementary metal-oxide semiconductor technologies for fast readouts to allow for fast flyby imaging are under way.

4.3.3. Outer Heliosphere Phase

Well before the heliospheric termination shock, the Interstellar Probe would spin up using thrusters and remain in this configuration until end of mission. Particle, fields, ENA, and UV imaging would be a primary objective in this phase. A spin rate of 1 minute up to 10 minutes could be acceptable because this also meets the need for IR observations of the CIB to achieve a sufficient signal while spinning.

As above, traversing the heliosheath during a significant part of a solar cycle would ensure that variabilities would be captured. Shocks propagating through the heliosheath and perturbing the environment even well beyond the HP are essential to study to fully understand the exotic interface to interstellar space. Traversing in much less than 3 years would decrease the number of such events in the boundary region and therefore is the scientific driver of an upper limit on asymptotic speed.

4.3.4. Interstellar Phase

The interstellar phase would conceivably be declared once no perturbations from solar variability could be detected (i.e., once the "pristine" LISM was reached). Because there are no precise estimates as to where this begins, this phase could begin as early as 300 au or at a point closer to the end of a nominal mission period. However, this phase would mark the important milestone of leaving our habitable astrosphere behind us and beginning the interstellar journey, where new discoveries would be waiting.

The design lifetime of Voyager 1 and 2 was 5 years, and yet they are still operational with sufficient power to observe and communicate after ~43 years in space. Both will likely last a few more years until their power supplies are no longer sufficient for operating one instrument and communicating, or until the temperature reaches a critically low point—the likely scenario for Voyager 2. With today's experience and heightened requirements on mission assurance, it is therefore reasonable to anticipate that an Interstellar Probe with appropriate margin philosophy would survive well beyond its nominal lifetime of ~50 years, and would continue gathering data long into the interstellar phase.

The second stage of the study will analyze these trades in more detail.

4.4. Section 4 References

Batygin, K., Morbidelli, A. (2017) Dynamical Evolution Induced by Planet Nine. *The Astronomical Journal* 154(6), 229. doi: 10.3847/1538-3881/aa937c

Kletzing, C.A., Kurth, W.S., Acuna, M., et al. (2013) The Electric and Magnetic Field Instrument Suite and Integrated Science (EMFISIS) on RBSP. *Space Science Reviews* 179, 127-181. Retrieved from https://ui.adsabs.harvard.edu/abs/2013SSRv..179..127K

McComas, D.J., Schwadron, N.A. (2014) Plasma Flows at Voyager 2 Away From the Measured Suprathermal Pressures. *The Astrophysical Journal* 795(1). doi: 10.1088/2041-8205/795/1/l17

Schwadron, N.A., Moebius, E., Fuselier, S.A., et al. (2014) Separation of the Ribbon From Globally Distributed Energetic Neutral Atom Flux Using the First Five Years of IBEX Observations. *The Astrophysical Journal Supplement Series* 215(1), 13. doi: 10.1088/0067-0049/215/1/13

5. Example Science Traceability Matrix

The basic science questions of an interstellar probe have not changed over the several decades since they were formed. This illustrates clearly that the groundbreaking science is purely enabled by location. The summary of goals, science questions, objectives, and associated measurements was put together mainly from community discussions held around the 1st Interstellar Probe Exploration Workshop at The Explorer's Club in New York City, 10–12 October 2018, where more than 55 scientists and engineers from around the world were gathered. Because the purpose of this study is to provide the trades and not the science definition, Table 5-1 is an overview of the science questions that could be addressed given appropriate measurements as listed in the rightmost column.

Table 5-1. Interstellar Probe Condensed Science Traceability Matrix as Presented During the 1st Interstellar Probe Exploration Workshop, New York City, 2018

Goals	Overarching Objectives	Specific Questions	Measurements
Our Heliosphere as a Habitable Astrosphere (Primary Goal)	**Nature of Interstellar Medium**	Interstellar medium (ISM) composition	Elemental and isotopic abundances
		Field, plasma, and neutral properties	Flows, temperatures, density, charge states, fields
		Cosmic ray origin	Cosmic ray ions/electrons, galactic gamma rays, radio
		Cosmic evolution	Isotopic abundances of He and other light elements
	Structure of the Heliosphere	Bubble or tail	Plasma, energetic particles, fields, energetic neutral atoms (ENAs), radio
		Shocks, hydrogen wall	Plasma, neutrals, ENAs, Lyman-alpha
		Effects of the heliosphere on the ISM	Plasma, energetic particles, galactic cosmic rays (GCRs), ENAs
	Dynamics of the Heliosphere	Response to solar (and ISM) variability	Thermal plasma, pickup ions (PUIs), waves, anomalous cosmic rays
		Effects of ISM on inner heliosphere	PUIs, ACRs, high-energy electrons
Origin and Evolution of Planetary Systems (Supporting Goal)	**How Did Matter in the Solar System Originate and Evolve?**	Zodiacal dust cloud structure	Dust, infrared (IR), plasma
		ISD composition and organic matter	Dust, IR (cross-reference to ISM comp.), PUI
		Edgeworth-Kuiper Belt grain composition	Dust
		Kuiper Belt Object and planetary (KBOP) geology, composition, history	IR, visible
		Evolutionary aspects and KBOP distribution	visible
		KBOP atmospheres, magnetospheres, and interiors	ultraviolet, IR, visible, mag, plasma
The Universe Beyond the Circumsolar Dust Cloud (Supporting Goal)	**How Did Galaxies Form and Evolve in the Universe?**	First-light galaxies, dust-obscured star formation Mass, distance of lensing targets	Optical/near infrared/far infrared beyond Zodi Optical μ-lensing parallax effect

6. Example Model Payload

After the discussion of the compelling science questions at the 1st Interstellar Probe Exploration Workshop in 2018, a preliminary, example baseline payload was discussed and documented. Resource requirements and measurement capabilities were drawn from the input of and presentations made by community members at the workshop. It was noted that the stated required resources were optimistic as compared to past flown instrumentation. The intention was to provide resource, spacecraft, and operational requirements to drive the design of a mission architecture. Trade-offs for a lighter, example threshold payload were also discussed but were not analyzed in detail.

6.1. Example Baseline Model Payload

Table 6-1. Example Baseline Model Payload as Discussed and Documented at the 1st Interstellar Probe Exploration Workshop, New York City, 2018, and presented at the AGU Fall Meeting 2018.

Instrument	Mass (kg)	Power (W)	Bitrate (bps)	Capabilities	Spacecraft Requirements	TRL and Heritage
Vector Helium Magnetometer	1	2	6	3 axes Dual configuration 0.01–10 nT, 10–60 s Power includes 1-W heater	Boom > 10 m Fiber optics integrated with sensor Spinning	TRL = 6 Cassini, rocket flights
Fluxgate Magnetometer	5.6	2.2	1200	3 axes	Boom > 10 m Spinning	TRL > 7 Voyager (3.6-m boom)
Plasma Wave Instrument	6	1.5	100	Includes sensor, wire antennas, shielding, harness	>10-m stacer antennas to support slow spin modes Spinning	TRL = 6 Van Allen Probes
Solar Wind and PUI (combined with below)				0.5–80 keV/q ΔE/E ~ 0.3 Interstellar PUI: ^{3}He+, ^{4}He+, N+, O+, ^{20}Ne+, ^{22}Ne+, Ar+ Inner source PUI: C+, O+, Mg+, Si+ Mass and charge state of H-Fe ions 1.4×10^{-3} cm^2 sr eV/eV 6° × 360°	Spinning Perpendicular to spacecraft spin axis Onboard processing to obtain PADs	TRL > 5 IMAP
Suprathermals and Energetic Ions	6.1	10.8	1000	0.03–5 MeV/nuc 1 – >60 amu 12° × 10° × 7° over 360° 0.2 cm^2 sr	Spinning Perpendicular to spacecraft spin axis Onboard processing to obtain PADs	TRL > 5 IMAP

Instrument	Mass (kg)	Power (W)	Bitrate (bps)	Capabilities	Spacecraft Requirements	TRL and Heritage
Cosmic-ray spectrometer: anomalous and galactic cosmic rays	3	2	2	H ~ 50 keV – 200 MeV (stopped in detector) H 0.2–2 GeV (penetrating) He ~200 keV – 1 GeV C, N, O, Ne 1 – 200 MeV/nuc e- ~50 keV – 30 MeV		TRL = 3 ACE
Dust Detector	14	25	579	M/ΔM > 200 <1° 1–70 km/s >0.3 µm	Deployable cover (TBD) Ram pointing	TRL = 6 Cassini/CDA, Europa Clipper, IMAP, NASA Matisse
Neutral Ion Mass Spectrometer	3.5	5	1	Isotope ratios: D/H, $^{3}He/^{4}He$, $^{13}C/^{12}C$, $^{18}O/^{16}O$, $^{22}Ne/^{20}Ne$, $^{38}Ar/^{36}Ar$ Li abundance m/Δm > 100 at 1σ Sensitivity: 0.1 cm^3	Ram direction	TRL = 7 BepiColombo, Rosetta, LADEE, MAVEN
Low-Energy ENA	3	3	100	10–2000 eV (32 energy channels) H, He, O, Ne 45° × 2° pixels using scanning platform	Scanning Platform	TRL = 6 IBEX-Lo comparison: 11.5 kg, 3.46 W, 122 bps
Medium-Energy ENA	7.37	0.65	99	0.38–6.0 keV 6.5° 3×10^{-3} cm^2 sr eV/eV at 2.2 keV (double coincidence, incl. eff.)	Spinning	TRL = 9 IBEX-Hi values shown Heritage: IBEX-Hi
High-Energy ENA	7.2	6.5	500	≥1.5° (electron optics limit) 90° × 120° ~1–300 keV/nuc (ENA) H, He, O, S GF: ≤1.8 cm^2 sr Efficiency: 0.2 (H)	Spinning	TRL > 7 Cassini/INCA, IMAGE/HENA, JUICE/JENI, IMAP-Ultra
Lyman-alpha Spectrograph	12.5	11.86	24	115–180 nm in 165 bins	Scanning Platform	TRL = 7 DMSP SSUSI; NASA TIMED/GUVI; SSUSI-Lite
VisNIR Imager	8.6	15	?	Panchromatic (~0.3–0.8 µm) and multispectral (~0.3–2 µm) 100 m/px at 10,000 km: <5 µrad (baselined ~LORRI optics) Framing (panchromatic) and pushbroom (multispectral) modes (baselined ~EIS electronics) Single-pass pushbroom stereo capability Millisecond to multiple second exposures Tolerance needed to observe planet-Sun transits beyond 30 AU as exoplanet analog. Also could observe moons crossing planets' disks.	Staring and pushbroom operations	TRL = 6 LORRI, DRACO, EIS heritage

Instrument	Mass (kg)	Power (W)	Bitrate (bps)	Capabilities	Spacecraft Requirements	TRL and Heritage
VISNIR/FIR Mapper	4	3		0.5–15.0 + 40–100 µm 10 µrad 7-cm diameter	Spinning spacecraft or scanning platform	TRL = 9 for VISNIR flight instrument design Voyager/IRIS, Galileo/NIMS, Cassini/VIMS, Rosetta/VIRTIS, New Horizons RALPH/LEISA TRL = 9 using H2RG Detector Deep Impact HRI/IR, OREX/OVIRS, JWST/NIRSpec TRL = 5 Using "Speckle" Low Mass/Power Design CIBER 2
Total	**81.87**	**88.51**	**3611**			

6.2. Discussions on an Example Threshold Payload

A threshold payload must be derived from a careful analysis of a threshold mission and its science value. At the 1st Interstellar Probe Exploration Workshop in 2018, a brief discussion was held among the participating community members to analyze and document the science loss of a few example trades. It is important to note that no consensus was reached on any particular threshold science or payload.

Although imaging of the circumsolar dust by an infrared (IR) detector would provide groundbreaking information on the large-scale structure, in situ detection by a dust analyzer would still provide unprecedented information on the size and compositional distribution along an outward trajectory. The only dust measurements accomplished to date in the outer solar system have been made by the Student Dust Counter on board New Horizons. Even though it did not resolve composition or size, it provided the community with a very important constraint, and the only one thus far.

A dust analyzer provides important elemental and, to some extent, isotopical compositional information about circumsolar dust and interstellar dusts (ISDs). This information would be particularly important crossing the heliopause (HP) into the local interstellar medium, providing insights into the properties of ISDs in our galaxy that could be an essential part of the building blocks of our and other solar systems, as well as galactic chemical evolution. Although a dust counter requires much less mass and power, it does not resolve any composition and would provide total number density as a function of distance from the Sun. Dust hits could also be counted by a plasma wave antenna and provide at least a rough relative number density.

The spectral resolution uniquely provided by a Lyman-alpha spectrograph would be the first to remotely differentiate the interstellar H flow and wall from the Lyman-alpha background and the hotter components believed to exist in the inner and outer heliosheath. Lyman-alpha intensity measurements that would not resolve the line shape would repeat the total column density measurements of H that have been performed by the Voyager/Ultraviolet Spectrometer (UVS) and New Horizons/Alice instruments that cannot uniquely resolve the interstellar flow but can be used for atmospheric observations during a potential flyby of a dwarf planet or Kuiper Belt Object.

Given the success of ENA observations from IBEX and Cassini, energetic neutral atom (ENA) imaging was generally agreed to be one of the more important and appropriate observations from an interstellar probe. The wide field of view (FOV) of a high-energy (approximately tens of kiloelectronvolts) ENA camera (Cassini/INCA and IMAP-Ultra) is required to capture the first unique image of the heliosphere shape from an external vantage point beyond the HP. Minimizing the FOV to a telescope-like configuration would save some mass but would severely impact the ability to derive any information on the global shape. In the medium 0.4- to 10-keV energy range, current instrument techniques (IBEX-Hi and IMAP-Hi) revolve around a narrow FOV, which necessitates the use of a scanning platform to achieve wide angular coverage. This is important to discern the source location and mechanisms of the ribbon by imaging from the changing vantage point that a trajectory out of the heliosphere would provide. Also, it would ensure that any temporal variations in emission strength could be captured globally. A telescope-like configuration mounted perpendicular to the spin axis without a scanning platform would cover a great circle in the sky that would scan the boundary along the outward trajectory, much like an MRI scan. However, this would severely limit the capability to discern global structure or ribbon source location and would make it difficult to differentiate between temporal versus spatial variations.

7. Mission Architecture: First Steps

Three foundational tasks dominated the systems engineering and mission architecture effort for the beginning of this study:

1. Multiple options for launch configurations were identified, based on existing hardware and new hardware being developed under the Space Launch System (SLS) development effort. This effort was accomplished by working closely with the payload accommodation team from NASA's SLS program.

2. Trajectories were developed and multiple flight paths out of the solar system were analyzed, maximizing hyperbolic escape velocity within the expected constraints on the launch and flight system.

3. Critical thermal conditions for the mission were scoped out, particularly for trajectories that fly close to the Sun on the way out of the solar system, and initial assessments of possible solution spaces were made (R. L. McNutt et al., 2019).

Along with the science scope and plan, the trajectory information, launch vehicle configurations, and conditions for surviving the thermal environment (if a solar Oberth maneuver were to be used) are the knowledge base upon which the team can now execute more in-depth design of the flight system, develop options for a concept of operations (CONOPS), and home in on an executable mission architecture.

To make an initial assessment of spacecraft performance, we drew upon the class of "smaller" outer-solar-system spacecraft flown to date—Pioneer 10/11 (251.8 kg), Ulysses (366.7 kg), and New Horizons (478.3 kg) (separated wet masses; Ralph L. McNutt, Jr. et al. (2014) and references therein)—supplemented with the large Voyager 1/2 spacecraft (825.4 kg) (Heacock, 1980) (Figure 7-1, from Ralph L. McNutt, Jr. et al. (2018)).

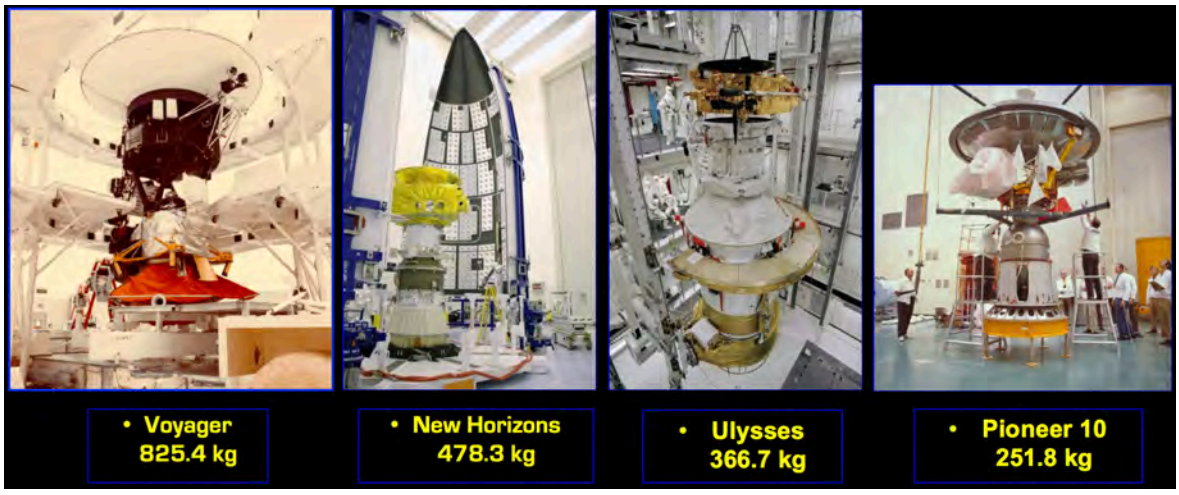

Figure 7-1. Deep-space scientific satellites have varied in mass by a factor of ~3.3.

Given APL's development of New Horizons (Fountain et al., 2008), which is the newest of these smaller spacecraft, the use of a general-purpose heat source radioisotope thermoelectric generator (GPHS RTG), and the availability of flight drawings, it was decided that the initial scoping studies would use the nominal 478.3-kg New Horizons mass along with the form, fit, and function of that spacecraft. This approach allowed an initial assessment of the various launch system and trajectory options to be made while a more mature "custom" spacecraft design proceeded in parallel.

7.1. Space Launch System Application: Methodology and Required Calculations

7.1.1. Requirements

At a technical exchange meeting held at Marshall Space Flight Center (MSFC) on 5 December 2017, requirements were articulated for "what is needed":

- *Good* performance numbers for SLS Block 1B (but see footnote 26) with various stage combinations
- Separated spacecraft mass of 300–800 kg "bounds the box" (increased from 200 kg to be more realistic, as of 1 May 2018)
- Kick-stage selections based on existing hardware

7.1.2. Background

This list of "needs" is based on previous work reported at the 65th International Astronautical Congress (IAC) in Toronto, Canada, in 2014 (Ralph L. McNutt, Jr. et al., 2014), the 66th IAC in Jerusalem, Israel, in 2015 (Ralph L. McNutt, Jr., Benson, et al., 2015), and at the 67th IAC in Guadalajara, Mexico, in 2016 (Ralph L. McNutt, Jr. et al., 2016); general issues relating to the SLS Block 1B usage were also presented at the 2016 IAC (Ralph L. McNutt, Jr. & Vernon, 2016). Follow-up general information was presented at the 68th IAC in Adelaide, Australia, in 2017 (Ralph L. McNutt, Jr. et al., 2017).

Ralph L. McNutt, Jr., Benson, et al. (2015) contains initial trade studies on upper stages—and this at a time when the SLS design itself was still undergoing significant changes. At that time, the study examined the SLS Block 1B 27000 (cargo) configuration with focus on what were then considered four "near-term" systems:

1. Interim Cryogenic Propulsion Stage (ICPS)
2. Star 48BV
3. CASTOR 30B: The Antares 220 Second Stage [Antares 122 per OSP-3 User's Guide, Release 1.1, July 2013]
4. CASTOR 30XL: The Antares 230 Second Stage [Antares 132 per OSP-3 User's Guide, Release 1.1, July 2013]

Best performance was found when "The STAR 48BV was used in conjunction with either an ICPS or Castor 30XL as the stage between the STAR 48BV and the EUS" (Ralph L. McNutt, Jr., Aleman, et al., 2015).

The ICPS is now off the option list, and the SLS Block 1B design has continued evolving, so please read further. (At the time, NASA pronouncements suggested that the SLS Block 1 with the ICPS rather than the Exploration Upper Stage (EUS) might be the only available launch combination in the near future.)

Earlier work (Ralph L. McNutt, Jr. et al., 2014) conducted a more general review of available upper stages combined with what was then known about the notional SLS configurations. Then, as later, the best choice for the "final" upper stage appeared to be the Star 48BV stage. The match is about correct for limiting the burnout acceleration, and a similar upper stage was then considered for—and is now implemented for—Parker Solar Probe, which launched on 12 August 2018.

At that time and through the 2015 calculations (Ralph L. McNutt, Jr., Benson, et al., 2015) and later unpublished ones, it became clear that the very high C_3s required can only be obtained with a sizable upper stage with an appropriate size and between the EUS of the SLS Block 1B and the Star 48BV powered stage. Higher performance by the notional (in 2015) SLS Block 2 would, of course, be preferable. However, we have chosen not to pursue that configuration because its exact performance and date of initial operational capability (IOC) remain undefined at this time. (At the time, it was thought to be worthwhile to look at the nominal Block 2 performance just to establish what might notionally be possible, but newer developments have led to the analysis using the Block 2 performance as now understood in January 2020 (Stough et al., 2019)).

7.1.3. Configurations

To "bound the box," we need to continue to look at final separated spacecraft masses of 300–800 kg, although 300 kg may be so light as to violate safe acceleration limits (one of the first items that requires evaluation).

Such a configuration would be used for a direct flight to Jupiter and a passive gravity assist there (i.e., "Option 1," cf. section 11.5.3). For that configuration, we need a robust, high-fidelity design with margins, adaptors, etc., and based on the currently best known SLS Block 1B parameters in order to provide a good injected mass versus C_3 curve for that best configuration and separated mass of 300–800 kg for the spacecraft.

In addition, there are two other configurations that need detailed evaluation and will require the convolution of mission design with launch vehicle staging and approach.

- Powered Jupiter flyby ("Option 2")
- Oberth maneuver (powered Sun flyby) ("Option 3")

To look at either of these options, we need to know the injected mass versus C_3 for the SLS Block 1B for trajectories that allow a stack of kick stages plus the satellite to actually reach Jupiter. A simplified, analytic, patched-conic model calculation (see the appendix of the 2014 IAC paper referenced above) in its current instantiation (of 5 December 2017) has been developed to provide some estimates. For Earth and Jupiter in coplanar, circular orbits (with orbital radii equal to their semimajor axes), the C_3 to reach Jupiter on a Hohmann transfer is 77.32 km^2/s^2 with a fly-out time from Earth of 2.73 years; the required C_3 can be lowered with a ΔV Earth gravity assist (ΔV-EGA) and/or additional EGAs and Venus gravity assists (VGAs). This approach was used with both Galileo and Cassini but is accomplished at the expense of additional fly-out time to Jupiter. Because minimization of mission time is a driving requirement and such maneuvers require additional large deep-space maneuvers (DSMs) with corresponding propulsion systems, we defer the use of such gravity assists to reach Jupiter initially to possible future studies.

7.1.4. Option 1, Option 2, and How They Trade

To deal with option 2, the appropriate trade is to use an optimized staging approach (i.e., determine optimal real stage stacks with a parameterized, separated spacecraft mass as a parameter that runs from 300 to 800 kg). Next, compare the asymptotic solar system escape speed for burning all stages during Earth launch followed by an optimized, passive, Jupiter flyby with the asymptotic solar system escape speed with a launch using all but the uppermost kick stage (presumably powered by a Star 48BV motor), and then optimizing the subsequent Jupiter flyby with an engine burn of that stage at perijove. This ignores the issue of stage maintenance during the Earth-to-Jupiter cruise. Finally—and only if energetically possible (which it likely is not)—boost the top two kick stages with the spacecraft to Jupiter and burn both of those stages there.

Rough calculations with the previously identified SLS Block 1B capability and the above-mentioned analytic work indicate that the powered Jupiter gravity assist (JGA) does not trade well against a passive JGA after a far larger launch C_3. To the best of our knowledge, such a result is not "obvious," nor has it ever been done. If the assertion is that one does far better with the higher launch energy, then this is an important result, not just for this study at hand, but in general.

Of course, Jupiter and Earth are not in coplanar, circular orbits. Those features do make a difference because optimized launch windows for the Earth-Jupiter system occur at the synodic period of 398.9 days (1.092 years) versus Jupiter's sidereal period of 11.86 years. Because there is no small number of synodic periods that are integral, the "pattern" of Earth-Jupiter transfers does not repeat on small timescales: Each optimal occurrence advances the ecliptic longitude by ~33.16°. After 11 synodic periods (i.e., after 12 years), the period is very close to repeating. Hence, within a given 12-year period, there should be a "best" case and a "worst" case for an optimized ("highest" = "best") asymptotic solar system escape speed to a given target. With Jupiter's small orbital inclination with respect to the plane of the ecliptic (1.303°), a "best" (most rapidly reached) target in the sky will always lie very near the plane of the ecliptic.

Hence, for trajectory comparison purposes, an approach could be to consider the period from 2015 to 2050 (2100 is a better choice to deal with any "but what ifs", e.g., programmatic), assume

an “optimal” SLS Block 1B plus kick stage(s) configuration for a separated spacecraft mass of 300–800 kg in, e.g., 50-kg increments (13 parameter values) and provide the corresponding C_3, and determine for each calendar year (for 50 [80 years from 2020 to 2100] years) (1) the optimal launch date and launch declination as well as the corresponding optimal ecliptic latitude and longitude of the resulting “aim-point” on the sky, (2) the optimal Jupiter encounter date (and hence fly-out time to Jupiter) and optimal perijove altitude and latitude (Jupiter-centric), and (3) the resulting asymptotic escape vector of the spacecraft (speed, ecliptic latitude, and ecliptic longitude). These data would complete the “scoping calculation” for what we can call Option 1.

The option 2 scenario consists of all of the same inputs and calculations as option 1, with the *significant exception* that the final kick stage would exercise its burn centered on perijove, rather than being used as part of the launch scenario. We will not worry about any changes that might be required for multiyear, deep-space “storage” of the kick-stage propellant—whether solid or liquid—as part of this exercise. The purpose is to provide a direct comparison of what can be achieved with the two launch approaches in some technologically ideal limit.

Depending on the difficulties of these calculations, we may want to redo them, with arbitrarily higher specific impulses for the final kick stage: a value of ~450 seconds (characteristic of a nonexistent liquid oxygen/liquid hydrogen [LOX/LH_2] engine of the same mass class) and a value of ~900 seconds (characteristic of a nonexistent nuclear thermal rocket engine with LH_2 propellant of the same mass class) (see further discussion of “advanced” upper stages in a separate document). Such engines likely cannot be built; the point of doing such calculations is to demonstrate in no uncertain terms that the relative performance of the two scenarios is independent of the specific impulse of the final kick stage.

7.1.5. Option 3

In this scenario, the Jupiter flyby is retrograde to enable a fall into the Sun by “killing off” the spacecraft’s solar system angular momentum. Option 3 uses the Oberth maneuver. As outlined above, (for now) we would only consider direct flights from Earth to Jupiter, i.e., no VGAs or EGAs either solely or in any combination (hence, no “extra propulsion system” to execute a DSM is considered in the mass stack-up). As with Options 1 and 2, there is a minimum launch C_3 required to reach Jupiter (and this will, of course, vary across our 80-year period with a periodicity of ~12 years, also as noted previously).

In this case, an upper kick stage must be carried to a close solar flyby. The launch C_3 sets the perihelion distance that can be reached. In addition, one must worry about appropriate thermal shielding for the spacecraft, and that will also vary with the perihelion point and will change the mass and, hence, available velocity change from the perihelion burn and ultimate asymptotic solar system escape speed.

We break the scenario into two pieces. The first is parameterized by the separated spacecraft mass and by the perihelion; the second adds in the required thermal shield mass to enable the spacecraft to survive the perihelion pass and fire the final kick stage. By bounding the perihelion between 1 solar radius, i.e., the photosphere, and 10 solar radii, just inside the nominal, final Parker

Solar Probe perihelion of 9.86 solar radii, the full range of possibilities can be viewed. N.B. All perihelion distances are in units of solar radii from the ***center*** of the Sun. Numbers from the model calculation indicate a fairly narrow range of C_3s: 104.2 km^2/s^2 to get to ~15.4 solar radii, increasing to 109.9 km^2/s^2 to reach 1 solar radius.

What we can call "Option 3a" uses this approach—with no thermal shield—to calculate performance as compared with those of Option 1 and Option 2. In "Option 3b," for each of a grid of perihelion values, say 1–10 solar radii by 0.5 solar radius increments, a thermal shield mass would be added for a given perihelion and the range of separated spacecraft masses. For this pass, we assume a geometrical configuration of the New Horizons spacecraft and its upper stage (and perihelion values of 3, 4, and 5 solar radii (R. L. McNutt et al., 2019)).

This approach separates detailed consideration of mission design plus launch vehicle, detailed spacecraft design, reliability, instrument contingent, and science goals from each other, but provides a parametric structure to link these parallel efforts together in what is essentially a "first run" at the overall task.

The preliminary calculation on the effect of the mass of the thermal shield is shown in Figure 7-2 (and again in Figure 11-3 with the supporting calculation detail).

This example is for a Star 48BV stage and illustrates the problem for the ideal case of a spacecraft falling in from infinity (rather than "just" from Jupiter). N.B. At 4 solar radii and no shield penalty, we are looking at ~8 astronomical units (au)/year asymptotic escape speed, based on this engine. This is a very rough calculation, but it nonetheless illustrates the type of calculation that is required with fairly high fidelity. A fully self-consistent solution will, of course, require a fairly complete spacecraft design, but this helps provide a good first cut in deciding which option or piece thereof to pursue.

It is worth noting that part of this is up against fundamental physical limits (see also section 11.1.3). The escape speed from the Sun's ***surface*** (i.e., the photosphere) is

$$V_{Sun} = \sqrt{\frac{2GM_S}{R_S}} = 617.6\ km/s.$$

The ideal Oberth maneuver limit is then

$$V_{esc,0} = (2V_{Sun}\,\Delta V)^{1/2}\ \left(\frac{R_S}{r_p}\right)^{1/4} = 35.14\left(\Delta V[\tfrac{km}{s}]\right)^{1/2}\ \left(\frac{R_S}{r_p}\right)^{1/4} km/s =$$

$$7.413\ \left(\Delta V[\tfrac{km}{s}]\right)^{1/2}\ \left(\frac{R_S}{r_p}\right)^{1/4} AU/yr. \quad (1)$$

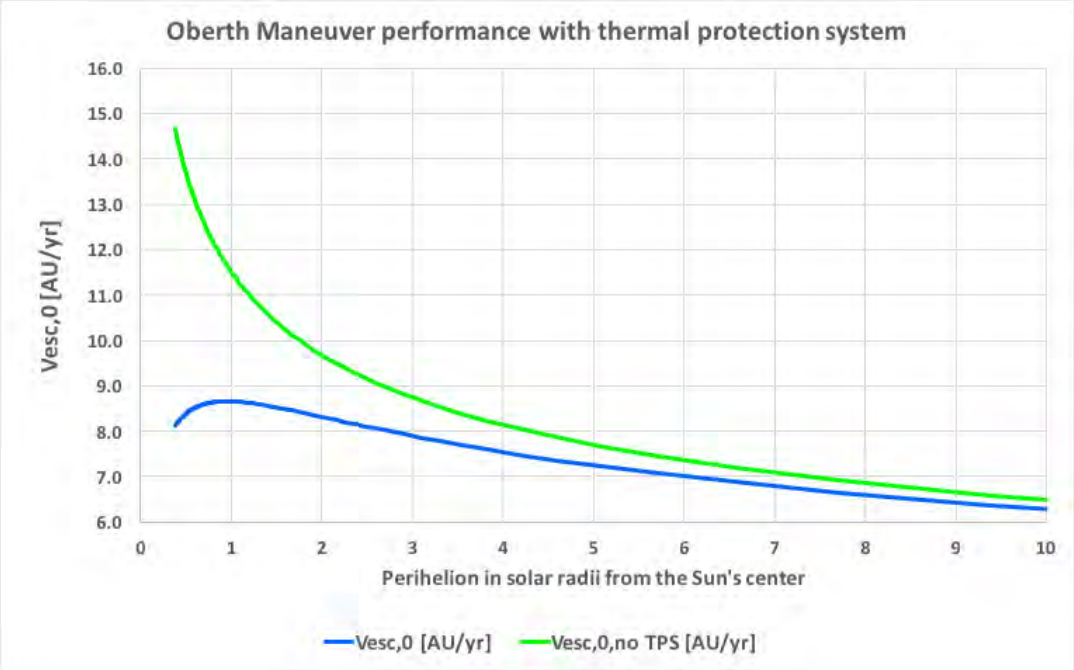

Figure 7-2. (See same figure and detail in current section 11.2.2 for details.) For a fixed solid kick stage, this figure illustrates the decrease in performance for a solar Oberth maneuver due to the added mass of a thermal protection system (TPS). Maximum performance can be expected as the distance to the Sun's center decreases and the potential gain in performance by going deeper into the Sun's gravity well is overtaken by the required increase in mass of the TPS. The exact location is heavily dependent on the details of the combined thermal, mechanical, and attitude control system design of the entire system.

Hence, in the ideal case, to achieve an asymptotic escape speed of 20 au/year, the requirement is

$$\left(\Delta V[\tfrac{km}{s}]\right)^{1/2}\left(\frac{R_S}{r_p}\right)^{1/4} = \frac{20}{7.413} = 2.69796 \tag{2}$$

or

$$\left(\Delta V[\tfrac{km}{s}]\right)\left(\frac{R_S}{r_p}\right)^{1/2} = 7.27900. \tag{3}$$

This provides the fundamental lower limit for the required ΔV by setting r_p = 1 R_S. Even for this case, such a large propulsive maneuver is not possible with a single-stage-solid or -cryogenic (LOX/LH_2) stage. Although within the range of a thermal nuclear rocket engine stage, such stages have never been developed to flight hardware status, and all designs have been for stage sizes about a factor of 10 too large for this application (e.g., Schnitzler & Borowski, 2007, 2008; Schnitzler et al., 2009).

This being said, if the asymptotic speed were backed off to 10 au/year (about three times that of Voyager 2 and somewhat less than three times that of Voyager 1, ~10.8 au/year), the constitutive relationships for the idea case change to

$$\left(\Delta V[\tfrac{km}{s}]\right)^{1/2}\left(\frac{R_S}{r_p}\right)^{1/4} = \frac{10}{7.413} = 1.34898 \quad (4)$$

or

$$\left(\Delta V[\tfrac{km}{s}]\right)\left(\frac{R_S}{r_p}\right)^{1/2} = 1.81975. \quad (5)$$

For a perihelion of 2.5 R_S, the ΔV is 2.87728 km/s. This is within the potential scope of what might be accomplished with a solid rocket motor stage. The driving question in this point design is what would be the required mass of the thermal shield for such a close perihelion distance.

At an asymptotic fly-out speed of 10 au/year, the mission would reach the solar gravitational lens distance (Eshleman, 1979) of ~550 au in just over 50 years of flight time. Although there are significant technical challenges in exploiting this feature (Turyshev & Andersson, 2003), the reach would still be approximately three times the expected penetration of Voyager 1 into the very local interstellar medium (VLISM) before its demise. As we show in the following sections, this high of an asymptotic fly-out speed remains "challenging" at best.

7.1.6. Summary, Characteristics, and Comparisons

A review of ultimate SLS Block 1B high-C_3 capabilities[1] and how those relate to existing kick stages is required, along with a baseline spacecraft design, for the input to Option 1 and Option 2 calculations. Such calculations would provide a basis for determining "current" capabilities, as well as the required starting point for the Option 3 calculations. Additional potential subjects include targeting close flybys of (known) large Kuiper Belt Objects (KBOs) as indicated in Figure 7-3 (reproduced from Ralph L. McNutt, Jr., Benson, et al. (2015)).

Insights can be drawn from New Horizons before its encounter with Arrokoth (Stern et al., 2019) when the spacecraft was within 2 au of its flyby of the small KBO 2014 MU69 ("Ultima Thule") (Figure 7-4). This small KBO has a slightly larger eccentricity than that of Quaoar (0.04815 versus 0.03756) and a slightly larger semimajor axis (44.52 au versus 43.62 au). The point is that with respect to lighting and sequencing, the New Horizons flyby of 2014 MU69 is almost a perfect dress rehearsal for a future flyby of Quaoar by an interstellar probe, albeit at a significantly faster (at least a factor of 2) flyby speed. Ixion, a similar larger KBO, is about the correct direction but somewhat closer to the Sun and in a higher eccentricity orbit (data from the Jet Propulsion Laboratory [JPL] Solar System Dynamics Small-Body Data Base Browser, as of 7 May 2018).

[1] As noted elsewhere in this report, the performance characteristics of the SLS and its variants continued to evolve during the early portion of this study. At the beginning of the study, the designation was SLS B1B BOLE (Booster Obsolescence Life Extension), which would be the enhanced performance B1B after the existing stockpile of boosters from the Space Transportation System (STS or "Space Shuttle") ran out in the mid-2020s. At the start of this study, these were also referred to as the SLS B1B+. As the design has matured, projected performance has increased, and the designation has been shifted to the SLS Block 2 (also SLS B2 (Stough et al., 2019)).

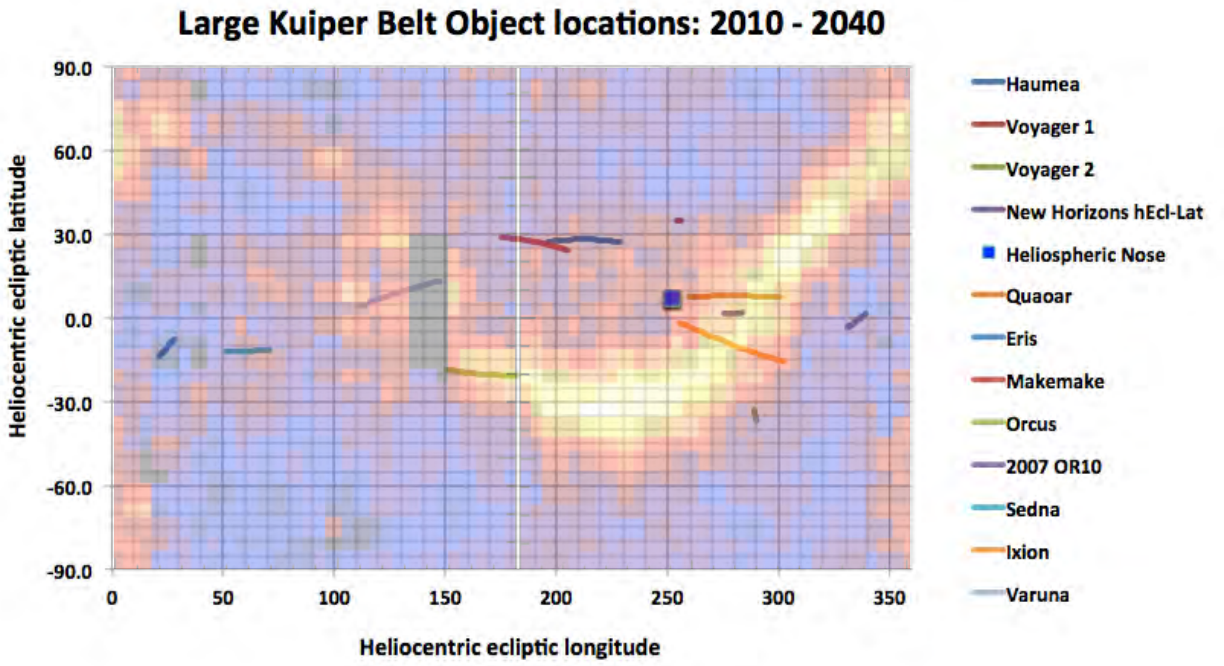

Figure 7-3. The background map shows the Interstellar Boundary Explorer (IBEX) "ribbon" source of energetic neutral atoms (ENAs). The location of Quaoar (and its moon Weywot) is near the ribbon and the plane of the ecliptic. Quaoar is about the same size as Pluto's large moon Charon and might make for a good flyby target on the way "out" of the solar system, the trade being the mass of appropriate flyby instruments, need for three-axis stabilization, etc. The New Horizons flyby of 2014 MU69 (as of this writing successfully accomplished) will make for a good test case (size versus flyby speed).

A final note is the possibility of using multiple gravity assists to increase further the asymptotic escape speed. Planetary locations between now and the end of the century drive the potential solution space, especially because of the very long orbital periods of Uranus and Neptune. For a limited number of aim-points on the sky, the solution space tends to be over-constrained (cf., e.g., figure 7 in Fiehler and McNutt (2006)). What has not been done is to look for possible trajectories with dual planetary flybys to maximize the fly-out speed without regard for the end point of the asymptotic trajectory on the sky. Such calculations would enable us to "bound the box" for such variations on the other scenarios. A Jupiter flyby appears to be required in any case; whether the limitations on launch windows would be worth potential gains of adding additional available flybys before the year 2100 has not yet been explored.

The physical limitations of simple ballistic trajectories are illustrated in the Figure 7-5. These are based on a simple analytic model (described in section 7.1.3 with additional details given in the appendix of (Ralph L. McNutt, Jr. et al., 2014) and compare fly-out times and asymptotic speeds both with and without optimized (passive) Jupiter flybys. The "direct" and "assist" (Jupiter flyby) curves merge eventually because the gravity assists become less and less effectual as the optimal

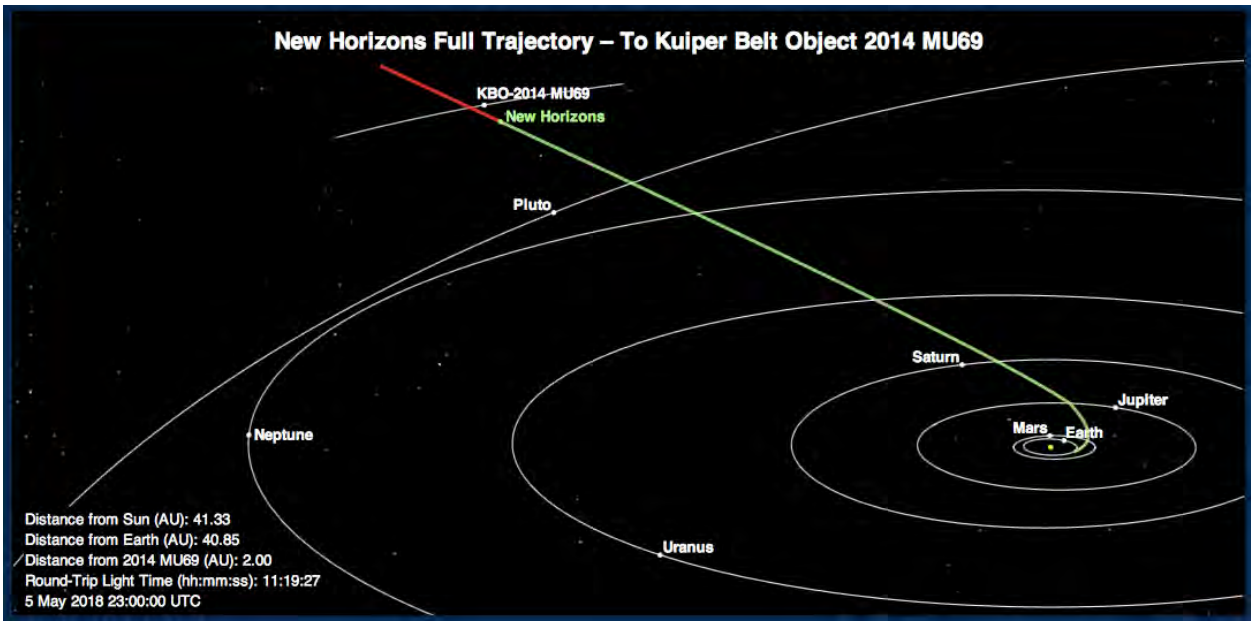

Figure 7-4. The location of New Horizons on 5 May 2018, after the successful Pluto system flyby in 2015 and before the flyby of the small KBO 2014 MU69 (now officially designated 486958 Arrokoth). This shows the period of intense planning for the flyby, largely driven by uncertainties in the heliocentric radial position of the object. This will be a common concern for all future KBO close flybys because of limited observation of their orbits, set by their relatively recent discoveries (this was also an issue with the Pluto flyby because the orbit of Pluto has only been tracked since its discovery in 1930 (Slipher, 1930; Strömgren, 1930), and that includes only a small fraction of its long orbit).

flyby closest approach distance moves farther and farther toward the center of a point-mass Jupiter,[2] whereas the actual closest approach is, of course, limited by the true planetary radius. The square root of the C_3 value simply indicates the post-Earth-escape speed being added and, for computing travel times, does not take into account the extra "boost" provided by the Earth's orbital speed about the Sun.

Altogether, six different ballistic trade options can be considered, if the goal is to maximize the fly-out speed from the Sun and into the near interstellar medium. The cases just described appear to be the only ones not dismissed fairly easily.

For a given launch vehicle configuration, other than the simple cases of a direct ascent or a passive JGA ("Minovitch maneuver," used by all five solar-system-escaping spacecraft launched to date), all other cases convolve significant engineering issues (primarily, but not exclusively, thermal and structural) with mission design. Of these, the powered-solar flyby ("Oberth maneuver") appears to offer the most potential promise but also provides the largest challenges:

[2] After these initial calculations, an error was found showing the gravity assist curves actually overestimate the escape speed and underestimate the flight times by a small amount for a value of C_3 > ~225 km^2/s^2.

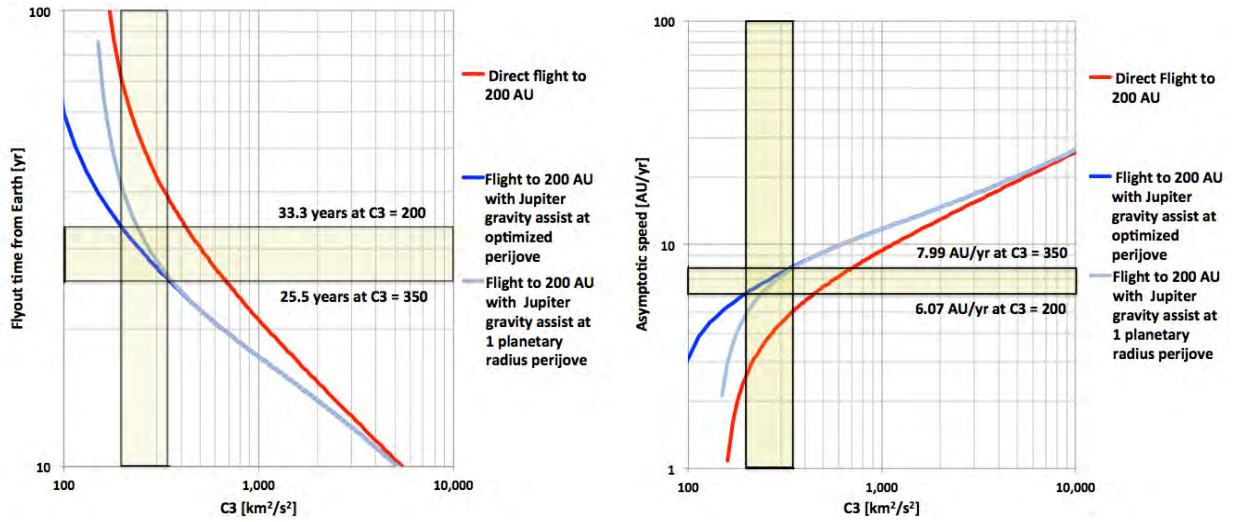

Figure 7-5. Calculations are based on the appendix of (Ralph L. McNutt, Jr. et al., 2014). (Left) Transit times from Earth launch to a heliocentric distance of 200 au using ballistic trajectories both with and without JGAs. The optimized solution targets a perijove such that the outgoing asymptote in the heliocentric frame is parallel to Jupiter's orbital velocity. An error in the optimized time calculation slightly underestimates the time for C_3 > ~225 km^2/s^2. (Right) Corresponding asymptotic speeds.

1. Its near-solar burn is a critical maneuver.
2. It cannot be tested in a "full-up" thermal and radiation environment.
3. It adds over three years up front to the mission (from launch to the Sun periapsis burn).
4. It requires thermal protection (for the rocket motor).
5. It increases the overall range of thermal requirements.

Even with all of these considerations, by far the most challenging issue—and an entirely separate topic—is dealing with these five items while also having a rocket stage (or stages) that can be built with today's or even near-term technology while satisfying whatever solar system escape speed requirement is imposed in equation 1 above. Put differently, if, for a given launch vehicle configuration, the optimized thermal shield/rocket-stage design can only provide a maximal performance such that the solar system escape speed is, at best, what can be provided by a passive JGA, then the Oberth maneuver can be ruled out as a viable technical approach because of the significant additional development and operational risks.

Hence, the most important issue to resolve in this study is precisely the viability of a solar Oberth maneuver because it will determine what can actually be accomplished with an all-ballistic approach. For reference, an asymptotic fly-out speed of 20 au/year using an optimized ("skimming the clouds") JGA would require a launch C_3 of ~4036 km^2/s^2 (an optimized Jupiter flyby is ~1.03 Jovian radii at a launch C_3 of ~476 km^2/s^2). For comparison, the fly-out speed of 20 au/year could also be provided using an Oberth maneuver with a ΔV of ~7.3 km/s at the edge of the photosphere (1 solar radius from the center of the Sun with a black body temperature of ~5780 K). Backing off

to 10 solar radii (closest approach to the Sun for the Parker Solar Probe) for the maneuver increases the required ΔV to ~23 km/s (estimated lower limit from equation 1). Such a requirement is, at best, well beyond current and near-term technology and, at worst, simply not achievable because of the physical and chemical properties of materials.

To set the scale, it is worth remembering that a speed of 1 au per (Julian) year is 4.740470461 km/s, and with 1 parsec (pc) = 206,264.806 au, at 20 au/year the distance to Proxima Centauri (4.246 light years or 1.302 pc) would be covered in some 13,428 years. This is at a speed of 94.81 km/s, at which one could cover the distance from Washington, DC, to New York City (328 km) in 3.46 seconds.

7.1.7. Are There Other Viable Approaches?

The short answer is no. Typically, this question is interpreted in terms of "low-thrust" or "in-space propulsion," which are different ways of expressing the same concept. These concepts break into "sails" and "electric propulsion."

The category of "sails" includes "solar sails" (using sunlight), "laser sails" (using illumination from a laser), "microwave sails" (using illumination from microwaves) (Forward, 1985), "radioisotope sails" (using asymmetric alpha-particle emission for propulsion) (Forward, 1996; Short & Sabin, 1959-60), and "electric sails" (Janhunen & Sandroos, 2007; Janhunen, 2008, 2014) or "magsails" (using wires to interact with the electric and magnetic fields in the solar wind) (Winglee, 1999). All of these suffer from structural support mass issues. General analysis could—and should—be done to rule out this class of purported "solutions."

The category of "electric propulsion" divides into three generally recognized thruster types—ion, Hall, and magnetoplasma dynamic (MPD)—and three types of electric power—nuclear fission, radioisotope, and solar (although some might argue nuclear fusion should be included, net energy gain from such systems remains to be demonstrated; in any case this is far-term technology and out of scope for this current effort (e.g., Bussard, 1990; Hilton et al., 1964; Hyde et al., 1972; Razin et al., 2014; Reinmann, 1971; Williams et al., 2001). Electric propulsion began its developmental history in the 1960s with the Space Electric Rocket Test I (SERT I—powered for ~1 hour with a battery). It was not "proven" in flight until the flight of the New Millennium Program Deep Space 1 (DS-1) mission to Comet Borrelly in 1998 (Rayman & Lehman, 1997; Rayman & Varghese, 2001). That flight paved the way for the subsequent NASA Discovery Program Dawn mission to Ceres and Vesta (Russell et al., 2004) and the European Space Agency (ESA) SMART-1 mission to the Moon. The other approaches have not fared so well. The first attempt at nuclear electric propulsion (NEP) was with the SNAPSHOT or SNAP-10A mission launched from Vandenberg Air Force Base (VAFB) on 3 April 1965; the ion propulsion part was secondary to the goal of running a reactor in space. An electrical malfunction led to the ejection of the neutron beryllium reflectors after 43 days of operation in space (Voss, 1984). The SP-100 program never came to fruition (*The SP-100 nuclear reactor program: Should it be continued?*, 1992), nor did the other nuclear engine concepts under Project Timberwind of the Strategic Defense Initiative (SDI). The subsequent Phase A study on

Project Prometheus for the Jupiter Icy Moons Orbiter (JIMO) identified technical issues for a robotic NEP spacecraft (Taylor, 2005), but the project was canceled, likely because of the projected multibillion dollar costs for retiring engineering uncertainties.

Radioisotope electric propulsion (REP) (Robert J. Noble, 1993; R. J. Noble, 1998, 1999) was considered for one of the NASA "Vision Mission" implementations of an interstellar probe (R. L. McNutt, Jr. et al., 2005), but the low-mass electric converters that enable the approach (have so far) failed to materialize.

Other thruster variants such as the Variable Specific Impulse Magnetoplasma Rocket (VASIMR) and the aforementioned MPD approach require significant electrical power (more than hundreds of kWe) that can only be achieved with nominal fission reactors of the Prometheus size or larger.

Given the structural issues with sails operating near a lightness number of unity, the cost and mass issues associated with NEP, and the high specific masses of REP, there are no near-term, viable, low-thrust propulsion options for a robotic interstellar probe.

7.1.8. What About Exotic Propulsion?

"Exotic propulsion" is terminology that is typically, but not always, used for types of "propulsion" that are based on physical principles but totally lacking in required technology development (Bruno et al., 2013) and demonstration. Some of many examples include, e.g., inertial confinement fusion (Hilton et al., 1964; Powell et al., 1973; Reinmann, 1971; Roth, 1961-62), muon catalyzed fusion, gas-core fission reactors (Grey, 1959; McLafferty, 1970a, 1970b; Moeckel, 1972; Ordway, 1970), and photon propulsion (Peschka, 1956; Sänger, 1961; Stuhlinger, 1959). Other proposed concepts are in apparent violation of known physics laws (e.g., "cold fusion") (Steinetz et al., 2020) or total violation of physics laws (e.g., the EM Drive) (White et al., 2016). The goal of the NASA Breakthrough Propulsion Physics Program (BPPP) was to uncover, but demonstrate the viability of, such concepts (M. G. Millis, 1999). The program cut a wide swath through many notional concepts (Marc G. Millis & Davis, 2009) but funding was shut down (in 2002) and the principals dispersed after documenting the funded program (~$1.2M) (Mark G. Millis, 2010; Wikipedia, 2020a). None of the identified concepts have moved to a state of even "promising" technology.

Previous "exotic" concepts have also been documented (Chew et al., 2001); all such efforts have had as their aim the identification of heretofore unknown means of implementing "fast" (equaling approximately within a human lifetime) interstellar travel.

7.1.9. The Conundrum of Human Interstellar Travel Remains

Speculations on the need for a way out of the solar system date to the beginning of the 20th century from Tsiolkovskii (Tsiolkovskiy, 1967) and Goddard (Goddard, 1983) (cf. section 11.1.2). After World War II, investigations began into the implications for special relativity for space travel in general (Ackeret, 1946, 1947) and interstellar travel in particular (Shepherd, 1952), with "atomic rockets" as the enabling technology (Shepherd & Cleaver, 1948a, 1948b, 1949). Considerations of the implications of power levels required to perform such missions (Peschka, 1956; Sänger, 1961)

had already led to an appreciation of the enormous technical difficulties such travel would impose (Purcell, 1963). The most eloquent exposition of the time used these features to argue for there being "general limits to space travel" (Sagan, 1963; von Hoerner, 1962) with the implication that to investigate the positive outcome possibility of "Fermi's paradox" (Jones, 1985), the human race should investigate communication with extraterrestrial intelligence (CETI) (Shklovskii & Sagan, 1968). That line of reasoning was rebranded as the search for extraterrestrial intelligence (SETI) (Tarter, 2001), which, it can be argued, now plays a large role in the *de facto raison d'être* of the accelerating field of exoplanet research.

With the only alternatives to "fast" interstellar travel being human—or robotic—"hibernation" or sufficiently large generational "world ships" (Asimov, 1966; Bernal, 1969), the initiative of an "Interstellar Probe" may look questionable to some. However, it is worth bearing in mind that even our voyages to the "nearby environs" of the solar system have already left an indelible mark on the human psyche and experience. Lao-Tzu is said to have remarked words to the effect that "a journey of a thousand miles begins with a single step" some 26 centuries ago. And there are examples of just that (on the Earth!), from Marco Polo's reported travel of 15,000 miles during 24 years (Wikipedia, 2020c) to Ibn Battuta's supposed journey of 75,000 miles during 29 years of travels across the world (Wikipedia, 2020b). Of course, Voyager 1 at almost 21 light hours from Earth after 43 years and 1 month of travel (as of October 2020), holds the current record for farthest distance traveled.

How far we will go in space—to echo Asimov's query of 52 years ago (Asimov, 1966) —is not clear, and will not be for some time to come. But that does not mean we should hesitate to take the first step. There is a universe waiting for us….

7.2. Maximizing Heliocentric Hyperbolic Escape Velocity: System Challenges

The three different architectures/considered in this study (sections 7.1.4–7.1.6; 7.2, and 11.5.3)—all hinging on a Jupiter flyby, and one with a close solar flyby—generally are recognized as the only ballistic alternatives (Jaffe et al., 1977).

The analysis of the passive Jupiter flyby scenario (Option 1) provides a baseline mission architecture that minimizes complexity. Although it does result in a fly-out speed that is significantly in excess of that of Voyager 1 (3.58 au/year = 17.00 km/s; cf. (Natha & Espinoza, 2020)), the speed for an "average" Jupiter flyby remains ~6–8 au/year for "typical" values of C_3 (200–350 km^2/s^2; Figure 7-5, right panel), which should be achievable with the SLS configurations being considered. Although some of the previous studies have noted significantly higher fly-out speeds (up to ~20 au/year), sections 4.3.2 and 4.3.3 discuss the potential value of slower fly-out speeds in terms of science data collection requirements.

This baseline also reveals important characteristics of the mission that apply to all three architectures under consideration, as discussed in the following subsections (7.2.1–7.2.3):

- The repetition of a maximum speed approximately every 13 months in sync with the relative motion of Earth and Jupiter

- Our ability to access any direction, in the plane of ecliptic, using Jupiter as a gravitational leverage point along the way
- Clear understanding of the duration of each launch window (around the local maxima on the curve)

This baseline also gives us minimum speeds to compare to in future iterations of this study as other mission requirements are added, such as targeting asymptotes that are out of plane with the ecliptic and variations of payload and, hence, separated spacecraft mass. For future analyses with trajectories that require flying out of the plane of the ecliptic, we will be able to compare the trade-off between achieving that targeted distance and the lower hyperbolic asymptotic escape velocity due to using some of the gravitational assist by Jupiter to accelerate upward (or downward) instead of simply speeding up. This analysis also reveals, through its comparison to the powered Jupiter assist, the answer to an old and important question: Where is the most advantageous place at a systems level to expend the mission's propellant to achieve a maximum escape speed?

We considered two identical systems. In one case (Option 1), every rocket stage is fired as part of an optimized launch sequence, targeting a passive Jupiter flyby. In the second case (Option 2), the final/uppermost kick stage is fired at Jupiter—hence, a powered JGA.

The result is not intuitively clear. In the first case, all the fuel is expended right away, close to Earth and much closer to the Sun, than in the second case. In the second case, a stack consisting of the separated spacecraft and the final stage, plus the adaptor between the two, supplementary heaters for the solid fuel in the upper stage, additional avionics as required, and other parasitic masses ends up on a slower trajectory to Jupiter before the final stage is ignited in the gravity well there. Hence, full-up self-consistent system designs are required for an "honest" comparison.

Our initial side-by-side analyses suggest that the powered Jupiter flyby provides an increased solar system asymptotic escape speed. However, this approach also requires a more complicated flight system and the additional requirement of long-term, in-space storage of a final kick stage, with a solid rocket motor, before use. Given initial projected capabilities of the SLS and a variety of upper stages (see also Figure 7-6 and Figure 7-7), pragmatic scenarios (i.e., based on existing flight hardware) are consistent with neither multiple solid stages nor liquid-propellant stages (including mono- and bipropellant) transported to Jupiter. These more complex solutions are ruled out by risk and the lack of a significant performance increase (cf., e.g., Ralph L. McNutt, Jr. and Vernon (2016)).

This trade is not merely of academic value. This result has profound programmatic impact. NASA, when considering this and future missions that require substantial launch and energy requirements as we explore our solar system and beyond, balances cost and risk against the value of each mission. These initial analyses suggest that by moving the firing time and position of one element in the system, effectively changing the system's complexity and therefore risk, a higher speed may be achieved. The cost and cost risk of development need further study, but the powered flyby appears to be superior if speed is the singular figure of merit.

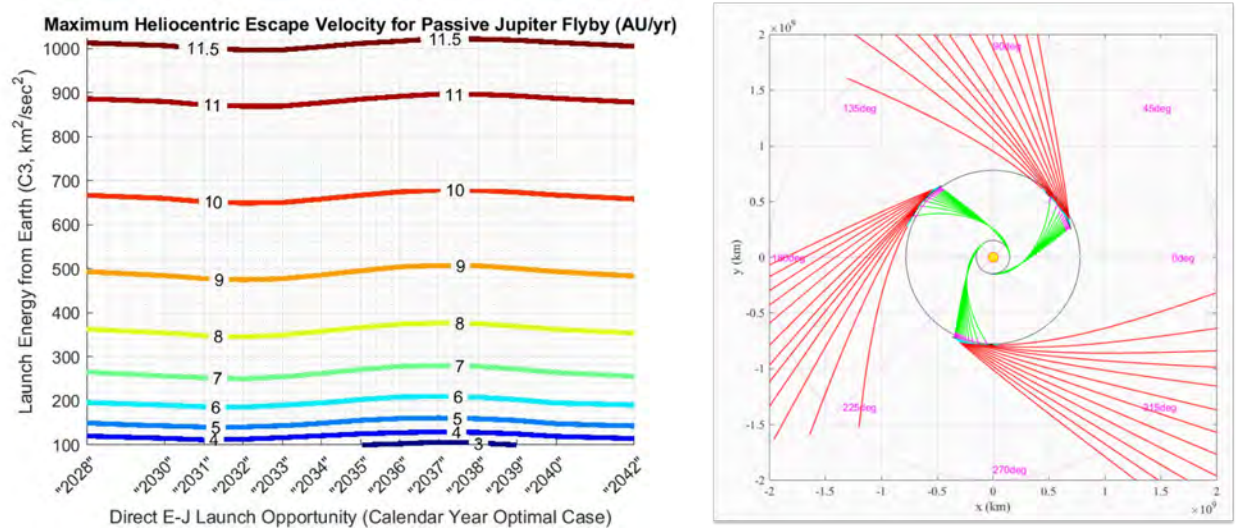

Figure 7-6. (Left) A passive JGA can achieve ~7 au/year with the simplest of systems and a launch C_3 of between 200 and 300 km²/s². (Right) Corresponding spread in distribution of fly-out directions as the C_3 is varied for three different fly-out windows. N.B. The years across the X-axis are listed in quotation marks ("...") because this pattern can be adjusted forward or backward in time by a sidereal Jupiter year (~11.86 Earth sidereal years), and the same pattern holds.

To explore these three mission architectures to characterize the balance among outbound speed, complexity, and mass, the payload mass was fixed at 60 kg, with a complete exploration spacecraft mass fixed at 487.3 kg, the (wet) mass of the New Horizons spacecraft at launch. Additional mass for kick stages and, where applicable, thermal control systems was added in addition to the 487.3-kg spacecraft mass. The fixed-mass spacecraft thus allows the three architectures to be compared initially across a range of launch years and outbound directions. More details of these comparisons follow.

7.2.1. Heliocentric Escape via Jupiter Passive Flyby (Option 1)

A direct method for solar system escape is to utilize the amount of Earth-escape launch energy along with the most opportune passage and acceleration assist provided by a Jupiter flyby trajectory. This study is focusing on launch opportunities within and around the decade of the 2030s; direct transfers with the shortest time of flight between Earth and Jupiter occur approximately every 13 months in the cycle of Jupiter's synodic period. With the objective of maximizing the heliocentric escape velocity of a spacecraft using a JGA, the best combinations of Earth launch energy and either passive or powered Jupiter flybys are analyzed over the period of interest. Figure 7-6 shows the variation of outbound speed across an entire Jupiter orbit as a function of launch C_3.

The most direct method for achieving a high-velocity escape from the solar system is to pair a maximized C_3 launch energy with a JGA. Our study focuses on launch opportunities beginning in

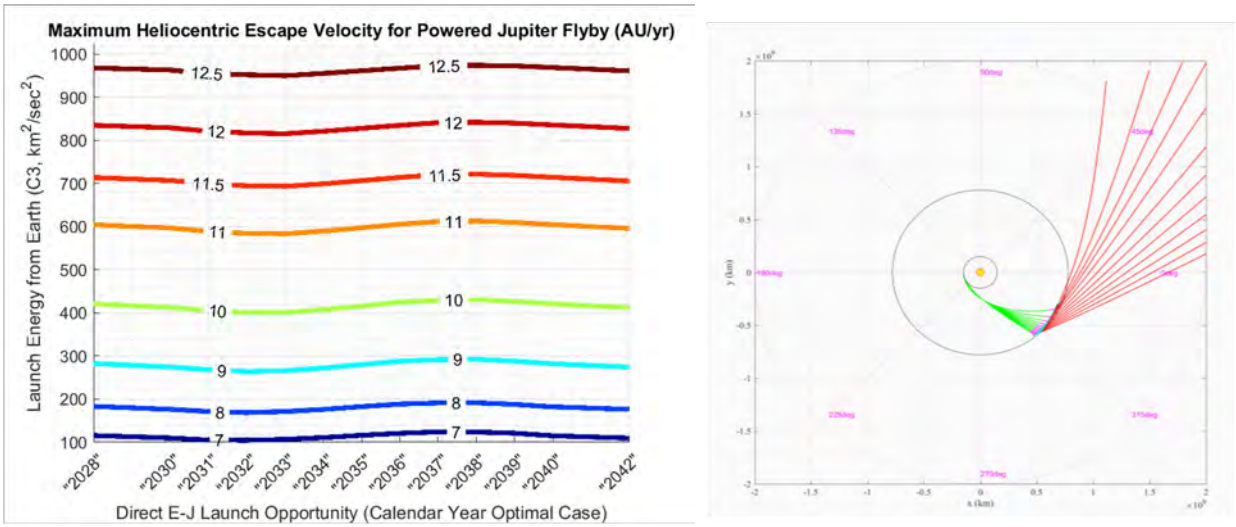

Figure 7-7. (Left) A powered JGA can, in principle, achieve ~9 au per year for conditions similar to those assumed for the passive JGA depicted in Figure 7-6. However, a consistent comparison requires correcting the available launch C_3 for the additional stage mass as well as other required mass increases associated with added guidance and control and thermal needs associated with getting the kick stage (here a Star 48BV) from Earth to Jupiter. (Right) Corresponding spread in trajectory directions associated with varying the launch C_3.

2030, optimized for short Earth-Jupiter transit times. The high C_3 requirement is met by minimizing spacecraft mass and optimizing the upper-stage configuration on NASA's SLS Block 2B. Analyses were performed on both passive Jupiter flybys and powered Jupiter flybys. These analyses deliver a solution space that can quickly adjust mission fly-out speeds for different launch vehicle configurations, by tying fly-out speed directly to launch C_3.

To consider the direct Earth-to-Jupiter transit opportunities in the time period of interest, an initial survey of patched-conic trajectories was performed between Earth and Jupiter by solving Lambert's problem. This leads to a derivation of the outgoing Earth departure energy and approach velocity conditions at Jupiter, with the assumptions of two-body mechanics (Figure 7-6).

7.2.2. Powered Jupiter Flyby (Option 2)

Increased heliocentric escape velocity can potentially be realized through a propulsive maneuver at Jupiter. The inclusion of the mass of the kick stage will increase the payload weight launched from Earth, reducing launch C_3 for a given launch configuration and reducing the incoming velocity at Jupiter. But analyses to date show that a perijove propulsive maneuver has greater positive impact on heliocentric escape velocity than the negative impact of the reduced launch C_3.

This analysis considered a number of existing, flight-proven kick stages (discussed below). The general criteria for kick-stage selection are relatively high performance with relatively low mass and overall volume that still fits in the launch vehicle payload fairing. A good example for analysis purposes is the solid rocket Star 48BV motor in a stage configuration, with relatively high specific impulse and high propellant mass fraction.

Similar to the passive flyby trajectory results above, the powered flyby trajectories progress from Earth to Jupiter on essentially the same type of transits. The departure launch energy is smaller for these trajectories given the addition of the kick-stage mass to the separated payload system weight (PSW). However, the same process is followed, parameterizing the launch-energy C_3 across a range of input values to produce variability curves for heliocentric escape velocity across a Jupiter orbit of the Sun. Because of the variation in imparted ΔV from the kick stage based on the payload mass, a series of results is created for the powered flyby trajectories based on a range of assumed payload mass sizes.

As with the passive Jupiter flyby cases, iterative trajectory calculations can be used to optimize the heliocentric escape velocity after the powered Jupiter flyby. In this analysis, the kick stage is fired impulsively at the periapse of the Jupiter flyby, and the imparted ΔV is based on the nominal stage performance characteristics and the given wet payload mass. An example of the performance using the Star 48BV kick-stage configuration is shown in Figure 7-7.

7.2.3. Solar Oberth Maneuver (Option 3)

The components and considerations discussed so far apply to the prograde Jupiter flyby Options 1 and 2. To consider Option 3, the Oberth maneuver, we first need to take up the subject of thermal shields—the thermal protection system (TPS)—and the associated mechanical mounting structure—the thermal structure assembly (TSA) —and the reality of taking a spacecraft very, very close to the Sun. Oberth pointed out in 1929 that the most rapid escape from the solar system could be effected by a powered spacecraft maneuver deep in the Sun's gravity well by a spacecraft that falls toward the Sun from a large distance (Oberth, 1970). A rough estimate of the effectiveness of such a maneuver can be estimated from conservation of energy by a spacecraft initially at infinite separation and negligibly small angular momentum as

$$V_{esc} \approx V_{esc,0} = (2V_{Sun}\,\Delta V)^{\frac{1}{2}} \left(\frac{R_S}{r_p}\right)^{\frac{1}{4}}$$

$$= 35.14\left(\Delta V\left[\frac{km}{s}\right]\right)^{\frac{1}{2}} \frac{\left(\frac{R_S}{r_p}\right)^{\frac{1}{4}} km}{s}$$

$$= 7.413\left(\Delta V\left[\frac{km}{s}\right]\right)^{1/2} \left(\frac{R_S}{r_p}\right)^{1/4} au/yr,$$

where r_p is the perihelion distance, R_S is the radius of the Sun, ΔV is the propulsive speed increment (applied at perihelion and in the direction of motion), V_{sun} = 617.6km/s is the escape speed from the visible "surface" of the Sun, and V_{esc} is the asymptotic escape speed from the Sun, with the subscript "0" denoting the approximate relation. See also section 11.1.3.

One problem (of several) is the need to shield appropriately both the spacecraft and the propulsion system from the thermal environment of the Sun, with the mass of any such shield increasing with decreasing distance to the Sun, as the distance to the Sun decreases and the finite solid angle

it subtends in the sky as viewed from the spacecraft assembly increases. To maximize the effect of the burn, it must be applied as close to perihelion as possible and at high thrust over a short (preferably minutes) period of time to minimize gravitational losses.

After many years of research and development, materials and concepts were developed (Potocki et al., 2006) to enable the Parker Solar Probe to approach a perihelion distance (from the center of the Sun) of 9.86 R_S. Given the specific impulse (I_{sp}) (Greenwood, 1975) of solid rocket fuel, a simple, solid kick stage might provide ~3 km/s for ΔV. At the eventual perihelion of Parker Solar Probe, this would provide $V \approx 7.25$ au/year, about twice the current escape speed of Voyager 1, the fastest object ever to leave the solar system.

The question is whether such a maneuver can be better exploited. Rough estimates suggest that for such a maneuver to be efficacious, the spacecraft perihelion must at least be as small as 5 R_S; as we shall show, perihelia less than ~3 R_S are problematic. Oberth had postulated a probe speed at perihelion of 500 km/s, a ΔV of 5 km/s, and a resulting exit from the solar system at 70.9 km/s or ~15 au/year. He noted the need to bring the craft "to the edge of the solar corona," and a perihelion speed of 500 km/s corresponds to a closest approach of ~1.5 R_S (R. L. McNutt et al., 2019).

This study included the analysis of several different configurations of spacecraft, kick stage, and thermal shield through this solar Oberth maneuver, using the form and initial mass (478.3 kg) of the New Horizons spacecraft as a starting point. The thermal shield, based on the Parker Solar Probe material and further analyses, was sized to protect the spacecraft and the kick stage across a range of perihelion distances and several kick stages (see Figure 7-14–Figure 7-17 in section 7.3.3).[3] The estimated mass of the shield was included in the overall performance estimate, and the results for these configurations are shown in Figure 7-8. A 4-solar-radii flyby of the Sun, firing a CASTOR 30XL engine, could apparently accelerate a New Horizons-scale spacecraft to >12.5 au/year. This speed can be achieved across an entire Jupiter orbit with small variation, giving the mission planners the opportunity to explore in whichever direction the science consensus leads.

However, one must carefully consider the aspects of all parts of the system. The three largest kick stages provide too massive a stack mass for the SLS to launch directly to Jupiter. The use of an Orion 50XL (or a Star 48GXV, not considered in this first iteration) may be possible from a mass viewpoint, but only for a New Horizons mass or less massive spacecraft, and this is still before a careful study of attitude control requirements during the burn.

[3] The Parker Solar Probe TPS is designed to withstand a temperature of 1400°C = 1673 K at a perihelion of 9.86 R_S. For a flat shield normal to the Sun direction, the temperature scales as the inverse square root of the perihelion distance from the Sun's center. Hence, that design would see a temperature of 4253 K or 3980°C and would not survive at that closer distance. Of the ultra-high-temperature ceramics, hafnium carbide (HfC) melts at 3958°C (Wikipedia, 2020d), and of the metals, tungsten melts at ~3400°C (EngineeringToolBox, 2005). Such investigations are also relevant to research into practical hypersonic flight (Cedillos-Barraza et al., 2016).

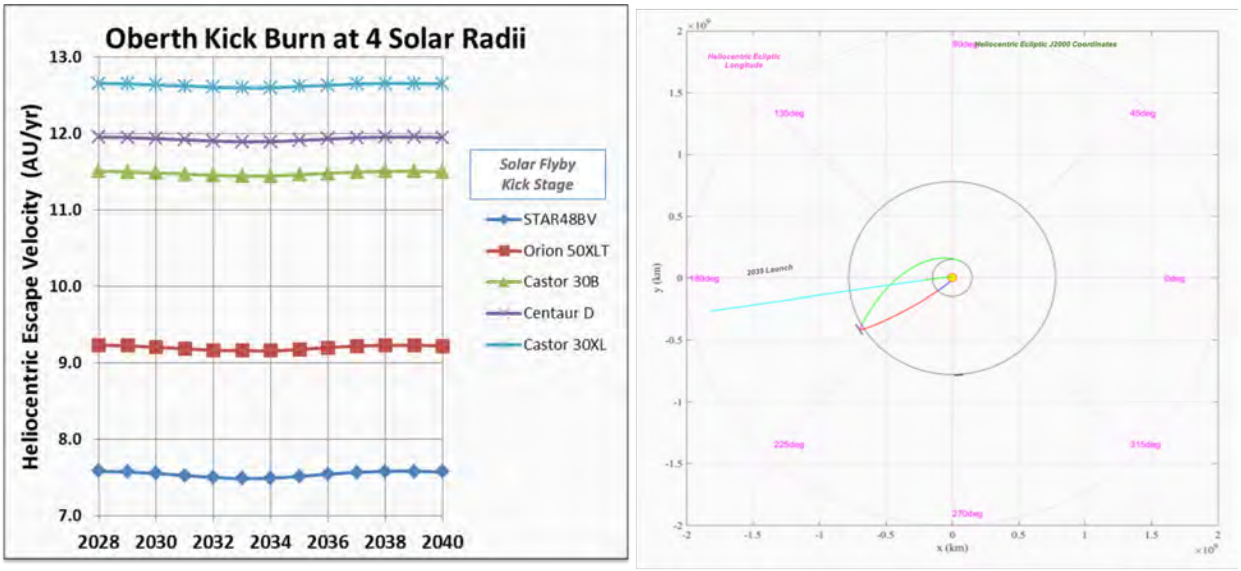

Figure 7-8. (Left) A powered-solar Oberth maneuver can, in principle, greatly accelerate the escape speed of a spacecraft from the solar system. The variation over the course of a Jupiter year is present but small. However, although these performance numbers take into account some initial mass estimates for the required thermal shield, they do not take into account the lift capability of the SLS. In particular, the apparently "best-performing" kick-stage cases are too heavy (even for the SLS!) to fly "Jupiter-direct" trajectories. (Right) A notional trajectory is shown here for a CASTOR 30XL kick stage. Note that while for the JGAs (passive and powered), the asymptotic fly-out direction is ~90° more in ecliptic longitude than the location of Jupiter at the gravity assist, the asymptotic fly-out longitude for the solar Oberth maneuver is toward an ecliptic longitude that is somewhat less than that of Jupiter for the precursor, and required, reverse JGA flyby. Hence, for a fixed ecliptic longitude "target," there is no "simple" switching back and forth of the selected architecture approach over the course of an ~12-year Jupiter orbit around the Sun.

A more detailed study of Option 3 possibilities is currently scheduled for a late-2020/early-2021 time frame once the spacecraft concept has matured past a New Horizons "model." Nonetheless, this first look has "set the stage" for more detailed consideration of its implementation issues.

7.3. Launch Configuration Trade Study

7.3.1. Engineering Ground Rules and Constraints

NASA's SLS is currently planned to serve as the heavy-lift vehicle for enabling humanity's return from low Earth orbit (LEO) to the surface of our Moon. However, its capacity for launching massive payloads is also enabling for very high-C_3 missions (Creech et al., 2019). The SLS Spacecraft/Payload Integration and Evolution Office (SPIE) at the Marshall Space Flight Center (MSFC) analyzed multiple upper-stage options mounted on the SLS Block 2 first and second stages. For the 2030s, the selected (appropriate) configuration studied was the SLS Block 2 (Figure 7-9).[4] A number of

[4] At the beginning of this study, the designation of the baseline configuration tested was designated SLS Block 1B+ (B1B+). With a launch aim-point of no earlier than 2030, the Block 1B was envisioned to be extended via an upgrade

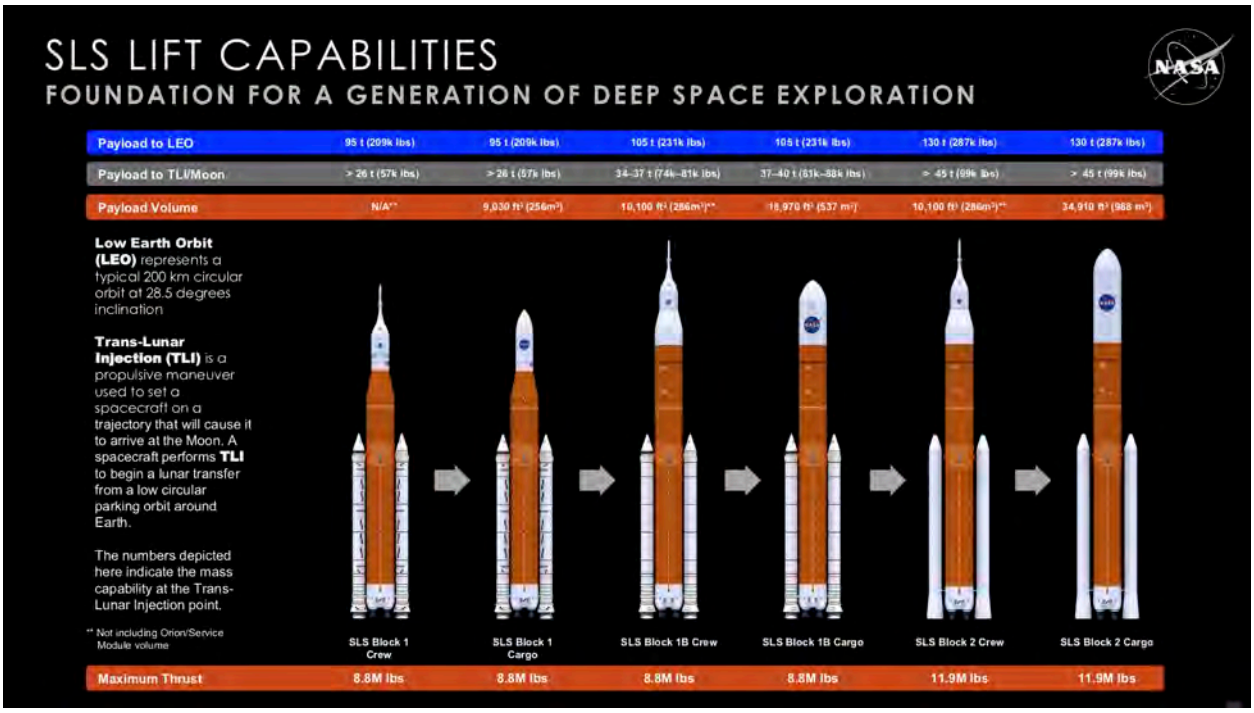

Figure 7-9. Multiple SLS variants were explored (Creech, 2019; Creech et al., 2019).

existing in-space propulsion systems were considered as third and fourth stages, firing in sequence as the spacecraft departed Earth. Initial estimates before the current study showed a considerably high C_3 could be achieved with SLS (Ralph L. McNutt, Jr. et al., 2014; Ralph L. McNutt, Jr., Benson, et al., 2015). At the beginning of the current study, as the analysis effort shifted to MSFC and the SLS design matured, the trend indicated by the initial calculations was confirmed.

The curves in Figure 7-10 show the initially calculated C_3 capability of SLS by MSFC with various upper stages across a range of spacecraft masses (performance data have been provided incrementally by the SLS program). The initial performance data, shown here, are from September 2018. Performance for this current study was finalized in December 2019 (Stough et al., 2019).[5] The SLS

of the solid boosters called the Booster Obsolescence Life Extension (BOLE). As the SLS design has matured, it became apparent that this configuration would already have the performance originally denoted by the designation "Block 2" (B2). Thus, by the end of 2019, the designation B1B+ had been replaced by B2. Hence, there has been an evolution of the notation over the initial course of this study conducted in conjunction with MSFC.

[5] After informal conversations in late July 2017 and at the subsequent International Astronautical Congress (IAC) in Adelaide, Australia, contacts were renewed with personnel at MSFC in mid-2018 after the initiation of funding on this project. MSFC made available some initial scoping runs ("v6") on 21 August 2018. A series of technical interchange meetings led to various iterations in parallel with evolution of SLS plans and predicted performance at MSFC. "v7" was made available on 7 September 2018 (including a new Manager's Reserve strategy); "v7.1" was made available (providing some corrections) on 14 September 2018; "v8," including a variety of baseline updates (as the SLS design performance evolved), was made available almost a year later on 22 August 2019; "v10" with most of the other requested configurations (Centaur D with fourth-stage runs still to be computed) was made available on 15 November 2019; and "v11," including the Centaur D runs, was made available on 19 November 2019. An updated supplement

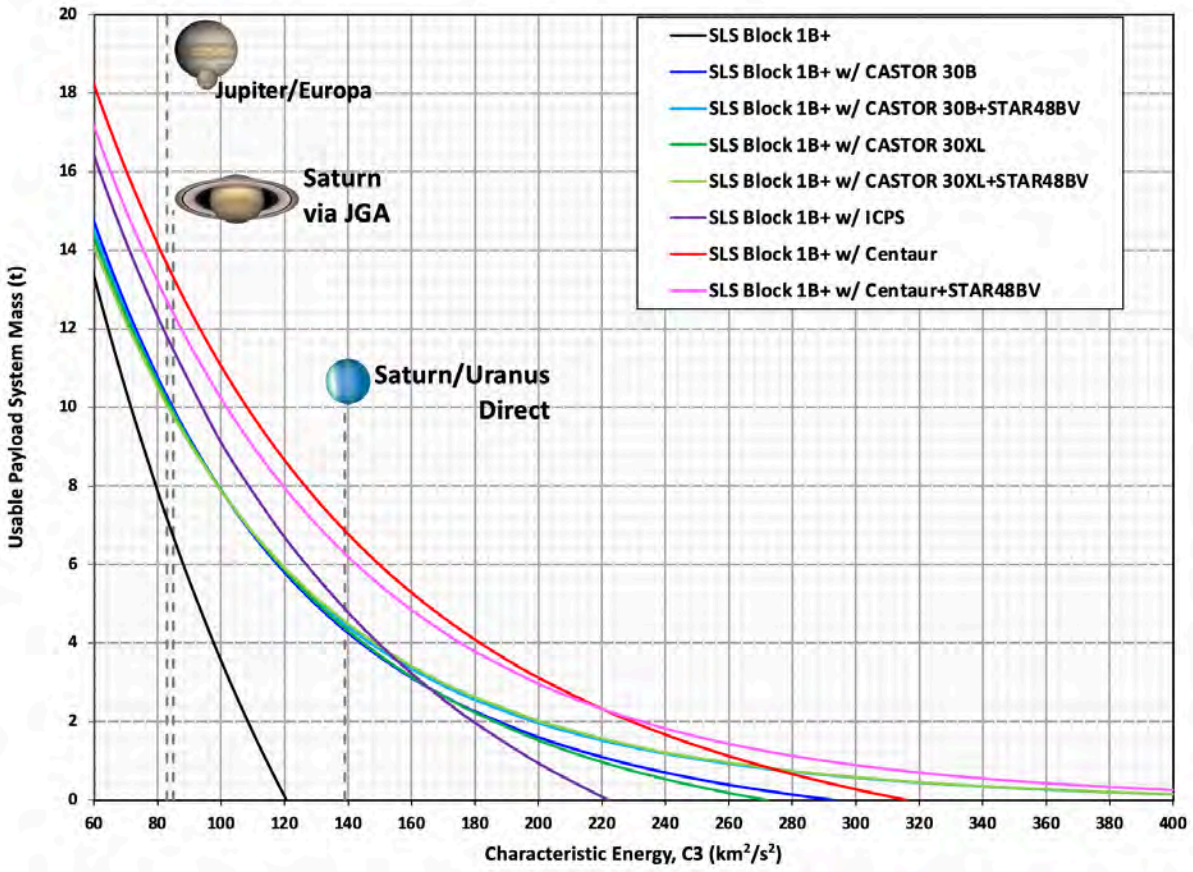

Figure 7-10. Initial calculated performance of the then SLS Block 1B+ launch vehicle by MSFC with an initial assortment of upper stages made in September 2018, soon after the start of the current effort.

program quotes vehicle performance relative to simulated trajectories using detailed models, low-performing vehicle characteristics, and manager's performance margin being withheld to ensure the quoted performance is achievable. New Horizons, at a C_3 of 157.7501 km^2/s^2 and a spacecraft mass of 478.3 kg, had the fastest Earth-escape velocity of any mission to date (Guo & Farquhar, 2008).[6] Had New Horizons been launched on SLS, characteristic energies >280 km^2/s^2 would have been achievable. This large energy is enabling for a mission to the interstellar medium.

for the information summary was received on 4 December (dated 3 December) 2019 at about the time of the fall 2019 meeting of the American Geophysical Union (AGU). 3 December materials were made available for public release on 30 June 2020. 1B BOLE (Booster Obsolescence Life Extension program), previously also known as Block 1B+, is now formally renamed as Block 2 in light of new, upgraded performance metrics (as the design performance has evolved). The performance curves of Figure 7-10 are from "v6," and those of Figure 7-6 and Figure 7-7 made use of calculations provided by personnel at Kennedy Space Center in July 2016, before this current (and funded) effort.

[6] With the possible—and disputed—exception (if one wants to call it a "mission") of the "manhole cover" (reportedly ~900 kg) used in the Pascal B nuclear weapons test of Operation Plumbob at the Nevada Test Site (NTS) on 27 August 1957. The estimated speed at the surface was five to six times Earth escape speed (i.e., ~60 km/s) (Brownlee, 2002; Hall, 2018; Harrington, 2016).The test is reportedly one of the motivations for the full-up investigation of nuclear-pulse propulsion (Dyson, 2002).

The basic exercise of stacking various stages and computing the relative velocities achieved for a range of various spacecraft-separated mass values, using the standard rocket equation, has been performed numerous times for decades. The earliest analyses (e.g., Boelter et al., 1959; Coleman, 1961; Goldsmith, 1957; Malina & Summerfield, 1947) focused on optimization of stages in general. With the rapid development of the astronautics industry, fairly standard stages have been developed, which can, in turn, be called on to approximate optimal performance. Truly "optimized" custom stages are, in general, not practical because of the costs of design, fabrication, and verification for "one-off" applications. There are, nonetheless, a wide, albeit finite, number of stage designs from which to choose (Ralph L. McNutt, Jr. & Vernon, 2016). Energy-based solutions are often applied for these studies, yielding order-of-magnitude solutions very quickly. These approaches often lend themselves to "spreadsheet"-based solutions with one to a very few trajectories assumed. Unfortunately, mission integration and flight experience gained on APL's very-high-characteristic-energy missions (New Horizons and Parker Solar Probe, with launch C_3s of 157.7501 km^2/s^2 (Guo & Farquhar, 2008) and 152.42 km^2/s^2, respectively) has demonstrated that this unique class of very-high-launch-energy missions is extremely sensitive to the effects of parasitic masses as well as their physical locations on the launch stack for these systems. This Interstellar Probe study has considered these parasitic mass impacts specifically related to the subsystems required to achieve very-high-launch-energy missions. Irrespective of trajectories and other orbit-related studies, this Interstellar Probe study has applied several "engineering-based" ground rules to the launch stack configurations considered. The general engineering ground rules applied are summarized in Table 7-1.

Table 7-1. Motor/Stage Ground Rules

#	Characteristic	Ground Rules	Exceptions
1	Motor or Stage Production Status	Motors and/or stage systems shall be in current production and/or funded for development for a first flight in the 2020s time frame.	Shuttle/Centaur exempted from production status
2	Propulsion System Technology Maturity Level	The Interstellar Probe study shall limit propulsion system technologies to systems currently in production and/or funded for a first flight in the 2020s time frame.	No exceptions identified
3	Fairing Volumetric Constraints	The configurations studied shall be volumetrically limited to the SLS 62-foot design.	No exceptions identified
4	Adaptors and Separation Systems	Interstellar Probe shall identify and provide mass allocations/estimates for all required adaptors and separation systems for each configuration studied.	No exceptions identified
5	Avionics, Harness, Guidance and Control Systems	Interstellar Probe shall identify and provide mass allocations/estimates for avionics, harness, and guidance and control systems for each configuration studied.	No exceptions identified
6	Special Cooling Systems, Thermal Shields, etc.	Interstellar Probe shall identify and provide mass estimates where thermal shields or special cooling systems are required for each configuration.	No exceptions identified
7	Spacecraft Separated Mass and Volume Constraints	The Interstellar Probe study shall assume the final, spacecraft separated mass will be 478 kg and volumetrically similar to the New Horizons spacecraft.	No exceptions identified

7.3.2. The Ground Rules

Several of the ground rules applied were designed to ensure the study considered basic engineering principles deemed critically necessary for very-high-launch-energy, stacked, launch-vehicle-performance estimates. To limit the scope of the study and still produce results that could be easily compared against one another, the constraints of Table 7-1 were applied. The rationales applied are as follows:

1. For Ground Rules #1 and #2, the study intentionally limited the systems studied and the propulsion technologies considered to systems and components currently in production or funded with emerging first flights (currently) planned in the 2020s.

2. Ground Rule #3, the fairing volume and physical size constraint, was applied to set an upper limit to ensure that the configurations are achievable in practice with current facilities and plans. Other fairings may be possible, but this constraint ensures an architecture will close.

3. Launch system engineering experience gained with the development of launch systems for NASA's New Horizons and Parker Solar Probe missions has demonstrated that one must also recognize and allocate mass and physical locations on the stack for mission-unique systems and/or hardware required by one particular trajectory versus another, as noted in Ground Rules #4, #5, and #6.

4. Ground Rule #7 (spacecraft physical size) was set as a constant to normalize the C_3 and/or ΔV results across the 31 launch system stack configurations studied.

7.3.3. Launch System Engineering and Staging and the Methodology Applied

Fairly reliable and consistent data are often readily available for most, if not all, solid rocket motors and solid-motor stage systems currently in production. For example, manufacturers of solid motors that have flown or have been ground tested usually will advertise the most basic information for inclusion in performance studies. Values for specific impulse (I_{sp}) and loaded and dry mass (kilograms) are generally available for motors when considered as components versus systems or stage systems. Corresponding liquid-stage data were more challenging to find to identify critical values needed to perform performance estimates. There are a variety of reasons for this, including protection of proprietary data, differing fuel loads used for various missions and trajectories, mission-unique modifications used, cryogenic depletion rates, as well as many other interrelated dependencies. The "laundry list" of very-high-launch-energy missions, specifically where the liquid upper stages are pressed to their performance limits, is actually quite small in practice. Thus, a systems engineering approach is required to ensure the launch-energy estimates produced are not overly optimistic and remain achievable with current technology as defined within the constraints of the ground rules applied. Furthermore, emerging systems such as the United Launch Alliance (ULA) Advanced Cryogenic Evolved Stage (ACES), the Blue Origin two- or three-stage vehicle, the ULA Centaur V, and the European Service Module (Orion propulsion module) are still in development, and securing reliable values can be problematic, with significant margin holdbacks assumed until the first flights are completed. Many funded emerging systems and their respective

performance values for "stand-alone" systems are usually reluctantly offered and manufacturers of "systems" prefer to deliver the "package" versus the individual component performance parameters. All of these issues are to be expected and simply reflect market (and marketing) realities. Nonetheless, this Interstellar Probe study effort has been able to secure the required performance values from almost all manufacturers.

7.3.3.1. Ground Rules #1 and #2

Table 7-2 provides a summary of the stages studied to date. Hence, these stages along with the SLS Block 1B and Block 2 follow from the application of Ground Rule #1 and Ground Rule #2.

Table 7-2. Stage and Motor Systems Considered

#	Stage/Motor	Type	Propellant	Current Production Status	Manufacturer
1	Star 48BV	Solid Motor	Solid	In production	Northrop Grumman
2	Star 48 GXV	Solid Motor	Solid	Completed one successful static fire test	Northrop Grumman
3	Orion 50 XL	Solid Motor	Solid	In production	Northrop Grumman
4	CASTOR 30B	Solid Motor	Solid	In production	Northrop Grumman
5	CASTOR 30XL	Solid Motor	Solid	In production	Northrop Grumman
6	Centaur D (Shuttle/ Centaur)	Liquid Stage	LH_2/LO_2	Engineering development model components produced	United Launch Alliance
7	ACES	Liquid Stage	LH_2/LO_2	In development	United Launch Alliance
8	Atlas V/Centaur 3	Liquid Stage	LH_2/LO_2	In production	United Launch Alliance
9	ICPS (SLS)	Liquid Stage	LH_2/LO_2	In production	United Launch Alliance
10	Vulcan/Centaur V	Liquid Stage	LH_2/LO_2	In development	United Launch Alliance
11	European Service Module (Orion)	Liquid Stage	MON/MMH	Awaiting first flight	Airbus

Launch vehicle systems considered to date (cutoff of 30 September 2019) in the study are listed in Table 7-3.

Table 7-3. "Core" Launch Vehicle Systems Considered

Identifier	# Stages	Current Production Status	Manufacturer
Space Launch System (SLS) Block 1B	2	In development	NASA
New Glenn	2	In development	Blue Origin
New Glenn	3	In development	Blue Origin
Delta IV Heavy	2	In production	United Launch Alliance
Falcon Heavy	2	In production	SpaceX

A ground rule, not specifically identified and labeled as such, but "derived" from the "*realistic and achievable*" theme of the study, was to also consider the launch services acquisition cycle for high-value-science flagship-class missions as part of our study constraints applied. Not only should a candidate launch vehicle and stage "system" be advertised and believed to exist by a certain date, but one simply must be able to procure such a system as well to meet NASA standards for a reasonable number of successful flights and other constraints applied. The 30- to 36-month launch service acquisition and/or build cycle typically applied to NASA spacecraft development projects

was applied to "realistic solutions" for the selection of various propulsion technologies studied.[7] Thus, nuclear rockets, solar sails, laser propulsion, "warp drives," and other exotic systems were not considered because they were "out of scope" for the time frame under consideration. The NASA SLS Block 1B system development and current manifest and funding schedule, coupled to its advertised launch-energy performance and volumetric fairing availability, appear to have met these criteria for now with a manifest and target dates funded and mandated by Congress.

7.3.3.2. Ground Rule #7

Proceeding to explain the application of Ground Rule #7 (out of chronological order of the ground rules applied), this rule (spacecraft-separated mass value) is a significant study-controlling rule whose application flows into staff hours and costs for a real flight system, and thus is discussed first. This rule was applied to all launch vehicle systems studied.[8] We note the rationale for selecting a *single, spacecraft-separated mass* value to study is significant. Performance analyses performed in previous Parker Solar Probe and New Horizons studies for these very-high-launch-energy missions have demonstrated that there are very clear "sweet spots" for stage stacking. These "sweet spots" are typically neither obvious nor intuitive. To achieve consistent and easily understood results across an almost infinite combination of trajectories and stack configurations, the study team concluded that by holding a fixed, spacecraft-separated mass across this initial study, the results developed would be consistent and could be understood easily and compared with a minimal number of caveats. The team assumed that one single stack combination and/or a family of solutions would then emerge, and the team then would be well prepared to vary other parameters such as spacecraft-separated mass, or to tailor solutions based on the conditions presented at a later date. With the separated-spacecraft mass target value set to ~500 kg, preliminary Earth-escape missions were first examined for the current vehicles that are in production.

Quick looks at the two largest domestic vehicles currently existing, the Delta IV Heavy and the Falcon Heavy, yielded only incremental increases in predicted C_3 for the notional Interstellar Probe spacecraft mass and mission, as compared with that of Parker Solar Probe, which achieved a C_3 of 152.42 km^2/s^2 and used a Star 48BV "kick stage" (entry 1 of Table 7-2). When studied, these two candidate vehicles simply did not offer solutions that were sufficiently energetic to satisfy a desirable C_3 launch-energy requirement of no less than 300–400 km^2/s^2, which, averaged over a Jupiter sidereal year, corresponds to asymptotic escape speeds from the Sun of ~7.4 to ~8.4 au/year for a passive JGA (Option 1). Figure 7-11 depicts the NASA National Launch Service II (NLS-II) performance curves currently advertised (30 September 2019) for the Heavy vehicles in that database (Atlas, Falcon Heavy, and Delta IV Heavy).

This study leveraged early Parker Solar Probe stacking studies that demonstrated that the Star 48BV upper stage is the most efficient very-high-launch-energy choice in this range of separated spacecraft masses and these available launch vehicles. For reference, Parker Solar Probe

[7] We note that the recent report on the SLS from the Office of the Inspector General (NASA) notes a 50-month current procurement cycle for the SLS "core" stage (Martin, 2018).
[8] The rationale for arriving at the mass bogy value of ~500 kg is explained elsewhere.

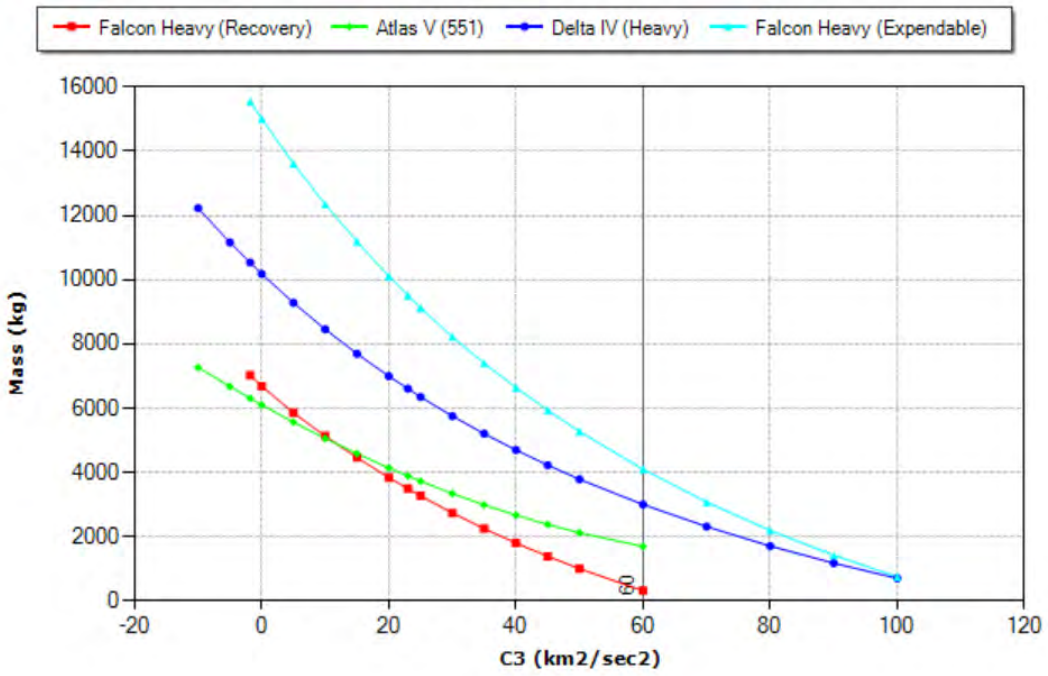

Figure 7-11. Performance comparisons for the "heavy" U.S. launch vehicles currently (as of 30 September 2019) in production. Note all curves depict only two-stage performance, and all will show better performance with additional upper stages. However, such additions will not affect the trends significantly. For high C_3 (>100 km^2/s^2) performance, the Delta IV Heavy and its all-LOX/LH_2 stages outperforms all other vehicles. The cut in Falcon Heavy performance for the "recovery" versus "expendable" mode is also clearly apparent.

advertised a not-to-exceed (NTE) spacecraft-separated design mass of 675 kg with a launch-energy requirement set at 154 km^2/s^2. After a brief review of Delta and Falcon Heavy vehicles, the Interstellar Probe study team quickly recognized that the significant SLS launch mass capability could be expected to provide some interesting options to explore. With its tremendous projected lift capability, the SLS Block 1B provided significant opportunities to incorporate stages/motors above and beyond Falcon and Delta IV Heavy vehicles. The capability potentially could achieve launch energies in the >300 km^2/s^2 range. Although the actual performance estimates will be discussed later, Figure 7-12 and Figure 7-13 depict several crude, quick-look comparisons that surfaced very early in these considerations (July 2016). Although lacking in precision, these preliminary estimates clearly justified the decision to involve MSFC and investigate the SLS as a priority over the other existing core vehicle systems available. It should be noted that these analyses were performed several years ago while the SLS performance characteristics were still evolving. As a result, the detailed numbers achievable with the current design will differ from those depicted here. However, the relative performance of the various staging approaches remains a good indicator of what could be achieved.

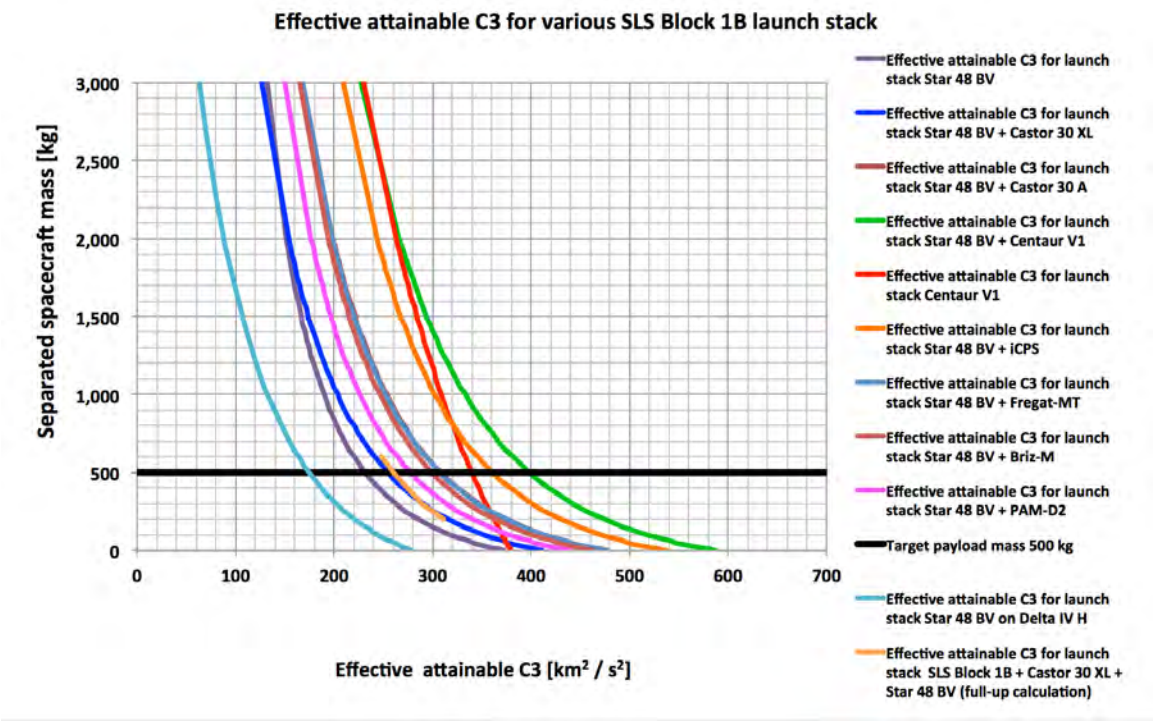

Figure 7-12. Preliminary launch-energy estimate curves. The black horizontal line indicates a separated spacecraft mass of 500 kg.

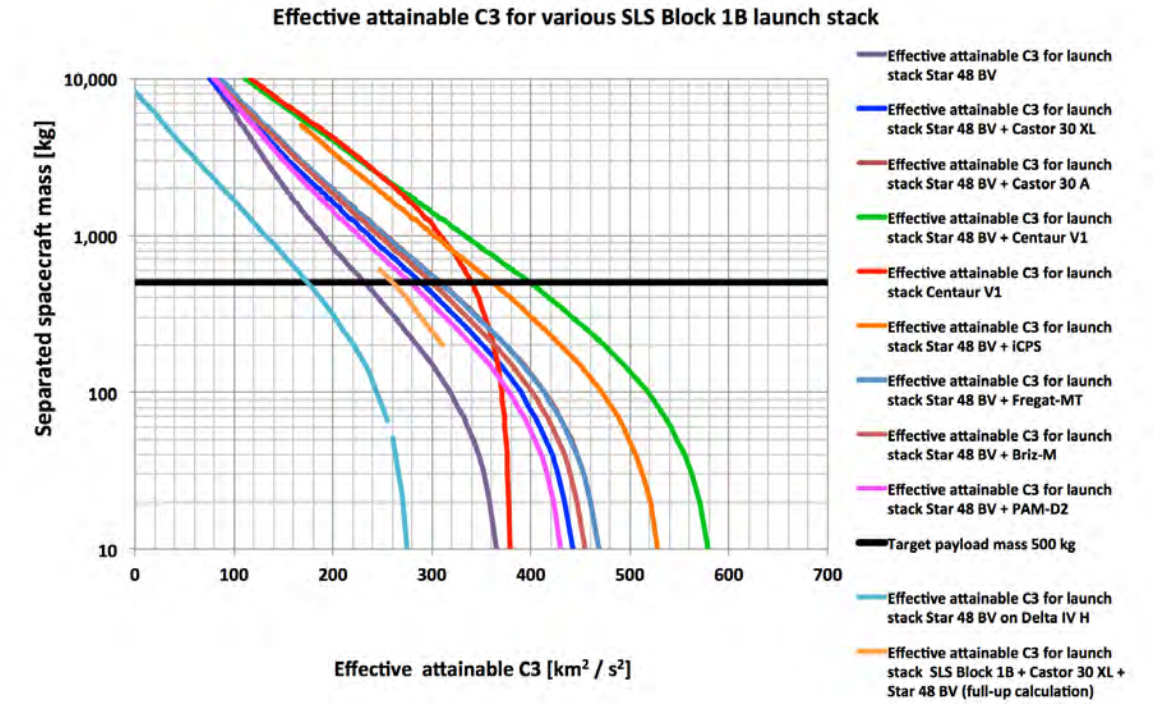

Figure 7-13. Same data as in Figure 7-12 but plotted on a semilog scale. This presentation provides better visual performance trending for the high C_3s available near the various performance cutoffs.

The least-effective performance in these calculations is for a Star 48BV on a Delta IV Heavy (aqua curve to the far left). All other launch stack configurations were based on performance numbers for the SLS Block 1B as available at the time from NASA's Launch Services Program in July 2016 using a simplified set of calculations. (Subsequent data obtained directly from the SLS program are of higher fidelity.) The next best performance is for a Star 48BV only. The red curve is for a Centaur V1 on an SLS Block 1B only; all other complete curves are based on the same simplified algorithms assuming an SLS Block 1B plus an intermediate third stage, plus a Star 48BV fourth stage (to which the final spacecraft is attached). Increasing performance (shift of the basic curve to the left) is provided by using the following for the intermediate (third) stage, in increasing order of performance: (1) PAM-D2 (stage for geosynchronous transfer orbit [GTO] from Shuttle cargo based on Star 63D motor); (2) CASTOR 30XL; (3) Briz-M (Russian liquid upper stage for Proton manufactured by Khrunichev State Research and Production Space Center; the S5.98M engine has a specific impulse of 326 seconds using nitrogen tetroxide [NTO] and unsymmetrical dimethyl hydrazine [UMDH] (Wikipedia, 2018a)); (4) Fregat-MT (Russian liquid upper stage for Soyuz manufactured by NPO Lavochkin; the S5.92 engine has a specific impulse of 333.2 seconds using NTO and UDMH) (Wikipedia, 2018b); (5) ICPS ("standard" second stage for the SLS Block 1); and (6) Centaur V1 (single-engine, second-stage variant for the Atlas V). Comparison of the red and green curves shows how the performance of a Centaur third stage is "stretched" by the inclusion of a Star 48BV fourth stage. The partial orange curve shows the decrease in performance with the CASTOR 30XL indicated by a more detailed calculation (compare with blue curve). Note that the "break" in the exponential decay of capability occurs once the payload mass is about the burnout mass of the top powered stage. The various stage combinations discussed are to illustrate technical trades only; actual implementation of some of the combinations, especially from non-U.S. vendors, might not prove possible for nontechnical reasons.

In general, it is worth noting that the quasi-exponentially decaying trendline indicates the upper envelope of what might be obtained by increasing the number of stages in an optimized fashion.

As noted, the methodology applied to the stacking of stages must ensure that particular attention is paid to parasitic mass impacts on performance. Basically, assembling an optimized stage stack combination with existing flight-proven (or nearly so) hardware is a "Goldilocks problem": the technical characteristics must be "just right" while adhering as closely as possible to existing, and preferably flight-proven, hardware, to minimize project cost.

7.3.3.3. Ground Rule #3

Returning to the original order of the ground rules, Ground Rule #3 led to the SLS 8.4-m, short (8.4-m-diameter, 19.1-m-long) fairing. This choice intentionally limits the volume space for stacking and thus sets an upper "physical" limit on stage choices. The choice of this particular fairing (and accompanying ground rule) was recommended by MSFC staff to ensure compatibility with (1) the SLS planned ground processing and (2) the currently available NASA payload processing facilities at the NASA Kennedy Space Center (KSC) launch site. The selection of the SLS Block 1B 8.4-m short fairing with 62.7-foot (19.1-m) fairing length is dictated by the overhead crane hook height available in the processing facilities at KSC. Corresponding mechanical layouts are shown

below after introducing more of the "ground rule" constraints. (Alternative approaches may be available by time of flight, but this ground rule ensures approach availability at time of flight.)

One of the most significant differences between this approach to Interstellar Probe and other NASA scientific spacecraft is the addition of multiple kick stages required to accommodate a rapid escape from the Sun's gravity field. Although the approach has been to pursue existing or near-existing stages, the implementation requires more attention to be paid up front to staging considerations than is typical on robotic, scientific missions.

The exercise of stacking stages as applied to this study included performing representative mechanical layouts of each of the configurations considered. Included in the exercise of performing these layouts was the identification of the "available" volume space for the candidate spacecraft, associated stages, and other hardware.

As a starting point, the candidate spacecraft was taken to be New Horizons. An actual spacecraft is the subject of future design and optimization studies, of course, but with a wet mass of ~500 kg as per the initial scoping studies (New Horizons had a wet mass at launch of 478.3 kg), a radioisotope power supply (New Horizons used the F-8 general-purpose heat source [GPHS] radioisotope thermoelectric generator [RTG] (Bennett et al., 2006; Cockfield, 2006)), a 2.1-m-diameter high-gain antenna (HGA), and structural integrity to comply with the loads from a Star 48B kick stage, New Horizons provided a good initial "model" for the spacecraft. As with Parker Solar Probe, the use of New Horizons as a "model" enabled leveraging of the flight drawings and derivative flight experience available at APL (Fountain et al., 2008). The available payload volume was derived from each configuration studied; the layouts included the representative adaptors and separation systems. Configurations that did not allow sufficient volume or height to accommodate a "New Horizons"-class spacecraft and payload were eliminated from the trade space. Actual accommodation of a payload will, of course, follow from future studies by a Science Definition Team (SDT) should a decision be made to pursue a particular strawman payload. However, New Horizons was again seen as a good, conservative starting place because the payload fractions for deep-space spacecraft are all relatively the same, and the "1-W/kg" rule for scientific instruments also tends to be a good starting point for scoping studies (R. L. McNutt, 2010).

7.3.3.4. Ground Rule #4

Engineering Ground Rule #4 requires allocations to be generated for all staging system adaptors and separation systems. The project elected to take several paths to produce these estimates for the various configurations. In most cases, these hardware systems did not exist, yet a realistic and achievable goal for mass was required. NASA SLS employed the Advanced Concepts Office (ACO) to generate estimated masses for the stage adaptors interfacing various upper stages. The adaptors are sized assuming a maximum payload on top of the last stage of 10 metric tons (mt) such that the analysis was simplified. The adaptors consist of two interface rings with composite face sheets and an aluminum honeycomb core. The composite structure sizing is consistent with NASA CR-1457 (Sullins et al., 1969) and NASA SP-8007 (Peterson et al., 1968). After the basic mass of each adaptor is estimated, 18% of mass growth allowance (MGA) is added. For other cases, for

which the adaptor/separation system existed, the existing systems were roughly evaluated for suitability (loads, interface features, etc.), and the allocations for mass were made. In several unique cases, for which sufficient data or tools did not exist, the adaptor/separation system mass value was developed by similarity and/or rules of thumb, dependent in all cases on the loads supported above the hardware systems.

7.3.3.5. Ground Rule #5

Referring to study Ground Rule #5, which refers to mass allocations for avionics, the associated wiring harness and avionics must be allocated and factored into the performance estimates. The methodology applied varied with the stacking. In cases in which the "final" or "upper stage" was a Star 48BV-based stage, the approach was based on the New Horizons and Parker Solar Probe experiences: an independent and separate "smart/guided stage" was a requirement to ensure injection accuracy and control were "in family" with high-C_3 missions. In cases of existing stage systems (Centaur, etc.), dry mass values carried mass set-asides for power, avionics, guidance and control (G&C), etc. These mass values were retained with the stage intact, in addition to the "upper stage" system. In cases in which a "solid motor" was devoid of "smart stage" components, the study added an avionics package mass allocation to the system where appropriate to control the stack.

7.3.3.6. Ground Rule #6

Ground Rule #6 required mass allocations to be produced and levied on performance estimates to identify mission-unique requirements primarily driven by a given trajectory. Two specific classes of parasitic mass allocations driven strictly by the trajectories chosen are the Oberth maneuver performed in close proximity to the Sun ("Option 3") and the powered solid motor firing near Jupiter ("Option 2"). For Option 3, thermal shield mass estimates were generated for each configuration studied and for each close approach to the Sun at closest passes of 3 R_S, 4 R_S, and 5 R_S. Figure 7-14–Figure 7-17 depict several physical configurations for shields that formed the geometric basis for the shield masses produced for these three cases and various kick stages. Note that each "stack" configuration and closest approach required a unique mass estimate to be produced to evaluate the mission-design performance.

Figure 7-14. Star 48BV stack with thermal shield for perihelia of 3 R_S (left), 4 R_S (center), and 5 R_S (right).

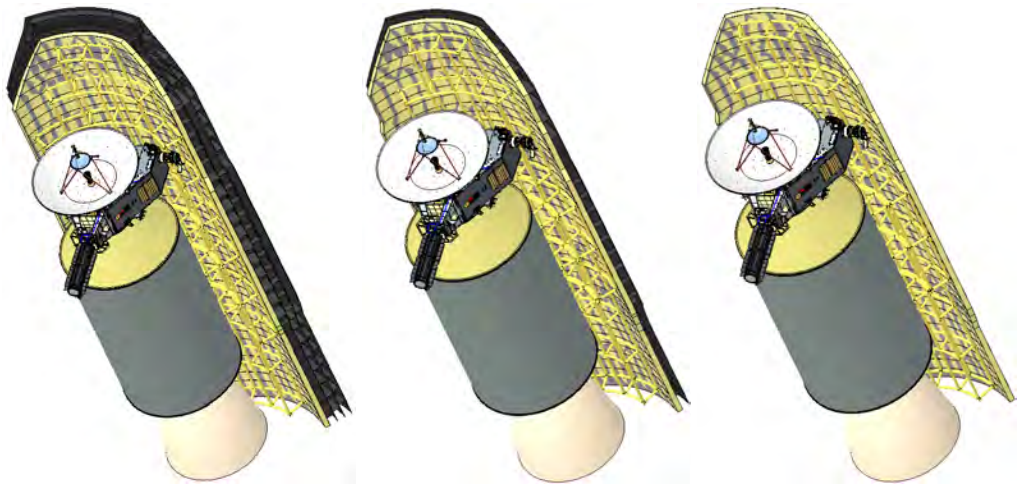

Figure 7-15. CASTOR 30XL stack with thermal shield for perihelia of 3 R_S (left), 4 R_S (center), and 5 R_S (right).

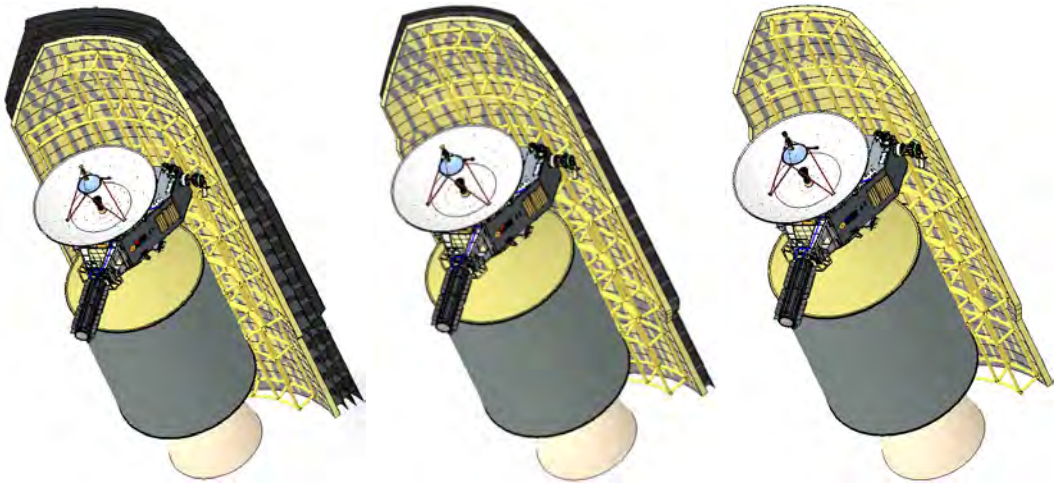

Figure 7-16. CASTOR 30B stack with thermal shield for perihelia of 3 R_S (left), 4 R_S (center), and 5 R_S (right).

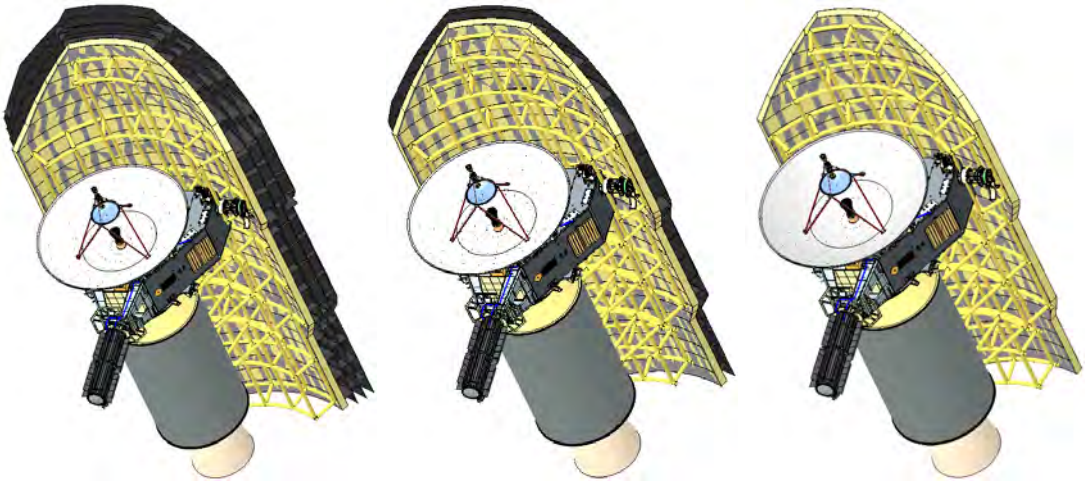

Figure 7-17. Orion 50XL stack with thermal shield for perihelia of 3 R_S (left), 4 R_S (center), and 5 R_S (right).

Several other trajectories analyzed suggested that a solid motor, carried during cruise and ignited well after launch in the vicinity of Jupiter, denoted as Option 2, offered interesting performance. In these cases, mass and power estimates were produced, based on Parker Solar Probe and Mars Science Laboratory (also known as Curiosity) hardware and systems, such that waste heat from the GPHS RTG would be harvested during cruise to provide a stable temperature environment for the solid motor up to the ignition point in the mission.

For a few of the selected trajectories studied, for which a solid motor is stored in space during the cruise phase before ignition, previous studies and solid-motor, long-term storage tests and evaluations (Hamlyn et al., 1991) have shown temperature control is required to ensure thermal cycles are minimized in both quantity and severity of the temperature swings. Additionally, studies and solid-motor flight experience have demonstrated that motor gradients should be minimal (2–3°C) in order to provide predictable performance.

7.3.4. Stage and Motor Technical Data Summary

Various sources were consulted (literature, vendor catalogs, etc.) to assemble a relevant database corresponding to the stage and motor systems listed in Table 7-2. This provided a basis for evaluating volume constraints, calculating thermal protection shield envelopes for the "Option 3" configuration, and evaluating stack-system performance. While numbers for systems in production are readily available, values for many of the parameters of systems in development are estimates or not available due to proprietary concerns.

7.3.5. Summary of Launch Vehicle Configurations Studied

Building on the mission-design options and the various staging possibilities, we identified 31 launch system configurations for further evaluation and potential further consideration as potential spacecraft detailed designs deviate from the New Horizons characteristics assumed for this initial baseline study.[9] Each configuration studied was assigned a unique configuration number and configuration name. Each was then coupled to the applicable trajectory for which the vehicle configuration could be flown in order to estimate performance. A comprehensive evaluation remains a work in progress, although some general conclusions can be drawn. 31 system configurations have been identified to date (30 September 2019) along with their identifying characteristics. Figure 7-18–Figure 7-23 display six of the nine corresponding physical layouts performed by MSFC staff for the SLS configurations through 30 September 2019.[10]

[9] In the following year, the count was reduced to 22 without loss of generality after identification and elimination of what were, effectively, duplicate entries.
[10] More details were given already in footnote 4.

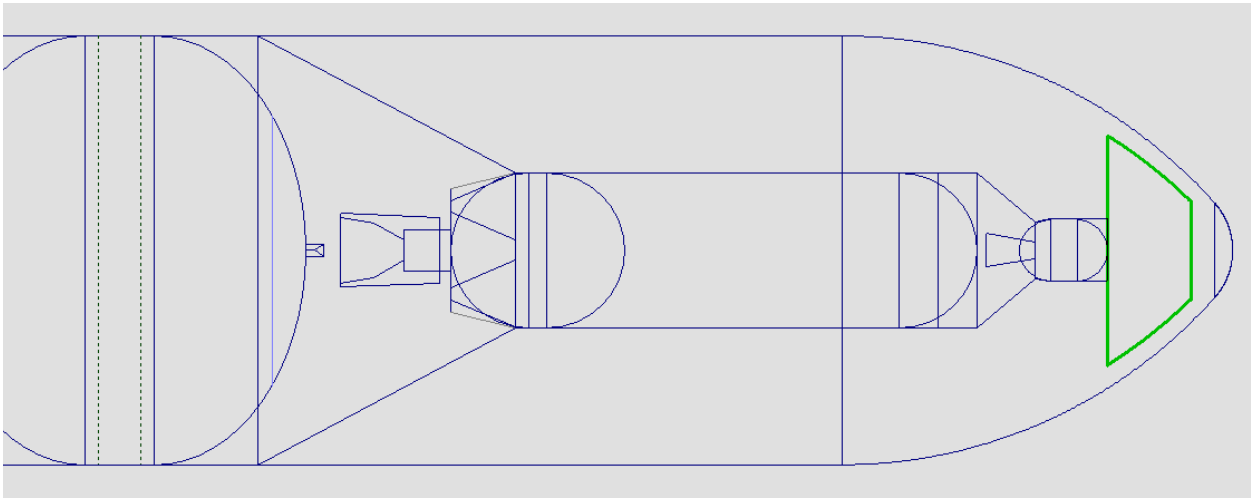

Figure 7-18. SLS-1 configuration: Atlas Centaur/48BV with SLS 8.4-m short fairing.

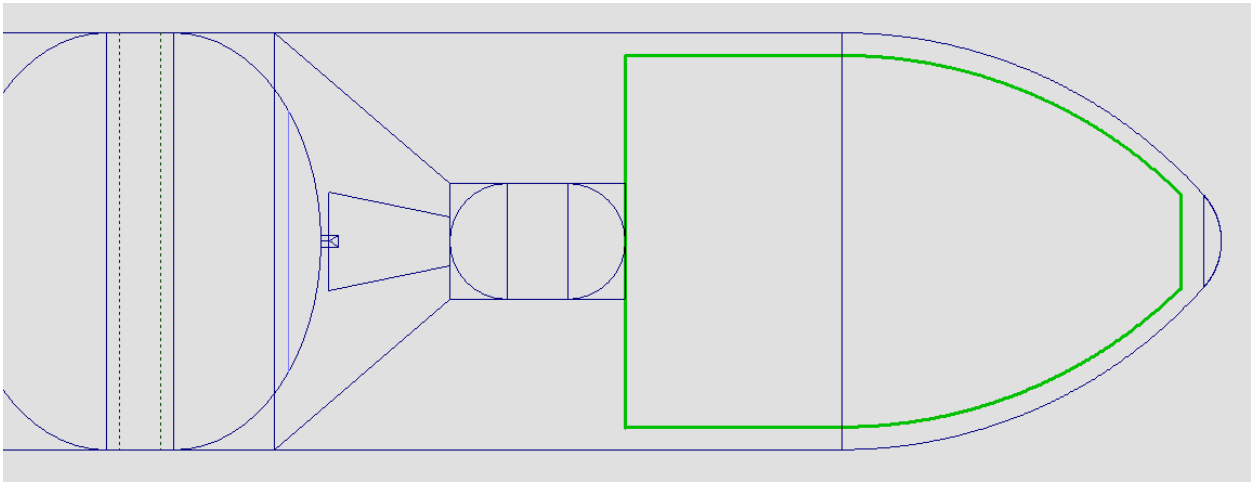

Figure 7-19. SLS-2 configuration: CASTOR 30XL with SLS 8.4-m short fairing.

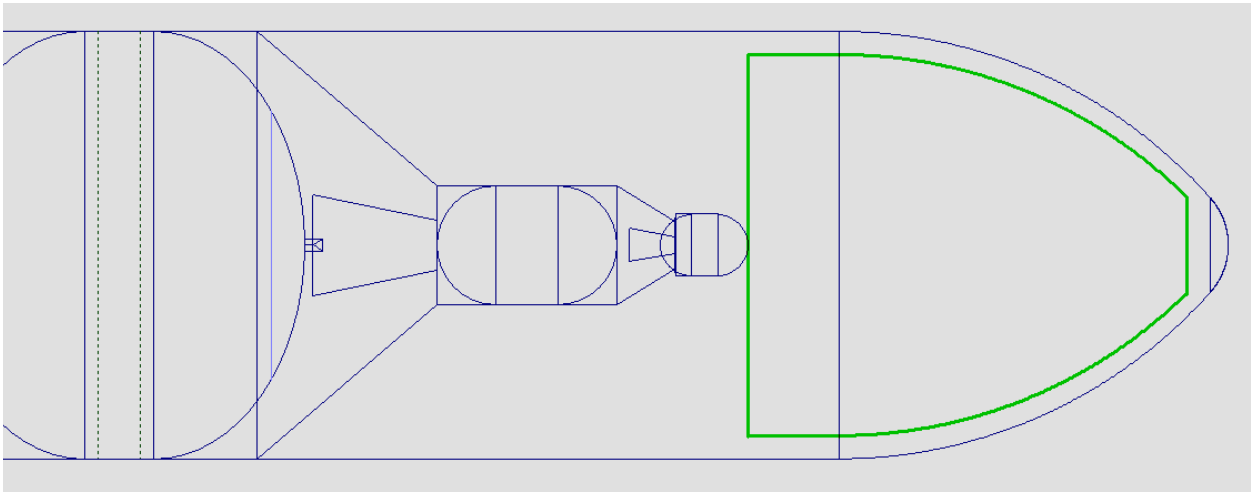

Figure 7-20. SLS-3 configuration: CASTOR 30XL/48BV with SLS 8.4-m short fairing.

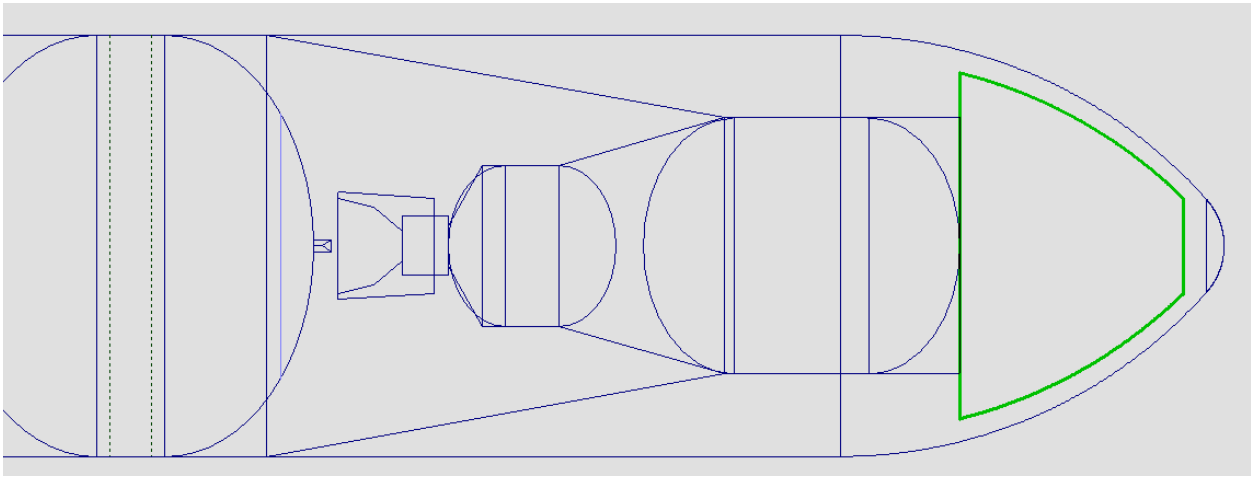

Figure 7-21. SLS-8 configuration: ICPS with SLS 8.4-m short fairing.

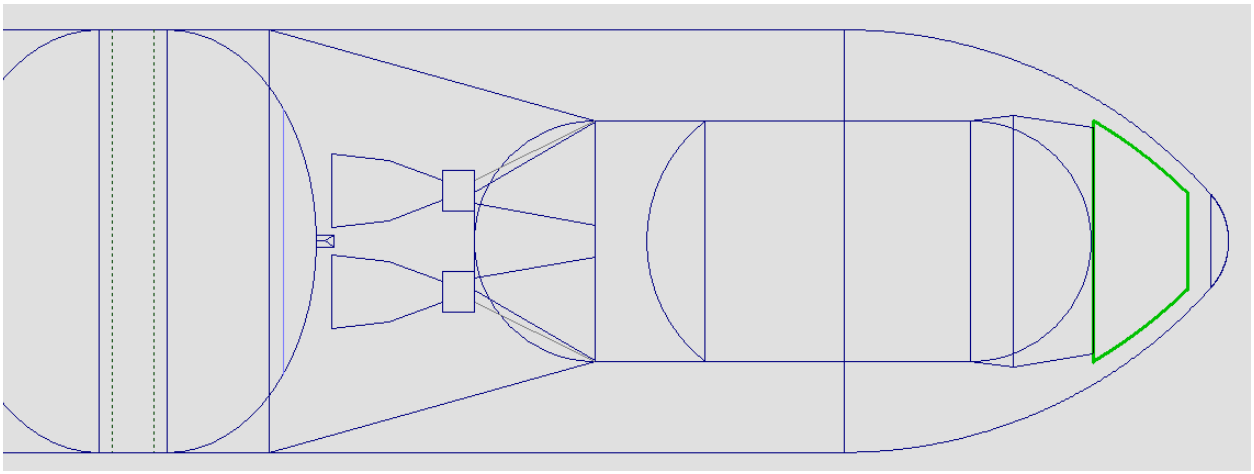

Figure 7-22. SLS-9 configuration: ACES with SLS 8.4-m short fairing.

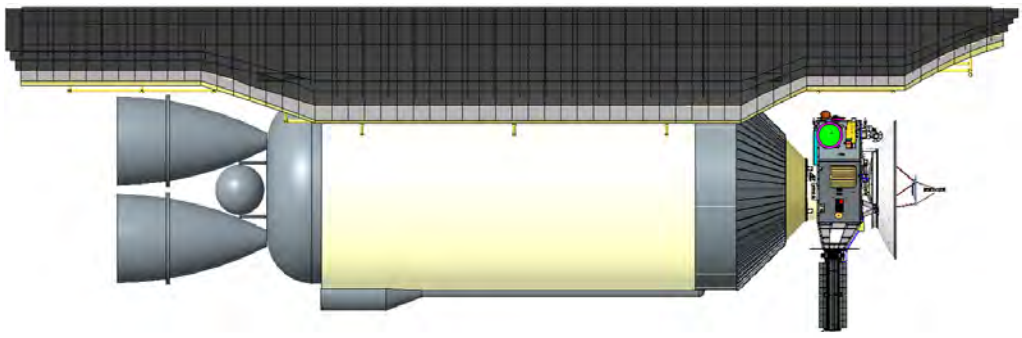

Figure 7-23. SLS-7 configuration: Centaur D with a thermal shield configured for 3 R_S perihelion. N.B. This is not a flyable design, for the following reasons: (1) It is too massive to launch directly to Jupiter on an SLS, (2) cryogenic propellants cannot be stored for cruise or especially for transport to 3 R_S from the center of the Sun, and (3) this "design" includes no means for maintaining a required attitude for the perihelion burn as the offset solar radiation pressure acts asymmetrically against the rapidly changing center of gravity of the assembly during the burn.

7.3.6. Interstellar Probe Launch System Development – Notional Schedule

We have performed a brief review of the Parker Solar Probe launch system development history and drafted a notional (and parallel) Interstellar Probe launch system development schedule. The Parker Solar Probe launch system development schedule actually began well before the project Phase "A" start date as part of "Pre-Phase A" studies. The system development effort started ~11 years before launch,[11] and the engineering-based studies employed a robust mix of trajectory analysis tasks and launch system engineering-based tasks. The launch system development tasks, although funded as a component of the Parker Solar Probe project effort, were performed before, and independently of, the science/instrument team selections and the spacecraft development schedule. Typically the spacecraft physical separating interface, volume, mass, and orbit requirements are the primary requirements the launch system development incorporates into early launch system studies. This separation of effort allowed the science community (including the Science and Technology Definition Team [STDT][12]) and selection processes to proceed almost independently of the launch system development.[13] Only the most critical requirements (spacecraft mass and C_3/orbit requirements) intersected the independent development paths early on. Table 7-4 provides a rough comparison of the Parker Solar Probe development schedule with a notional Interstellar Probe launch system development schedule.

The Parker Solar Probe launch system development team recognized, and exploited, the fact that the intersections and dependencies existing between estimating launch system ultimate performance values (velocity) and a fully matured spacecraft design can be tempered properly with allocations for parasitic masses attributed to fairings, adaptors, avionics, and power systems, etc., factored in.

The case of an Interstellar Probe mission is little different from other large missions (e.g., New Horizons and Parker Solar Probe) in that appropriate technical risk retirement up front and adequate planning for large, critical hardware pieces are critical to successful implementation.

[11] Parker Solar Probe launched from Cape Canaveral Air Force Station on 12 August 2018. The mission was assigned to APL by NASA' Office of Space Science (OSS), roughly equivalent to the current SMD, in 2001. That assignment was followed by ~4 years of a risk-mitigation study for the thermal protection system (TPS), which was seen as the primary technical risk for the mission (Potocki et al., 2006). Other engineering studies were also performed during this period to decrease technical, cost, and schedule risk to the mission plan.

[12] The original Solar Probe STDT was established within the Living With a Star (LWS) program at NASA in early 2004. After completing its initial report, the team was reconstituted as the Solar Probe Plus STDT to deal with a reconfiguration necessitated by the lack of RTGs to power the spacecraft. That team was disbanded on 9 April 2008. An Announcement of Opportunity was released on 3 December 2009, and proposals for instruments were due on 26 March 2010, some 8.5 years before launch.

[13] On a reduced scale, this is not unlike the issues faced during the early days of Apollo (Von Braun, 1962).

Table 7-4. Notional Interstellar Probe Development Schedule and Actual Parker Solar Probe Development Schedule

Parker Solar Probe						Interstellar Probe Parallels
L- Years		L- Months	Note: Dates Are Notional Task Start Dates	Notional Dates	L- Years	
11		132	Mission Formulation Start	1-Jun-18	11	
10		125	Launch System Configuration and Performance Trades (start)	30-Jul-18	10	
9		103	Engagement Studies with Launch Vehicle and Stage Providers	9-Jun-20	9	
9		103	Launch System Configuration, Trajectory, and Performance Trades (with NASA KSC)	9-Jun-20	9	
9		103	Spacecraft Phase "A" Start	9-Jun-20	9	
8		94	Program Cost, Performance, and Risk Trade Studies	2-Mar-21	8	
7		79	Spacecraft Phase B Start	24-May-22	7	
3		41	Launch Vehicle System Selection (by NASA)	6-Aug-25	3	
3		41	Spacecraft Mission Phase C Start	6-Aug-25	3	
2		27	Spacecraft Integration and Testing Start	20-Sep-26	2	
1		11	Spacecraft Environmental Testing Start	15-Feb-28	1	
0		5	Launch Campaign Start at the Launch Site	27-Jul-28	0	
0		0	Launch Date	1-Jan-29		

In this case, the launch vehicle itself is perhaps the most daunting risk. To carry a GPHS RTG, a certain number of successful prior missions are required as a matter of current policy (September 2019), and adequate time is required to comply with the Nuclear Launch Safety Approval Process. The latter has been well vetted in recent years by the launches of New Horizons, Curiosity, and Mars 2020.[14] The successful planned use of the SLS as a launch vehicle for the Europa Clipper mission will provide a good start, along with planned human missions to the Moon (Artemis program), for certification of the launch vehicle for an Interstellar Probe at the end of the 2020s, while also watching for developments with other (commercial) launch vehicles of similar capability.

[14] Mars 2020, now known as *Perseverance*, successfully launched 30 July 2020 and has a now-planned landing on Mars on 18 February 2021 (NASA, 2020).

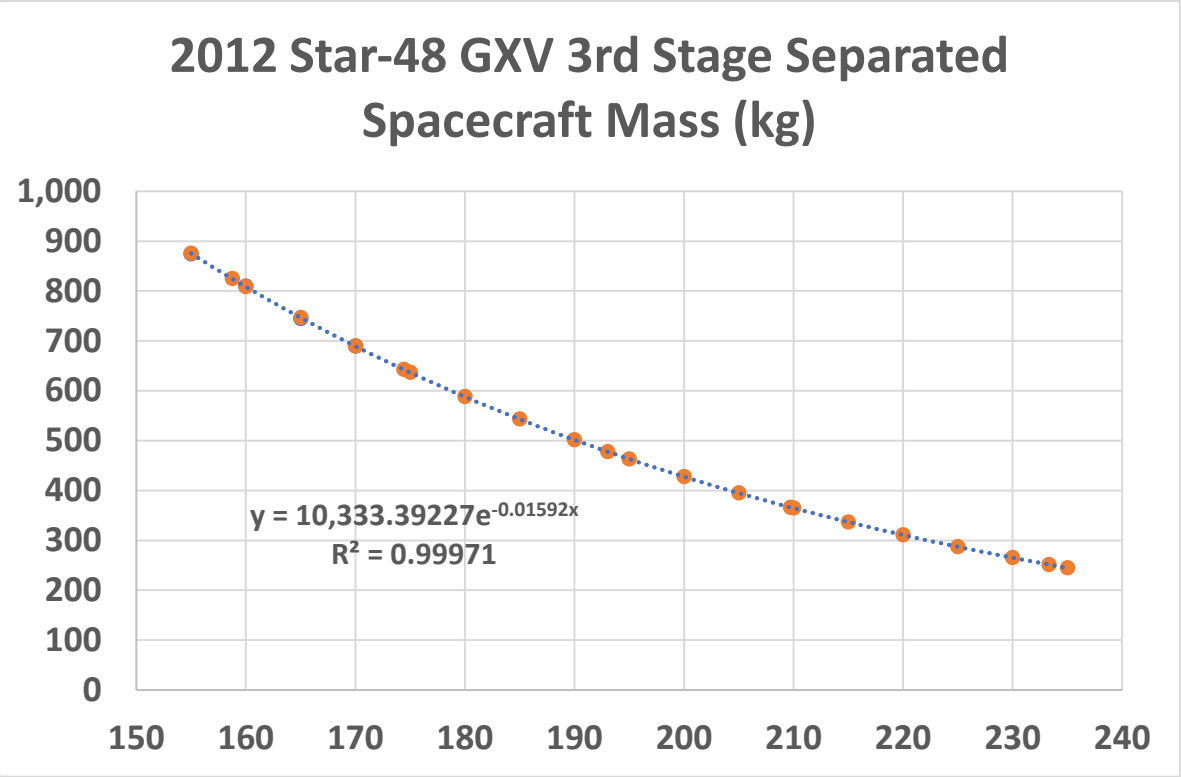

Figure 7-24. Injected mass versus C_3 for a combination of a Delta IV Heavy and a Star 48GXV kick stage.

7.3.7. Mission Examples with Existing and Vintage Flight Hardware

Some perspective on the use of the SLS Block 1B+[15] and Options 2 and 3 on bettering performance can be seen from using previous spacecraft and existing launch options. Currently, the most powerful, high-C_3 launch vehicle in the world is the Delta IV Heavy.[16] The highest performance "new" kick stage is the Star 48GXV. The solid stage has ~50% more propellant mass than the Star 48BV and was under development for use with an Atlas V for the Parker Solar Probe mission. Although it safely passed a hot fire test (5 December 2013), further flight qualification was stopped in favor of using the more powerful Delta IV Heavy (as compared with the Atlas V) and less capable, but multiply flight-proven Star 48BV-based stage.

Rough performance numbers can be calculated based on the Star 48GXV plus Delta IV Heavy combination. Figure 7-24 shows a spacecraft-separated mass curve versus C_3 for this combination, along with an approximate fit to a decaying exponential.

[15] Now denoted as "Block 2" – "Cargo" configuration.

[16] The Delta IV Heavy outperforms the Falcon Heavy (expendable version) at high C_3s (see Figure 7-11) because of its use of LOX/LH_2 in all stages.

To provide some idea of current capability using such a system, Table 7-5 provides approximate fly-out speeds for previous deep-space satellites, which could be obtained with such a system. This provides potential asymptotic fly-out speeds obtainable with an ideal, optimized, prograde JGA.

Table 7-5. Asymptotic Fly-Out Speeds of Vintage Spacecraft on a Delta IV Heavy plus Star 48GXV Stack

Spacecraft	C_3 (km²/s²)	Spacecraft Mass (fit) (kg)	Asymptotic Speed (au/yr)	Asymptotic Speed/3.6 au/yr (Voyager 1)
Voyager 1/2	158.75	825.4	5.25	1.46
Parker Solar Probe	174.43	643.0	5.59	1.55
New Horizons	193.02	478.3	5.95	1.65
Ulysses	209.71	366.7	6.24	1.73
Pioneer 10/11	233.32	251.8	6.60	1.83

This type of system could suffice to take a robust spacecraft up to ~1.5 times the asymptotic fly-out speed of Voyager 1 with a passive, prograde JGA (Option 1). Current NASA performance numbers for high-performance rockets in the absence of an upper stage (Figure 7-25) are limited to the Delta IV Heavy and Falcon Heavy for direct flights to Jupiter with no inner-solar-system gravity assists (required $C_3 \geq$ ~80 km²/s²).

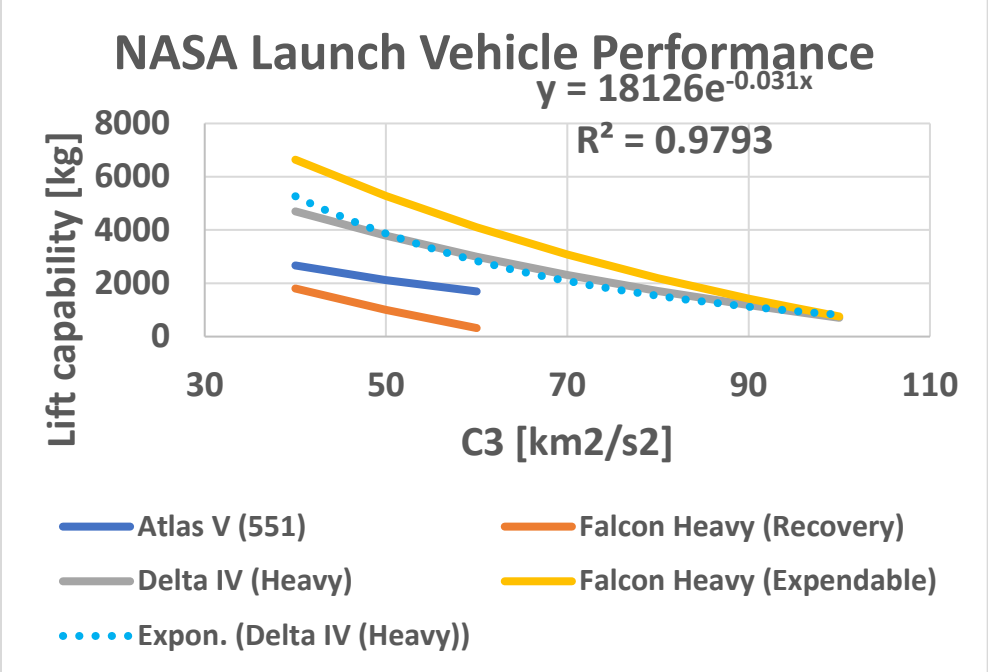

Figure 7-25. Injected mass versus C_3 for current high-energy vehicles covered by NASA's Launch Services Program Launch Vehicle Performance Planning Assessment (data from queries made to website tool on 10 July 2019). Compare with Figure 7-11.

To compare with the case shown in Figure 7-24, for a burn of the final stage at Jupiter (Option 2), we note that a stack consisting of a New Horizons-mass spacecraft on a Star 48GXV-powered stage would have a mass of ~3775 kg. The corresponding Delta IV Heavy capability is <70 km²/s², so Option 2 is not even feasible for this case.

7.4. Section 7 References

Ackeret, J. (1946) Zur Theorie der Raketen. *Helv. Phys. Acta* 19(April 1946), 103-112. Retrieved from http://www.e-periodica.ch/cntmng?pid=hpa-001:1946:19::571

Ackeret, J. (1947) Zur Theorie der Raketen (English Translation). *J. Brit. Int. Soc.* 6, 116-123.

Asimov, I. (1966) How Far Will We Go in Space? In *The 1966 World Book Year Book* (pp. 148-163). Chicago, IL: Field Enterprises Educational Corporation,.

Bennett, G.L., Lombardo, J.J., Hemler, R.J., et al. (2006) *Mission of Daring: The General-Purpose Heat Source Radioisotope Thermoelectric Generator, AIAA 2006-4096*. Paper presented at the 4th International Energy Conversion Engineering Conference and Exhibit (IECEC), San Diego, CA.

Bernal, J.D. (1969) The World, the Flesh, and the Devil: An Enquiry into the Future of the Three Enemies of the Soul (2nd ed.). Bloomington, IN: Indiana Univ. Press.

Boelter, L.M.K., Stever, H.G., Summerfield, M., et al. (1959) *Space Technology* (Seifert, H.S. Ed.). New York: John Wiley and Sons, Inc.

Brownlee, R.R. (2002) Learning to Contain Underground Nuclear Explosions. 2. Retrieved from http://nuclearweaponarchive.org/Usa/Tests/Brownlee.html

Bruno, C., Dachwald, B., Genta, G., et al. (2013) *Key Technologies to Enable Near-Term Interstellar Scientific Precursor Missions* (Bruno, C., Matloff, G.L. Eds.). China: China Aeospace Science and Technology Corporation.

Bussard, R.W. (1990) Fusion as Electric Propulsion. *Journal of Propulsion and Power* 6(5), 567-574. doi: 10.2514/3.23257

Cedillos-Barraza, O., Manara, D., Boboridis, K., Watkins, T., Grasso, S., Jayaseelan, D.D., Konings, R.J.M., Reece, M.J., Lee, W.E. (2016) Investigating the Highest Melting Temperature Materials: A Laser Melting Study of the TaC-HfC System. *Scientific Reports* 6, 37962. doi: 10.1038/srep37962

Chew, G., Doyle, M., Stancati, M. (2001) *Interstellar Spaceflight Primer*. Schaumburg, Illinois:

Cockfield, R. (2006) Preparation of RTG F8 for the Pluto New Horizons Mission. In *4th International Energy Conversion Engineering Conference and Exhibit (IECEC)*: American Institute of Aeronautics and Astronautics.

Coleman, J.J. (1961) Technical Notes: Optimum Stage-Weight Distribution of Multistage Rockets. *ARS Journal* 31(2), 259-261. doi: 10.2514/8.5447

Creech, S.D. (2019) Space Launch System - Payload Opportunities for Lunar Exploration, Science Missions (Funding Grant NM07AA70C). Washington, D.C.: Center, M.S.F.

Creech, S.D., Robinson, K.F., Stough, R.W. (2019) *NASA's Space Launch System - Payload Opportunities for Lunar Exploration, Science Missions*. Paper presented at the International Astronautical Congress (IAC), Washington, D.C. https://ntrs.nasa.gov/citations/20190033316.

Dyson, G. (2002) *Project Orion: The True Story of the Atomic Spaceship*. New York: Henry Holt and Company.

EngineeringToolBox (2005) Metals and Alloys - Melting Temperatures. Retrieved from https://www.engineeringtoolbox.com/melting-temperature-metals-d_860.html.

Eshleman, V.R. (1979) Gravitational Lens of the Sun: Its Potential for Observations and Communications over Interstellar Distances. *Science* 205(4411), 1133-1135. doi: 10.1126/science.205.4411.1133

Fiehler, D.I., McNutt, R.L., Jr. (2006) Mission design for the Innovative Interstellar Explorer vision mission. *Journal of Spacecraft and Rockets* 43(6), 1239-1247. doi: 10.2514/1.20995

Forward, R.L. (1985) Starwisp - An Ultra-Light Interstellar Probe. *Journal of Spacecraft and Rockets* 22(3), 345-350. doi: 10.2514/3.25754

Forward, R.L. (1996) Radioisotope Sails for Deep Space Propulsion and Power. *J. Brit. Int. Soc.* 49, 147-149.

Fountain, G.H., Kusnierkiewicz, D.Y., Hersman, C.B., et al. (2008) The New Horizons Spacecraft. *Space Science Reviews* 140, 23-47. Retrieved from http://adsabs.harvard.edu/abs/2008SSRv..140...23F

Goddard, R.H. (1983) The Ultimate Migration. *Journal of the British Interplanetary Society* 36, 552-554.

Goldsmith, M. (1957) On the Optimization of Two-Stage Rockets. *Journal of Jet Propulsion* 27(4), 415-428. doi: 10.2514/8.12799

Greenwood, S.W. (1975) Definition of Specific Impulse. *Journal of Spacecraft and Rockets* 12(1), 62-62. doi: 10.2514/3.27809

Grey, J. (1959) Gaseous-core nuclear rockets. *Astronautics* 4(10), 23.

Guo, Y., Farquhar, R.W. (2008) New Horizons Mission Design. *Space Science Reviews* 140(1), 49-74. doi: 10.1007/s11214-007-9242-y

Hall, M. (2018) In Memoriam: Robert R. Brownlee. 14. Retrieved from https://nationalatomictestingmuseum.org/2018/06/01/in-memoriam-robert-r-brownlee/

Hamlyn, K., McGrath, D., Lara, M. (1991) Venus Orbit Insertion of the Magellan Spacecraft Using a Thiokol STAR 48B Rocket Motor. In *27th Joint Propulsion Conference*: American Institute of Aeronautics and Astronautics.

Harrington, R. (2016) The Fastest Object Ever Launched Was a Manhole Cover — Here's the Story from the Guy Who Shot it into Space. *Business Insider,* (28). Retrieved from https://www.businessinsider.com/fastest-object-robert-brownlee-2016-2

Heacock, R.L. (1980) The Voyager Spacecraft. *Proceedings of the Institution of Mechanical Engineers* 194, 211-224. Retrieved from http://stickings90.webspace.virginmedia.com/voyager.pdf

Hilton, J.L., Luce, J.S., Thompson, A.S. (1964) Hypothetical Fusion Propulsion Rocket Vehicle. *J. Spacecraft* 1(3), 276-282.

Hyde, R., Wood, L., Nuckolls, J. (1972, 29 Nov - 1 Dec 1972) *Prospects for rocket propulsion with laser-induced fusion microexplosions.* In AIAA/SAE 8th Joint Propulsion Specialist Conference, New Orleans, LA.

Jaffe, L.D., Ivie, C.V., Lewis, J.C., Lipes, R., Norton, H.N., Stearns, J.W., Stimpson, L.D., Weissman, P. (1977) *An Interstellar Precursor Mission*. Pasadena, California: Laboratory, J.P.

Janhunen, P., Sandroos, A. (2007) Simulation Study of Solar Wind Push on a Charged Wire: Basis of solar Wind Electric Sail Propulsion. *Ann. Geophys.* 25, 755-767.

Janhunen, P. (2008) The Electric Sail - A New Propulsion Method Which May Enable Fast Missions to the Outer Solar System. *J. Brit. Int. Soc.*(61), 322-325.

Janhunen, P. (2014) Electric Sail, Photonic Sail and Deorbiting Applications of the Freely Guided Photonic Blade. *Acta Astronautica* 93(0), 410-417. doi: http://dx.doi.org/10.1016/j.actaastro.2013.07.041

Jones, E.M. (1985) *"Where Is Everybody?" An Account of Fermi's Question* (UC-34B). Los Alamos, New Mexico: Laboratory, L.A.N.

Malina, F.J., Summerfield, M. (1947) The Problem of Escape from the Earth by Rocket. *Journal of the Aeronautical Sciences (Institute of the Aeronautical Sciences)* 14(8), 471-480. doi: 10.2514/8.1417

Martin, P.K. (2018) NASA's Management of the Space Launch System Stages Contract. Washington, D.C.:

McLafferty, G.H. (1970a) Gas-Core Nuclear Rocket Engine Status. *J. Spacecraft* 7(12), 1391-1396.

McLafferty, G.H. (1970b) Gas-Core Nuclear Rocket Engine Technology Status. *Journal of Spacecraft and Rockets* 7(12), 1391-1396. doi: 10.2514/3.30179

McNutt, R.L. (2010) Science Satellites: Interplanetary Spacecraft. In *Encyclopedia of Aerospace Engineering*: John Wiley & Sons, Ltd.

McNutt, R.L., Wimmer-Schweingruber, R.F., Gruntman, M., et al. (2019) Near-Term Interstellar Probe: First Step. *Acta Astronautica* 162, 284-299. doi: https://doi.org/10.1016/j.actaastro.2019.06.013

McNutt, R.L., Jr., Gold, R.E., Krimigis, S.M., et al. (2005, 13 Jul 2005) *Innovative Interstellar Explorer: Radioisotope Propulsion to the Interstellar Medium.* In 41st AIAA/ASME/SAE/ASEE Joint Propulsion Conference & Exhibit, AIAA, Tucson, AZ.

McNutt, R.L., Jr., Elsperman, M.S., Gruntman, M., Klaus, K.K., Krimigis, S.M., Roelof, E.C., Smith, D.B., Vernon, S.R., Wimmer-Schweingruber, R.F. (2014) *Enabling Insterstellar Probe with the Space Launch System (SLS)*. Paper presented at the 65th International Astronautical Congress, Toronto, Ontario, Canada.

McNutt, R.L., Jr., Aleman, S.M., Amato, M.J., et al. (2015) *Nuclear Power Assessment Study - Final Report*. Laurel, MD: Center, N.G.R.

McNutt, R.L., Jr., Benson, W.W., Gruntman, M., Krimigis, S.M., Roelof, E.C., Vernon, S.R., Wimmer-Schweingruber, R.F. (2015) *Enabling Interstellar Probe: Space Launch System (SLS) trades*. Paper presented at the 66th International Astronautical Congress, Jerusalem, Israel.

McNutt, R.L., Jr., Vernon, S.R. (2016) *Enabling Solar System Science with the Space Launch System (SLS)*. Paper presented at the 67th International Astronautical Congress, Guadalajara, Mexico. https://iafastro.directory/iac/paper/id/35548/ext/appendix/IAC-16,A3,1,4,x35548.pdf.

McNutt, R.L., Jr., Zurbuchen, T.H., Gruntman, M., Krimigis, S.M., Roelof, E.C., Vernon, S.R., Wimmer-Schweingruber, R.F. (2016) *Interstellar Probe: Requirements*. Paper presented at the 67th International Astronautical Congress, Guadalajara, Mexico. https://iafastro.directory/iac/paper/id/35475/ext/appendix/IAC-16,D4,1,9,x35475.pdf.

McNutt, R.L., Jr., Wimmer-Schweingruber, R.F., Gruntman, M., Krimigis, S.M., Roelof, E.C., Zank, G.P., Stone, E.C., Brandt, P.C., Vernon, S.R. (2017) *Near-Term Exploration of the Interstellar Medium*. Paper presented at the 68th International Astronautical Congress, Adelaide, Australia.

McNutt, R.L., Jr., Wimmer-Schweingruber, R.F., Gruntman, M., et al. (2018) *Near-Tem Interstellar Probe - First Step*. Paper presented at the 69th International Astronautical Congress, Bremen, Germany.

Millis, M.G. (1999) NASA Breakthrough Propulsion Physics Program. *Acta Astron.* 44, 175-182.

Millis, M.G. (2010) *Progress in Revolutionary Propulsion Physics*. Paper presented at the 61st International Astronautical Congress,, Prague, Czech Republic. http://arxiv.org/ftp/arxiv/papers/1101/1101.1063.pdf

http://www.iafastro.net/iac/archive/browse/IAC-10/C4/8/8526/.

Millis, M.G., Davis, E.W. (Eds.) (2009) *Frontiers of Propulsion Science* (Vol. 227). Reston, Virginia: American Institute of Aeronautics and Astronautics.

Moeckel, W.E. (1972) Comparison of Advanced Propulsion Concepts for Deep Space Exploration (NASA TN D-6968). Cleveland, OH:

NASA (2020) Mars 2020 Perseverance Rover. Retrieved from https://mars.nasa.gov/mars2020/.

Natha, A., Espinoza, L. (2020) Voyager Mission Status. Retrieved from https://voyager.jpl.nasa.gov/mission/status/.

Noble, R.J. (1993) *Radioisotope-Powered Electric Propulsion of Small Payloads for Regular Access to Deep Space*. Paper presented at the 29th Joint Propulsion Conference and Exhibit, Monterey, California. http://dx.doi.org/10.2514/6.1993-1897.

Noble, R.J. (1998) *Radioisotope Electric Propulsion of Sciencecraft to the Outer Solar System and Near-Interstellar Space.* In Missions to the Outer Solar System and Beyond; 2nd IAA Symposium on Realistic Near-Term Advanced Scientific Space Missions, International Academy of Astronautics,, Aosta, Italy.

Noble, R.J. (1999) Radioisotope Electric Propulsion of Sciencecraft to the Outer Solar System and Near-Interstellar Space. *Acta Astron.* 44(2-4), 193-199.

Oberth, H. (1970) *Ways to Spaceflight* (Agence Tunisienne de Public-Relations, T., Tunisia, 1970, Trans.): National Aeronautics and Space Administration. Retrieved from https://ia600503.us.archive.org/21/items/nasa_techdoc_19720008133/19720008133.pdf

Ordway, F.I. (1970) 2001: A Space Odyssey. *Spaceflight* 21(3), 110-117.

Peschka, W. (1956) Über die Überbrückung interstellarer Entfernungen. *Astron. Acta* 2, 191-200.

Peterson, J.P., Seide, S., Weingarten, V.I. (1968) *Buckling of Thin-Walled Circular Cylinders* (NASA SP-8007). Hapton, Virginia: NASA.

Potocki, K.A., Dantzler, A., Mehoke, D., Drewry, D. (2006) Solar probe thermal protection system risk mitigation study: FY 2006 final report. Laurel, Maryland:

Powell, C., Hahn, O.J., McNally, J.R., Jr. (1973) Energy balance in fusion rockets. *Astron. Acta* 18, 59-69.

Purcell, E. (1963) Radioastronomy and communication through space. In Cameron, A.G.W. (Ed.), *Interstellar communication: A collection of reprints and original contributions* (Cameron, A. G. W. ed., pp. 121 - 143). New York: W. A. Benjamin, Inc.

Rayman, M.D., Lehman, D.H. (1997) Deep Space One: NASA's First Deep-Space Technology Validation Mission. *Acta Astronautica* 41(4), 289-299. doi: http://dx.doi.org/10.1016/S0094-5765(98)00073-3

Rayman, M.D., Varghese, P. (2001) The Deep Space 1 Extended Mission. *Acta Astronautica* 48(5), 693-705. doi: http://dx.doi.org/10.1016/S0094-5765(01)00044-3

Razin, Y.S., Pajer, G., Breton, M., Ham, E., Mueller, J., Paluszek, M., Glasser, A.H., Cohen, S.A. (2014) A direct fusion drive for rocket propulsion. *Acta Astronautica* 105(1), 145-155. doi: http://doi.org/10.1016/j.actaastro.2014.08.008

Reinmann, J.J. (1971) *Fusion Rocket Concepts* (NASA TM-X-67826). Cleveland, OH:

Roth, J.R. (1961-62) A Preliminary Study of Thermonuclear Rocket Propulsion. *J. Brit. Int. Soc.* 18, 99-108.

Russell, C.T., Coradini, A., Christensen, U., et al. (2004) Dawn: A Journey in Space and Time. *Planetary and Space Science* 52(5–6), 465-489. doi: http://dx.doi.org/10.1016/j.pss.2003.06.013

Sagan, C. (1963) Direct Contact Among Galactic Civilizations by Relativistic Interstellar Spaceflight. *Planet. Space Science* 11, 485-498.

Sänger, E. (1961) 21.4 Photon propulsion. In Koelle, H.H. (Ed.), *Handbook of Astronautical Engineering*. New York: McGraw-Hill Book Company, Inc.

Schnitzler, B., Borowski, S. (2007) Neutronics Models and Analysis of the Small Nuclear Rocket Engine (SNRE). In *43rd AIAA/ASME/SAE/ASEE Joint Propulsion Conference & Exhibit*: American Institute of Aeronautics and Astronautics.

Schnitzler, B., Borowski, S. (2008) Small Nuclear Rocket Engine and Stage Benchmark Model. In *44th AIAA/ASME/SAE/ASEE Joint Propulsion Conference & Exhibit*: American Institute of Aeronautics and Astronautics.

Schnitzler, B., Borowski, S., Fittje, J. (2009) A 25,000-lbf Thrust Engine Options Based on the Small Nuclear Rocket Engine Design. In *45th AIAA/ASME/SAE/ASEE Joint Propulsion Conference & Exhibit*: American Institute of Aeronautics and Astronautics.

Shepherd, L.R., Cleaver, A.V. (1948a) The Atomic Rocket - 2. *Journal of the British Interplanetary Society* 7, 234-241.

Shepherd, L.R., Cleaver, A.V. (1948b) The Atomic Rocket - 1. *Journal of the British Interplanetary Society* 7, 185-194.

Shepherd, L.R., Cleaver, A.V. (1949) The Atomic Rocket - 3. *Journal of the British Interplanetary Society* 8, 23-37.

Shepherd, L.R. (1952) Interstellar Flight. *Journal of the British Interplanetary Society* 11(4), 149 - 167.

Shklovskii, I.S., Sagan, C. (1968) *Intelligent Life in the Universe* (Fern, P., Trans. 1st ed.). New York: Dell Publishing Co., Inc.

Short, W., Sabin, C. (1959-60) A Radioisotope Propulsion System. *J. Brit. Int. Soc.* 17, 453-458.

Slipher, V.M. (1930) The Discovery of a Solar System Body Apparently Trans-Neptunian. Mars Hill, Flafstaff, Arizona:

The SP-100 nuclear reactor program: Should it be continued?, U.S. House of Representatives. 15 (1992).

Steinetz, B.M., Benyo, T.L., Chait, A., et al. (2020) Novel Nuclear Reactions Observed in Bremsstrahlung-Irradiated Deuterated Metals. *Physical Review C* 101(4), 044610. doi: 10.1103/PhysRevC.101.044610

Stern, S.A., Weaver, H.A., Spencer, J.R., et al. (2019) Initial Results from the New Horizons Exploration of 2014 MU69, a Small Kuiper Belt Object. Science 364(6441), eaaw9771. doi: 10.1126/science.aaw9771

Stough, R.W., Hitt, D., Holt, B., Philips, A., Patrick, M. (2019) *Supporting Material for APL's Interstellar Probe Final Report* (M20-7868). NASA Technical Reports Server:

Strömgren, E. (1930) *Transneptunian planet*. Obervatoire de Copenhague: Internationale, l.U.A.

Stuhlinger, E. (1959) Photon rocket propulsion. *Astronautics*, 36 + 69-78.

Sullins, R.T., Smith, G.W., Spier, E.E. (1969) *Manual for structural stability analysis of sandwich plates and shells* (NASA CR-1457). Washington, D.C.: Corporation, G.D.

Tarter, J. (2001) The Search for Extraterrestrial Intelligence (SETI). *Annual Review of Astronomy and Astrophysics* 39, 511. doi: 10.1146/annurev.astro.39.1.511

Taylor, R. (2005) *Prometheus Project: Final Report* (982-R120461). Pasadena, CA:

Tsiolkovskiy, K.E. (1967) *Study of Outer Space by Reaction Devices*. Washington, D.C.:

Turyshev, S.G., Andersson, B.G. (2003) The 550-au Mission: A Critical Discussion. *Monthly Notices of the Royal Astronomical Society* 341(2), 577-582. doi: 10.1046/j.1365-8711.2003.06428.x

Von Braun, W. (1962) *Appendix B, Manned Lunar Landing Program Mode Comparison* (NASA TM-74929). Washington, D.C.:

von Hoerner, S. (1962) The General Limits of Space Travel: We may never visit our neighbors in space, but we should start listening and talking to them. *Science* 137(3523), 18-23. doi: 10.1126/science.137.3523.18

Voss, S.S. (1984) *SNAP Reactor Overview*. Kirtland Air Force Base, New Mexico: Command, A.F.S.

White, H., March, P., Lawrence, J., Vera, J., Sylvester, A., Brady, D., Bailey, P. (2016) Measurement of Impulsive Thrust from a Closed Radio-Frequency Cavity in Vacuum. *Journal of Propulsion and Power*, 1-12. doi: 10.2514/1.B36120

Wikipedia (2018a) Briz (rocket stage). Retrieved from https://en.wikipedia.org/wiki/Briz_(rocket_stage).

Wikipedia (2018b) Fregat. Retrieved from https://en.wikipedia.org/wiki/Fregat.

Wikipedia (2020a, 7 January 2020) Breakthrough Propulsion Physics Program. Retrieved from https://en.wikipedia.org/wiki/Breakthrough_Propulsion_Physics_Program.

Wikipedia (2020b, 30 October 2020) Ibn Battuta. Retrieved from https://en.wikipedia.org/wiki/Ibn_Battuta.

Wikipedia (2020c, 16 October 2020) Marco Polo. Retrieved from https://en.wikipedia.org/wiki/Marco_Polo.

Wikipedia (2020d) Ultra-high-temperature ceramics. Retrieved from https://en.wikipedia.org/wiki/Ultra-high-temperature_ceramics.

Williams, C., Dudzinski, L., Borowski, S., Juhasz, A. (2001) Realizing "2001: A Space Odyssey" - Piloted spherical torus nuclear fusion propulsion. In *37th Joint Propulsion Conference and Exhibit*: American Institute of Aeronautics and Astronautics.

Winglee, R.M. (1999) *Mini-Magnetospheric Plasma Propulsion (M2P2)* (NIAC Award No. 07600-010, Final Report)

8. Long-Duration Mission Challenges and a Path to Solutions

The science goals of heliospheric and planetary missions are continuing to require increased mission durations. Voyager's mission requirement was for 4.5 (Draper et al., 1975) years, and, in its various mission extensions, it has operated for a total of 43 years to date (e.g., Matsumoto, 2016). Cassini took 7 years to reach the Saturnian system and then operated in orbit an additional 13 years for a total of 20. The New Horizons mission required over 9 years to reach Pluto and has now continued into the Kuiper Belt for the past 4 years. The goals of the Interstellar Probe mission (R. L. McNutt et al., 2019) will require the spacecraft to operate for 50 years or more to meet the science goals being discussed (Brandt et al., 2019). To meet this requirement, greater care and planning will be required. The challenges fall into three categories: spacecraft reliability, sustainment of a ground system, and ensuring that a team with its knowledge base intact (the human element) is available to support the mission throughout its duration.

In 2018 and 2019, the Interstellar Probe study concentrated on some of the overarching organizational and structural issues that will challenge the mission. This report provides a status of the work on the challenges of a long-duration mission as of the end of calendar year (CY) 2019. Those overarching issues are documented below.

In 2019, work started on spacecraft reliability and on many of the ground segment's practical challenges that need to be met based on mission architecture. A review of the literature indicated that Voyager was the most well-known long-term mission with regard to lifetime but not the only one (Fox et al., 2013). The literature noted that if spacecraft continue to operate for a few years (no infant mortality), they tend to function for a very long time. The often-assumed constant failure rate models are not appropriate for such long-term missions, and a Weibull distribution of failure rates (i.e., failure rate decrease over time) is a better model (Saleh & Castet, 2011). As the details of mission requirements and the spacecraft architecture progress, a statistical analysis of Interstellar Probe reliability will be developed and mitigations then will be recommended where that analysis indicates additional work will be required to ensure the reliability risk is acceptable.

The ground segment for an Interstellar Probe mission will be based on a concept of operations (CONOPS) whose initial outlines are described in section 4. Experience from past and current missions such as Voyager and New Horizons will provide guideposts to help and form the basis for the challenges for the ground segment described below; however, these challenges will be refined into specific issues based on the currently (or soon to be) available ground assets and the spacecraft resources to be defined by the ongoing work described in section 7. The resulting implications, in more specific terms for the ground segment, will be documented in future reports.

As stated above, prior missions such as Voyager, Cassini, and New Horizons have operated for long periods of time. Other missions are currently planning for eventual workforce transitions, such as NASA's Europa Clipper (Weber, 1968) and the European Space Agency's (ESA's) Jupiter Icy Moons Explorer (JUICE). The timeline of an interstellar mission, however, is so extreme as to largely eclipse any and all prior activities. Arrival at the target destination will not take place for 50 years, a period

longer than Voyager's operational timeline, now expected to terminate 45 years after launch. Several of Voyager's initial principal investigators (PIs) have already passed away (Bradford A. Smith, 2018; Rudolf A. Hanel, 2015; Herbert S. Bridge, 1995; Von R. Eshleman, 2017; James Warwick, 2013; Frederick L. Scarf, 1988), with deputies taking on leadership roles only once the PI has died, akin to a form of kingship or inheritance (Weber, 1968). Voyager data management and updating efforts began over 20 years after launch. On Cassini, those who joined after selection and became the lifeblood of mission planning and operations had to wait until several years into the mission before they were offered an official mission role; while PIs could add newcomers to their teams, facility instrument leaders on Cassini could not do so without NASA Headquarters' approval. A late addition of a participating scientist's program enabled some mobility of these juniors into official roles. New Horizons is still under the command of its PI, with deputies in charge of encounter planning experiencing role turnover in extended-mission phases. As such, many of the innovations that enable such mission longevity have been implemented on an ad hoc basis, according to the timeline of mission extension or need, and were not part of the initial mission plan, personnel assignments, or proposal, as driven by budgetary limits.

This ad hoc approach to temporality and change will simply not work on the Interstellar Probe mission. Most of the original team will be dead by the time the spacecraft reaches its targeted end of mission of 50 years past launch. Even if the spacecraft arrives fully operational at the interstellar medium, without appropriate operational plans in place, the initial team that operated it will have dissolved into postmortem factions, with potentially archaic data standards that are no longer supported and little to no resources to support the upkeep of essential equipment or the successful promotion of juniors to leadership roles, and the mission will be a failure. Just as extreme distance drives technical parameters associated with speed and trajectory, which, in turn, impact instrumentation and design, ***the extreme temporality associated with the mission lifetime must drive the mission's teaming and data architectures because they are essential to enable full mission success.***

NASA-funded spacecraft teams have not yet faced the considerations associated with such long periods of cruise and operations, except on an ad hoc, extended-mission basis. Sociologists, anthropologists, and historians who have studied collaborations organized for expected long periods have identified several features in common. Importantly, the most successful of these communities conceptualize their built instrumentation as *research infrastructure*. Research infrastructures must not only be planned and built, they must be maintained over time, with budgetary resources put aside for upgrades and upkeep (Matthew J Bietz et al., 2010; Borgman et al., 2016; Edwards, 2013; Karasti et al., 2010; Lee et al., 2006; Millerand et al., 2013; Star & Ruhleder, 1996; Star, 1999).

In addition, such infrastructures are *organized* to support expected and regular leadership turnover. Navies and fleets demonstrate hierarchical structures that support strong leadership, effective and efficient communication, and delivery of results. This means that although instrumentation is bespoke and individuals forge strong associations with their detectors, ships, or devices, they anticipate that these tools of their trade will be *shared* and *passed onward* to successive waves of participants (M. Cohn, 2013; Charlotte Linde, 2001; C. Linde, 2009; Ribes & Finholt, 2007,

2009). These new members of the community are trained in how to use the research infrastructure and take on more responsibility as their careers mature. Instrument management, too, is also frequently decoupled from scientific investigations, with PIs leading groups of investigators without taking charge of a particular instrument (Traweek, 1988).

Finally, research infrastructures establish *standards* for data management and transfer that look to the long term (Matthew J. Bietz & Lee, 2009; Birnholtz & Bietz, 2003; Endersby, 2008; Millerand et al., 2013; Pasquetto et al., 2016; Ribes & Jackson, 2013). Data stewardship considerations therefore begin at the outset of the collaboration. They are not addressed in a post hoc manner once formats become out of date or system upgrades render important files useless.

These principles, which enable research collaborations to endure over many decades, inform our discussion of the planned social order of the Interstellar Probe team. We first describe the *organization* of the human element that takes these considerations into account. We then describe our plan for long-term maintenance with respect to *funding* and for *data management*.

8.1. Organizing for the Long Term

Many scientists in the planetary science, astrophysics, and heliophysics communities are used to a model of PI ownership in which individuals become charismatically associated with their instruments and that instrument's success. Transition from one leader to another can prove difficult or even destructive to the instrument as the loss of knowledge and perceived leadership is devastating for the instrument and for the team. *This model will not work for a mission that must, by definition, outlive all of its original leadership team before it becomes fully operational*. The team must therefore meet this challenge head-on, with considerable forethought. Fortunately, examples from organizational sociology and the sociology of science offer opportunities to innovate in order to ensure scientific success.

8.1.1. A Bureaucratic Structure

Over a hundred years ago, Max Weber explained that the charismatic form of leadership does not endure beyond the lifetime of the charismatic individual—unless the organization successfully transitions to a bureaucratic hierarchy (Weber, 1968). While the former social form is characterized by leadership through forceful "personality" and individual participants' adherence to the leader, bureaucracies are seen as more legitimate and efficient social forms, characterized by strong centralized authority and a clear chain of command and communication such as that seen in military operations or among a fleet of ships. Such systems rely on individual expertise but also provide clear roles for participants, opportunities for advancement should this be desired, and clear mechanisms for training and evaluating candidates. They also provide meaningful employment and connection to the cause. Individuals move in and out of roles (or "bureaus") with clearly defined tasks, and their evaluation is based on their performance of the role's tasks, not their personality. Newcomers have the opportunity to enter and to move up the chain, criteria for advancement are clear, and decision-making is comparatively transparent.

This model has already been used to great effect in voyages of exploration and discovery, which took place under social structures that endure for generations, such as national navies or private companies. This includes the voyages initiated by the Hudson's Bay Company (e.g., the voyage of the *Nonsuch* in 1668) or the Dutch East India Company (Vereenigde Oostindische Compagnie; VOC, e.g., the voyages of Henry Hudson); the three Pacific voyages of James Cook, while he was an officer in the Royal Navy (Great Britain); the circumnavigation of the globe by the Imperial Russian Navy under Admiral Fabian Gottlieb von Bellingshausen; or the voyages of the Chinese Treasure Fleet under the command of Zheng He (鄭和). While now remembered for certain charismatic discoverers and captains, these expeditions were actually organized under the rubric of large, national-level institutions, and not undertaken by isolated entrepreneurs.

There are advantages to this model of group operations. Ship operations led cognitive scientist Ed Hutchins to develop the notion of "distributed cognition," which relies on clear roles and communication pathways between members of such a well-oiled machine. There is even evidence that bureaucratic hierarchies may be better for women and minorities because of these criteria, unlike other models of hiring and promotion that operate based on perceived "fit" and that persistently conflate this standard with merit (Castilla & Benard, 2010; Freeman, 1972; Rivera, 2012). Most importantly for the Interstellar Probe mission, however, such social systems endure much longer than corporations, militias, or religions that are predicated on following single, charismatic individuals, and that are likely to fizzle out once that leader is gone.

Most NASA teams in the directed or Flagship class provide strong structures in the form of individual instrument teams. However, leadership on these instrument teams is often charismatic in form and does not change hands. There is no single role at the top of the chain, equivalent to a CEO or an admiral. The "project scientist" (PS) role is more subservient, transmitting the concerns of the PI to those constructing instrumentation, with no functional hierarchical authority—a form of "structural powerlessness" (Kanter, 1993). While some PSs have managed a form of control due to charisma (i.e., Ed Stone of the Voyager project), others have stayed within the traditional confines of the role. To follow the ship analogy, what is necessary is for each instrument to be managed by a captain and the overall fleet by an admiral. While individuals in these roles can be replaced through formal procedures, the roles and their authority remain.

To convert the common NASA Flagship team structure into one with staying power to last multiple generations of scientists, we recommend the following modifications:

- Write contracts to allow the PI-ship to exchange hands over the lifetime of the instrument. Instrument leadership should be promoted from within the instrument team and/or competed participating scientist programs, not necessarily within the institution; contracts and instrument development plans must be written accordingly.
- Formalize deputy roles for all PI-ships, and formalize mechanisms for their replacement.
- Formalize procedures for PI and PS replacement through the ranks.

- Create and classify clear roles on the mission team (beyond simply co-investigator [Co-I] or instrument engineer) that allow the responsibilities to remain with the roles.
- Assign formal deputies, apprenticeships, or assistantships to all roles for junior scientists to build mentorship and continuity into the architecture of the mission.
- Formalize mechanisms and procedures for advancement (i.e., selection of the next PI or PS, rotation of deputies through the ranks, mobility of juniors among roles and up the chain of command). The mission must not be allowed to grow stale in its leadership or among its membership ranks.

8.1.2. Instrumentation and Leadership

An essential property of such organizations is the ability to draw a clear distinction between instrument development, leadership, and management on the one hand and individual scientific investigations on the other. This model is already in place in related research infrastructures that support particle physics and astronomy. Observatories, for instance, are founded on the premise that they will produce a shared resource that is managed by a scientific community, that is kept reasonably up-to-date in terms of operational capacity and instrumentation, and that enables community participation and observation (e.g., the Space Telescope Science Institute [STSci], established for the Hubble Space Telescope in 1981). While groups of technicians manage the physical upkeep of the equipment, groups of scientific experts decide which investigators may use the instrumentation (McCray, 2000; Traweek, 1988). Meanwhile, particle accelerators, synchrotrons, and neutrino detectors (Doing, 2004; Knorr Cetina, 1999; Pinch, 1986; Traweek, 1988) are also built to support the long-term goals of physicists working in a collaborative environment over a long duration. This includes particle accelerator facilities, such as the Stanford Linear Accelerator (SLAC)—now the SLAC National Accelerator Laboratory—begun in 1962 at Stanford University; the High Energy Accelerator Research Organization (高エネルギー加速器研究機構 *Kō Enerugī Kasokuki Kenkyū Kikō*), known as KEK, established in 1997; and CERN (derived from *Conseil européen pour la recherche nucléaire*), established in 1954. At these facilities, which have been studied by social scientists (Knorr Cetina, 1999; Traweek, 1988), the goal is to provide an infrastructure for long-term scientific work, that supports multiple scientists' investigative goals, and that cares for and provides regular upkeep and upgrades for equipment.

Thus far, this has not been the model on NASA spacecraft teams. On such teams, individuals naturalize the notion that PIs expect the data from their instruments in return for their hard work and investment. They assume that the kind of detailed knowledge of the instrument necessary for design, construction, maintenance, and use can *only* be held by the PI. Given the proclivity of other scientific fields to structure themselves differently, this assumption is false; it is instead the outcome of an organization in which individuals are permitted to possess charismatic leadership roles with the "special powers" that presumes. Should instruments be built instead with the express assumption that they are to outlive their progenitors and that the role of the PI is one of an instrument steward amid generations of leadership, these assumptions will change.

We therefore recommend something that will sound outrageous to many NASA scientists and PIs: that instruments may begin under the purview of a charismatic individual, but within 10 years of their construction, they must transition to more of a "facility"-style instrument: one managed over the long term by an institution and series of technicians. These technicians may initially be selected and trained by the PI, but the contract must go to an institution and laboratory with the capability to host and manage instrumentation over generations of instrumental stewards. To that end, we recommend the following:

- Clear instructions to proposers stipulating that even if the instruments are at first built by individual PIs, they must transition to facility support in the early stages of the mission, such that an institution can robustly manage the instrument's continued operations. *The goal is to produce instruments that will outlive their creators, and for the creators to imbue them with qualities that will enable that transition.*

- Successive generations of PIs may be responsible for guarding and safeguarding the institutional instrumentation and making decisions as to its management.

- Scientists in charge of facility instrumentation must not be subject to structural powerlessness (i.e., saddled with the responsibility for instrumentation but having limited true authority over its construction or management). Akin to new captains put in charge of existing vessels in a fleet, they must be allowed to make decisions regarding the operations, care, and maintenance of the instrument entrusted to their care.

- Future rounds of PI selection may disentangle instrumentation management entirely from investigation management, as is the case with research infrastructures at locations such as CERN or at large telescope centers. This would enable cross-collaboration among instrument groups within the project science group through cross-functional teams.

8.1.3. Ritualized Role Turnover

Most missions do not plan for promotions or shifting roles. PI-ships are rarely transferred, and contracts are established with institutions with the understanding that the named individuals and organizations will endure. In reality, many missions must confront this problem should a team member retire or pass away, and must work at cross-purposes with contracts and institutions to resolve the problem. An interstellar mission that goes beyond the life expectancy of any of its founders can and indeed must plan for such a reality in advance by building this expectation into its sociotechnical structure.

Far from a disadvantage, role turnover can be advantageous if considered well enough in advance to establish appropriate organizational structures and practices. However, this turnover cannot simply happen once, or when a PI dies or retires. This would cause too much of an exogenous shock to the team system, with uncontrollable effects (Haveman et al., 2001). The team must instead ritualize role and leadership turnover, such that it becomes part of the team's temporal rhythm (Jackson et al., 2011). Research in the Carnegie School of organizational sociology indicates that routines can be a source of both stability and change (Feldman, 2000; Feldman & Pentland, 2003).

As such, routinized and ritualized handover of instrumental authority can be a source of stability for the Interstellar Probe team even as it allows for some administrative fresh air. Further, if elements at the core of the organization—its social structure and its technical resources—do not change, then social theory suggests that the organization will develop a strong degree of structural inertia that enables flexibility and adaptability without compromising the durability and success of the organization as a whole (Hannan & Freeman, 1984).

Taking these considerations into account, we suggest a novel approach to the problem of team turnover on the Interstellar Probe mission team. Instead of treating turnover as an ad hoc or exogenous event, we propose its routine ritualization as part of the core of the mission structure. Ideally such leadership transitions should take place with a regular cadence and a regular set of predictable activities. They should enable a leader to have enough charge over an instrument to come to know it intimately, but without developing such a close relationship that the instrument cannot effectively be handed over (indeed, the instrument *must* be developed with handover in mind). Such transitions must allow a leader to make an impact in their position, but not be in power for so long that the instrument's operation is unimaginable without them. Much like how mission teams require an operational readiness test to practice and perfect their operational constraints and concerns, role transitions must occur more than once over the lifetime of the mission, and certainly more than once before arrival at the interstellar medium.

We recommend a *decadal cadence* to satisfy these requirements. By the time of the mission's arrival, leadership will have changed hands four times, allowing for much room for the transition's improvement. This also offers the opportunity to align leadership periodicity with naturally occurring changes on the mission, for instance:

- Years 1–10: PIs selected; spacecraft and instruments built and launched; initial databases established for data collection.
- Years 11–20: Deputy promoted to PI; new deputies and internal leads promoted. Appoint 10 participating scientists to use instrumentation; conduct planetary science exploration phase throughout solar system cruise. User testing in situ of databases, software, and hardware required for data collection and circulation.
- Years 21–30: Deputy promoted to PI; new deputies and internal leads promoted. Deploy lessons learned from initial solar system cruise.
- Years 31–40. Review to ensure continuity by initiating a new wave of participating scientists. Produce and promote cross-functional teams for physical sciences that deploy multiple instruments.
- Years 41–50. New wave of participating scientists. New PI-level leaders for cross-functional teams. Implement lessons learned and system upgrades based on operations to date.

The team must spell out the rules for instrument delivery and transition in advance so that PIs, team members, and community members know what to expect in terms of the legacy of their instrumentation.

All phases of transition require robust transfer of knowledge, skills, and institutional memory—what is typically called "knowledge management." Work by anthropologists and sociolinguists at NASA Ames Research Center to support the former Constellation program considered these same concerns with respect to human spaceflight, many of which apply here:

- Rotate mission roles among a roster of apprenticed teammates, with members appointed and transitioning from roles on regular basis on multiyear terms. This reinforces that knowledge is localized to the role, not to the individual, and also spreads embodied knowledge of the mission and its particulars among more team members, especially those who may move up into positions of decision-making authority.

- Develop an onboarding process for all newly appointed team members that introduces them to the customs, culture, and instrumentation of the mission team.

- Ensure a robust online-and-offline document and information repository for knowledge capture.

- Encourage blogging, oral histories, and memoir writing by members of the team to encourage the relay of stories and information across generations (Charlotte Linde, 2001). The "spirit" of the team has to transition to the next generation, along with specific technical knowledge.

8.2. Plan for Infrastructural Aging

Given that there are no "magic hands" in space to tinker with or otherwise change the spacecraft after launch, considering these issues well in advance is essential to mitigating the challenges that can—and will—arise during flight and operations, decades into an unknowable future. These challenges are not entirely unknown, however. Studies of long-term scientific collaborations have revealed several common concerns about long-duration collaborations associated with data management, software, and hardware. For instance, individuals planning the MESSENGER mission spent 3 years trying to read Mariner 10 tracking tapes to help develop their mission; restoration efforts resulted in the conclusion that the 40-year-old tapes were not "easily" readable.

Aging with the spacecraft will require dealing with aging standards for software code and for data formats and storage to anticipate the need for backward compatibility many years in the future. Such problems are routinely dealt with post-mission by NASA's Planetary Data System (PDS), and they have been, and continue to be, challenging (R. L. McNutt, Jr. et al., 2017). Dealing with such issues has been done on a best-effort, ad hoc basis with the Voyager spacecraft during the Voyager Interstellar Mission (VIM), which commenced 4 June 1990 (Belcher, 1990). For Interstellar Probe, a more deliberate, planned, and appropriately funded approach is required.

8.2.1. Data Management

Data management must encompass curation and compatibility policies in addition to more typical cleaning, calibration, and release dates (Matthew J. Bietz & Lee, 2009; Borgman et al., 2016; R. L. McNutt, Jr. et al., 2017). The mission should carefully consider and implement the following:

- Data storage and management standards that do not change with time
- Budgeting for compatibility systems in the future such that new machines can read old file formats
- Careful and complete documentation of such systems as they develop and age
- Use of redundant hardware systems (e.g., disk readers)
- Plans for periodic system upgrades in advance
- Consistent use of NASA, NSSDCA (NASA Space Science Data Coordinated Archive), and NARA (National Archives and Records Administration) archives, standards, and best practices in collaboration with pre-mission NASA arrangements and requirements
- Best practices regarding the use of archiving standards and metadata documentation, including use of digital object identifiers (DOIs) for data sets and archiving of analysis software as applicable (e.g., with GitHub, equivalents, and/or successors)

Maintenance and repair should be core factors of all work on long-duration missions and should be explicitly and contractually built into mission plans by confirmation at the latest (Steinhardt, 2016). One potential approach would be to consider including a maintenance crew bureau that supports scientific and technical endeavors across the team (such a structure is more common in National Institutes of Health (NIH)-funded collaborations that implement a coordination bureau). Care should also be taken to build a system with relative simplicity that relies on preexisting standards, with robustness and reduplication built in, to enable long-distance troubleshooting and repair. In addition, information technology (IT) cybersecurity threats must be appropriately dealt with such that digital resilience (Rothrock, 2018) is built into the data systems and archives from the start in order to protect the long-term integrity of the data obtained.

In addition, the team must anticipate software patch build up, to include updates or upgrades to earlier standards, possibly written in new programming languages (M. L. Cohn, 2016). Adopting ISO (International Organization for Standardization) standards and compiling a software dictionary up front for each mission instrument can assist in this regard and should follow NASA PDS best practices or equivalent. Onboard training for old programming languages will be essential for newcomers who, years in the future, will not be familiar with today's languages. The team might choose to standardize use of a small group of languages across their infrastructure to better enable problem-solving by future computer engineers or the crafting of software patches for use with old file format standards in data analysis.

8.2.2. Funding Management

By their nature, "large strategic missions" (aka "Flagship" missions) provide significant funding challenges to go with their significant scientific opportunities (National Academies of Sciences, 2017). Precisely because they are large, cost overruns and/or schedule slips can have a significant negative impact on all stakeholders in a variety of ways outside of just monetary impact (Zelizer, 2017). An example of what to avoid is that of the James Webb Space Telescope [JWST]). Originally proposed as the Next Generation Space Telescope (NGST) by the Astrophysics Decadal Survey in 2001 for a cost of $1 billon (Council, 2001), JWST is now planned to be launched in March 2021 with a mission cost of $9.7 billion. There are two challenges. The first is that NASA "bookkeeps" the mission cost as that established as the baseline at mission confirmation, which follows the Preliminary Design Review. However, costs at that point can already be in excess of the estimates put forth in initial planning documents such as the Decadal Surveys, and that in itself can be problematic for keeping large missions sold. Up-front cost estimates are difficult to make for cutting-edge large missions, but they can be mitigated to some extent by advanced engineering studies of critical technologies, such as that begun here. A quantitative predictor remains problematic, although NASA's establishment of the CADRe (Cost Analysis Data Requirement) system and the use of the CATE (cost and technical evaluation) process are given a measure of credit in eliminating cost surprises (National Academies of Sciences, 2015). The previous methodology that NASA investigated as embodied by "Gruhl's Rule" (Honour, 2004) makes qualitative sense (the more money spent on initial concept engineering, the less the final overrun), but its quantitative validity has been called into question by some.

Funding management is a multisided issue with any large mission, and this one will be no exception. In any event, no mission can ever be considered solidly sold until it is successfully launched. Research is underway to characterize the effects of shifting budgetary conditions on spacecraft development and operations (Vertesi, 2016). With considerable mismatch between Congressional cycles of funding allocation and the life expectancy of an interstellar mission as well as an inability to predict long-term fiscal and political realities, there will be significant challenges both in the development phase and in the cruise phase for the project and its management. Such periods of uncertainty are not new, but the long timescale of this project by design will exacerbate difficulties experienced by previous long-term projects.

To that end, the mission must involve budgetary practices that allow for long-term planning from the outset, including the following:

- Build funding requests into the mission profile for periodic system upgrades. This includes ground-based infrastructure, data infrastructure, and spacecraft operating systems. This future-minded approach must also form part of the software architecture from the outset such that systems are not working with multiple "reverse salients" at a time as well as continual breakdowns (Hughes, 1999; Star, 1999). Redundancy and repair must be essential characteristics of spacecraft and ground system construction (Jackson et al., 2012; Rosner & Ames, 2014; Steinhardt & Jackson, 2015; Steinhardt, 2016).

- Streamline the mission profile to keep costs as low as realistically feasible; include margins for the "unknown unknowns."
- Provide an honest, accurate, and robust cost estimate well before mission confirmation (e.g., as early as the appropriate Decadal Survey deliberations). Continue to perform cost estimations at regular intervals as the mission proceeds.
- Do not "upscale" the mission after stakeholder buy-in if this would lead to significant budget requirement increases (e.g., both the developers and NASA management must pro-actively avoid "bait and switch" tactics as opposed to solid stakeholder buy-in during early development).
- After launch, during the development phase, avoid shifting costs from development to operations that add complexity to operations, as with deletion of the Cassini scan platform.
- Characterize budget-cutting processes in advance (i.e., instrument descopes and operational stand-downs), and secure concurrence in these processes from all stakeholders in advance as well.
- Consider an appropriate international partnership with formally agreed-to and documented, well-defined, and mission-enabling roles for non-NASA partners as part of the pre-decisional mission development.

8.3. Section 8 References

Belcher, J.W. (1990) *Overview of VIM-5*. Voyager Memorandum. Massachusetts Institutte of Technology. Center for Space Research.

Bietz, M.J., Lee, C.P. (2009) *Collaboration in Metagenomics: Sequence Databases and the Organization of Scientific Work*, Springer London, London.

Bietz, M.J., Baumer, E.P.S., Lee, C.P. (2010) Synergizing in Cyberinfrastructure Development. *Computer Supported Cooperative Work (CSCW)* 19(3-4), 245-281. doi: 10.1007/s10606-010-9114-y

Birnholtz, J.P., Bietz, M.J. (2003, 2003) *Data at Work: Supporting Sharing in Science and Engineering*, ACM Press.

Borgman, C.L., Sands, A.E., Darch, P.T., Golshan, M.S. (2016) The Durability and Fragility of Knowledge Infrastructures: Lessons Learned from Astronomy. *Proceedings of the Association for Information Science and Technology* 53(1), 1-10. doi: 10.1002/pra2.2016.14505301057

Brandt, P.C., McNutt, R., M. V. Paul, M.V., et al. (2019) Humanity's First Explicit Step in Reaching Another Star: The Interstellar Probe Mission. *Journal of the British Interplanetary Society* 72, 202-212.

Castilla, E.J., Benard, S. (2010) The Paradox of Meritocracy in Organizations. *Administrative Science Quarterly* 55(4), 543-576. doi: 10.2189/asqu.2010.55.4.543

Cohn, M. (2013) *Lifetimes and Legacies: Temporalities of Sociotechnical Change in a Long-Lived System.* (Ph.D. Thesis). University of California, Irvine, Irvine, CA.

Cohn, M.L. (2016, 27 February - 2 March) *Convivial Decay: Entangled Lifetimes in a Geriatric Infrastructure.* In CSCW 2016, ACM, San Francisco, California.

Council, N.R. (2001) *Astronomy and Astrophysics in the New Millennium*. Washington, DC: The National Academies Press. doi:10.17226/9839

Doing, P. (2004) 'Lab Hands' and the 'Scarlet O': Epistemic Politics and (Scientific) Labor. *Social Studies of Science* 34(3), 299-323.

Draper, R., Purdy, W., Cunningham, G. (1975) The Outer Planet Mariner Spacecraft. In *Conference on the Exploration of the Outer Planets*: American Institute of Aeronautics and Astronautics.

Edwards, P.N. (2013) *A Vast Machine: Computer Models, Climate Data, and the Politics of Global Warming*: MIT Press. Retrieved from https://mitpress.mit.edu/books/vast-machine

Endersby, J. (2008) *Imperial Nature: Joseph Hooker and the Practices of Victorian Science*. Chicago: University of Chicago Press,.

Feldman, M.S. (2000) Organizational Routines as a Source of Continuous Change. *Organization Science* 11(6), 611-629. Retrieved from http://www.jstor.org/stable/2640373

Feldman, M.S., Pentland, B.T. (2003) Reconceptualizing Organizational Routines as a Source of Flexibility and Change. *Administrative Science Quarterly* 48(1), 94. doi: 10.2307/3556620

Fox, G., Salazar, R., Habib-Agahi, H., Dubos, G.F. (2013, 2-9 March 2013) *A Satellite Mortality Study to Support Space Systems Lifetime Prediction.* In 2013 IEEE Aerospace Conference.

Freeman, J. (1972) The Tyranny of Structurelessness. *Berkeley Journal of Sociology* 17, 151-164. Retrieved from http://www.jstor.org/stable/41035187

Hannan, M., Freeman, J. (1984) Structural Inertia and Organizational Change. *American Sociological Review* 49(2), 149-164.

Haveman, H.A., Russo, M.V., Meyer, A.D. (2001) Organizational Environments in Flux: The Impact of Regulatory Punctuations on Organizational Domains, CEO Succession, and Performance. *Organization Science* 12(3), 253-273. doi: 10.1287/orsc.12.3.253.10104

Honour, E.C. (2004) 6.2.3 Understanding the Value of Systems Engineering. *INCOSE International Symposium* 14(1), 1207-1222. doi: 10.1002/j.2334-5837.2004.tb00567.x

Hughes, T.P. (1999) The Evolution of Large Technological Systems. In Biagioli, M. (Ed.), *The Science Studies Reader* (pp. 202-223). New York: Routeledge.

Jackson, S.J., Ribes, D., Buyuktur, A., Bowker, G.C. (2011, 2011) *Collaborative rhythm: Temporal Dissonance and Alignment in Collaborative Scientific Work*, ACM Press.

Jackson, S.J., Pompe, A., Krieshok, G. (2012) *Repair Worlds: Maintenance, Repair, and ICT for Development in Rural Namibia.* In Proceedings of the ACM 2012 Conference on Computer Supported Cooperative Work (CSCW'12) Association for Computing Machinery, New York, NY, Seattle, Washington.

Kanter, R.M. (1993) *Men and Women of the Corporation*. New York, NY: Basic Books.

Karasti, H., Baker, K.S., Millerand, F. (2010) Infrastructure Time: Long-term Matters in Collaborative Development. *Computer Supported Cooperative Work (CSCW)* 19(3-4), 377-415. doi: 10.1007/s10606-010-9113-z

Knorr Cetina, K. (1999) *Epistemic Cultures: How the Sciences Make Knowledge*. Cambridge, MA: Harvard University Press,.

Lee, C.P., Dourish, P., Mark, G. (2006, 2006) *The Human Infrastructure of Cyberinfrastructure*, ACM Press.

Linde, C. (2001) Narrative and Social Tacit Knowledge. *Journal of Knowledge Management* 5(2), 160 - 170. Retrieved from http://www.emerald-library.com/ft

Linde, C. (2009) *Working the Past: Narrative and Institutional Memory*. Oxford ; New York: Oxford University Press.

Matsumoto, S.K. (2016) Voyager Interstellar Mission: Challenges of flying a very old spacecraft on a very long mission. In *SpaceOps 2016 Conference* (pp. 12): AIAA.

McCray, W.P. (2000) Large Telescopes and the Moral Economy of Recent Astronomy. *Social Studies of Science*. Retrieved from http://www.jstor.org/stable/285761

McNutt, R.L., Wimmer-Schweingruber, R.F., Gruntman, M., et al. (2019) Near-Term Interstellar Probe: First Step. *Acta Astronautica* 162, 284-299. doi: https://doi.org/10.1016/j.actaastro.2019.06.013

McNutt, R.L., Jr., Gaddis, L.R., Law, E., et al. (2017) *Planetary Data System Roadmap Study for 2017 – 2026*. Greenbelt, Maryland: Center, N.G.S.F.

Millerand, F., Ribes, D., Baker, K.S., Bowker, G.C. (2013) Making an Issue out of a Standard: Storytelling Practices in a Scientific Community. *Science, Technology & Human Values* 38(1), 7-43. doi: 10.1177/0162243912437221

National Academies of Sciences, Engineering, and Medicine (2015) *The Space Science Decadal Surveys: Lessons Learned and Best Practices*. Washington, DC: The National Academies Press. https://doi.org/10.17226/21788

National Academies of Sciences, Engineering, and Medicine (2017) *Powering Science: NASA's Large Strategic Science Missions*. Washington, DC: The National Academies Press. https://doi.org/10.17226/24857

Pasquetto, I.V., Sands, A.E., Darch, P.T., Borgman, C.L. (2016, 2016) *Open Data in Scientific Settings: From Policy to Practice*, ACM Press.

Pinch, T. (1986) *Confronting Nature: The Sociology of Solar-Neutrino Detection*. Dordrecth, The Netherlands: D. Reidal.

Ribes, D., Finholt, T.A. (2007, 2007) *Tensions Across the Scales: Planning Infrastructure for the Long-Term.* In 2007 International ACM conference, ACM Press.

Ribes, D., Finholt, T.A. (2009) The Long Now of Technology Infrastructure: Articulating Tensions in Development. *Journal of the Association for Information Systems* 10(5), 375-398. doi: 10.17705/1jais.00199

Ribes, D., Jackson, S.J. (2013) Data Bite Man: The Work of Sustaining a Long-Term Study. In Gitelman, L. (Ed.), *Raw Data Is an Oxymoron* (pp. 147-166). Cambridge MA: MIT Press.

Rivera, L.A. (2012) Hiring as Cultural Matching: The Case of Elite Professional Service Firms. *American Sociological Review* 77(6), 999-1022. Retrieved from http://www.jstor.org/stable/41723081

Rosner, D.K., Ames, M. (2014, 2014) *Designing for Repair?: Infrastructures and Materialities of Breakdown*, ACM.

Rothrock, R.A. (2018) *Digital Resiliance*. New York, New York: American Management Association. Retrieved from https://www.amazon.com/Digital-Resilience-Company-Ready-Threat/dp/0814439241

Saleh, J.H., Castet, J.-F. (2011) *Spacecraft Reliability and Multi-State Failures*: John Wiley & Sons, Ltd. 10.1002/9781119994077

Star, S.L., Ruhleder, K. (1996) Steps Toward an Ecology of Infrastructure: Design and Access for Large Information Spaces. *Information Systems Research* 7(1), 111-134.

Star, S.L. (1999) The Ethnography of Infrastructure. *American Behavioral Scientist* 43(3), 377-391. doi: 10.1177/00027649921955326

Steinhardt, S.B., Jackson, S.J. (2015, 2015) *Anticipation Work: Cultivating Vision in Collective Practice*, ACM.

Steinhardt, S.B. (2016, 7-12 May) *Breaking Down While Building Up: Design and Decline in Emerging Infrastructures.* In CHI 2016, ACM, San Jose, CA.

Traweek, S. (1988) *Beamtimes and Lifetimes: The World of High Energy Physicists*. Cambridge, MA: Harvard University Press.

Vertesi, J. (2016) Pricing the Priceless Spacecraft: The Social Life of Money in Robotic Planetary Exploration. Retrieved from https://www.nsf.gov/awardsearch/showAward?AWD_ID=1633314.

Weber, M. (1968) *Economy and Society: An Outline of Interpretive Sociology* (Fischoff, E., Trans.). New York: Bedminster Press.

Zelizer, V.A. (2017) *The Social Meaning of Money: Pin Money, Paychecks, Poor Relief, and Other Currencies*. Princeton, NJ: Princeton University Press. Retrieved from https://press.princeton.edu/titles/11007.html

9. Management

9.1. Stage 1: Basic Feasibility (2018)

The first phase of study for the Pragmatic Interstellar Probe mission concept began in spring 2018.[1] The initial task allowed the study team, along with over 50 additional collaborators (i.e., unpaid participants) from around the country and also Europe, to determine (1) that a spacecraft of modest size and power, propelled by NASA's Space Launch System (SLS), could indeed reach the termination shock of the solar system within about a decade and (2) that communications and operations could continue many tens of additional astronomical units (au) beyond the heliopause.

This funding also helped support a special session on interstellar studies, including Interstellar probe concepts, at the 2018 meeting of the Committee on Space Research (COSPAR) held in Pasadena, California, on 14–22 July 2018. The session was organized by the Panel on Interstellar Research (PIR) in 2015 with R. L. McNutt Jr. as chair; T. Zurbuchen was co-chair until his appointment as NASA associate administrator for the Science Mission Directorate (SMD), at which time Professor R. Wimmer-Schweingruber of the University of Kiel in Germany assumed that role. In addition, ahead of the regular COSPAR meeting, a presentation on Interstellar Probe was given to the International Academy of Astronautics (IAA) as part of the Academy Day program on 14 July 2018 in Pasadena.

The COSPAR meeting report follows.[2] A full list of meetings, presentations, conferences, and talks is available at interstellarprobe.jhuapl.edu.

9.1.1. COSPAR 2018 Meeting Report: Panel on Interstellar Research (PIR)

The PIR convened three half-day sessions during the 42nd COSPAR Scientific Assembly held 14–22 July 2018 in Pasadena, California. A business meeting of the panel was also held (13:00–14:00 on Tuesday, 17 July). The planned Panel Session "PIR.1: Near-Term Exploration of the Interstellar Medium" included 26 oral presentations and nine posters. The oral sessions were held in room SR 26 of the Hilton Hotel and attracted about ~35 attendees (audience size varied between ~40 and ~25 across the three sessions). The timing was negotiated so as not to overlap with talks in another session (session D1.2, Large-Scale Heliospheric Structure: Theory, Modelling, and Data), the science content of which was complementary to the PIR.1 talks; it also was preferred, and worked well, that the PIR.1 sessions were contiguous in time.

[1] Contract Number NNN06AA01C, Order Number 80MSFC18F0139, dated 13 June 2018: Form 336 NNN06AA01C Task Order First Pragmatic Interstellar Probe Mission Study, Purchase Requisition: 4200656072 Fund: SCEX22018D Appropriation: 8018/190120. This contract followed from a Request for Proposal (RFP) issued to APL by NASA on 4 April 2018 ("Request for Proposal for New Task under NNN06AA01C - Interstellar Probe Mission Study," issued by Marshall Space Flight Center [MSFC] on that date).

[2] Submitted to COSPAR on or about 14 March 2018.

The program was divided into six 90-minute-long sessions; five of those sessions accommodated two 25-minute talks and two 20-minute talks, one session accommodated six 15-minute talks.

Table 9-1. Organization of the PIR.1 Event at COSPAR 2018

Time Slot	Session Name	Solicited Talks		Contributed Talks	
		Number	Duration	Number	Duration
Monday, 16 July, a.m.	Science, Mission, and Implementation – I	2	25		
		2	20		
	Science, Mission, and Implementation – II	2	25		
		1	20	1	20
Monday, 16 July, p.m.	Scientific Perspectives and the Conditions in the Very Local Interstellar Medium	1	25	1	25
		1	20	1	20
	Lessons for Other Systems from Nearby Observations	2	25		
				2	20
Tuesday, 17 July, a.m.	Instrumentation and Engineering Challenges – I	2	25		
				2	20
	Instrumentation and Engineering Challenges – II	1	15	5	15
Totals	Three half-day slots of two sessions each	14		12	

One contributed 15-minute oral talk was withdrawn at the last minute, and so one of the nine poster authors was invited to give a 15-minute talk in that time slot. The poster authors were in attendance at poster sessions on the evenings of Monday, 16 July, and Tuesday, 17 July (PCC EXHIBIT HALL C POSTER).

The 26 oral presentations were given by scientific and institutional leaders in the field from 11 different institutions from five different nations. Revolving around the pragmatic implementation and science of an interstellar probe to the local interstellar medium (LISM), the presentations covered the plasma physical interactions with the LISM, planetary and Kuiper Belt Object (KBO) science opportunities, science of the circum-solar debris disk, and astrophysical opportunities, including measurement of the extragalactic background light (EBL) and exoplanetary sciences. Thus, a remarkable breadth of science opportunities was represented from the three major space disciplines (heliophysics, planetary sciences, and astrophysics) that would all be enabled by a probe leaving the solar system to go beyond the heliopause. A few other sessions dealt with detailed science results from various parts of the outer heliosphere, given the recent results from Voyager 1 and 2, the Interstellar Boundary Explorer (IBEX), and Cassini. However, the PIR.1 session was unique in its mission-driven focus that served to collect the compelling science case from the global science community; this will become a valuable asset to any future Science Definition Team (SDT) and serve to raise the importance of this science in the U.S. Decadal Surveys and documents alike worldwide. In addition, five presentations were directly reporting on the implementation of a pragmatic interstellar probe using available or near-term technology. Several international stake-

holders participated in the session together with the ~40 attendees, including NASA program managers and several directors of institutions from around the world. Since the 42nd COSPAR Assembly, the Interstellar Probe concept and the groundbreaking, cross-disciplinary science it enables have seen dramatically increased traction: A dedicated Interstellar Probe Exploration Workshop was conducted subsequently in New York City (NYC) in October 2018, with 55 international scientists representing all three disciplines (heliophysics, planetary sciences, and astrophysics), and a special session was conducted at the American Geophysical Union (AGU) Fall Meeting held in December 2018, in Washington, DC. Several upcoming sessions and presentations are being planned in both the United States and Europe, including the Planetary Exploration Horizon 2061 Synthesis Workshop in Toulouse, France, in June 2019; a special session at the joint European Planetary Science Congress (EPSC)-Division for Planetary Sciences (of the American Astronomical Society) (DPS) Meeting in Geneva, Switzerland, in September 2019; a planned second Interstellar Probe Exploration Workshop in NYC in November 2019; and a proposed third Interstellar Probe Special Session at the AGU Fall Meeting in San Francisco inn December 2019. Given this global momentum, the organizing committee of PIR.1 looks forward to another successful session at the 43rd COSPAR Assembly in Sydney, Australia, in 2020.

9.1.2. Other Meetings in Calendar Year (CY) 2018

The COSPAR meeting aligned with the proposed effort, i.e., to reach out and engage both the domestic (U.S.) and international communities to assess their scientific interest in, and encourage them to contribute ideas to, the ongoing study.

Interstellar Probe was presented 30 July 2018 at the Solar, Heliospheric, and INterplanetary Environment (SHINE) Town Hall in Cocoa Beach, Florida, and at a Future In-Space Operations (FISO) seminar on 5 September 2018 (invited). The study effort was presented to the Voyager science team at the Voyager Science Steering Group (SSG) meeting (11–12 September 2018 at APL) and at the 69th International Astronautical Congress (IAC) Session D4.4 (5 October 2018 in Bremen, Germany). The conference paper was subsequently invited for publication in *Acta Astronautica* and was published there the next year (Ralph L. McNutt et al., 2019).

9.1.3. First Annual Interstellar Probe Exploration Workshop

The 1st Interstellar Probe Exploration Workshop was held on 10–12 October 2018 at the Explorers Club in NYC. This first meeting was “invitation only” because of limited meeting room at the club. The agenda is shown in Figure 9-1. There were 46 presentations plus discussion sessions over the course of 2.5 days to a capacity crowd of ~80 attendees.

HUMANITY'S JOURNEY TO INTERSTELLAR SPACE

INTERSTELLAR PROBE

Interstellar Probe Exploration Workshop, Explorers Club, NYC, 10-12 October, 2018.

Day 1

Time	Duration	Title	Presenter	Chair
11:00	0:15	Welcome and Introductions	Michael V. Paul	Michael V. Paul
11:15	0:45	Interstellar Probe History and Overview	Ralph McNutt	|
12:00	0:45	**Lunch in Room**		|
12:45	0:15	NASA HQ Perspective	Arik Posner	|
13:00	0:30	Outbrief of Engineering Analysis	Michael V. Paul	|
13:30	0:30	NASA SLS: Enabler of Interstellar Probe	Rob Stough	|
14:00	0:30	Interstellar Probe Team Work	Janet Vertesi	|
14:30	0:15	Scope, Format and Outcome of Workshop	Pontus Brandt and Kathy Mandt	|
14:45	0:10	**Coffee**		|
15:05	0:10	Helio/LISM - Introduction	Elena Provornikova	Elena Provornikova and Pontus Brandt
15:20	0:10	The Global Heliosphere	Merav Opher	|
15:30	0:10	Global Heliospheric Structure in ENAs	Robert DeMajistre	|
15:40	0:10	Interstellar O and O+ Flows	Jee-Woo Park	|
15:50	0:10	Ion and Neutral Gas Analyzer	Nicholas Paschalidis	|
16:00	0:10	Sources of Heliospheric ENAs	Eberhardt Moebius	|
16:10	0:10	Solar-wind, Pickup, Suprathermal, Energetic Ion Comp.	Mihir Desai	|
16:20	0:10	Characterizing Thermal Plasma	Michel Blanc	|
16:30	0:10	Interstellar Gas Composition	Stefano Livi	|
16:40	0:10	Ly-alpha Spectrograph	Eric Quemerais	|
16:50	0:10	Collisionality of VLISM	Parisa Mostafavi	|
17:00	0:10	Measuring Interstellar Magnetic Fields	Adam Szabo	|
17:10	0:10	Radio and Plasma Waves on the Interstellar Probe	Bill Kurth	|
17:20	0:10	Astrophysics Connection	Michel Blanc	|
17:30	0:05	Wrap-Up	Michael V. Paul	
17:35		Adjourn Day 1		

Day 2

Time	Duration	Title	Presenter	Chair
8:30	0:30	Coffee and Recap	Elena Provornikova	Elena Provornikova and Pontus Brandt
9:00	0:10	In-Situ Investigations of the ISM	Bob Wimmer-Schweingruber	|
9:10	0:10	Particle Measurements on the Interstellar Probe	George Gloeckler	|
9:20	0:10	Science of Space Weather Along the Way	Kelly Korreck	|
9:30	0:10	Galactic Cosmic Ray Anisotropies	Matt Hill	|
9:40	0:20	**Coffee**		
10:00	1:00	Discussion Session - Helio/LISM	All	Elena Provornikova and Pontus Brandt
11:00	0:20	Team Photo		
11:20	0:45	**Lunch in room**		
12:05	0:10	Circum-Solar Debris Introduction	Casey Lisse	Casey Lisse and Andrew Poppe
12:15	0:10	Solar System Debris Disk	Andrew Poppe	|
12:25	0:10	Transformative Astrophysics Measurements	Michael Zemcov	|
12:35	0:10	Astrophysics With an Interstellar Probe	Charles "Chas" Beichman	|
12:45	0:10	Presentation	Reserve	
12:55	0:10	Measurement of Dust in the Interstellar Medium	Kelvin Long	|
13:05	0:10	Dust Measurements On Board an Interstellar Probe	Jamey Szalay	|
13:15	0:20	**Coffee**		
13:35	1:00	Discussion Session - Debris Disk	All	Casey Lisse and Andrew Poppe
14:35	0:10	KBO/Planetary/Exoplanets - Introduction	Kirby Runyon and Abi Rymer	Kirby Runyon and Abi Rymer
14:45	0:10	Planetary and KBO Targets in 2030-2050	John Cooper	|
14:55	0:10	Ice Giants Science Opportunities	Kathy Mandt	|
15:05	0:10	KBO and (Exo) Planetary Science Opportunities	Kirby Runyon	Abi Rymer and Kirby Runyon
15:15	0:10	Hypothetical Planet X Orbital Paramaters and Science	Elizabeth Bailey	|
15:25	0:10	Exploring Exoplanets from the Interstellar Medium	Lou Friedman	|
15:35	0:10	Earth as an Exoplanet	Sonny Harman	|
15:45	0:10	Trade-offs at the Solar Gravity Lens Focal Point	Steinn Sigurdsson	|
15:55	0:05	Dinner Logistics	Michael Paul	Michael Paul
16:00		Adjourn Day 2		
18:00		Cocktail Hour		
19:00		Dinner and Public Panel		

Day 3

Time	Duration	Title	Presenter	Chair
8:30	1:00	KBO/Planetary/Exoplanets - Discussion Session	All	Kirby Runyon and Abi Rymer
9:30	0:45	Science Summary Discussion	All	Pontus Brandt and Kathy Mandt
10:15	0:30	**Coffee**		
10:45	0:45	Model Payload Discussion	All	Ralph McNutt and Pontus Brandt
11:30	0:30	Next Steps and Actions	Michael Paul	Michael Paul
12:00	1:00	**Lunch in Room**		
13:00		Adjourn Meeting		

Figure 9-1. The 1st Interstellar Probe Exploration Workshop drew broad support from a diverse set of science and engineering experts.

Finally, for CY 2018 there was a special session on Interstellar Probe at the 2018 AGU Fall Meeting of the AGU, held 10–14 December 2018 in Washington, DC. Session SH32C, "The Interstellar Probe Mission: Study Findings and Next Steps I" (held on 12 December 2018 from 10:20 to 12:20) consisted of 10 talks. A poster session, Session SH33C, "The Interstellar Probe Mission: Study Findings and Next Steps Posters" (also held on 12 December but from 13:40 to 18:00) consisted of 18 poster presentations.

9.2. Stage 2: Concept Development Study (2019)

9.2.1. Presentation Efforts and Community Engagement

On 27 February 2019, the Interstellar Probe idea was introduced to the space nuclear community as a (small) part of the keynote dinner address at the Nuclear and Emerging Technologies for Space (NETS) meeting held at Pacific Northwest National Laboratory in Richland, Washington.

In the second quarter of fiscal year (FY) 2019, the government shutdown (midnight EST on 22 December 2018, until 25 January 2019 [35 days]) led to a depletion of funds and a significant delay in the study team's out-brief of the initial feasibility study to the leadership at the NASA Heliophysics division. On 7 March 2019, the details were delivered by the study team to the Heliophysics leadership at NASA Headquarters (meeting 2–4 p.m. in MIC 7A [7H41]). Although NASA had returned to operations, the disruption of the shutdown continued to delay resumption of the study effort, even though presentations and meetings continued. This included an invited presentation as part of a panel on "Future Directions in Heliophysics" at the 2019 Goddard Memorial Symposium of the American Astronautical Society on 21 March 2019 in Silver Spring, Maryland.

There were a variety of other presentations, including two poster presentations at the 50th Lunar and Planetary Science Conference (LPSC) in The Woodlands, Texas, on 19 March 2019. There was also a poster-paper presentation on 11 April 2019 at the European Geosciences Union (EGU) General Assembly in Vienna, Austria. Interstellar Probe was also briefed to the Outer Planets Assessment Group (OPAG) at their meeting in Washington, DC, on 24 April 2019.

Members of the study team were invited to Moscow to participate in a workshop, "Perspective of the Global Heliospheric Studies: Open Questions and Future Space Missions (Including Interstellar Probe)," sponsored by the Center of Advanced Studies of the Russian Academy of Sciences, Moscow, Russia, 25 May 25 to 1 June 2019. Attendance was approved by NASA, and an amendment was provided to the initial task order (then out of funds) on 21 May 2019 to cover attendance (Amendment/Modification Number P00003).

With negotiations in progress for additional funding, the team accepted an invitation from the organizers of a special session (ST05,-"From the Heliosphere to Interstellar Exploration") at the 16th Annual Meeting of the Asia Oceania Geosciences Society (AOGS) held 28 July to 2 August 2019. The team provided the lead talk of that session on 1 August 2019 in Singapore. A paper on the engineering status was delivered at the American Institute of Aeronautics and Astronautics (AIAA) Propulsion and Energy 2019 Forum (19–22 August 2019 in Indianapolis, Indiana) (Paul et al., 2019).

Invited talks were also delivered in Toulouse, France, on 11 September 2019 at the Horizon 2061 meeting (5–7 June 2019) and in a special session on "Interstellar Probe: Science, Mission Designs, Opportunities and Challenges" on 17 September 2019 at the EPSC-DPS Joint Meeting 2019, held in Geneva, Switzerland, on 15–20 September 2019. At the latter meeting, there were four talks total and one poster presentation on Interstellar Probe.

This includes all of the presentation venues between the start of funding and the end of FY 2019 (30 September 2019). The second workshop and other meetings during the end of CY 2019 are covered in the 2020 report.

9.2.2. Task Order Increase in Value and Lengthened Period of Performance

Only days before departure for Singapore for the Asia Oceania Geosciences Society (AOGS) meeting, funding was augmented (per Amendment/Modification Number P00005 of 25 July 2019). This action changed the end of the period of performance (beginning 13 June 2018) from 30 June 2019 to 30 April 2022. The obligated funding at that point was estimated to cover the period of performance through 31 July 2020.

This augmentation allowed the team to resume already planned conference attendance and science-driven development, while also ramping up the corresponding engineering effort. The latter also included the negotiation and issuance of two subcontracts: (1) to Advanced Ceramic Fibers (ACF) LLC (of Idaho Falls, Idaho) and (2) to the Center for Advanced Life Cycle Engineering (CALCE) at the University of Maryland.

ACF was selected to help extend the materials and processes used in the Parker Solar Probe thermal protection system (TPS) to the higher temperatures that would be encountered in a solar Oberth maneuver. This effort included application of some of ACF's patented processes to determine limiting temperatures and outgassing rates of the state of the art of ultra-high-temperature (UHT) materials.

CALCE was selected to bring their well-recognized expertise as "reliability science leader in the areas of failure mechanism identification and modeling, accelerated test methods, prognostics and health management approaches, supply chain management techniques, as well as the application of artificial intelligence for remaining life and fault prediction of electronic devices and assemblies"[3] to the problem of designing ab initio a scientific spacecraft with a design lifetime of 50 years. See CALCE's website for more information: https://calce.umd.edu/about-calce.

9.2.3. Organization, Tasks, and Baseline Schedule

The 2019 effort built on the work begun in June 2018 by expanding the engineering and the scientific discussion to a concept of operations level. The second workshop held in fall 2019 was planned so as to allow the engineering team to set parameters for the size and scope of notional science instruments, data volume, operational sequencing, and mission phases. These inputs, in

[3] Description from https://calce.umd.edu/about-calce

turn, will allow upgrading the initial "form and fit" of the example New Horizons spacecraft (as discussed in section 7) to a "self-consistent" Interstellar Probe engineering design.

The study team, led by Principal Investigator (PI) Dr. Ralph L. McNutt, Jr. (APL), is staffed by APL employees and subcontractors. The team draws on many collective decades of experience designing, building, and flying exploration space systems. All of these people have some level of experience with actual flight hardware, and most have supported and/or continue to support the New Horizons and Parker Solar Probe, development, build, checkout, and science operations. In addition, many people who are *not* APL staff have contributed to the effort, augmenting the outcome with their expertise and bringing a wider perspective to the current effort.

9.2.3.1. Study Team Organization

The study team has been organized along the lines of a flight mission to ensure that all elements of the conceptual flight system are well represented. The funding for this team is also organized by work breakdown structure (WBS) elements in a flight-mission-like fashion per NASA practices to allow traceability from this study.

The organization chart is shown in Figure 9-2. Boxes shaded light blue indicate APL-centric development tasks, which are also populated by APL personnel. Boxes shaded light orange indicate external personnel and/or activities interfacing with the external science and technical community; some of the latter are also led by APL personnel.

9.2.3.2. Interaction with NASA Marshall Space Flight Center (MSFC)

Significant contributions from MSFC (no exchange of funds basis) have been key enablers for this study. Informal conversations were initiated in 2017 and continued at the 2018 IAC in Adelaide, Australia. The effort that began there was completed in September 2019, submitted for public clearance in December 2019, and cleared for release at the end of January 2020 (Stough et al., 2019). Details are provided in footnote 4 (in section 7.3.1). This provides the baseline for all launch vehicle studies currently envisioned that use the SLS.

9.2.3.3. Baseline Study Schedule

The baseline study schedule is shown in Figure 9-3. This provides a rollup of top-level tasks in this study. The percentages are approximately how much of the task is complete as of 5 October 2020. The quarters are referenced to the displayed calendar years.

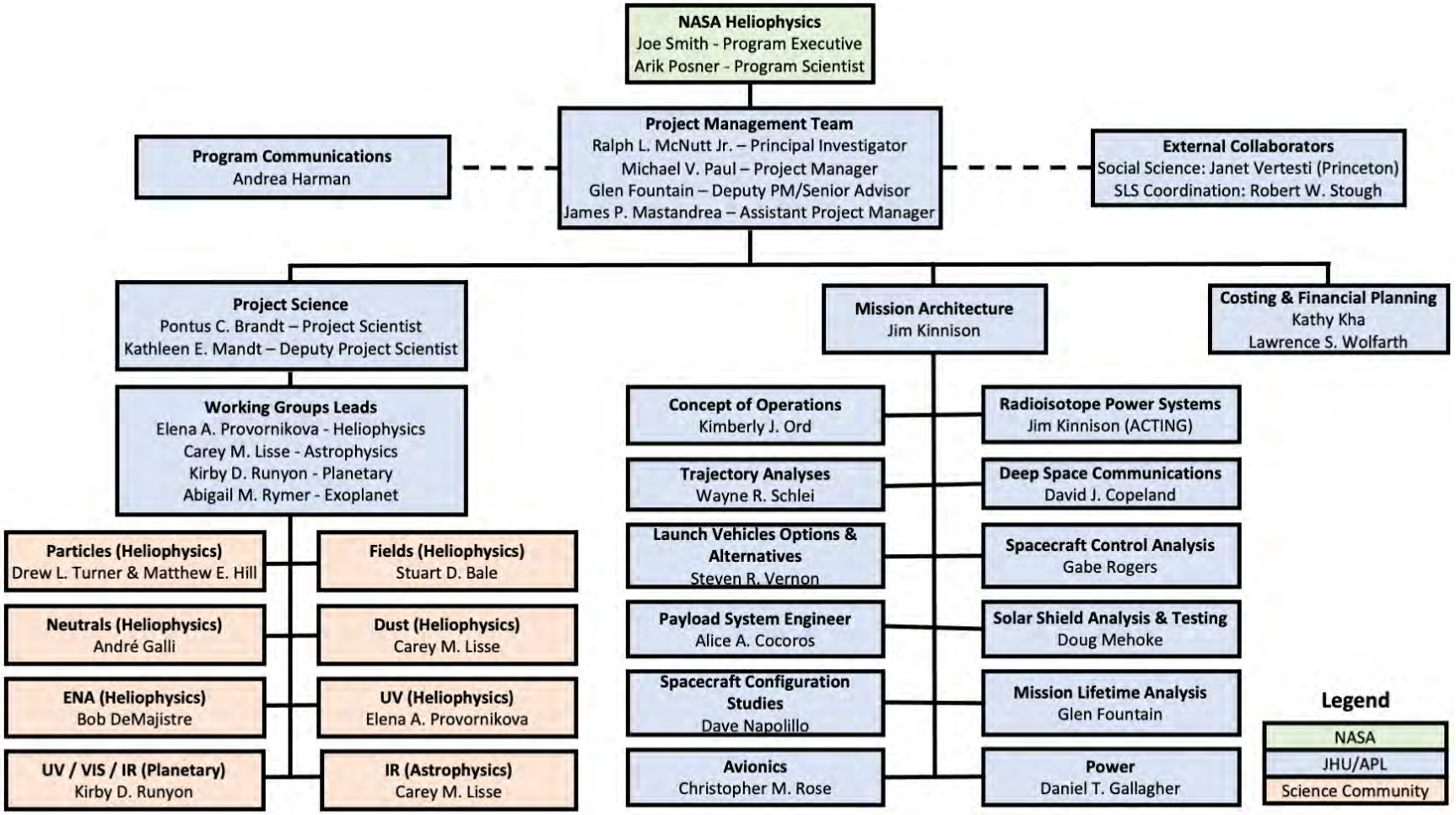

Figure 9-2. Organization chart of the current study. Most of the structure could be similar to or the starting point for that of an actual flight project.

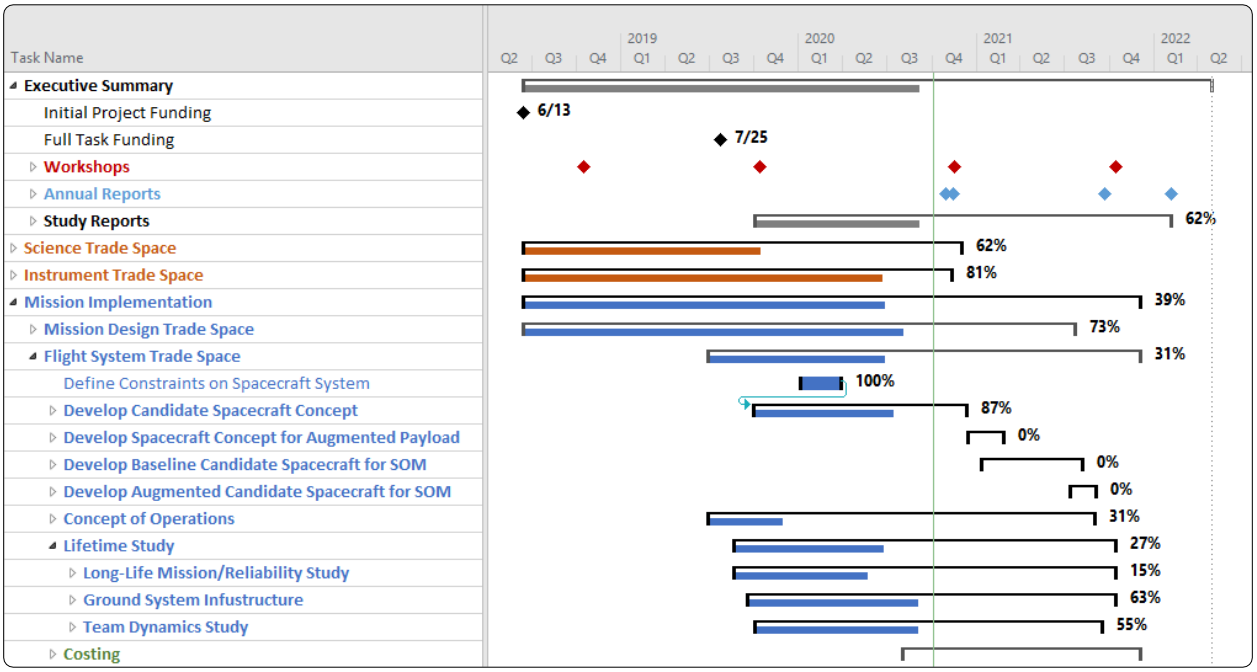

Figure 9-3. Top-level task schedule for the study. The tasks are planned and sequenced to provide for all final reporting to be delivered no later than the first CY quarter of 2022.

As noted previously, original funding for this task was provided on 13 June 2018, but in July 2019, the task order was increased in scope and duration per the Interstellar Probe Next Stage Concept Development contract modification. The first funding portion of the new task order, which is represented on the calendar as "Full Task Funding," was received 25 July 2019. The final funding portion is planned to be delivered in 2021.

9.2.4. Outreach Opportunities in CY2019

The Keck Institute for Space Studies (KISS) held a workshop in 2014–2015 with a smaller group of researchers who considered a longer mission timeline (Alkalai et al., 2017; Stone et al., 2015; Weinstein-Weiss et al., 2018). Building on the historic body of work on outbound exploration missions, the KISS study began a diverse, broad, science-community-wide effort to focus on a near-term interstellar probe mission. This pragmatic approach ensures that all points of view on science goals, measurements, mission implementation, and formal requirements are considered.

Outreach opportunities in CY 2019 are shown in Table 9-2.

Table 9-2. Targeted and Planned Activities for CY 2019 (as of April 2018)

Meeting	Date(s)	Venue	Presentation(s)
The Space Astrophysics Landscape for the 2020s and Beyond	1–3 April	William F. Bolger Center, Potomac, Maryland, USA	
EGU General Assembly	7–12 April	Austria Center Vienna, Vienna, Austria	One presentation accepted

Meeting	Date(s)	Venue	Presentation(s)
Perspective of the Global Heliospheric Studies: Open Questions and Future Space Missions	27–31 May	Uzkoe Hotel, Moscow, Russia	Four invitations
13th Low-Cost Planetary Missions Conference	3–5 June	Grand amphithéatre de l'Université Paul Sabatier, Toulouse, France	
11th IAA Symposium on the Future of Space Exploration	17–19 June	Politecnico di Torino – Lingotto Campus, Torino, Italy	
AbSciCon 2019	24–28 June	Hyatt Regency Bellevue, Bellevue, Washington, USA	
16th International Planetary Probe Workshop	8–12 July	Oxford University, Oxford, UK	Abstract submitted
AOGS 16th Annual Meeting	28 July – 2 August	Suntec Singapore Convention & Exhibition Centre, Singapore	One invited and accepted
EPSC-DPS Joint Meeting 2019	15–20 September	Centre International de Conférences de Genève (CICG), Geneva, Switzerland	Session proposal submitted
AIAA/SAE/ASEE Joint Propulsion Conference	19–22 August	JW Marriott, Indianapolis, Indiana	Abstract accepted
Interstellar Probe Exploration Workshop	October	Explorers Club, New York City, USA	In planning
70th International Astronautical Congress	21–25 October	Walter E. Washington Convention Center, Washington, DC, USA	Special session proposal and abstracts submitted
AGU Fall Meeting 2019	9–13 December	Moscone Center, San Francisco, California, USA	Special session proposal and abstracts to be submitted

Of these 13 events, all were attended with presentations save (1) The Space Astrophysics Landscape for the 2020s and Beyond, (2) the 13th Low Cost Planetary Mission Conference, (3) the 11th IAA Symposium on the Future of Space Exploration, (4) AbSciCon 2019, and (5) the 16th International Planetary Probe Workshop. These are all well-attended events, and several of the team's appearances resulted in invitations for follow-on presentations at future conferences.

9.3. Mission Study Relevance

The study team's work in 2019 resulted in a full "menu" of options, some combination of which could be technically realized by an interstellar probe mission during the time span of the next Solar and Space Physics Decadal Survey. Previous work had provided an updated, notional science traceability matrix (STM) as well as notional instruments, which could accomplish some of the required measurements. This survey of the state of the art in instrumentation (i.e., technology readiness level [TRL] of 6 or higher) suggests that a full "wish list" of science instrumentation may be too high by a factor of ~2–3 in mass and power. The situation is not unlike that encountered in the previous Interstellar Probe Science and Technology Definition Team (IPSTDT) work of 1999 or in

equivalent NASA studies conducted for various similar studies for Parker Solar Probe (e.g., Axford et al., 1995; Feldman et al., 1989; Gloecker et al., 1999; McComas et al., 2005, 2008).

Previous work also considered a "slate" of ideal mission trajectories to map out "performance" versus launch dates, where "performance" was quantified by the asymptotic escape speed from the Sun's gravitational field. This included a first cut across three mission options, all of which required close flybys of the planet Jupiter. A total of 31 launch-stage configurations were identified, but these were not thoroughly vetted across all possibilities because of lack of time and funding. In addition to a fairly in-depth consideration of the SLS Block 1B Cargo configuration, initial conversations were carried out with Blue Origin and Airbus. This follow-on work has enabled more detailed discussions with launch vehicle suppliers and kick-stage/upper-stage vendors as well as more robust performance estimates, e.g., by looking at radiation exposure limits at Jupiter, keep-out zones for trajectories due to Jupiter's dust rings, limitations imposed by realistic launch windows and delivery of radioisotope power systems (RPSs), and consideration of a variety of targeting and mission strategies.

All such studies help to better inform the next Solar and Space Physics Decadal Survey, other communities (e.g., the Outer Planets Assessment Group [OPAG]), and competed NASA panels such as a future potential Science Definition Team (SDT) and/or Science and Technology Definition Team (STDT), which NASA may or may not choose to convene in the future in considering an interstellar probe.

The team's progress and output produced sufficient interest to garner an invitation to provide a briefing on the study to date to a joint session of the Committee on Solar and Space Physics (CSSP) and the Committee on Astrobiology and Planetary Sciences (CAPS). The briefing took place on 27 March 2019 in Washington, DC, as part of the Space Science Week meetings of space science discipline committees of the Space Studies Board (SSB).

9.4. Building on the Parker Solar Probe Experience

Given the institutional experience of APL (dating back to 1977) and of the PI of this proposal (dating back to 1993, cf. R. L. McNutt et al. (1995)) with Parker Solar Probe, we believe it important in the proposed work to continue to use the lessons of Parker Solar Probe development up through the last Heliophysics Decadal Survey. The initial idea of a solar probe only predates that of an "outer-solar-system probe" by ~2 years (Chamberlain et al., 1958; Haviland, 1958) (and appendix of R. L. McNutt, Jr. et al. (2017)), yet the former was some 60 years in the making and went through four SDT/STDT studies before the final such study, begun in fall 2007, led to the basic configuration that became Parker Solar Probe, which was successfully launched on 12 August 2018 and came in under budget. That effort began as a 1-year engineering study in CY 2002 with a notional launch date of 2010.

The stated core science goals changed little from the Solar Probe Science Workshop of May 1977 through the final SDT exercise, which concluded in April 2008. Some of the most technically diffi-

cult investigations were dropped, namely the direct measurement of the solar gravitational quadrupole moment (J_2), a very-high-resolution imaging system for resolving small-scale photospheric features, and using the tracking system to search for low-frequency gravitational waves. Two other goals, the measurement of solar neutrons and interplanetary dust near the Sun, were also considered. The penultimate STDT report considered a white-light imager for the baseline payload to view the solar poles (McComas et al., 2005); the trajectory change that followed from the elimination of an RPS for the power supply led to the deletion of that instrument in the final STDT report (McComas et al., 2008). NASA elected not to select either a dedicated neutron detector or a dust detector for the final payload as flown.

9.5. Next Steps

This experience maps fairly well into providing for early, robust feasibility assessment of the widest set of interstellar probe options that could be selected from by a future STDT and/or successfully used for reference by Decadal Survey panel members. Appropriate items for proposed and continued study include, but are not limited to, the following:

1. Further compilation of an appropriate "catalog" of high-TRL instrument types either previously flown or in advanced development for flight for missions now in flight development. This activity began with many of the talks and posters, both invited and contributed, at the (then) most recent (2018) COSPAR and AGU Interstellar Probe sessions and at the (first in 2018) Mission Science Definition Workshop.

2. Higher-fidelity studies of the three identified mission options, including closure of staging designs for a variety of launch vehicles (including commercial), and higher-fidelity analysis of deep-space "storage" of kick stages (Options 2 and 3).

3. In-depth exploration of coating materials, technology, and manufacturability for cost and lower mass for the TPS of Option 3.

4. Case studies of sample mission targets and payload example masses across the mission options, including finite launch windows and changes in overall spacecraft mass beyond the notional "New Horizons"-like spacecraft used in the ideal studies just completed.

5. Further and continuing engagement of MSFC as the SLS architecture and implementation plans mature. This also involves the early introduction of the SLS team to appropriate understanding of Department of Energy (DOE) and other NASA and national policy issues that arise for a launch with an RPS. Because a high-energy launch vehicle that can be nuclear certified by the end of the decadal period is enabling for Interstellar Probe, as is the Next-Generation Radioisotope Thermoelectric Generator (RTG), early identification of issues is of importance to a robust mission study. The Multi-Mission RTG (MMRTG) and the enhanced MMRTG (eMMRTG) both have insufficient design lifetimes (17-year design life) for Interstellar Probe. As a backup, a refurbished general-purpose heat source (GPHS) RTG with new $^{238}PuO_2$ fuel may prove acceptable, but further engagement of appropriate people at both NASA and DOE will be required.

6. Assessment of downlink capabilities using Ka-band and presumed Deep Space Network (DSN) assets as now projected for 2030 and beyond. This will draw on hardware implementation on, and flight experience with, the telecommunications capabilities being used in flight on both the ongoing New Horizons and Parker Solar Probe missions.

7. A comprehensive mission engineering report and programmatic cost estimate using an experienced APL team.

9.6. Section 9 References

Alkalai, L., Arora, N., Turyshev, S., Shao, M., Weinstein-Weiss, S., Opher, M., Redfield, S. (2017) *A Vision for Planetary and Exoplanets Science: Exploration of the Interstellar Medium - The Space Between the Stars*. Paper presented at the 68th International Astronautical Congress, Adelaide, Australia.

Axford, W.I., Feldman, W., Forman, M.A., Habbal, S.R., Ling, J.C., Moses, S., Title, A., Woo, R., Young, D.T. (1995) *Close Encounter with the Sun - Report of the Minimum Solar Mission Science Definition Team, Scientific Rationale and Mission Concept*. Pasadena, CA: Jet Propulsion Laboratory.

Chamberlain, J.W., Kraushaar, W., Vestine, E.H., Winckler, J., Van Allen, J., Simpson, J.A. (1958) *Interim Report fo the Space Science Board from Committee 8, Physics of Fields and Particles in Space*

Feldman, W., Mellott, M., Tsurutani, B., et al. (1989) *Solar Probe Scientific Rationale and Mission Concept: A Report of the 1989 Solar Probe Science Study Team* (JPL D-6797). Pasadena, CA:

Gloecker, G., Feldman, W., Habbal, S.R., et al. (1999) *Solar Probe: First Mission to the Nearest Star*. Laurel, MD: The Johns Hopkins University Applied Physics Laboratory.

Haviland, R.P. (1958, 25-30 August) *Considerations of the Solar Probe.* In IXth International Astronautical Federation Congress, Springer-Verlag, Amsterdam.

McComas, D.J., Acton, L.W., Balat-Pichelin, M., et al. (2005) *Solar Probe: Report of the Science and Technology Definiiton Team*. Greenbelt, MD: NASA.

McComas, D.J., Acton, L.W., Balat-Pichelin, M., et al. (2008) *Solar Probe Plus: Report of the Science and Technology Definiiton Team*. Greenbelt, MD: NASA.

McNutt, R.L., Reynolds, E.L., McAdams, J.V., Bokulic, R.S., Bhatnagar, V., Williams, B.D., Willey, C.E., Myers, R., Gefert, L.P. (1995) Mission to the Sun - The Solar Pioneer. *Anticipating a Solar Probe* 17(3), 21-30. Retrieved from <Go to ISI>://WOS:A1995BD47J00003

McNutt, R.L., Wimmer-Schweingruber, R.F., Gruntman, M., et al. (2019) Near-Term Interstellar Probe: First Step. *Acta Astronautica* 162, 284-299. doi: https://doi.org/10.1016/j.actaastro.2019.06.013

McNutt, R.L., Jr., Wimmer-Schweingruber, R.F., Gruntman, M., Krimigis, S.M., Roelof, E.C., Zank, G.P., Stone, E.C., Brandt, P.C., Vernon, S.R. (2017) *Near-Term Exploration of the Interstellar Medium*. Paper presented at the 68th International Astronautical Congress, Adelaide, Australia.

Paul, M.V., McNutt, R.L., Stough, R.W., Hitt, D., Vernon, S.R., Alvarez, E., Brandt, P.C., Lathrop, B. (2019) *Enabling a Near-Term Interstellar Probe with the Space Launch System*. Paper presented at the AIAA Propulsion and Energy 2019 Forum. https://arc.aiaa.org/doi/abs/10.2514/6.2019-4048.

Stone, E., Alkalai, L., Friedman, L., et al. (2015) *Science and Enabling Technologies for the Exploration of the Interstellar Medium*. Pasadena, CA:

Stough, R.W., Hitt, D., Holt, B., Philips, A., Patrick, M. (2019) *Supporting Material for APL's Interstellar Probe Final Report* (M20-7868). NASA Technical Reports Server:

Weinstein-Weiss, S., Rayman, M., Turyshev, S., et al. (2018) A Science-Driven Mission Concept to an Exoplanet. *Journal of the British Interplanetary Society* 71, 140-150.

10. Summary

In 2019, the Interstellar Probe study was funded through approximately April 2020 and approved for the funding proposed through the end of April 2022. This allowed the study team to advance significantly the discussion of science goals and corresponding instrument candidates and to support the remainder of the tasks associated with spacecraft architecture and lifetime analysis. Given that the level and timing of funding was assured, the team could develop a more robust plan with appropriate milestones. The general plan, discussed above in section 9, has been in place for over a year (as of late 2020), and that plan continues to be the baseline for the study.

The first two study workshops (in 2018 and 2019) have provided forums for the science and engineering communities to provide input to the study. That input has resulted in the general goals described in section 2. Section 3 discusses the expansion of the study trade space by reviewing cross-divisional science objectives that might be leveraged by an Interstellar Probe spacecraft as it traverses regions of the solar system on its way to the very local interstellar medium. Instrumentation is divided into two categories: a baseline (heliophysics only) mission and an augmented payload capable of meeting other cross-divisional science objectives, including those of both planetary science and astrophysics. A survey of instrumentation on past missions provides a basis for identifying instrument options for an Interstellar Probe baseline mission. Candidate instrumentation for the augmented payload will be developed in late 2020 and early 2021. As examples, a science traceability matrix and model baseline payload are discussed in sections 5 and 6. These have been used as a starting point, as the spacecraft architecture is developed and mission-design constraints are identified in the next phase of the study (in 2020 and 2021). The traceability from science objectives to corresponding measurement requirements discussed in this report will be further refined in 2020 and then used to begin the discussion of what could constitute notional mission success.

Options for mission trajectories and how those options would impact science options are discussed in section 4. As appropriate for this study, the rationale for choosing an asymptotic fly-out direction is based on data collected by the Voyagers, New Horizons, IBEX, and Cassini. Data from the latter two missions suggest trajectories that would allow in situ measurements of the “ribbon” or “belt” of energetic neutral atom (ENA) emission that intersects the ecliptic plane. In addition to satisfying the primary objectives of an Interstellar Probe mission, the trajectory could be designed to fly by one of the dwarf planets located in the Kuiper Belt (an augmented mission option). All of these options will be considered as the trajectory trade space is analyzed in more detail in 2020.

The historical and technical background that motivates the current Interstellar Probe study, the analysis of mission-design options, and, from that, a set of guidelines for down-selecting “pragmatic” design options are provided in section 7. Section 11 contains a detailed history of the Interstellar Probe concept, beginning with the growth of human understanding of the scale of the Earth to the distance to the nearest stars to put the idea of an interstellar probe into perspective.

The evolution of the idea of an interstellar probe as a practical space science mission, starting with the Simpson Committee's 1960 report, through its many iterations leads into the review of mission-design options. With the supporting analyses, these define the boundaries of practical solutions to the mission-design problem and the resulting trade spaces as input into the spacecraft architecture studies to be undertaken in 2020. The general trajectory options are a Jupiter flyby directly onto a solar system escape trajectory and a solar Oberth maneuver. The Jupiter flyby can be either passive or active (if an upper stage is carried until the spacecraft reaches Jupiter). Initial analyses have provided the results of a parametric study for multiple configurations of upper stages showing fly-out velocities for a passive Jupiter flyby as a function of launch energy (C_3). For example, a C_3 of ~300 km^2/s^2 would allow a fly-out velocity of > 7 au/year. Similar analyses were performed (and documented in section 7) for a powered Jupiter flyby and for a solar Oberth maneuver. These last two options have engineering challenges, which affect the attainable fly-out asymptotic speeds. They will be analyzed in more detail and documented in 2020 and 2021.

In addition to the development of the trade space defined by science and the trajectory, an additional requirement of the study was specified to be a flight duration of 50 years. This duration allowed sufficient time for the spacecraft to reach the very local interstellar medium (distances of >120 au, the distance at which both of the Voyagers are generally thought to have passed the heliopause) and penetrate that region significantly past the projected distance anticipated for Voyager 1 (not greater than ~180 au from the Sun). Such distances are well within the mission-design boundary conditions defined in section 7. A lifetime study team has been established to understand better the challenges of a 50-year (by design) mission. This element of the Interstellar Probe study first focused on the "human element" (section 8) by drawing on experiences from the missions of Voyager and Cassini as well as from the associated academic literature. The "human element" work will be continued in 2020 to distill the lessons to be garnered from this work into recommendations for mitigating the challenges implied for a 50-year mission. Two other aspects of the lifetime study task are to understand better the spacecraft reliability and ground sustainment challenges for an Interstellar Probe mission. These two elements of the lifetime study were begun near the end of 2019, and their status will be documented in the 2020 report.

The 2019 effort has set the stage for trade studies to be performed in 2020 and 2021 to understand what options within the Interstellar Probe trade space are technically viable. With these options in hand, a cost estimate of a number of mission options will be developed in 2021. Cost estimates of a mission with the baseline instrumentation and passive Jupiter flyby and a mission with an augmented payload and passive Jupiter flyby will be developed. Depending on technical feasibility, both active Jupiter flybys and missions using a solar Oberth maneuver will also be costed.

11. Appendices: Background and Beginnings, Oberth Maneuver, and Escaping the Solar System

11.1. Background and Beginnings

11.1.1. How Far to a Star?

What is rarely appreciated is how far our knowledge of distances has come over just the last century. In particular, actually knowing how far away even the nearest stars are is relatively new knowledge.

As of the dawn of the 21st century, the scale of the universe is fairly well known. Details continue to be worked and surveys continue, but in terms of the basic distance ladder, from nearer stars directly measured, to absolute luminosity from Cepheid variable stars, to the standard candle of Type Ia supernovae, to the recession of galaxies and Hubble's Law, the scales out to hundreds of megaparsecs are well known and understood (cf., e.g., Wikipedia, 2020c).

This state of knowledge has been hard won over many years and operating at the edge of measurement technology. The story of the calculation of the size of the Earth by Eratosthenes is well known, although his book was lost in the fire of the library at Alexandria. The report of the story is known through a textbook by Cleomedes, who lived at least a century later and placed Eratosthenes' calculation as having been made ~240 BCE.

Distances to, and the sizes of, the Moon, Sun, and planets were the subject of speculation, which was accelerated by the acceptance of the Copernican, heliocentric model of the solar system with the then-known six planets. With Kepler's Laws and Newton's insights and mathematical theory of gravity and its consequences for planetary motion, the relative locations of the planets were well known by the early 18th century, but the absolute sizes of the planetary orbits continued to be debated.

The astronomer Edmund Halley recognized that the observation of the transit of the planet Venus across the disk of the Sun by Horrocks in 1639 (cf. Chapman, 1990) revealed a way forward.

Halley noted that by observing the upcoming transits of Venus in 1761 and 1769 from widely separated locations of the Earth with the proviso that both ingress and egress be observed by the same observer, the parallax of the Sun, and hence distance thereto, could be measured (Halleio, 1714; see also translation into English at Halley, 1809). The observations made during the transit of 1769 were of better character than those of 1761. Lalande (de Lalande, 1770a, 1770b, 1771) and others (M. K. Anderson, 2012; Vaquero & Vázquez, 2009) published coordinated calculations. By 1771, Hornsby (Hornsby, 1771) had provided a succinct summary of the various attempts and evaluation of the solar distance as "93,726,900 English miles." More data and further refinements were made possible by the Venus transits in 1874 and 1882 (Harkness, 1891).

With an accurate value of the solar distance from Earth, a baseline could be established for searching for the parallax of stars, and then inferring their absolute distances from those measurements. Criteria for efficiently looking for stellar parallaxes were given by Struve in 1837 (Perryman, 2012):

1. the star should be bright;
2. it should be moving with a large angular rate across the sky (although this could be a rapidly moving star at a large distance, it was more likely to be "nearby"); and
3. if the star was one of a binary pair, the two components should be well separated as judged by the time taken to orbit each other.

Struve presented a parallax measurement for the bright star Vega, close to the correct value, but skepticism prevailed until his analysis using far more observations was presented in 1840. Credit for the first successful measurement of a stellar distance went to Friedrich Bessel for his measurements of the star 61 Cygni, the fastest moving star in the plane of the sky visible without a telescope. The measurement yielded a distance of 10 light years (F. W. Bessel, 1838; Friedrich Wilhelm Bessel, 1839, 1840). Soon thereafter, Henderson provided a distance to Alpha Centauri from measurements made several years earlier but only more recently analyzed, after his return from the Cape of Good Hope, as well as for the brightest star Sirius (Henderson, 1840).

As with the initial measurements of Kuiper Belt Objects (KBOs) and exoplanets, initial stellar parallax determinations were hard won, with less than 100 observations by 1901. In the same way that charge-coupled devices (CCDs) have provided a revolution in modern astronomy, photographic plates provided a revolution as the 20th century dawned and helped to enable more rapid growth in the knowledge of stellar distances (Perryman, 2012).

Of interest with respect to the nearer stars is the discovery of the (still) fastest moving star in the plane of the sky as viewed from Earth, aptly still referred to as Barnard's Star (Barnard, 1916). Barnard discovered the star on photographic plates (it is not visible without a telescope), and it is a dim red dwarf. Given Struve's second criterion (for large proper motion), Barnard shared the location data with Russell, who derived a parallax of 0".70 ± 0".06, "which makes it nearer than any other known star except *α Centauri*" (Russell, 1917). A large parallax value was soon confirmed by Mitchell and others (Mitchell, 1917). Subsequent observations showed progression to a smaller value of 0".555 (Wilson, 1921), close to the modern value.

In 1915, Innes identified a faint star of large proper motion in the vicinity of Alpha Centauri (R. Innes, 1915). Voûte measured the parallax (Voûte, 1917), noted the similarity to that of Alpha Centauri, and suggested an association. Innes made a measurement of the parallax, announced that the star was closer to the Sun than Alpha Centauri, and so suggested the name "Proxima Centauri" (R. T. A. Innes, 1917). By 1928, the association was established and the name Proxima Centauri was established for the then-closest star to the Sun (Alden, 1928); that "closest" designation remains to this day.

One of the most difficult problems in the discussion of interstellar travel is providing an appropriate connection of the vast distances involved to "everyday" human experience. To provide this for the solar system "model" installed along the mall in Washington, DC, the "Voyage" project adopted a scale of 10 billion to one (Roman, 2020). That is, one astronomical unit, 149,597,870,700 m (IAU, 2012, 2020) is just under 15 m. The current best parallax for Proxima Centauri is 766.41 ± 0.91 mas (but see also the values listed in Benedict et al., 1999; Lurie et al., 2014), and hence at a distance of 1.3048 pc (1.3063 pc to 1.3032 pc), the corresponding range in light years (ly) is 4.2506 ly to 4.4207 ly. The corresponding "Voyage" model distance range is 4021 km to 4031 km, about the distance from Portland, Maine, to Vancouver, British Columbia (4026 km per (Time and Date AS, 2020b)). The corresponding "model speed of light" would be ~3 cm/s in the model. For the 40-ly goal set by Daniel Goldin in 1997 (to encompass 1000 stars), the scaled distance is 37,842 km—comparable to the ~40,000-km circumference of the Earth (hence 20 ly corresponds to 18,921 km, about the distance from Monaco to Wellington, New Zealand—18,948 km (Time and Date AS, 2020a).

It is against this backdrop that the discussion of realistic space missions must commence. But if this is the backdrop, the stage was already being set by a remarkable group of creative and inventive people as the 19th century turned to the 20th. And their ideas and insights were just as important in getting us to the present day of consideration of such missions to leave the solar system.

11.1.2. Voyages extraordinaires, Исследование мировых пространств реактивными приборами, Wege zur Raumschiffahrt

No one has ever thought that traveling to other stars—or even "just" planets—would be easy, but, that said, the physical realization is a lot harder still. Although the terminology "astronautics" was not introduced to the field by Robert Esnault-Pelterie until 1930 (Mike Gruntman, 2007), he in 1913 (Esnault-Pelterie, 1913), Robert H. Goddard in 1919 (Goddard, 1919), Konstantin E. Tsiolkovsky in 1903 (Tsiolkovskiy, 1967), and Herman J. Oberth in 1929 (Oberth, 1970), all working mostly in isolation, originated the field. Passage to a new generation was effected by mentorship: Friedrich A. Tsander (Zander) by Tsiolkovsky and Wernher von Braun by Oberth.

Of the four, Esnault-Pelterie, an aircraft designer and the fourth licensed pilot in France, used aeronautics and airplanes to approach rockets and astronautics. Goddard, Tsiolkovsky, and Oberth all approached rocketry and astronautics ab initio, but they had two things in common: Jules Verne and a dream of traveling to the stars.

History—the history of true events—is seldom simple, and this was certainly true of the evolution of Verne to his literary career. The keys were his notions of writing—and the long march to his literary debut; his idea "of inventing a new kind of novel, a 'Roman de la Science' ('novel of science'), which would allow him to incorporate large amounts of the factual information he so enjoyed researching in the Bibliothèque"; and his to-be publisher Pierre-Jules Hetzel's idea of the "Voyages extraordinaires (Extraordinary Voyages or Extraordinary Journeys)" series to which Verne was contractually bound (Wikipedia, 2020h). Of those, the key was the fourth, published in 1865: *From the Earth to the Moon: A Direct Route in 97 Hours, 20 Minutes* (French: *De la Terre à*

la Lune, trajet direct en 97 heures 20 minutes)" (Wikipedia, 2020d), a fictional novel of a large gun in Florida and a fictional Baltimore Gun Club.

Oberth read the book while recovering from scarlet fever in Italy while in his teens (NASA, 2010); Tsiolkovsky was at least partially inspired to write his 1903 tome to show that such a gun for space travel would not technically work ("The aspiration for the cosmic voyages was founded in me by the well known scientific fiction writer Jules Verne. He aroused my mind to work in this direction. Behind the desires, the activity of brain sprang up. Of course, it could have led to nowhere, if assistance from science had not been forthcoming" (Tsiolkovskiy, 1967); but the case of Goddard was more complicated.

Verne inspired H. G. Wells, who had captured the public imagination with his novel *The Time Machine* in 1895. With an education in biology, in speculating about the causes and consequences of something that depopulated London: "during a walk on nearby Horsell Common near his home in Woking, Surrey, 'there came to me suddenly a vivid picture, clean into my head, of the invaders just arrived in one of those inter-planetary cylinders which I borrowed from their inventor, Jules Verne.' For him, Mars was the obvious choice as it was the only planet like Earth. He acknowledged that the evolutionary process would make the Martians different, so he did not make them human. Finally, the heat-ray was used by Archimedes, and chemical black smoke was an old idea of Wells" (HistoryHouse, 2020). *The War of the Worlds* was published by Wells in 1898. Goddard read the novel, and on 19 October 1899, he began his own quest to begin the road to Mars (Lehman, 2020).

In the transition from the 19th to the 20th century, there was one other key ingredient, coming from research in basic physics. The beginning of that thread began with Becquerel's discovery of radioactivity in 1896 (Becquerel, 1896). This began the long road to nuclear physics with the discovery of polonium and the invention of the word "radioactivity" (Cai, 2008; P. Curie & Curie, 1898) and the discovery of radium (P. Curie et al., 1898) and its isolation and the identification of it as an element (Curie, 1902), followed by the isolation of the element itself (M. P. Curie & Debierne, 1910). The discoveries and new speculations came rapidly, including the identification of the activity of radium as due to transmutation of elements involving the ejection of extremely energetic helium nuclei (Rutherford & Soddy, 1902a, 1902b).

The possible applications for space travel were seized on immediately first by Tsiolkovsky and soon after by Goddard.

Tsiolkovsky's seminal work *Исследование мировых пространств реактивными приборами* "*Issledovaniye mirovykh prostranstv reaktivnymi priborami*," translated into English as "*Study of outer space by reaction devices*" (Tsiolkovskiy, 1967), was published in Russia (and in Russian) in 1903. This English collection version (also published together in the Soviet Union in 1967) is the translation of "Investigation of outer space by rocket devices" of 1911. In the section "Future of reactive devices" of that work, Tsiolkovsky notes (p. 185) (Moiseyev, 2015):

> It is thought, that radium, disintegrating continuously into more elementary matter, liberates from it particles of different masses, moving with amazing, unconceivable velocities, close to the velocity of light. For example, the helium atoms being released at this stage, move with a velocity of 30-100 thousands kilometers/second, the atoms of helium

> are four times heavier than the atoms of hydrogen; other little particles liberated by radium are 1000 times lighter than hydrogen, but they move with velocities of 150-250 thousand kilometers/second; the total mass of these particles (electrons) is considerably less than the mass of the atoms of helium. These velocities are 6-50 thousand times greater than the velocities of gases, flying out of the muzzle of our reaction pipe.
>
> Therefore, it [sic] it were possible to accelerate sufficiently the disintegration of radium or other radioactive bodies, (such are probably all the bodies), then its use might give-in similar other conditions, see formula (35) a velocity of the reactive device, by which access to the closest Sun (star) would come down to 10-40 years.
>
> Then, a pinch of radium (see formula 16) would be sufficient, to enable the rocket weighing a ton, to break all relations with the solar system.
>
> It is possible that future advancement of science will show, that all this, is far from reality but it is good that we can even now dream of it.
>
> It may be, that with the help of electricity, it will be possible by and by, to impart tremendous velocity to the particles, being ejected from the reactive devices. And now, we know, that cathode rays in Crook's tube, like the rays of radium, are accompanied by a flux of electrons, the mass of each of which, as we have mentioned, is 4000 times less than the mass of an atom of helium, and whose velocity reaches 30-100 thousand km/sec, that is, it is 6-20 thousand times the velocity of the common combustion products, flying out from our reaction pipe.

The problem, of course, with a "radium rocket" is that while the exhaust speed has the right magnitude, the effective mass ratio is exceedingly low (and the "engine" is extremely radioactive (Forward, 1996; Short & Sabin, 1959-60)).

On 14 January 1918, Robert Goddard initiated the discussion of interstellar travel when he asked: "Will it be possible to travel to the planets which are around the fixed stars, when the Sun and the Earth have cooled to such an extent that life is no longer possible on the Earth?" (Goddard, 1983). He posed an answer as well:

> To answer this question, it is necessary to answer two others; first, will it be possible to unlock, and control, intraatomic energy? and second, if the first cannot be answered in the affirmative, will it be possible to reduce the protoplasm in the human body to the granular ·state, so that it can withstand the intense cold of interstellar space? It would probably be necessary to desiccate the body, more or less, before this state could be produced. Awakening may have to be done very slowly. It might be necessary to have people evolve, through a number of generations, for this purpose….
>
> If it is possible to unlock, and to control, intra-atomic energy, or even to store up to great quantities of energy in artificial atoms, the transportation can be a comparatively simple matter.
>
> …If it is not possible to obtain and control atomic energy, hydrogen and oxygen, burned and ejected from a magazine rocket apparatus must be used, aided by solar energy, to get up speed, and leaving the Solar System with such a velocity that, at a great distance from the Solar System, the speed will be 3 to 1 0 miles per second. This will, of course, necessitate a very large apparatus, initially, unless solar energy can be used over a considerable time, to get up speed, either by passing through the Solar System from end to end, crossing as far from the Sun as possible, or spiraling outward until sufficient speed has been obtained.
>
> The pilot should be awakened, or animated, at intervals, perhaps of 10,000 years for a passage to the nearer stars, and 1,000,000 years for great distances, or for other stellar systems. To accomplish this, a clock operated by the change in weight (rather than by electric charges, which produce too rapid effects) of a radioactive substance, should be used. Any substances to be used as a spring should be tested for permanent set at low temperatures. It might be necessary to use the pressure of the gases generated by the radioactivity. This would amount to a radium alarm clock.

The later idea was explored in 1929 by J. D. Bernal (1969), who echoed these sentiments with the idea of a huge "world ship" that could take an appreciable fraction of humanity to another star system. The problem of the extinction of the Sun was also touched on by Tsiolkovsky by 1926. However, the quantitative magnitude of the problem was not addressed by Goddard, Tsiolkovsky, or Bernal.

The "world ship" idea (Figure 11-1) continued to surface ever so often both in futurist writings (Asimov, 1966; Cole, 1965) as well as in science fiction (Aldiss, 1960; Heinlein, 1965).

Figure 11-1. Hollowed out "world ship" for human space transport. External (left) and internal (right) views. Original artwork by Roy G. Scarfo and text by Dandridge M. Cole (Cole, 1965).

In reviewing a table of contents for a planned book *Flights to Other Planets and the Moon* in 1925, Tsander touches on relativity, atomic power, and interstellar flight for two chapter titles (Tsander, 1967):

> XII. Reaching other solar systems by atomic energy or special energy from decomposition of radium.
> XIII. Slowing of life and possibility of returning to earth alive after millions of years, by flying at velocity near the speed of light, according to Einstein's theory of relativity.
> Possibility of flying through all of interstellar space.

This is perhaps the first written reference of making use of relativistic speeds and time dilation to enable human flight within a lifetime between different star systems. In his 1929 essay, Bernal considered the speed issue in the context of his "world ships" (Bernal, 1969):

> Interstellar distances are so large that high velocities, approaching those of light, would be necessary; and though high velocities would be easy to attain—it being merely a matter of allowing acceleration to accumulate—they would expose the space vessels to very serious dangers, particularly from dispersed meteoric bodies.

Extensions of both the special and general theories of relativity to uniformly accelerated reference frames (Marder, 2008; Marsh, 1965) had been well known for over a decade by that time (Born, 1909; Kottler, 1914a, 1914b, 1916, 1918; Romain, 1963) but applied only to problems of fundamental physics.

The study of relativistic space travel and its consequences for rocket systems began in earnest in 1946 (Ackeret, 1946, 1947), soon followed by considerations of nuclear energy for powering rockets (Shepherd & Cleaver, 1948a, 1948b, 1949). An explicit in-depth study of these two combined fields was carried out by the founder of modern Chinese astronautics H. S. Tsien (Tsien, 1949). Shepherd considered the general problem of relativistic interstellar travel (Shepherd, 1952) and noted the "ultimate" propulsive concept of the "photon rocket," as introduced by Sänger (Sänger, 1961, 1961-2, 1963; Ernst Stuhlinger, 1959) and also studied by Peschka (Peschka, 1956). Even more novel was Bussard's concept of using fusion of interstellar matter in a "ram-jet" mode (Bussard, 1960).

Although studies of the general problem continued (Dole, 1964; Forward, 1975), it became clear that even with multiple nuclear stages (Spencer & Jaffe, 1962), the profound energy requirements for relativistic travel were, and continue to be, a significant limitation (Asimov, 1966; Purcell, 1963; Sagan, 1963; Sebastian von Hoerner, 1962).

11.1.3. Oberth Maneuver

A means for rapid solar system escape appears to have originated with Hermann Oberth in the publication of his work *Wege zur Raumschiffahrt* (*Ways to Spaceflight*) published in Germany in 1929 (Oberth, 1970). On page 198 of the referenced translation, Oberth provides the following *gedanken* experiment with the introduction: "As is apparent, we have so far dealt with matters of pure definition. That changes, however, as soon as we are dealing with a body moving between different reference systems. Let us demonstrate it by means of a mental experiment." (It is perhaps interesting to note that the comment about the different reference frames foreshadows the use of gravity assists for enabling space missions, a concept that was not put forth until the early 1960s by Minovitch.)

Oberth posits an astronaut living on an asteroid 900 astronomical units (au) from the Sun. He notes that the orbital speed will be 1 km/s and the period of revolution about the Sun will be 27,000 years. The astronaut wants to fly to a fixed star 10^{15} km away (which Oberth notes is about the distance to "Regulus in the Lion"). The target star lies in the orbital plane of the asteroid, and the astronaut has at his disposal a rocket capable of delivering a velocity change of 6 km/s. The Sun, asteroid, and target star are in a line in that order. Oberth poses the question "How can our astronaut get to the distant fixed star fastest?"

Oberth gives the answers in "obvious" order:

1. Start right now because you are closest; reach the star in 5,555,000 years, or
2. Wait for 20,000 years—¾ of an orbit—so that the asteroid's velocity adds to the velocity of the astronaut's ship; reach the star in 4,760,000 years plus the 20,000-year wait.

But he then concludes that neither of these is correct and the correct answer is to use 1 km/s of propellant capability in the direction opposite to that of the asteroid's motion and fall to "the edge of the solar corona" in a very elongated ellipse. At perihelion, the speed will be ~500 km/s, at which time the remaining rocket fuel is used to boost the speed to 505 km/s. The difference in incoming and outgoing kinetic energy amounts to an asymptotic speed away from the Sun of 70.9 km/s, cutting the transit time to a mere 470,000 years.

Oberth remarks:

> The first time I made this calculation, I believed nothing else in the first minute but that here the law of the conservation of energy was broken, or at least that one could gain work at the cost of energy stimulating the field of gravity somewhat similar to the work performed by an electromagnet which is counterbalanced by weakening of the stimulating current. But neither is the case. The fuels have performed the whole work alone. Beside their energy of combustion, they contained potential energy, since they were so high above the sun to begin with.

The real issue, of course, is how close one can really get a spacecraft to the Sun to take advantage of a propulsive maneuver in the Sun's gravity well given the thermal environment. Nonetheless, the invention of "the Oberth maneuver" was as fundamental a recognition as were Hohmann's discovery of minimum energy transfer orbits some 4 years earlier (Hohmann, 1960),[1] and Minovitch's discovery of the (passive) gravity assist in the early 1960s (Dowling et al., 1990, 1991, 1999; M.A. Minovitch, 1961; Michael A. Minovitch, 1963).

Aside from a few discussions of interstellar travel based on some version of nuclear power (Ackeret, 1946; Bussard, 1960; Peschka, 1956; Shepherd, 1952), discussions of solar-system-escaping probes came onto the scene gradually[2] and always within the context of a *solar probe* going inward from the Earth and toward the Sun (Charles F. Hall et al., 1962; Ralph L. McNutt, Jr. et al., 2017).[3] A spacecraft with sufficient launch energy to launch toward the Sun and reach a perihelion of 0.2 au could launch outward and escape the Sun's gravity altogether (Matthews & Erickson, 1964). The key problem was propulsive capability; a Saturn C-1 plus upper stages using liquid hydrogen (LH_2) fuel and liquid fluorine propellant (LF_2) were suggested to provide the propulsive capability (Charles F. Hall et al., 1962). Subsequently, Minovitch pointed out that a Jupiter gravity assist (JGA), the mass of Mars being insufficient to provide the required trajectory deflections (M.A. Minovitch, 1965), could enable all three of the difficult "special probes" flagged by the Space

[1] Originally published in German: *Die Erreichbarkeit der Himmelskörper*. R. Oldenbourg (Munich, Berlin), 1925.

[2] The first written mention seems to have been at the 7th meeting of the Space Studies Board (SSB) in Washington, DC, in March 1960. One of the committee reports notes a group of "Special Probes" including "b. Outer solar system probe: to be aimed away from the Sun in the plane of the ecliptic. (It is hoped that motion away from the Sun to the extent of 5 or 6 astronomical units per year could be accomplished by 1965)." The speeds noted would be sufficient for solar system escape.

[3] More details on the studies performed are given by Matthews and Erickson (Matthews & Erickson, 1964). They note: "The studies of this mission were made at the NASA-Ames Research Center and by Ames contractors in 1963. Four contractual studies were made -- one, under the direction of Dr. R. Grant Athay and Lewis L. House of the High Altitude Observatory at Boulder, Colo., reviewed possible experiments oriented principally to solar physics for a close-in solar probe. The other three were four-month studies by industrial contractors -- Missile and Space Div. of General Electric at Valley Forge, Pa., Martin Co., Space Programs Div., Baltimore, Md., and the Western Development Laboratories of Philco Corp., Palo Alto, Calif. The Minneapolis-Honeywell Regulator Co. also studied this mission and made the results available to NASA. … The initial constraints placed on the studies were that the spacecraft and its subsystems have an operational lifetime of one year, that the communications and tracking systems be compatible with the operation of the Deep Space Information Facility (DSIF) of NASA, that launch be from the Atlantic Missile Range (AMR), and that boosters be restricted to the Atlas/Agena and the Atlas/Centaur, both with a solid rocket motor as a final injection stage. Subsequently, the studies were expanded to include some work on the mission directed away from the Sun (antisolar mission)."

Studies Board (SSB) in its 1960 meeting[4] without relying on such large and exotic launch vehicles and stages.[5]

The use of a close solar flyby (CSF) was revisited by Ehricke in 1971 (Krafft A. Ehricke, 1971) but with cautionary notes on the required near-Sun thermal and propulsive technologies that would be required to implement it.

On the technology side, the renewed interest in "interstellar precursor missions" (Jaffe et al., 1977; Jaffe & Ivie, 1979; Jaffe et al., 1980; Jaffe & Norton, 1980) (largely spurred by the upcoming Pioneer 10 mission) led to a focus in the 1970s and 1980s on the use of nuclear electric propulsion (NEP) to achieve the large solar system ejection speeds from long periods of low thrust (Etchegaray, 1987; Nock, 1987; Pawlik & Phillips, 1977; Phillips & Pawlik, 1978) with specific implementations looking forward to the SP-100 nuclear space reactor, which had begun development (Deininger & Vondra, 1988, 1991).[6]

It had become clear that any use of an NEP system for propulsion would be heavy, and expensive, and the science community, already looking to a more ambitious mission before the Pioneer 10 launch (Dessler & Park, 1971), had begun to focus on a small and, hence, less-expensive ("cheap") implementation of such a mission (Allen et al., 1976).[7] With such "boundary conditions," the use

[4] Item b "outer solar system probe" became the center of the Advanced Pioneer program and was flown as Pioneer 10 (C. F. Hall, 1974). Item c "probe 'perpendicular' to the ecliptic" was investigated in the United States using the Pioneer bus (Christiansen et al., 1971). Item a "solar probe" was changed from a Jupiter-flyby strategy (McComas et al., 2005) to a multiple-Venus-flyby strategy (McComas et al., 2008) because of the lack of radioisotope power supplies for the mission.

[5] Rocket stages using LF_2 as the oxidizer were found by both the U.S. Air Force and Soviet Strategic Rocket Forces to be entirely too dangerous to use in a practical system (Sutton, 2006).

[6] The SP-100 project was eventually canceled (along with the other Strategic Defense Initiative tasks) at the beginning of the Clinton administration in the early 1990s in the wake of significant schedule slippages, cost overruns, and management issues (*The SP-100 Nuclear Reactor Program: Should It Be Continued?*, 1992). A thorough vetting of NEP for flight by NASA under Project Prometheus in the 2000s confirmed the large mass and high cost of such systems and revealed gaps in technical readiness for flight (Ashcroft & Eshelman, 2006; Burdge & Levine, 2006; Taylor, 2005; Wollman & Zika, 2006); NEP is no longer under active consideration by NASA for any uses in the future.

[7] See page B-92:

1069. Solar System Escape spacecraft:

Small spacecraft with particles-and-fields instrumentation launched in 1980 by Titan-Centaur plus high-performance upper stages on a trajectory escaping solar system in general direction of solar apex. If mission launched in late 80's, electric propulsion, solar sailing, and/or Jupiter swingby could be used to reduce transit time to heliosphere boundary. Mission duration ten years or more.

See page B-74 for traceability entries.

Overlaps are with theme 9 (091, 093, and 094) and theme 10 (101 and 104).

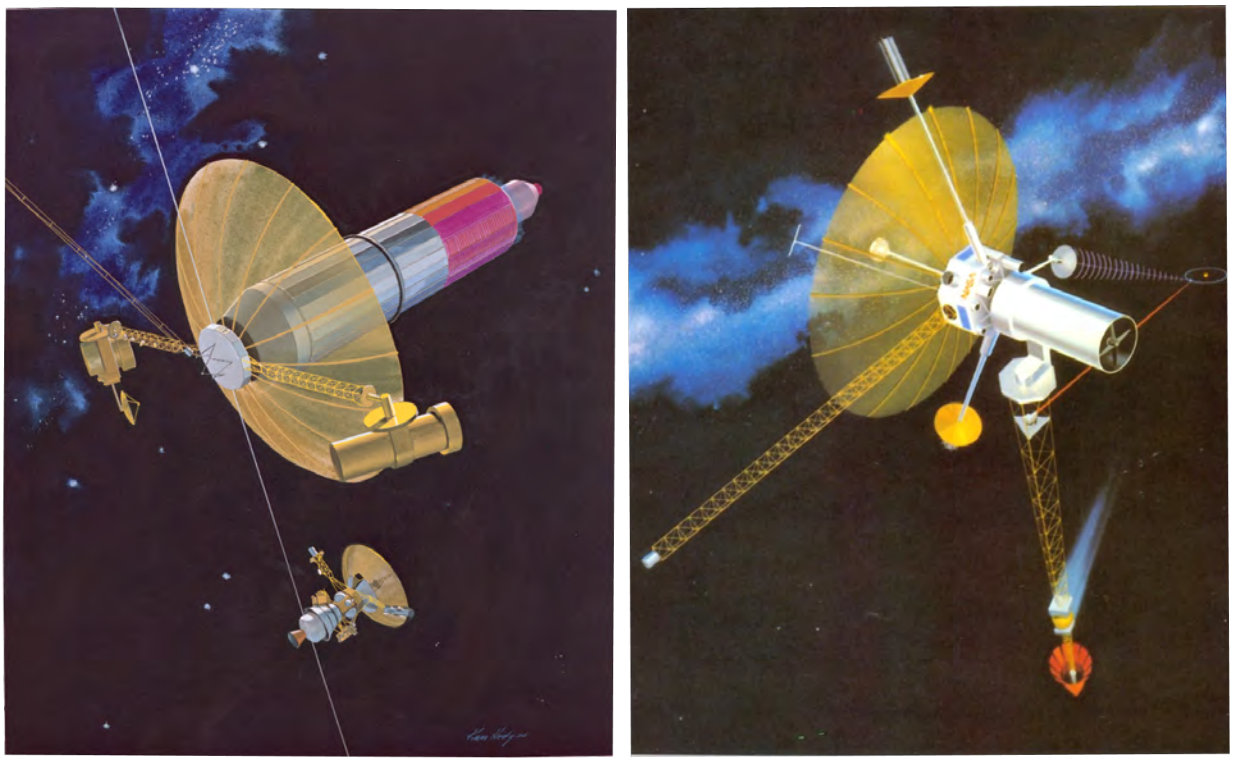

Figure 11-2. (Left) NEP Interstellar Probe spacecraft concept of 1978 (Jaffe et al., 1980), shown dropping off Pluto Orbiter. The reactor and its coolant system and 15-m-diameter mesh high-gain antenna (HGA) (40 W, X-band system) dominate the configuration. (Right) The NEP system (using a reactor advanced past the "baseline" SP-100 design concept) for the Thousand Astronomical Unit (TAU) mission of almost a decade later (Nock, 1987) is dominated by a 5-m-diameter radio antenna for doing very-long baseline interferometry (VLBI) for studying interstellar scintillation and compact radio sources. Data downlink is via a 1-m-diameter optical communications system (Etchegaray, 1987).

of an Oberth maneuver near the Sun was again under consideration (T. E. Holzer et al., 1990) (see also the Report of the *Cosmic and Heliospheric Panel* in volume 1 of the *Space Physics Strategy – Implementation Study* report to the Space Physics Subcommittee of NASA's Space Science and Applications Advisory Panel, second edition, April 1991). A follow-up technical study noted (Mewaldt et al., 1995):

> To accomplish its scientific objectives, an Interstellar Probe should acquire data out to a heliocentric distance of ~200 AU. To reach 200 AU within a reasonable mission lifetime (e.g., ~25 years or less), the spacecraft velocity must be several times greater than those of Pioneer-10 and the Voyagers, which range from 2.4 to 3.5 AU/yr. In order to minimize the time and distance to the heliopause, the general direction of the trajectory should be toward the nose of the heliosphere, which corresponds to the ram direction of the inflowing interstellar gas. In the rest frame of the sun, the direction from which the interstellar flow is coming has ecliptic coordinates of +7.50 latitude and 254.50 longitude.

"Advanced propulsion" was also considered, with the authors noting:

> The requirement to achieve escape velocities of -10 AU/year suggests that advanced propulsion concepts should be considered. Nuclear electric propulsion would appear to be well suited, but the time scale on which it will become available is unclear. Solar electric propulsion would appear to have limited utility for a mission that must venture so far from the Sun. RTG-powered electric propulsion is an interesting possibility that warrants further study, since there will clearly

be excess RTG power early in the mission. Finally, calculations indicate that a solar sail might also provide more than the required acceleration if unfurled at several tenths of an AU from the Sun. While it is unlikely that the costs associated with the development of any of these new propulsion technologies could be borne by this mission alone, Interstellar Probe might provide a very attractive opportunity to test a new propulsion system prior to its use in other applications, such as a manned mission to Mars.

These suggestions set the stage for further lines of inquiry during the following two decades for means of providing rapid solar system escape.

One response to a NASA Research Announcement[8] was to study a dual-use "standardized" spacecraft for implementing both a solar probe and an interstellar probe mission. The idea was to look at a small probe that could fire a kick stage at perihelion prograde to escape the solar system and retrograde to provide an aphelion of <1 au for a solar probe mission (the latter being an approach that had been discussed previously).

Although the proposal was not selected for funding, preliminary work considered a perihelion distance of ~4 solar radii (R_S), as had been discussed for a solar probe mission, enabled by a retrograde JGA as discussed initially by Minovitch (M.A. Minovitch, 1965). It was estimated that a speed increase of ~3.6 km/s would be required at 4 R_S to provide a solar system escape speed of ~10 au/year (R. L. McNutt, Jr. et al., 1997).

A very simple scaling illustrates the magnitude of the issue. Suppose the solar perihelion distance is r_p, the mass of the spacecraft is m, the Newtonian Gravitational constant is G, the asymptotic escape speed of the spacecraft after the Oberth burn is V_{esc}, and the burn has an ideal impulsive value of ΔV (i.e., the impulse is applied instantaneously at perihelion with no gravity loss corrections). A final consideration is that the spacecraft "falls" to the Sun, beginning from rest, and so, on a parabolic orbit from infinity ("close" to Oberth's 900 au); in the real case, the probe will be on a highly eccentric orbit with an aphelion at Jupiter (from the location of the retrograde Minovitch maneuver). Then, if V is the (tangential) spacecraft speed at perihelion when the impulsive burn is implied, we have (also neglecting the spacecraft mass with respect to the mass of the Sun M_S):

$$E = 0 = \tfrac{1}{2}mV^2 - \frac{GM_S m}{r_p} \tag{1}$$

$$E + \Delta E = \tfrac{1}{2}mV_{esc}^2 = \tfrac{1}{2}m(V + \Delta V)^2 - \frac{GM_S m}{r_p} = \tfrac{1}{2}m(V + \Delta V)^2 - \tfrac{1}{2}mV^2 \approx mV\Delta V, \tag{2}$$

[8] NASA Research Announcement NRA 96-0SS-03 released 20 February 1996; proposal submission deadline 20 May 1996: "SPACE PHYSICS NEW MISSION CONCEPTS PROGRAM. This NASA Research Announcement (NRA) solicits proposals for concept studies for future U.S. flight missions in space physics whose subdisciplines are cosmic and heliospheric physics; solar physics; magnetospheric physics; and ionospheric, thermospheric, and mesospheric physics. Grants of up to about $100K per year for up to two years will be provided to support studies of innovative missions that NASA might sponsor that promise breakthrough advances in one or more of these subdisciplines. Especially desirable are mission concepts that focus on interdisciplinary objectives for integrated research in space physics. Since low cost is a particularly important factor for the successful initiation of new space science programs, proposals for mission concepts that utilize hardware systems and/or management approaches promising minimal cost are especially encouraged. Also encouraged are concepts that promote the development and/or use of new technologies to achieve miniaturization, cost reduction, and/or light-weighting compared to the current state of the art."

where we have used the fact that $\Delta V << V$. Hence

$$V_{esc} \approx V_{esc,0} \equiv (2\Delta V)^{1/2} \left(\frac{R_S}{r_p}\right)^{1/4} \left(\frac{2GM_S}{R_S}\right)^{1/4}. \quad (3)$$

Introducing the escape speed V_{Sun} from the "surface" of the Sun (defined as the distance from the Sun's center to a solar radius of 695,700 km, from resolution B3 passed by the International Astronomical Union in 2015), we have

$$V_{Sun} = \sqrt{\frac{2GM_S}{R_S}} = 617.6\ km/s. \quad (4)$$

And so[9]

$$V_{esc,0} = (2V_{Sun}\,\Delta V)^{1/2} \left(\frac{R_S}{r_p}\right)^{1/4} = 35.14\left(\Delta V[\tfrac{km}{s}]\right)^{1/2} \left(\frac{R_S}{r_p}\right)^{1/4} km/s =$$

$$7.413\left(\Delta V[\tfrac{km}{s}]\right)^{1/2} \left(\frac{R_S}{r_p}\right)^{1/4} AU/yr. \quad (5)$$

In any event, the performance can never exceed what would be obtained for a spacecraft that "skimmed" the photosphere at $r_p = 1\ R_S$. For an escape speed of 21 au/year (100 km/s), one would require a ΔV of 8.1 km/s. To provide a rough estimation of the problem, if we set the required ΔV to the exhaust velocity of the rocket engine, the implied specific impulse is then $\Delta V/g$ = 825 s, just above the demonstrated value (~820 s) for the Phoebus 2A nuclear thermal propulsion (NTP) engine (containing ~300 kg of uranium) demonstrated in June 1968 under the Nuclear Engine for Rocket Vehicle Application (NERVA) program (LASL, 1969).

11.2. General Issues for Implementing an Oberth Maneuver

11.2.1. Jupiter Gravity Assist

It can easily be shown that optimal performance for outgoing trajectories makes use of a Minovitch maneuver at Jupiter (prograde JGA); while tying the aim-point for the trajectory on the sky to the location of Jupiter, there is a significant gain in fly-out speed over the case of not using an optimized Jupiter flyby.

What is not so obvious is that there is likely better performance in using all propulsive capability during the launch sequence from Earth while the launch stack is within Earth's gravity well, rather than "saving" a stage to use a combined Minovitch-Oberth maneuver at Jupiter (powered, prograde Jupiter flyby). Spot checks with some simple assumptions indicate this is indeed the case, but a more definitive study is required because the properties of the launch stack used are not separable from the mission-design performance.

[9] Standard definitions of units are used, including c = 2.99792458 × 10^8 ms^{-1}; 1 (Julian) year = 365.25 days = 8766 hours; 1 au = 1.495 9787066 × 10^{11} m; 1 pc = 206,264.806 au. Thus, 1 au/(Julian) year = 4.740470461 km/s.

Here the only potential thermal issue is that of "storing" an upper stage in a cold soak during the transit from Earth to Jupiter, if it is not to be used until the Jupiter flyby (this is, of course, in addition to the addition of a critical event deep in Jupiter's radiation environment from which there is no graceful recovery, and that cannot be tested before launch).

11.2.2. Oberth Maneuver

To execute an Oberth maneuver, it can easily be shown that a Minovitch maneuver at Jupiter (retrograde) is required to delete the heliocentric angular momentum picked up by a spacecraft from its launch at Earth in order to penetrate sufficiently close to the Sun to take advantage of the maneuver. This issue is well known from the multiple considerations of solar probe trajectories over almost six decades[10] (to counteract the Earth's orbital speed with a direct launch at 1 au, the required C_3 would be ~900 km^2/s^2). The required C_3 is ~100 km^2/s^2 to reach Jupiter on a direct trajectory. Without this large a launch energy, multiple Earth and/or Venus gravity assists are required to reach Jupiter; in those cases, deep-space maneuvers (DSMs) are required and additional fly-out time to the Sun is required up front). Hence, for an Oberth maneuver, minimization of the time from launch to the maneuver requires a direct trajectory from Earth to Jupiter, followed by a "fall" of the spacecraft to its perihelion near the Sun. The launch energy then limits the allowable mass of the spacecraft/kick stage stack that must be injected into orbit to Jupiter.

An Oberth maneuver intimately ties together the mission design, spacecraft and kick-stage mass, and required thermal design. From equation 5, we want to maximize $\Delta V/r_p^{1/2}$. However, there is an implied trade due to the thermal constraint that the spacecraft and kick stage(s)—the latter providing the ΔV—must survive perihelion. The high temperatures require that some type of TPS must protect the stack through the perihelion pass. The closer the pass, the higher the temperature on the TPS and the larger the solid angle subtended by the stack. Both considerations will make the mass of the TPS, m_{TPS}, a monotonically, but probably non-linear, decreasing function f of the perihelion distance r_p (i.e., the TPS mass *increases with decreasing perihelion distance*).

Before the burn, the kick stage (we assume a single stage, but the result can be generalized in a straightforward, if somewhat clumsy, way) has a total mass

$$m_{initial} = m_{spacecraft} + m_{kick-stage,empty} + m_{propellant} + m_{TPS}, \quad (6)$$

[10] The use of Venus gravity assists for both Parker Solar Probe and Solar Orbiter was entirely driven by the lack of radioisotope power systems (RPSs) for these missions. An interstellar probe will require an RPS in any case, and the Venus gravity assists are far less efficient, would require multiple Venus passes versus a single Jupiter pass, and thus require more "up front" time before an Oberth maneuver (Niehoff, 1966). Even for an infinite number of Venus flybys, the smallest perihelion reachable is set by the initial launch energy (Tanabe & Yokota, 1980).

and so, the ΔV is given (assuming no gravity losses) by

$$\Delta V = \mathrm{g} I_{sp} ln\left(\frac{m_{spacecraft}+m_{kick-stage,empty}+m_{propellant}+m_{TPS}}{m_{spacecraft}+m_{kick-stage,empty}+m_{TPS}}\right). \quad (7)$$

As noted before, the escape speed V_{esc} is bounded from above by $V_{esc,0}$ from equation 5, and we also have

$$m_{TPS} = f(r_p). \quad (8)$$

Combining equations 5, 7, and 8, we obtain

$$V_{esc} \lesssim V_{esc,0} = \left(2V_{Sun}\, \mathrm{g} I_{sp} ln\left(\frac{m_{spacecraft}+m_{kick-stage,empty}+m_{propellant}+f(r_p)}{m_{spacecraft}+m_{kick-stage,empty}+f(r_p)}\right)\right)^{\frac{1}{2}} \left(\frac{R_S}{r_p}\right)^{\frac{1}{4}}. \quad (9)$$

To simplify the notation—and better reveal the dependencies—introduce the propellant mass fraction of the spacecraft plus kick-stage stack

$$\eta \equiv \frac{m_{propellant}}{m_{spacecraft}+m_{kick-stage,empty}+m_{propellant}} \quad (10)$$

and the mass of the TPS normalized to the fueled stack mass

$$\hat{f}(r_p) \equiv \frac{m_{TPS}}{m_{spacecraft}+m_{kick-stage,empty}+m_{propellant}}. \quad (11)$$

Equation 9 then becomes

$$V_{esc} \lesssim V_{esc,0} = \left(2V_{Sun}\, \mathrm{g} I_{sp} ln\left(\frac{1+\hat{f}(r_p)}{1-\eta+\hat{f}(r_p)}\right)\right)^{1/2} \left(\frac{R_S}{r_p}\right)^{1/4}. \quad (12)$$

In principle, there is a maximum (at least an extremum, which is presumably a maximum) at

$$\frac{dV_{esc,0}}{dr_p} = 0 \quad (13)$$

(again, ignoring the slight dependence of $V_{esc,0}$ itself on r_p); we then find

$$\left(1+\hat{f}\right)\left(1+\hat{f}-\eta\right) ln\left(\frac{1+\hat{f}}{1+\hat{f}-\eta}\right) = -2\eta r_p \frac{d\hat{f}}{r_p}. \quad (14)$$

For an exercise based on the New Horizons spacecraft and its upper stage, we found (Ralph L. McNutt, Jr. et al., 2017)

$$m_{TPS} \simeq 1773 \left(\frac{R_S}{r_p}\right)^{1.13} kg. \quad (15)$$

If we estimate the Interstellar Probe wet mass with margin as ~585 kg, the third-stage wet mass as ~2950 kg, the propellant mass as ~2010 kg, V_{Sun} = 617.6 km/s, g = 9.81 m s^{-2}, and the I_{sp} as 292 s, then we can solve equation 14 using equation 15.

Using equations 11 and 15, we obtain

$$\hat{f} = \frac{1773}{585+2950}\left(\frac{R_S}{r_p}\right)^{1.13} = \frac{1}{1.994}\left(\frac{R_S}{r_p}\right)^{1.13}. \tag{16}$$

And so

$$r_p \frac{d\hat{f}}{r_p} = -\frac{1}{1.994}\, r_p \left(\frac{R_S^{1.13}}{r_p^{2.13}}\right) = -\frac{1}{1.994}\left(\frac{R_S}{r_p}\right)^{1.13} = -\hat{f}. \tag{17}$$

Equation 14 now becomes a transcendental equation for $\hat{f}$ with the parameter η, where from equation 10:

$$\eta \equiv \frac{m_{propellant}}{m_{spacecraft}+m_{kick-stage,empty}+m_{propellant}} = \frac{2010}{585+2950} = \frac{2010}{3535} = 0.568. \tag{18}$$

The optimum is then found via the solution of

$$\left(1+\hat{f}\right)\left(1+\hat{f}-\eta\right) ln\left(\frac{1+\hat{f}}{1+\hat{f}-\eta}\right) = 2\eta\hat{f}. \tag{19}$$

We can note that if $\hat{f} = 0$, there is no solution (i.e., with no "constraint" of a thermal shield mass, there is no "optimal" solution). The best one could do would be to "skim the photosphere" at r_p = R_S. Equation 12 becomes

$$V_{esc} \lesssim V_{esc,0} = \left(2V_{Sun}\, \mathrm{g} I_{sp} ln\left(\frac{1}{1-\eta}\right)\right)^{\frac{1}{2}} \left(\frac{R_S}{r_p}\right)^{\frac{1}{4}} = 54.5\,\frac{km}{s} = 11.5\,\frac{AU}{yr}. \tag{20}$$

This is close to the number that Oberth derived in 1929, but it still falls short of the 20 au/year we have been seeking. Again, this is with *no* TPS.

The optimal solution of equation 19 for the given value of η is $\hat{f} = 0.67667$, for which r_p = 0.767 R_S (i.e., inside of the Sun). The solution is, of course, nonphysical, because $\hat{f} \leq 1/1.994$ from equation 16. This is similar to the well-known geometrical constraint in the Minovitch maneuvers that one cannot approach closer to the center of the planet than the planet's surface!

In terms of the normalized perihelion distance

$$\widehat{r_p} \equiv \frac{r_p}{R_S}, \tag{21}$$

and writing generically,

$$\hat{f} = \widehat{f_0}\left(\frac{1}{\widehat{r_p}}\right)^{\alpha}. \tag{22}$$

Equation 12 becomes

$$V_{esc} \lesssim V_{esc,0} = \left(2V_{Sun}\, \mathrm{g}I_{sp} ln\left(\frac{1+\hat{f}}{1-\eta+\hat{f}}\right)\right)^{\frac{1}{2}} \left(\frac{\hat{f}}{\widehat{f_0}}\right)^{\frac{1}{4\alpha}} = \left(2V_{Sun}\, \mathrm{g}I_{sp}\right)^{1/2} F\left(\hat{f}; \alpha, \eta, \widehat{f_0}\right), \tag{23}$$

where the various masses and their scalings are isolated in the function *F*:

$$F\left(\hat{f}; \alpha, \eta, \widehat{f_0}\right) \equiv \left(ln\left(\frac{1+\hat{f}}{1-\eta+\hat{f}}\right)\right)^{\frac{1}{2}} \left(\frac{\hat{f}}{\widehat{f_0}}\right)^{\frac{1}{4\alpha}}, \tag{24}$$

and the characteristic Oberth speed can be defined as

$$V_{Oberth} \equiv \left(2V_{Sun}\, \mathrm{g}I_{sp}\right)^{1/2}. \tag{25}$$

This parameterization separates the propulsion means (as embodied in the specific impulse) from the structural characteristics (which includes the thermal shield). The function *F* will change with most robust thermal and engine designs, while the characteristic speed is simply set by the maneuver itself and the rocket equation (ignoring gravity losses from finite burn time for the maneuver).

For our case with a solid rocket engine, V_{Oberth} = 59.48 km/s = 12.55 au/year. The degradation due to the inclusion of the TPS can be evaluated by defining

$$F(0; 0, \eta, 0) \equiv \left(ln\left(\frac{1}{1-\eta}\right)\right)^{\frac{1}{2}} \left(\frac{1}{\widehat{r_p}}\right)^{\frac{1}{4}} \tag{26}$$

and using this in conjunction with equation 23. For the parameters assumed here, the performances with and without the TPS are shown in Figure 11-3.

These curves provide an upper bound on the performance for the case cited. Note that twice the current Voyager 1 escape speed is ~7.2 au/year.

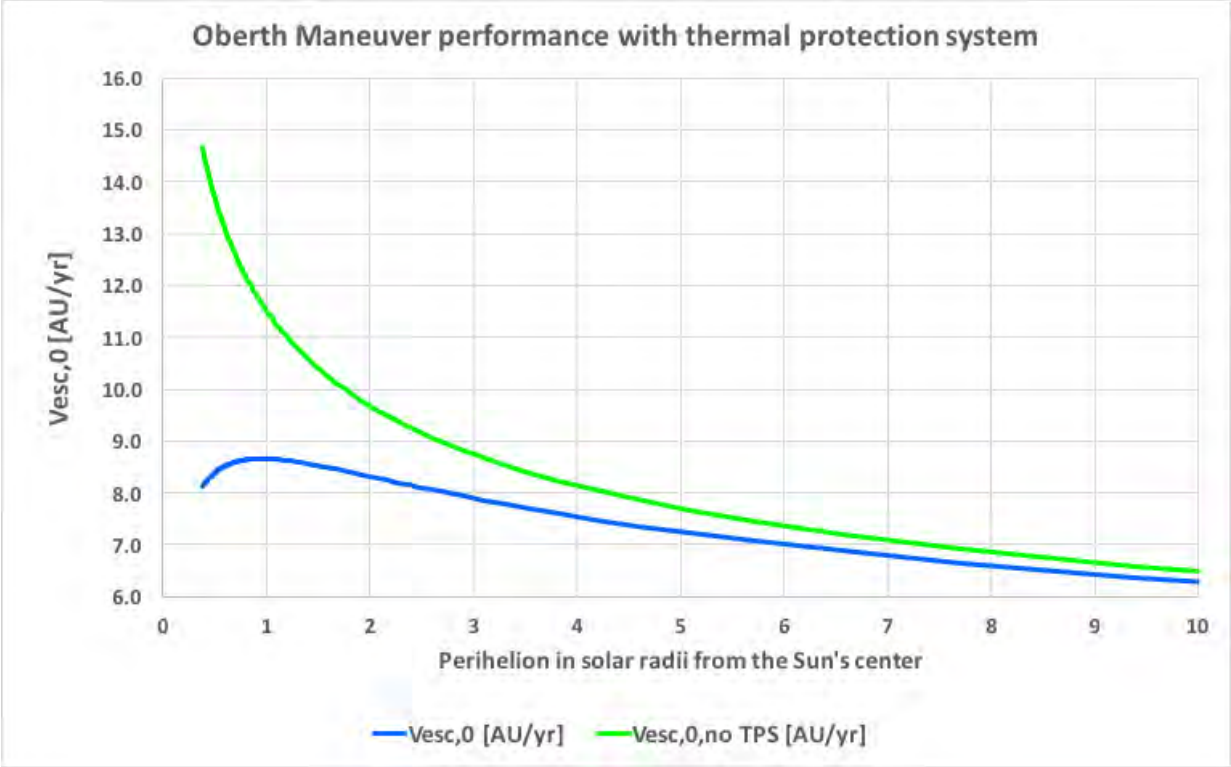

Figure 11-3. Variation of solar system asymptotic escape speed as a function of perihelion distance for asset of example Interstellar Probe parameters (see text). The green curve shows what could be obtained in the absence of a TPS. The blue curve shows the increasing impact of a notional TPS on performance as the perihelion distance decreases.

11.2.2.1. Relativistic Oberth Maneuver

Another idea that has surfaced from time to time that one should at least explore is how far one could really push the Oberth maneuver by making use of objects with even stronger gravitational fields than that of the Sun. A quick review of web entries shows that this is not a new idea, having been considered by others before. For completeness, it seems reasonable to at least take up the subject.

The real question is then not only how higher gravity fields affect the results but also how these results are modified further by the effect of the super-strong gravity of a black hole, for which the full panoply of relativistic effects will also come into play. Because this is a *gedanken* experiment at best, we limit the treatment to that for a probe dropped into the gravity field of an uncharged black hole with no intrinsic angular momentum. The appropriate metric for our purposes is then the Schwarzschild metric (Schwarzschild, 1916)

$$ds^2 = c^2 d\tau^2 = \left(1 - \frac{r_s}{r}\right) c^2 dt^2 - \frac{dr^2}{\left(1 - \frac{r_s}{r}\right)} - r^2 d\theta^2 - r^2 sin^2\theta d\varphi^2,$$

where the Schwarzschild radius r_s is defined by

$$r_s \equiv \frac{2GM}{c^2}.$$

As per standard procedure, we consider the orbit possibility of a test particle with $m << M$ in the plane $\theta = \frac{\pi}{2}$.

There are two constants of the motion, the total energy E and the specific angular momentum $h \equiv \frac{L}{\mu} = r^2 \frac{d\varphi}{d\tau}$. For the case here, we can take the reduced mass μ to be that of the (vanishingly small mass of the) test particle m.

This allows the metric to be written as

$$c^2 = \left(1 - \frac{r_s}{r}\right) c^2 \left(\frac{dt}{d\tau}\right)^2 - \frac{1}{\left(1 - \frac{r_s}{r}\right)} \left(\frac{dr}{d\tau}\right)^2 - r^2 \left(\frac{d\varphi}{d\tau}\right)^2$$

and so yields an equation for the radial observer coordinate as a function of the proper time of the test particle

$$\left(\frac{dr}{d\tau}\right)^2 = \frac{E^2}{m^2 c^2} - \left(1 - \frac{r_s}{r}\right)\left(c^2 + \frac{h^2}{r^2}\right).$$

From this equation and the definition of the constant of motion of the energy in terms of the proper time τ, both the coordinate time t and the proper time τ can be reduced to quadrature for the radial coordinate r as

$$\tau = \int \frac{dr}{\sqrt{\frac{E^2}{m^2 c^2} - \left(1 - \frac{r_s}{r}\right)\left(c^2 + \frac{h^2}{r^2}\right)}}$$

$$t = \int \frac{dr}{c\left(1 - \frac{r_s}{r}\right)\sqrt{1 - \left(1 - \frac{r_s}{r}\right)\left(c^2 + \frac{h^2}{r^2}\right)\frac{m^2 c^2}{E^2}}}.$$

Fairly simple analytic forms can be derived for cases for which the specific angular moment is zero. For the case at hand (we want to go near the hole, perform a propulsive maneuver, and then look at the final asymptotic state), the angular momentum is *not* zero.

Hence, we can eliminate the dependence on proper time and derive a differential equation for the coordinate r as a function of the azimuthal coordinate φ

$$\left(\frac{dr}{d\varphi}\right)^2 = \left(\frac{dr}{d\tau}\right)^2 \left(\frac{d\tau}{d\varphi}\right)^2 = \left(\frac{dr}{d\tau}\right)^2 \left(\frac{r^2}{h}\right)^2 = \left[\frac{E^2}{m^2 c^2} - \left(1 - \frac{r_s}{r}\right)\left(c^2 + \frac{h^2}{r^2}\right)\right]\left(\frac{r^2}{h}\right)^2$$

$$= \frac{r^4}{\left(\frac{hmc}{E}\right)^2} - \left(1 - \frac{r_s}{r}\right)\left(r^2 + \frac{r^4}{\left(\frac{h}{c}\right)^2}\right).$$

As with the time coordinate and proper time, the solution for the angular coordinate as a function of the radial coordinate can be reduced to quadrature

$$\varphi = \int \frac{dr}{r^2\sqrt{\frac{1}{\left(\frac{hmc}{E}\right)^2} - \left(1 - \frac{r_s}{r}\right)\left(\frac{1}{\left(\frac{h}{c}\right)^2} + \frac{1}{r^2}\right)}}.$$

A complete analytic solution is available (Wikipedia, 2020f) using the standard technique for solving the Kepler problem in classical physics by using the inverse radius *u*:

$$u \equiv \frac{1}{r},$$

and so

$$\left(\frac{dr}{d\varphi}\right)^2 = \left(\frac{d\left(\frac{1}{u}\right)}{d\varphi}\right)^2 = \frac{1}{u^4}\left(\frac{du}{d\varphi}\right)^2.$$

Hence, we can obtain

$$\left(\frac{du}{d\varphi}\right)^2 = \frac{1}{\left(\frac{hmc}{E}\right)^2} - (1 - ur_s)\left(u^2 + \frac{1}{\left(\frac{h}{c}\right)^2}\right)$$

or

$$\left(\frac{du}{d\varphi}\right)^2 = \left[\frac{1}{\left(\frac{hmc}{E}\right)^2} - \frac{1}{\left(\frac{h}{c}\right)^2}\right] + u\frac{r_s}{\left(\frac{h}{c}\right)^2} - u^2 + r_s u^3$$

or

$$\left(\frac{du}{d\varphi}\right)^2 = \left[\left(\frac{E}{mc^2}\right)^2 - 1\right]\left(\frac{c}{h}\right)^2 + ur_s\left(\frac{c}{h}\right)^2 - u^2 + r_s u^3.$$

Denoting the three roots of this cubic polynomial as u_1, u_2, and u_3, we can rewrite this equation as

$$\left(\frac{du}{d\varphi}\right)^2 = r_s(u - u_1)(u - u_2)(u - u_3),$$

and from the standard properties of cubic equations we have for the sums and products of the roots

$$u_1 + u_2 + u_3 = \frac{1}{r_s} \text{ and } u_1 u_2 u_3 = \frac{1}{r_s}\left[\left(\frac{E}{mc^2}\right)^2 - 1\right]\left(\frac{c}{h}\right)^2.$$

If all the roots are real, then let $u_1 < u_2 < u_3$, and if there is only one real root, let that root be u_3. The solution is then given by the Jacobi elliptic sine, or *sinus amplitudinis*, sn, via

$$u = u_1 + (u_2 - u_1)\text{sn}^2\left(\frac{1}{2}\varphi\sqrt{r_s(u_3 - u_1)} + const\right),$$

with *const* being the constant of integration and the elliptic modulus *k* (the square root of the parameter *m*) being given by

$$k \equiv \sqrt{\frac{(u_2 - u_1)}{(u_3 - u_1)}}.$$

For computational purposes, the Jacobi elliptic functions, which are related to the inverse of the incomplete elliptic integral of the first kind, are standard and given by, e.g., Wolfram, viz. Jacobi SN[u,m] gives the value of sn(u|m) (Wolfram, 2020).

The full set of solutions is quite rich. The usual solutions for the precession of the planet Mercury (Einstein, 1916) and the bending of light by the Sun (F. W. Dyson et al., 1920), which were used as the initial tests of general relativity theory, the gravitational red shift (Popper, 1954), as well as the time delay due to the Sun's gravity field (Shapiro et al., 1968) have all been based on the weak-gravity limit of the Schwarzschild metric. Here we are interested in the opposite situation t*o ascertain how the Oberth maneuver would be modified by strong gravity* (and aside from the hazardous radiation and accretion disk environments near the event horizon of a real black hole).

For the case at hand, we wish to consider a massive (i.e., non-photonic) test particle that comes in from a given separation and then goes back to an unbound infinite separation with a larger energy. To consider the analog to the limit of an Oberth maneuver, we take the initial condition to also be of an infinite separation but with zero speed relative to the attractive black hole mass. Hence, the initial total energy is just the rest mass (i.e., $E_{initial} = mc^2$). The final energy will be greater than this at a potential energy of zero. In the classical case, this simply corresponds to an incoming parabolic orbit and an outgoing hyperbolic one, the two being connected by a finite momentum increase provided by a rocket engine burn at closest approach to the gravitating object. In this initial treatment, we ignore the dissipation of any energy of motion inbound or outbound due to gravitational radiation, consistent with the small mass limit of our test mass (the spacecraft) compared with the mass of the black hole. Furthermore, we assume that the change in momentum due to the burn is itself sub-relativistic, i.e., $\Delta p << mc$, with *m* being the spacecraft proper mass before the burn (hence the relationship holds subsequent to the burn as well).

The magnitude of the evolution of the radial coordinate location with proper time is

$$\left(\frac{dr}{cd\tau}\right)^2 = \left(\frac{E}{mc^2}\right)^2 - \left(1 - \frac{r_s}{r}\right)\left(1 + \frac{\left(\frac{h}{c}\right)^2}{r^2}\right),$$

but the actual variation must change from negative (initial ingoing) to positive (final outgoing) at closest approach (and the rocket burn). Hence, the general equation will have only one real route (corresponding to unbounded motion).

We can rewrite the equation as

$$\left(\frac{dr}{cd\tau}\right)^2 = \left[\left(\frac{E}{mc^2}\right)^2 - 1\right] + \frac{r_s}{r} - \frac{\left(\frac{h}{c}\right)^2}{r^2} + \frac{r_s\left(\frac{h}{c}\right)^2}{r^3}.$$

For the incoming trajectory, the total conserved energy is just the rest mass and we have

$$\left(\frac{dr}{cd\tau}\right)_{inbound} = -\frac{h}{c}\sqrt{\frac{r_s}{r}}\sqrt{\left(\frac{c}{h}\right)^2 - \frac{\frac{1}{r_s}}{r} + \frac{1}{r^2}}.$$

The turnaround point is fixed by the finite specific angular momentum *h* and is given by

$$\frac{1}{r_{limit}} = \frac{1}{2r_s} \pm \frac{1}{2}\sqrt{\left(\frac{1}{r_s}\right)^2 - 4\left(\frac{c}{h}\right)^2}.$$

For the limit to be real, we also require $\left(\frac{1}{r_s}\right)^2 > 4\left(\frac{c}{h}\right)^2$, i.e., $\frac{h}{c} > \frac{1}{2}r_s$. In practice, the angular momentum cannot simply go to zero without escaping the black hole. Indeed, as with the limiting minimal value for the Oberth maneuver at the Sun (one cannot go closer to the center of the Sun than 1 R_S), similarly, there is a limit here. We can note that at $r = r_s$, the derivative can no longer change sign for a finite energy and so an inbound particle cannot escape the black hole.

We can cast the radial "equation of motion" in terms of a pseudo-potential V, which we express in units of the Schwarzschild radius

$$\left(\frac{dr}{cd\tau}\right)^2 = \left[\left(\frac{E}{mc^2}\right)^2 - 1\right] + \frac{1}{\left(\frac{r}{r_s}\right)} - \frac{\left(\frac{h}{cr_s}\right)^2}{\left(\frac{r}{r_s}\right)^2} + \frac{\left(\frac{h}{cr_s}\right)^2}{\left(\frac{r}{r_s}\right)^3}$$

$$\left(\frac{dr}{cd\tau}\right)^2 = \left[\left(\frac{E}{mc^2}\right)^2 - 1\right] - 2V(r),$$

where

$$-2V(r) \equiv \frac{1}{\left(\frac{r}{r_s}\right)} - \frac{\left(\frac{h}{cr_s}\right)^2}{\left(\frac{r}{r_s}\right)^2} + \frac{\left(\frac{h}{cr_s}\right)^2}{\left(\frac{r}{r_s}\right)^3}.$$

The resulting roots are

$$\frac{r_{inner,outer}}{r_s} = \left(\frac{h}{cr_s}\right)^2 \left[1 \mp \sqrt{1 - 3\left(\frac{cr_s}{h}\right)^2}\right],$$

which for $r_s \ll \frac{h}{c}$ reduce to $r_{inner} \approx \frac{3}{2} r_s$ and $r_{outer} \approx 2r_s \left(\frac{h}{cr_s}\right)^2$. These also locate two possible circular orbits: an unstable inner one and a stable outer one. In any case, h/c must exceed $\sqrt{3}r_s$, for which otherwise the angular momentum is insufficient for the test particle to evade capture (a metastable circular orbit exists at $3r_s$ for this case).

But all of this introduces another complication. For test particles with finite mass, the potential barrier must have at least a value of zero to prevent capture of a particle falling from infinity. We have two equations connected by the speed change, which increases both the energy and angular momentum at the point at which the proper radial motion is zero.

$$\left(\frac{dr_{inbound}}{cd\tau}\right)^2 = \left[\left(\frac{E_{inbound}}{mc^2}\right)^2 - 1\right] + \frac{1}{\left(\frac{r}{r_s}\right)} - \frac{\left(\frac{h_{inbound}}{cr_s}\right)^2}{\left(\frac{r}{r_s}\right)^2} + \frac{\left(\frac{h_{inbound}}{cr_s}\right)^2}{\left(\frac{r}{r_s}\right)^3}$$

$$\left(\frac{dr_{outbound}}{cd\tau}\right)^2 = \left[\left(\frac{E_{outbound}}{mc^2}\right)^2 - 1\right] + \frac{1}{\left(\frac{r}{r_s}\right)} - \frac{\left(\frac{h_{outbound}}{cr_s}\right)^2}{\left(\frac{r}{r_s}\right)^2} + \frac{\left(\frac{h_{outbound}}{cr_s}\right)^2}{\left(\frac{r}{r_s}\right)^3}.$$

Suppose the initial total energy is just the rest mass. Then the radial proper velocity is just twice negative of the potential, i.e., the inbound equation is

$$\left(\frac{dr_{inbound}}{cd\tau}\right)^2 = \frac{1}{\left(\frac{r}{r_s}\right)} - \frac{\left(\frac{h_{inbound}}{cr_s}\right)^2}{\left(\frac{r}{r_s}\right)^2} + \frac{\left(\frac{h_{inbound}}{cr_s}\right)^2}{\left(\frac{r}{r_s}\right)^3}.$$

The corresponding roots are just

$$\frac{r_{01,02}}{r_s} = \frac{1}{2}\left(\frac{h_{inbound}}{cr_s}\right)^2 \left[1 \pm \sqrt{1 - 4\left(\frac{cr_s}{h_{inbound}}\right)^2}\right].$$

For an approaching unbound orbit, the closest approach to the black hole that can be reached is just twice the Schwarzschild radius, and this occurs for $\frac{h_{inbound\ minimum}}{cr_s} = 2$. Smaller values of the inbound angular momentum result in the test particle going over the event horizon into the hole.

At this location, the proper velocity is entirely azimuthal, and the speed increase will occur parallel to that velocity, increasing both the angular momentum and the energy. At the turning point, the energy and angular momentum after the burn are related by

$$\left(\frac{dr}{cd\tau}\right)^2 = \left(\frac{E_{outbound}}{mc^2}\right)^2 - \left(1 - \frac{r_s}{r}\right)\left(1 + \frac{h_{outbound}{}^2}{c^2 r^2}\right),$$

and with the proper velocity all azimuthal and the transition occurring at twice the Schwarzschild radius, we have

$$0 = \left(\frac{E_{outbound}}{mc^2}\right)^2 - \frac{1}{2}\left(1 + \frac{h_{outbound}{}^2}{4c^2 r_s^2}\right)$$

or

$$\left(\frac{E_{outbound}}{mc^2}\right)^2 - 1 = \frac{1}{2}\left(-1 + \frac{h_{outbound}{}^2}{4c^2 r_s^2}\right).$$

The components of the proper velocity, or celerity, provide the increments in radial and transverse (azimuthal) distance per increment of clock time on the moving observer. As such, they provide the components of momentum per unit mass of the moving test object, and they can also be related back to the constants of the motion *E* and *h* via the components of the local velocity *v* (being the components of the rate of change of the test object as referred to the distant, stationary coordinate clock time).

We can write

$$\frac{dr}{d\tau} = v_r \sqrt{\frac{1 - \frac{r_s}{r}}{1 - \frac{v^2}{c^2}}}$$

$$\frac{r d\varphi}{d\tau} = \frac{v_\varphi}{\sqrt{1 - v^2/c^2}}$$

$$\frac{d\tau}{dt} = \sqrt{\left(1 - \frac{r_s}{r}\right)\left(1 - \frac{v^2}{c^2}\right)}$$

and

$$h \equiv \frac{L}{m} = \frac{r v_\varphi}{\sqrt{1 - \frac{v^2}{c^2}}}$$

$$E = mc^2 \sqrt{\frac{1 - \frac{r_s}{r}}{1 - \frac{v^2}{c^2}}}$$

with components

$$E_{rest} = mc^2$$

$$E_{kinetic} = mc^2 \left(\frac{1}{\sqrt{1 - v^2/c^2}} - 1 \right)$$

$$E_{potential} = \frac{\sqrt{1 - r_s/r} - 1}{\sqrt{1 - v^2/c^2}} mc^2.$$

At the turning point (periapsis about the block hole), $v_r = 0$ and $v_\varphi = v$, so that

$$\frac{h_{inbound}}{c r_s} = \frac{\frac{r_{01} v}{r_s \, c}}{\sqrt{1 - v^2/c^2}}$$

and, from above,

$$\frac{r_{01}}{r_s} = \frac{1}{2} \left(\frac{h_{inbound}}{c r_s} \right)^2 \left[1 + \sqrt{1 - 4 \left(\frac{c r_s}{h_{inbound}} \right)^2} \right].$$

From these formulae, we can calculate the speed at the time of the maneuver burn as

$$\frac{v}{c} = \frac{\frac{h_{inbound}}{c r_s} \frac{r_s}{r_{01}}}{\sqrt{1 + \left(\frac{h_{inbound}}{c r_s} \right)^2 \left(\frac{r_s}{r_{01}} \right)^2}}.$$

Three sample analytic values are given by

$\frac{h_{inbound}}{c r_s}$	$\frac{r_{01}}{r_s}$	$\frac{v}{c}$
2	2	$1/\sqrt{2}$ = 0.70711
5/2 = 2.5	5	$1/\sqrt{5}$ = 0.44721
29/10 = 2.9	29/4 = 7.25	$2/\sqrt{29}$ = 0.37139

At the Oberth burn, the angular momentum per unit mass and the energy are both changed in a discontinuous fashion. Some more thought regarding how this works in the various reference frames is warranted, but suppose the burn is a very sub-relativistic 4 km/s as could be applied with a simple solid rocket engine. As a fraction of light speed, the burn is 1.33426×10^{-5}. For the closest and therefore most pressing case, the speed is 0.707107, and a simple addition gives the resultant speed as 0.707120. However, a proper addition of speeds related to the far frame yields a speed of "only" 0.707113 due to the finite speed of light in the local frame at the burn time. From the increased energy, we can deduce a speed of 1302.26 km/s far from the black hole. For the Sun, the Schwarzschild radius is 2.953 km, and the nominal solar radius is ~235,572 times the Schwarzschild radius. For the same burn at perihelion there, we obtain an asymptotic fly-out speed of 70.41 km/s.

If we go back to equation 5, we see that for a burn of 4 km/s applied at 1 R_S, the simple treatment gives an asymptotic fly-out speed of 2 × 35.14 km/s = 70.28 km/s. Similarly, reducing the closest approach distance by a factor of 235,572 (to the Sun's Schwarzschild radius) would increase this speed by the fourth root of that factor (i.e., by a factor of 22.031) to 22.03 × 70.28 = 1548 km/s, higher than the relativistic correct speed. In this case, the smaller value is due to the application of the burn at an already relativistic speed of ~70% *c*, limiting the advantage of the 4 km/s burn due to the finite speed of light.

In any event, even if one did have a "local" black hole with a benign environment near the horizon, a classic chemical rocket, in the best case of an ideal point burn, could only accelerate the vehicle to ~2000 km/s for a burn of 10 km/s, and this falls short of the possibility of "rapid" interstellar travel, given stellar distances in our local region of the Milky Way galaxy.

11.2.2.2. The Orbit of a Free-Falling Massive Object from Rest at Infinite Separation

The orbital equation in the Schwarzschild metric is

$$\left(\frac{du}{d\varphi}\right)^2 = \left[\left(\frac{E}{mc^2}\right)^2 - 1\right]\left(\frac{c}{h}\right)^2 + ur_s\left(\frac{c}{h}\right)^2 - u^2 + r_s u^3.$$

For our case of interest, the first term is identically zero and

$$\left(\frac{du}{d\varphi}\right)^2 = u\left(\frac{1}{r_s}\left(\frac{r_s c}{h}\right)^2 - u + r_s u^2\right),$$

so that the root u_1 in the general solution is zero. The other two roots are given by the solution of the quadratic term and, therefore, are

$$u_{2,3} = \frac{1 \pm \sqrt{1 - 4\left(\frac{r_s c}{h}\right)^2}}{2r_s}.$$

For the closest approach solution $u_2 = u_3 = \frac{1}{2r_s}$ and

$$\frac{du}{d\varphi} = \pm\sqrt{r_s}\sqrt{u}\left(u - \frac{1}{2r_s}\right),$$

so

$$\varphi = \pm\frac{1}{\sqrt{r_s}}\int \frac{du}{\sqrt{u}\left(u-\frac{1}{2r_s}\right)} = \mp\frac{1}{\sqrt{r_s}}\frac{2\tanh^{-1}\left(\sqrt{2r_s u}\right)}{\sqrt{\frac{1}{2r_s}}} = \mp 2\sqrt{2}\tanh^{-1}\left(\sqrt{2r_s u}\right),$$

which is easily inverted to yield

$$r_s u = \frac{1}{2}\tanh^2\left(\frac{\varphi}{2\sqrt{2}}\right)$$

or

$$\frac{r}{r_s} = 2\coth^2\left(\frac{\varphi}{2\sqrt{2}}\right).$$

The corresponding orbit is plotted in Figure 11-4.

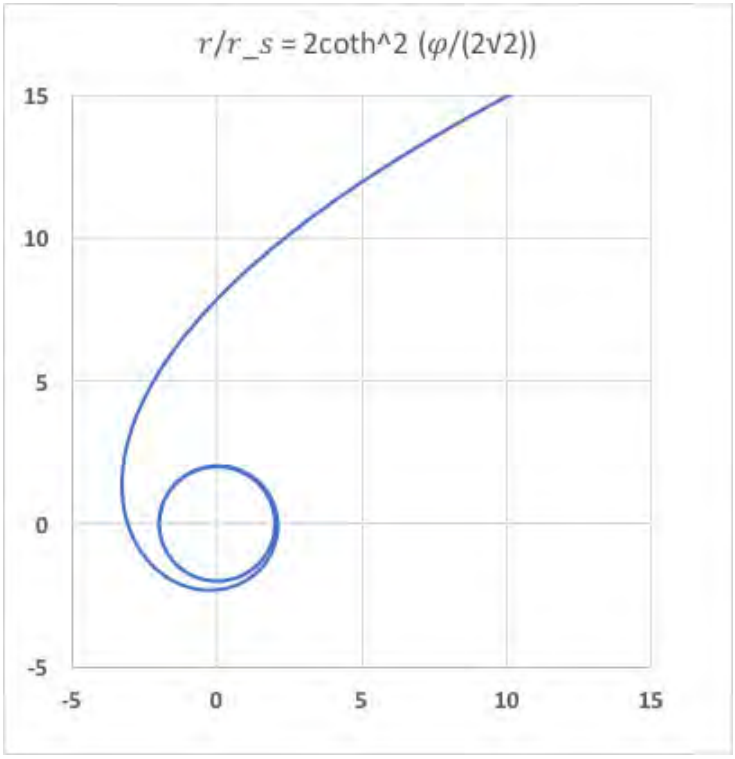

Figure 11-4. Orbit of a massive (i.e., non-photonic) mass, falling from rest at infinity toward a black hole. For angular momentum tuned to a minimum orbital radius of twice the Schwarzschild radius, the object never escapes back to an infinite separation.

No further simplifications follow, for $r(t)$, $r(\tau)$, or $r(\varphi)$, for the next set of algebraically simple roots $u_{2,3} = \frac{1}{5r_S}$ and $\frac{4}{5r_S}$, for which

$$u = \tfrac{1}{5}\mathrm{sn}^2\left(\tfrac{\varphi}{\sqrt{5}}\right) \text{ with } k = \tfrac{1}{2}.$$

Although inclusion of rotation can provide frame dragging within the Kerr metric (Kerr, 1963), especially outside of the event horizon but still within the ergosphere (Wikipedia, 2020e), there is no readily obvious way one could take advantage of this effect via a rocket maneuver, and the interpretation of the effects near the event horizon is nontrivial (cf., e.g., Carter, 1968).

(And do not even think of contributing to the income of one certain author (Essig, 2016); the multiple repetitions of text and the pseudoscience promulgated through such works are yet one more problem in actually trying to accomplish technical things while an ill-educated (at best) audience holds the purse strings.)

In terms of scaled coordinates:

$$\hat{r} \equiv \tfrac{r}{r_S} \qquad \hat{u} \equiv \tfrac{r_S}{r} = r_S u \quad \hat{t} \equiv \tfrac{t}{r_S} \quad \hat{\tau} \equiv \tfrac{\tau}{r_S}$$

$$\left(\frac{d\hat{u}}{d\varphi}\right)^2 = \left[\left(\tfrac{E}{mc^2}\right)^2 - 1\right]\left(\tfrac{r_S c}{h}\right)^2 + \hat{u}\left(\tfrac{r_S c}{h}\right)^2 - \hat{u}^2 + \hat{u}^3.$$

And from

$$\left(\frac{dr}{cd\tau}\right)^2 = \left(\tfrac{E}{mc^2}\right)^2 - \left(1 - \frac{r_S}{r}\right)\left(1 + \frac{h^2}{c^2 r^2}\right)$$

$$\left(\frac{dr}{cd\tau}\right)^2 = \left[\left(\frac{E}{mc^2}\right)^2 - 1\right] + \frac{r_S}{r} - \frac{\left(\frac{h}{c}\right)^2}{r^2} + \frac{r_S\left(\frac{h}{c}\right)^2}{r^3}$$

$$\left(\frac{dr}{d\varphi}\right)^2 = \left(\frac{d\left(\frac{1}{u}\right)}{d\varphi}\right)^2 = \frac{1}{u^4}\left(\frac{du}{d\varphi}\right)^2,$$

we obtain

$$\frac{1}{\hat{u}^4}\left(\frac{d\hat{u}}{cd\hat{\tau}}\right)^2 = \left[\left(\tfrac{E}{mc^2}\right)^2 - 1\right] + \hat{u} - \left(\tfrac{h}{r_S c}\right)^2 \hat{u}^2 + \left(\tfrac{h}{r_S c}\right)^2 \hat{u}^3,$$

and with

$$\left(\frac{cd\hat{t}}{cd\hat{\tau}}\right)^2 = \left(\tfrac{E}{mc^2}\right)^2 \frac{1}{(1-\hat{u})^2},$$

we obtain the equation set to solve of

$$\left(\frac{d\hat{u}}{d\varphi}\right)^2 = \left[\left(\frac{E}{mc^2}\right)^2 - 1\right]\left(\frac{r_S c}{h}\right)^2 + \hat{u}\left(\frac{r_S c}{h}\right)^2 - \hat{u}^2 + \hat{u}^3$$

$$\frac{1}{\hat{u}^4}\left(\frac{d\hat{u}}{cd\hat{t}}\right)^2 = \left[\left(\frac{E}{mc^2}\right)^2 - 1\right] + \hat{u} - \left(\frac{h}{r_S c}\right)^2 \hat{u}^2 + \left(\frac{h}{r_S c}\right)^2 \hat{u}^3$$

$$\frac{1}{\hat{u}^4}\left(\frac{d\hat{u}}{cd\hat{t}}\right)^2 = \left(\frac{mc^2}{E}\right)^2 (1-\hat{u})^2 \left\{\left[\left(\frac{E}{mc^2}\right)^2 - 1\right] + \hat{u} - \left(\frac{h}{r_S c}\right)^2 \hat{u}^2 + \left(\frac{h}{r_S c}\right)^2 \hat{u}^3\right\},$$

For a particle falling into the black hole from rest (from outside the event horizon), we have $E = mc^2$, and so

$$\left(\frac{d\hat{u}}{d\varphi}\right)^2 = \hat{u}\left[\left(\frac{r_S c}{h}\right)^2 - \hat{u} + \hat{u}^2\right]$$

$$\left(\frac{d\hat{u}}{cd\hat{t}}\right)^2 = \left(\frac{h}{r_S c}\right)^2 \hat{u}^5 \left[\left(\frac{r_S c}{h}\right)^2 - \hat{u} + \hat{u}^2\right]$$

$$\left(\frac{d\hat{u}}{cd\hat{t}}\right)^2 = \left(\frac{h}{r_S c}\right)^2 (1-\hat{u})^2 \hat{u}^5 \left[\left(\frac{r_S c}{h}\right)^2 - \hat{u} + \hat{u}^2\right].$$

Let $\alpha \equiv \frac{r_S c}{h}$, and put $\hat{u} \equiv x^2$. Then $d\hat{u} \equiv 2x\,dx$. Then $\frac{du}{\sqrt{\hat{u}}} = 2dx$, and so

$$\varphi = 2\int \frac{dx}{\sqrt{\alpha^2 - x^2 + x^4}}$$

$$c\tau = 2\alpha \int \frac{dx}{x^4\sqrt{\alpha^2 - x^2 + x^4}}$$

$$ct = 2\alpha \int \frac{dx}{x^4(1-x^2)\sqrt{\alpha^2 - x^2 + x^4}}.$$

All three integrals for arbitrary energy E can be integrated in terms of incomplete elliptic integrals of the first, second, and third kinds.

The goal is to find a "compact" version of the integrals in terms of standard functions to ease calculation and minimize the possible chance of transcription errors. At least part of this effort can be mitigated with additional definitions of intermediate algebraic forms that show up in multiple places in the nominal solution.

For simplicity, use $z \equiv \hat{u}$, $\alpha \equiv \frac{r_S c}{h}$ as before, and $\varepsilon \equiv \left(\frac{E}{mc^2}\right)^2 - 1$, so that a test particle with no velocity at infinite separation has only its rest energy, which is a constant of the motion and for which case $\varepsilon = 0$.

The various alternative forms to be investigated can be written as

$$\varphi = \int \frac{dz}{\sqrt{\varepsilon\alpha^2 + \alpha^2 z - z^2 + z^3}}$$

$$c\tau = \alpha \int \frac{dz}{z^2\sqrt{\varepsilon\alpha^2 + \alpha^2 z - z^2 + z^3}}$$

$$ct = \frac{\alpha}{\varepsilon + 1} \int \frac{dz}{(1-z)z^2\sqrt{\varepsilon\alpha^2 + \alpha^2 z - z^2 + z^3}}.$$

In each of these, there is a characteristic cubic polynomial $P(z) = \varepsilon\alpha^2 + \alpha^2 z - z^2 + z^3$ with non-zero roots z_1, z_2, z_3, such that

$$z_1 + z_2 + z_3 = 1$$

and

$$z_1 z_2 z_3 = -\varepsilon\alpha^2.$$

For the special case of $\varepsilon = 0$ (test particle falling from infinity), the expressions simplify to

$$\varphi = \int \frac{dz}{\sqrt{z}\sqrt{\alpha^2 - z + z^2}}$$

$$c\tau = \alpha \int \frac{dz}{z^{5/2}\sqrt{\alpha^2 - z + z^2}}$$

$$ct = \alpha \int \frac{dz}{(1-z)z^{5/2}\sqrt{\alpha^2 - z + z^2}},$$

with the two non-zero roots of the characteristic polynomial given by

$$z_1 + z_2 = 1$$

and

$$z_1 z_2 = \alpha^2.$$

Solutions can comparatively easily be written down for $\varphi(z)$ and then inverted to yield $z(\varphi)$:

$$\varphi = \int \frac{dz}{\sqrt{\varepsilon\alpha^2 + \alpha^2 z - z^2 + z^3}}$$

$$\varphi = 2 \int \frac{dx}{\sqrt{\alpha^2 - x^2 + x^4}}$$

$$c\tau = 2\alpha \int \frac{dx}{x^4\sqrt{\alpha^2 - x^2 + x^4}}$$

$$ct = 2\alpha \int \frac{dx}{x^4(1-x^2)\sqrt{\alpha^2 - x^2 + x^4}}.$$

A search of the web with Google led to a posting on the Mathematics Stack Exchange (StackExchange, 2010). Although the subject integrand is the inverse of the case here, the steps given are the same required for the problem at hand, in both cases making use of a Möbius transformation of the integration variable. For the record, the calculation given at the referenced website is duplicated here using slightly different notation.

The integral of interest is

$$\int \frac{dz}{\sqrt{P(z)}}$$

with

$$P(z) = (a-z)(b-z)(c-z) \; where \; a > b > c \geq z.$$

The substitution is the transformation

$$z \equiv \frac{b - c(\frac{a-b}{a-c})x}{1 - (\frac{a-b}{a-c})x} = \frac{b - ck^2x}{1 - k^2x} \; with \; m = k^2 \equiv \frac{a-b}{a-c},$$

so that

$$P(z) = \frac{(a-b)^2(b-c)^2}{(a-c)^{\frac{3}{2}}} \frac{x(1-x)}{(1-k^2x)^3}$$

and

$$dz = \frac{(a-b)(b-c)}{(a-c)} \frac{1}{(1-k^2x)^2} dx.$$

Then

$$\int \frac{dz}{\sqrt{P(z)}} = \frac{1}{\sqrt{a-c}} \int \frac{dx}{(1-k^2x)^{1/2}\sqrt{x(1-x)}} = \frac{2}{\sqrt{a-c}} \int \frac{ds}{\sqrt{(1-k^2s^2)(1-s^2)}} = \frac{2}{\sqrt{a-c}} \int \frac{d\vartheta}{\sqrt{(1-k^2sin^2\vartheta)}} = F(\vartheta, k).$$

To write the incomplete elliptical integral of the first kind with no additional constant offset, the angular integral should run from 0 to ϑ. This corresponds to the limits of 0 to sin ϑ for the integral in *s*, a lower limit of 0 in the integral over *x*, and a lower limit of *b* in the integral over *z*.

Consider the general form

$$P(z) = \varepsilon\alpha^2 + \alpha^2 z - z^2 + z^3,$$

with $z \equiv \hat{u} \equiv \frac{r_S}{r} = r_S u$, $\alpha \equiv \frac{r_S c}{h}$, and $\varepsilon \equiv \left(\frac{E}{mc^2}\right)^2 - 1$. Hence, $\alpha > 0$, $\varepsilon \geq 0$, and r varies between infinity and the outermost turning point in the motion, the largest value of r for which $dr/d\tau = 0$. This condition corresponds to the smallest root c of $P(z)$.

From Descartes's rule of signs, there are at most two positive roots, and there is one negative root unless $\varepsilon = 0$. If we write

$$t \equiv z + \frac{1}{3}$$

$$p = \alpha^2 - \frac{1}{3}$$

$$q = \varepsilon\alpha^2 + \frac{1}{3}\alpha^2 - \frac{2}{27},$$

then

$$P(t) = t^3 + \left(\alpha^2 - \frac{1}{3}\right)t + \left(\frac{1}{3}\alpha^2 + \varepsilon\alpha^2 - \frac{2}{27}\right).$$

The nature of the roots (two complex conjugates or all real) are determined by the sign of

$$\left(\frac{p}{3}\right)^3 + \left(\frac{q}{2}\right)^2 = \left(\frac{\alpha^2 - 1/3}{3}\right)^3 + \left(\frac{\frac{1}{3}\alpha^2 + \varepsilon\alpha^2 - \frac{2}{27}}{2}\right)^2,$$

which must be negative for all three roots to be real.

The error in the treatment above is that we ***always*** have the ordering in z-space of $a > b > z \geq 0 \geq c$ for the roots of $P(z)$ as long as $\varepsilon \geq 0$, which is the case at hand here. This follows from the result of Descartes' rule of signs, which, as we have noted, says that there must be one negative root. And, in the limiting case of our initial condition that $\varepsilon = 0$, the minimum root is $c = 0$, and the ordering still stands. Hence, for both the incoming and outgoing trajectories, the mapping deduced above applies with the ordering and limits of equation 3.131.3 of (Gradshteyn & Ryzhik, 1980), viz.

$$\int_c^z \frac{dx}{\sqrt{(a-x)(b-x)(x-c)}} = \frac{2}{\sqrt{a-c}} F\left(\sin^{-1}\sqrt{\frac{u-c}{b-c}}, \sqrt{\frac{b-c}{a-c}}\right),$$

so that we obtain

$$F\left(\sin^{-1}\sqrt{\frac{z-c}{b-c}}, \sqrt{\frac{b-c}{a-c}}\right) = \frac{\varphi(u)-\varphi(c)}{2}\sqrt{a-c}$$

or

$$\sqrt{\frac{z-c}{b-c}} = \sin\left[F^{-1}\left(\frac{\varphi(u)-\varphi(c)}{2}\sqrt{a-c}, \sqrt{\frac{b-c}{a-c}}\right)\right] = \mathrm{sn}\left(\frac{\varphi(u)-\varphi(c)}{2}\sqrt{a-c}, \sqrt{\frac{b-c}{a-c}}\right),$$

so that

$$z = c + (b-c)\mathrm{sn}^2\left(\frac{\varphi(u)-\varphi(c)}{2}\sqrt{a-c}, \sqrt{\frac{b-c}{a-c}}\right),$$

which is the form (Wikipedia, 2020f)

$$u = u_1 + (u_2-u_1)\mathrm{sn}^2\left(\frac{1}{2}\varphi\sqrt{r_s(u_3-u_1)} + const\right) \; with \; k \equiv \sqrt{\frac{(u_2-u_1)}{(u_3-u_1)}},$$

although now the meaning of the *const* entry is clear. Without loss of generality, we can set $\varphi(c) = 0$ and write the inverted equation as

$$z(\varphi) = c + (b-c)\mathrm{sn}^2\left(\frac{\varphi}{2}\sqrt{a-c}, \sqrt{\frac{b-c}{a-c}}\right).$$

If we now take $c = 0$ for $\varepsilon = 0$, we have

$$z(\varphi) = b\,\mathrm{sn}^2\left(\frac{\varphi}{2}\sqrt{a}, \sqrt{\frac{b}{a}}\right).$$

sn (0) = 0 and sn(K) = 1, where $K = K(k) = K\left(\frac{b}{a}\right)$ is the value of the complete elliptic integral of the first time. Hence

$$\varphi_{max} = \frac{2}{\sqrt{a}}K\left(\sqrt{\frac{b}{a}}\right).$$

Note that $\varphi_{max} \to \infty$ as $b \to a$, that is, for test particles at the limit, the orbit is executed an infinite number of times without the test particle approaching more closely. Next, set $\tau = 0$ at $\varphi = 0$ (and hence at $z = 0$); then we can write

$$\frac{c\tau}{r_s} = \frac{\alpha}{b^2}\int_0^{\varphi(\tau)} \frac{d\varphi}{\mathrm{sn}^4\left(\frac{\varphi}{2}\sqrt{a}, \sqrt{\frac{b}{a}}\right)} = \frac{\alpha}{b^2}\int_0^{\varphi(\tau)} \mathrm{ns}^4\left(\frac{\varphi}{2}\sqrt{a}, \sqrt{\frac{b}{a}}\right) d\varphi.$$

All of the integrals of interest with information can be located in (Byrd & Friedman, 1971), commencing with equation 233.00 (for $z(\varphi)$), 233.18 for $c\tau$ (referring to 366.03 with $m = 2$), and no explicit form for what we need for the integral for ct. Using equation 311.04, we can use the expression for B_4 for the expression for $c\tau$. Explicitly

$$\frac{c\tau}{r_s} = \frac{2\alpha}{b^2\sqrt{a}} \int_0^{\varphi(\tau)\sqrt{a}/2} \mathrm{ns}^4(u)\, du$$
$$= \frac{2\alpha}{3b^2\sqrt{a}} \left[\left(2 + \frac{b}{a}\right) \frac{\varphi\sqrt{a}}{2} - 2\left(1 + \frac{b}{a}\right) E\left(\frac{\varphi\sqrt{a}}{2}, \sqrt{\frac{b}{a}}\right) - dn\left(\frac{\varphi\sqrt{a}}{2}\right) cs\left(\frac{\varphi\sqrt{a}}{2}\right) \left\{ ns^2\left(\frac{\varphi\sqrt{a}}{2}\right) + 2 + 2\frac{b}{a} \right\} \right].$$

So for

$$\varphi_{max} = \frac{2}{\sqrt{a}} K\left(\sqrt{\frac{b}{a}}\right)$$

$$\frac{c\tau_{max}}{r_s} = \frac{2\alpha}{3b^2\sqrt{a}} \left[\left(2 + \frac{b}{a}\right) K\left(\sqrt{\frac{b}{a}}\right) - 2\left(1 + \frac{b}{a}\right) E\left(\sqrt{\frac{b}{a}}\right) \right].$$

The forms for $c\tau$ and ct are types of hyperelliptic integrals. We can try the same approach for ct. Proceeding the same way as for the proper time, we obtain

$$\frac{ct}{r_s} = \frac{\alpha}{(\varepsilon+1)b^2} \int_0^{\varphi(\tau)} \frac{d\varphi}{\mathrm{sn}^4\left(\frac{\varphi}{2}\sqrt{a}, \sqrt{\frac{b}{a}}\right) \left[1 - b\,\mathrm{sn}^2\left(\frac{\varphi}{2}\sqrt{a}, \sqrt{\frac{b}{a}}\right)\right]}$$
$$= \frac{2\alpha}{(\varepsilon+1)\sqrt{a}b^2} \int_0^{\varphi(t)\sqrt{a/2}} \frac{du}{\mathrm{sn}^4\left(u, \sqrt{\frac{b}{a}}\right) \left[1 - b\,\mathrm{sn}^2\left(u, \sqrt{\frac{b}{a}}\right)\right]}.$$

What we actually want to compute is the complete integral

$$\frac{ct_{max}}{r_s} = \frac{2\alpha}{(\varepsilon+1)\sqrt{a}b^2} \int_0^K \frac{du}{\mathrm{sn}^4\left(u, \sqrt{\frac{b}{a}}\right) \left[1 - b\,\mathrm{sn}^2\left(u, \sqrt{\frac{b}{a}}\right)\right]},$$

and for ct:

$$ct = \frac{\alpha}{\varepsilon+1} \int \frac{dz}{(1-z)z^2\sqrt{\varepsilon\alpha^2 + \alpha^2 z - z^2 + z^3}} = \frac{\alpha}{\varepsilon+1} \int \frac{dx}{(1-x)x^2\sqrt{(a-x)(b-x)(c-x)}},$$

and with $c = 0$, an analytic representation can be written down, albeit a very complicated one, which we do not include here.

It is now clear that the appropriate integrals can all be reduced to standard transcendental functions. However, for the case at hand, those forms are not very user friendly.

The key reference is the general solution of (Hagihara, 1931). Hagihara provides a solution and the history of that solution in references in chapter IV of his paper. His version of our three equations is given as his equation 49 with the function $U(u)$ given in his equation 39a:

$$U(u) = u^3 - u^2 + \frac{\alpha^2}{{h_1}^2}u + \frac{\alpha^2\left({h_3}^2 - 1\right)}{{h_1}^2}.$$

His corresponding system of equation 49 is

$$\frac{h_1}{\alpha^2}ds = \frac{du}{u^2\sqrt{U(u)}}$$

$$0 = \frac{du}{\sqrt{U(u)}} - d\psi$$

$$0 = \frac{du}{(1-u)u^2\sqrt{U(u)}} - \frac{h_1 c_0}{\alpha^2 h_3}.$$

Here α is just the Schwarzschild radius r_s with $u \equiv \frac{1}{r}$; h_1, h_2, and h_3 are constants of the motion; c_0 is the speed of light; and the line element ds is just the speed of light times the proper time, viz. $ds \equiv cd\tau$. By rotating the coordinate system so that the planar particle orbit is aligned with that system, the constant h_2 can be eliminated and we can see that

$$u \to \hat{u},\ \alpha \to r_s,\ c_0 \to c,\ ds/c_0 \to d\tau,\ h_1 \to \frac{h}{r_s c} \equiv \frac{1}{\alpha},\ \text{and}\ h_3 \to \frac{E}{mc^2} \equiv \sqrt{\varepsilon + 1}$$

in going from his paper to this one.

Hagihara notes that (Forsyth, 1920) provided the exact general equation for the orbit (in terms of Jacobi elliptic functions). Forsyth also provided the small angle approximations of the general solution to recapture the advance in the perihelion of Mercury. (Morton, 1921) elaborates on those results to illustrate some of the extreme non-Newtonian orbits allowed mathematically in the Schwarzschild metric. Hagihara also notes that the variation of the radial coordinate with proper time was considered along with orbit itself by (Droste, 1917), who takes the equations of motion over into the formalism of Weierstrauss's elliptical function $\wp(z)$, which can also be related back to the Jacobi elliptic functions.

The approach is as follows. Let u_1, u_2, and u_3 be the roots of $U(u) = 0$ (hence the same as our a, b, and c introduced above). Define $x \equiv u - \frac{1}{3}$ and $e_i \equiv u_i - \frac{1}{3}$ for $i = 1, 2, 3$. Then

$$d\psi = \frac{dx}{\sqrt{(x-e_1)(x-e_2)(x-e_3)}}$$

and with

$$|\wp'(z)|^2 = 4|\wp(z)|^3 - g_2\wp(z) - g_3$$

for

$$U(x) = x^3 - x\left(\frac{1}{3} - \frac{\alpha^2}{{h_1}^2}\right) + \frac{\alpha^2\left({h_3}^2 - \frac{2}{3}\right)}{{h_1}^2} - \frac{2}{27}$$

$$\frac{\psi + \beta_1}{2} = \int \frac{dx}{\sqrt{4x^3 - x\left(\frac{4}{3} - \frac{4\alpha^2}{{h_1}^2}\right) + \frac{4\alpha^2\left({h_3}^2 - \frac{1}{3}\right)}{{h_1}^2} - \frac{8}{27}}},$$

with which we can immediately write the solution

$$x = \wp\left(\frac{\psi + \beta_1}{2}\right),$$

with β_1 being a constant of integration and

$$g_2 = \frac{4}{3} - \frac{4\alpha^2}{{h_1}^2}$$

$$g_3 = \frac{8}{27} - \frac{4\alpha^2\left({h_3}^2 - \frac{2}{3}\right)}{{h_1}^2}.$$

The equations for the proper time and the coordinate time now become

$$\frac{h_1}{\alpha^2}ds = \frac{d\psi}{\left[\wp\left(\frac{\psi + \beta_1}{2}\right) + \frac{1}{3}\right]^2} = \frac{dx}{\left(x + \frac{1}{3}\right)^2\sqrt{(x - e_1)(x - e_2)(x - e_3)}}$$

$$\frac{h_1 c_0}{\alpha^2 h_3} = \frac{d\psi}{\left[\frac{2}{3} - \wp\left(\frac{\psi + \beta_1}{2}\right)\right]\left[\wp\left(\frac{\psi + \beta_1}{2}\right) + \frac{1}{3}\right]^2} = \frac{dx}{\left(\frac{2}{3} - x\right)\left(x + \frac{1}{3}\right)^2\sqrt{(x - e_1)(x - e_2)(x - e_3)}}.$$

Recalling the associated functions (cf. equations 8.171.1 and 8.171.2 of Gradshteyn & Ryzhik, 1980)

$$\zeta(u) \equiv \frac{1}{u} - \int_0^u \left(\wp(z) - \frac{1}{z^2}\right) dz$$

$$\sigma(u) \equiv u \exp\left\{\int_0^u \left(\zeta(z) - \frac{1}{z}\right) dz\right\}.$$

Note that

$\frac{d\zeta(u)}{du} = -\wp(u)$ and $\frac{d\ln\sigma(u)}{du} = \zeta(u)$ such that $\lim_{z\to 0}\left(\zeta(z) - \frac{1}{z}\right) = 1$ and $\lim_{z\to 0}\frac{\sigma(z)}{z} = 1,$

so we have the identity (cf. equation 8.177.3 of Gradshteyn & Ryzhik, 1980)

$$\zeta(x+y) - \zeta(x-y) - 2\zeta(y) = -\frac{\wp'(y)}{\wp(x) - \wp(y)},$$

which upon differentiation yields

$$\wp(x+y) + \wp(x-y) - 2\wp(y) = -\frac{\wp'(y)^2}{\left(\wp(x) - \wp(y)\right)^2} + \frac{\left(\wp''(y)\right)}{\wp(x) - \wp(y)}.$$

These relations allow integration of both equations. Go back to Hagihara's equation 59 and choose *y* and *z* such that

$$\wp(y) = -\frac{1}{3}$$

$$\wp(z) = \frac{2}{3}.$$

The invariants are then

$$g_2 = -4(e_1e_2 + e_2e_3 + e_3e_1) = \frac{4}{3} - \frac{4\alpha^2}{{h_1}^2}$$

$$g_3 = 4e_1e_2e_3 = \frac{8}{27} - \frac{4\alpha^2\left({h_3}^2 - \frac{2}{3}\right)}{{h_1}^2},$$

and with

$$\Delta = {g_2}^3 - 27{g_3}^2,$$

the expressions for the proper time and coordinate time can be integrated to yield

$$\frac{h_1}{\alpha^2}(s+\beta_0) = \frac{1}{\wp'(y)^2}\left[-\zeta\left(\frac{\psi+\beta_1}{2} + y\right) - \zeta\left(\frac{\psi+\beta_1}{2} - y\right) - (\psi+\beta_1)\wp(y) + \frac{\wp''(y)}{\wp'(y)}\left\{\log\frac{\sigma\left(\frac{\psi+\beta_1}{2} + y\right)}{\sigma\left(\frac{\psi+\beta_1}{2} - y\right)} - (\psi+\beta_1)\varsigma(y)\right\}\right]$$

$$\frac{h_1}{\alpha^2 h_3}(c_0 t + \beta_3)$$
$$= \frac{1}{\wp'(z)}\left\{(\psi+\beta_1)\varsigma(z) - \log\frac{\sigma\left(\frac{\psi+\beta_1}{2}+z\right)}{\sigma\left(\frac{\psi+\beta_1}{2}-z\right)}\right\}$$
$$-\frac{1}{\wp'(y)}\left\{(\psi+\beta_1)\varsigma(y) - \log\frac{\sigma\left(\frac{\psi+\beta_1}{2}+y\right)}{\sigma\left(\frac{\psi+\beta_1}{2}-y\right)}\right\}\left(1-\frac{\wp''(y)}{[\wp'(y)]^2}\right)$$
$$+\frac{1}{[\wp'(y)]^2}\left\{\zeta\left(\frac{\psi+\beta_1}{2}+y\right)+\zeta\left(\frac{\psi+\beta_1}{2}-y\right)+(\psi+\beta_1)\wp(y)\right\}$$

with

$$u-\frac{1}{3}=\wp\left(\frac{\psi+\beta_1}{2}\right).$$

One relationship to the Jacobi elliptic functions is (Wikipedia, 2020b)

$$\wp(z)=e_3+\frac{e_1-e_3}{\mathrm{sn}^2 w},$$

where

$$w=z\sqrt{e_1-e_3}$$

and the modulus of the Jacobi function is

$$k\equiv\sqrt{\frac{e_2-e_3}{e_1-e_3}}.$$

Look again at the various cases in Hagihara's summary. In his notation, the constants are

$$\lambda=\frac{\alpha^2}{{h_1}^2}$$

$$\mu={h_3}^2,$$

where the connection back with our original notation is $h_1 \to \frac{h}{r_s c} \equiv \frac{1}{\alpha}$, and $h_3 \to \frac{E}{mc^2} \equiv \sqrt{\varepsilon+1}$. For the case at hand, our interest is in the ingoing quasi-parabolic case and the outgoing quasi-hyperbolic case, corresponding to $\mu = 1$ and $\mu > 1$, respectively (and in practice for $0 < \mu - 1 <<< 1$).

The incoming case—a particle at rest at infinity falling inward but with a sufficiently large angular momentum per unit mass—corresponds to Hagihara's case IX ($\mu = 1$, $1 < \lambda < ¼$), which he labels as

"pseudo-parabolic" with the special value $e_3 = -1/3$ and lying on the boundary of his regions I and II (his Figure 13).

Consider case IX. We really have case IXb, "quasi-parabolic," which refers back to case V. There is no "easy" means of evaluation, so going back to

$$\varphi = \int \frac{dx}{\sqrt{(a-x)(b-x)(x-c)}}$$

$$c\tau = \alpha \int \frac{dx}{x^2\sqrt{(a-x)(b-x)(x-c)}}$$

$$ct = \frac{\alpha}{\varepsilon+1}\int \frac{dx}{(1-x)x^2\sqrt{(a-x)(b-x)(x-c)}},$$

recall we found the solution to the first equation by integrating from 0 to c and inverting the result to obtain

$$\varphi(z) = \int_c^z \frac{dx}{\sqrt{(a-x)(b-x)(x-c)}} = \frac{2}{\sqrt{a-c}} F\left(\sin^{-1}\sqrt{\frac{u-c}{b-c}}, \sqrt{\frac{b-c}{a-c}}\right)$$

$$F\left(\sin^{-1}\sqrt{\frac{z-c}{b-c}}, \sqrt{\frac{b-c}{a-c}}\right) = \frac{\varphi(u)-\varphi(c)}{2}\sqrt{a-c}$$

$$z(\varphi) = c + (b-c)\mathrm{sn}^2\left(\frac{\varphi}{2}\sqrt{a-c}, \sqrt{\frac{b-c}{a-c}}\right),$$

where we also put $\varphi(c) = 0$. Hence the second equation can, in general, be written

$$c\tau = \alpha\int_c^z \frac{dx}{x^2\sqrt{(a-x)(b-x)(x-c)}} = \alpha\int_{\varphi(c)}^{\varphi(z)} \frac{d\varphi\left(\frac{dx}{d\varphi}\right)}{x^2\sqrt{(a-x)(b-x)(x-c)}} = \alpha\int_{\varphi(c)}^{\varphi(z)} \frac{d\varphi}{x(\varphi)^2}.$$

Similarly, for the third equation, we can, in principle, write

$$ct = \frac{\alpha}{\varepsilon+1}\int_c^z \frac{dx}{x^2(1-x)\sqrt{(a-x)(b-x)(x-c)}} = \frac{\alpha}{\varepsilon+1}\int_{\varphi(c)}^{\varphi(z)} \frac{d\varphi}{x(\varphi)^2[1-x(\varphi)]}$$

$$= \frac{\alpha}{\varepsilon+1}\int_{\varphi(c)}^{\varphi(z)} \frac{cd\tau\left(\frac{d\varphi}{d(c\tau)}\right)}{x(\varphi)^2[1-x(\varphi)]} = \frac{\alpha}{\varepsilon+1}\int_{t(c)}^{t(z)} \frac{cd\tau}{\left[1-x\left(\varphi(\tau)\right)\right]}$$

$$c\tau = \alpha\int_{\varphi(c)}^{\varphi(z)} \frac{d\varphi}{x(\varphi)^2}$$

$$x(\varphi) = c + (b-c)\mathrm{sn}^2\left(\frac{\varphi}{2}\sqrt{a-c}, \sqrt{\frac{b-c}{a-c}}\right),$$

and so

$$c\tau = \alpha\int_{\varphi(c)}^{\varphi(z)} \frac{d\varphi}{\left[c + (b-c)\mathrm{sn}^2\left(\frac{\varphi}{2}\sqrt{a-c}, \sqrt{\frac{b-c}{a-c}}\right)\right]^2} = \frac{\alpha}{\mathrm{c}^2}\int_{\varphi(c)}^{\varphi(z)} \frac{d\varphi}{\left[1 + \frac{(b-c)}{c}\mathrm{sn}^2\left(\frac{\varphi}{2}\sqrt{a-c}, \sqrt{\frac{b-c}{a-c}}\right)\right]^2}.$$

This is valid only for $c \neq 0$ and is given by V_2, which is equation 336.02 of (Byrd & Friedman, 1971), viz.

$$V_2 \equiv \int \frac{du}{(1-\alpha^2\mathrm{sn}^2 u)^2}$$
$$= \frac{1}{2(\alpha^2-1)(k^2-\alpha^2)}\Big[\alpha^2 E(u) + (k^2-\alpha^2)u$$
$$+ (2\alpha^2k^2 + 2\alpha^2 - \alpha^4 - 3k^2)\Pi(\varphi, \alpha^2, k) - \frac{\alpha^4 \mathrm{sn}\, u\, \mathrm{cn}\, u\, \mathrm{dn}\, u}{1-\alpha^2\mathrm{sn}^2 u}\Big].$$

Also note

$$V_1 \equiv \int \frac{du}{1-\alpha^2\mathrm{sn}^2 u} = \Pi(\varphi, \alpha^2, k).$$

For the case $c = 0$, we have instead

$$c\tau = \frac{\alpha}{b^2}\int_{\varphi(c)}^{\varphi(z)} \frac{d\varphi}{\left[\mathrm{sn}^2\left(\frac{\varphi}{2}\sqrt{a-c}, \sqrt{\frac{b-c}{a-c}}\right)\right]^2} = \frac{\alpha}{b^2}\int_{\varphi(c)}^{\varphi(z)} \mathrm{ns}^4\left(\frac{\varphi}{2}\sqrt{a-c}, \sqrt{\frac{b-c}{a-c}}\right) d\varphi,$$

and from equation 311.04 of (Byrd & Friedman, 1971), we have

$$B_4 = \int \mathrm{ns}^4\, u\, du = \tfrac{1}{3}[(2+k^2)u - 2(1+k^2)E(u) - \mathrm{dn}\, u\, \mathrm{cs}\, u\, (\mathrm{ns}^2 u + 2 + 2k^2)].$$

Suppose

$$x(u) = \alpha^2\mathrm{sn}^2 u,$$

then

$$\int \frac{du}{\big(1-x(u)\big)x(u)^2} = \int \frac{du}{(1-\alpha^2\mathrm{sn}^2u)\,\alpha^4\mathrm{sn}^4u}$$
$$= \frac{1}{\alpha^4}\int \frac{\mathrm{ns}^4u\,du}{1-\alpha^2\mathrm{sn}^2u} = \frac{1}{\alpha^4}\int \mathrm{ns}^4u\; d\big(\Pi(\varphi,\alpha^2,k)\big)$$
$$= \Pi(\varphi,\alpha^2,k)\;\mathrm{ns}^4u + 4\int \Pi(\varphi,\alpha^2,k)\,\mathrm{ns}^3u\;cs\;u\;\mathrm{ds}\;u\;du.$$

Compare with 310.04

$$A_4 = \int \mathrm{sn}^4\,u\;du = \tfrac{1}{3k^4}[(2+k^2)u - 2(1+k^2)E(u) + k^2\;\mathrm{dn}\;u\;cn\;u\;\mathrm{sn}\;u\;].$$

It is worth noting that neither the incomplete elliptic integral of the second or third kind (Legendre's form) have an inverse in terms of standard functions.

Within WolframAlpha, we find two items, which are real and well behaved:

$$iE(\sin^{-1}(iu),m)$$

and

$$i\;\Pi(n,\sin^{-1}(iu),m),$$

where, again, one must be careful with the various differing notation conventions.

From equation 17.4.9 of (Abramowitz & Stegun, 1972), we can obtain

$$i\;E(i\varphi\backslash\alpha) = E\left(\theta\backslash\tfrac{\pi}{2}-\alpha\right) - F\left(\theta\backslash\tfrac{\pi}{2}-\alpha\right) - \tan\theta\sqrt{1-\cos^2\alpha\,\sin^2\theta},$$

where tan ϑ = sinh φ = –i sin $i\varphi$ and the functions are defined by

$$E(\varphi\backslash\alpha) \equiv E(u|m) \equiv \int_0^{u=\sin\varphi} \frac{\sqrt{1-mt^2}}{\sqrt{1-t^2}}dt = \int_0^{\varphi} \sqrt{1-\sin^2\alpha\,\sin^2\theta}\;\;d\theta = \int_0^u \mathrm{dn}^2\;w\;dw$$

$$F(\varphi\backslash\alpha) \equiv F(u|m) \equiv \int_0^{u=\sin\varphi} \frac{1}{\sqrt{(1-t^2)(1-mt^2)}}dt = \int_0^{\varphi} \frac{d\theta}{\sqrt{1-\sin^2\alpha\,\sin^2\theta}} = \int_0^u dw = u$$

$$\Pi(n;\varphi\backslash\alpha) \equiv \Pi(n;u|m) \equiv \int_0^{u=\sin\varphi} \frac{dt}{(1-nt)\sqrt{(1-t^2)(1-mt^2)}}$$
$$= \int_0^{\varphi} \frac{d\theta}{(1-n\sin^2\theta)\sqrt{1-\sin^2\alpha\,\sin^2\theta}} = \int_0^u \frac{du}{1-n\;\mathrm{sn}^2u},$$

and where these are the notations used in (Abramowitz & Stegun, 1972) (cf. 17.2.6–17.2.10 and 17.7.1).

Note that for the case of $c = 0$, the Wolfram solution includes the argument

$$i \sinh^{-1}\left(\sqrt{\tfrac{x}{a}-1}\right) = \sin^{-1}\left(\sqrt{1-\tfrac{x}{a}}\right)$$

and we obtain

$$\int \frac{dx}{x^{5/2}\sqrt{(a-x)(b-x)}}$$

$$= \frac{2(a-x)}{3a^2b^2x^{3/2}\sqrt{(a-x)(b-x)}}\Bigg[(x-b)(a\{b+2x\}+2bx)$$

$$+ \frac{x\sqrt{\frac{b-x}{a-b}}}{\sqrt{\frac{a}{x}-1}}\Big\{2(a^2-b^2)iE\left(\sin^{-1}\left(\sqrt{1-\tfrac{x}{a}}\right)\Big|\tfrac{a}{a-b}\right)$$

$$+ b(a+2b)iF\left(\sin^{-1}\left(\sqrt{1-\tfrac{x}{a}}\right)\Big|\tfrac{a}{a-b}\right)\Big\}\Bigg].$$

The issue is with

$$m = \frac{a}{a-b} > 1,$$

which can be remedied by using 17.4.15 and 17.4.16, but there is still an extra factor of i.

N.B. The expressions are fundamentally different in the two cases of $c = 0$ and $c \neq 0$.

After a few more false starts, one can tease well-behaved solutions from WolframAlpha. The zero and non-zero results may be identical in the limit of $c \to 0$, but that would take additional work to demonstrate.

Start with the $c = 0$ case, which corresponds to the energy being equal to the rest mass only at infinity as the initial boundary condition.

The integrals for both the proper time τ and the coordinate time t can be written as a single integral depending on the parameter η. The setting $\eta = 0$ yields the required expression for the proper time, and the setting $\eta = 1$ yields the required expression for the coordinate time. In both cases, $c = 0$ and $0 \le x \le b \le a$ in principle, although the equality cases still need to be checked for convergence at those points. WolframAlpha yields (*note the leading minus sign on the left*, which was moved there to reduce the braces count on the right in the Wolfram result)

$$-\int \frac{dx}{(1-\eta x)x^2\sqrt{(a-x)(b-x)x}}$$
$$= \frac{\left\{2\left[\sqrt{\frac{x}{b}}\sqrt{\frac{a-x}{a-b}}\begin{pmatrix} -3a^2b^3\eta^2 x\sqrt{1-\frac{x}{a}}\sqrt{\frac{x(b-x)}{b^2}}\Pi\left(b\eta;\ \sin^{-1}\left(\sqrt{\frac{x}{b}}\right)\middle|\frac{b}{a}\right)+ \\ ab^2x\sqrt{1-\frac{x}{a}}\sqrt{\frac{x(b-x)}{b^2}}F\left(\sin^{-1}\left(\sqrt{\frac{x}{b}}\right)\middle|\frac{b}{a}\right)+ \\ (a-x)(b-x)[a(3b\eta x+b+2x)+2bx] \end{pmatrix}+ \right.\right.}{\left.\left. x^2(x-a)[a(3b\eta+2)+2b]\sqrt{\frac{x-b}{a-b}}E\left(\sin^{-1}\left(\sqrt{\frac{x-b}{a-b}}\right)\middle|1-\frac{a}{b}\right)\right]\right\}}$$
$$3a^2b^3\left(\frac{x}{b}\right)^{\frac{3}{2}}\sqrt{\frac{a-x}{a-b}}\sqrt{(a-x)(b-x)x}.$$

This is the Wolfram result, except we have moved the minus sign to the left and changed the factor under the radial in the denominator from $(x-a)(x-b)$ to $(a-x)(b-x)$ to keep the quantities explicitly positive. The issues for computation purposes are that the argument of the incomplete elliptic integral of the second kind is imaginary, the parameter is greater than unity, and the coefficient is imaginary.

The first term is well behaved in both cases because for the characteristic being 0, we have

$$\Pi\left(0;\ \sin^{-1}\left(\sqrt{\frac{x}{b}}\right)\middle|\frac{b}{a}\right) = \mathrm{F}\left(\sin^{-1}\left(\sqrt{\frac{x}{b}}\right)\middle|\frac{b}{a}\right)$$

(cf. Abramowitz and Stegun (1972), equation 17.7.18) and, at $x = b$,

$$\Pi\left(b;\ \sin^{-1}\left(\sqrt{\frac{x}{b}}\right)\middle|\frac{b}{a}\right) = \Pi\left(b\middle|\frac{b}{a}\right),$$

which is also well behaved (cf. Abramowitz and Stegun (1972), equation 17.7.2). In the fourth term, we have

$$\sqrt{\frac{x-b}{a-b}}E\left(\sin^{-1}\left(\sqrt{\frac{x-b}{a-b}}\right)\middle|1-\frac{a}{b}\right) = i\sqrt{\frac{b-x}{a-b}}E\left(\sin^{-1}\left(i\sqrt{\frac{b-x}{a-b}}\right)\middle|1-\frac{a}{b}\right).$$

The parameter can be dealt with using (Abramowitz & Stegun, 1972) equation 17.4.16 to obtain

$$\sqrt{\frac{x-b}{a-b}}E\left(\sin^{-1}\left(\sqrt{\frac{x-b}{a-b}}\right)\middle|1-\frac{a}{b}\right) = i\sqrt{\frac{b-x}{a-b}}E\left(\sin^{-1}\left(i\sqrt{\frac{b-x}{a-b}}\right)\middle|1-\frac{a}{b}\right)$$
$$= i\sqrt{\frac{b-x}{a-b}}\left[\sqrt{1-\frac{a}{b}}E\left(u\sqrt{1-\frac{a}{b}}\middle|\frac{1}{1-\frac{a}{b}}\right)+\frac{a}{b}u\right],$$

where

$$\operatorname{sn} u = \sin\varphi = i\sqrt{\frac{b-x}{a-b}}.$$

That is,

$$u = F\left(\sin^{-1}\left(i\sqrt{\frac{b-x}{a-b}}\right)\middle|1-\frac{a}{b}\right).$$

We also need to correct the parameter for this function, so (with (Abramowitz & Stegun, 1972) equation 17.4.15) we can obtain

$$u = F\left(\sin^{-1}\left(i\sqrt{\frac{b-x}{a-b}}\right)\middle|1-\frac{a}{b}\right) = \frac{1}{\sqrt{1-\frac{a}{b}}}F\left(\sin^{-1}\left(i\sqrt{\frac{b-x}{a}}\right)\middle|\frac{1}{1-\frac{a}{b}}\right)$$
$$= \sqrt{\frac{b}{b-a}}F\left(\sin^{-1}\left(i\sqrt{\frac{b-x}{a}}\right)\middle|\frac{b}{b-a}\right),$$

but the parameter is *also* negative.

After more algebra, we find that by transforming from the negative parameter first and then from imaginary arguments, we can make the next step in transforming all to standard forms with the usual magnitudes of the various items.

Put

$$-m \equiv 1-\frac{a}{b}$$

and put

$$\varphi \equiv i\sinh^{-1}\left(\sqrt{\frac{b-x}{a-b}}\right) = \sin^{-1}\left(i\sqrt{\frac{b-x}{a-b}}\right) = \sin^{-1}\left(\sqrt{\frac{x-b}{a-b}}\right)$$

so that

$$\frac{iE(iu|-m)}{\sqrt{m+1}} = E\left(u\sqrt{m+1}\,\middle|\frac{1}{m+1}\right) - u - \operatorname{dn}\left(u\sqrt{1+m}\,\middle|\frac{1}{m+1}\right)\operatorname{sc}\left(u\sqrt{1+m}\,\middle|\frac{1}{m+1}\right)$$
$$+\frac{m\ \operatorname{sc}\left(u\sqrt{1+m}\middle|\frac{m}{m+1}\right)}{\sqrt{m+1}\operatorname{dn}\left(u\sqrt{1+m}\middle|\frac{m}{m+1}\right)}$$

and so

$$i\sqrt{\frac{b}{a}}E\left(iu\,\middle|\frac{a}{b}-1\right) = E\left(u\sqrt{\frac{a}{b}}\,\middle|\frac{b}{a}\right) - u - \operatorname{dn}\left(u\sqrt{\frac{a}{b}}\,\middle|\frac{b}{a}\right)\operatorname{sc}\left(u\sqrt{\frac{a}{b}}\,\middle|\frac{b}{a}\right) + \left(\frac{a}{b}-1\right)\sqrt{\frac{b}{a}}\frac{\operatorname{sc}\left(u\sqrt{\frac{a}{b}}\middle|1-\frac{b}{a}\right)}{\operatorname{dn}\left(u\sqrt{\frac{a}{b}}\middle|1-\frac{b}{a}\right)}.$$

There are no obvious simplifications, but the calculation is, in principle, doable.

For comparison of various cases, the closest approach angle needs to be used as the origin. The pattern rotates with varying angular momentum due to the variation of the period of the sn function with α. Even with α values close to the limit of ½, the relativistic effects only become acute for values close to the limit for $\alpha = \frac{\sqrt{2}}{3} \sim 0.47$, and there is only one additional "loop" in the trajectory near the center of attraction while that number goes to infinity as the limit of ½ is approached. Although these features are implicit in Hagihara's analysis (Hagihara, 1931), the plots available with current computational tools (which were nonexistent in 1930) are really needed to get a "feel" for the patterns. Unfortunately, as illustrated in the starts and stops in this documented analysis, even the application of these to the solutions is not trivial.

The maximum in *u* is also the minimum in *r* and occurs at the maximum of

$$\mathrm{sn}^2\left(\frac{\varphi}{2}\sqrt{a-c}, \sqrt{\frac{b-c}{a-c}}\right)$$

or, for $c = 0$, at the maximum of

$$\mathrm{sn}^2\left(\frac{\varphi}{2}\sqrt{a}, \sqrt{\frac{b}{a}}\right),$$

where $K(m)$ is the quarter period of $\mathrm{sn}(x,m)$ and hence, the half-period of $\mathrm{sn}^2(x,m)$, i.e., the maximum of the latter. Thus, we should have

$$\varphi_{max} = \frac{2}{\sqrt{a}}\boldsymbol{K}\left(\sqrt{\frac{b}{a}}\right).$$

So as φ goes from 0 to $2\varphi_{max}$, the argument of the sn function goes from 0 to $2\boldsymbol{K}$, which takes the trajectory inward from ∞ to closest approach to the gravitating mass and the back out to ∞. Hence, the trajectory will complete *n* full rotations about the gravitating mass for *n* being the largest integer for which

$$2\varphi_{max} = \frac{4}{\sqrt{a}}\boldsymbol{K}\left(\sqrt{\frac{b}{a}}\right) \geq 2\pi n$$

or

$$n \leq \frac{\varphi_{max}}{\pi} = \frac{2}{\pi\sqrt{a}}\boldsymbol{K}\left(\sqrt{\frac{b}{a}}\right).$$

Thus, we can, in principle, solve the transcendental equation for *n* as a function of α. The "roots" α_n are given by

$$n\frac{\pi}{2} = \frac{1}{\sqrt{a}}\boldsymbol{K}\left(\sqrt{\frac{b}{a}}\right)\Bigg|_{\alpha=\alpha_n}.$$

We also have $a + b = 1$, and so can solve for a.

Alternatively, we can write

$$= \mathrm{sn}^{-1}\left(1, \sqrt{\frac{b}{a}}\right)$$

so that

$$\frac{1-a}{a} = \mathrm{sn}^2\left(1, n\frac{\pi}{2}\sqrt{a}\right).$$

In the limit of large angular momentum per unit mass, i.e., $\alpha \to 0$, we have $a \to 1$, $b \to 1$, and $K(0) = \frac{\pi}{2}$, so that $n \to 1$. Hence, there is always one loop about the gravitating center. The threshold for two loops requires α~0.497761, with a~0.547269, b~0.452731. As both of these values approach the limiting value of ½, the number of windings increases, and the limit goes to ∞, with the test particle trapped in an asymptotic circular orbit with a radius twice that of the event horizon. It is from such an orbit that the best performance Oberth maneuver could be made such that the test particle is "nudged" to a value of α just lower than ½ and, thus allowing escape."

Recall—from above—that for this special limiting case, we have

$$\varphi = \int \frac{dx}{\sqrt{(a-x)(b-x)(x-c)}}$$

$$c\tau = \alpha \int \frac{dx}{x^2\sqrt{(a-x)(b-x)(x-c)}}$$

$$ct = \frac{\alpha}{\varepsilon+1} \int \frac{dx}{(1-x)x^2\sqrt{(a-x)(b-x)(x-c)}},$$

with $a = b = a = ½$ and $c = \varepsilon = 0$. These three equations become

$$\varphi = \frac{2}{\sqrt{a}}\tanh^{-1}\left(\sqrt{2x}\right)$$

$$\frac{c\tau}{\alpha} = \int \frac{dx}{x^{5/2}(a-x)} = \frac{2}{a^2\sqrt{a}}\tanh^{-1}\left(\sqrt{\frac{x}{a}}\right) - \frac{2}{3}\left(\frac{a+3x}{a^2x^{\frac{3}{2}}}\right) = \frac{\varphi}{a^2} - \frac{2}{3}\left(\frac{a+3x}{a^2x^{\frac{3}{2}}}\right)$$

$$\frac{ct}{\alpha} = \int \frac{dx}{(1-x)x^{\frac{5}{2}}(a-x)} = \frac{2}{a^2(1-a)\sqrt{a}}\tanh^{-1}\left(\sqrt{\frac{x}{a}}\right) - \frac{2}{3}\left(\frac{3ax+a+3x}{a^2x^{\frac{3}{2}}}\right) + \frac{1}{1-a}\log\left(\frac{1-\sqrt{x}}{1+\sqrt{x}}\right)$$

$$= \frac{2}{a^2(1-a)\sqrt{a}}\tanh^{-1}\left(\sqrt{\frac{x}{a}}\right) - \frac{2}{3}\left(\frac{3ax+a+3x}{a^2x^{\frac{3}{2}}}\right) - \frac{2}{1-a}\tanh^{-1}\left(\sqrt{x}\right),$$

and with a = ½, we obtain

$$\varphi = 2\sqrt{2}\tanh^{-1}\left(\sqrt{2x}\right)$$

$$\frac{c\tau}{\alpha} = 8\sqrt{2}\tanh^{-1}\left(\sqrt{2x}\right) - \left(\frac{\frac{4}{3}+8x}{x^{\frac{3}{2}}}\right)$$

$$\frac{ct}{\alpha} = 16\sqrt{2}\tanh^{-1}\left(\sqrt{2x}\right) - \left(\frac{12x+\frac{4}{3}}{x^{\frac{3}{2}}}\right) - 4\tanh^{-1}\left(\sqrt{x}\right).$$

We also used Wolfram to look at the case of a = 3/2; again, there were no simplifications.

At this point the case is closed. One can cross-reference equations on the relativistic rocket equation by (Ackeret, 1946) and the paper by Dyson on extraction of gravitational energy from a rotating white dwarf binary (in Cameron's book *Interstellar Communication* (Freeman J. Dyson, 1963)).

11.3. Escaping the Solar System

The scientific goal of probing the outer heliosphere and nearby interstellar medium beyond is almost as old as NASA itself, cf. the "Outer Solar System Probe" of Committee 8 – Physics of Fields and Particles in Space of the Space Science Board of the National Academy of Sciences (the "Simpson Committee" (Simpson et al., 1960)). With the evolution of NASA's science program and our knowledge of the heliosphere driven by the Pioneer 10 and 11 and Voyager 1 and 2 missions to date, the call for a dedicated probe to the near interstellar medium has evolved but nonetheless persisted as a scientific priority (J. F. Clarke et al., 1968; Dessler & Park, 1971).

Previous recent work carried out under NNN06AA01C (Task Order: "First Pragmatic Interstellar Probe Mission Study") under Order Number 80MSFC18F0139 dated 13 June 2018 for $680,000 (requisition number 4200656072) has identified reviewed, summarized, and extended these past efforts while focusing on near-term implementation.

Continuing work capitalized on this work by continuing to refine and identify the scientific impact of such a mission not only for heliophysics but also across planetary science and astrophysics as well. We made major inroads into breaking down traditional cross-divisional barriers beginning with the Mission Science Definition Workshop held under the previous effort last October (2018) as well as at the 2018 Committee on Space Research (COSPAR) Scientific Assembly in Pasadena, California, and the Fall 2018 AGU meeting held in Washington, DC. Major goals of this effort include (1) build on growing momentum in the international science community (invitations from multiple scientific conference organizers and requests for the second Mission Science Definition Workshop, held in 2019), (2) continue investigating cross-disciplinary opportunities (the workshop referred to led to interest from the astrophysics community in observations possible from well outside the solar system's dust environment), (3) explore synergies with new observations from the Voyager 1 and 2 spacecraft (now that there is general agreement that both have entered interstellar space) and from insights in progress about Kuiper Belt Objects (especially from the New Horizons flyby of 2014 MU69, aka "Ultima Thule"), (4) continue to explore how looking back on

the solar system can further inform our understanding of how the terrestrial planets can inform our inferences about the growing population of exoplanets, and (5) provide a definitive, technical answer to the question "What can the Interstellar Probe do that no other mission can do?" (the same question posed by Harold Glaser, the head of NASA's Solar Terrestrial Program Office, about "a Solar Probe" at a mission science definition workshop for that mission in 1977 (Neugebauer & Davies, 1978)) for the time frame of the next decade to provide appropriate input to the upcoming Solar and Space Physics Decadal Survey as to heliophysics science, cross-disciplinary science contributions, technical readiness and implementation possibilities, and associated costs.

It should be noted that there are three threads of work running though previous Interstellar Probe studies:

1. The notional goal of a mission to escape rapidly from the solar system
2. The engineering means
3. Mission studies, including both measurements and instrumentation

11.3.1. Goals for Escaping the Solar System

With respect to point 1, the earliest analysis was the *gedanken* experiment of Oberth, who noted that the most rapid escape would be enabled by (1) using a propulsive maneuver at a great distance from the Sun to cancel the orbital angular momentum and thus enable it to fall into the near vicinity of the Sun, followed by (2) a larger propulsive maneuver at perihelion. In 1929, he showed that such a set of maneuvers would provide the most rapid escape for a given propulsive capability (Oberth, 1970). Oberth's example includes a "start" from 900 au with a total ΔV capability of 6 km/s. Of this, he notes that one can use a 1 km/s maneuver to remove the orbital speed. He notes that one could then apply a 5 km/s maneuver at "the edge of the solar corona," increasing the vehicle speed there from ~500 km/s to 505 km/s. The difference in incoming and outgoing kinetic energy amounts to an asymptotic speed away from the Sun of 71 km/s (~15 au/year); the implied perihelion is ~1.5 R_S from the center of the Sun (so certainly at the "edge" of the visible corona during a total solar eclipse).

From the time of the 1960 "Simpson Committee" report (Simpson et al., 1960), there were no technical details discussed (other than a somewhat protracted discussion of a need for very sensitive magnetometers, but with no numbers mentioned). A requirement of sorts was stated as "(It is hoped that motion away from the Sun to the extent of 5 or 6 astronomical units per year [i.e., ~24 to 28 km/s] could be accomplished by 1965)" (Simpson et al., 1960). The idea of a probe to escape the solar system was an outgrowth of the Solar Probe studies carried out at NASA's Ames Research Center in the early 1960s (Charles F. Hall et al., 1962) and constituted the "anti-solar mission" option of the Advanced Pioneer mission studies (Matthews & Erickson, 1964). All orbits considered simply used launch from Earth with no gravity assists with bound orbits about the Sun; there was some discussion of use of Saturn launch vehicles with "high-energy" upper stages.

11.3.2. Engineering Means for Escaping the Solar System

Latter analyses combined points 1 and 2, that is, the studies included identifiable engineering means to inform the mission goals.

The first mission that "congealed" from these early works was the Galactic Jupiter Probe mission using a launch direct from Earth to Jupiter and then a (passive) JGA (M.A. Minovitch, 1965) "so that it may escape the gravitational control of the sun" (J. F. Clarke et al., 1968). For the envisioned mission, "The planetary encounter occurs between seventeen and twenty months after launch (Figure 11-5), and the probe reaches ten Astronomical Units in about three years. This distance would approximate the range limit of the communication system under consideration for the first flight."

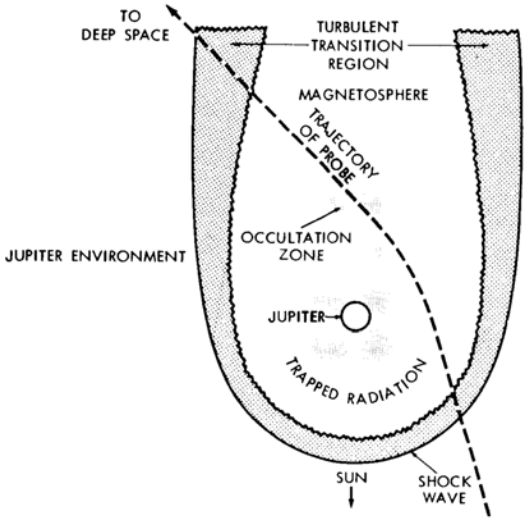

Figure 5 – Jupiter Encounter.

Figure 11-5. Passive Jupiter flyby schematic for the Galactic Jupiter Probe mission. (Reproduced from J. F. Clarke et al. (1968).)

The issue of speed was raised again by Kraft Ehricke (originator of the Centaur upper stage). The use of what he termed as a "close solar flyby (CSF)" was revisited by Ehricke in 1971 (Krafft A. Ehricke, 1971), but with cautionary notes on the required near-Sun thermal and propulsive technologies that would be required to implement it. Within the context of what he term the "ultraplanetary probe," Ehricke noted the following:

> In the stellar/interstellar frame of reference, space can be divided into a number of zones. In the order of increasing distance, these are: the stellar magnetosphere, circumstellar zone, stellar gravisphere, suboptical zone (SOZ), quasi-optical zone (QOZ) and zone of isolation (ZI). The innermost zone is determined by the extent to which the stellar magnetic field determines the motion of stellar plasma. In relation to the sun this zone is referred to as the heliosphere[11]. The circumstellar zone comprises the star's wider vicinity and represents a transition zone between the inner region filled

[11] The original definition and terminology are those of Dessler (Dessler, 1967).

with plasma emanating from the star and "free" interstellar space. As such, it contains the bulk of the residual primordial proto-stellar cloud of which the star was formed. In the case of our Sun (and other stars owning planetary systems) this is referred to as ultraplanetary zone (UZ), whose limit is set tentatively at 0.1 years (ly) or 6320 astronomical units (AU)[12]. Scientifically interesting features in ultraplanetary space include the heliospheric tail, long-periodic cometary matter and behavior (although cometary orbits extend far beyond the UZ) and the ultraplanetary environment proper – a mixture of protosolar cloud and interstellar matter in the local galactic region.

The solar gravisphere is the zone in which the path of an object is determined primarily by the Sun's gravity field. It is not a symmetric sphere, because of the uneven distribution of galactic masses around the Sun. However, the helio-gravisphere extends at least 1 ly out and should in some directions reach as far out as 2 to 3 ly.

Ehricke's SOZ, QOZ, and ZI are all concerned with travel to other star systems by employing means of relativistic flight speeds. Such issues have been addressed by many (Ackeret, 1946, 1947) (Sagan, 1963; Shepherd, 1952; S. von Hoerner, 1962) but are of no relevance here because there are no current or near-term propulsion means capable of reaching such speeds (e.g., Chew et al., 2001). Ehricke's "solar gravisphere," extending well into the Oort's cloud of long-period comets (Oort, 1950), is also beyond the reach of propulsion technology that can be implemented in the near term. This leaves his "stellar magnetosphere" and "circumstellar zone," also known as the heliosphere and, for the inner portion, the very local interstellar medium (VLISM), respectively. The "circumstellar zone" includes what are currently referred to as the heliosheath and VLISM, which together make up what Ehricke also refers to the "ultraplanetary zone" or UZ, extending to 6320 au. These terms are somewhat misleading today because the termination shock extends farther, by a factor ~8, than that deduced by Ehricke, and the current record holder for the largest aphelion, 2017 MB_7, travels as far as ~2800 au from the Sun (barycentric elements) on a highly inclined, highly eccentric orbit (Wikipedia, 2020a).

In a consideration of Ehricke's ideas for escape from the solar system, we limit ourselves to his considerations of "ultraplanetary probes" (i.e., probes to UZ).

The SOZ is defined as the region whose extent is determined primarily by the spacecraft's acceleration pattern and the allowable time to receipt by Earth of the radio signal of the vehicle's arrival at the target star (turn-around time). The flight speeds encountered extend into the relativistic regime, but are essentially sub-optical. The maximum practical extent of the SOZ, consistent with a turn-around time of 50 years, is 7 parsecs (23 ly). This spherical zone contains over 100 stars. The nearer ones among these, out to 12 ly, can still be reached with peak speeds in the sub-relativistic flight regime (0.2 to 0.8 light velocity) by starprobes on one-way (acceleration/deceleration) missions with a 50 year turn-around time. For Tau Ceti (11.8 ly) the required peak speed is $\beta = v/c \sim 0.55$, for Alpha Centauri $\beta \sim 0.2$. Reaching the outer limits of the SOZ requires a peak speed well in the relativistic flight regime ($0.8 \leq \beta < 1.0$), namely, $\beta > 0.95$. Formidable propulsion demands must be met, unless turn-around times of a sizeable fraction of a millennium are acceptable.

The QOZ requires sustained speeds at quasi-optical speeds ($\beta > 0.95$). Turn-around times are longer than 50 years and, in fact, are proportional to the distances involved (rather than to the accelerations, as in the SOZ—approaching for very large distances (≥ 100 ly) the turn-around time of a radio message. To the severe propulsion requirements are added formidable environmental problems, due to extensive ionization and sputtering from the impact of elementary particles and cosmic dust at relativistic speeds. Unbiased measurements of the free space environment are no longer possible at such speeds. Therefore, these starprobes can only serve stellar exploration, following slowdown near the target ster.

The QOZ has no definite limit. However, turn-around times become eventually so long that meaningful relations to Earth cease. Star travelers are separated from terrestrial civilization (and any other civilization) by such an enormous gulf

[12] Subsequently, Holzer defined the "very local interstellar medium," or VLISM, as the region of interstellar space within 0.01 parsec (pc) of the Sun generally taken as 0.01 pc = 2,062.65 au = 11.91 light days = 0.0326 light years (Thomas E. Holzer, 1989); this terminology "stuck" in the scientific literature while that of Ehricke did not, although the quantitative definition is typically used only loosely in the literature.

through time dilatation as to be virtually isolated from all other civilizations. Thus, at a distance of perhaps 300 to 1000 ly, the ZI becomes superimposed over the QOZ.

Ehricke notes:

Starprobes must rely on propulsive capabilities exclusively. But for ultraplanetary missions, the use of gravitational effects within the solar system is still meaningful. Several modes of ejecting the ultraplanetary probe from the solar system are available. The three principal ones are (1) direct departure from Earth orbit, (2) departure via Jupiter gravity assist (GA)[13], and (3) departure via close solar flyby (CSF)[14]. Mode (1) is expensive in terms of propulsion requirements, but allows readily the use of low-thrust high-I_{sp} systems. From Earth orbit, the probe spirals out directly into the cryospace environment of the outer solar system and beyond.

(Below we discuss the issues of "low-thrust, high-I_{sp} systems" which, with the implied distance from the Sun for ultraplanetary missions, must be limited to NEP and/or REP systems rather than a solar electric propulsion (SEP) system. The use of such systems is problematic because the expectations of Ehricke and others on their technical maturation have not materialized.)

Mode (2) is noticeably more efficient for launch speeds out of Earth orbit of some 50 km/s. Jupiter GA reaches maximum efficiency for out-of-Earth-orbit launch velocity of 18.3 km/s, in which case the speed imparted the probe by interaction with Jupiter permits exploration of the UZ out to 14 solar system radii (600 AU) or 9 percent of ultraplanetary space. Mode (2) also permits readily the application of low-thrust, high-I_{sp} systems if started following flyby or if operating beyond flyby.

The use of Mode (2) in conjunction with an REP system in the way suggested was considered and studied in some depth under the NASA Vision Mission studies (R. L. McNutt, Jr. et al., 2005).

Mode (3), CSF, is the potentially most efficient mode, but its worthwhileness depends on the closeness of the perihelion and its engineering feasibility depends on both the speed of approach and the availability of a high-I_{sp} system of sufficiently high thrust acceleration to impart to the spacecraft a significant velocity pulse in the general vicinity of the perihelion (approximately inside 0. 3 AU).

Mode (3), for the reason of efficiency noted, has been looked at multiple times using chemical rockets (T. E. Holzer et al., 1990; Mewaldt et al., 1995), nuclear pulse propulsion (R. L. McNutt, Jr. et al., 2004), and solar thermal propulsion (STP) (Lyman et al., 2001).

Three methods are available in Mode (3). The first is to drop from Earth orbit to the perihelion. This yields a brief ejection process but is propulsively expensive, and most significantly, the approach speed is critically slow for the required perihelion distances of less than 0.1 AU. The second method involves Jupiter rebound. This takes somewhat longer (~1000 days) but is more efficient propulsively, and the approach speed is closer to solar parabolic, but still fairly slow.

This latter version of Mode (3) is the same as our Option 3.

The third is a newly suggested method, using Saturn to reverse the probe's orbiting orientation from direct to retrograde (clockwise), running it into the Jovian gravity field where it receives a tremendous "kick", sending it toward perihelion at solar hyperbolic speed[15]. This method involves the longest ejection process, is propulsively most efficient, requires, however, virtually complete reliance on high-thrust systems (for maneuvers near Saturn and Sun)[16]. Because it yields the highest approach speed, the duration of the heat pulse accompanying the close perihelion transit may be

[13] This mode, Mode (2), includes what we later refer to as Options 1 and 2.

[14] Ehricke's Mode (3) (CSF) is what we refer to as Option 3, aka a powered solar Oberth maneuver.

[15] The subject of the paper by Ehricke in the *Journal of the British Interplanetary Society* (K. A. Ehricke, 1972)

[16] These required magnitudes are, it turns out, a significant issue; see following text.

> reduced sufficiently to design a probe capable of passing through perihelion distances between 0.1 and 0.01 AU[17]. To reach the outer limit of the UZ in 50 years, the probe must achieve a speed of 600 km/s (β = 0.002). The Saturn-Jupiter-Sun mode can reduce the associated perihelion requirement to 300 km/s (for solar-parabolic approach speed), or to about 210 km/s (for e = 2 hyperbolic approach speed), following a peri-Saturn maneuver of 30 to 40 km/s and a near-Earth departure maneuver of about 9 km/s. If a speed of 600 km/s[18] is to be attained in a 7-year powered flight in direct departure from Earth orbit (average thrust acceleration $2.8 \cdot 10^{-4}$ g), a very high power/mass ratio is required (~1700 kw/kg)/ This means that 14.8 billion kwh must be usefully expended annually for each ton of spacecraft mass; in other words, 100 tons of spacecraft require about the same annual power generation as the United States in 1966 (~1250 billion kwh). This underscores the importance of the flyby maneuvers to aid in the ejection for the solar system. But these, in turn, require high thrust accelerations for which the specific impulse tend to be lower, since many factors tend to limit the rate of power transfer from primary source to vehicle in the form of kinetic energy. For propulsive ejection speeds of 80 to 300 km/sec[19], a combination of gas core reactor[20] first stage and nuclear-electric (NE) ion-powered, or controlled thermonuclear reactor (CTR) powered second stage can be used. For higher propulsive speeds, nuclear pulse[21], NE and CTR drives are needed in two- or three-stage combinations. Among the propulsion systems now known to be within technological reach in the next 30 years, only the nuclear pulse can possibly attain very high propulsive ejection speeds (100 to 300 km/sec) inside the solar system. Low- thrust systems of both the NE and CTR variety require long propulsion periods that interfere with environmental measurements and, therefore, must either be discontinued periodically or require ejection of sub-probes at desired points.

Ehricke's analyses are all sound, but the ΔV requirements of "as low as" 30 km/s in deep space (at Saturn) at high thrust remain out of reach today, and the higher requirements (e.g., 210 km/s near the Sun) even more so. In summary, for an escape from the solar system of 600 km/s (126 au/year) without the complications of the Saturn rebound, we would need a maneuver near the Sun of 300 km/s. Ehricke does not mention the perihelion distance, but these numbers imply 1.06 R_S (i.e., just above the photosphere).

> The road to ultraplanetary and precursory interstellar mission capability is paved most expeditiously (from the standpoint of planning by key objectives and synergistic effectiveness) by the outer solar system probe so as mission specific payloads and nuclear-electric drives are concerned; and by the development of very advanced propulsion systems (primarily nuclear pulse and controlled thermonuclear reactor) for manned solar system mission capabilities.

While this philosophy has been oft repeated, the promised/required "advanced propulsion systems" have failed—and continue to fail—to materialize.

These same issues were reexamined within the decade as part of the JPL Interstellar Precursor study (Jaffe et al., 1977; Jaffe & Ivie, 1979; Jaffe et al., 1980; Jaffe & Norton, 1980). That mission baselined an NEP propulsion system, although what we have labeled as Options 1, 2, and 3 were also considered along with solar sails and a variety of combinations of these (Jaffe et al., 1980). Options included one or two NEP stages as well as inclusion of a "drop-off" Pluto orbiter (Figure 11-2, left panel). The baseline was a 20-year mission that could reach 400 au with an extended mission lifetime to 50 years to 1000 au. The propulsion was to be powered by a 500-kWe NEP system with a 20% conversion efficiency. The system used mercury for propellant, had a specific mass of 17 kg/kWe, and had an initial mass in LEO of 32,000 kg (see also more details at Pawlik &

[17] That is, between ~21.5 and ~2.15 R_S

[18] 600 km/s ~ 126 au/year

[19] That is, ~17 au/year to ~63 au/year

[20] Gas-core fission engines have been problematic and were never developed (Grey, 1959; McLafferty, 1970).

[21] e.g., Orion (cf. F. J. Dyson, 1965, 1968; G. Dyson, 2002)

Phillips, 1977). Hence, the "design point" for asymptotic escape from the solar system was set at 20 au/year (~95 km/s).

This asymptotic escape speed was carried forward to the Thousand Astronomical Unit (TAU) mission of the mid 1980s (Etchegaray, 1987; Nock, 1987). The final speed, after a 10-year "burn" using an NEP system at 1 MWe power, specific mass of the power plant of 12.5 kg/kW, specific impulse of 12,500 seconds (using liquid xenon, LXe), and an initial mass of 61.5 mt, would be 106 km/s (22.4 au/year) to reach 1000 au 50 years after launch.

To formulate a "cheap" approach, as compared to the NEP systems just mentioned, a new look was taken at conventional propulsion and the use of the solar Oberth maneuver (T. E. Holzer et al., 1990):

> For the Interstellar Probe to accomplish its scientific objectives, it should acquire data out to a heliocentric distance of ~200 AU. A reasonable duration for spacecraft operation is ~25 years. Thus, after allowing for a few years of trajectory maneuvers in the inner solar system, an escape velocity on the order of 10 AU/year is required.

The accompanying trajectory studies included passive prograde JGAs ("Minovitch maneuver") and a combined retrograde JGA, to put the spacecraft on a near-Sun ("solar-probe-like") trajectory, followed by a propulsive maneuver at perihelion ("Oberth maneuver"). This combined "Minovitch-Oberth trajectory" offered the best performance of the all-chemical propulsion approaches. Although details were not included, a fly-out speed of 14 au/year was derived for a 200-kg probe and two-stage solid rocket at perihelion (distance not specified and specific impulse I_{sp} of 290 s assumed) launched with a Titan IV/Centaur, again with the cautionary note "the large maneuver near the Sun (several km/sec) will pose a significant technical challenge."

This approach had been highlighted in the report *Space Science in the Twenty-First Century* (Donahue et al., 1988):

> An Interstellar Probe, that could be launched about the year 2000, should reach beyond about 100 AU in a time interval of less than 10 years, preferably about 5 years. Several possible schemes, including Jupiter gravity assist and swingby of the Sun at 4 solar radii (see Figure 4-4) as well as use of megawatt nuclear electric propulsion, could provide the necessary acceleration for spacecraft velocities varying from about 50 to 100 km/s (11 to 21 AU/yr). The spacecraft should be instrumented redundantly with plasma, field, particle, and wave instruments, depending on detailed definition of science objectives and spacecraft capabilities. The fully instrumented spacecraft mass is likely to be in the range of 500 to 1000 kg.

For the example of a ΔV of 5 km/s applied at 4 R_S, the rough escape speed can be estimated as 11.7 au/year (55.5 km/s),[22] with the other end of the range corresponding to the 1-MWe NEP system of the TAU mission.

In the next iteration (Mewaldt et al., 1995), the goals were captured as follows:

[22] For some perspective, a ΔV of 5 km/s applied at 1 R_S (i.e., the photosphere) would boost the asymptotic escape speed to ~16.6 au/year. To reach ~20 au/year with a 1-R_S periapsis would require a ΔV of ~7.3 km/s—either the thermal or propulsive requirements of which are already prohibitive to execute. A similar performance at 4 R_S increases the required ΔV to ~14.6 km/s, which is well out of reach for a high-thrust single stage.

To accomplish its scientific objectives, an Interstellar Probe should acquire data out to a heliocentric distance of ~200 AU. To reach 200 AU within a reasonable mission lifetime (e.g., ~25 years or less), the spacecraft velocity must be several times greater than those of Pioneer-10 and the Voyagers, which range from 2.4 to 3.5 AU/year.

The updated scenario used a DSM to achieve a Venus flyby followed by two Earth flybys (the trajectory followed by Galileo to reduce the launch-energy requirements) to reach Jupiter. A subsequent retrograde Jupiter flyby is used along with single-stage and two-stage propulsion near the Sun. The distance and Δ*V*s are not given, but asymptotic solar system escape speeds of ~6–14 au/year are noted along with a mass for the spacecraft of "~200 kg."

11.3.2.1. The "Goldin Challenge" and the Reemergence of Photon Sails

In 1998, NASA Administrator Daniel Goldin challenged JPL to determine a means to reach near star systems within 40 ly of the Sun in no more than 100 years (Frisbee & Leifer, 1998). As part of NASA's new Origins program, this would also correspond to reaching the nearest star system, that of Alpha Centauri A/B / Proxima Centauri, within ~10 years (Wallace, 1999). An initial "roadmap" was proposed based on solar sail and then laser sail technologies (Marzwell & Harris, 1998), with the first step being a Heliosphere Explorer robotic probe to 200 au (Wallace, 1999) (Figure 11-6). As the roadmap concept evolved, the focus on sails with the ultimate goal of beamed laser energy came into greater focus because this path was considered to be the most technically advanced of all those considered (J. L. Anderson, 1999).

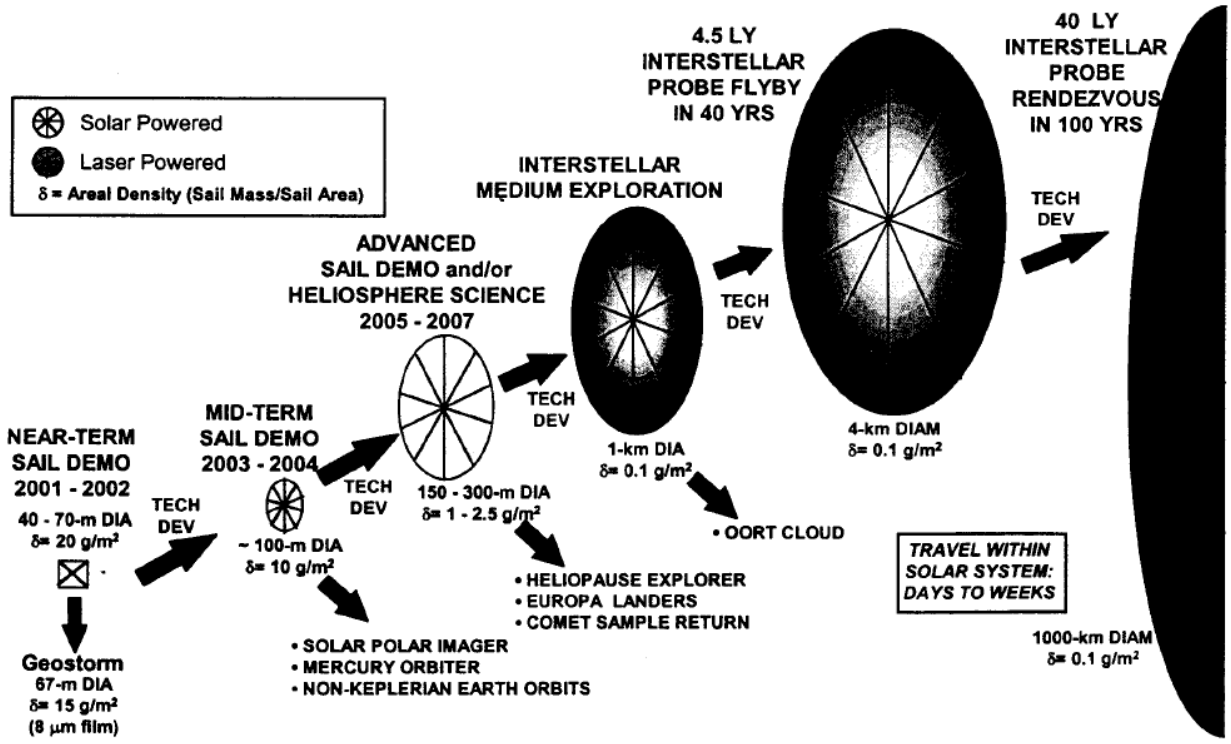

Figure 11-6. Sail roadmap of 1999 in response to the interstellar travel "challenge" of then-NASA Administrator Daniel Goldin. (Reprinted from Wallace (1999) with permission; © 1999 IEEE.)

11.3.2.2. Interstellar Probe Science and Technology Definition Team of 1999

An Interstellar Probe Science and Technology Definition Team (IPSTDT) was established and had three meetings at JPL, on 15–17 February 1999, 29–31 March 1999, and 17–19 May 1999. Baseline mission requirements were set as reaching 200 au within 15 years of launch. A Sun-approaching solar sail was baselined as the launch mode for meeting the requirements (Liewer et al., 2000; Liewer et al., 2001; R. A. Mewaldt & P. C. Liewer, 2000; Mewaldt & Liewer, 2001).

11.3.2.3. NASA Institute for Advanced Concepts

At the same time, the NASA Institute for Advanced Concepts (NIAC) funded a new concept study that revisited the use of the retrograde JGA-Oberth maneuver, based on a perihelion distance of 4 R_S. The requirement was for an asymptotic solar system escape speed of 20 au/year, requiring a ΔV of ~15 km/s (McAdams & McNutt, 2002, 2003). Such an impulse is about that imported to the Ulysses spacecraft in LEO, following Shuttle deployment (STS-41 mission) with the ~20,000-kg three-stage solid rockets of the two-stage IUS plus Payload Assist Module – Special (PAM-S) stage. For the study, such a massive stage was out of scope. After a brief assessment of using small nuclear charges against a pusher plate (the Orion concept (G. Dyson, 2002)), the study focused on adapting the thermal input into the TPS to run a solar thermal propulsion system with LH_2 as the propellant (Lyman et al., 2001). There were problems in getting the engineering analysis to close while maintaining the large, required ΔV; not surprisingly, the main issue was the mass of the spacecraft and all of its systems (R. L. McNutt et al., 2003). Additionally, there was the realization that such a system could never be tested realistically before flight.

11.3.2.4. NASA "Vision Mission" Studies

Different approaches were taken under NASA's "Vision Mission" program in looking at approaches to interstellar precursors: a very low specific mass NEP system (Zurbuchen et al., 2008) and an REP (Robert J. Noble, 1993; R. J. Noble, 1998, 1999) system (Fiehler & McNutt, 2005, 2006; M. Gruntman et al., 2004; M. Gruntman et al., 2006; R. L. McNutt et al., 2005; R. L. McNutt et al., 2006; R. L. McNutt, Jr. et al., 2005). Both of these launched outward from the Earth; the REP concept ("Innovative Interstellar Explorer") did incorporate a prograde Minovitch maneuver at Jupiter to provide a significant increase in the asymptotic escape speed.

11.3.2.5. Large Launch Vehicles–Ares V and the Space Launch System

Renewed consideration of what role—if any—very large launch vehicles could play in the "Interstellar Probe" mission was prompted by a request for a presentation at a meeting of the Committee on Science Opportunities Enabled by NASA's Constellation System of the National Research Council on 21 February 2008 (NRC, 2008). Some further refinements of this approach were presented at the Heliophysics Town Hall held 19–20 May 2008 in College Park, Maryland, and at the Ares V Solar System Science Workshop held at the NASA Ames Conference Center on 16 and 17 August 2008 (Langhoff et al., 2008). Further discussions of this approach have been carried out at various IACs: with the Ares V at the 60th IAC in 2009 in Daejeon, South Korea (Ralph L. McNutt, Jr. & Wimmer-Schweingruber, 2011) and the 61st IAC in 2010 in Prague, Czech Republic (Ralph L.

McNutt, Jr. et al., 2011), and then changing to the SLS at the 65th IAC in 2014 in Toronto, Canada (Ralph L. McNutt, Jr. et al., 2014) and the 66th IAC in 2015 in Jerusalem, Israel (Ralph L. McNutt, Jr., Benson, et al., 2015).

Continuing with the SLS as a baseline launch vehicle, at the 67th IAC in Guadalajara, Mexico, trades using the Oberth maneuver versus other approaches were reviewed (R. L. McNutt, Jr. et al., 2016) and at the 68th IAC in 2017 Adelaide, Australia, some preliminary scalings making use of the Oberth maneuver and a Star 48-powered perihelion stage with rough thermal shield mass estimates, based on the TPS being implemented on Parker Solar Probe, were discussed (Ralph L. McNutt, Jr. et al., 2017). This was the first time the required TPS mass was explicitly modeled as a function of perihelion distance from the Sun's center in a parametric fashion.

11.3.2.6. Keck Institute for Space Studies and Solar Thermal Propulsion

Point designs using the Oberth maneuver were also been considered by JPL, first in conjunction with a workshop at the Keck Institute of Space Studies (KISS) on 8–11 September 2014 and 13–15 January 2015 (Alkalai & Arora, 2015; E. Stone et al., 2015) and more recently at the 68th IAC. Several designs have been studied using multiple inner heliosphere gravity assists to enable a fast solar system escape. One design used an STP system running at 3400 K (I_{sp} ~1350 s). The separated spacecraft wet mass is ~561 kg with a payload of ~42 kg. Most of the escape speed is provided by a ΔV of 11.2 km/s performed by the STP system at ~3 R_S. The total initial stack dry mass of 11,278 kg and 15,732 kg of LH_2 gives a total launch mass of ~28,000 kg (including a 43% margin) (Alkalai et al., 2017).

11.3.2.7. Low-Thrust, In-Space Propulsion Approaches

All low-thrust schemes are underdeveloped and face significant technical and physical challenges for use in expelling spacecraft rapidly from the solar system. Almost all of these issues can be traced to materials properties and strength, long-term autonomous operations or both. All sail concepts (solar sails, laser sails, electric sails, and their variants) tend to trace to the former, and nuclear electric propulsion traces to the latter. REP occupies a special case—where the problem is with the specific mass of the power system. The difficulty in dealing with that issue is illustrated by the technical failures in and cancellation of the Advanced Stirling Radioisotope Generator (ASRG) program. Many of the problems with NEP for long-term robotic space missions were identified by Project Prometheus but were not solved during that effort, which was canceled as the costs for getting to and launching an NEP-based craft reached $10 billion and continued to rise.

Regarding the use of radiation pressure, whether from the Sun or a laser, and in principle on charge wires, it is not a question of whether it "works" but, rather, whether it can be used effectively for the primary source of propulsion. Solar radiation pressure was used to conserve propellant on NASA's MESSENGER mission (O'Shaughnessy et al., 2014) and was used on the Japan Aerospace Exploration Agency's (JAXA's) Interplanetary Kite-craft Accelerated by Radiation Of the Sun (IKAROS) technology demonstration mission. IKAROS had a mass of ~300 kg and sail area of ~200 m^2, and, hence an effective areal mass density of ~1500 g m^{-2}, roughly a factor of 1000 too heavy to enable an interstellar probe, and then only if perfect reflectivity is assumed.

Aside from the question of sail properties, manufacture, and guidance and control, one can ask how well such a system might perform by combining the technical difficulties into a single lightness number λ, defined as the ratio of the outward acceleration of the entire system by radiation pressure from the Sun for normal incidence to the inward acceleration of the entire system due to solar gravity.

One can bracket solar sail performance while capturing the salient features of more complex scenarios, for which numerical integration of the trajectories is required, by making a few simple assumptions. If the sail is always pointed radially to the Sun, after its deployment, the sail acts simply to reduce the effective gravitation attraction of the probe by the Sun in a discontinuous manner. Hence, for whatever stable orbit the probe is in, the net energy will change with no change in the angular momentum, allowing for the probe to move to a greater aphelion or escape the system entirely. For a simple example, consider a probe in a heliocentric circular orbit of radius 1 au. Suppose a sail is abruptly deployed with its normal toward the Sun with a lightness number of unity. The situation is akin to that of a stone on a string swung in a circle, with the string abruptly cut and then moving in a straight line with its previously circular speed. The probe released at 1 au will similarly move off in a straight line, with an impact parameter of 1 au and now traveling at $v_0 = 2\pi$ au/year, i.e., 29.7859 km/s, the mean orbital speed of the Earth. The trouble is that one needs a higher speed. For an initial orbit at 0.25 au, the fly-out speed is increased by a factor of 2; further increases can be obtained with a higher speed at the release point, a larger lightness number, or both. It is worth noting that a sailcraft (spacecraft "powered" by a solar sail) released from any circular orbit with a lightness number of ½ will execute a parabolic orbit, reaching infinite separation from the Sun at zero heliocentric speed after infinite time.

Thus, an ideal deployment of an ideal sail with λ = 1 in a heliocentric circular orbit of 0.25 au radius would provide a solar system escape speed of 4π au/year ~ 60 km/s, a speed sufficing to reach 200 au in just over 15 years. The thermal issues of taking a spacecraft into 0.25 au are already suggested by the experience of MESSENGER at Mercury and the designs of ESA's BepiColombo and Solar Orbiter missions. Suffice it to say, these pale in comparison with the issues associated with the operation of a unity lightness number sailcraft deployed at that distance because of the stress on the sail supports, which must be dealt with while maintaining the low system mass.

There are sufficient complexities that this is a subject that needs to be taken up separately; ultimately there are significant materials issues that must be dealt with for this scheme to work, regardless of the nature of the sail, its deployment mechanism, or the source of the propulsive force acting on it. Suffice it to say, although lightness numbers exceeding unity would be even more preferred from a kinematics perspective, their implementation is even more challenging from a materials perspective.

Work has continued (Johnson, 2016), but real progress continues to be hampered by the lack of a flight mission that can demonstrate the required lightness numbers and structural integrity that would be need for an Interstellar Probe (cf. Figure 11-7).

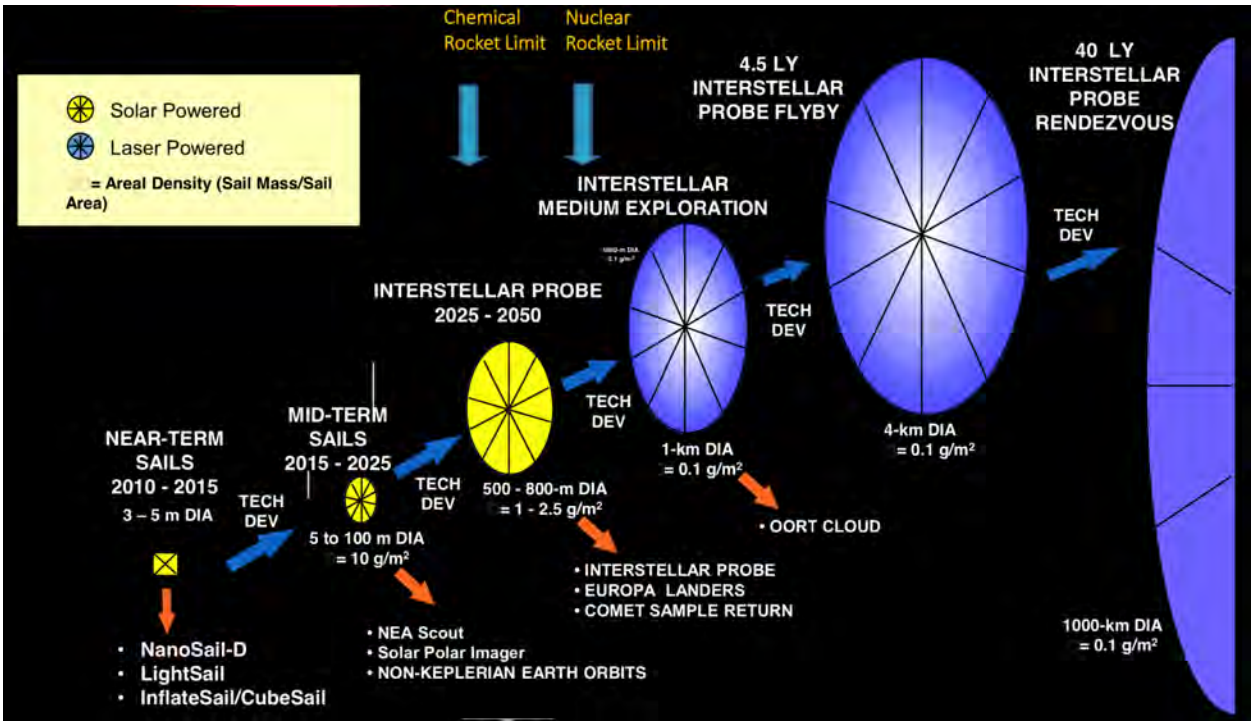

Figure 11-7. Sail roadmap of 2016. Although some smaller projects (Nanosail-D2, Interplanetary Kite-craft Accelerated by Radiation of the Sun (IKAROS) of the Japan Aerospace Exploration Agency [JAXA], and LightSail 2 of The Planetary Society [TPS]) have successfully flown, they are still small and heavy compared to what would be required for the advertised sail for the Interstellar Probe sail mission. When compared with the 1999 roadmap (Figure 11-6), the roadmap goals are largely unchanged, but the timetable has "slipped" by at least one to two decades, making technological readiness for flight as early as the 2030s a questionable proposition at the present time. (Image credit: NASA.)

11.3.2.8. Current Engineering Status—A Summary

A summary of the various studies, considered with various levels of detail, is given in Table 11-1. These 18 concepts vary in terms of study details but are typically defined by similar, if not the same, science goals, as discussed in section 11.3.3. Fly-out distances, times, and speeds are all heavily modulated by the posited propulsion means. There are still no definitive/funded low-thrust, in-space propulsion technologies that can enable the posited performances accompanying those approaches.

Table 11-1. Summary of Interstellar Probe Mission Concepts, 1960–2019

Study Year	Study	Escape Speed	Means	Distance	Probe Mass (Initial Wet)
1960	Simpson Committee	5 or 6 au/yr	Not specified	Not specified	Not specified
1968	Galactic Jupiter Probe – GSFC	10 au in 3 yr	Passive JGA	10 au (communications limit)	500 lbs (~230 kg)
1971	Ultraplanetary Probe – Ehricke	126 au/yr	Close solar flyby; 1.06 R_S at ΔV = 300 km/s; nuclear pulse	6320 au (0.1 ly) in 50 yr	Not specified

Study Year	Study	Escape Speed	Means	Distance	Probe Mass (Initial Wet)
1977	Interstellar Precursor – JPL	20 au/yr	500 kWe NEP at 17 kg/kWe with Hg propellant	400 au nominal (20 yr); 1000 au extended (50 yr)	32,000 kg
1987	TAU – JPL	22.4 au/yr	1 MWe NEP at 12.5 kg/kWe with LXe propellant at I_{sp} of 12,500 s	1000 au	61,500 kg
1988	*Space Science in the Twenty-First Century* – Scarf et al.	11.7 au/yr	Solar Oberth at 4 R_S at ΔV = 5 km/s	>100 au in less than 20 yr	500–1000 kg
1990	Interstellar Probe/Frontier Probe – Holzer et al.	14.7 au/yr	Two-stage solar Oberth with I_{sp} = 290 s	200 au	200 kg
1995	Small interstellar probe – Mewaldt et al.	14 au/yr	Solar Oberth maneuver with chemical stage after ΔV-Venus-Earth-Earth gravity assist (VEEGA) to Jupiter	200 au in 25 yr or less	~200 kg
1999	IPSTDT – NASA/JPL	~15 au/yr	400-m-diameter solar sail from 0.25 au	>200 au in 15 yr	150 kg
2000	Realistic Interstellar Explorer, NIAC Phase I – McNutt et al., APL	20.2 au/yr	Solar Oberth maneuver at 4 R_S at ΔV = 15.4 km/s; nuclear pulse/NTP/STP	1000 au toward ε Eri	50 kg
2002	Realistic Interstellar Explorer, NIAC Phase II – McNutt et al.	~12 au/yr	Solar Oberth maneuver at 4 R_S using STP	1000 au toward ε Eri	147 kg
2005	ISP Vision Mission using NEP – Zurbuchen et al. University of Michigan	Not specified	NEP with LXe and I_{sp} = 5000 s; 17,050 kg for Prometheus spacecraft with JGA	150 au in 20.5 yr	36,000 kg
2005	ISP Vision Mission using REP (aka Innovative Interstellar Explorer [IIE]) – McNutt et al., APL	8.3 au/yr	Outbound JGA + 1.0 kWe REP with LXe at I_{sp} of 3734 s	200 au in 28.8 yr	1135 kg
2009	IIE extension to use of Ares V launch vehicle at large C_3 = 270.0 km^2/s^2 – McNutt et al., APL	9.7 au/yr	Large launch vehicle (Ares V) with Centaur upper stage and REP system + JGA	200 au in 23.2 yr	1230 kg
2014	Use of SLS – McNutt et al., APL	>7.4 au/yr	All ballistic with unpowered JGA	200 au in 25–30 yr	~500 kg
2015	KISS Workshops – JPL	>13 au/yr	SLS Block 1B + ΔV-EGA and solar Oberth with STP	200 au in 20.5 yr	16,766 kg launch with 544 kg spacecraft
2017	SLS Block 2 launch vehicle; Updated JPL – Alkalai et al.	19.1 au/yr	SLS Block 1B + ΔV-VVEEGA and solar Oberth with STP (3400K/I_{sp} ~1350 s) + electric propulsion and LXe I_{sp} ~1800 s; at 3 R_S at ΔV = 11.2 km/s; advanced segmented-modular radioisotope thermoelectric generators (SMRTGs) for power; 1.2 kWe needed for cryocooler for LH_2	200 au within 20 yr of launch	~28,000 kg launch including ~550 kg spacecraft and 15,720 kg LH_2
2019	SLS Block 1B launch vehicle; Part 1 of this study – McNutt et al., APL	Variation with launch epoch for given vehicle and C_3	Conventional stages for all options: Passive JGA Powered JGA Solar Oberth One GPHS RTG for power	1000 au	New Horizons spacecraft 478.3 kg wet at launch as baseline

11.3.3. Mission Studies: Measurements and Instrumentation

With respect to point 3, explicit identification of measurements and instruments to obtain them were historically disjointed from mission studies, especially the earlier studies.

11.3.3.1. Galactic Jupiter Probe–1967

For example, in his remarks on the Galactic Probe (J. F. Clarke et al., 1968), Parker noted the following:

> The two ultimate questions are the distance which the solar wind extends outward from the sun and the cosmic ray intensity in interstellar space.... Theoretical estimates suggest that the solar wind extends ten to one thousand Astronomical Units beyond Earth, so that the cosmic ray intensity surrounding the solar system in interstellar space may easily be two or more times higher than here at Earth. Considerations involving the observed dynamical state of the galaxy suggest only that cosmic rays above one billion electron volts per nucleon are not ten times as numerous as here, else their pressure would burst the galaxy.
>
> Altogether, then, it appears that, with the ongoing exploring and monitoring of particles and fields at the orbit of Earth over the sunspot cycle, the next step in the scientific inquiry involves missions to large distances … particularly to many AU beyond the orbit of Earth ...

11.3.3.2. Missions Beyond the Solar System–1971

Science objectives were discussed by Ehricke (refer to previous remarks on "zone" definitions and locations at the beginning of section 11.3.2).

> COSMIC "ZONING"
>
> Space beyond the solar system is so vast that a breakdown into "zones" becomes necessary to bound objectives, problems and solutions (Fig. 1).
>
> Helio-Magnetosphere (Heliosphere)
>
> In immediate stellar vicinity, zoning can be governed by environmental characteristics. In terms of the solar magnetosphere (or heliosphere) the outermost planets Neptune and Pluto are located already in interstellar space--at least temporarily. Our Sun is the center of a spinning magnetic field, moving through interstellar gas (galactic wind) and through a galactic magnetic field whose vector angle relative to the Sun's motion is uncertain at this time. The Sun moves through an interstellar medium whose extreme conditions could be described as (a) an[d] H I (absorbing) condition at a gas temperature of 125 °K in which the neutral hydrogen atom density is much higher than the proton density; or (b) an H II (emitting) condition at 10^4°K in which protons predominate. In either case, the total particle density (atoms and protons) is of the order of 0.7 per cc. Considered a perfect gas, the velocity of sound is 1.32 km/s and 11.8 km/s in H I and H II regions, respectively. Since the solar velocity is 20 km/s, the flow of the interstellar medium relative to the Sun's magnetic field is, therefore, supersonic, causing a bow shock wave bounding the heliosphere in the direction of motion (zero azimuth angle), and a transition zone (magnetopause). At azimuth angles between 90 and 180 deg., the magnetopause will eventually dissolve as the galactic wind diffuses into the tail of the heliosphere. The thickness of the magnetopause (possibly several astronomical units (AU)) and the amount of ionization of galactic hydrogen by solar ultraviolet are not known. Relations between solar and galactic winds have been investigated by various authors. Weddell (Ref. 1) in particular, has shown that the size of the heliosphere (radial distance r at low azimuthal angles) under H II interstellar conditions is too small ($2 \leq r \leq 3.45$ AU) to be consistent with observed diffusion and solar modulation of galactic cosmic rays at 1 AU and slightly beyond (Refs. 2, 3). For H I conditions he found, for high solar conditions, conservatively $9.15 \leq r \leq 12.04$, compared with a value of $r \sim 7.43$ (Ref. 2) for low solar conditions.
>
> Thus, transition into the interstellar environment for outward flights of small azimuth angles may be assumed to occur at a heliocentric of between 8 and 16 AU. At 180 deg. azimuth (heliospheric tail) unperturbed interstellar conditions may not be restored at distances less than 400 to 600 AU for low and high solar activity, respectively. The orientation of the longitudinal axis of the heliosphere is not exactly known. If coincident with the Sun's vector of motion, the axis points toward the celestial Coordinates R.A. 18 h 4 m, Decl. + 30 deg. On the basis of cometary statistics, Robey (Ref. 4) showed evidence that the axis may be pointed at R.A. 21 h 0 m, Decl. + 32 deg. The multiple-planet missions into the outer solar system in 1976 to 1979 (launch years) cross the orbit of Saturn (10 AU) at R.A. 11 h to 12 h, the orbits of Neptune or

Pluto at R.A. 14 h to 17 h. Thus these probes move toward the forward half of the he1iosphere and may provide the first sampling of the interstellar medium.

Helio-Gravisphere

Gravitationally speaking, interstellar space is the region in which the galactic field rather than a particular stellar field dominates. At Sun's distance from the galactic center (8200 pc) galactic parabolic velocity is 290 km/sec (Ref. l2). From these values one can compute the radius of the Sun's nominal activity sphere to be about 1.14 ly. The galactic field is not strictly radially oriented because of the large dimensions of the central mass and because of the masses in the spiral arms beyond Sun's distance. Moreover, the basic galactic field shows local variations because of inhomogeneous stellar clustering. Therefore, no simple relation exists for the extent of the solar activity sphere. But the above figure shows at least that the solar field dominates out to about 1 light year distance--far beyond the mere 5-lh radius of the known solar system. The dimensions of the orbits of near-parabolic comets attest to this fact.

Ultraplanetary Zone (UZ)

In addition to magnetic and gravitational fields, micromatter and nucleonic matter is an important environmental factor. In, the comparative proximity of the Sun, dust and plasma density is likely to be higher than the average interstellar value. In order to account for a transition region between interplanetary and interstellar environmental conditions, we define an ultraplanetary zone (UZ). For want of definite data we postulate that the UZ extends to a distance of 0.1 ly from the Sun, that is, 158 solar system radii (1 ssr = 40 AU) or 6320 AU.

Sub-Optical Zone (SOZ)

At interstellar ranges that include other stars, the space-time continuum and the flight speed through which the two components are interrelated begin to assert themselves….

OBJECTIVES

Exploration beyond the limits of this solar system has two fundamental objectives (Fig. 2): scientific exploration and search for galactic intelligences in other solar systems. The objectives of scientific exploration into four disciplines: stellar physics, space physics, astroplanetology and astrobiology. While solar system exploration also involves the search for life, the scope of interstellar operation is far greater because of the wide variety of living organisms that may have arisen during the past 5 or more billion years on alien planets around stars more or less different from our Sun. Astroplanetology covers a virtually unlimited number and variety of planetary systems, from formative to fossil worlds circling dying or dead stars….

Similar musings were in play at the same 1971 conference by others in addition to Ehricke. For locations "near" the Sun, Despain et al. identified "big picture" items, including (Despain et al., 1971):

…the purpose of missions to the edge solar system as:

- Explore the boundary of the sun's sphere of influence.
- Seek the primordial conditions of the solar nebula.
- Explore fields, particles, gas, and dust in the extended solar nebula
- Provide correlations with near-Earth Observations of particles and fields to develop a solar-system-wide picture of solar system processes.

Missions into interstellar space will extend observations into the great distances between stars. In this tenuous environment sensitive measurements will be needed for such programs as:

- An interstellar monitoring platform to conduct long-term observations of fields, particles, gas, and dust.
- Long-baseline observations made jointly with earth-based or near earth instruments such as radio inter-ferometers, and studies of large scale correlations of interstellar fields.
- Astrophysics experiments in relativity, interstellar chemistry and physics in the relatively field-free regions far from any star.

They categorized both scientific objectives and measurement techniques based on the emphasis of a given robotic mission:

Table 11-2. Objectives and Techniques from "Missions Beyond the Solar System"—1971

Stellar Emphasis	Planetary Emphasis	Life Emphasis
Stellar Integral and Surface Prop	Planet ARV System Detection	Life Detection Prop
Stellar Structural Detail	Planetary System Structure	Nonequilibrium Prop
Stellar Nebula Prop	Interior or Bulk Properties	Atmospheric Environment Prop
Stellar Environmental Relationships	Planetary Atmospheric Prop	Surface Environment Prop
Binary Interactions	Surface Prop	Organic/Biotic Record
Interstellar Medium Prop	Interplanetary Prop	UFE Biochemistry, Behavior, etc.

Edge of Solar System	Interstellar Space	Stellar Emphasis	Planetary System and Life
Charged Particle Tech	Charged Particle Tech	Imaging	Imaging
Magnetic Mapping	Magnetic Mapping	Spectrometry	Surface Lander Tech
Tracking	RF Tech	Radiom/Phot	Spectrometry
Particulate Analysis	Tracking	X- and γ-Ray Tech	Tracking
RF Tech	Interferometry	Charged Particle Tech	Magnetic Mapping
Interferometry	Astrometry	RF Tech	Sounding Tech
Astrometry	X- and γ-Ray Tech	Magnetic Mapping	Radiom/Phot
	etc.	Tracking	etc.

Dessler and Park focused on "The First Step Beyond the Solar System" (Dessler & Park, 1971) in considering the then-current notions of the interaction of the solar wind and interstellar medium (Dessler, 1967) and the types of new knowledge expected from the upcoming Pioneer F and G launches (denoted as Pioneer 10 and 11, respectively, after those launches), after their Jupiter flybys.

11.3.3.3. JPL Interstellar Precursor–1976

The discussions continued to evolve as the focus settled on the idea of an interstellar precursor mission. In the JPL-led consideration of such a mission, the primary objectives focused on the heliosphere and its interaction with the local interstellar medium and the use of the long observation baseline possible from such a spacecraft; secondary objectives focused on a close observation of Pluto, characteristics of galactic and extragalactic objects, and observations of a solar system from a spacecraft (Jaffe & Ivie, 1979). Corresponding observations were planned, and others were rejected:

Table 11-3. Objectives and Techniques from JPL Interstellar Precursor—1976

Scientific Objectives	
Primary Objectives	
1	Characterize the heliopause, where the solar wind presumably terminates against the incoming interstellar medium
2	Determine characteristics of the interstellar medium
3	Improve the stellar and galactic distance scale, through measurements of the distance to nearby stars
4	Determine characteristics of cosmic rays at energies excluded by the heliosphere
5	Determine characteristics of the solar system as a whole, such as its interplanetary gas distribution and total mass

Secondary Objectives	
1	Determine characteristics of Pluto and its satellites and rings, if any If by 2000 there had been a mission to Pluto, this objective would be modified.
2	Determine characteristics of distant galactic and extragalactic objects
3	Evaluate problems of scientific observations of another solar system from a spacecraft
Planned Observations	
Heliopause and Interstellar Medium	Magnetic, electric, and plasma measurements with conventional instrumentation but high sensitivity
	Plasma blobs via radio scintillation at wavelengths ~1 m
	Radiation temperature via detector cooled to "a few Kelvins"
	Dust via impact-ionization mass spectrometer
	Mass spectrometer + plasma analyzer for ions
	Neutral gas spectrometer needs greater sensitivity and signal-to-noise ratio than now available
	Gas composition via absorption spectroscopy looking back at the Sun: D/H, H/H_2/H^+, He/H, He^3/He^4, C, N, O, and Li, Be, and B if possible
Stellar and Galactic Distance Scale	Baseline of a few hundred to a few thousand astronomical units to triangulate to Cepheid variables a few thousand parsecs away; need resolution of a fraction of an arc sec → 1M objective diameter
Cosmic Rays	Low-energy cosmic rays; measure to energies below 10 MeV and to 10 keV or lower; can use conventional instrumentation
Solar System as a Whole	Spatial distribution of neutral and ionized gases and of dust
	Mass of entire solar system via dual-frequency Doppler tracking
	Continuum observations to see dust; fluorescent observations of spectral to see neutral gas
Observations of Distant Objects	Optical observations of faint extended objects without background of reflected light from gas and dust in solar system
	Observations of distant objects via radio astronomy below 1 kHz with very-low-frequency (VLF) receiver and long dipole or monopole antenna
	Radio and gamma-ray event timing for triangulation across Earth to spacecraft baseline
	Measure galactic hydrogen distribution via ultraviolet/visible (UVV) spectrophotometry outside of local concentration due to the Sun
Pluto	Measurements with TV camera, infrared (IR) radiometer, UVV spectrometer, particle and field instruments, and IR spectrometer for a flyby only
	Atmospheric properties via ultraviolet (UV) observations during solar occultation and radio observations of Earth occultation; radio tracking to provide mass
	Addition of an altimeter for surface features and a gamma-ray spectrometer for surface composition if an orbiter mission is included
Gravity Waves	Long baseline and precision two-way Doppler measurements between the spacecraft and Earth
Simulated Stellar Encounter	Look at operational choices and observations during approach – only if motion is revered and the spacecraft is directed back to the solar system

Measurements Not Planned	
Detecting the Oort Cloud of Comets	Comet encounters would be accidental – all fluxes, particle and photon, are too low
Very-Long Baseline Interferometry	Would require very high data transmission rates to Earth that are not feasible
	Ambiguities not resolvable with only two receivers
	Structures resolvable with such baselines are likely low flux, and coherence may not be maintained because of irregularities in the interstellar medium
Issues	
Two spacecraft with asymptotic trajectories at right angles would give better heliospheric structure information and better baseline for transient radio and gamma-ray transient source location	
Neutral gas mass spectrometer – difficult sensitivity issues, C, N, O at ~10^{-5} to 10^{-4} atom/cm^3; Li, Be, and B at ~10^{-10} atom/cm^3	

A corresponding set of instruments was posited, but with no specifications provided:

Vector magnetometer	Electric field meter
Plasma spectrometer	Camera(s), long and short focus (aperture about 1 m)
Ultraviolet/visible spectrometers	Gamma-ray transient detector
Dust impact detector and analyzer	If a Pluto flyby or orbiter is planned:
Low-energy cosmic-ray analyzer	Infrared radiometer
Dual-frequency radio tracking (including low frequency with high-frequency uplink)	Infrared spectrometer
Radio astronomy/plasma wave receiver (including VLF; long antenna)	If a Pluto orbiter is planned:
Mass spectrometer	Gamma-ray spectrometer
Microwave radiometer	Altimeter

11.3.3.4. Thousand Astronomical Unit (TAU) Mission—1986

Scientific goals for the TAU mission were formulated at the TAU Thinkshop, held 29 September 1986 at JPL (Etchegaray, 1987). These had a heavy focus on what could be accomplished with a 1000-au baseline for astronomical/astrophysics observations (and need to be rethought in light of what has been accomplished with the Gaia mission).

Table 11-4. Goals and Instrumentation for TAU—1986 (Etchegaray, 1987)

3.1 Visible and IR Stellar Parallax
- 3.1.1 Uncertainty in the Expansion Rate of the Universe
  - The period luminosity relation
- 3.1.2 Age of the Galaxy
  - Ages of the globular clusters
- 3.1.3 Galactic Structure
  - The gravitational mass of the Galaxy
  - Dynamic temperature of the disk and halo of the Galaxy
  - Distance to the galactic center
- 3.1.4 Stellar Evolution
  - Early stellar evolution and resolution of cloud complexes
  - The initial mass function
  - Binary star evolution
  - Late stages of stellar evolution
  - Study of peculiar objects
    - a. Carbon Stars
    - b. Young Protostars

3.1.5 Targets of Opportunity

Objects with unknown distance:

O-B Associations
Regions of high polarization (filamentary)
Nuclei of planetary nebulae
Nova during observation
Nova remnants
Supernovae
Pulsars
Open clusters, young and very old
Local Group - dwarf galaxies
Local Group - M31 bright members
M33
M81
S Doradus - LMC
47 Tucanae - LMC
Supernova remnants
Intergalactic objects in LMC and SMC
Infrared objects discovered by IRAS, SIRTF, LDR
New interesting objects identified by HST, AXAF, LDR, GRO

3.2 Astronomy, Astrophysics, and Cosmology

3.2.1 Interstellar Gases

Cosmic abundance of hydrogen
Abundance and distribution of He3/He4, D/H, and Li6/Li7
Abundance and distribution of H, He, C, N, and O
Radio Science - VLBI studies of interstellar scintillation

3.2.2 Astronomy

Radio Science - VLBI studies of very compact radio sources
Low frequency radio astronomy
Gamma-ray burst timing and positioning
Gravitational lensing - quasar studies

Among the projects TAU will be able to accomplish are the following (Ref. 13 [Jones, D., memo, January 16, 1987.]).

a. Test the hypothesis that high amplitude events are caused by gravitational lensing by individual stars in an intervening galaxy.
b. Determine the size of the region responsible for the optical continuum emission of quasars by observing spacial [sic] luminosity differences during high amplification events (HAE).
c. Observe brightness variations in quasars due to the transverse motion of the lensing star (and the intervening galaxy) with respect to the background quasar.
d. Determine the number of bodies causing the gravitational lensing of observable quasars. A large sampling of quasars is required to do this study.

3.2.3 Cosmology

Gravitational wave detection
Spatial variations of G
IR background

3.2.4 Solar System Studies

Zodiacal light
Planetary system

As TAU leaves the solar system, it could study the zodiacal light from a distance, in visible as well as IR wavelengths. The study of what a “solar system dust cloud” looks like from a distance could be used to correlate with detections of other dust clouds, such as those surrounding Vega and Beta Pictoris, which have recently been made (Ref. 26 [Dumont, R. and A-C. Levasseur-Regourd, “Gradients of Temperature, Albedo and Density in the Zodiacal Cloud, as Deduced from the Available Thermal and Optical Observations,” Astronomy and Astrophysics, in press, 1987]).

Determination of the total solar system mass

By the time the spacecraft reaches 1000 AU a substantial amount of the mass of the inner Oort Cloud will be inside the orbit of TAU. A more accurate determination of the mass of the solar system than has been done to date can be done with TAU (Ref. 28 [Hanner, M., memo, December 18, 1986.]).

3.3 Space Plasma Physics

3.3.1 Dust

Solar system
Heliopause
Interstellar Medium

3.3.2 Plasma and Energetic Particles Distribution

Heliosphere
Interstellar medium

3.3.3 Low-energy Cosmic Rays

3.3.4 Magnetic Field Morphology

Heliosphere/Heliopause
Interstellar medium

3.3.5 Plasma Waves

Heliosphere/Heliopause
Interstellar medium

4.0 SCIENCE INSTRUMENTATION

The scientific objectives listed in the previous section define the need for a specific complement of scientific instruments. Below is a preliminary list of the instruments that were suggested to accomplish the proposed investigations.

Strawman science payload:

Optical/IR Telescope
Cosmic Ray Detector
Dust Detector
Energetic Particle Detector
Ion/Neutral Particle Detector
Gamma-Ray Spectrometer
Magnetometer
Plasma Particle Detector
Plasma Wave Instrument
Ultraviolet Spectrometer
Very Low Frequency Radio Astronomy Antenna

a. Dipole antenna
b. Pointable dish

Much more effort is necessary to establish the interactions of these various instruments with each other and their effect on the overall spacecraft design.

11.3.3.5. Interstellar Probe—1990 and Forward

Beginning with the 1990 report by Holzer et al. discussing an Interstellar Probe mission (T. E. Holzer et al., 1990), concept payloads were accompanied by mass and power estimates. The pattern is typical for difficult missions in formulation: low-risk instrumentation characteristics typically lead to an over-subscribed payload, while instruments posited by the spacecraft and mission developers typically lead to optimistically low mass and power numbers. Table 11-5 duplicates and adds to that found in (Ralph L. McNutt, Jr. et al., 2011).

Notes: Instrument names are from Innovative Interstellar Explorer (IIE) (Table 2 of R. L. McNutt, Jr. et al., 2005), and the spacecraft mass is that of the Option 1 baseline, not including the REP system, yielding a total wet mass of 1249.9 kg. Equivalences to payload elements on other spacecraft are notional and sometimes very divergent with respect to capabilities; they provide a rough guide only. Interstellar Probe 1990 is from (T. E. Holzer et al., 1990); Pioneer instrument masses are from *Pioneer H Jupiter Swingby Out-of-the-Ecliptic Mission Study*, NASA Technical Memorandum NASA-TM-108108 (1971) including 0.3 kg (0.272 kg) for the high-field fluxgate magnetometer flown on Pioneer 11 but not on Pioneer 10 (also brings the total mass up to 252.1 kg) (Christiansen et al., 1971); Voyager masses are originally from the National Space Science Data Center (NSSDC), and updated numbers are from (Heacock, 1980); New Horizons masses are from *Space Sci. Rev.*, 140 (1–4), 2008; Ulysses masses are from *Astron. Astrophys. Suppl. Series*, 92, 207 *et seq.*, 1992; IBEX masses are from (McComas et al., 2009), and the wet mass for the overall flight system with kick motor is 457.7 kg; STEREO masses are from *Space Sci. Rev.*, 136 (1–4), 2008; Helios masses are from *Raumfahrtforschung*, Band 19, Heft 5, September/Oktober 1975 (not all are available; marked "NA") and fact sheets in *Raumfahrtforschung*, Band 19, Heft 4, Juli/August 1975; and Interstellar Heliopause Probe (IHP) masses are from (Wimmer-Schweingruber, McNutt, Schwadron, et al., 2009); the launch mass of 517 kg includes margins. Advanced Composition Explorer (ACE) masses are from (E. C. Stone et al., 1998). Van Allen Probes masses are from (Kirby et al., 2013). Masses for IMAP are from the white paper submitted to the last Heliophysics Decadal Survey (there is an addition error of 2 kg in the total). IIE (technology readiness level [TRL] 9) refers to instruments identified with close functional capabilities that have flown; NEP (2008) refers to the entries in Table 2 (entitled "Instrumentation of the daughter probes") of the Zurbuchen et al. NASA Space Science Vision Missions study (Zurbuchen et al., 2008).

The entries for "Small Interstellar Probe (1994)" are the corresponding entries from (Mewaldt et al., 1995). The "A Sole/Ad Astra 1997" configuration of 1997 (R. L. McNutt, Jr. et al., 1997) was the precursor to the NIAC Realistic Interstellar Probe effort; the wet mass of 311.9 kg does not include the 216-kg Star 20B kick stage (brings the total stack mass to 527.9 kg). Entries for NASA's IPSTDT of 1999 are from that study, and the spacecraft mass of 150 kg (~246 kg with solar sail) is from (Liewer et al., 2001); entries for NIAC (2004) refer to the Phase II "Realistic Interstellar Explorer" (R. L. McNutt et al., 2004).

Table 11-5. Instrument Masses on Deep-Space Robotic Spacecraft

Spacecraft → / Instrument →	Interstellar Probe 1990	Small Interstellar Probe 1994	A Sole/Ad Astra 1997	IPSTDT 1999	NIAC II (2004)	IIE Vision (2005)	IIE (TRL 9) (2005)	NEP Vision (2008)	IHP (2007)	Helios (1974)	Pioneer (1972)	Voyager (1997)	ACE (1997)	New Horizons (2006)	Ulysses (1986)	IBEX (2008)	STEREO (2006)	Van Allen Probes (2012)	IMAP (Decadal)
Magnetometer (type not specified)	4	1	0.25	0.5	1.89			1.8										20.9	3
Vector helium magnetometer						8.81			1.5	4.40	2.7				2.332				
Fluxgate magnetometer							5.6			4.75	0.3	5.6	4.1		2.4		0.27		
Plasma wave sensor	11	3	2.25	0.5	1.48	10.0	7.17	7	5.8	NA		9.1			7.4		13.23	27.4	
Plasma	20	10	2	8.5	0.97	2.00	6.2	16	2	15.696	5.5	9.9	6.8	3.3	6.7		2.37	65.6	7
Plasma composition	17						5.97	8	1.5				14.6		5.584		11.4		
Energetic particle spectrometer	8	3	0.5	1.5	0.80	1.50	37.4	15	3.0	3.50	3.3	7.5	60.2	1.5	5.8		1.63	6.6	10
Cosmic-ray spectrometer: anomalous and galactic cosmic rays	22			2.5	0.84	3.50	51.1	12	3.5		3.2	7.5	54.0		14.6		1.92		5
Cosmic-ray spectrometer: electrons/positrons, protons, helium	10	2.5		2.4		2.30	14.6	4	1.5	7.15	1.7		12.8				1.98	9.2	3
Geiger tube telescope											1.6								
Meteoroid detector										8.93	3.2								
Cosmic dust detector	8	1.5		1.5	0.70	1.75	16.36	25	1.1		1.6			1.6	3.8				8
Solar X-rays and gamma-ray bursts		0.5			2.05										2.0				
Neutral atom detector	4	3		2.3		2.50	20.75	8								12.09			15
Energetic neutral atom detector				3.5		2.50	13.9	7	4.5						4.3	7.70			27
Lyman-alpha detector/UV measurements	1	0.5	2	0.4	3.43	0.30	6.6	5	1.2		0.7	4.5		4.4					4

Spacecraft → / Instrument →	Interstellar Probe 1990	Small Interstellar Probe 1994	A Sole/Ad Astra 1997	IPSTDT 1999	NIAC II (2004)	IIE Vision (2005)	IIE (TRL 9) (2005)	NEP Vision (2008)	IHP (2007)	Helios (1974)	Pioneer (1972)	Voyager (1997)	ACE (1997)	New Horizons (2006)	Ulysses (1986)	IBEX (2008)	STEREO (2006)	Van Allen Probes (2012)	IMAP (Decadal)
Infrared measurements	20			3			34	15			2.0	30.2							
Imaging photopolarimeter											4.3	4.4		8.6					
Imaging system								30		8.93		38.2		10.5			48.1		
Common electronics, harness, boom, etc.		2	3					20					3.9			5.42	19.1		24
Totals	125	27	10	26.6	12.16	35.2	219.65	173.8	25.6	73.2/ 76.5	30.1	116.9	156.4	29.9	54.9	25.21	100.0	129.7	106
Spacecraft wet mass	N/A	~200	311.9	~246	147.15	549.5	N/A	N/A	517	370.0/ 376.5	252.1	825.4	756.54	478.3	366.7	104.9	623/ 658	665.4	N/A
Payload/Wet mass (fraction)	--	0.135	0.032	0.108	0.083	0.064	--	--	0.049	0.198/ 0.203	0.119	0.142	0.207	0.063	0.150	0.240	0.160/ 0.152	0.195	--
B – as built; N – notional	N	N	N	N	N	N	N	N	N	B	B	B	B	B	B	B	B	B	N

11.3.3.6. The Enduring Questions

Beginning with the Holzer et al. report, there was a shift in emphasis toward heliospheric science objectives. From the Scarf et al. report of the Task Group on Solar and Space Physics, Space Science Board, Commission on Physical Sciences, Mathematics, and Resources, National Research Council *Solar and Space Physics: Space Science in the Twenty-First Century – Imperatives for the Decades 1995 to 2015* (Scarf et al., 1988), the identified scientific measurement priorities were as follows:

1. *Heliopause and Interstellar Medium:* Determination is needed of the characteristics of the solar wind just inside the heliopause, of the heliopause itself, of the accompanying shock (if one exists), and of the region between the heliopause and the shock.
2. *Cosmic Rays:* Measurements should be made of low-energy cosmic rays, which the solar magnetic field excludes from the heliosphere.
3. *Pluto:* If a Pluto flyby is contemplated, measurements should include optical observations of the planet to determine its diameter, surface and atmosphere features, and an optical search for and observations of any satellites or rings.

These were summarized as:

> The objectives of the mission are to determine the characteristics of the heliopause, interstellar medium, low-energy cosmic rays excluded from the heliosphere, and global interplanetary gas and mass distribution of the solar system, and possibly, a much more precise determination of the stellar and galactic distance scale through parallax measurements of the distance to nearby stars.

The exploration of Pluto—and Kuiper Belt Object 2014 MU69—has now, of course, been accomplished with the New Horizons spacecraft as a dedicated mission. The SWAP, PEPSSI, and VB SDC instruments continue to make heliospheric observations of note of the solar wind, energetic particles, pickup ions, and dust. The other two objectives continue to be the focus of the Voyager 1 and Voyager 2 missions, with both of those coming to the end of their lifetimes, as their power supplies continue to decline.

Holzer et al (1990) shortened these to the following:

1. Explore the nature of the interstellar medium and its implications for the origin and evolution of matter in the galaxy.
2. Explore the structure of the heliosphere and its interaction with the interstellar medium.
3. Explore fundamental astrophysical processes occurring in the heliosphere and the interstellar medium.

There is also discussion of measuring the infrared flux so that “dust and comet clouds near the Sun could be recognized by their parallax and there is a good chance of seeing individual comets as the spacecraft passes through the Kuiper Belt. Getting outside the zodiacal dust may also be critical for cosmology if the cosmic IR background is too faint to recognize through the foreground dust in the inner solar system. This instrument might have some heritage from the COBE DIRBE experiment” (T. E. Holzer et al., 1990).

The IPSTDT of 1999 formulated the scientific objectives as follows (Liewer et al., 2001; R. Mewaldt & P. Liewer, 2000):

1. Explore the nature of the interstellar medium and its implications for the origin and evolution of matter in our Galaxy and the Universe;
2. Explore the influence of the interstellar medium on the solar system, its dynamics, and its evolution;

3. Explore the impact of the solar system on the interstellar medium as an example of the interaction of a stellar system with its environment;
4. Explore the outer solar system in search of clues to its origin, and to the nature of other planetary systems.

These flowed from four corresponding questions formulated as part of the development of Quest 3 of the Sun-Earth Connection (SEC) Roadmap, as it was discussed at the Third IPSTDT meeting at JPL on 17–19 May 1999 (also cf. Table 1 of R. L. McNutt, Jr. et al., 2005):

1. What is the nature of the nearby interstellar medium?
2. How do the Sun and galaxy affect the dynamics of the heliosphere?
3. What is the structure of the heliosphere?
4. How did matter in the solar system and interstellar medium originate and evolve?

The science objectives have evolved over the intervening years (e.g., Zurbuchen et al., 2008):

1. Explore the nature of the interstellar medium and its implications for the origin and evolution of matter in our galaxy and the Universe
2. Explore the influence of the interstellar medium on the Solar System, its dynamics, and its evolution
3. Explore the impact of the Solar System on the interstellar medium as an example of the interaction of a stellar system with its environment
4. Explore the outer Solar System in search of clues to its origin and to the nature of other planetary systems
5. Explore the Universe from a unique vantage point beyond the zodiacal light and far from Earth

The objectives have consistently focused on science questions and scientific measurements that can be addressed in no other way than with an Interstellar Probe.

11.4. Interstellar Probe Trajectory Trades–Ballistic Options

The idea of using a large launch vehicle to provide a ballistic solution for propulsion for an Interstellar Probe mission grew from a question posed by the National Academies in 2008. The question—and subsequent report—were sponsored by NASA to address the question of what science could be enabled with the Ares V launch vehicle. This was the large rocket component of the Constellation program. The presentation on the concept was made 21 February 2008 at the Keck Building in Washington, DC, to the Committee on Science Opportunities Enabled by NASA's Constellation System (NRC, 2008). This was followed by a workshop on the same topic at NASA's Ames Research Center in August 2008 (Langhoff et al., 2008). None of these "quick-look" efforts were funded by NASA; all work derived from internal APL overhead funds.

The February presentation built on the previously funded NASA "Vision Mission" effort for using REP (Fiehler & McNutt, 2006; R. L. McNutt, Jr. et al., 2005). With respect to the use on an Ares V, the following points were noted:

11.4.1. Constellation Architecture Changes (Some of the) Launch Vehicle "Rules"

- Ares V can only provide C_3 of ~70 km^2/s^2.
  - Average Earth orbital speed v_0 = 29.79 km/s = 6.28 au/year
  - Let v_∞ = asymptotic escape speed from solar system
  - With no gravity assist or REP: $C_{3,\min} = v_0^2 (2^{1/2} - 1)^2 = 153$ km^2/s^2

  - In general, $v_\infty = v_0 \left[(1 + C_3^{1/2}/v_0)^2 - 2 \right]^{1/2}$

- Optimized launch (higher C_3) requires a cryogenic upper stage.
  - These are expensive.
  - These are heavy.
  - A customized design would be required for the Delta IV Heavy; existing Centaur is too heavy.
- Ares V provides more lift capability for an upper stage, needed for high-energy launch.
- Ares I upper stage has too high a dry mass to use.

11.4.2. Constellation "Quick Look"

- Key to performance is high-energy launch → need upper kick stage with the "right" dry mass.
  - Ares I upper stage is too large to be launched by the Ares V to LEO
  - Looked at just the Ares V to a positive C_3 and only got to a C_3 of ~70 km^2/s^2 because of the large dry mass of the Ares V upper stage
  - Added a Centaur from the Atlas V and got a C_3 of ~ 270 km^2/s^2
  - Ran that trajectory out and got to 200 au in ~25 years with a JGA
  - Quick look at fitting the Centaur in the Ares V shroud; appears to fit
  - May have to use the ogive at the top for the IIE, but there should be room
- So, the "quick-look" launch architecture is as follows:
  - The baseline Constellation Ares V vehicle launches the IIE + Centaur + Ares V upper stage to LEO.
  - The Ares V upper stage sends the stack to a "low" positive C_3.
  - The Ares V upper stage is then jettisoned, and the Centaur stage is fired to provide the remainder of the energy delivering 1500 kg to a C_3 of 270 km^2/s^2.

A "quick-look" analysis was also performed using the NERVA gamma stage rather than a Centaur. Aside from the TRL, the nuclear stage was not a good technical fit. This approach was presented at the 60th IAC in Daejon, South Korea (2009) (Ralph L. McNutt, Jr. & Wimmer-Schweingruber, 2011) and at the 61st IAC in Prague, Czech Republic (2010) (Ralph L. McNutt, Jr. et al., 2011).

With the termination of the ASRG project (Ralph L. McNutt, Jr., Aleman, et al., 2015) and the absence of a sufficiently low mass, long-lived isotopic power source for an REP system, the focus turned to what might be accomplished using a large ballistic launcher alone. Although Constellation and Ares V had been canceled, a new large launch vehicle for human deep-space missions, the SLS, was beginning development.

Initial assessments of carrying out an Interstellar Probe mission with the SLS were reported at the 65th IAC (2014) in Toronto, Canada (Ralph L. McNutt, Jr. et al., 2014) and the 66th IAC in Jerusalem, Israel (2015) (Ralph L. McNutt, Jr., Benson, et al., 2015). A reexamination of mission requirements and the current state of the art of propulsion requirements was discussed at the 67th IAC in Guadalajara, Mexico (2016) (R. L. McNutt, Jr. et al., 2016). Most recently, a renewed focus on methods toward near-term implementation (as well as a summary of the past history of Interstellar Probe concepts) was presented at the 68th IAC in Adelaide, Australia (2017) (Ralph L. McNutt, Jr. et al., 2017).

11.5. Next Step(s)

With the maturation of the SLS design and its variants, particularly that of the "Block 1B" and the "Block 1B+ ('plus')," and the award of study money from NASA's Heliophysics Division (13 June 2018 through 28 February 2019), it is imperative that a robust "snapshot" be made of SLS capabilities for an Interstellar Probe. Such information about realistic, near-term possibilities is imperative for informing the science community well in advance of the next Heliophysics Decadal Survey, which will nominally cover the decade 2023–2032.

Propulsion implementation has been a significant discriminator in "putting off" an Interstellar Probe during the past two decades. With the Voyager spacecraft now nearing the end of their lives because of the decay of their power sources (driven by Pu-238 in the Multi-hundred Watt Radioisotope Thermoelectric Generators [MHW-RTGs]), it is more important than ever that this line of scientific exploration of near interstellar space be reconsidered.

11.5.1. Decadal Surveys

In the Decadal Survey covering 2003–2012 (NRC, 2003), Table 2.4, "Deferred High-Priority Flight Missions (Listed Alphabetically)," lists one large mission: Interstellar Probe with the "Reason for Deferral" as "Advanced propulsion technology needed."

The context is given in the "Integrated Research Strategy" under "The Heliosphere and Its Components" (pp. 57–58):

> The boundary between the solar wind and the local interstellar medium (LISM) is one of the last unexplored regions of the heliosphere. Very little is currently known about this boundary or the nature of the LISM that lies beyond it. The outer boundary of the heliosphere will eventually be sampled directly by an Interstellar Probe mission. Advances in propulsion technology are expected to make such a mission feasible during the decade 2010-2020. Although it cannot yet be included in the program recommended by the committee, an Interstellar Probe is a high-priority future mission for which the required technology investments should begin as soon as possible. In the meantime, certain aspects of the heliospheric boundary and the LISM can be studied by a combination of remote sensing and in situ sampling techniques. This investigation could be accomplished by an Interstellar Sampler mission traveling to distances of several AU to measure the neutral atoms of the LISM that penetrate well into the heliosphere and to obtain energetic neutral atom images and extreme ultraviolet images of the heliospheric boundary. Such a mission is gauged to be feasible within the resources of the Explorer program and so is not prioritized separately in this report.

Discussion of the technology concepts referred to can be found on page 85 along with a recommendation to NASA:

Missions to the outer planets and beyond, including an Interstellar Probe, require propulsion capabilities that significantly exceed those of the present fleet of launch vehicles. Nuclear electric propulsion (NEP) is being considered as a promising solution to the problem of providing the high-performance propulsion capabilities that such deep-space missions will need. The NASA 2003 budget submitted to Congress contains funding to support the study of NEP technology, and the ROSS-2002 NASA research announcement solicits proposals for propulsion and power studies that will lead eventually to the development of an NEP capability. When such a propulsion technology becomes available, there is little doubt that an Interstellar Probe will become one of the most exciting of the future missions that could reach beyond the solar system.

Although recent advances in high-efficiency solar arrays can support small- and moderate-scale missions to Jupiter, radioisotope thermoelectric generators (RTGs) are needed for most missions to the outer solar system. They might also simplify the design of a Solar Probe mission and make multiple passes into ~4 solar radii a possibility. Pioneers 10 and 11, Voyagers 1 and 2, and the Ulysses, Galileo, and Cassini missions have all used RTGs as the source of their electrical power, with the Voyager and Pioneer missions having demonstrated long-term (>25-year) reliability. The 2003 NASA budget provides funding for the renewed production of RTGs.

Recommendation: NASA should assign high priority to the development of advanced propulsion and power technologies required for the exploration of the outer planets, the inner and outer heliosphere, and the local interstellar medium. Such technologies include solar sails, space nuclear power systems, and high-efficiency solar arrays. Equally high priority should be given to the development of lower-cost launch vehicles for Explorer-class missions and to the reopening of the radioisotope thermoelectric generator (RTG) production line.

These advanced technologies include solar sails, space nuclear power systems, and high-efficiency solar arrays. Equally high priority should be given to the development of lower-cost launch vehicles for Explorer-class missions and to reopening the RTG production line.

In the next Decadal Survey (NRC, 2013), comments on an Interstellar Probe were relegated to the "Report of the Panel on Solar and Heliospheric Physics," with no mention in the main body of the report. In section 10.2.1, "Prioritized Imperatives for NASA," the last two priorities were as follows (p. 265):

8. Carry out advanced planning for the Solar Polar Imager and Interstellar Probe missions (§10.5.2.6, §10.5.2.7).
9. To develop solar-sail propulsion for future Heliophysics Division missions, invest about $50 million as "seed money" in a full-scale solar sail demonstration mission by partnering with the Office of the Chief Technologist's Technology Demonstration Missions program (§10.5.2.8).

Section 10.5.2, "New Imperatives for NASA" (p. 299) states: "Sections 10.5.2.5-10.5.2.7 discuss one high-priority concept (L5) that should be considered for the following decade and two concepts—the Solar Polar Imager and the Interstellar Probe—that address high-priority goals but require new propulsion technology and possibly other new technologies." The contents of section 10.5.2.7, "Interstellar Probe Mission Concept" (pp. 309–310) read:

Recent in situ measurements by the Voyagers, combined with all-sky heliospheric images from IBEX and Cassini, have made outer-heliospheric science one of the most exciting and fastest-developing fields of heliophysics. The measurements have transformed knowledge of the boundaries of the heliosphere. The Voyagers are now deep in the heliosheath, and one or both may cross the heliopause in the next decade. Although they have performed spectacularly, the Voyager instruments are 1970s-vintage and, for example, are unable to measure suprathermal heavy ions or interstellar-plasma elemental and ionic charge-state composition. The interstellar probe[19] would make comprehensive, state-of-the-art, in situ measurements of plasma and energetic-particle composition, magnetic fields, plasma waves, ionic charge states, energetic neutrals, and dust that are required for understanding the nature of the outer heliosphere and exploring our local galactic environment.

Advanced scientific instrumentation for an interstellar probe does not require new technology, as the principal technical hurdle is propulsion. (Also required are electric power from a low-specific-mass radioactive power source and reliable, sensitive, deep-space Ka-band communications.) Advanced propulsion options, which could be pursued with international cooperation, should aim to reach the heliopause considerably faster than Voyager 1 (3.6 AU/year). Possibilities include solar sails and solar electric propulsion alone or in conjunction with radioisotope electric propulsion.[20,21] The panel did not find either the ballistic or the nuclear electric power approach to currently be credible. In summary, to

enable achievement of this decadal survey's key science goals in the coming decades, the SHP panel believes high priority should be given by NASA toward developing the necessary propulsion technology for visionary missions like SPI and interstellar probe.

---

[19] R. McNutt et al., Interstellar Probe, white paper submitted to the Decadal Strategy for Solar and Space Physics (Heliophysics), Paper 195 [cf. Table I.1: "Proposes an interstellar probe that can be launched during the coming decade."]

[20] R. McNutt et al., Interstellar Probe, white paper submitted to the Decadal Strategy for Solar and Space Physics (Heliophysics), Paper 195.

[21] L. Johnson et al., Solar Sail Propulsion: Enabling New Capabilities for Heliophysics, white paper submitted to the Decadal Strategy for Solar and Space Physics (Heliophysics), Paper 122 cf. Table I.1: "Reports on a sampling of missions enabled by solar sails, the current state of the technology, and what funding is required to advance the current state of technology such that solar sails can enable these missions."].

Within Appendix B, "Instrumentation, Data Systems, and Technology," the subsection entitled "Propulsion – Solar Sails" reads as follows:

Heliophysics can benefit from observations of the Sun, Earth, and heliosphere from orbits requiring continuous propulsive activity to maintain or reach in a timely fashion. Vantage points above Earth's poles, at sub-L1 locations, and at high ecliptic latitudes have unique properties that enable important observations. Six community white papers advocated science enabled by this technology, and previous strategic studies have advocated solar sails. Past heliophysics mission concepts include a solar polar imager, a stationary Earth polar observatory, upstream solar wind monitoring at a sub-L1 location, an L5 mission, Solar Sentinels, and Interstellar Probe.

Significant investments have already been made in the United States and abroad. The Japan Aerospace Exploration Agency (JAXA) and NASA carried out dedicated tests of solar sailing for primary thrust using the IKAROS spacecraft and NanoSail-D2. Without an appropriate demonstration mission that goes beyond the small-scale, heavy-sail tests to date, the possibility of using this technology in the future will remain in doubt. NASA's Office of the Chief Technologist has suggested a technology demonstration line that could cover 75 percent of the cost of a $200 million solar sail demonstration mission. The committee strongly urges that this potential opportunity be pursued to demonstrate a 25 g m^{-2}, ~40-m solar sail.[1]

---

[1] See Section 2.4.4.4 of NASA, In-Space Transportation Capability Portfolio, 2005.

There are also Decadal Mid-Term Assessments centered between the Decadal Surveys to assess progress against those documents. A new mid-term assessment is about to be stood up for heliophysics (indeed this ongoing study can help address "NASA Imperative" number 8 already noted above and will hopefully be noted as such).

From the previous Mid-Term Assessment for Heliophysics (NRC, 2009b), much of the progress—or lack thereof—as noted was funding driven. The following is from page 4 (the text is expanded on pp. 38–39):

Technology Development

Grade: C

Finding: NASA is planning to add new small and medium launch capabilities and has made some progress in developing advanced spacecraft systems and command-and-control and data acquisition technologies for spacecraft constellations. But NASA's progress in developing solar sails is limited, and NASA has only recently begun studying the feasibility of advanced space nuclear power systems and the availability of the necessary radioactive isotopes. These technologies

have been identified as strategic needs for upcoming missions. It is also unclear if the rate of technological progress in spacecraft systems can be sustained in the absence of a replacement for NASA's canceled New Millennium Program, which provided a testbed for new technologies. NASA has also not followed up on decadal survey recommendations regarding advanced scientific instrumentation.

11.5.2. Propulsion Options

11.5.2.1. Nuclear Electric Propulsion and Project Prometheus

Part of the context worth noting is the contemporaneous National Academies report on the restoration of radioisotope power supply capabilities (NRC, 2009a) as well as the closeout report on the Project Prometheus Nuclear Electric Propulsion (NEP) study (Ashcroft & Eshelman, 2006; Taylor, 2005; Wollman & Zika, 2006). The latter, with Phase A funding of $463,897,341 (grand total per Table 13.3-1, which appears on p. 179 of the final report), identified major outstanding technological development requirements, including providing for adequate reactor lifetime and a final mission life-cycle cost estimate (LCCE) for the Jupiter Icy Moons Orbiter (JIMO) mission of $12.751 billion plus $3.565 billion for science and $5.161 billion for launch costs—a grand total of $21.478 billion (real-year dollars, following the completion of Phase A in 2005). However, as noted on page 4, the project was ***NOT*** allowed to continue into Phase B despite its extensive accomplishments:

> In FY 05, the project successfully completed Phase A, passing the JPL Project Mission and Systems Review (PMSR) in July 2005. Supporting this review was the Prometheus reference Spaceship design and project life cycle cost estimate, 68 "gate product" documents, and an extensive library of other documentation. Prometheus also completed an Analysis of Alternatives (AoA) study for ESMD and performed planning activities for a DSV Demonstration Mission to the Moon.
>
> However, NASA re-evaluated its priorities in light of available funding. NASA indicated that Return to Flight, International Space Station, and Crew Exploration Vehicle were the highest priority tasks for the Agency. The Agency nuclear initiatives were postponed to a large extent, and work within the nuclear systems program was reprioritized. NEP was given third priority behind nuclear surface power and nuclear thermal propulsion. Consequently the Prometheus Project was directed to not proceed into Phase B. In addition, the Project was asked to support a major Agency study, the Exploration Systems Architecture Study (ESAS), in the area of lunar surface power. The Project delivered the Lunar Fission Surface Power Station Study Final Report on August 17, 2005.
>
> The Project was officially discontinued effective October 2, 2005. This Final Report and all project documentation are the final deliverables for the Project.
>
> Precursors to the Prometheus Project include the Space Power-100kW (SP-100) Project, the Deep Space One (DS1) mission, the NASA Evolutionary Xenon Thruster (NEXT) project, and the X2000/Deep Space Avionics (DSA) project. SP-100 was a Department of Defense (DOD)-NASA-DOE multi-party development that provided valuable experience and technology in developing a spaceborne nuclear reactor. The DS1 mission provided valuable experience in ion-propulsion development and mission operations. NEXT is an ongoing electric-powered ion thruster development involving JPL in collaboration with GRC and MSFC. X2000/DSA provided valuable experience in identifying and developing electronics and materials that will function in an extreme radiation environment. Precursors to the JIMO mission include Project Voyager and Project Galileo. Voyager and Galileo were science explorations of Jupiter and provided considerable experience in understanding its harsh radiation environment.

Although SEP continues under development, the Prometheus effort, coupled with the failure of the earlier SP-100 reactor program (*The SP-100 Nuclear Reactor Program: Should It Be Continued?*, 1992), effectively was the death knell for NASA's implementation of NEP into space systems, which had been long pursued as a means of achieving large spacecraft speeds for a variety of missions and for which Prometheus was to be the capstone pushing toward implementation on real systems (NRC, 2006).

Ultimately, the effort was defeated by the lack of true autonomy in nuclear fission systems (ongoing maintenance is required to provide the long lifetimes of the systems) and the mass of the associated thermal radiator and other auxiliary systems required to deal with rejected heat in space. Unlike on the ground, where waste heat from both commercial and military fission systems can be dealt with efficiently via location on waterways or in water, or with nearby cooling towers, waste heat in space can be rejected only by radiation, and one is at the mercy of the Stefan-Boltzmann law, essentially turning all heat rejection problems into material problems. In addition, and importantly, low-thrust, long-duration propulsion systems are also at the mercy of their specific mass, i.e., the mass-to-electric-power ratio of the power-plant mass, including all radiators, convertors, and support equipment, or its inverse, the specific power α (E. Stuhlinger, 1964, 1967).

(E. Stuhlinger, 1964) defined a "characteristic velocity"

$$v_{char} \equiv \sqrt{2\alpha\tau}$$

and showed that for the optimum performance of a low-thrust system, this characteristic velocity needs to be about equal to the exhaust velocity and, in turn, about equal to the final velocity change. Here τ is the operational time over which the speed change ΔV is put into the vehicle. The point has also been emphasized by (Shepherd, 1999) with a focus on nuclear systems:

> Nuclear electric propulsion systems suffer from serious limitations to achievable specific power, which results in a limit being set to the specific impulse that may be usefully exploited, thereby setting limits to the range of missions that would be of viable duration. This range could be of the order of a thousand AU, well beyond the planetary boundary but insignificant in terms of interstellar distances. The limited level of specific impulse would be well within the capacity of nuclear fission and would not require fusion.

Here, Shepherd points to technologies not yet fully wrung out at the time of this writing, as shown, less than a decade, later through the analysis of alternatives (AoA) studies done with Prometheus (Appendix F, section F.2 of Taylor (2005)). This issue is apart from that already mentioned regarding autonomous reactor operation over at least a decade.

11.5.2.2. The Solar Sail Conundrum

The idea of large sails to trap the momentum of the radiation in the Sun—and later at potentially higher power levels from lasers—is not a new one. The idea of using light pressure from the Sun to propel a spacecraft through interplanetary space appears to have been originated by Tsander in the Soviet Union in 1924 (see NASA Technical Translation of Из научного наследия (Tsander, 1967)).

In the summary of Tsander's work, on page 18 under "Outline of Lecture on My Spaceship Read at Theoretical Section of Moscow Society of Astronomy Enthusiasts" (noted as from 20 January 1924), Item B.VI. translates as "VI. Usages of mirrors and screens in place of rockets in interplanetary space. Calculations and benefits." Further, an excerpt from page 29 (from "Report of Engineer F. A. Tsander Concerning Interplanetary Voyages") reads:

> For flights in interplanetary space, I am working on the idea of flying using tremendous mirrors of very thin sheets, capable of achieving favorable results (see drawing of mirror and dust, and sphere).
>
> In case people might later construct interplanetary stations in interplanetary space which would revolve around the earth like the moon, except closer to the earth, receiving travelers from the earth and sending out large interplanetary

spaceships for further travel, equipped with all the comforts, according to my calculations, the following design can be used. The interplanetary ships to be sent to other planets should be equipped with large mirrors almost one square kilometer in area; the interplanetary stations should also have mirrors, but even larger (see drawing). The light is collected by these mirrors and sent to the mirror of the interplanetary space-ship in flight. The low pressure of light over the tremendous distances of travel will result in tremendous flight speeds, thereby shortening flight durations. The greatest time required for flight to the nearest outer planet, to Mars, the so-called Red Star, will be about 2S6 days; the flight time to the nearest inner planet, Venus, will be about 14S days (flight drawing). There are other sources for the production of the velocities, investigation of which is in progress and will be reported on in our interplanetary Society. If we fly around a planet in space, the planet will attract us, curve our flight trajectory and so to speak pull us after itself, so that our flight speed after passing the planet will be greater than before; in the best case, flight around the earth might yield an increase of 10 km/sec, around Mars -- 4.S km/sec, around the largest planet of our solar system, Jupiter -- 24 km/sec and around our moon -- 2 km/sec (see diagram). Furthermore, if we approach a planet, then circle around it within its atmosphere, we can achieve high flight speeds: as when a small sphere strikes another large, rapidly moving sphere, the speed of the small sphere can be strongly increased. With this type of flight around the earth, we might receive an increment in flight velocity of about 50 km/sec, which should be quite important in performing various tasks in flights to other planets. However, this question of flying around a planet within its atmosphere requires further development (see drawing of flight in atmosphere).

Let us analyze now the question of the effect of the force of attraction of the earth, planets and sun. We know that the force of attraction of the earth at a height equal to its radius, i.e., 6370 km over the surface, is only one fourth of the force which acts upon us on the surface; if the altitude is two radii, the force is only one ninth that which acts upon us at the surface, etc. Due to this, the work which must be performed in order to fly away from the earth into space is not infinite, but is only a finite quantity. However, if we were to perform infinite work on a stone, it would have the speed of light, i.e., 300,000 km/sec. In order to overcome the entire gravitational attraction of the earth, a speed of 11 km/sec is required. At a lower speed, we will rotate around the earth in an ellipse, at a higher speed we will fly away on a hyperbola to infinity (see drawing).

If we overcome the attraction of the earth, we still retain the speed of the earth around the sun, i.e., approximately 29 km/sec. If, for example, we add 3 km/sec to this velocity for a rocket, we attain very extended flight around the sun, our interplanetary spacecraft will move away from the sun and will reach the planet Mars at the furthest point on its trajectory, Mars being 1.5 times further from the sun than is the earth. If still more additional velocity is given to our ship by a rocket or by light pressure or by circling around Mars, we can reach the other planets.

An excerpt from another report (*Flights to Other Planets*, beginning on p. 32 and then following from p. 34) reads:

According to my calculations, the acceleration of these flights in interplanetary space can be performed using the pressure of light falling on thin sheets. If these sheets are made in the form of large circles and rotated, they will hold their flat form due to centrifugal force, in spite of the pressure of the light. Over the tremendous distances between planets, the slight pressure of the light will be sufficient for the acceleration required.

The time of a flight to Mars, if we desire to save fuel, would be 256 days for a rocket. To do this, the rocket would have to take off from the earth in the direction of the earth's movement around the sun [15], adding 3 km/sec of additional speed [16] to the 29 km/sec at which the earth rotates around the sun. This would cause the spacecraft to move in an orbit which according to my calculations would take it to the planet Mars. If we decrease the speed of 29 km/sec by 2.5 km/sec, the spacecraft would move on an inward trajectory, somewhat closer to the sun and would reach the planet Venus in 145 days. If more fuel is expended, in order to give the spacecraft additional speed greater than the 3 or 2.5 km/sec, we will reach these planets more rapidly.

The area of rocket design is still very little developed. It would be desirable to continue energetic work in this area, to make it possible for us to enter interplanetary space by orbiting around the earth as described above, then to reach new freedom, new capabilities and new worlds.

11 August 1924 F. A. Tsander

Thus, Tsander can be credited with both the concept of propulsion by light (“thin mirrors”) and the gravity assist, apparently rediscovered independently by Minovitch almost four decades later (M.A. Minovitch, 1961; Michael A. Minovitch, 1963).

The “solar sail” idea was bought up (also apparently independently) by (Garwin, 1958) and brought into the popular literature by (A. C. Clarke, 1964). The concept of using a laser for propulsion (Marx, 1966) followed soon after the first demonstration of a laser. A great deal of discussion of the use of solar sails for various missions has occurred during the intervening years. Solar sails were baselined for the NASA IPSTDT effort in 1999 (Liewer et al., 2001; Mewaldt & Liewer, 2001) as well as for a proposed Cosmic Visions mission for ESA (Wimmer-Schweingruber, McNutt & IHP/HEXTeam, 2009; Wimmer-Schweingruber, McNutt, Schwadron, et al., 2009).

Incident sunlight on the body of a spacecraft alters the trajectory of that spacecraft. This has been observed by and well documented by a variety of missions, e.g., MESSENGER (O'Shaughnessy et al., 2014), IKAROS (Wikipedia, 2011), and NanoSail D (Johnson et al., 2011). In principle, the concept of the solar sails and solar sailing works. Less well studied are the mechanical constraints on sail configurations that are sufficiently low mass to enable high-speed Interstellar Probe missions.

At the simplest level—an interstellar “sailcraft” powered by solar radiation pressure—the ratio of the solar radiation force to the gravitational force on the craft (the “lightness number” λ) should be equal to or greater than unity, with the sail deployed face on to the Sun. This enables gravity to at least be “nullified” (for a unity lightness number), in which case the craft will simply exit the solar system at its heliocentric orbital speed. For example, a sailcraft in orbit at 1 au could exit the system at the orbital speed of the Earth, ~2π au per year, ~6.3 au/year, or not quite twice the 3.6 au/year current speed of Voyager 1. To go faster, one needs to deploy the sail from a heliocentric orbit closer to the Sun. Because the (circular) heliocentric orbital speed is proportional to the inverse square root of the orbital radius, increasing the escape speed by a factor of 3–6π au/year (~18.8 au/year) requires the initial heliocentric orbital radius to be 1/9th of an astronomical unit (~24 R_S).

A different approach is easily derivable from the vis-viva equation for which the velocity v can be expressed in terms of the mean orbital speed v_0 of the Earth, the radial location of the spacecraft r (in astronomical units), and the semimajor axis of its orbit a (in astronomical units) by

$$v = v_0\sqrt{\tfrac{2}{r}-\tfrac{1}{a}}.$$

Hence, the speed at perihelion v_p is given by

$$v_p = v_0\sqrt{\tfrac{2}{r_p}-\tfrac{2}{1+r_p}} = v_0\sqrt{\frac{2}{r_p(1+r_p)}}$$

or

$$r_p = \frac{-1+\sqrt{1+8\left(\frac{v_0}{v_p}\right)^2}}{2}.$$

So the increase by the factor of 3 could be achieved by reaching inward to 0.187 au or 40.2 R_S with a ballistic launch from Earth before deployment of the solar array.

Perhaps as a better example, consider Parker Solar Probe, with a total spacecraft mass of 685 kg launched with a Star 48BV kick stage atop a Delta IV Heavy launch vehicle. The spacecraft reached first perihelion on 5 November 2018 at 35.7 R_S (0.166 au). The speed was ~3.2 times the Earth's mean orbital speed or 20.2 au/year.

To be "neutrally buoyant" with an ideally reflective sail, the sailcraft would require an effective surface areal density of 1.539 g m^{-2} (see, e.g., section 3.1.1 of Ralph L. McNutt, Jr. et al., 2011). For a total sailcraft mass of 685 kg including the sail mass, support booms, and deployment mechanisms, the implied sail area is 0.44 km^2, e.g., a perfectly reflecting square sail 667 m on a side, a number not unlike that first discussed by Tsander. This mass budget would have to contain a thermal shield for the spacecraft proper more capable than that of the MESSENGER mission to Mercury, and the sail structure and sails themselves would have to equally have such a thermal capability. Structural robustness of the sail under the loads experienced at the launch also needs to be considered; this introduces additional constraints on the mechanical strength required for the sail supports when considered along with the lightness number constraints (Greschik & Mikulas, 2002). Such constraints tend to drive up the mass fraction of the sailcraft that must be devoted to the sail support structure, further limiting the available mass of the spacecraft proper to smaller values than a zeroth-order initial analysis typically implies, and complicating any executable design.

Although sailcraft per se are achievable today, sailcraft of lightness numbers near unity remain at low TRLs because of such considerations.

11.5.2.3. All-Ballistic Options

With the less-than-promised specific mass capabilities of in-space propulsion schemes, both the promised performance and TRL levels of such schemes for an Interstellar Probe have remained short of expectations with low TRLs. Significant targeted technology developments for science missions are not credible given the budget levels that have shown little change since the end of the Apollo program. Simply put, cost does matter (National Academies of Sciences, 2017), and to maximize payload development needed to maximize the new science, spacecraft and launch hardware remain tied to already-developed approaches; this applies especially to means of propulsion. The aforementioned termination of the Prometheus program is a case in point.

In any case, the use of the largest launch vehicles, while potentially enabling, also provides a cautionary note. Such usage must be truly enabling as the experience of trying to use Saturn Vs for Mars exploration under the Voyager program revealed before that program's cancellation (Cortright, 1967).

Given a compelling science case for an Interstellar Probe, along with the potential capability for implementation using the SLS or a near-term variant, the motivation has been present for some years to explore the possibilities (as outlined previously). With the upcoming Space and Solar Physics Decadal Survey and the maturing—and funded—work on the SLS, coupled with a stated NASA desire to use the SLS for science as well as crewed missions, the ongoing study for a pragmatic interstellar probe seems a worthwhile one. The cautionary note is that one must also be realistic—

and that means conservative—in designing a mission architecture. In turn, that means making use of existing, qualified launchers and kick stages/upper stages. Such items are significant cost and schedule drivers even when operational, and totally new systems are simply not a realistic schedule/cost option. In particular, this rules out custom "small" NTP stages and deep-space, long-lived, cryogenic systems (e.g., liquid oxygen [LOX]/LH_2), both of which are still on the drawing board at any rate and, of those initiatives, at stage sizes that are simply too large to provide adequate performance with a single SLS launch.

The use of thermal shields attached to stages and the deep-space use of solid motors are already developmental and monetary risks, but certainly not to the extent of a totally new stage development program.

The best-performing SLS variant on the horizon (currently) is the Block 1B+ Cargo configuration, which will have significant design commonality with the deep-space version to be used with the crewed Orion spacecraft. The Block 2 "first-use" date is already at the end of the 2020s and so is simply not consistent with a baseline approach for consideration during the next decadal period. Similarly, the contemplated spacecraft mass range of ~300–800 kg, as informed by the work on the ballistic approach to date, strongly biases the choice of a "final" upper stage to one similar to that being used on Parker Solar Probe and powered by a Star 48BV motor, although the Star 48GXV developed as an alternative early in the Parker Solar Probe program is another potential candidate. The question is then, does one also need to include yet another stage between the Exploration Upper Stage (EUS), the second stage of the SLS Block 1B and Block 1B+, and the upper Star 48BV/48GXV stage?

Initial indications are that the answer is "yes." Because currently existing stages in a "good" mass range are preferred, these considerations have led to the current focus on the Centaur stage (second stage of the Atlas V) and the CASTOR 30B and CASTOR 30XL used in variants of the Antares launch vehicle. Use of SpaceX vehicles currently seems to be excluded because of the lack of cryogenic upper stages leading to poor performance at high C_3s. Blue Origin launch vehicles are currently under design with cryogenic upper stages, but these lag the EUS and Centaur (and the ICPS is too heavy, as is the Airbus Vinci stage being designed for the Ariane 6). The commercial sector remains fluid and so bears continued investigation, but the options they offer currently are not components of the current baseline based on performance as it currently exists for those vendors.

11.5.3. Trajectory Considerations

As is well known from the flight performance of the five solar-system-escaping spacecraft (namely Pioneer 10, Pioneer 11, Voyager 1, Voyager 2, and New Horizons), the velocity from the Sun's gravity well is significantly enhanced by a "prograde" JGA, a fact apparently first noticed by Tsander and first studied in detail by Minovitch. More planets mean even better performance but far fewer launch opportunities, a point brought home by the discovery of Grand Tour possibilities by (Flandro, 1966).

An even more efficient escape scheme was first identified and studied by Oberth in 1929: a powered spacecraft maneuver while deep in the gravity well of the Sun after having fallen to the Sun

from a great distance away (Oberth, 1970). In practice, the Oberth maneuver requires a retrograde JGA in order to shed enough of the angular momentum of the Earth to pass sufficiently close to the Sun, along with a sufficiently robust TPS to survive that close passage.

A potential "intermediate" case is a powered, prograde JGA.

All of these schemes require gravity assists at Jupiter, and so the performance of launch opportunities to a fixed direction in the sky is modulated by Jupiter's sidereal period of 11.8 years as well as the synodic period of 399 days that controls the Earth-to-Jupiter leg of the trajectory. For a given launch vehicle, outbound trajectories near the plane of the ecliptic have the best performance because they maximize the JGA angular momentum and energy transfer to the spacecraft.

The significant question at hand—that must be answered up front—is which of these three general options can provide the most rapid exit from the solar system given current launch vehicles, kick stages, and TPS capabilities.

11.5.3.1. Option 1: Prograde Jupiter Gravity Assist (Passive)

The "simplest" ballistic option for rapid solar system escape is to make use of an optimized prograde JGA near the plane of the ecliptic. The basic calculation of how to relate the launch energy (C_3) to an optimized Jupiter flyby distance and the asymptotic speed away from the solar system is documented in the appendix of (Ralph L. McNutt, Jr. et al., 2014) for a simplified patched-conic model. In principle, sufficient launch energy (direct to Jupiter) causes the spacecraft energy to intersect Jupiter's orbit at an angle α with respect to Jupiter's orbital velocity vector. By targeting an appropriate flyby altitude from Jupiter, the gravitational field of the planet will then rotate the spacecraft trajectory, so that it is aligned with the velocity vector of Jupiter, adding the planet's speed to that of the spacecraft. As the launch energy increases, the required closest approach to Jupiter to effect the bending also increases. At a sufficiently large launch energy, the closest approach reaches the Jovian cloud tops. Further increases in launch energy are less and less effective as a result. Using a simple, patched-conic approximation with Earth and Jupiter assumed to be in coplanar, circular orbits yields a minimum C_3 of ~77.324 km^2/s^2 for a Hohmann transfer and a C_3 of ~494 km^2/s^2 to drive the optimal flyby distance down to Jupiter's cloud tops. Retrograde JGAs to allow close perihelion passages are ~100–120 km^2/s^2 (the simple model gives 102.403 km^2/s^2 for a perihelion pass of 9.5 R_S and 109.887 km^2/s^2 for 1 R_S, with corresponding perihelion, transverse, speeds of 199.56 km/s up to 617.43 km/s). Voyager 1 and 2 launch C_3s were 105.5 km^2/s^2 and 102.4 km^2/s^2, respectively (Heacock, 1980). Lower launch energies to enable large masses are possible by making use of multiple Earth and/or Venus gravity assists (e.g., by Galileo and Cassini) at the expense of multi-hundreds of meters per second DSMs and extra years of time within the inner solar system. So the trade is one of time and orbital complexity versus larger launch vehicle (e.g., the use of the Delta IV Heavy and gravity assists versus the use of the SLS Block 1 for the Europa Clipper mission).

For all the examples here, we consider direct fly-outs to Jupiter with an SLS Block 1B or Block 1B+.[23] Even with upper stages, this vehicle is not going to be capable of launching a multi-hundred-kilogram spacecraft to a C_3 of >470 km^2/s^2, which means there is always a clear (mathematical) path to an optimized Jupiter flyby, but the constraint of Jupiter's size must be taken into account at the highest launch energies.

"Optimal" trajectories to Jupiter occur roughly once every synodic period of 398.88 days versus its sidereal period of 365.256 days. Hence, the optimal "aim-point" of the fastest trajectory will advance each launch opportunity by ~(398.88/365.256 − 1) × 360° = 33.14°. After 11 such "best" opportunities, the aim-point will have advanced in heliolongitude by 364.541°, being ~4.5° advanced from the previous cycle (of 11 × 398.88/365.256 = 12.0126 synodic years of the Earth). The 4.5° advance means that the "best" orbital parameters will not be reproduced exactly but will not vary greatly over several 12-year periods.

11.5.3.2. Option 2: Prograde Jupiter Gravity Assist (Active)

The first variation makes use of an active, prograde rocket burn at closest approach to Jupiter. This is the exact reverse of the capture burns made by the Galileo and Juno orbital missions to orbit Jupiter. Hence, such burns are critical, but no more so than for orbital capture.

Deep-space use of solid rocket motors has been a topic of debate for many years. Maintenance of propellant form stability is crucial for eventual—and successful—operation. This includes maintaining both a minimum ambient storage temperature and minimal thermal gradients across the motor. Without active heating, and the associated mass, power, and other complexities associated with such a system, the use of solid kick stages in deep space is viewed with suspicion by many. However, a Star 48B motor was used successfully after 462 days in deep space to insert NASA's Magellan mission into Venus orbit on 10 August 1990 (Hamlyn et al., 1991).

A similar problem was encountered during orbit insertion for the Galileo spacecraft after its launch from the Space Shuttle Atlantis on 18 October 1989 (D'Amario et al., 1992). After launch via the IUS after deployment in LEO, Galileo underwent a Venus-Earth-Earth gravity assist (VEEGA) trajectory to Jupiter because the IUS could not provide sufficient C_3 for a direct-to-Jupiter orbit; the initial launch mass of Galileo was 2717 kg, for which the IUS could provide a C_3 of only 17 km^2/s^2. This did compare favorably with the 1989 VEEGA minimum requirement of ~13 km^2/s^2. The Jupiter orbit insertion (JOI) maneuver was made 2.6 hours after perijove at 4 Jovian radii (using 1 R_J = 71,492 km). The 49-minute burn slowed the spacecraft by 630 m/s (spacecraft speed relative to Jupiter is not given).

For Galileo, a dedicated, custom retropropulsion model (RPM) was developed and provided by the Federal Republic of Germany. Messerschmitt-Boelkow-Blohm GmRH (MBB) designed, built, and tested the RPM, with project management provided by the Deutsche Forschungs- und Versuchsanstalt fuer Luft- und Raumfahrt e. V. (DFVLR) (Hagenest et al., 1984). The system used a 400-N

[23] What was designated as Block 1B+" is now (as of December 2019) designated as "Block 2."

motor and had a burnout mass of 205.89 kg. The 935 kg of propellant (MON-1/monomethyl hydrazine [MMH]) provided a vacuum-specific impulse of 308 seconds. The same type of propulsion system attached to a nominal 478.3-kg Interstellar Probe could, therefore, provide a total ΔV of ~2.603 km/s. Modern components could likely provide somewhat better performance with space-storable liquid fuel and oxidizer.

To provide an "apples-to-apples" comparison of performance with Option 1, a full set of data on the stack masses is required. For Option 1, asymptotic solar system escape speed can be calculated on the basis of the C_3 possible for a set spacecraft mass and a given upper stage. To compare with Option 2, the injected stack must now consist of the spacecraft plus the upper stage, whatever that is, which together will be launched toward Jupiter with a lower C_3. The trajectory at Jupiter must then be designed to optimize the asymptotic escape speed once the kick stage is now fired at perijove. This is presumably given by selecting the perijove such that the outgoing spacecraft asymptote in the heliocentric frame is—as with Option 1—aligned with Jupiter's orbital velocity vector in the heliocentric frame. In principle, one could launch a stack of two powered stages to Jupiter and use both at perijove versus using both at launch. The comparison intimately ties the launch vehicle and stage performances to the mass of the final separated probe, and the properties of the powered stages vary in a non-linear fashion for which numerical calculations are required.

11.5.3.3. Option 3: Retrograde Jupiter Gravity Assist (Passive) Followed by Active Sun Gravity Assist ("Oberth Maneuver")

The "Oberth maneuver" was Oberth's answer to his *gedanken* experiment of how to escape the solar system most rapidly, a problem he addressed in his 1929 book, *Wege zur Raumschiffahrt* or Ways to Spaceflight (Oberth, 1970). Simply put, by dropping from a far distance deep into the gravity field of the Sun, a rocket acquires a very large speed. A rocket burn that augments this speed only slightly provides a significant net energy to the rocket, so that there is now a net large energy increase enabling a rapid escape from the system. Beginning on page 198 of NASA's technical translation, Oberth writes (as translated):

> As is apparent, we have so far dealt with matters of pure definition. That changes, however, as soon as we are dealing with a body moving between different reference systems. Let us demonstrate it by means of a mental experiment.
>
> An asteroid is to circle the earth at a distance of 900 radii of the earth's orbit. Then, according to the rules of astronomy, its velocity equals 1 km/sec, and its period of revolution is 27000 years. Let us suppose there is a long-living astronaut on the asteroid. He wishes to fly to a fixed star 10^{15} (that is one quadrillion) km away (that is about the distance of the regulus in the Lion). The fixed star is not supposed to move relative to the sun and is to lie in the trajectory plane of the asteroid. The asteroid is to stand exactly at point A' (cf. Fig. 66) between the sun and the fixed star (A indicates the direction to the fixed star), and the available fuels of the rocket are to correspond to an ideal propulsion of 6 km/s. Here, the parabolic velocity with reference to the sun is p = 1.4 km/s. Later in the chapter, I will show that we can completely ignore this quantity in the following calculation; the parabolic velocity with reference to the asteroid is likewise to be irrelevant. Now the question is: How can our astronaut get to the distant fixed star fastest?

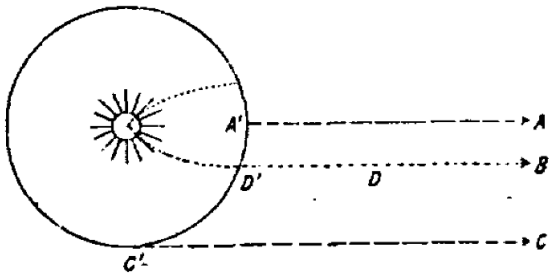

Fig. 66

Some laymen will say: He must start right now. 1) In so doing, he loses no time waiting. 2) This is the best time to leave anyway, for the asteroid is nearest to the fixed star. Then he will arrive in $\frac{10^{15}}{6\cdot 3\cdot 10^{7}} = 5{,}555{,}600$ years (in this connection compare the answer given by the astronomic observatory in JULES VERNE'S novel, "From the Earth to the Moon", Point 4).

Others will say: No, he must wait until another 20000 years; then the planet has completed ¾ of its revolution and its motion aims exactly at the fixed star. If the rocket starts then (that is on the line C'C), the asteroid's velocity of 1 km/s is added to its own velocity. It covers the distance in $\frac{10^{15}}{7\cdot 4\cdot 10^{7}} = 4{,}760{,}000$ years and makes up for the 20000 years of waiting. – Who is right?

No one. It is best for the rocket to start a few centuries after this period with a velocity exactly opposite to the velocity of the asteroid and not quite as great. In so doing, it uses a propelling force of 1 km/sec and describes an elongated ellipse around the sun that is to bring it to the edge of the solar corona, In the perihelion (that is the trajectory point nearest the sun) it should have a velocity of 500 km/sec. Now, the astronaut adds the remaining 5 km/sec to this velocity and travels toward the fixed star with the hyperbolic velocity of 505 km/sec on trajectory D'D. The velocity of 500 km/sec corresponds to the kinetic energy used up in order to bring the rocket back up to the trajectory of the asteroid again. That would require energy amounting to $-\frac{1}{2}m500^2$. This additional kinetic energy which the rocket has at 505 km/s is expressed in the fact that it does not stop when it reaches the range of the asteroid but flies on with a velocity whose kinetic energy is equal to the difference between the energy present at 505 km/sec and at 500 km/s. If this velocity is *x*, then

$$\tfrac{1}{2}\cdot m\cdot x^2 = \tfrac{1}{2}\cdot m\cdot 505^2 - \tfrac{1}{2}\cdot m\cdot 500^2.$$

From that follows

$$x = 70.9 \text{ km/s}.$$

With this velocity, our astronaut gets to the unknown fixed star in 470,000 years, which is 1/12 or 1/10 of the time stated above.

It is most remarkable that, at 70.9 km/s, the kinetic energy of the rocket can be greater than the total chemical energy of the fuels carried along. For example, if it was filled with hydrogen and oxygen, which result in and exhaust velocity of ca 4000 km/sec, and we let the mass of the empty rocket equal *m*, then the mass of the full rocket (according to formula (6)) equaled $e^{6/4} = 4.48m$, and the mass of the fuels carried along was 3.48 m. The mechanical equivalent of the heat of combustion was 30.5-35.9 million mkg/kg. When returning from the sun, on the other hand, the kinetic energy of the rocket, when it was as far from the sun as the asteroid, amounted to

$$\tfrac{1}{2}\cdot m\cdot 70{,}000^2 = \tfrac{5}{2}10^9\cdot m \text{ mkg},$$

which is 70-100 times more than the chemical energy of the fuels!

The first time I made this calculation, I believed nothing else in the first minute but that here the law of conservation of energy was broken, or at least that one could work at the cost of energy stimulating the field of gravity somewhat similar to the work performed by an electromagnet which is counterbalanced by weakening of the stimulating current. But neither is the case. The fuels have performed the whole work alone. Beside their energy of combustion, they contained potential energy, since they were so high above the sun to begin with.

By the drop, that was converted to kinetic energy, which now was considerably diminished by the exhaust velocity of 1 km/s, The gases trailing behind are still flying away from the sun, but they no longer come to the height of the

> asteroid; and because we brought them nearer to the sun, energy was released which is now evident in the more rapid motion of the rocket.
>
> In the case of the burning rocket, we are also dealing with two different reference systems. The exhaust gas attains velocity *c* with reference to the rocket, but the rocket gets its propulsion with respect to the earth. With that we move from the area of mental experiments to the sphere of the tangible.
>
> …

(The text that follows is a long discussion of errors and misconceptions held at the time in the published literature, with regard to how the concepts of energy and work can be—and were—misapplied to explanations of rocketry and the question of whether interplanetary flight was feasible.)

It is perhaps worth noting that the identification of hydrogen and oxygen as the "best" fuel and oxidizer for rocket applications was made by Tsiolkovsky, who also discussed the problems of storage of hydrogen, especially with respect to both temperature and volume (Tsiolkovskiy, 1967).

It is also sobering to note that in coming up to the centenary of Oberth's discovery, we are still plagued by the same technical problems of 1929 in trying to implement the scheme, namely, passage "to the edge of the solar corona" and providing the requisite speed change. Oberth's identified probe speed of 500 km/s corresponds to a periapsis of 1.526 R_S, and a 5 km/s spacecraft maneuver would eject the spacecraft from the solar system at an asymptotic speed of ~15 au/year.[24] Furthermore, for a LOX/LH_2 system, the specific impulse could be as high as 465.5 s,[25] for which the required mass ratio would be 2.989. The problem with such a "design" is, of course, the need to store the LH_2 and LOX in deep space for many years while thermally shielding the spacecraft down to the requisite distance above the Sun.[26]

For this option, the C_3 requirements appear to span a somewhat narrow "band" from ~115 to 125 km^2/s^2. For a solid kick stage near the Sun, fine tuning the mass and propellant loading may well be problematic in any event, along with the longer in-space "storage" time before stage use. Control of the burn direction will also be critical along with integration of the TPS into the spacecraft/stage stack. Again, a custom, space-storable propellant system may be preferable, if significantly more costly.

Some comparison can be made with the Cassini propulsion system (Barber & Cowley, 2002; Leeds et al., 1996): "The Cassini Propulsion Module Subsystem (PMS) features a stand-alone, modular configuration, designed to be assembled, tested, and loaded independently from the remainder of the S/C." The system dry mass was 491.9 kg. Expendables included 8.7 kg of helium (pressurant),

[24] Escape speed from the solar "surface" of 1 R_S with 1 R_S = 695,700 km is 617.6 km/s (Williams, 2018). The escape speed goes as the inverse square root of the perihelion, so Oberth's speed of 500 km/s corresponds to a closest approach of 1.526 R_S. For a ΔV of 5 km/s, the usual simple approximation (equation 1 of Ralph L. McNutt, Jr. et al., 2017) gives the asymptotic escape speed as 70.77 km/s or 14.92 au/year.

[25] RL 10B-2 (cf. AerojetRocketdyne, 2020)

[26] The Parker Solar Probe TPS is designed to withstand a temperature of 1400°C = 1673 K at a perihelion of 9.86 R_S. For a flat shield normal to the Sun direction, the temperature scales as the inverse square root of the perihelion distance from the Sun's center. Hence, that design would see a temperature of 4253 K or 3980°C and would not survive at that closer distance. Of the ultra-high-temperature ceramics, hafnium carbide (HfC) melts at 3958°C (Wikipedia, 2020g), and of the metals, tungsten melts at ~3400°C (EngineeringToolBox, 2005). Such investigations are also relevant to research into practical hypersonic flight (Cedillos-Barraza et al., 2016).

132.0 kg of hydrazine for the monopropellant system, and 1132.0 kg of MMH and 1868.0 kg of nitrogen tetroxide (NTO) for the bipropellant system, yielding a total wet mass of 3632.6 kg. For operating the system, the worst-case power consumption was estimated as 241.77 W (from Table 4, "Mass and Power Summary," Leeds et al., 1996). For Cassini, the monopropellant and bipropellant systems were separated (as compared with the dual-mode systems used on other spacecraft such as MESSENGER). Total planned pre-launch ΔV requirements totaled 2.0392 km/s. The specific impulse of the two systems is not given.

The programmatic approach is worth noting for comparison with Galileo:

> In keeping with the international flavor of CRAF/Cassini from its inception, the earliest S/C Propulsion Subsystem was to be built by the Federal Republic of Germany (FRG). Technically, the Germans were contributing one propulsion subsystem for the CRAF Mission and a spare subsystem that was to be used for the Cassini Mission. From the start, the Propulsion Subsystem consisted of a large, helium regulated bipropellant system, and a much smaller hydrazine system for reaction control and smaller AV maneuvers.
>
> Due to budget cuts in 1992, the Cassini Program was downsized, and the CRAF S/C was canceled. Following this decision, the FRG elected to end their participation in the Program. At that point, the decision was made at JPL to procure the entire Propulsion Subsystem from industry. This propulsion contract was eventually won by Lockheed Martin Astronautics in Denver and started in April 1993.

Overall, the total Cassini initial mass was 5574 kg; the orbiter's dry mass was 2113 kg, the Huygens probe's mass was 320 kg, bipropellant mass was 3000 kg (1869 kg oxidizer and 1131 kg fuel), bipropellant helium mass was 8.6 kg, monopropellant mass was 132 kg, and monopropellant helium mass was 0.4 kg. The launch general-purpose heat source radioisotope thermoelectric generator (GPHS RTG) power was 879 W (Barber & Cowley, 2002). Subsequent performance assessments of the system report an effective specific impulse of 301 seconds for the bipropellant system and 217 seconds for the monopropellant (hydrazine) system (Sturm et al., 2015).

As a rough (very rough) estimate, suppose we estimate a spacecraft dry mass of 478.3 kg plus 491.1 kg (Cassini PMS dry mass) with a propellant load of 3000 kg and a specific impulse of 301 seconds. We can estimate a ΔV of 4.2 km/s for such a system (the monopropellant system needs to be nearly as sophisticated, which would bring the dry mass down, but the need for power for the system would also bring the dry mass up); for now we use the 491.1 kg as an estimate and note that it is about the same as the estimated spacecraft (wet) mass of 478.3 kg. It is worth noting that such a deep-space, bipropellant kick stage has not been built before.

The use of such a "custom" stage for a maneuver near the Sun would have the added advantage that the TPS could be built in from the start, rather than "retrofit" into an existing solid propellant stage. The TPS mass would, of course, also bring the performance down. With a 500-kg TPS, the velocity performance would drop from 4.2 km/s to 3.3 km/s; with a 1000-kg TPS, it would drop to 2.7 km/s, and so on.

11.6. Section 11 References

Abramowitz, M., Stegun, I.A. (1972) *Handbook of Mathematical Functions* (Tenth Printing ed. Vol. 55). Washington, D.C.: U.S. Government Printing Office.

Ackeret, J. (1946) Zur Theorie der Raketen. *Helv. Phys. Acta* 19(April 1946), 103-112. Retrieved from http://www.e-periodica.ch/cntmng?pid=hpa-001:1946:19::571

Ackeret, J. (1947) Zur Theorie der Raketen (English Translation). *J. Brit. Int. Soc.* 6, 116-123.

AerojetRocketdyne (2020) RL10 engine. Retrieved from https://www.rocket.com/space/liquid-engines/rl10-engine.

Alden, H.L. (1928) Alpha and Proxima Centauri. *Astronomical Journal* 39(913), 20-23. doi: 10.1086/104871

Aldiss, B. (1960) *Starship*. New York: Signet Books.

Alkalai, L., Arora, N. (2015) *The Interstellar Medium (ISM) – The Next Frontier in Space Science and Exploration*. Paper presented at the IAA Symposium on the Future of Space Exploration: Towards New Global Programs, Torino, Italy.

Alkalai, L., Arora, N., Turyshev, S., Shao, M., Weinstein-Weiss, S., Opher, M., Redfield, S. (2017) *A Vision for Planetary and Exoplanets Science: Exploration of the Interstellar Medium – The Space Between the Stars*. Paper presented at the 68th International Astronautical Congress, Adelaide, Australia.

Allen, J.P., Baker, J.L., Bannister, T.C., et al. (1976) *Outlook for Space: Report to the NASA Administrator by the Outlook for Space Study Group* (NASA SP-386). Washington, D. C.:

Anderson, J.L. (1999) Roadmap to a Star. *Acta Astronautica* 44, 91-97. Retrieved from https://www.sciencedirect.com/science/article/pii/S0094576599000338

Anderson, M.K. (2012) *The Day the World Discovered the Sun: An Extraordinary Story of Scientific Adventure and the Race to Track the Transit of Venus*. Boston, Massachusetts: Da Capo Press. Retrieved from https://books.google.com/books?id=ZVRhuXJVHyAC&pg=PP1&lpg=PP1&dq=The+Day+the+World+Discovered+the+Sun:+An+Extraordinary+Story+of+Scientific&source=bl&ots=Qo0QxiNMHZ&sig=jw8V4F-OJMHxjElBcc9I9JlcaLk&hl=en&sa=X&ei=XPz9VImRNMmeggT4vISIBg&ved=0CCoQ6AEwAjgK#v=onepage&q=Lalande&f=false

Ashcroft, J., Eshelman, C. (2006) *Summary of NR Program Prometheus Efforts* (LM-05K188; TRN: US0602908 United States10.2172/881290TRN: US0602908Thu Jun 28 07:51:34 EDT 2012KAPLEnglish)

Asimov, I. (1966) How Far Will We Go in Space? In *The 1966 World Book Year Book* (pp. 148-163). Chicago, IL: Field Enterprises Educational Corporation, Publishers.

Barber, T.J., Cowley, R.T. (2002) Initial Cassini Propulsion System In-Flight Characterization. In *38th AIAA/ASME/SAE/ASEE Joint Propulsion Conference & Exhibit*: American Institute of Aeronautics and Astronautics.

Barnard, E.E. (1916) A Small Star with Large Proper-Motion. *Astonomical Journal* 29(695), 181-183. doi: 10.1086/104156

Becquerel, H. (1896) Surles radiations emises par phosphorescence. [On radiation emitted by phosphorescence]. *Comptes rendus hebdomadaires des séances de l'Académie des sciences / publiés... par MM. les secrétaires perpétuels* 122(2), 420-421. Retrieved from https://gallica.bnf.fr/ark:/12148/bpt6k30780/f419.item#

Benedict, G.F., Barbara, M., Chappell, D.W., et al. (1999) Interferometric Astrometry of Proxima Centauri and Barnard's Star Using HUBBLE SPACE TELESCOPE Fine Guidance Sensor 3: Detection Limits for Substellar Companions. *The Astronomical Journal* 118(2), 1086. Retrieved from http://stacks.iop.org/1538-3881/118/i=2/a=1086

Bernal, J.D. (1969) *The World, the Flesh, and the Devil: an Enquiry into the Future of the Three Enemies of the Soul* (2nd ed.). Bloomington, IN: Indiana Univ. Press.

Bessel, F.W. (1838) II. A letter from Professor Bessel to Sir J. Herschel, Bart., dated Konigsberg, Oct. 23, 1838. *Monthly Notices of the Royal Astronomical Society* 4(17), 152-161. doi: 10.1093/mnras/4.17.152

Bessel, F.W. (1839) Bestimmung der Entfernung des 61sten Sterns des Schwans. *Astronomische Nachrichten* 16(5-6), 65-96. doi: 10.1002/asna.18390160502

Bessel, F.W. (1840) Fernere Nachricht von der Bestimmung der Entfernung von 61 Cygni. *Astronomische Nachrichten* 17(18), 273-276. doi: 10.1002/asna.18400171802

Born, M. (1909) Die Theorie des starren Elektrons in der Kinematik des Relativitätsprinzips. *Annalen der Physik* 335(11), 1-56. doi: 10.1002/andp.19093351102

Burdge, W.D., Levine, B.L. (2006) *Space Nuclear Power Plant Pre-Conceptual Design Report, For Information* (SPP-67210-0010; TRN: US0603406 United States10.2172/883378TRN: US0603406Mon Dec 02 07:34:19 EST 2013KAPLEnglish)

Bussard, R.W. (1960) Galactic Matter and Interstellar Flight. *Astron. Acta* 6, 179-194.

Byrd, P.F., Friedman, M.D. (1971) *Handbook of Elliptic Integrals for Engineers and Scientists*(2 ed., Vol. 67, pp. xvi+360). 10.1007/978-3-642-65138-0

Cai, S.-y. (2008) Polonium and Radium Started Up the Era of Nuclear Science and Technology: Commemorating the 110th Anniversary of the Discovery of Po & Ra by M. Curie and P. Curie. *Journal of Isotopes* 21(4), 242-248.

Carter, B. (1968) Global Structure of the Kerr Family of Gravitational Fields. *Physical Review* 174(5), 1559-1571. Retrieved from https://link.aps.org/doi/10.1103/PhysRev.174.1559

Cedillos-Barraza, O., Manara, D., Boboridis, K., Watkins, T., Grasso, S., Jayaseelan, D.D., Konings, R.J.M., Reece, M.J., Lee, W.E. (2016) Investigating the Highest Melting Temperature Materials: A Laser Melting Study of the TaC-HfC System. *Scientific Reports* 6, 37962. doi: 10.1038/srep37962

Chapman, A. (1990) Jeremiah Horrocks, the Transit of Venus, and the 'New Astromnomy' in Early Seventeenth-Century England. *Quarterly Journal of the Royal Astonomical society* 31, 333-357. Retrieved from http://articles.adsabs.harvard.edu/pdf/1990QJRAS..31..333C

Chew, G., Doyle, M., Stancati, M. (2001) *Interstellar Spaceflight Primer*. Schaumburg, IL: Science Applications International Corporation.

Christiansen, R.A., Jackson, R.W., Sperans, J., Tendeland, T., Wolfe, J.H. (1971) *Pioneer H Jupiter Swingby Out-of-the-Ecliptic Mission Study – Final Report* (NASA-TM-108108). Moffett Field, CA: National Aeronautics and Space Administration.

Clarke, A.C. (1964) The Sumjammer. *Boy's Life,* 8.

Clarke, J.F., Hymowitz, E.W., Trainor, J.H. (1968) *Galactic Jupiter Probes*. Paper presented at the Fifth Goddard Memorial Symposium, Washington, D.C.

Cole, D.M. (1965) *Beyond Tomorrow:The Next 50 Years in Space* (1st ed.). Amherst, WI: Amherst Press.

Cortright, E.M. (1967, 14-15 March) *The Voyager Program.* In Americal Astronautical Society Annual Goddard Memorial Symposium, AAS Publications Office, Washington, D.C.

Curie (1902) Sur le Poids Atomique du Radium. [On the atomic weight of radium]. *Comptes rendus hebdomadaires des séances de l'Académie des sciences / publiés... par MM. les secrétaires perpétuels* 135, 161 - 163. Retrieved from https://gallica.bnf.fr/ark:/12148/bpt6k64435428/f167.item.r=Curie

Curie, M.P., Debierne, M.A. (1910) Sur le Radium Métallique. [On metallic radium]. *Comptes rendus hebdomadaires des séances de l'Académie des sciences / publiés... par MM. les secrétaires perpétuels* 151, 523 - 525. Retrieved from https://gallica.bnf.fr/ark:/12148/bpt6k31042/f523.item.r=1910CurieDebierne%201910%20Curie%20Debierne

Curie, P., Curie, P., Bémont, G. (1898) Sur une Nouvelle Substance Fortement Radio-Active, Contenue dans la Pechblende. [On a New, Strongly Radio-active Substance Contained in Pitchblende]. *Comptes rendus hebdomadaires des séances de l'Académie des sciences / publiés... par MM. les secrétaires perpétuels* 127(7), 1215-1217. Retrieved from https://gallica.bnf.fr/ark:/12148/bpt6k3083q/f1217.item

Curie, P., Curie, S. (1898) Sur une Substance Nouvelle Radio-Active, Contenue dans la Pechblende. [On a New Radioactive Substance Contained in Pitchblende]. *Comptes rendus hebdomadaires des séances de l'Académie des sciences / publiés... par MM. les secrétaires perpétuels* 127(7), 175-178. Retrieved from https://gallica.bnf.fr/ark:/12148/bpt6k3083q/f177.item

D'Amario, L.A., Bright, L.E., Wolf, A.A. (1992) Galileo Trajectory Design. *Space Science Reviews* 60(1), 23-78. doi: 10.1007/bf00216849

de Lalande, J.-J.L. (1770a) Mémoire sur la parallaxe du Soleil, qui résulte du passage de Vénus, observé en 1769. *Mémoires de l'Académie royale des sciences*, 9-14. Retrieved from http://www.academie-sciences.fr/activite/archive/dossiers/Lalande/Lalande_pdf/Mem1770_p9.pdf

de Lalande, J.-J.L. (1770b) Mémoire sur la parallaxe du Soleil, qui résulte du passage de Vénus, observé en 1769. *Histoire de l'Académie royale des sciences*, 74-76. Retrieved from http://www.academie-sciences.fr/activite/archive/dossiers/Lalande/Lalande_pdf/Hist1770_p74.pdf

de Lalande, J.-J.L. (1771) Mémoire sur la parallaxe du Soleil, déduite des observations faites dans la mer du Sud, dans le Royaume d'Astracan, et à la Chine. *Mémoires de l'Académie royale des sciences*, 776-799. Retrieved from http://www.academie-sciences.fr/activite/archive/dossiers/Lalande/Lalande_pdf/Mem1771_p776.pdf

Deininger, W.D., Vondra, R.J. (1988) Arcjet Propulsion System for an SP-100 Flight Experiment. *Journal of Spacecraft and Rckets* 25(6), 427-432. doi: 10.2514/3.26023

Deininger, W.D., Vondra, R.J. (1991) Spacecraft and mission design for the SP-100 flight experiment. *J. Brit. Int. Soc.* 44, 217-228.

Despain, L.G., Hennes, J.P., Archer, J.L. (1971, 28-30 June) *Scientific Goals of Missions Beyond the Solar System.* In 17th Annual Meeting American Astronautical Society, Seattle, WA.

Dessler, A.J. (1967) Solar Wind and Interplanetary Magnetic Field. *Reviews of Geophysics* 5(1), 1-41.

Dessler, A.J., Park, R.A. (1971, 28-30 June) *The First Step Beyond the Solar System.* In 17th Annual Meeting American Astronautical Society, Seattle, WA.

Dole, S.H. (1964) *Habitable Planets for Man*. New York: Blaisdell Publishing Co.

Donahue, T.M., Anderson, D., Baker, D.J., et al. (1988) *Space Science in the Twenty-First Century: Imperatives for the Decades 1995 to 2015 - Report of the Study Steering Group, Space Science Board, Commission on Physical Sciences, Mathematics, and Resources*: National Research Council. Retrieved from http://www.nap.edu/catalog/748.html

Dowling, R.L., Kosmann, W.J., Minovitch, M.A., Ridenoure, R.W. (1990, 1997) *Chapter 2 - The Origin of Gravity-Propelled Interplanetary Space Travel.* In Twenty-Fourth Symposium of the International Academy of Astronautics, Univelt, Incorporated, Dresden, Germany.

Dowling, R.L., Kosmann, W.J., Minovitch, M.A., Ridenoure, R.W. (1991) *Chapter 2 - Gravity Propulsion Research at UCLA and JPL, 1962-1964.* In Twenty-Fifth History Symposium of the International Academy of Astronautics, Univelt, Incorporated, Montreal, Canada.

Dowling, R.L., Kosmann, W.J., Minovitch, M.A., Ridenoure, R.W. (1999) *The Effect of Gravity-Propelled Interplanetary Space Travel on the Exploration of the Solar System: Historical Survey, 1961 to 2000.* In Thirty-Third History Symposium of the International Academy of Astronautics, Univelt, Incorporated, Amsterdam, The Netherlands.

Droste, J. (1917) The field of a single centre in Einstein's theory of gravitation and the motion of a particle in that field. *Proceedings of the Royal Netherlands Academy of Arts and Sciences (KNAW)* 19(1), 197-215. Retrieved from http://www.dwc.knaw.nl/DL/publications/PU00012346.pdf

Dyson, F.J. (1963) Gravitational Machines. In Cameron, A.G.W. (Ed.), *Interstellar Communication* (First ed., pp. 115-120). New York: W. A. Benjamin, Inc.

Dyson, F.J. (1965) Death of a Project. *Science* 149, 141-144.

Dyson, F.J. (1968) Interstellar Transport. *Phys. Today*, 41-45.

Dyson, F.W., Eddington, A.S., Davidson, C. (1920) A Determination of the Deflection of Light by the Sun's Gravitational Field, from Observations Made at the Total Eclipse of May 29, 1919. *Philosophical Transactions of the Royal Society of London. Series A, Containing Papers of a Mathematical or Physical Character* 220(571-581), 291-333. doi: 10.1098/rsta.1920.0009

Dyson, G. (2002) *Project Orion: The True Story of the Atomic Spaceship*. New York: Henry Holt and Company.

Ehricke, K.A. (1971, 28-30 June) *The Ultraplanetary Probe.* In 17th Annual Meeting American Astronautical Society, Seattle, WA.

Ehricke, K.A. (1972) Saturn-Jupiter Rebound. *Journal of the British Interplanetary Society* 25, 561-571.

Einstein, A. (1916) Die Grundlage der allgemeinen Relativitätstheorie. *Annalen der Physik* 354(7), 769-822. doi: 10.1002/andp.19163540702

EngineeringToolBox (2005) Metals and Alloys - Melting Temperatures. Retrieved from https://www.engineeringtoolbox.com/melting-temperature-metals-d_860.html.

Esnault-Pelterie, M. (1913) Considérations sur les résultats d'un allégement indéfini des moteurs. [A consideration of the effect of indefinitely reducing the weight of motors.]. *Journal de Physique Théorique et Appliquée* 3(1), 218-230. doi: 10.1051/jphystap:019130030021800

Essig, J. (2016) *Call of the Cosmic Wild. Relativistic Rockets for the New Millennium*(Third ed., pp. 6792). Retrieved from https://play.google.com/store/books/details?id=WAX3CwAAQBAJ&rdid=book-WAX3CwAAQBAJ&rdot=1&source=gbs_vpt_read&pcampaignid=books_booksearch_viewport

Etchegaray, M.I. (1987) *Preliminary Scientific Rationale for a Voyage to a Thousand Astonomical Units* JPL.

Fiehler, D.I., McNutt, R.L., Jr. (2005) *Mission Design for the Innovative Interstellar Explorer Vision Mission* (NASA/CR-2005-214017 IEPC-2005-211). Cleveland, OH:

Fiehler, D.I., McNutt, R.L., Jr. (2006) Mission Design for the Innovative Interstellar Explorer Vision Mission. *Journal of Spacecraft and Rockets* 43(6), 1239-1247. doi: 10.2514/1.20995

Flandro, G.A. (1966) Fast Reconaissance Missions to the Outer Solar System Utilizing Energy Derived from the Gravitational Field of Jupiter. *Astron. Acta* 12(4), 329-337.

Forsyth, A.R. (1920) Note on the Central Differential Equation in the Relativity Theory of Gravitation. *Proceedings of the Royal Society of London. Series A* 97(682), 145-151. doi: 10.1098/rspa.1920.0019

A National Space Program for Interstellar Exploration, 94th United States Congress, First Sess. 279-387 (1975).

Forward, R.L. (1996) Radioisotope Sails for Deep Space Propulsion and Power. *J. Brit. Int. Soc.* 49, 147-149.

Frisbee, R., Leifer, S. (1998) Evaluation of Propulsion Options for Interstellar Missions. In *34th AIAA/ASME/SAE/ASEE Joint Propulsion Conference and Exhibit*: American Institute of Aeronautics and Astronautics.

Garwin, R.L. (1958) Solar Sailing - A Practical Method of Propulsion Within the Solar System. *Jet Propulsion* 28(3), 188-189. Retrieved from https://www.fas.org/rlg/030058-SS.pdf

Goddard, R.H. (1919) A Method of Reaching Extreme Altitudes. *Smithsonian miscellaneous collections* 71(2), 82. Retrieved from https://library.si.edu/digital-library/book/smithsonianmisce711921smit

Goddard, R.H. (1983) The Ultimate Migration. *Journal of the British Interplanetary Society* 36, 552-554.

Gradshteyn, I.S., Ryzhik, I.M. (1980) *Table of Integrals, Series, and Products* (Scripta Technica, I., Trans. Corrected and enlarged edition of Alan Jeffrey incorporating the fourht edition prepared by Yu. V. Geronimus and M. Yu. Tseytlin ed.). New York: Academic Press.

Greschik, G., Mikulas, M.M. (2002) Design Study of a Square Solar Sail Architecture. *Journal of Spacecraft and Rockets* 39(5), 653-661. doi: 10.2514/2.3886

Grey, J. (1959) Gaseous-Core Nuclear Rockets. *Astronautics* 4(10), 23.

Gruntman, M., McNutt, R.L., Jr., Gold, R.E., Krimigis, S.M., Roelof, E.C., Gloeckler, G., Koehn, P.L., Kurth, W.S., Oleson, S.R. (2004) *Innovative Interstellar Explorer.* In 55th International Astronautical Congress, Vancouver, CA.

Gruntman, M., McNutt, R.L., Gold, R.E., et al. (2006) Innovative Explorer Mission to Interstellar Space. *Jbis-Journal of the British Interplanetary Society* 59(2), 71-75. Retrieved from <Go to ISI>://WOS:000234975900008

Gruntman, M. (2007) *From Astronautics to Cosmonautics - Space Pioneers Robert Esnault-Pelterie and Ary Sternfeld*. North Charleston, SC: Booksurge. Retrieved from http://www.astronauticsnow.com/astrocosmo/index.html

Hagenest, W., Sola, F., Tyler, W. (1984) Development of a Bipropellant Propulsion Module for the Galileo Spacecraft. In *20th Joint Propulsion Conference*: American Institute of Aeronautics and Astronautics.

Hagihara, Y. (1931) Theory of the Relativistic Trajectories in a Gravitational Field of Schwarzschild. *Japanese Journal of Astronomy and Geophysics* 8, 67 - 176. Retrieved from http://adsabs.harvard.edu/abs/1930JaJAG...8...67H

Hall, C.F., Nothwang, G.J., Hornby, H. (1962) Solar Probes - A Feasibility Study. *Aeorspace Engineering*, 22-30.

Hall, C.F. (1974) Pioneer 10. *Science* 183, 301-302.

Halleio, E. (1714) Methodus singularis qua solis parallaxis sive distantia a terra, ope veneris intra solem conspiciendoe, tuto determinari poterit. *Philosophical Transactions of the Royal Society* 29, 454-464. Retrieved from http://rstl.royalsocietypublishing.org/content/29/338-350/454

Halley (1809) A New Method of Determining the Parallex of the Sun, or His Distance from the Earth; by Dr. Halley, Sec. R. S. No. 348, p.454. Translated from the Latin. In *The Philosophical Transactions of the Royal Society of London, from Their Commencement in 1665, in the Year 1800* (Vol. 29, pp. 243-249): London, Printed by and for C. and R. Baldwin.

Hamlyn, K., McGrath, D., Lara, M. (1991) Venus Orbit Insertion of the Magellan Spacecraft Using a Thiokol STAR 48B Rocket Motor. In *27th Joint Propulsion Conference*: American Institute of Aeronautics and Astronautics.

Harkness, W. (1891) *The Solar Parallax and Its Related Constants: Including the Figure and Density of the Earth*. Washington, D.C. Retrieved from https://play.google.com/store/books/details?id=ZRVAAAAAYAAJ&rdid=book-ZRVAAAAAYAAJ&rdot=1

Heacock, R.L. (1980) The Voyager Spacecraft. *Proceedings of the Institution of Mechanical Engineers* 194, 211-224. Retrieved from http://stickings90.webspace.virginmedia.com/voyager.pdf

Heinlein, R.A. (1965) *Orphans of the Sky*. New York: Signet Books.

Henderson, T. (1840) XVI. On the Parallax of Sirius. *Memoirs of the Royal Astronomical Society* 11, 239-248.

HistoryHouse (2020) The Inspirations for the Invaders from Mars. Retrieved from http://www.historyhouse.co.uk/articles/hg_wells.html.

Hohmann, W. (1960) *The Attainability of Heavenly Bodies* (NASA, Trans. Vol. F-44). Washington, D.C.: National Aeronautics and Space Administration. Retrieved from http://large.stanford.edu/courses/2014/ph240/nagaraj1/docs/hohmann.pdf

Holzer, T.E. (1989) Interaction Between the Solar Wind and the Interstellar Medium. *Annual Review of Astronomy and Astrophysics* 27(1), 199-234. doi: 10.1146/annurev.aa.27.090189.001215

Holzer, T.E., Mewaldt, R.A., Neugebauer, M. (1990) *The Interstellar Probe: Scientific Objectives for a Frontier Mission to the Heliospheric Boundary and Interstellar Space*. Ballston, VA:

Hornsby, T. (1771) The Quantity of the Sun's Parallax, as Deduced from the Observations of the Transit of Venus, on June 3, 1769: By Thomas Hornsby, M. A. Savilian Professor of Astronomy in the University of Oxford, and F. R. S. *Philosophical Transactions* 61, 574-579. doi: 10.1098/rstl.1771.0054

IAU (2012) *Resolution B2 on the Re-Definition of the Astronomical Unit of Length* Union, I.A.

IAU (2020) Measuring the Universe - The IAU and Astronomical Units. Retrieved from https://www.iau.org/public/themes/measuring/.

Innes, R. (1915) A Faint Star of Large Proper Motion. *Circular of the Union Observatory*(30), 235-236. Retrieved from http://adsabs.harvard.edu/abs/1915CiUO...30..235I

Innes, R.T.A. (1917) Parallax of the Faint Proper Motion Star Near Alpha of Centaurus. *Circular of the Union Observatory*(40), 331-336. doi: 1917CiUO...40..331I

Jaffe, L.D., Ivie, C.V., Lewis, J.C., Lipes, R., Norton, H.N., Stearns, J.W., Stimpson, L.D., Weissman, P. (1977) *An Interstellar Precursor Mission*. Pasadena, CA: Laboratory, J.P.

Jaffe, L.D., Ivie, C.V. (1979) Science Aspects of a Mission Beyond the Planets. *Icarus* 39, 486-494.

Jaffe, L.D., Ivie, C.V., Lewis, J.C., Lipes, R., Norton, H.N., Stearns, J.W., Stimpson, L.D., Weissman, P. (1980) An Interstellar Precursor Mission. *J. Brit. Int. Soc.* 33, 3-26.

Jaffe, L.D., Norton, H.N. (1980) A Prelude to Interstellar Flight. *Astro. Aero.* 18, 38-44.

Johnson, L., Whorton, M., Heaton, A., Pinson, R., Laue, G., Adams, C. (2011) NanoSail-D: A Solar Sail Demonstration Mission. *Acta Astronautica* 68(5–6), 571-575. doi: http://dx.doi.org/10.1016/j.actaastro.2010.02.008

Johnson, L. (2016) *Solar Sails for Spacecraft Propulsion*. Paper presented at the The University of Tennessee, Tickle College of Engineering Distinguished Lecture Series, Room 622, Min Kao Electrical Engineering and Computer Science Building. https://ntrs.nasa.gov/citations/20160005683.

Kerr, R.P. (1963) Gravitational Field of a Spinning Mass as an Example of Algebraically Special Metrics. *Physical Review Letters* 11(5), 237-238. Retrieved from https://link.aps.org/doi/10.1103/PhysRevLett.11.237

Kirby, K., Artis, D., Bushman, S., et al. (2013) Radiation Belt Storm Probes—Observatory and Environments. *Space Science Reviews* 179(1-4), 59-125. doi: https://doi.org/10.1007/s11214-012-9949-2

Kottler, F. (1914a) Fallende Bezugssysteme vom Standpunkte des Relativitätsprinzips. *Annalen der Physik* 350(20), 481-516. doi: 10.1002/andp.19143502003

Kottler, F. (1914b) Relativitätsprinzip und beschleunigte Bewegung. *Annalen der Physik* 349(13), 701-748. doi: 10.1002/andp.19143491303

Kottler, F. (1916) Über Einsteins Äquivalenzhypothese und die Gravitation. *Annalen der Physik* 355(16), 955-972. doi: 10.1002/andp.19163551605

Kottler, F. (1918) Über die physikalischen Grundlagen der Einsteinschen Gravitationstheorie. *Annalen der Physik* 361(14), 401-462. doi: 10.1002/andp.19183611402

Langhoff, S., Spilker, T., Martin, G., Sullivan, G. (2008) *Workshop Report On Ares V Solar System Science* (NASA/CP–2008-214592). Moffett Field, CA: NASA Ames Research Center.

LASL (1969) *Phoebus 2A Preliminary Report*. Los Alamos, NM: Atomic Energy Commission.

Leeds, M., Eberhardt, R., Berry, R. (1996) Development of the Cassini Spacecraft Propulsion Subsystem. In *32nd Joint Propulsion Conference and Exhibit*: American Institute of Aeronautics and Astronautics.

Lehman, M.K. (2020) Robert Goddard, American Professor and Inventor. Retrieved from https://www.britannica.com/biography/Robert-Goddard.

Liewer, P.C., Mewaldt, R.A., Ayon, J.A., Wallace, R.A. (2000) *NASA's Interstellar Probe Mission.* In Space Technology and Applications International Forum (STAIF)-2000, Albuquerque, NM.

Liewer, P.C., Mewaldt, R.A., Ayon, J.A., Gamer, C., Gavit, S., Wallace, R.A. (2001) Interstellar Probe Using a Solar Sail: Conceptual Design and Technological Challenges. In Scherer, K., Fichtner, H., Fahr, H.-J., et al. (Eds.), *COSPAR Colloquium on The Outer Heliosphere: The Next Frontiers COSPAR Colloquia Series* (Vol. 11, pp. 411-420). New York: Pergamon Press.

Lurie, J.C., Henry, T.J., Jao, W.-C., Quinn, S.N., Winters, J.G., Ianna, P.A., Koerner, D.W., Riedel, A.R., Subasavage, J.P. (2014) The Solar Neighborhood. XXXIV. ASearch for Planets Orbiting Nearby M Dwarfs Using Astrometry. *The Astronomical Journal* 148(5), 91. Retrieved from http://stacks.iop.org/1538-3881/148/i=5/a=91

Lyman, R.W., Ewing, M.E., Krishnan, R.S., Lester, D.M., McNutt, R.L., Jr. (2001, 8-11 July 2001) *Solar Thermal Propulsion for an Interstellar Probe.* In 37th AIAA/ASME/SAE/ASE Joint Propulsion Conference, Salt Lake City, UT.

Marder, L. (2008) On Uniform Acceleration in Special and General Relativity. *Mathematical Proceedings of the Cambridge Philosophical Society* 53(1), 194-198. doi: 10.1017/S0305004100032114

Marsh, L.M. (1965) Relativistic Accelerated Systems. *American Journal of Physics* 33(11), 934-938. doi: 10.1119/1.1971081

Marx, G. (1966) Interstellar Vehicle Propelled By Terrestrial Laser Beam. *Nature* 211(5044), 22-23. Retrieved from http://dx.doi.org/10.1038/211022a0

Marzwell, N., Harris, H. (1998, 28-31 July) *Interstellar Science, Technology, Mission Roadmap*, Jet Propulsion Laboratory, Pasadena, CA.

Matthews, H.F., Erickson, M.D. (1964) *The NASA Advanced Pioneer Mission*. http://dx.doi.org/10.4271/640228.

McAdams, J.V., McNutt, R.L., Jr. (2002) Ballistic Jupiter Gravity-Assist, Perihelion-ΔV Trajectories for a Realistic Interstellar Explorer. *Adv. Astron. Sci.* 112, 725-737.

McAdams, J.V., McNutt, R.L., Jr. (2003) Ballistic Jupiter Gravity-Assist, Perihelion-ΔV Trajectories for a Realistic Interstellar Explorer. *J. Astron. Sci.* 51, 179-193.

McComas, D.J., Velli, M., Lewis, W.S., et al. (2005) Solar Probe: Humanity's First Visit to a Star. *Proceedings of the Conference Solar Wind 11 - SOHO 16* 592, 279-286. Retrieved from <Go to ISI>://WOS:000235471300042

McComas, D.J., Acton, L.W., Balat-Pichelin, M., et al. (2008) *Solar Probe Plus: Report of the Science and Technology Definiiton Team*. Greenbelt, MD: National Aeronautics and Space Administration.

McComas, D.J., F. Allegrini, F., Bochsler, P., et al. (2009) IBEX - Interstellar Boundary Explorer. *Space Sci. Rev.* 146, 11-33. doi: 10.1007/s11214-009-9499-4

McLafferty, G.H. (1970) Gas-Core Nuclear Rocket Engine Status. *J. Spacecraft* 7(12), 1391-1396.

McNutt, R.L., Andrews, G.B., McAdams, J., Gold, R.E., Santo, A., Oursler, D., Heeres, K., Fraeman, M., Williams, B. (2003) Low-cost interstellar probe. *Acta Astronautica* 52(2-6), 267-279. doi: 10.1016/s0094-5765(02)00166-2

McNutt, R.L., Andrews, G.B., Gold, R.E., et al. (2004) A Realistic Interstellar Explorer. *To the Edge of the Solar System and Beyond* 34(1), 192-197. doi: 10.1016/j.asr.2003.03.053

McNutt, R.L., Gold, R.E., Krimigis, S.M., et al. (2005) Innovative Interstellar Explorer. *Proceedings of the Conference Solar Wind 11 - SOHO 16* 592, 693-696. Retrieved from <Go to ISI>://WOS:000235471300139

McNutt, R.L., Gold, R.E., Krimigis, T., et al. (2006) Innovative Interstellar Explorer. *Physics of the Inner Heliosheath: Voyager Observations, Theory, and Future Prospects* 858, 341-347. Retrieved from <Go to ISI>://WOS:000242532200051

McNutt, R.L., Jr., Gold, R.E., Roelof, E.C., Zanetti, L.J., Reynolds, E.L., Farquhar, F.W., Gurnett, D.A., Kurth, W.S. (1997) A Sole/Ad Astra: From the Sun to the Stars. *J. Brit. Int. Soc.* 50, 463-474.

McNutt, R.L., Jr., Andrews, G.B., Gold, R.E., et al. (2004) A Realistic Interstellar Explorer. *Adv. Space Res.* 34, 192-197.

McNutt, R.L., Jr., Gold, R.E., Krimigis, S.M., et al. (2005, 13 Jul 2005) *Innovative Interstellar Explorer: Radioisotope Propulsion to the Interstellar Medium.* In 41st AIAA/ASME/SAE/ASEE Joint Propulsion Conference & Exhibit, AIAA, Tucson, AZ.

McNutt, R.L., Jr., Gruntman, M., Krimigis, S.M., Roelof, E.C., Wimmer-Schweingruber, R.F. (2011) Interstellar Probe: Impact of the Voyager and IBEX Results on Science and Strategy. *Acta Astronautica* 69(9-10), 767-776. doi: 10.1016/j.actaastro.2011.05.024

McNutt, R.L., Jr., Wimmer-Schweingruber, R.F. (2011) Enabling Interstellar Probe. *Acta Astronautica* 68(7-8), 790-801. Retrieved from http://www.sciencedirect.com/science/article/B6V1N-50T9475-1/2/fa0fc0accdbcee487278c47c06797bec

McNutt, R.L., Jr., Elsperman, M.S., Gruntman, M., Klaus, K.K., Krimigis, S.M., Roelof, E.C., Smith, D.B., Vernon, S.R., Wimmer-Schweingruber, R.F. (2014) *Enabling Insterstellar Probe with the Space Launch System (SLS)*. Paper presented at the 65th International Astronautical Congress, Toronto, Ontario, Canada.

McNutt, R.L., Jr., Aleman, S.M., Amato, M.J., et al. (2015) *Nuclear Power Assessment Study - Final Report*. Laurel, MD: NASA Glenn Research Center.

McNutt, R.L., Jr., Benson, W.W., Gruntman, M., Krimigis, S.M., Roelof, E.C., Vernon, S.R., Wimmer-Schweingruber, R.F. (2015) *Enabling Interstellar Probe: Space Launch System (SLS) trades*. Paper presented at the 66th International Astronautical Congress, Jerusalem, Israel.

McNutt, R.L., Jr., Wimmer-Schweingruber, R.F., Gruntman, M., Krimigis, S.M., Roelof, E.C., Zank, G.P., Stone, E.C., Brandt, P.C., Vernon, S.R. (2017) *Near-Term Exploration of the Interstellar Medium*. Paper presented at the 68th International Astronautical Congress, Adelaide, Australia.

McNutt, R.L., Jr. , Zurbuchen, T.H., Gruntman, M., Krimigis, S.M., Roelof, E.C., Vernon, S.R., Wimmer-Schweingruber, R.F. (2016) *Interstellar Probe: Requirements*. Paper presented at the 67th International Astronautical Congress, Guadalajara, Mexico. https://iafastro.directory/iac/paper/id/35475/ext/appendix/IAC-16,D4,1,9,x35475.pdf.

Mewaldt, R., Liewer, P. (2000) An interstellar probe mission to the boundaries of the heliosphere and nearby interstellar space. In *Space 2000 Conference and Exposition*: American Institute of Aeronautics and Astronautics.

Mewaldt, R.A., Kangas, J., Kerridge, S.J., Neugebauer, M. (1995) A Small Interstellar Probe to the Heliospheric Boundary and Interstellar Space. *Acta Astronautica* 35, Supplement 1(0), 267-276. doi: http://dx.doi.org/10.1016/0094-5765(94)00192-O

Mewaldt, R.A., Liewer, P.C. (2000, 19-21 Sep 2000) *An Interstellar Probe Mission to the Boundaries of the Heliosphere and Nearby Interstellar Space.* In AIAA Space 2000 Conference and Exposition, Long Beach, CA.

Mewaldt, R.A., Liewer, P.C. (2001) Scientific Payload for an Interstellar Probe Mission. In Scherer, K., Fichtner, H., Fahr, H.-J., et al. (Eds.), *The Outer Heliosphere: The Next Frontier* (pp. 451-464). New York: Pergamon.

Minovitch, M.A. (1961) *A Method for Determining Interplanetary Free-Fall Reconnaissance Trajectories*. Pasadena, CA: Jet Propulsion Laboratory.

Minovitch, M.A. (1963) *The Determination and Characteristics of Ballistic Interplanetary Trajectories Under the Influence of Multiple Planetary Attractions* (Technical Report Number 32-464). Pasadena, CA: Jet Propulsion Laboratory.

Minovitch, M.A. (1965) *Utilizing Large Planetary Perturbations for the Design of Deep-Space, Solar-Probe, and Out-of-Ecliptic Trajectories*. Pasadena, CA: Jet Propulsion Laboratory.

Mitchell, S.A. (1917) Preliminary parallax of Barnard's star of large propoer-motion. *Astronomical Journal* 30(710), 126-127. Retrieved from http://adsabs.harvard.edu/abs/1917AJ.....30..126M

Moiseyev, I. (2015) The Real Interstellar - Space Travel Theories from Tsiolkovsky to Wormholes. *Room - The Space Journal, 2(4),* 38-41. Retrieved from https://room.eu.com/article/The_real_Interstellar_space_travel_theories_from_Tsiolkovsky_to_wormholes.

Morton, W.B. (1921) LXI. The Forms of Planetary Orbits on the Theory of Relativity. *The London, Edinburgh, and Dublin Philosophical Magazine and Journal of Science* 42(250), 511-522. doi: 10.1080/14786442108633793

NASA (2010) Hermann Oberth. Retrieved from https://www.nasa.gov/audience/foreducators/rocketry/home/hermann-oberth.html.

National Academies of Sciences, Engineering, and Medicine (2017) *Powering Science: NASA's Large Strategic Science Missions*. Washington, DC: The National Academies Press. doi:10.17226/24857

Neugebauer, M., Davies, R.W. (1978) *A Close-Up of the Sun* (JPL Publication 78-70). Pasadena, CA: Jet Propulsion Laboratory.

Niehoff, J.C. (1966) Gravity-Assisted Trajectories to Solar-System Targets. *Journal of Spacecraft and Rockets* 3(9), 1351-1356. doi: 10.2514/3.28659

Noble, R.J. (1993) *Radioisotope-Powered Electric Propulsion of Small Payloads for Regular Access to Deep Space*. Paper presented at the 29th Joint Propulsion Conference and Exhibit, Monterey, CA. http://dx.doi.org/10.2514/6.1993-1897.

Noble, R.J. (1998) *Radioisotope Electric Propulsion of Sciencecraft to the Outer Solar System and Near-Interstellar Space.* In Missions to the Outer Solar System and Beyond; 2nd IAA Symposium on Realistic Near-Term Advanced Scientific Space Missions, International Academy of Astronautics, Aosta, Italy.

Noble, R.J. (1999) Radioisotope Electric Propulsion of Sciencecraft to the Outer Solar System and Near-Interstellar Space. *Acta Astron.* 44(2-4), 193-199.

Nock, K. (1987) TAU - A Mission to a Thousand Astronomical Units. In *19th International Electric Propulsion Conference*: American Institute of Aeronautics and Astronautics.

NRC (2003) *The Sun to the Earth - and Beyond: A Decadal Research Strategy in Solar and Space Physics*. Washington, D.C.: The National Academies Press. Retrieved from http://www.nap.edu/catalog/10477.html

NRC (2006) *Priorities in Space Science Enabled by Nuclear Power and Propulsion*. Washington, D.C.:

NRC (2008) *Launching Science: Science Opportunities Provided by NASA's Constellation System*. Wasington, D.C.: The National Academies Press. Retrieved from http://www.nap.edu/catalog/12554.html

NRC (2009a) *Radioisotope Power Systems: An Imperative for Maintaining U.S. Leadership in Space Exploration*. Washington, D.C.: The National Academies Press. Retrieved from http://www.nap.edu/openbook.php?record_id=12653

NRC (2009b) *A Performance Assessment of NASA's Heliophysics Program*. Washington, D.C.: The National Academies Press. Retrieved from http://www.nap.edu/catalog/12608/a-performance-assessment-of-nasas-heliophysics-program

NRC (2013) *Solar and Space Physics: A Science for a Technological Society* Washington, D.C.: The National Academies Press. Retrieved from http://www.nap.edu/catalog.php?record_id=13060

O'Shaughnessy, D.J., McAdams, J.V., Bedini, P.D., Calloway, A.B., Williams, K.E., Page, B.R. (2014) MESSENGER's Use of Solar Sailing for Cost and Risk Reduction. *Acta Astronautica* 93(0), 483-489. doi: http://dx.doi.org/10.1016/j.actaastro.2012.10.009

Oberth, H. (1970) *Ways to Spaceflight* (Agence Tunisienne de Public-Relations, T., Tunisia, 1970, Trans.): National Aeronautics and Space Administration. Retrieved from https://ia600503.us.archive.org/21/items/nasa_techdoc_19720008133/19720008133.pdf

Oort, J.H. (1950) The Structure of the Cloud of Comets Surrounding the Solar System and a Hypothesis Concerning Its Origin. *Bulletin of the Astronomical Institutes of the Netherlands* 11, 91-110.

Pawlik, E.V., Phillips, W.M. (1977) A Nuclear Electric Propulsion Vehicle for Planetary Exploration. *J. Spacecraft* 14(9), 518-525.

Perryman, M. (2012) The History of Astrometry. *The European Physical Journal H* 37(5), 745-792. doi: 10.1140/epjh/e2012-30039-4

Peschka, W. (1956) Über die Überbrückung interstellarer Entfernungen. *Astron. Acta* 2, 191-200.

Phillips, W., Pawlik, E. (1978) *Design Consideration for a Nuclear Electric Propulsion System.* In 13th International Electric Propulsion Conference, American Institute of Aeronautics and Astronautics, San Diego, CA.

Popper, D.M. (1954) Red Shift in the Spectrum of 40 Eridani B. *Astrophysical Journal* 120, 316-321. doi: 10.1086/145916

Purcell, E. (1963) Radioastronomy and Communication Through Space. In Cameron, A.G.W. (Ed.), *Interstellar communication: A Collection of Reprints and Original Contributions* (Cameron, A. G. W. ed., pp. 121-143). New York: W. A. Benjamin, Inc.

Romain, J.E. (1963) Time Measurements in Accelerated Frames of Reference. *Reviews of Modern Physics* 35(2), 376-388. Retrieved from https://link.aps.org/doi/10.1103/RevModPhys.35.376

Roman, D. (2020) The Experience. *Voyager, A Journey Through Our Solar System.* Retrieved from http://voyagesolarsystem.org/the-experience/.

Russell, H.N. (1917) Preliminary Parallax of Barnard's Star of Large Proper-Motion. *Astronomical Journal* 30(705). Retrieved from http://adsabs.harvard.edu/abs/1917AJ.....30...73R

Rutherford, E., Soddy, F. (1902a) LXIV. The Cause and Nature of Radioactivity.—Part II. *The London, Edinburgh, and Dublin Philosophical Magazine and Journal of Science* 4(23), 569-585. doi: 10.1080/14786440209462881

Rutherford, E., Soddy, F. (1902b) XLI. The Cause and Nature of Radioactivity.—Part I. *The London, Edinburgh, and Dublin Philosophical Magazine and Journal of Science* 4(21), 370-396. doi: 10.1080/14786440209462856

Sagan, C. (1963) Direct Contact Among Galactic Civilizations by Relativistic Interstellar Spaceflight. *Planet. Space Science* 11, 485-498.

Sänger, E. (1961) 21.4 Photon Propulsion. In Koelle, H.H. (Ed.), *Handbook of Astronautical Engineering*. New York: McGraw-Hill Book Company, Inc.

Sänger, E. (1961-2) Some Optical and Kinematical Effects in Interstellar Astronautics. *J. Brit. Int. Soc.* 18, 273-277.

Sänger, E. (1963) *Space Flight: Countdown for the Future*. New York: McGraw-Hill Book Co.

Scarf, F., Bonnet, R.M., Brueckner, G.E., et al. (1988) *Space Science in the Twenty-First Century: Imperatives for the Decades 1995 to 2015*. Washington, D.C.: Press, T.N.A.

Schwarzschild, K. (1916) Über das Gravitationsfeld eines Massenpunktes nach der Einsteinschen Theorie. [On the gravitational field of a mass point according to Einstein's theory]. *Sitzungsberichte der Königlich Preussischen Akademie der Wissenschaften* 1, 189-196. Retrieved from http://de.wikisource.org/wiki/%C3%9Cber_das_Gravitationsfeld_eines_Massenpunktes_nach_der_Einsteinschen_Theorie

Shapiro, I.I., Pettengill, G.H., Ash, M.E., Stone, M.L., Smith, W.B., Ingalls, R.P., Brockelman, R.A. (1968) Fourth Test of General Relativity: Preliminary Results. *Physical Review Letters* 20(22), 1265-1269. Retrieved from https://link.aps.org/doi/10.1103/PhysRevLett.20.1265

Shepherd, L.R., Cleaver, A.V. (1948a) The Atomic Rocket - 2. *Journal of the British Interplanetary Society* 7, 234-241.

Shepherd, L.R., Cleaver, A.V. (1948b) The Atomic Rocket - 1. *Journal of the British Interplanetary Society* 7, 185-194.

Shepherd, L.R., Cleaver, A.V. (1949) The Atomic Rocket - 3. *Journal of the British Interplanetary Society* 8, 23-37.

Shepherd, L.R. (1952) Interstellar flight. *Journal of the British Interplanetary Society* 11(4), 149-167.

Shepherd, L.R. (1999) Performance criteria of nuclear space propulsion systems. *Journal of the British Interplanetary Society* 52(9 / 10), 328 - 335.

Short, W., Sabin, C. (1959-60) A Radioisotope Propulsion System. *J. Brit. Int. Soc.* 17, 453-458.

Simpson, J.A., Chamberlain, J.W., Kraushaar, W., et al. (1960) *Interim Report No. 3*. Washington, D.C.: Committee 8 - Physics of Fields and Particles in Space.

The SP-100 Nuclear Reactor Program: Should It Be Continued?, U.S. House of Representatives. 15 (1992).

Spencer, D.F., Jaffe, L.D. (1962) Feasibility of Interstellar Travel. *Astronautica Acta* 9, 49-58.

StackExchange (2010) Integrals of the Square Root of a Cubic Polynomial. Retrieved from https://math.stackexchange.com/questions/9127/integrals-of-the-square-root-of-a-cubic-polynomial.

Stone, E., Alkalai, L., Friedman, L., et al. (2015) *Science and Enabling Technologies for the Exploration of the Interstellar Medium*. Pasadena, CA: Studies, K.I.f.S.

Stone, E.C., Frandsen, A.M., Mewaldt, R.A., Christian, E.R., Margolies, D., Ormes, J.F., Snow, F. (1998) The Advanced Composition Explorer. In Russell, C.T., Mewaldt, R.A., Rosenvinge, T.T. (Eds.), *The Advanced Composition Explorer Mission* (pp. 1-22): Springer Netherlands.

Stuhlinger, E. (1959) Photon Rocket Propulsion. *Astronautics*, 36 + 69-78.

Stuhlinger, E. (1964) *Ion Propulsion for Space Flight*. New York: McGraw-Hill Book Company.

Stuhlinger, E. (1967) Electric Space Propulsion Systems. *Space Sci. Rev.* 7, 795-847.

Sturm, E.J., Barber, T.J., Roth, D. (2015, 7-14 March 2015) *Ensuring Cassini's End-of-Mission Propellant Margins.* In 2015 IEEE Aerospace Conference.

Sutton, G.P. (2006) *History of Liquid Propellant Rocket Engines*. Reston, VA: AIAA.

Tanabe, T., Yokota, H. (1980) *Optimal Multiple Venus Swingby Sequence in Solar Probe Missions*. Paper presented at the 31st International Astronautical Congress, Tokyo, Japan.

Taylor, R. (2005) *Prometheus Project: Final Report* (982-R120461). Pasadena, CA:

Time and Date AS (2020a) Distance from Monaco to Wellington. Retrieved from https://www.timeanddate.com/worldclock/distanceresult.html?p1=264&p2=674.

Time and Date AS (2020b) Distance from Portland to …. Retrieved from https://www.timeanddate.com/worldclock/distances.html?n=1081.

Tsander, F.A. (1967) *From a Scientific Heritage* (NASA TT F-541). Moscow: NASA), N.P.t.b.

Tsien, H.-S. (1949) Rockets and Other Thermal Jets Using Nuclear Energy with a General Discussion on the Use of Porous Pile Materials. In Goodman, C. (Ed.), *The Science and Engineering of Nuclear Power* (First ed., Vol. 2, pp. 177-195). United States of America: Adison-Wesley Press, Inc.

Tsiolkovskiy, K.E. (1967) *Study of Outer Space by Reaction Devices*. Washington, D.C.:

Vaquero, J.M., Vázquez, M. (2009) The solar diameter and the astonomical unit. In *The Sun Recorded Through History*: Springer.

von Hoerner, S. (1962) The General Limits of Space Travel. *Science* 137, 18-23.

von Hoerner, S. (1962) The General Limits of Space Travel: We May Never Visit Our Neighbors in Space, But We Should Start Listening and Talking to Them. *Science* 137(3523), 18-23. doi: 10.1126/science.137.3523.18

Voûte, J. (1917) A 13th Magnitude Star in Centaurus, with the Same Parallax as α Centauri. *Monthly Notices of the Royal Astronomical Society* 77(9), 650-651. doi: 10.1093/mnras/77.9.650

Wallace, R.A. (1999, 03/06/1999 - 03/13/1999) *Precursor Missions to Interstellar Exploration.* In Aerospace Conference 1999, IEEE, Aspen, CO.

Wikipedia (2011) IKAROS. Retrieved from http://en.wikipedia.org/wiki/IKAROS.

Wikipedia (2020a, 15 October 2020) 2017 MB7. Retrieved from https://en.wikipedia.org/wiki/2017_MB7.

Wikipedia (2020b) Weierstrass's elliptic functions. Retrieved from https://en.wikipedia.org/wiki/Weierstrass%27s_elliptic_functions.

Wikipedia (2020c, 19 September 2020) Cosmic distance ladder. Retrieved from https://en.wikipedia.org/wiki/Cosmic_distance_ladder.

Wikipedia (2020d) From the Earth to the Moon. Retrieved from https://en.wikipedia.org/wiki/From_the_Earth_to_the_Moon.

Wikipedia (2020e, 23 October 2020) Kerr metric. Retrieved from https://en.wikipedia.org/wiki/Kerr_metric#Open_problems.

Wikipedia (2020f, 20 October 2020) Schwarzschild geodesics. Retrieved from https://en.wikipedia.org/wiki/Schwarzschild_geodesics.

Wikipedia (2020g) Ultra-high-temperature ceramics. Retrieved from https://en.wikipedia.org/wiki/Ultra-high-temperature_ceramics.

Wikipedia (2020h) Jules Verne. Retrieved from https://en.wikipedia.org/wiki/Jules_Verne.

Williams, D.R. (2018) Sun Fact Sheet. *Planetary Fact Sheets.* Retrieved from https://nssdc.gsfc.nasa.gov/planetary/factsheet/sunfact.html.

Wilson, D.T. (1921) On the Parallax of Barnard's Proper-Motion Star. *Astronomical Journal* 34(793). doi: 10.1086/104476

Wimmer-Schweingruber, R.F., McNutt, R.L., Jr., IHP/HEXTeam (2009) The Interstellar Heliopause Probe: Heliospheric Boundary Explorer Mission to the Interstellar Medium. *Earth Moon Planet* 104, 17-24. doi: DOI 10.1007/s11038-008-9249-8

Wimmer-Schweingruber, R.F., McNutt, R.L., Jr., Schwadron, N.A., Frisch, P.C., Gruntman, M., Wurz, P., Valtonen, E., IHP/HEXTeam (2009) Interstellar Heliospheric Probe/Heliospheric Boundary Explorer Mission—A Mission to the Outermost Boundaries of the Solar System. *Exp. Astron.* 24, 9-46. doi: 10.1007/s10686-008-9134-5

Wolfram (2020, Not available) JacobiSN. Retrieved from https://reference.wolfram.com/language/ref/JacobiSN.html.

Wollman, M.J., Zika, M.J. (2006) *Prometheus Project Reactor Module Final Report, For Naval Reactors Information* (SPP-67110-0008 United States10.2172/884680Tue Feb 05 05:16:18 EST 2008KAPLEnglish)

Zurbuchen, T.H., Patel, P., Fisk, L.A., Zank, G.P., Malhotra, R., Funsten, H.O., Mewaldt, R.A. (2008) Leaving the Heliosphere: A Nuclear-Powered Interstellar Probe. In Allen, M.S. (Ed.), *NASA Space Science Vision Missions* (Vol. 224, pp. 434). Reston, Virginia.

12. Acronyms and Abbreviations

AA	Associate Administrator (NASA)
AAS	(1) American Astronautical Society
AAS	(2) American Astronomical Society
ACE	Advanced Composition Explorer
ACE Lab	APL Concurrent Engineering Laboratory
ACES	Advanced Cryogenic Evolved Stage
ACF	Advanced Ceramic Fibers (LLC)
ACO	Advanced Concepts Office
ACR	Anomalous Cosmic Ray
AGU	American Geophysical Union
AIAA	American Institute of Aeronautics and Astronautics
ALMA	Atacama Large Millimeter/submillimeter Array
AMR	Atlantic Missile Range
AoA	Analysis of Alternatives
AOGS	Asia Oceania Geosciences Society
APL	The Johns Hopkins University Applied Physics Laboratory
ASEE	American Society for Engineering Education
ASME	The American Society of Mechanical Engineers
ASRG	Advanced Stirling Radioisotope Generator
au	Astronomical Unit, defined as exactly 149,597,870,700 meters
B2	Block 2 (of the Space Launch System)
BCE	Before Common Era
BOLE	Booster Obsolescence Life Extension
BPPP	Breakthrough Propulsion Physics Program

C_3	Square of the Excess Hyperbolic Escape Speed from the Earth
CALCE	(The) Center for Advanced Life Cycle Engineering (at the University of Maryland)
CAPS	Committee on Astrobiology and Planetary Sciences, committee of the SSB
CATE	Cost and Technical Evaluation
CCD	Charge-Coupled Device
CDA	Cosmic Dust Analyzer
CENA	Chandrayaan-1 Energetic Neutrals Analyzer
CETI	Communication with Extraterrestrial Intelligence
CFC	Chlorofluorocarbon
CIB	Cosmic Infrared Background
CIBER	Cosmic Infrared Background Experiment
CIBR	Cosmic Infrared Background Radiation
CICG	Centre International de Conférences de Genève
CIR	Corotating Interaction Regions
CMBR	Cosmic Microwave Background Radiation
CME	Coronal Mass Ejection
CMOS	Complementary Metal-Oxide Semiconductor
COB	Cosmic Optical Background
CoDICE	Compact Dual Ion Composition Experiment
COBE	Cosmic Background Explorer
CONOPS	Concept of Operations
COSPAR	Committee on Space Research
CSF	Close Solar Flyby (per Ehricke)
CSSP	Committee on Solar and Space Physics, committee of the SSB
CTR	Controlled Thermonuclear Reactor (controlled fusion with net energy gain)
CY	Calendar Year

DFVLR	Deutsche Forschungs- und Versuchsanstalt fuer Luft- und Raumfahrt e. V.
DGL	Diffuse Galactic Light
DIRBE	Diffuse InfraRed Background Experiment
DMSP	Defense Meteorological Satellite Program
DOD	Department of Defense (U.S.)
DOE	Department of Energy (U.S.)
DOI	Digital Object Identifier
DPS	Division for Planetary Sciences (of the American Astronautical Society)
DRACO	Didymos Reconnaissance and Asteroid Camera for OpNav
DS1	Deep Space One, science and electric propulsion technology test mission
DSA	Deep Space Avionics
DSIF	Deep Space Information Facility
DSM	Deep-Space Maneuver
DSN	Deep Space Network
EBL	Extragalactic Background Light
ΔV-EGA	Delta-V, Earth Gravity Assist
EGU	European Geosciences Union
EIS	Europa Imaging System
EKB	Edgeworth-Kuiper Belt
EMFISIS	Electric and Magnetic Field Instrument Suite and Integrated Science
eMMRTG	Enhanced Multi-Mission Radioisotope Thermoelectric Generator
ENA	Energetic Neutral Atom
EPD	Energetic Particle Detector
EPSC	European Planetary Science Congress
ESA	(1) Electrostatic Analyzer
ESA	(2) European Space Agency

ESAS	Exploration System Architecture Study
EUS	Exploration Upper Stage
EUV	Extreme Ultraviolet
FIR	Far Infrared
FISO	Future In-Space Operations
FOV	Field of View
FRG	Federal Republic of Germany, aka “West Germany” (1949–1990)
FY	Fiscal Year
GA	Gravity Assist
G&C	Guidance and Control
GCR	Galactic Cosmic Ray
GMIR	Global Merged Interaction Region
GPHS	General-Purpose Heat Source
GTO	Geosynchronous Transfer Orbit
GUVI	Global Ultraviolet Imager
HAE	High-Amplification Event, continuum emission from quasars
HENA	High-Energy Neutral Atom
HfC	Hafnium Carbide
HGA	High-Gain Antenna
HP	Heliopause
HRI	High Resolution Instrument
HST	Hubble Space Telescope
HTC	Halley-Type Comet
HUT	Hopkins Ultraviolet Telescope
H-wall	Hydrogen Wall
IAA	International Academy of Astronautics

IAC	International Astronautical Congress
IAU	International Astronomical Union
IBEX	Interstellar Boundary Explorer, Heliophysics Small Explorer
ICPS	Interim Cryogenic Propulsion Stage
IDEX	Interstellar Dust Experiment
IEEE	Institute of Electrical and Electronics Engineers
IHP	Interstellar Heliopause Probe
IIE	Innovative Interstellar Explorer, APL Interstellar precursor “Vision Mission” study
IKAROS	Interplanetary Kite-craft Accelerated by Radiation of the Sun
IMAP	Interstellar Mapping and Acceleration Probe
IMF	Interplanetary Magnetic Field
INCA	Ion and Neutral Camera
INMS	Ion and Neutral Mass Spectrometer
IOC	Initial Operational Capability
IPD	Interplanetary Dust
IPSTDT	Interstellar Probe Science and Technology Definition Team (three meetings at JPL in 1999)
IR	Infrared
IRAS	Infrared Astronomy Satellite
ISD	Interstellar Dust
ISM	Interstellar Medium
ISMF	Interstellar Magnetic Field
ISO	Infrared Space Observatory
I_{sp}	Specific Impulse
IT	Information Technology
IUS	Inertial Upper Stage

IUVS	Imaging Ultraviolet Spectrograph
IW	Interstellar Wind
JAXA	Japan Aerospace Exploration Agency
JENI	Jupiter Energetic Neutrals and Ions
JFC	Jupiter-Family Comet
JGA	Jupiter Gravity Assist
JIMO	Jupiter Icy Moons Orbiter
JoEE	Jovian Energetic Electrons
JOI	Jupiter Orbit Insertion
JPL	Jet Propulsion Laboratory
JUICE	Jupiter Icy Moons Explorer
JWST	James Webb Space Telescope
KBO	Kuiper Belt Object
kEV	Kiloelectronvolt
KISS	Keck Institute for Space Studies
KSC	Kennedy Space Center
λ	“Lightness Number,” Photon Sails
LADEE	Lunar Atmosphere and Dust Environment Explorer
LANL	Los Alamos National Laboratory, designation since 1981
LASL	Los Alamos Scientific Laboratory, designation from 1945 to 1980 (1943–1945 “Project Y”)
LBTI	Large Binocular Telescope Interferometer
LCCE	Life-Cycle Cost Estimate
LCPMC	Low-Cost Planetary Missions Conference
LDEX	Lunar Dust Experiment
LECP	Low-Energy Charged Particle

LEISA	Linear Etalon Imaging Spectral Array
LENA	Low-Energy Neutral Atom Imager
LEO	Low Earth Orbit
LF_2	Liquid Fluorine, energetic cryogenic rocket oxidizer, notional
LHB	Late Heavy Bombardment
LH_2	Liquid Hydrogen, cryogenic rocket fuel
LIC	Local Interstellar Cloud
LISM	Local Interstellar Medium
LLC	Limited Liability Company (or Corporation)
LORRI	Long Range Reconnaissance Imager
LOS	Line of Sight
LOX	Liquid Oxygen, cryogenic rocket oxidizer
LPSC	Lunar and Planetary Science Conference
LST	Lifetime Study Team
LWS	Living With a Star, program within NASA's Heliophysics Division
LXe	Liquid Xenon, space-storable rocket propellant for low-thrust, electric engines
ly	Light Year, = 9,460,730,472,580,800 meters (exactly) ≈ 63,241.077 au (per IAU)
MAG	Magnetometer
mas	Milliarc Second
MAVEN	Mars Atmosphere and Volatile Evolution
MBB	Messerschmitt-Boelkow-Blohm GmRH
MENA	Medium-Energy Neutral Atom
MESSENGER	Mercury Surface, Space Environment, Geochemistry, and Ranging
MGA	Mass Growth Allowance
MHD	Magnetohydrodynamic
MHW	Multi-Hundred Watt

MLI	Multilayer Insulation
MMH	Monomethyl Hydrazine, space-storable rocket fuel
MMRTG	Multi-Mission Radioisotope Thermoelectric Generator
MMS	Magnetospheric Multiscale Mission
MON	Mixed Oxides of Nitrogen, space-storable rocket oxidizer
MPD	Magnetoplasma Dynamic, notional, in-space, high-power electric rocket engine
MSFC	Marshall Space Flight Center
MSL	Mars Science Laboratory, aka *Curiosity*
mt	Metric Ton, defined as 1000 kg
MVIC	Multispectral Visible Imaging Camera
Myr	Million Years
NARA	National Archives and Records Administration
NASA	National Aeronautics and Space Administration
NE	Nuclear Electric
NEOCAM	Near-Earth Object Camera
NEP	Nuclear Electric Propulsion
NERVA	Nuclear Engine for Rocket Vehicle Application
NETS	Nuclear and Emerging Technologies for Space
NEXT	NASA Evolutionary Xenon Thruster
NGMS	Neutral Gas Mass Spectrometer
NGST	Next Generation Space Telescope
NIAC	NASA Institute for Advanced Concepts
NIRSpec	Near Infrared Spectrograph
NLS – II	NASA Launch Service – II
NMS	Neutral Mass Spectrometer
NRA	NASA Research Announcement

NRC	National Research Council
NSSDC	National Space Science Data Center
NTE	Not-to-Exceed
NTO	Nitrogen Tetroxide, space-storable rocket oxidizer
NTP	Nuclear Thermal Propulsion
NYC	New York City
OCC	Oort-Cloud Comets
OPAG	Outer Planet Assessment Group
OSIRIS-REx	Origins, Spectral Interpretation, Resource Identification, Security, Regolith Explorer
OSS	Office of Space Science
OVIRS	OSIRIS-REx Visible and Infrared Spectrometer
PACS	Photodetector Array Camera and Spectrometer
PAM	Payload Assist Module, kick stage designator
PAM – S	Payload Assist Module – Special, unique build for Ulysses (ESA) mission
pc	Parsec, distance at which a star exhibits an Earth-based parallax of 1” (of arc)
PDS	Planetary Data System
PEPSSI	Pluto Energetic Particle Spectrometer Science Investigation
PI	Principal Investigator
PIR	Panel on Interstellar Research
PMS	Propulsion Module Subsystem
PMSR	Project Management and System Review
PPD	Protoplanetary Disk
PS	Project Scientist
PSP	Parker Solar Probe
PSW	Payload System Weight

PUI	Pickup Ion
PWS	Plasma Wave Spectrometer
px	Pixel
QOZ	Quasi-Optical Zone (per Ehricke)
QTN	Quasi-Thermal Noise
REP	Radioisotope Electric Propulsion
R_J	Jovian Radius, using 1 R_J = 71,492 km
ROSINA	Rosetta Orbiter Spectrometer for Ion and Neutral Analysis
RPM	Retropropulsion Model
RPS	Radioisotope Power System
RPWS	Radio and Plasma Wave Science
R_S	Solar Radius, with 1 R_S taken herein as 695,700 km
RTG	Radioisotope Thermoelectric Generator
SAE	(formerly) Society of Automotive Engineers; now “SAE International”
SARA	Sub-keV Atom Reflecting Analyzer
SDC	Student Dust Counter
SDI	Strategic Defense Initiative
SDT	Science Definition Team
SEC	Sun-Earth Connection
SEP	Solar Electric Propulsion
SEPICA	Solar Energetic Particle Ionic Charge Analyzer
SERT I	Space Electric Rocket Test I
SETI	Search for Extraterrestrial Intelligence
SHINE	Solar, Heliospheric, and INterplanetary Environment
SIS	(1) Solar Isotope Spectrometer
SIS	(2) Suprathermal Ion Spectrograph

SIT	Suprathermal Ion Telescope
SLAC	Stanford Linear Accelerator
SLS	Space Launch System
SMD	Science Mission Directorate
SNR	Signal-to-Noise Ratio
SNRE	Small Nuclear Rocket Engine
SOHO	Solar and Heliospheric Observatory
SOZ	Suboptical Zone (per Ehricke)
SPICE	Spectral Imaging of the Coronal Environment
SPIE	SLS Spacecraft/Payload Integration and Evolution (Office)
SSB	Space Studies Board, derived from Space Science Board in 1989
SSG	Science Steering Group (Voyager Project)
ssr	Solar System Radius, using 40 au (per Ehricke)
SSUSI	Special Sensor Ultraviolet Spectrographic Imager
STDT	Science and Technology Definition Team
STIS	Space Telescope Imaging Spectrograph
STM	Science Traceability Matrix
STP	Solar Thermal Propulsion
STS	Space Transportation System, aka *Space Shuttle*
SUDA	Surface Dust Analyzer
SW	Solar Wind
SWAN	Solar Wind Anisotropies
SWAP	Solar Wind Around Pluto
SWEAP	Solar Wind Electrons Alphas and Protons
SWEPAM	Solar Wind Electron Proton Alpha Monitor
SWICS	Solar Wind Ion Composition Spectrometer

TAU	Thousand Astronomical Units, interstellar precursor mission concept at JPL, late 1980s
TDI	Time-Delay Integration
TESS	Transiting Exoplanet Survey Satellite
3D	Three-Dimensional
TIMED	Thermosphere Ionosphere Mesosphere Energetics and Dynamics
TOF	Time-of-Flight
TPS	(1) The Planetary Society
TPS	(2) Thermal Protection System
TRL	Technology Readiness Level
TS	Termination Shock
TSA	Thermal Structure Assembly
UDMH	Unsymmetrical Dimethylhydrazine, space-storable rocket fuel
UHT	Ultra-High Temperature
ULA	United Launch Alliance
ULEIS	Ultra Low Energy Isotope Spectrometer
UV	Ultraviolet
UVS	Ultraviolet Spectrometer
UVV	Ultraviolet/Visible
UZ	Ultraplanetary Zone (per Ehricke)
VAFB	Vandenberg Air Force Base
VAP	Van Allen Probes
VASIMR	Variable Specific Impulse Magnetoplasma Rocket, developmental rocket engine
vdf	Velocity Distribution Function
VEEGA	Venus-Earth-Earth Gravity Assist
VGA	Venus Gravity Assist

VIM	Voyager Interstellar Mission
VIMS	Visible and Infrared Mapping Spectrometer
VIRTIS	Visible and Infrared Thermal Imaging Spectrometer
VISNIR	Visible Near Infrared
VLBI	Very-Long Baseline Interferometry
VLF	Very Low Frequency
VLISM	Very Local Interstellar Medium, original definition of within 0.01 pc of the Sun
W	Watt
WBS	Work Breakdown Structure
WISE	Wide-field Infrared Survey Explorer
WMAP	Wilkinson Microwave Anisotropy Probe
ZI	Zone of Isolation (per Ehricke)